MODELING THE EARTH SYSTEM

Dennis Ojima, Editor

Papers arising from the 1990 OIES Global Change Institute

Snowmass, Colorado
16–27 July 1990

UCAR/Office for Interdisciplinary Earth Studies
Boulder, Colorado
1992

OIES

UCAR

Office for Interdisciplinary Earth Studies
Global Change Institute Volume 3

Produced by the Office for Interdisciplinary Earth Studies of the University Corporation for Atmospheric Research through support from the U.S. Department of Energy, Environmental Protection Agency, U.S. Geological Survey, National Aeronautics and Space Administration, National Oceanic and Atmospheric Administration, and National Science Foundation.

Table of Contents

Preface

The 1990 Global Change Institute on Earth System Modeling is the third of a series organized by the Office for Interdisciplinary Earth Studies to look in depth at particular issues critical to developing a better understanding of the earth system. The first institute focused on how the biosphere interacts with atmospheric chemistry, how terrestrial and marine biological processes have contributed to the makeup of the atmosphere, and how these processes may be modified by projected global environmental changes. The second conference concentrated on past earth system changes and how understanding these may assist us in our study of future changes. It also addressed the questions of what major processes interact during global environmental change and what various measurements from the earth's history can tell us about the earth system.

The 1990 Global Change Institute focused on the role of modeling in developing a better understanding of the earth system. Models play a vital role in the study of the earth system. They represent our understanding of natural processes, prompt specific questions, suggest further measurements, and permit forecasting of future conditions. Mathematical models have the added advantage of quantifying interactive processes, as well as describing the inputs, forcing conditions, and internal parameters that control the behavior of these systems. They allow us to estimate how changes in any part of the system will affect not only that part but those attached to it, even distantly, through the vast web of interactions.

The complexity of these interactions among subcomponents is immense. To study all of them would be an impossible and futile task. Creating a strategy of how to best study the earth system raises the questions of what we know of the earth system, how to model the system, and how to test these models. Simplified representations of our understanding of critical processes that influence the earth system are fundamental tools for global change scientists.

We are still in the early stages of dynamically linking the components of the earth system in our models. The basic subcomponent models vary considerably in sophistication and success. In many cases, the observations necessary to validate the dynamics of the fully coupled models, or even of the smaller subcomponent models, do not exist.

We are faced with two challenges: not being able to study the full complexity of the earth system, and not possessing a full enough understanding to know what is essential to include in earth system models. Models can be only as accurate as the knowledge of those who build them. In other words, any gap in our knowledge of the workings of the earth system can result in a flaw in our ability to predict changes, especially changes of a magnitude or type that has not been experienced for hundreds of thousands of years, if ever. Thus, the first question that modelers must ask of themselves is: "What do we not know?"

As in most complex systems, the processes controlling the state and evolution of the earth system operate on different space and time scales. In order to study their behavior, it is necessary to build a hierarchy of models to try to match these different scales. Both simple models and complex models have a role in this work. Neither can be considered superior; both have valid uses.

Simple or toy models are useful in developing basic understanding of how processes may respond to perturbations to the system, or how linkages between subcomponents are dynamically altered through modeled feedbacks. Toy models are limited in scope but easier to design and understand; if they are time dependent, they can be integrated over longer periods. Their results may be more readily interpreted. We must recognize, however, that our interpretation incorporates preconceived and simplified notions of what we assume the system to be, not the system itself.

Complex models include many more processes than toy models and may be more realistic. They are, however, intrinsically more expensive to design and operate, difficult to parameterize, and challenging to validate. Often, they cannot run simulations covering very long time periods. The number and complexity of the processes included in these models also render interpretation of the results more difficult.

No model, simple or complex, exists that can faithfully mimic the "real world"; rather, models represent an idealization of reality. All models must therefore be validated. This is a process in which model results and predictions are compared to the actual evolution of the modeled system. The means of validation must be carefully chosen and designed if the process is to offer a true reality check.

Environmental change on a global scale and over time scales of decades to centuries is a very complex subject, the modeling of which requires the collaboration of scientists in many disciplines. Participants from a variety of disciplines, such as atmospheric chemical and physical researchers, oceanographers, hydrologists, pedologists, marine and terrestrial biologists and ecologists, and social scientists, must work together to advance our understanding of the processes affecting changes in the earth system. These collaborations have recently begun to take place.

The 1990 Global Change Institute on Modeling the Earth System offered a timely opportunity to promote cooperation among scientists attempting to simulate the earth's subsystems (atmosphere, land, and oceans) and their interactions. Like all Global Change Institutes, the 1990 symposium offered about 45 scientists from many disciplines the opportunity to work together, to listen to each other's knowledge and needs, in the belief that each would carry away more than he or she brought.

The 1990 GCI on Earth System Modeling was organized around three themes: defining critical gaps in our knowledge of the earth system, developing simplified working models, and validating comprehensive system models. This book is divided into three sections that reflect these themes. Each section begins with a set of background papers offering a brief tutorial on the subject, followed by working group reports developed during the institute. These reports summarize the joint ideas and recommendations of the participants and bring to bear the interdisciplinary perspective that imbued the institute

Since the conclusion of the 1990 Global Change Institute, research programs, nationally and internationally, have moved forward to implement a number of the recommendations made at the institute, and many of the participants have maintained collegial interactions to develop research projects addressing the needs identified during the two weeks in Snowmass.

Acknowledgments

The 1990 Global Change Institute and the publication of this volume were made possible by the continuing and generous support of the U.S. Department of Energy, Environmental Protection Agency,

National Aeronautics and Space Administration, National Oceanic and Atmospheric Administration, National Science Foundation, and U.S. Geological Survey.

We are proud to give credit to Jack Eddy as the originator and motivator, not only of the 1990 institute but of the entire series. Additional thanks are due to the many individuals who gave a special impetus to this project: co-directors Bert Bolin and Francis Bretherton, editor Carol Rasmussen, and the members of the Organizing Committee for the institute: Barbara Anderson, Andre Berger, Kirk Bryan, Bob Dickinson, Ron Prinn, and Dave Schimel. As always, we thank the OIES staff, whose support makes the institutes possible: Lisa Butler, Sarah Danaher, Diane Ehret, Paula Robinson, and Pamela Witter.

Finally, we are indebted to all who came to Snowmass, especially to the rapporteurs for spending countless hours pulling together the material for the working group reports, and to the moderators of the various sessions for guiding the discussions toward the purpose assigned. In addition, a special thanks is due to those scientists who have taken time to review the manuscripts contained in the 1990 GCI volume. Without their efforts, the scientific worth of this volume would have been lessened.

Dennis Ojima

Introduction

Bert Bolin and Francis Bretherton

To advance our knowledge about the structure and behavior of the global geosphere-biosphere system, the development of models is essential. The great complexity of the earth's system promotes the use of models to synthesize in a meaningful manner the huge number of data that already are available as well as the even more extensive data bases of the future. Models also serve as essential tools to predict future changes in the earth's system, natural or anthropogenic. Any model is a simplification of reality, but it provides means to ascertain internal consistency in our attempts to interpret observations and to test the plausibility and compatibility of hypotheses concerning the interactions of key processes in a system.

It is useful as a starting point to construct a reasonably detailed qualitative picture of basic interactions that take place in the earth system—a so-called wiring diagram. In this way we can impose on our models the overall requirements of key processes such as energy balance and other dynamical constraints on the system as a whole, as well as mass continuity in the biogeochemical cycling of all significant elements. This is, however, only a first step. We must select the essential interconnections and assess the possible feedback mechanisms in order to proceed from the complexity of the real earth system to the simplified world of the model. Eventually, we will need to include more complex representations of these processes in the model to "understand" the fundamental characteristics of the earth system. To do so we must analyze in more detail the nature of these processes at work. Model development thus

means determining how the key processes interact at specific regions and under the constraints defined by the overall characteristics of the system.

Neglecting in the present context the slowly acting geological processes, the earth's system may be considered as the interactions among the atmosphere, the oceans, and the terrestrial system including snow and ice (called the cryosphere). Models for these three subsystems are in various stages of development.

Atmospheric models were first developed in the 1950s for weather forecasting, i.e., predicting the physical behavior of the atmosphere. The inclusion of chemical processes was begun a decade or two later, and now quite elaborate models are available for the study of the physical and chemical behavior of the atmosphere. Most of these are, however, still essentially weather forecasting models that are integrated over extended periods of time with prescribed constant or changing boundary conditions and external forcing (changing solar radiation, modified composition of the air, etc.).

Model development for the oceans started somewhat later than that of atmospheric models but has proceeded in a similar manner. Rather elaborate models that deal with the physics of the oceans are available, and the inclusion of geochemical and biological interactions has begun. During the last decade more consideration has been given to the role of the oceans in climate.

Basic model development for the atmosphere and ocean subsystems has by no means been completed. Particularly, the oceanic models are not yet able to produce rates of transfer of matter in the sea that are adequate for analysis of the ocean's biogeochemistry.

Model development for the ocean and atmosphere is based on the application of the basic hydrodynamical equations. A corresponding basis for analysis of the terrestrial system is not available, as the stationary characteristics of the terrestrial biosphere are wholly different. We are therefore confronted with the need to develop a fundamental methodology to describe this very heterogeneous and complex system. The initial attempt to describe and understand the global characteristics of terrestrial ecosystems was simply based on the application of continuity equations for the fluxes of water and energy and the basic elements necessary for the maintenance of the major terrestrial ecosystems. Global analyses of the terrestrial ecosystem are now being undertaken to investigate the dynamic feedback between the biosphere and the atmosphere through exchanges of energy and CO_2, H_2O, and other radiatively active gases.

The recent realization that human activities may have major impacts on the earth's climate has stimulated increased research within the various disciplines involved (meteorology, ecology,

oceanography, atmospheric chemistry, sociology, and many others). It is becoming increasingly clear that the proper approach for studying climate and climate change requires the use of models that permit mutual interactions among all three components of the earth system—the land, ocean, and atmosphere—with proper consideration of the cryosphere. Relaxing the constraints implied by fixed boundaries between the different subsystems introduces additional degrees of freedom for the system as a whole, and the compatibility of the model formulations for the interacting processes becomes a crucial issue.

One can now envisage a development that would lead to the construction of elaborate coupled models including all basic components of the system; but, as indicated above, major difficulties would arise during this process. Much care must be exercised to ensure that the different submodels that are employed are indeed coupled appropriately, i.e., that the formulations for the three respective subsystems are mutually compatible. In developing these coupled models, it will be important to formulate very simplified models ("toy models") of the particular interactions and possible feedback mechanisms that are introduced, and to verify that these representations are in agreement with available observations.

Attempts to proceed in the direction of full coupled models have been hampered by insufficient interaction among scientists in the relevant fields of research and particularly by inadequacies of fundamental concepts and terminology linking these fields. The differences among the characteristic spatial and temporal scales used to model the various subsystems have been another obstacle for progress.

Considerations of this kind served as a basis for choosing the three scientific goals for the 1990 Global Change Institute, which was intended to further the development of earth system models. These goals were:

- Locate any important gaps in our knowledge of basic earth system interactions
- Define simplified or toy models that could assist in the long-term development of more complex earth system models
- Specify the best validation methods for earth system models.

The structure of this volume also follows these three themes. For each topic, background papers are followed by the reports of the working groups that discussed aspects of each theme, offering an overview of the institute's deliberations.

Atmosphere, Ocean, and Land: Critical Gaps in Earth System Models

Ronald G. Prinn and Dana Hartley

Introduction

The earth's unique environment for life is determined by an interactive system comprising the atmosphere, ocean, land, and the living organisms themselves. We know from observations that this system is not static but changing. Our ability to understand past changes and predict future changes is hampered by insufficient understanding of at least five fundamental processes in the earth system: (1) convection, condensation nuclei, and cloud formation; (2) oceanic circulation and its coupling to the atmosphere and cryosphere; (3) land surface hydrology and hydrology-vegetation coupling; (4) biogeochemistry of greenhouse gases; and (5) upper atmospheric chemistry and circulation.

We need to improve our knowledge of each of these processes through a combination of observations and theory (model development). We then need to incorporate realistic models for these processes into climate prediction models with special attention to potential feedbacks to climate change involving these processes (Figure 1). In each case it is not just a matter of explaining the present state but also of understanding how each of the processes contributing to this state will change when one or more of the external forcing mechanisms changes. In this paper we briefly review current knowledge and pinpoint some of the major areas of uncertainty for each of the above five fundamental processes.

Convection, Condensation Nuclei, and Cloud Formation

Clouds and water vapor play a major role in the heat budget of the earth's surface. Clouds contribute to surface cooling by reflect-

ing sunlight back to space. In fact, cloud albedo doubles the albedo of the entire earth over what it would be in the absence of clouds (Ramanathan et al., 1989). Furthermore, both water vapor and clouds contribute to surface heating by absorbing and re-emitting infrared radiation (greenhouse effect). Indeed, the contribution to

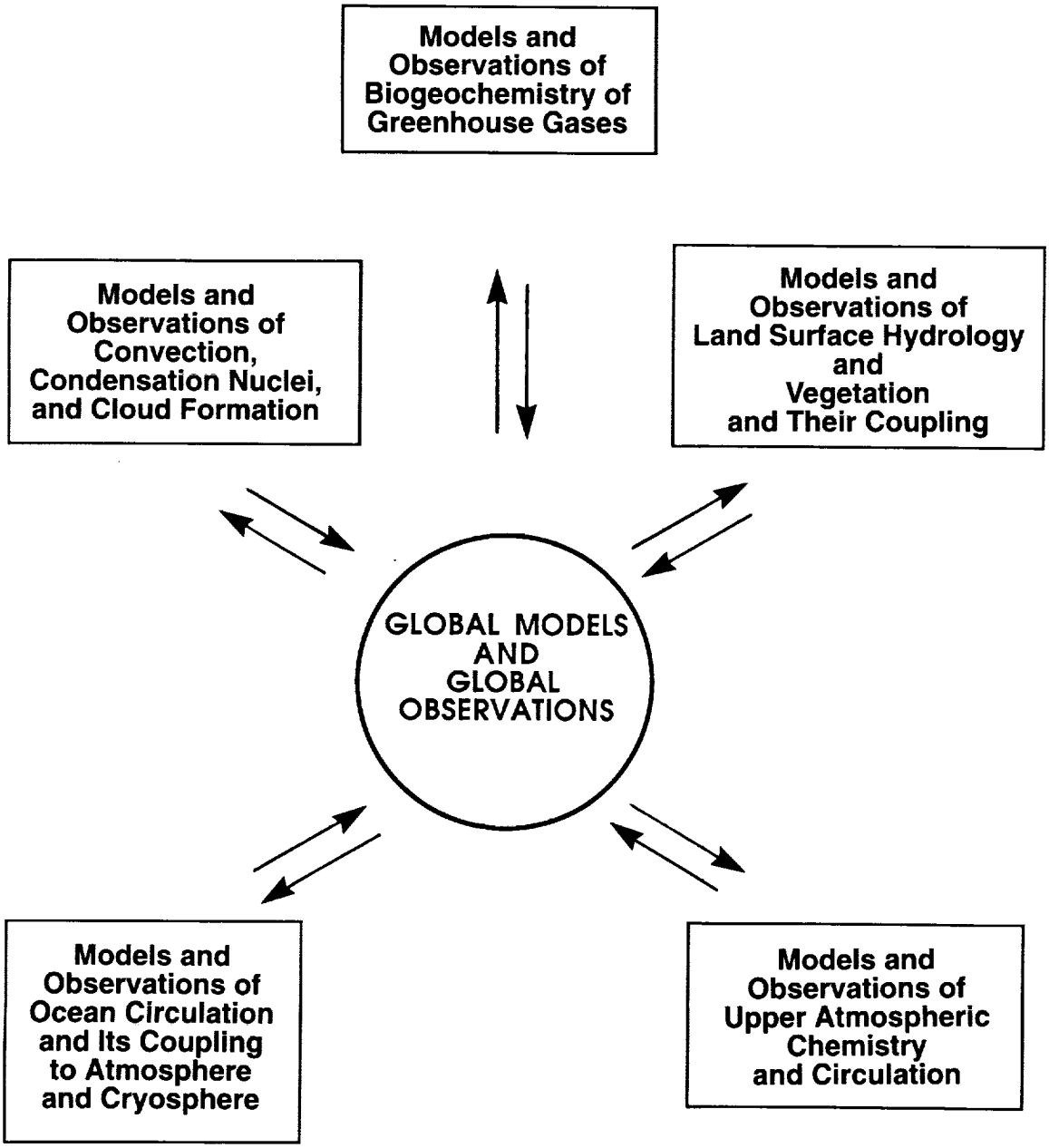

Figure 1. Schematic illustrating required research for improving current climate models.

the greenhouse effect of clouds and water vapor is far greater than that caused by CO_2 (see Table 1 for chemical names and formuli) and the other long-lived greenhouse gases.

Table 1: Chemicals named in this chapter

^{12}C	carbon-12
^{13}C	carbon-13
$CFCL_3$	trichlorofluoromethane (CFC-11)
CF_2Cl_2	dichloro-difluoromethane (CFC-12)
$CF_2ClCFCl_2$	1-chlorodifluoro-2-dichlorofluoroethane (CFC-113)
$CHClF_2$	chlorodifluoromethane (HCFC-22)
$CHCl_2CF_3$	1-dichloro-2-trifluoroethane (HCFC-123)
CH_2FCF_3	1-trifluoro-2-fluoroethane (HCFC-134a)
CH_3CCl_3	1-trichloroethane (methyl chloroform)
CH_35Cl_3 (DMS)	dimethyl sulfide
CH_4	methane
Cl	chlorine atom
ClO	chlorine monoxide
$ClONO_2$	chlorine nitrate
ClOOCl	chlorine monoxide dimer
Cl_2	molecular chlorine
CO	carbon monoxide
CO_2	carbon dioxide
HCl	hydrogen chloride
HNO_3	nitric acid
HO_2	hydroperoxyl free radical
H_2O	water
H_2O_2	hydrogen peroxide
NO	nitric oxide
NO_2	nitrogen dioxide
N_2O	nitrous oxide
$O(^1D)$	electronically excited oxygen atom
OH	hydroxyl free radical
O_2	molecular oxygen
O_3	ozone
RH	generic hydrocarbon
RO_2	generic organic peroxy free radical
ROOH	generic organic hydroperoxide
SO_2	sulfur dioxide

The net effect of clouds is determined by the opposing effect of the albedo of the cloud and its opacity to infrared radiation. Theory and observations have shown that the net effect of clouds is to lower the surface temperature relative to the cloud-free state (Somerville and Remer, 1984; Ramanathan et al., 1989). However, there are still difficulties in representing the present cloud forcing in large-scale general circulation models (GCMs). A recent comparison between GCM results and present-day observations illustrates some of the weaknesses in present parameterizations of cloud formation (Kiehl and Ramanathan, 1990). Figure 2 in particular shows that there is too much solar radiance reaching the surface near the poles and too little near the tropics in the community climate model (CCM) of the

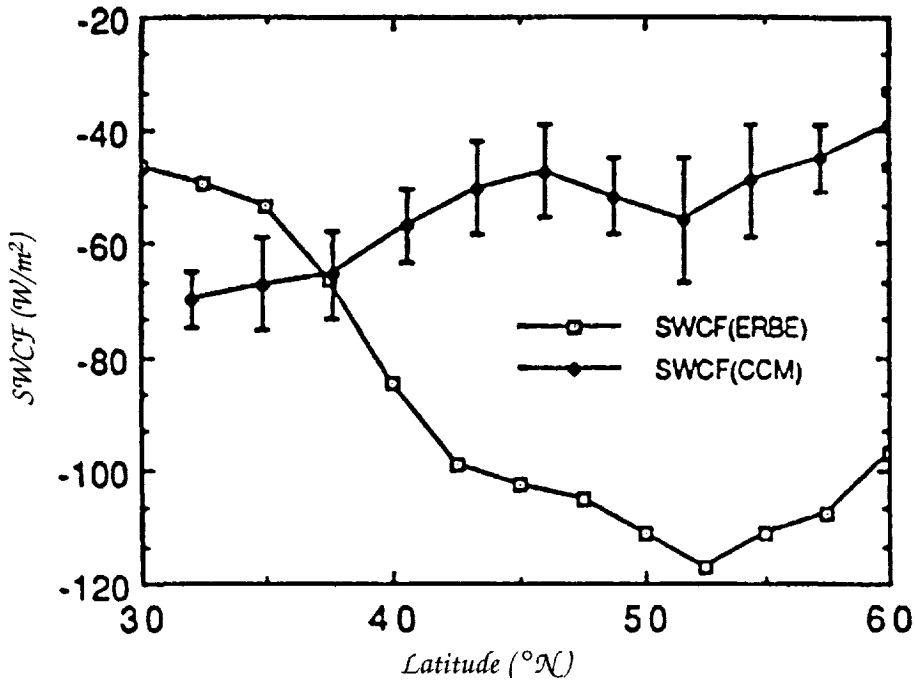

Figure 2. Shortwave cloud radiative forcing (SWCF) as a function of latitude in the western North Atlantic from ERBE data and from the NCAR community climate model (adapted from Kiehl and Ramanathan, 1990).

National Center for Atmospheric Research as compared to Earth Radiation Budget Experiment (ERBE) data. Some of this difference is associated with the surface albedo's being too large in the model tropics and some with obvious gaps in the ability of the CCM to parameterize the cloud formation process. Furthermore, for predictions of future climate change, we want to be capable of determining how the cloud/radiative balance may change, which requires a fundamental understanding of the cloud formation process. We then need realistic models for linking cloud microphysics and atmospheric dynamics to yield accurate predictions of the global three-dimensional structure of clouds.

The microphysics of clouds is determined to a large extent by the ambient concentrations of cloud condensation nuclei (CCN). Over land the presence of CCN is often due to dust or aerosol emissions by humans. Over the oceans the predominant source of CCN is either land-derived CCN and CCN precursors like SO_2 advected off the land, or the CCN precursor dimethyl sulfide (DMS), which is produced in the surface ocean itself by planktonic algae (see, e.g., Charlson et al., 1987). The more CCN available, the smaller the cloud

droplets will be. Twomey (1977) demonstrates in addition that for a fixed volume of cloud water, the smaller the particles, the greater the albedo. Charlson et al. (1987) have specifically calculated (Figure 3) the change in cloud-top albedo as compared to a reference cloud as the droplets either grow or become smaller with the same total liquid water content. The top axis in Figure 3 indicates how this change is related to the number of droplets. Thus, as the number of droplets

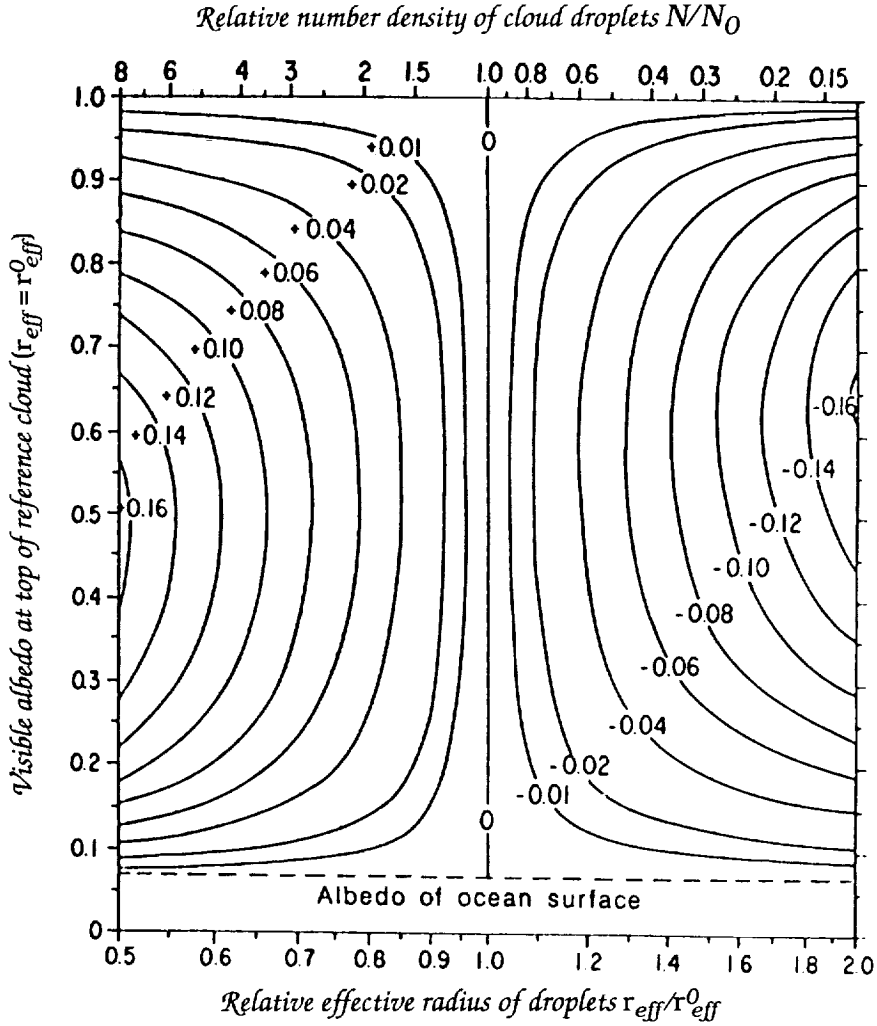

Figure 3. Contours showing change of visible albedo caused by changing droplet number density N or equivalently droplet effective radius r_{eff} relative to a reference cloud (N_0, r^0_{eff}). Albedo at top of reference cloud given on left-hand vertical scale (adapted from Charlson et al., 1987; reprinted by permission from Nature, © 1987 Macmillan Magazines Ltd.).

increases, as would be the case if more CCN were available due to increased DMS emissions, the albedo increases. Therefore, any climate changes that influence the emissions of DMS over the oceans may induce a cloud-climate feedback associated with them. Understanding how CCN may change is therefore an important aspect of predicting future cloud cover and rainfall.

The three-dimensional structure of optically thick clouds is important. For very deep clouds, the downward emission from the warm cloud base significantly exceeds the upward emission from the cool cloud top. Very shallow clouds, on the other hand, exhibit much smaller differences between these fluxes, so the greenhouse effect due to them is much smaller. This influences the competition between the albedo and greenhouse effect of clouds. For example, Ramanathan and Collins (1991) have recently argued that relatively thin, highly reflective cirrus clouds formed during El Niño may effectively limit the magnitude of the sea surface temperature increase being forced by the greenhouse effect of water vapor and clouds. The three-dimensional structure of clouds depends on both mesoscale processes (convection) and the larger-scale circulation and is poorly predicted in current climate models.

Convection also has a large influence on the surface heat budget. Evaporation and subsequent convection serve to cool and dry the surface and lower troposphere. In turn, the middle and upper troposphere are warmed by condensation. The distribution of water vapor and also many chemically important trace species is strongly influenced by convection and its subsequent motions. As shown by Dickerson et al. (1987), the convective motions tend to transport tracers from the lower troposphere to upper levels. Figure 4 illustrates the redistribution of carbon monoxide. To the left of the cloud the normal vertical distribution is evident, with the CO mixing ratio decreasing with height. However, within the cloud, the situation has reversed as the high-CO air in the boundary layer has been transported to the upper troposphere, leaving the lower levels depleted in CO relative to the normal situation.

For climate prediction models we clearly need realistic models for convection, including its roles in heat, momentum, and trace species (e.g., water vapor) transport, and in cloud formation. The first step in developing a cloud model is to understand the basic processes, and the second step is to parameterize these processes for inclusion in GCMs, in which they are subgrid-scale phenomena. Previous attempts at producing convective parameterizations have had their drawbacks. For example, Manabe et al. (1965) used a straightforward convective adjustment scheme that adjusts the atmospheric lapse rate back to an observed neutral state for satu-

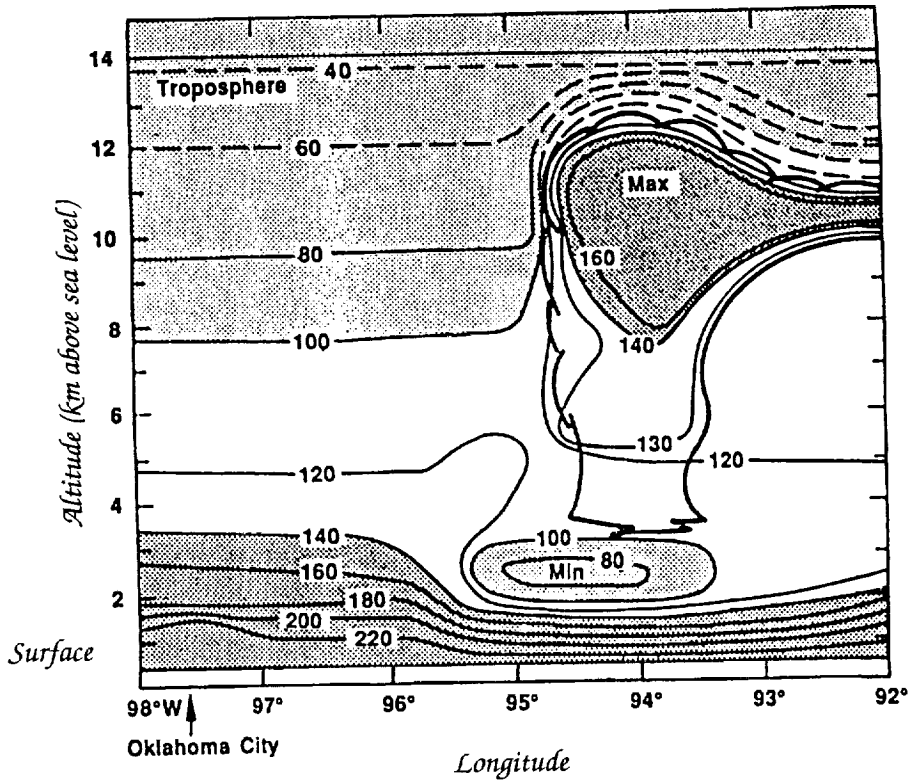

Figure 4. Concentration of carbon monoxide (ppbv) as a function of altitude and latitude over Oklahoma City, Oklahoma, both outside and within a thunderstorm (adapted from Dickerson et al., 1987; © 1987 by the AAAS).

rated regions. Unfortunately, this means instability can build up in unsaturated regions. A recent parameterization by Betts (1986) allows for adjustment in unsaturated regions, but it still does not predict the profiles of temperature or water vapor. Instead, these are adjusted to observed profiles. Emanuel (1990) allows for the prediction of water vapor content but relies on a specified vertical distribution of precipitation. The major drawback of the above schemes is that they are all based on adjusting the atmosphere back to an observed structure. For purposes of climate change models, this type of parameterization is quite suspect since certain potentially important climate changes are omitted. The Kuo (1974) scheme is more physical. In this scheme convection occurs when there is moisture convergence. However, this also has its problems. Regions can get extremely unstable, yet unless there is a transport of moisture into that region, no convection occurs. Realistic models for convection and cloud formation are clearly an important requirement for GCMs to be used for future climate change predictions.

Oceanic Circulation and Its Coupling to the Atmosphere and Cryosphere

The oceanic circulation has major influences on the climate system. In the energy balance of the earth, the ocean circulation is important in the heat transport from equator to pole. Figure 5 shows the heat transport for both the oceans and the atmosphere as determined by Carissimo et al. (1985) and earlier workers. The oceanic and atmospheric heat transport have comparable strengths. Thus, it is evident that the ocean is crucial to consider and without it the latitudinal temperature gradient would probably be significantly larger. The ocean circulation also contributes to the determination in space and time of the latent, sensible, and radiative heating of the troposphere. For studying possible climate changes, the changes in water vapor input from the ocean with changing sea surface temperature are a critical feedback (Ramanathan, 1981). Another way the ocean circulation affects the heating in the troposphere is in its interaction with sea ice. Figure 6 gives some results from Hibler (1990) and earlier papers which show how important it is to consider the ice dynamics. There is about 50% more ice when there is no ice dynamics. The greater the extent of the sea ice, the more it can decrease the heat flux between the ocean and the atmosphere (Bentley, 1984). Since generally, in the polar regions, the ocean is warmer than the atmosphere, the extent of sea ice can greatly influence the temperature of the tropospheric air. Furthermore, the albedo of sea ice is about 0.9 whereas that of sea water is about 0.1. Thus, the radiative heating of the troposphere is influenced by sea ice cover, which in turn is affected by the ocean circulation.

The ocean circulation is essential for transporting nutrients to the surface of the open oceans in order to feed phytoplankton and other marine organisms (Broecker and Peng, 1982). An example of the importance of this process is seen during an El Niño year when the usual East Pacific equatorial upwelling is suppressed. As a consequence there are no new nutrients, and the fish die off, which is devastating for the Peruvian fishing industry (Philander and Rasmusson, 1985).

Finally, the ocean serves as a sink for thermal energy and carbon dioxide as they increase in the atmosphere. The ability of the ocean to do this depends greatly on the strength of its circulation. Figure 7 is a result from Hansen et al. (1985) showing the different temperature increases expected with different vertical diffusion rates in a highly simplified ocean model. Obviously, the ocean serves as a large heat sink since its heat capacity is so much greater than the atmosphere's, but its ability to do so depends on its circulation. This is also true in the uptake of CO_2. Siegenthaler (1983) explored the effects of circulation on the uptake of CO_2, and one of his results is shown in Figure 8 which illustrates how much more CO_2 is taken

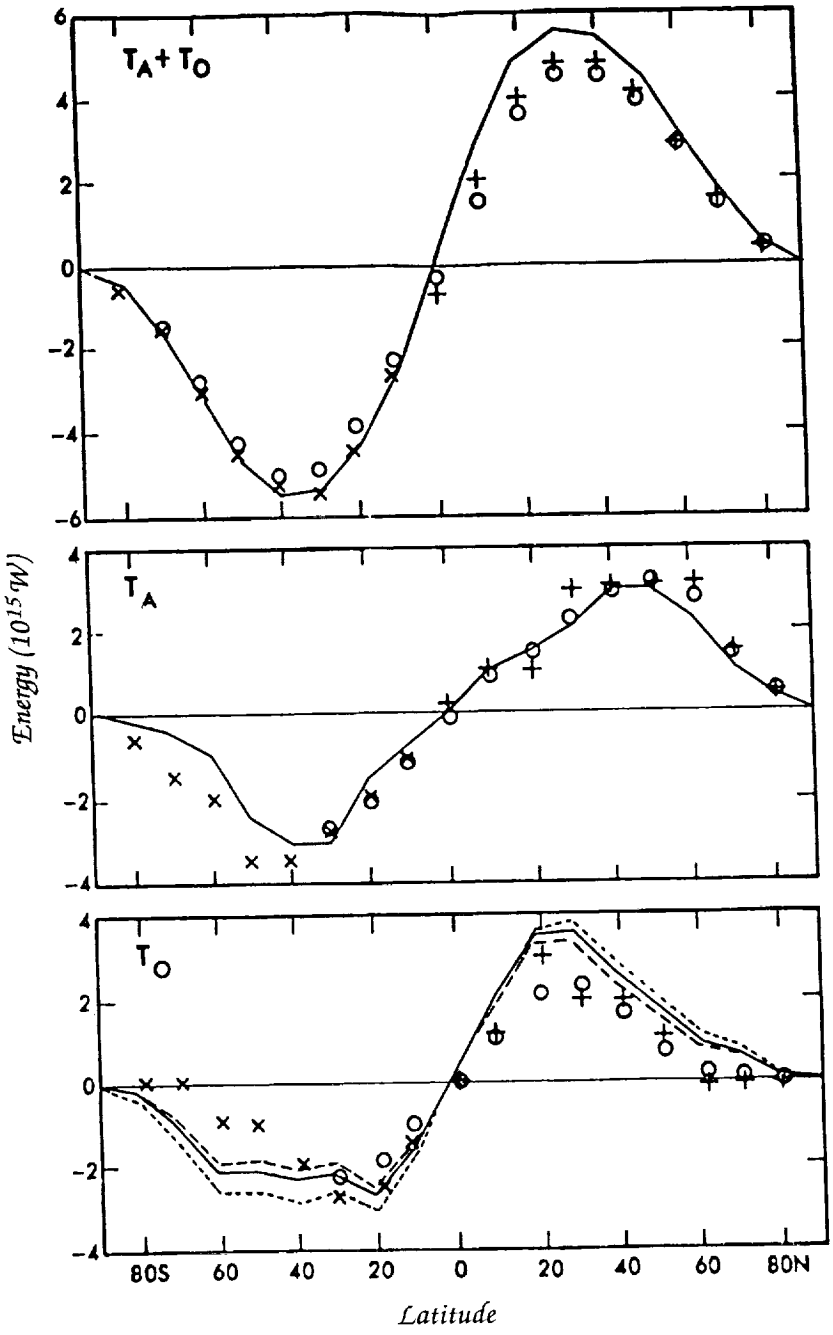

Figure 5. Annual meridional transport of energy (10^{15} W) in the atmosphere plus ocean ($T_A + T_O$), atmosphere (T_A), and ocean (T_O) computed by Carissimo et al. (1985) and compared to previous investigators: (+) Oort and Vonder Haar, 1976; (x) Trenberth, 1979; (O) Newell et al., 1972 (adapted from Carissimo et al., 1985; © American Meteorological Society).

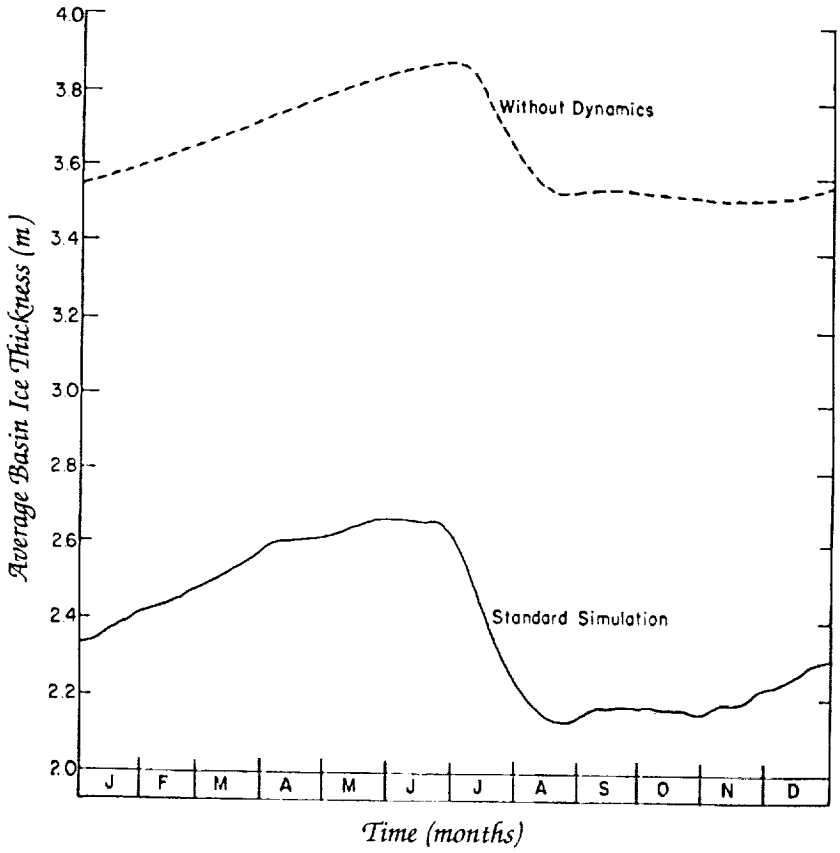

Figure 6. Comparison of Arctic basin average ice thickness (m) for a two-level model without dynamics and with dynamics (standard) (adapted from Hibler, 1990; © American Meteorological Society).

into the ocean when there is efficient downward advection in "outcrop" regions like the Norwegian and Weddell seas.

The atmosphere also influences the ocean since the upper ocean circulation is forced by atmospheric winds. This coupling is exemplified by the El Niño/Southern Oscillation (ENSO) phenomenon, during which the warming of the eastern equatorial Pacific is accompanied by slowing of the trade winds and by an eastward extension of the western Pacific convection zone. Slowing of the trade winds decreases the upwelling associated with Ekman drift, thus contributing to the warming of the eastern Pacific. The assignment of cause and effect in this coupled ocean-atmosphere phenomenon is difficult to make (Philander and Rasmusson, 1985).

The ocean circulation and sea ice are also coupled. When ice is formed, the ocean becomes more saline, tending to increase the

oceanic overturning (Hibler, 1990). If the ice is transported by the combined effects of the winds and the ocean circulation (which are related) and then melts in another region, this latter region becomes less saline, and overturning is inhibited there. One possible consequence of this could be changes in the northern Atlantic climate. The Gulf Stream transports warmer water northward. When it reaches the North Atlantic the water cools, thereby warming the tro-

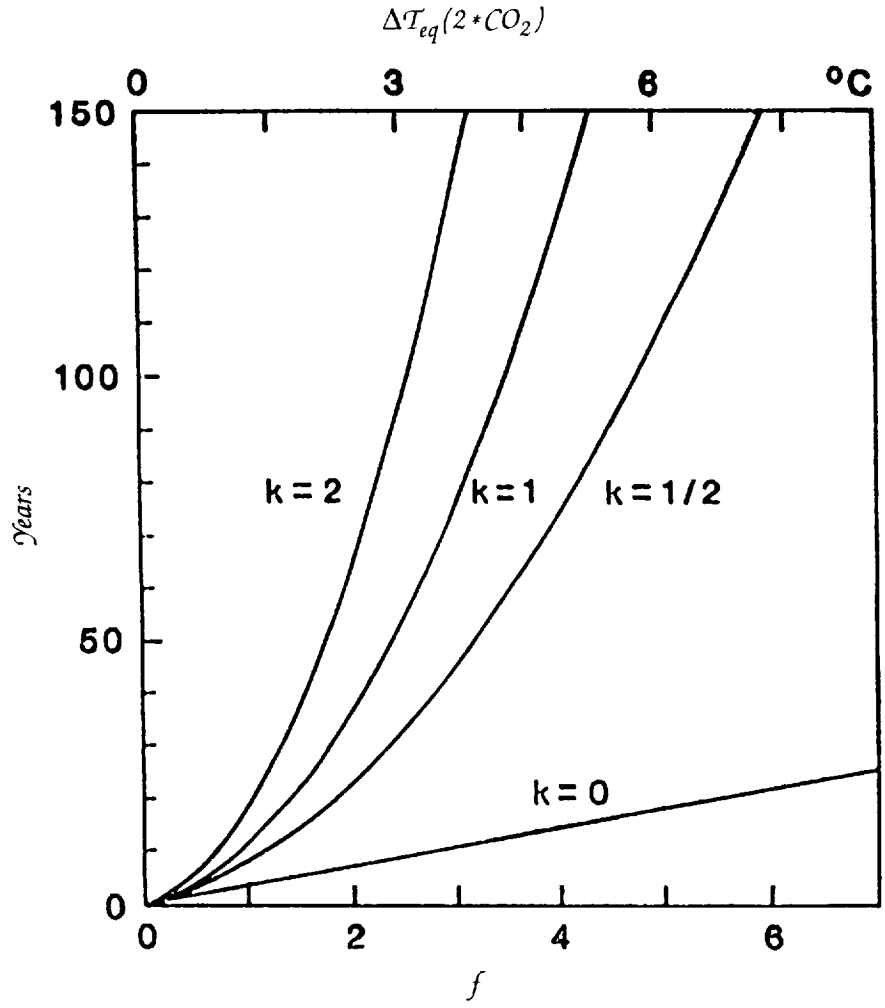

Figure 7. Ocean surface response time (time to reach $1 - e^{-1}$ of equilibrium response) for a one-dimensional diffusive ocean model as a function of climate sensitivity to doubled CO_2 [ΔT_{eq} ($2*CO_2$)] or equivalently as a function of the climate feedback factor f. Mixed layer depth is 100 m and results for various vertical diffusion coefficients k (cm^2/s) are shown (adapted from Hansen et al., 1985; © 1985 by the AAAS).

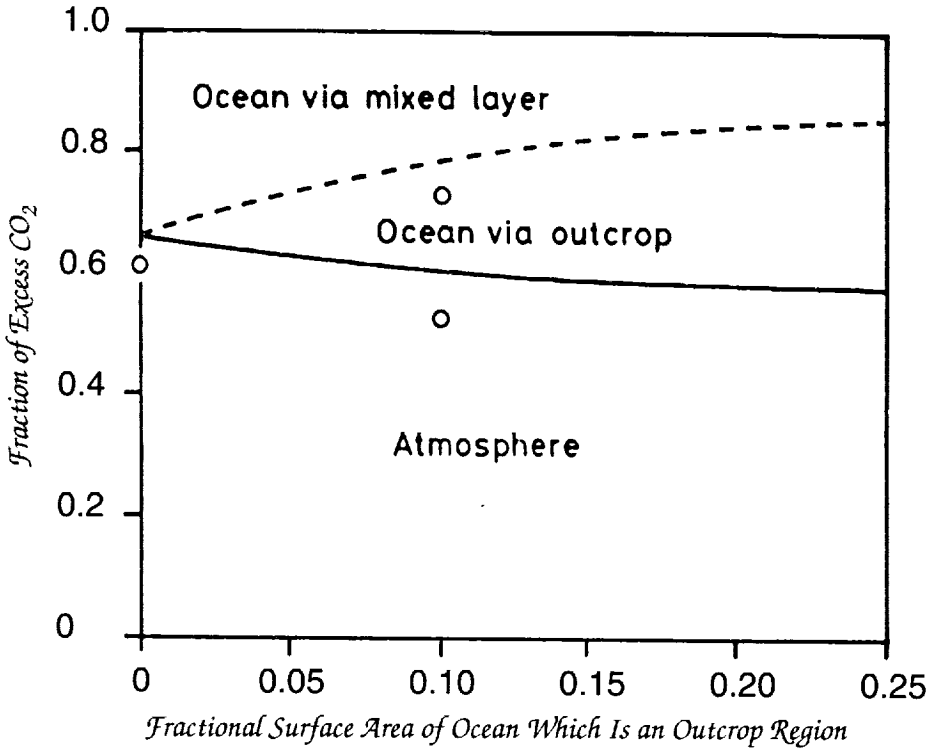

Figure 8. Fractions of the CO_2 added exponentially with an e-folding time of 22.5 years which are taken up by the ocean (diffusion into mixed layer plus simulated advection into deep water via an outcrop) as a function of the relative area of the outcrop. Circles denote fractions of bomb-produced ^{14}C taken up by the different media for relative outcrop areas of 0.0 and 0.1 (adapted from Siegenthaler, 1983).

posphere. As the water cools, it sinks, to be replaced by more warm water from the south (Broecker, 1987; Broecker and Denton, 1990). This northward flow of warm water in a "conveyor belt" keeps Europe warm during its winters. However, if sea ice invaded the North Atlantic and melted there, this would inhibit sinking (e.g., by the same mechanism in which the thermohaline circulation weakened due to increased river runoff and precipitation in the coupled ocean-atmosphere climate model of Stouffer et al., 1989). This would tend to decelerate the conveyor belt and cool Europe. This is just a hypothesis, but it could mean that one signal of greenhouse warming may actually be a cooling in some locations, which draws attention to the different results that could arise in a coupled ocean-atmosphere model but not in a model with prescribed sea surface temperatures or a horizontally static oceanic mixed layer. In fact, many ocean models that do have a circulation force the model to

observed climatology, which short-circuits many potential feedbacks when the climate is changing. We ultimately need realistic models that predict the changes in the ocean circulation as the climate changes and the resultant feedbacks to the climate and nutrient budgets (i.e., phytoplankton populations). The phytoplankton play a role in the uptake of CO_2 as well as the release of DMS, which, as discussed earlier, may be an important influence on the formation and radiative properties of clouds.

Land Surface Hydrology and Hydrology-Vegetation Coupling

The relationship between vegetation, soils, water flow, and weather patterns is complex and fundamental to life on the continents. The large-scale correlations between seasonal vegetation index, deep convective clouds (Warren et al., 1986), and surface albedo (Ramanathan et al., 1989) are quite evident. Vegetation is a major contributor to the absorption of sunlight over the land and, thus, to the local and global radiation budget. The albedo over vegetation is less than half that over bare land (Charney et al., 1975). Changing land vegetation cover can thus alter the net solar absorption. In addition, vegetation pumps water from soils into the atmosphere through evapotranspiration, thereby regulating the relative amounts of water in the atmosphere and in the soils. Thus, the vegetation affects the local and downstream water and latent heat budget. Shukla and Mintz (1982) illustrate the control vegetation could have on the regional climate. Figure 9 shows the significant effect soil moisture can have on precipitation patterns, with Figure 9a having a wet soil and Figure 9b having a dry soil boundary. Shukla and Mintz (1982) also show the effects of the soil moisture on surface temperature and pressure. The dry soil causes the land to be warmer and produces lower pressures because the energy from solar insolation cannot go into evaporation at the surface. Furthermore, there are fewer clouds (since there is less water to feed them), and therefore even more solar radiation reaches the surface. Thus vegetation is a major influence on regional climate.

On the other hand, vegetation is itself dependent on the climate. Different vegetation types thrive in different climates (Running and Coughlin, 1988; Clark, 1990, 1991). Some species are very sensitive to precipitation and solar input. Therefore, as these change, so will the vegetation. Furthermore, as regions become more dry the fire potential increases, and large areas of vegetation can potentially be cleared by burning. This can then influence what new vegetation will grow (Clark, 1990, 1991). Thus, changes in climate can both directly

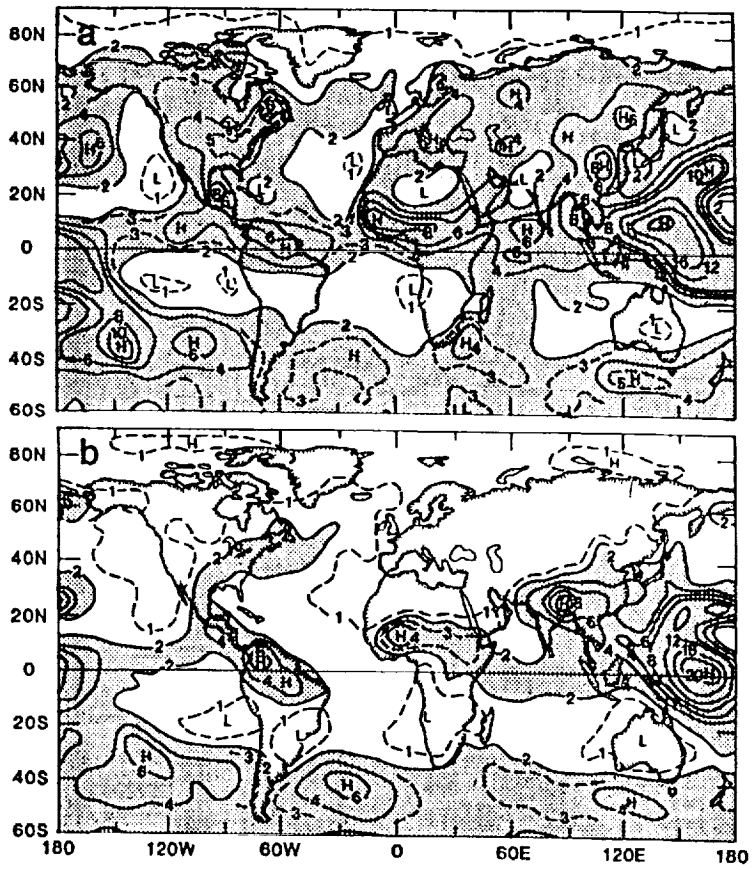

Figure 9. Model simulated July precipitation (mm/day) in (a) the wet soil and (b) the dry soil case (adapted from Shukla and Mintz, 1982; © 1982 by the AAAS).

and indirectly alter the vegetation. One feedback mechanism is illustrated in a well-known theory of desertification (Charney et al., 1975). Charney et al. (1975, 1977) show that as vegetation is cleared, the albedo increases, evapotranspiration decreases, subsidence occurs, and the normal precipitation is suppressed. Thus, this feedback dries out the surface, and recovery of the vegetation is severely inhibited. It is apparent, therefore, that accurate models for predicting future climate change cannot merely specify the vegetation at the surface, but instead must include vegetation as an internal variable.

For the current global GCMs, the effects of vegetation need to be parameterized since the scale of the relevant ecosystems is much smaller than that of a model grid box. These parameterizations must take account of local topography, water sources, and soil types since these are some of the crucial influences on vegetation cover. Various

simple vegetation/hydrology schemes in the GCMs of today give predictions that do not agree well with observations or with one another on a regional scale. Figure 10 shows the different predictions of soil moisture from several different GCMs. For these calculations, both the subgrid-scale convective and vegetation parameterizations contribute to the distinct differences.

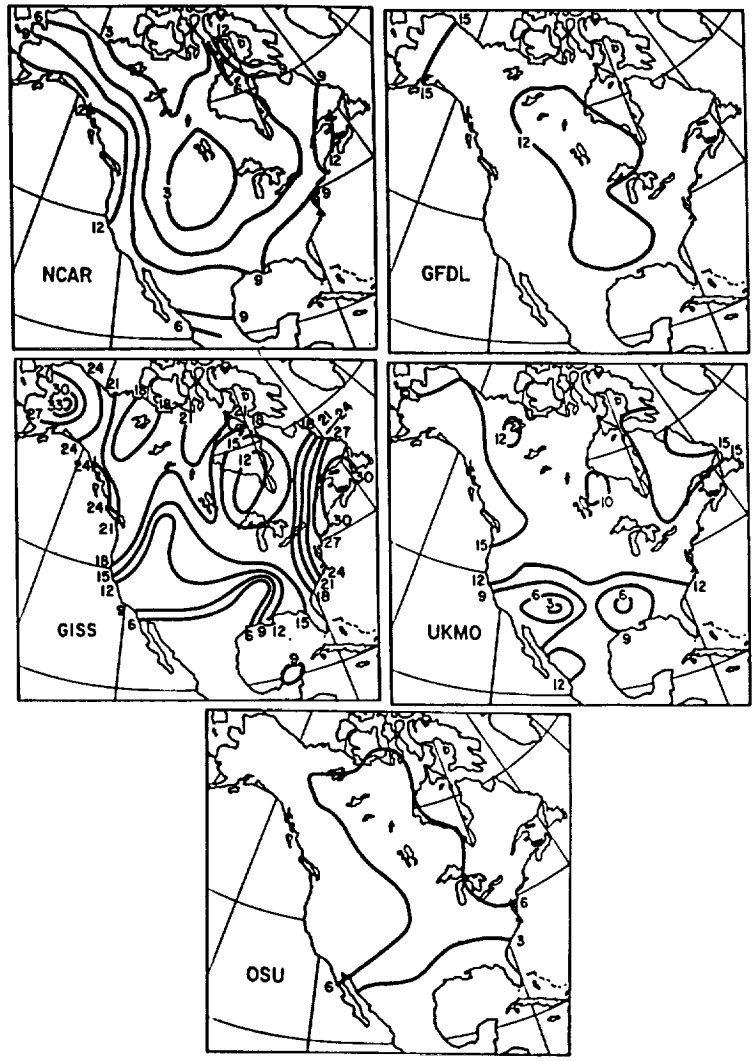

Figure 10. Present-day simulations of soil moisture in winter for North America obtained in general circulation climate models from the National Center for Atmospheric Research, Geophysical Fluid Dynamics Laboratory, Goddard Institute for Space Studies, U.K. Meteorological Office, and Oregon State University. Units are cm of water (adapted from Kellogg and Zhao, 1988).

Biogeochemistry of the Long-Lived Greenhouse Gases

Current concerns about future climate change are driven in large part by the undeniable observational evidence that several of the so-called long-lived greenhouse gases (CO_2, CH_4, N_2O, chlorofluorocarbons) are increasing presently at very significant rates. These increases, coupled with expected feedbacks increasing the concentration of the major greenhouse gas, the short-lived H_2O molecule, are predicted to lead to a significant warming over the next century (e.g., Dickinson and Cicerone, 1986). However, we lack the detailed biogeochemical and physical knowledge of individual sources and sinks for the long-lived greenhouse gases (with the exception of the chlorofluorocarbons) needed to explain quantitatively these present trends and to project them accurately into the future.

The long-lived greenhouse gases can be conveniently divided into three categories based on their chemical reactivity:

- *First category:* Some of the long-lived species are very inert (lifetimes exceeding 70 years) because they can be destroyed only by mixing up into the stratosphere above 25 kilometers altitude. Here, they can be dissociated by solar ultraviolet photons with wavelengths less than 250 nm. In this category are the industrial chlorofluorocarbons $CFCl_3$, CF_2Cl_2, and $CF_2ClCFCl_2$, which are widely used as refrigerants, propellants, plastic foaming agents, and solvents and which have lifetimes of around 45, 125, and 110 years respectively at the present time (Golombeck and Prinn, 1986, 1989, 1991, personal communication). Measurements made in the Atmospheric Lifetime Experiment/Global Atmospheric Gases Experiment (ALE/GAGE) network of automated stations (located in Ireland, Oregon, Barbados, Samoa, and Tasmania; Prinn, 1988; Prinn et al., 1983) indicate that $CFCl_3$, CF_2Cl_2, and $CF_2ClCFCl_2$ are currently increasing at rates of about 5%, 5%, and 10% per year respectively over the globe (Figure 11). Also in this class is N_2O, which has a present-day lifetime of about 130 years and is increasing at 0.2 to 0.3% per year (Figure 11) and has both natural (soils, ocean) and anthropogenic (disturbed and fertilized soil, combustion) sources. Analysis of ALE/GAGE N_2O data using inverse methods yields the conclusion that tropical sources of this gas compose 52–68% of the global total (Prinn et al., 1990). We need to understand these sources better and discern their sensitivity to climate changes. Another point worth noting is that all of the gases in this first category, when dissociated in the stratosphere, yield reactive species that catalytically destroy ozone, and some of them play a major role in the processes causing the Antarctic ozone hole. Destruction of

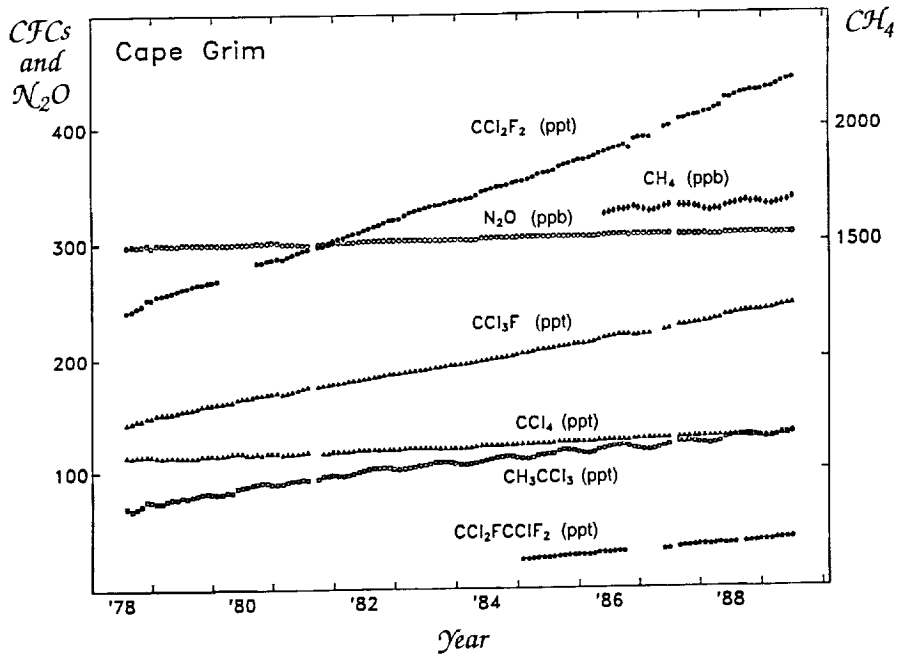

Figure 11. Monthly average concentrations of various long-lived trace gases measured at the Cape Grim, Tasmania, station of ALE/GAGE. Left vertical axis gives numerical values for mixing ratios of all compounds except CH_4, for which values are on the right vertical axis. Units are given on the data lines (from R. Prinn, P. Fraser, P. Simmonds, R. Rasmussen, F. Alyea, D. Cunnold, A. Crawford, and R. Rosen, personal communication).

stratospheric ozone in turn increases ultraviolet dosages at the surface, affecting living organisms and influencing the oxidation process in the lower atmosphere by accelerating photodissociation of O_3 to produce $O(^1D)$.

- *Second category:* Long-lived species in this category are less inert (lifetimes typically less than 15 years) because they can be destroyed by reaction with OH in the lower atmosphere. In this category is atmospheric CH_4 with a lifetime of 9.6 years (Prinn et al., 1987), which is increasing today at about 1% per year (Figure 11; see also Blake and Rowland, 1988). Methane (like N_2O) has both natural (wetlands, tundra) and human-controlled (cattle, combustion, rice agriculture) sources (Ehhalt, 1988; Cicerone and Oremland, 1988). Also in this category is the widely used industrial solvent and cleaning agent methyl chloroform (CH_3CCl_3) with a lifetime of 6.3 years (Prinn et al., 1987), which is increasing globally at about 4% per year (Figure 11). Finally, in this category are the hydrochlorofluorocarbons such as $CHClF_2$ (16-year present-day lifetime), currently increasing at about 10% per year, and

$CHCl_2CF_3$ (1.5 year steady-state lifetime), and CH_2FCF_3 (15-year steady-state lifetime), proposed as industrial replacements for the chlorofluorocarbons $CFCl_3$ and CF_2Cl_2.

As reviewed by Crutzen (1979), the concentrations of OH radicals are determined to a significant extent by short-lived species whose life cycles begin and end on local and regional scales (e.g., NO, NO_2, O_3, CO, hydrocarbons, etc., in Figure 12). Thus the global atmospheric chemistry of the long-lived species in the second category is linked in very important ways to the local and regional-scale atmospheric chemistry of the short-lived species that determine OH levels. One important implication of this linkage is that the positive trends in species like CH_4 may in part be

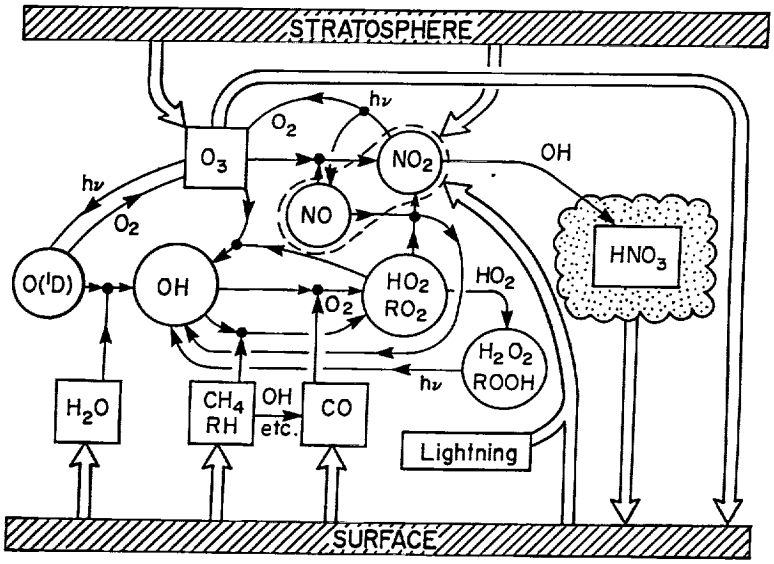

Figure 12. Schematic outlining the major recognized gas-phase chemistry in the troposphere. Black dots denote occurrence of chemical reactions. Thin arrows denote pathways for chemical reactions, while thick arrows denote fluxes of species from sources or to sinks. In continental air, rich in nitrogen oxides, NO is a major reactant for recycling HO_2 to OH and photodissociation of the resultant NO_2 is a major source for ozone. The dashed line enclosing NO and NO_2 signifies that both are produced from surface sources and lightning. In remote marine air, where nitrogen oxide levels are low, the major recycling of HO_2 to OH occurs through peroxide (H_2O_2, ROOH) formation and subsequent photodissociation. Reaction of HO_2 with O_3 provides another OH recycling mechanism in both environments. The OH and NO_2 are removed by formation of HNO_3, which is scavenged by clouds, indicated by the dotted area.

due to a decrease in OH radicals and thus a decrease in CH_4 loss rates rather than exclusively to an increase in CH_4 emission rates. Another implication is that the destruction of long-lived gases in this second category is weighted heavily to the hot tropical lower atmosphere whose local and regional chemistry we are only beginning to be informed about (Donahue and Prinn, 1990).

- *Third category:* CO_2 requires a category of its own. It is essentially chemically inert in the atmosphere and is cycled between atmosphere, upper ocean, green vegetation, and soils on decadal time scales and between the upper ocean and deep ocean on a time scale of a few hundred years. It is currently increasing at a rate of about 0.34% per year (Figure 13; Keeling, personal communication) and possesses a significant annual cycle driven by uptake of CO_2 by photosynthesizing vegetation in spring and summer and release of CO_2 by decaying vegetation in fall and winter. Classical ideas, as reviewed by Oeschger and Siegenthaler (1988), had the oceans playing the major role as a sink for carbon dioxide. A typical global budget has the current fossil fuel combustion source (5300 Tg C/yr) opposed by an oceanic sink (2300 Tg C/yr) to yield the observed atmospheric increase (3000 Tg C/yr). The land biosphere was generally considered to be a small contributor to the budget, although estimates of the deforestation source ranged from 400 to 2600 Tg C/yr. A recent comparison of the observed CO_2 latitudinal gradient with a global model containing only an ocean sink (Tans et al., 1990) showed poor agreement (Figure 14).

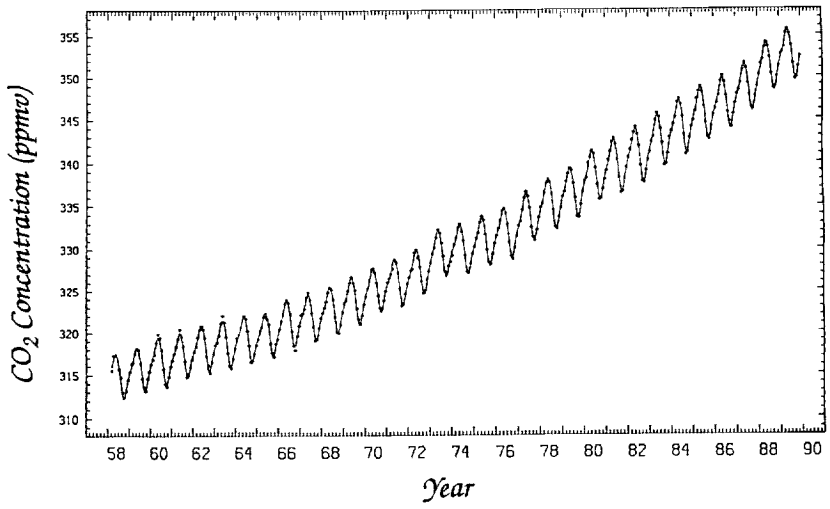

Figure 13. Concentration of CO_2 (ppmv) measured at Mauna Loa Observatory, Hawaii (C.D. Keeling, personal communication).

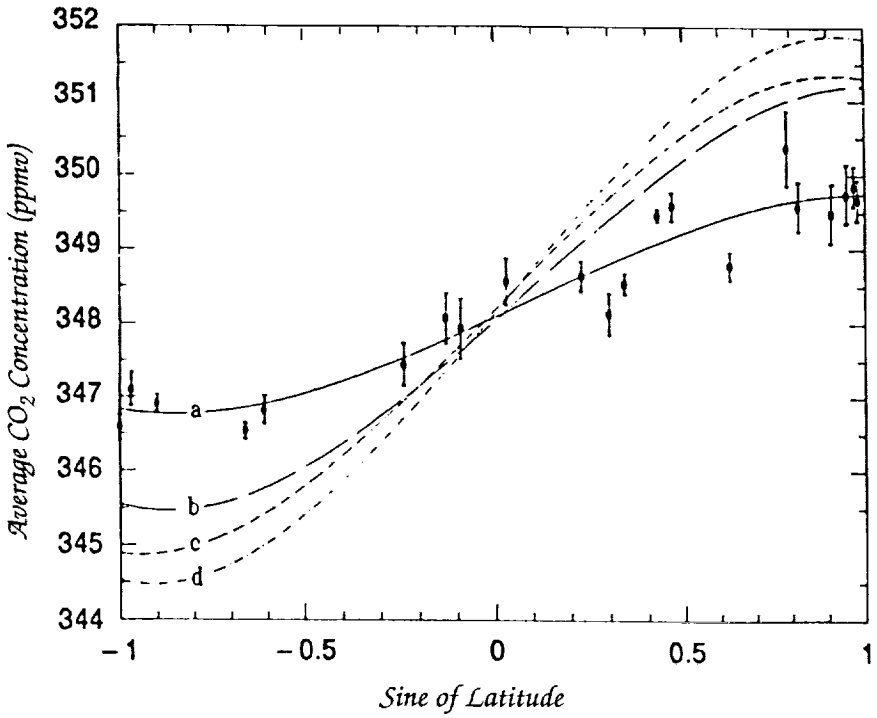

Figure 14. Observed CO_2 mixing ratios (circles with 1 sigma error bars), a cubic polynomial fit to observed CO_2 (line a), and predicted CO_2 in three GCM model runs (lines b, c, d). In the model runs the ocean is the only CO_2 sink, and this sink is computed in different ways in the three runs. A good fit (not shown) to the observations is obtained if a large Northern Hemisphere continental sink is included and the ocean sink decreased appropriately (adapted from Tans et al., 1990; © 1990 by the AAAS).

A new, significant Northern Hemispheric sink is needed to fit the data, but the available ocean uptake estimates do not allow the Northern Hemispheric oceans to provide this sink. Tans et al. concluded therefore that a significant Northern Hemispheric continental sink (about 2700 Tg C/yr) augmented by a smaller oceanic sink (about 1000 Tg C/yr) was needed to balance the atmospheric accumulation (3000 Tg C/yr), the fossil fuel input (5300 Tg C/yr), and the deforestation input (1400 Tg C/yr). Thus the ocean sink and the *net* biospheric sink (2700 −1400 = 1300 Tg C/yr) are comparable. If correct, this implies that continental forest regrowth and soil carbon uptake will need to be understood and appropriately modeled. Of particular interest is the possibility of CO_2 fertilization. Perhaps related to this is the increasing amplitude of the CO_2 annual cycle in recent years (Figure 13). It is worth noting, however, that the available $^{13}C/^{12}C$ data do not indicate a biospheric sink of the size needed here (Keeling et al., 1989).

Better knowledge of the controlling mechanisms and magnitudes of the individual sources and sinks for the greenhouse gases is essential for developing the needed models for reliable prediction of future emissions and for inclusion of potential feedbacks between these source and sink rates and climate change. Of particular importance is improved understanding of the role of the biota as trace gas sources and sinks and the effects of climate change on these sources and sinks (see, e.g., Prinn, 1992). The potential for such biogeochemical feedbacks is seen in the analyses of gases trapped in ice cores, which show this effect over the past 150,000 years where variations in concentrations of both methane and carbon dioxide are *correlated* with variations of temperature (Chappellaz et al., 1990). In particular, CH_4 and CO_2 are generally low during the ice ages and high during the warm interglacial epochs (Figure 15). This suggests the existence of a biogeochemical-climate feedback whereby increases in temperature or greenhouse gas concentrations lead to increases in greenhouse gas emissions or global warming respectively.

Upper Atmospheric Chemistry and Circulation

Changes in surface trace gas emissions, stratospheric-tropospheric exchange rates, and stratospheric temperatures and circulation will all affect the ozone layer. N_2O, methane, industrial chlorofluorocarbons like $CFCl_3$ and CF_2Cl_2, and water vapor are transported from the surface up into the stratosphere where photochemical reactions driven by solar ultraviolet radiation can decompose them to form a number of very reactive species (NO, NO_2, Cl, ClO, OH, HO_2) which can catalytically destroy ozone. Because stratospheric ozone is produced essentially exclusively by ultraviolet dissociation of O_2, its rate of global production is set externally by the supply of ultraviolet radiation from the sun. The global rate of destruction of ozone depends, however, on the supply of catalysts, which is rapidly rising due to continued chlorofluorocarbon emissions at the surface. Removal of the catalysts from the stratosphere occurs through their (partially reversible) conversion to harmless reservoir species (HNO_3, $ClONO_2$, HCl, etc.), many of which can be transported down again to the troposphere ultimately to rain out or deposit at the surface.

A dramatic illustration of the fact that the global chemical system is changing is provided by the Antarctic ozone hole phenomenon (Figure 16). This phenomenon can occur because temperatures in

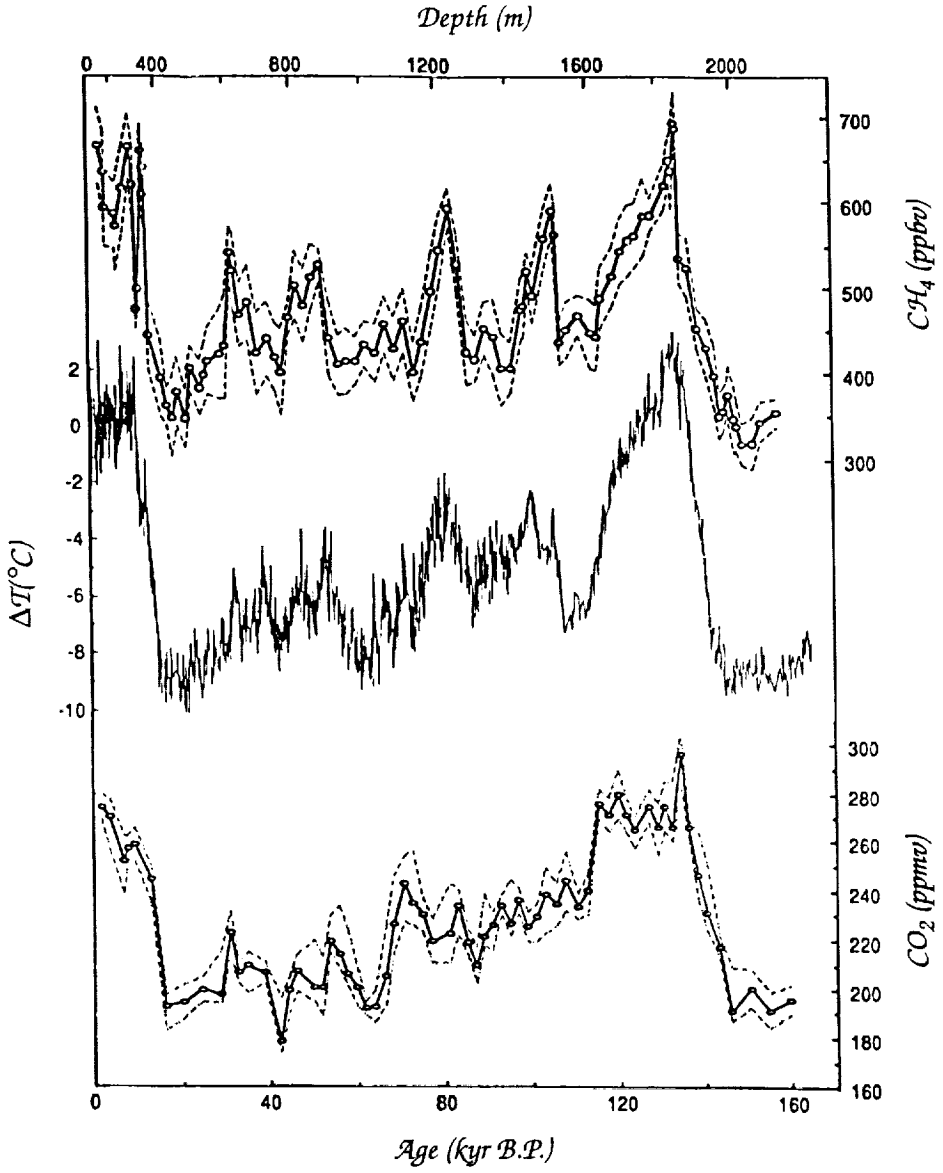

Figure 15. Vostok ice-core analyses of CH_4 (upper curves, 2 sigma errors), temperature relative to present as deduced from H_2O isotopes (middle curve), and CO_2 (lower curve, 2 sigma errors). Depth scale applies to CO_2 and CH_4. Due to downward diffusion the gases are younger than the ice in which they are trapped (adapted from Chappellaz et al., 1990; © 1990, Macmillan Magazines Ltd.).

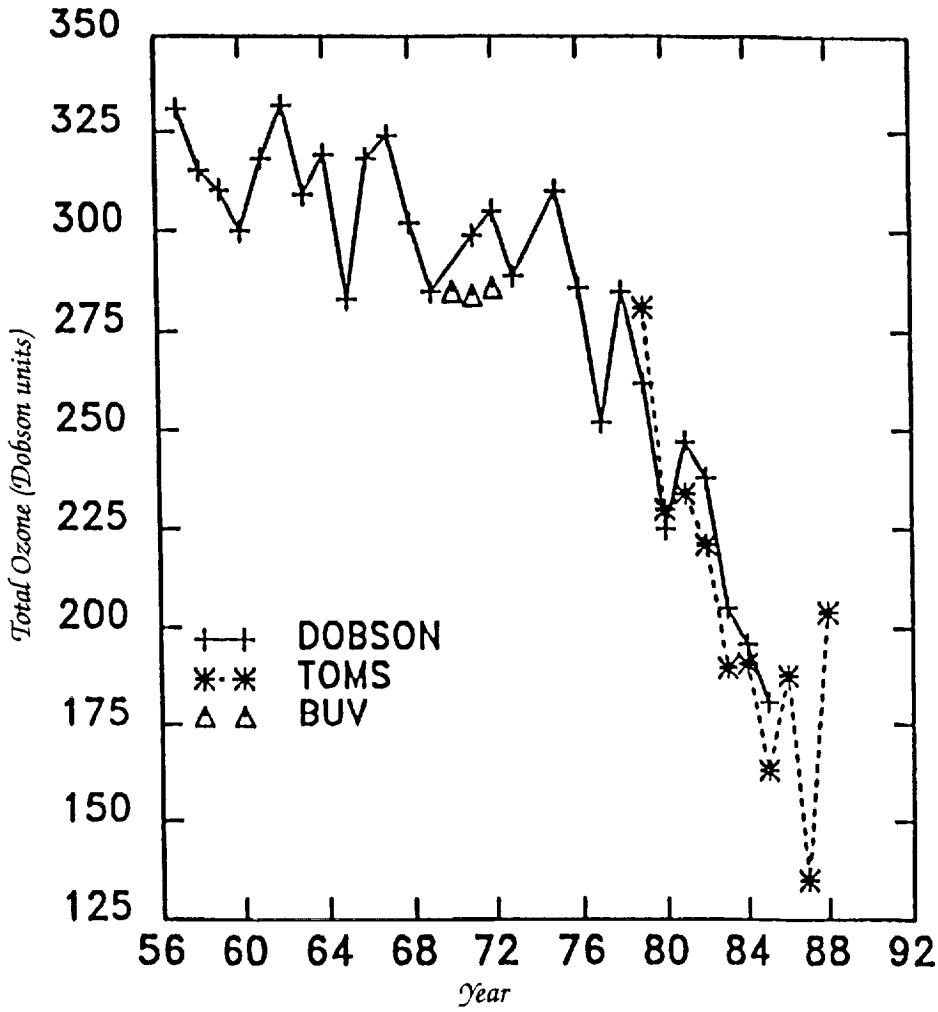

Figure 16. October monthly mean total ozone measurements over Halley Bay as measured by Halley Bay Dobson and Nimbus 4 BUV (backscatter ultraviolet) instruments. The polar minimum values for TOMS (total ozone mapping spectrometer) for October are also shown. Dobson unit is 2.7×10^{16} ozone molecule per cm^2 (Schoeberl et al., 1989; Stolarski, 1988).

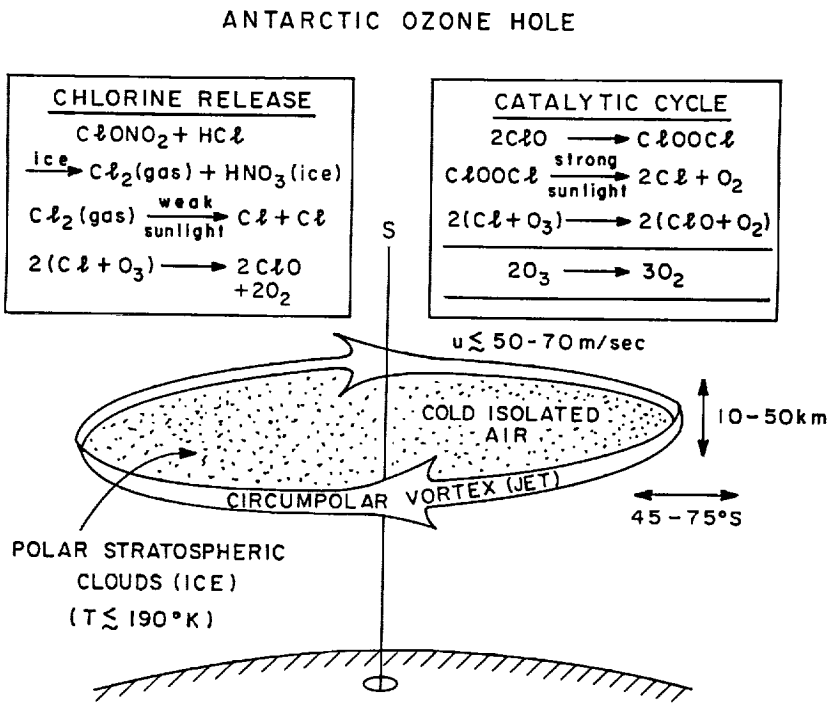

Figure 17. Schematic showing the vortex circulation, ice clouds, chlorine release reactions, and catalytic ozone destruction reactions involved in the Antarctic ozone hole.

the meteorologically isolated air mass lying between 10 and 30 km altitude in the Antarctic winter become so low (less than 190 K) that ice crystals condense in this region (Figure 17). Decomposition of some of the catalyst reservoir species occurs on and within these ice crystals, producing ClO in the early Antarctic spring. The ClO levels become very high because HNO_3 remains in the ice and is therefore not available to contribute to the conversion of ClO back to its relatively harmless reservoir compound $ClONO_2$. The scarcity in the Antarctic spring of ultraviolet radiation capable of decomposing O_3 means that different catalytic cycles operate here than the ones operating in tropical regions, which require O atoms produced by O_3 photodissociation (e.g., Rowland and Molina, 1975). The reaction sequence shown in Figure 17 serves to efficiently destroy O_3 without requiring O_3 photodissociation and without destroying ClO (Molina et al., 1987).

Theoretical models of the greenhouse effect indicate that a rise in the level of the greenhouse gases will tend not only to warm the earth's surface and lower atmosphere but also to *cool* the stratos-

phere, due to either the rise in a greenhouse gas, as is the case for CO_2, or the depletion of ozone, as in the case of rising chlorofluorocarbons (e.g., Ramanathan et al., 1985; Wang et al., 1991). This cooling of the stratosphere is expected to affect the ozone layer by decreasing ozone destruction in equatorial regions by slowing down the destruction reactions in these regions and increasing ozone destruction in the Antarctic (and also in the Arctic if cooling is sufficiently large) by increasing the extent of the polar ice clouds. These effects would be added to the increased ozone destruction expected due to the still rising chlorofluorocarbon concentrations. The stratospheric cooling by the greenhouse gases combined with these ozone layer changes will in turn affect the circulation at this level and conceivably at lower levels also. Also, changes in the intensity of tropical convection and midlatitude storms associated with a global warming are likely to alter significantly tropospheric-stratospheric exchange rates of trace gases involved in the ozone layer chemistry.

We therefore need realistic models of stratospheric circulation and chemistry that can be coupled with models of the lower atmosphere to improve the accuracy of tropospheric as well as stratospheric predictions.

Concluding Remarks

Understanding and modeling the above five fundamental processes provides a major interdisciplinary challenge with both observational and theoretical components. Several ongoing projects of the World Climate Research Program and the International Geosphere-Biosphere Program will all make large contributions. These projects include among others the International Global Atmospheric Chemistry (IGAC) project, Joint Global Ocean Flux Study (JGOFS), Global Energy and Water Cycle Experiment (GEWEX), Global Change and Terrestrial Ecosystems (GCTE) project, Tropical Oceans and Global Atmosphere (TOGA) project, and the World Ocean Circulation Experiment (WOCE). Later this decade the Earth Observing System (EOS) of the National Aeronautics and Space Administration will add a major satellite remote sensing capability relevant to many of these projects.

Acknowledgments

We thank M. Heimann for his constructive review of this paper and D. Sykes for help in manuscript preparation. This research is

supported by the National Science Foundation and the National Aeronautics and Space Administration.

References

Bentley, C.R. 1984. Some aspects of the cryosphere and its role in climate change. In *Climate Processes and Climate Sensitivity* (J.E. Hansen and T. Takahashi, eds.), Geophysical Monograph 29, American Geophysical Union, Washington, D.C., 207–220.

Betts, A.K. 1986. A new convective adjustment scheme. Part I: Observational and theoretical basis. *Quarterly Journal of Research of the Meteorological Society 112*, 677–691.

Blake, D., and S. Rowland. 1988. Continuing world-wide increase in tropospheric methane, 1978 to 1987. *Science 239*, 1129–1131.

Broecker, W.S. 1987. Unpleasant surprises in the greenhouse? *Nature 328*, 123–126.

Broecker, W.S., and G.H. Denton. 1990. What drives the glacial cycles? *Scientific American 262*, 49–56.

Broecker, W.S., and T.H. Peng. 1982. *Tracers in the Sea.* Lamont-Doherty Geological Observatory, New York.

Carissimo, B.C., A.H. Oort, and T.H. Vonder Haar. 1985. Estimating the meridional energy transports in the atmosphere and ocean. *Journal of Physical Oceanography 15*, 82–91.

Chappellaz, J., J. Barnola, D. Raynand, Y. Korotkevich, and C. Lorius. 1990. Ice core record of atmospheric methane over the past 160,000 years. *Nature 345*, 127–131.

Charlson, R.J., J.E. Lovelock, M.O. Andreae, and S.G. Warren. 1987. Oceanic phytoplankton, atmospheric sulphur, cloud albedo and climate. *Nature 326*, 655–661.

Charney, J., P.H. Stone, and W.J. Quirk. 1975. Drought in the Sahara: A biogeophysical feedback mechanism. *Science 187*, 434–435.

Charney, J., W.J. Quirk, S. Chow, and J. Kornfield. 1977. A comparative study of effects of albedo changes on drought in semi-arid regions. *Journal of the Atmospheric Sciences 34*, 1366–1385.

Cicerone, R., and R. Oremland. 1988. Biogeochemical aspects of atmospheric methane. *Biogeochemical Cycles 2*, 299–327.

Clark, J.S. 1990. Fire and climate change during the last 750 years in north-western Minnesota. *Ecological Monographs 60(2)*, 135–139.

Clark, J.S. 1991. Ecosystem sensitivity to climate change and complex responses. In *Global Climate Change and Life on Earth* (R. Wyman, ed.), Chapman and Hall, New York.

Crutzen, P. 1979. The role of NO and NO_2 in the chemistry of the troposphere and stratosphere. *Annual Review of Earth and Planetary Science 7*, 443–472.

Dickerson, R.R., G.J. Huffman, W.T. Luke, L.J. Nunnermacker, K.E. Pickering, A.C.D. Leslie, C.G. Lindsey, W.G.N. Slinn, T.J. Kelly, P.H. Daum, A.C. Delaney, J.P. Greenberg, P.R. Zimmerman, J.F. Boatman, J.D. Ray, and D.H. Stedman. 1987. Thunderstorms: An important mechanism in the transport of air pollutants. *Science 235*, 460–465.

Dickinson, R., and R. Cicerone. 1986. Future global warming from atmospheric trace gases. *Nature 319*, 109–115.

Donahue, N., and R. Prinn. 1990. Non-methane hydrocarbon chemistry in the remote marine boundary layer. *Journal of Geophysical Research 95*, 18387–18411.

Ehhalt, D.H. 1988. How has the atmospheric concentration of CH_4 changed? In *The Changing Atmosphere* (F. Rowland and I. Isaksen, eds.), John Wiley and Sons, Chichester, England, 25–32.

Emanuel, K.A. 1990. *A Scheme for Representing Cumulus Convection in Large-Scale Models.* Report No. 3, Center for Global Change Science, Massachusetts Institute of Technology, Cambridge.

Golombeck, A., and R. Prinn. 1986. A global three-dimensional model of the circulation and chemistry of $CFCl_3$, CF_2Cl_2, CH_3CCl_3, CCl_4, and N_2O. *Journal of Geophysical Research 91*, 3985–4001.

Golombeck, A., and R. Prinn. 1989. Global 3-dimensional model calculations of the budgets and present-day atmospheric lifetimes of $CF_2ClCFCl_2$ and $CHClF_2$. *Geophysical Research Letters 16*, 1153–1156.

Hansen, J., G. Russel, A. Lacis, I. Fung, D. Rind, and P. Stone. 1985. Climate response times: Dependence on climate sensitivity and ocean modelling. *Science 229*, 857–859.

Hibler, W.D. 1990. *Sea Ice Response to Global Climate Change.* Review Document for Brookhaven Workshop on Global Climate Feedbacks.

Keeling, C.D., S.C. Piper, and M. Heimann. 1989. A three dimensional model of atmospheric CO_2 transport based on observed winds: 4. Mean annual gradients and interannual variations. In *Aspects of Climate Variability in the Pacific and the Western Americas* (D.H. Peterson, ed.), Geophysical Monograph 55, American Geophysical Union, Washington, D.C., 305–363.

Kellogg, W.W., and Z.-C. Zhao. 1988. Sensitivity of soil moisture to doubling of carbon dioxide in climate model experiments. Part I: North America. *Journal of Climate 1*, 348–366.

Kiehl, J.T., and V. Ramanathan. 1990. Comparison of cloud forcing derived from the Earth Radiation Budget Experiment with that simulated by the NCAR Community Climate Model. *Journal of Geophysical Research 95*, 11679–11698.

Kuo, H.L. 1974. Further studies of the parameterization of the influence of cumulus convection on large-scale flow. *Journal of the Atmospheric Sciences 31*, 1232–1240.

Manabe, S., J. Smagorinsky, and R.F. Strickler. 1965. Simulated climatology of a general circulation model with a hydrologic cycle. *Monthly Weather Review 93*, 769–798.

Molina, M., T. Tso, L. Molina, and F. Wang. 1987. Antarctic stratospheric chemistry of chlorine nitrate, hydrogen chloride, and ice: Release of active chlorine. *Science 238*, 1253–1257.

Newell, R.E. J.W. Kidson, D.G. Vincent, and G.J. Boer. 1972. *The General Circulation of the Tropical Atmosphere* (Vol. 1). MIT Press, Cambridge, Massachusetts, 258 pp.

Oeschger, H., and U. Siegenthaler. 1988. How has the atmospheric concentration of CO_2 changed? In *The Changing Atmosphere* (F. Rowland and I. Isaksen, eds.), John Wiley and Sons, Chichester, England, 5–23.

Oort, A.H., and T.H. Vonder Haar. 1976. On the observed annual cycle in the ocean-atmosphere heat balance over the Northern Hemisphere. *Journal of Physical Oceanography 6*, 781–800.

Philander, G.S., and E.M. Rasmusson. 1985. The Southern Oscillation and El Niño. *Advances in Geophysics 28A*, 197–215.

Prinn, R. 1988. How have the atmospheric concentrations of the halocarbons changed? In *The Changing Atmosphere* (F. Rowland and I. Isaksen, eds.), John Wiley and Sons, Chichester, England, 33–48.

Prinn, R. 1992. Cyclic closure of biogeochemical cycles: Vernadsky Loops. In *Trace Gases and the Biosphere* (B. Moore and D. Schimel, eds.), Global Change Institute Volume 1, UCAR/Office for Interdisciplinary Earth Studies, Boulder, Colorado, 79–86.

Prinn, R., P. Simmonds, R. Rasmussen, R. Rosen, F. Alyea, C. Cardelino, A. Crawford, D. Cunnold, P. Fraser, and J. Lovelock. 1983. The Atmospheric Lifetime Experiment, I: Introduction, instrumentation and overview. *Journal of Geophysical Research 88*, 8353–8368.

Prinn, R., D. Cunnold, R. Rasmussen, P. Simmonds, F. Alyea, A. Crawford, P. Fraser, and R. Rosen. 1987. Atmospheric trends in methyl chloroform and the global average for the hydroxyl radical. *Science 238*, 945–950.

Prinn, R., D. Cunnold, R. Rasmussen, P. Simmonds, F. Alyea, A. Crawford, P. Fraser, and R. Rosen. 1990. Atmospheric trends and emissions of nitrous oxide deduced from ten years of ALE/GAGE data. *Journal of Geophysical Research 95*, 18369–18385.

Ramanathan, V. 1981. The role of ocean-atmosphere interaction in the CO_2 climate problem. *Journal of the Atmospheric Sciences 38*, 918–930.

Ramanathan, V., and W. Collins. 1991. Thermodynamic regulation of ocean warming by cirrus clouds deduced from observations of the 1987 El Niño. *Nature 351*, 27–32.

Ramanathan, V., R. Cicerone, H. Singh, and J. Kiehl. 1985. Trace gas trends and their potential role in climate change. *Journal of Geophysical Research 90*, 5547–5566.

Ramanathan, V., R.D. Cess, E.F. Harrison, P. Minnis, B.R. Barkstrom, E. Ahmad, and D. Hartmann. 1989. Cloud-radiative forcing and climate: Results from the Earth Radiation Budget Experiment. *Science 243*, 57–63.

Rowland, F., and M. Molina. 1975. Chlorofluoromethanes in the environment. *Reviews of Geophysics and Space Physics 13*, 1–35.

Running, S.W., and J.C. Coughlan. 1988. A general model of forest ecosystem processes for regional applications. I. Hydrologic balance, canopy gas exchange and primary production processes. *Ecological Modelling 42*, 125–154.

Schoeberl, M., R. Stolarski, and A. Krueger. 1989. The 1988 Antarctic ozone depletion: Comparison with previous year depletions. *Geophysical Research Letters 16*, 377–380.

Shukla, J., and Y. Mintz. 1982. Influence of land-surface evapotranspiration on the Earth's climate. *Science 215*, 1498–1501.

Siegenthaler, U. 1983. Uptake of excess CO_2 by an outcrop-diffusion model of the ocean. *Journal of Geophysical Research 88*, 3599–3608.

Somerville, R.C.J., and L.A. Remer. 1984. Cloud optical thickness feedbacks in the CO_2 climate problem. *Journal of Geophysical Research 89*, 9668–9672.

Stolarski, R. 1988. Changes in ozone over the Antarctic. In *The Changing Atmosphere* (F. Rowland and I. Isaksen, eds.), John Wiley and Sons, Chichester, England, 105–119.

Stouffer, R., S. Manabe, and K. Bryan. 1989. Interhemispheric asymmetry in climate response to a gradual increase of atmospheric CO_2. *Nature 342*, 660–662.

Tans, P., I. Fung, and T. Takahashi. 1990. Observational constraints on the global atmospheric CO_2 budget. *Science 247*, 1431–1438.

Trenberth, K.E. 1979. Mean annual poleward energy transports by the oceans in the Southern Hemisphere. *Dynamics of the Atmosphere and Oceans 4*, 57–64.

Twomey, S. 1977. *Atmospheric Aerosols*. Elsevier, Amsterdam.

Wang, W.-C., M. Dudek, X.-Z. Liang, and J. Kiehl. 1991. Inadequacy of effective CO_2 as a proxy in simulating the greenhouse effect of other radiatively active gases. *Nature 350*, 573–577.

Warren, S., C. Hahn, J. London, R. Chervin, and R. Jenne. 1986. *Global Distribution of Total Cloud Cover and Cloud Type over Land*. Technical Note TN-273+STR, National Center for Atmospheric Research, Boulder, Colorado.

Towards Coupled Physical-Biogeochemical Models of the Ocean Carbon Cycle

Stephen R. Rintoul

Introduction

The purpose of this review is to discuss the critical gaps in our knowledge of ocean dynamics and biogeochemical cycles. I will start with the assumption that our ultimate goal is the design of a model of the earth system that can predict the response to changes in the external forces driving climate. The prediction aspect is important; simplifying tricks that can be used to describe the present biogeochemical state of the ocean may not be sufficient for predicting future changes. It will also become clear that the design of such a model depends on the time scale it is intended to simulate.

The ocean circulation plays two direct roles in the climate system. First, the poleward flow of warm water and equatorward flow of colder water at depth in the thermohaline circulation results in a heat flux from equator to pole that is roughly equal to that of the atmosphere. Second, the ocean has a large heat capacity relative to that of the atmosphere, so that the timing of any change in global temperatures due to external forcing is largely determined by the thermal inertia of the ocean. Consequently, changes in ocean circulation can lead directly to changes in climate.

The ocean's ability to store and transport heat is perhaps its most important feature with regard to the physical climate system. However, the aim of this review is to focus on those aspects of the climate system that involve the interaction between ocean dynamics and marine biogeochemistry. In particular, I will try to identify those aspects of marine biogeochemistry that need to be included in the

ocean component of a coupled model of the earth system if we are to obtain useful predictions of future climatic change.

To focus the discussion even further, I will limit myself to consideration of the ocean carbon cycle. Carbon participates in active organic and inorganic chemical systems in the ocean, and most other biogeochemical cycles are linked to that of carbon by the marine biota. In addition, much effort has been devoted to modeling the carbon cycle due to conern over the climatic impact of the anthropogenic input of carbon dioxide.

The discussion here, however, will not be limited to the oceanic uptake of anthropogenic CO_2. Rather, I will assume that we have a broader interest in understanding how and why the carbon cycle functions as it does at present, and in learning its capacity for change over a range of time scales, from seasons to glacial cycles. The goal is not a comprehensive review, but a personal view of issues that need to be considered to move toward useful, predictive coupled models of the earth system.

Implicit in most carbon cycle modeling to date is an assumption that the system was in steady state prior to the anthropogenic invasion and has remained so in postindustrial times. In particular, the input of CO_2 due to fossil fuel burning and deforestation is often treated as a small perturbation to the equilibrium carbon system. This is despite the fact that the increase in atmospheric CO_2 since industrialization is already half that since the last glaciation, when evidence suggests that the ocean circulation and carbon system may have been very different than they are today. To be confident of our model predictions, we need to move beyond the assumption that the carbon system will remain in steady state. This requires a model of how the ocean circulation and carbon cycle interact.

In the following sections, I will review some of the coupled biological-physical models that have been used to date. The models generally represent two extremes of scale. Highly simplified box models have been used to study global phenomena on long time scales, such as the changes in climate between the glacial and interglacial. At the other extreme, more detailed models that explicitly resolve the nonlinear interactions between the biological and physical systems have focused on limited regions and short time scales. By reviewing the results of both types of models, I hope to shed some light on the issue of the most appropriate carbon cycle model for climate studies. In particular, what biological-physical interactions must be included to reproduce the essential processes on the time scales of interest? Modeling is by nature an art of compromise, and the appropriate balance between faithful reproduction of system dynamics and the simplifications that allow increased understanding will depend on the problem considered.

Oceanic Uptake of Carbon

The uptake of atmospheric CO_2 by the ocean is limited by several factors: the exchange of CO_2 across the air-sea interface, the buffer capacity of the oceanic carbonate system, and the transfer between the surface layers of the ocean and the deep sea. In this section, these fundamental aspects of the oceanic uptake of carbon are briefly reviewed.

Gas Exchange

The exchange of CO_2 between the atmosphere and the ocean can be expressed as the product of the difference in the partial pressure of CO_2 between the air and the surface ocean (δpCO_2) and a gas transfer coefficient. The gas transfer coefficient increases with increasing wind speed, but the exact form of the wind speed dependence is not well known; present formulations give an uncertainty of about a factor of two in the transfer coefficient (Liss and Merlivat, 1986; Tans et al., 1990). Even if we knew the wind speed-dependence of the transfer coefficient exactly, we would still have problems, because we do not know the wind distribution very well over large parts of the ocean, and we have even fewer observations of oceanic pCO_2. Consequently we cannot even "predict" the present exchange of CO_2 between the ocean and the atmosphere very accurately. Over large areas we are uncertain whether the ocean is a net source or sink.

If we knew the winds and the dependence of the transfer coefficient on wind speed, the problem would be reduced to one of predicting pCO_2 in the surface ocean. The partial pressure of CO_2 in the ocean is primarily a function of temperature and the concentrations of alkalinity (ALK) and total dissolved inorganic carbon (DIC).

Due in part to the temperature dependence of the solubility of CO_2 in sea water, the dominant factor in determining δpCO_2 is ocean upwelling and downwelling (Keeling, 1968). Upwelled water warms at the sea surface and releases CO_2; water cooled at high latitudes takes up CO_2. Maps of oceanic pCO_2 from the scarce data presently available agree with this broad-brush picture of the ocean as a sink for atmospheric CO_2 at high latitudes and a source at low latitudes (Figure 1).

The temperature dependence of pCO_2 implies that the physical factors that determine the temperature of the mixed layer also affect pCO_2. Therefore, to be able to predict oceanic pCO_2 we need to model the physical mechanisms that affect temperature (lateral and vertical advection and mixing, and heating and evaporation at the sea surface) and the biochemical mechanisms that determine the concentrations of alkalinity and DIC.

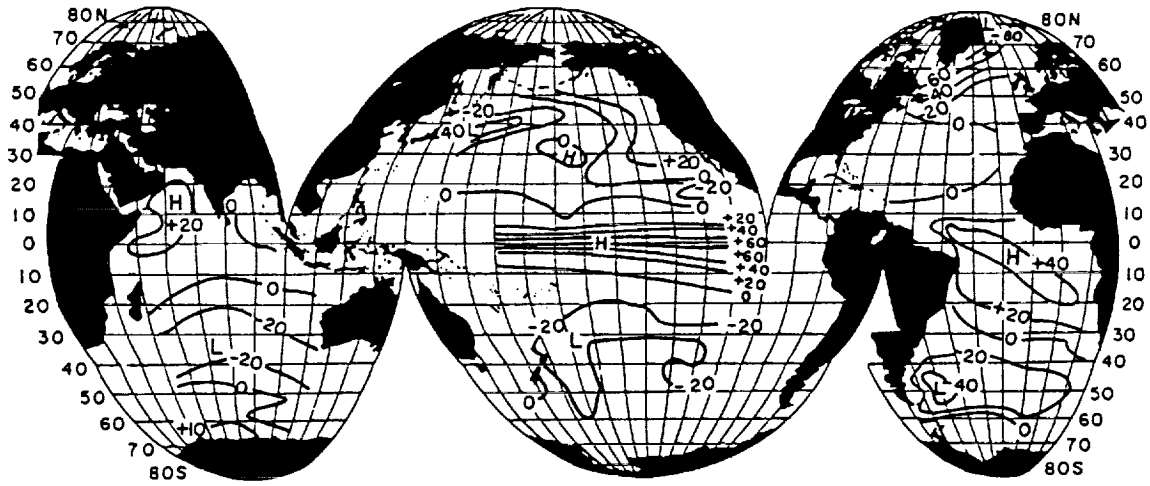

Figure 1. Map showing the difference in pCO_2 (in μatm) between the surface ocean and the atmosphere. Positive values indicate that the ocean is a source of CO_2 to the atmosphere; negative values indicate an oceanic sink. Based on data collected during the GEOSECS expedition (from Broecker and Takahashi, 1984).

The Buffer Factor

While CO_2 in the atmosphere is nonreactive, CO_2 in the ocean is involved in a variety of inorganic and organic reactions. DIC is made up of bicarbonate and carbonate ions, as well as CO_2. The three pools are related through the reversible reaction:

$$CO_3^{=} + CO_2 + H_2O \leftrightarrow 2HCO_3^{-}$$

Most of the dissolved carbon in sea water is in the form of bicarbonate ion (90%), with the remainder made up primarily of carbonate ion. Less than 1% of the total DIC in the sea occurs as dissolved CO_2 gas. As a result, the carbon system in the ocean is well buffered. The strength of this buffering is described by the Revelle factor, which is about 10 for most of the world ocean. A 10% increase in atmospheric CO_2 requires only a 1% increase in oceanic pCO_2 to restore equilibrium.

The Biological Pump

The partial pressure of CO_2 in the surface ocean is also influenced by biological productivity. Phytoplankton in the sunlit surface layers of the ocean take up CO_2 and nutrients, and release O_2, in forming organic matter by photosynthesis. Most of the primary production is quickly recycled through plant and animal respiration in the upper ocean, replacing the carbon removed by photosynthesis. The "regenerated" production thus does not result in a net removal of CO_2 from the euphotic zone. The fraction of the primary production that sinks

out of the euphotic zone is known as the new production. If the carbon and nutrient distributions are in steady state, then the carbon and nutrients exported as new production must be replaced by the mixing up of carbon- and nutrient-rich water from below.

Because nutrient concentrations are close to zero in most of the mid- and low-latitude surface ocean, the supply of nutrients has traditionally been considered the limiting factor for phytoplankton growth. In the equatorial Pacific and at high latitudes, however, there are measurable levels of nitrate and phosphate in the surface ocean. The limiting factor in these regions has been assumed to be light limitation. Recently Martin and co-workers (Martin and Fitzwater, 1988; Martin and Gordon, 1988; Martin et al., 1990) have suggested that iron is the limiting factor in many areas far from land (see Peng et al., this volume, for a discussion on limits to the proposed effect of iron).

Nitrogen, phosphorus, oxygen, and carbon are believed to occur in marine organic matter in fixed ratios known as the Redfield ratios (Redfield et al., 1963). In a nutrient-limited system typical of most of the ocean, the net carbon export, or new production, can thus be equivalently expressed in terms of a net input of nitrate.

As the particulate matter exported from the euphotic zone sinks through the water column, it dissolves or decomposes, consuming oxygen and releasing carbon. The downward transfer of carbon from the sea surface to the deep water is known as the biological pump. In the present-day ocean, the biological pump is responsible for maintaining deep ocean concentrations of dissolved inorganic carbon at levels 10–15% higher than surface values (Broecker and Peng, 1982). Because nutrients are also taken up in the formation of organic matter and regenerated at depth, the concentrations of nitrate and phosphate (as well as other minor nutrients needed for plant growth) increase with depth in a way similar to DIC. However, the maximum DIC concentration lies deeper in the water column than the nutrient maxima. This reflects the dissolution of calcium carbonate tests, which occurs at greater depths than the regeneration of organic soft tissue. The sinking and dissolution of calcium carbonate particles carries carbon but not nutrients to the deep sea. The difference in carbon regeneration depths resulting from the "soft-tissue pump" and the "carbonate pump" (Volk and Hoffert, 1985) will be seen to provide an essential mechanism by which biological productivity can influence atmospheric pCO_2.

Recent observations of larger concentrations of dissolved organic matter (DOM) than previously assumed have thrown the traditional one-dimensional view of the biological pump, as sketched above, into doubt. In particular, the existence of a large reservoir of non-sinking organic matter with an intermediate lifetime (longer than

days and shorter than centuries) implies that lateral transport may be an essential element of marine biogeochemical cycles (Sugimura and Suzuki, 1988; Toggweiler, 1989).

The Role of Ocean Transport

As mentioned in the introduction, the ocean plays a direct role in the climate system through the storage and transport of heat. The ocean circulation also plays a more indirect role in the climate system through its impact on the carbon cycle. Once CO_2 has reached equilibrium between the atmosphere and ocean, there are two main pathways for carbon between the surface ocean and the interior: a biologically mediated path (the biological pump described above) and a path mediated by physical processes. The biological pump is, of course, itself controlled by physical processes (Figure 2); since the new production is, by definition, equal to the rate of supply of nutrients to the upper ocean, the rate of vertical exchange between deep and surface water is the rate-determining step in the biologically mediated uptake of carbon.

The wide variety of physical mechanisms that lead to an exchange between surface and subsurface waters also contribute to the net

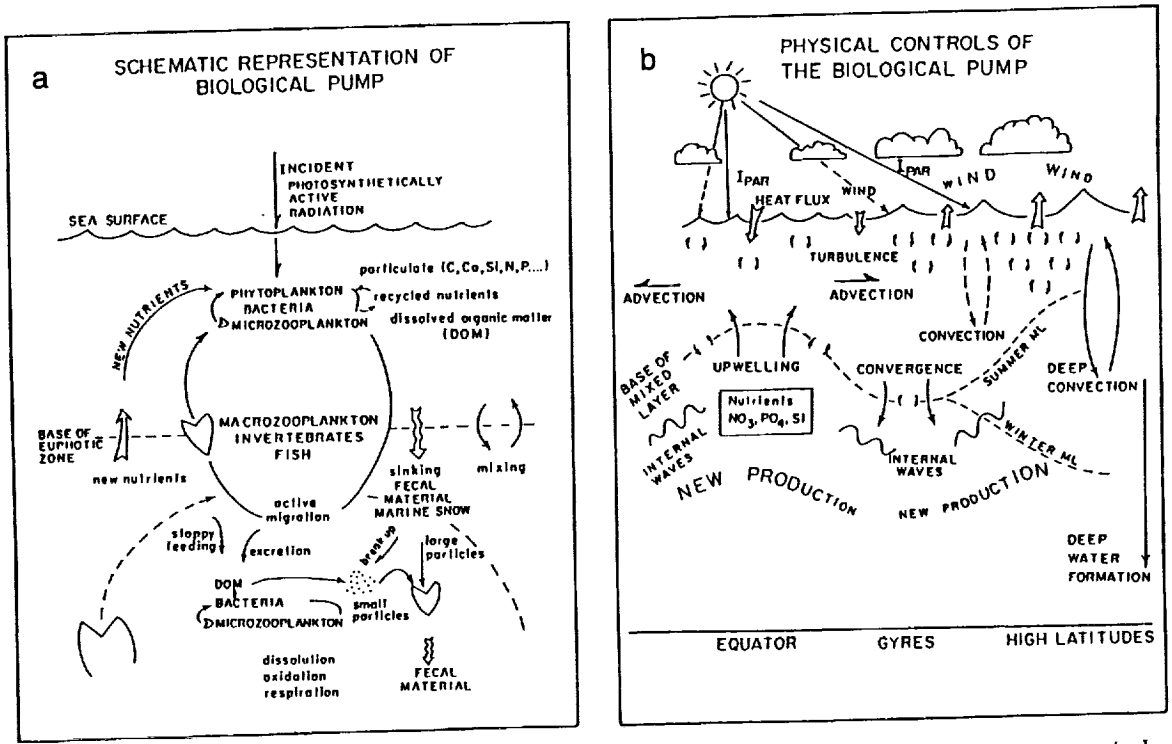

Figure 2. Schematic representation of (a) the biological pump and (b) the physical processes controlling the biological pump (from Bishop, 1989).

exchange of carbon with the ocean interior. Each of these ventilation mechanisms (e.g., subduction, Ekman pumping, the formation of deep and intermediate water masses) has its own characteristic overturning time, which determines the period for which carbon carried into the interior is sequestered from contact with the atmosphere. The physical processes that need to be resolved in a coupled biological-physical climate model therefore depend on the time scale of interest.

As a consequence of the temperature dependence of the solubility of CO_2, the thermohaline circulation plays a role in the redistribution of carbon analagous to the role it plays in the global heat balance. Surface water cooled at high latitudes picks up CO_2; when this water loses sufficient bouyancy to sink from the surface layer to the ocean interior, it carries CO_2 with it. The CO_2 sequestered by the formation of deep water masses is ultimately given back to the atmosphere through upwelling at low latitudes. Volk and Hoffert (1985) have termed this mechanism of downward carbon transport the "solubility pump."

Another example of how ocean physics and biology interact in the transport of carbon out of the surface layer involves seasonal variability. Codispoti et al. (1982) have shown that in the Bering Sea, biological productivity can draw down surface pCO_2 by 200 ppmv in two months (Figure 3). Ocean ventilation processes also vary on seasonal time scales. Consequently, biological processes can play an important role in determining the carbon concentration of surface waters carried into the deep ocean by physical mechanisms (Brewer, 1986). Few carbon cycle models presently represent the seasonal cycle of the physics or biology.

Summary

To sequester atmospheric CO_2 in the ocean interior requires, first, exchange across the air-sea interface and, second, transfer from the sea surface to the deep ocean. The second transfer is achieved by one of two primary mechanisms: a biologically-mediated path known as the biological pump and a variety of physical processes that result in exchange of water between the upper and lower layers of the sea.

For the purpose of constructing coupled physical-biogeochemical carbon cycle models, it is necessary to look more closely at the relative importance of each of these barriers to the uptake of atmospheric CO_2 by the ocean. First, concerning gas exchange, the surface ocean and the atmosphere equilibrate with respect to CO_2 in about one year (Broecker and Peng, 1982), so that gas exchange is not the rate limiting step in the oceanic uptake of CO_2. Rather, the rate of vertical exchange between the surface and deep ocean appears to limit the rate at which CO_2 is taken up by the ocean (Oeschger et al., 1975; Sarmiento et al., 1990). This suggests that

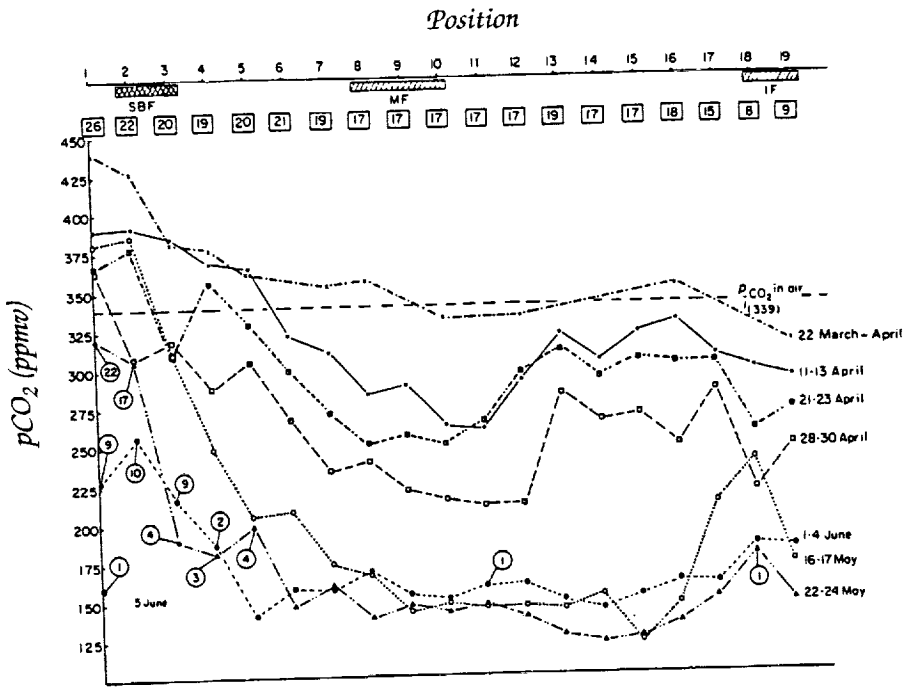

Figure 3. The temporal evolution of pCO_2 in the surface water along a transect in the Bering Sea. The hatched boxes mark the location of three fronts. Initial nitrate concentrations (in μg-atom/L) at the surface are given in the squares. Surface nitrate concentrations >1 between May 22 and June 5 are shown in circles (from Codispoti et al., 1982).

the remaining uncertainties in the gas transfer coefficient are not critical for the prediction of CO_2 uptake. Supporting evidence for this conclusion is provided by some of the models discussed below, in which the uptake of carbon is found to be insensitive to changes in the gas exchange rate.

The second issue that it is important to make clear concerns the efficiency of the biological pump in the sequestering of carbon. The ocean biota undoubtedly play a critical role in determining the preindustrial, unperturbed, distribution of carbon in the sea. As mentioned above, the downward flux of carbon fixed by marine plants and repackaged by heterotrophs maintains deep ocean concentrations of DIC at levels 10–15% higher than those in the surface ocean. As a result, atmospheric CO_2 concentrations are significantly lower than they would be if the atmosphere overlay an abiotic ocean.

However, the fact that the marine biota play a crucial role in the natural, unperturbed carbon cycle does not automatically imply that it is essential to include biology in climate models designed to

predict the response to changing external forcing, such as the anthropogenic input of CO_2. The models discussed in the following section show that the question of whether biology is important depends on the time scale of interest. The marine biota have little *direct* effect on the ocean's uptake of *anthropogenic* CO_2. Primary production in the sea is limited by light and nutrients, not carbon. Increasing the CO_2 concentrations in the surface ocean therefore has no direct effect on primary production. It is also important to realize that *in equilibrium* the biological pump plays *no role* in the sequestering of carbon in the deep ocean. By definition, if the system is in steady state, the biologically mediated export of organic carbon from the surface ocean is compensated for by an input of inorganic carbon supplied by vertical mixing.

Ocean biology may have an important indirect effect on oceanic uptake of the "excess" CO_2 supplied by human activities. Changes in the atmospheric circulation due to CO_2-induced changes in the radiative forcing will force changes in the ocean circulation. Changes in the circulation, for example, a change in the strength of the thermohaline overturning, may lead to a redistribution of nutrients which will affect the marine biology.

The important point is that changes in the ocean biogeochemical system of relevance to the uptake of carbon from the atmosphere can occur only on relatively long time scales. A global redistribution of nutrients, for example, requires a time equal to the turnover time of the deep ocean, about 1000 years. Therefore, the importance of the role played by marine biogeochemistry depends on the time scale considered; for the prediction of oceanic uptake of carbon on decadal time scales, physical exchange processes are probably most important, while on time scales of 100–1000 years and longer the role of marine biota may be critical.

Gaps in Present Physical and Biogeochemical Models

Gaps in the Physical Models

Before considering particular examples of coupled biogeochemical-physical models, it is worth considering in a general way the characteristics of the physical and biological models that are to be coupled. Most models of ocean biogeochemistry start with a conservation equation for some biologically active component (e.g., phytoplankton or nitrate). The conservation equation includes terms for advection and diffusion, both lateral and vertical, and a biological source/sink term. The first step, then, is an accurate description of the transport field in the ocean. Are there gaps in our knowledge of ocean dynamics?

Modelers of ocean dynamics have an immediate advantage over biogeochemical modelers: The equations are known. We are confident that the Navier-Stokes equations describe the physics of ocean flow accurately. However, it is not possible to resolve every scale of motion, from basin scale to molecular scale. The art of the modeler lies in the parameterization of subgrid-scale processes in a way that maintains the essential nature of the unresolved processes while simplifying the problem enough to make it tractable.

In ocean models, small-scale processes are usually parameterized by relying on an analog to Fick's law of diffusion (Bryan, 1979). The net effect of small-scale mixing is expressed as an eddy coefficient multiplied by the large-scale property gradient. Mixing in the ocean is the result of a large variety of processes acting on different scales (e.g., breaking internal waves, shear instability, convection, double diffusion, wind stirring). It is not clear that the same parameterization should apply to the net effect of each of these processes. To make matters worse, the magnitude of the diffusion coefficient is generally chosen for numerical stability, rather than on physical grounds; the coarser the resolution, the larger the diffusion coefficients must be. Consequently, in coarse-resolution models the thermocline tends to be too diffuse, fronts tend to be too broad, and inertial effects are too strongly damped.

The results of a model are generally sensitive to the magnitude of the diffusion coefficient. Bryan (1987), for example, has demonstrated the sensitivity of the thermohaline circulation and meridional heat flux to the magnitude of the vertical diffusivity in a coarse-resolution general circulation model (GCM). Given the importance of the thermohaline circulation in the climate problem, as discussed above, such sensitivity is cause for concern.

As the model grid size decreases and more scales of motion are explicitly resolved, the relative magnitudes of "advection" and "diffusion" change. Eddy resolving GCMs do not have to parameterize as much of the eddy field and can use smaller eddy coefficients. However, such calculations are extremely computationally intensive, and it is not possible to integrate long enough for the thermohaline circulation to reach equilibrium or to do multiple experiments to test the sensitivity to the model parameterizations.

A final issue related to the parameterization of mixing in ocean circulation models regards the orientation of the mixing tensor. Mixing in the ocean occurs much more efficiently along neutral surfaces than across them, since motions across neutral surfaces are opposed by buoyant restoring forces. In most ocean models, lateral mixing is represented as a strictly horizontal process. Since neutral surfaces are generally inclined to the horizontal, mixing in the

model does not truly represent the effect of turbulent motions on the transport of physical and chemical properties. Lin (1988), for example, has shown that heat penetrates into the ocean interior more efficiently in a model with isopycnal diffusion than in one with horizontal diffusion. Similarly, the injection of chemical properties such as CO_2 will be sensitive to the orientation of the mixing tensor.

A second major problem encountered by an ocean modeler is the fact that the forcing at the ocean boundary (wind stress, heat flux, and freshwater flux) is usually poorly known. Wind stress and precipitation are notoriously difficult to measure accurately from ships. The heat flux and evaporation rate also depend critically on the wind speed. Generally the fluxes have been so poorly known that modelers have resorted to tricks such as restoring the surface temperature and salinity to "observed" values with some time constant. There are several potential problems with this approach: The "climatological" average values used as observations generally are highly smoothed and may not reflect the spatial/temporal scales of the real surface fluxes; the time constant introduces an additional free parameter; and there is the possibility that one can mask some fundamental deficiency in the model physics by preventing the model solution from drifting too far from the "truth." Perhaps the main problem is that we cannot use such a model to predict the response to changing conditions in the future, for which observations are not available, or to couple to an atmospheric model.

Gaps in the Biological Models

If our goal is the design of a coupled model that is able to predict the carbon export from the euphotic zone, what kind of biological model is required, and where are the gaps in present models?

Given that CO_2 is not limiting in the surface ocean environment, the two fundamental requirements for primary production are light and nutrients. At a minimum, then, a coupled biological-physical model for studies of the oceanic carbon cycle must reproduce the light and nutrient environment experienced by primary producers. The light and nutrient regimes are functions of the vigor of vertical mixing in the upper ocean. If the vertical mixing is very weak, the absence of an input of nutrients will limit primary production; if the vertical mixing is deep and energetic, phytoplankton spend only a short time in the euphotic zone, and production is again limited.

In addition, the structure of marine communities, or the relative abundance of different species, changes as the vertical mixing regime changes to take maximum advantage of the resources available. For example, stably stratified regimes resulting from weak vertical mixing tend to favor small phytoplankton, while energetic

regimes characterized by episodic pulses of nutrients tend to be dominated by large phytoplankton with rapid growth rates (Williams and von Bodungen, 1989). The former community type efficiently recycles the limited supply of nutrients, and only a small fraction of the total primary production is exported. In contrast, the communities dominated by large cells such as diatoms export a relatively large fraction of the primary production. Therefore changes in the physical mixing regime can lead to changes in community structure and the efficiency with which biological processes export carbon from the euphotic zone.

Note, however, that while a shift from low mixing to high mixing at a particular location may lead to shifts in community structure and changes in the new production, the net uptake of carbon is unchanged; the supply of "new" nutrients by mixing will be accompanied by a supply of DIC in the Redfield proportion. The only way this constraint can be removed is if the ratios of C:N:P are not constant in marine organic matter. Although observations suggest that the Redfield ratios are relatively constant, the extent to which the Redfield ratios may vary spatially, temporally and by species is not well known.

An accurate description of the time history of the nutrient distribution and the mixed-layer depth would therefore appear to be essential for a coupled biological-physical model. An additional step is necessary to translate the supply of nutrients and light into a net export of carbon. A variety of "rules" have been used to relate the export production to the physical mixing, light, and nutrient distributions.

The simplest "rule" is to simply equate the export production to the input of "new" nutrients by mixing, using the Redfield ratio to convert the flux of nitrate or phosphate into an equivalent carbon flux. The majority of the models discussed in the next section adopt this approach. It has the advantage of simplicity and serves as an integral constraint that may be applied without a knowledge of the details of the biological system. However, there are several limitations to this approach. First, the method implicitly assumes that nutrients are the sole factor limiting primary production. This is not true at high latitudes, or even at midlatitudes during the winter, when light is limiting. Second, the method assumes that the Redfield ratio is constant and accurately known. Third, it does not take into account some evidence that other nutrients, including silicate, and elements needed in trace quantities, such as iron, may be limiting in some regions at some times of year. Finally, the method is of no use if we are interested in issues other than the net export production, such as the standing stock of phytoplankton or the dynamics of the spring bloom.

At the opposite extreme lie ecosystem models that attempt to explicitly resolve the different classes of organisms, and the transfers between them, that make up the marine food web. The immense complexity of the biological system is usually reduced to a set of pools of carbon or nitrogen representing the components of the food web (e.g., phytoplankton, zooplankton, bacteria, nitrate) (Fasham, 1985; Venzina and Platt, 1987; Michaels and Silver, 1988). Each of these pools can be advected and diffused. In addition, biochemical processes transfer material from one pool to another, but the equations describing these transfers are not well known. A large number of parameters, which generally are poorly constrained by observations, are needed to describe such factors as the efficiency of carbon transfer between trophic levels, the sinking and regeneration rate of particles, and the physiological characteristics of individual cells (e.g., maximum growth rate, photosynthetic response to light). Plankton adapt to changing environmental conditions, so that these parameters may also change in time depending on the past history of the cell.

The minimum ingredients necessary to model a food web are light, nutrients, a primary producer (to fix carbon), and a secondary producer (to package the fixed carbon for export). Additional elements that may be critical to model a particular phenomenon include multiple size classes of phytoplankton and zooplankton, multiple phytoplankton species (e.g., diatoms forming silicious tests vs. coccolithophores forming calcium carbonate tests), ammonium as well as nitrate as a substrate, trace nutrients such as iron, vertical migration, particle aggregation to form "marine snow," caprophagy, higher trophic levels, and production of dissolved organic matter. To include these additional pools or processes, the transfer of carbon between each of the pools must be parameterized. However, the rate of transfer between various reservoirs is extremely difficult to observe, and the parameterizations are thus highly uncertain.

Therefore, one category of gaps in present biological models is rooted in the question of how to parameterize the many interactions in a complex biological system that is patchy in space and time. More fundamentally, we do not have a clear understanding of which of these processes are essential and which can be safely ignored. We have even less feeling for the importance of resolving the nonlinear interactions occurring between physical and biological processes that are varying on similar spatial and temporal scales.

To consider a specific example, the box models discussed in the next section suggest that changes in biological productivity at high latitudes, where surface nutrient concentrations are not equal to zero, can have a profound impact on atmospheric pCO_2 on the time scale of centuries. One question we might want to ask of our cou-

pled ocean circulation–carbon cycle model is this: Given the changes in wind stress and heat flux expected at the sea surface due to CO_2-induced changes in the radiative forcing of the atmosphere over the next 100 years, how will high-latitude circulation, productivity, and distribution of nutrients and carbon change? (Ultimately, of course, the atmospheric model would be coupled directly to the ocean carbon model). At the present time, we have no idea what elements of the marine food web—or, for that matter, of the physical model—need to be included to answer this question.

Summary

Basin-scale ocean circulation models have generally focused on the large-scale flow. The limited spatial resolution achievable in these models has meant that several aspects of the ocean that are potentially the most important in determining the role of the ocean in the global carbon cycle have been neglected. In particular, the dynamics of the mixed layer and exchange between the mixed layer and the ocean interior are not well reproduced in present coarse-resolution models. Deficiencies in the way present models simulate ocean ventilation processes, together with uncertainties in the surface forcing, make model-based predictions of the oceanic uptake of carbon by physical processes highly uncertain.

The difficulties are enhanced when one contemplates coupling the physical and biogeochemical subsystems in a model. The biogeochemistry is most sensitive to exactly those aspects of the ocean that coarse-resolution models have the most trouble reproducing: the physical and chemical properties of the mixed layer and vertical exchange processes. Accurate representation of upper-ocean mixing and knowledge of the surface forcing are critical to simulate both the physically and biologically mediated transfer of carbon to the ocean interior.

It is clear that the circulation will depend on the resolution of the model, but we do not understand the biogeochemical processes well enough to know what features of the circulation we need to get right. For example, even the eddy resolving models do not accurately reproduce some basic features, such as the location of the separation of the Gulf Stream from the coast. The Gulf Stream plays a major role in determining the pattern of mixed layer depth in the North Atlantic; is getting the Gulf Stream separation right therefore important for modeling the carbon cycle? How much trust can we have in the biogeochemical implications of a circulation model that has clear physical inadequacies? The remainder of this paper reviews a variety of attempts to model aspects of marine biogeochemical cycles in the search for answers to these questions.

Examples of Coupled Ocean Dynamics-Biogeochemical Models

Box Models

The use of box models to study the carbon cycle has a long history (e.g., Revelle and Suess, 1957; Craig, 1957; Nydal, 1968; Oeschger et al., 1975). The box-diffusion model of Oeschger et al., in which the ocean is represented as a deep diffusive reservoir capped by a well-mixed surface box in communication with the atmosphere, has proved particularly useful. Sixteen years after its introduction, the box-diffusion model (with some modifications) is still the primary tool used to predict the carbon cycle's response to different CO_2 scenarios (e.g., Houghton et al., 1990).

The analysis of trapped air bubbles in ice cores, which showed that atmospheric pCO_2 increased at the end of the last glacial period from 200 ppm to 280 ppm in only a few hundred years (Neftel et al., 1982), sparked a renaissance in biogeochemical box modeling. This observation demonstrated that the carbon system was capable of much more rapid change than had been previously thought. A series of simple box models was developed to explore the role that the oceans might play in producing such rapid changes in atmospheric pCO_2 (Broecker, 1982; Sarmiento and Toggweiler, 1984; Knox and McElroy, 1984; Siegenthaler and Wenk, 1984). These models provide some of the clearest suggestions of how ocean circulation and biology may interact to determine atmospheric pCO_2.

In box models the ocean is reduced to a small number of well-mixed reservoirs, and the net effect of all ocean transport processes is parameterized as a few exchange terms between reservoirs. The magnitude of the "circulation" is fixed by fitting to the basin-averaged vertical profile of a tracer such as ^{14}C. Biology also enters in the simplest possible way: The export from the surface box is proportional to the nutrients supplied by mixing between the surface box and the nutrient-rich deep box.

Broecker (1982) used a two-box model of oceanic phosphate to study the increase in atmospheric pCO_2 that occurred at the end of the ice age. In this model, the "physics" consists of a single term, the exchange between the boxes. Broecker proposed that during the glacial period, phosphate concentrations increased due to oxidation of organic matter deposited on the continental shelves. Increased oceanic phosphate led to an increased efficiency of the biological pump and a larger transport of carbon to the deep sea. More recent work, however, has shown that the changes in atmospheric pCO_2 preceded the changes in ice volume (Shackleton and Pisias, 1985)

and occurred too rapidly (Siegenthaler and Wenk, 1984) to be consistent with this hypothesis.

The next generation of box models overcame these difficulties by dividing the surface ocean into a high- and a low-latitude box (Knox and McElroy, 1984; Sarmiento and Toggweiler, 1984; Siegenthaler and Wenk, 1984). Phosphate at high latitude (P_{hl}) is determined by the balance between the input of nutrient-rich water from below and the export of nutrients in sinking organic matter. When convective exchange between the surface and deep boxes at high latitude increases, P_{hl} increases, which in turn leads to increases in surface DIC and alkalinity, and thus atmospheric pCO_2. Increases in high-latitude productivity export more nutrients to the deep sea, P_{hl} decreases, and hence so does atmospheric pCO_2. The presence of a high-latitude outcrop allows more direct communication between the atmosphere and the carbon reservoir in the deep ocean. This in turn permits relatively rapid exchange between the atmospheric and oceanic carbon reservoirs.

A somewhat different three-box model was used by Dymond and Lyle (1985) and Sarmiento et al. (1988) to investigate the effect of differences in the regeneration depth of organic carbon and calcium carbonate on atmospheric pCO_2. The simplest model they could devise that still contained the essential features consisted of three stacked boxes, one each for surface, thermocline, and deep water. All organic matter was assumed to be regenerated in the thermocline box, and all calcium carbonate was assumed to regenerate in the deep water box. In this model, atmospheric pCO_2 is changed by sequestering or releasing ALK in the deep ocean; an increase in the sequestering of ALK in the deep sea or an increase in the surface mixing will lead to an increase in atmospheric pCO_2.

Recently the number of boxes included in such models has continued to grow (e.g., Broecker and Peng, 1986; Keir, 1988; Boyle, 1988; Volk, 1989). The models with additional boxes are constructed in the same way as the two- and three-box models: The circulation is postulated a priori, and the resulting atmospheric pCO_2 and carbon and nutrient distributions are calculated. However, additional boxes do reveal phenomena that are hidden in the simpler models. For example, Keir (1988) stressed the essential difference between the Mediterranean-type high-latitude circulations typical of the North Atlantic (and of the three-box models above) and the estuarine-type circulations thought to be characteristic of the Antarctic. In the first case, changing the productivity at high latitudes decreases atmospheric pCO_2 but has little effect on low-latitude productivity, since the nutrient concentration of deep water upwelling into the low-latitude surface box has not changed signifi-

cantly. In the second case, increasing productivity in the Antarctic leads to trapping of carbon and nutrients in the circumpolar deep water. This decreases both atmospheric pCO_2 and productivity in the warm surface waters, since the preformed nutrient concentration of the intermediate water upwelling to supply the warm surface box is decreased.

The primary justification for box models is that they provide insight into the essential mechanisms controlling pCO_2 and help to identify those parameters to which the properties of interest are most sensitive. For example, the box models have indicated that high-latitude production, the "alkalinity pump," and the magnitude of vertical mixing all may play an important role in determining atmospheric pCO_2. However, the results of box models should be viewed with caution; even in these simple systems there may be multiple scenarios consistent with a particular observation (such as the fact that atmospheric pCO_2 was 80 ppm lower in glacial times). The comparison of different box models also demonstrates the sensitivity of the results to the model configuration and "physics" assumed, such as the magnitude and sense of the overturning circulation. For example, the two-box model suggested that ocean biology played a small role in determining atmospheric pCO_2; dividing the surface ocean into a high- and a low-latitude box, as in the three-box models, suggested instead that biological productivity at high latitude could have a major impact (Sarmiento et al., 1988). Most of the present box models have been calibrated with a single tracer, usually natural ^{14}C. Models calibrated with other tracers such as bomb-produced ^{14}C or tritium result in different values for the mixing coefficients and circulation (Sundquist, 1985). Furthermore, none of these tracers is a perfect analog for CO_2. Finally, such models cannot tell us how the system might change. This suggests the need for models with less extreme parameterization.

Diagnostic Box Models

Diagnostic or inverse models differ from box models primarily in that some ocean dynamics is included. Diagnostic models attempt to deduce the circulation, mixing, and biochemical transformation rates consistent with a set of physical, biological or chemical observational constraints (e.g., Riley, 1951; Garcon and Minster, 1988; Schlitzer, 1988; Bolin et al., 1989; Metzl et al., 1990; Rintoul and Wunsch, 1991). The inverse calculations share some of the advantages and disadvantages of box models: Such models are often useful for identifying important physical or biochemical mechanisms, but are of little use in determining how the system may change in the future.

Furthermore, like those of box models, the conclusions reached by these models may depend on the degree of resolution or averaging of the data. For example, Schlitzer (1988) concluded from a low-resolution model of the North Atlantic that dissolved organic matter played no role in the basin-scale nitrogen balance. Schlitzer avoided the Gulf Stream, realizing that the highly smoothed data he used would not adequately represent the sharp front of the western boundary current. Rintoul and Wunsch (1991), on the other hand, considered a smaller area but with high-resolution hydrographic data. They found that the western boundary current played a critical role in the transport of nitrate and that a sizeable dissolved organic nitrogen (DON) pool was required to balance the nitrogen budget in the North Atlantic. When the data were smoothed prior to the inversion, the meridional fluxes of nitrate and silicate were changed significantly.

Although inverse models are by nature not predictive tools, once a solution has been found, it can be used to perform transient or predictive calculations by assuming the circulation and mixing remain in steady state. For example, Bolin et al. (1989) estimated the transient uptake of tritium, ^{14}C, and CO_2 from the atmosphere by the Atlantic Ocean (Figure 4). They found that large-scale advection was primarily responsible for the transport of carbon into the ocean interior. A second experiment with a more energetic circulation led to greater uptake of carbon.

A great advantage of inverse models lies in the variety of information that can be used to constrain the solution. One also obtains useful information concerning what features of the solution have been well determined by the available information, and explicit error estimates. However, since the primary goal is the development of a predictive coupled model, I will not discuss diagnostic models further.

Mixed-Layer Models

At the opposite extreme of model scale, models of the mixed layer use high resolution (a few meters) in the upper 100–300 m of the water column and treat the rest of the ocean as a bottom boundary condition. In the open oligotrophic ocean, the input of nutrients into the euphotic zone, and thus new production, is controlled by turbulent vertical transport through the base of the mixed layer. Several attempts have been made in recent years to use models of mixed-layer physics together with some representation of biologically important processes to study the interaction between physics and biology in the upper ocean. Perhaps the most valuable insight that has been gained from these one-dimensional models is an apprecia-

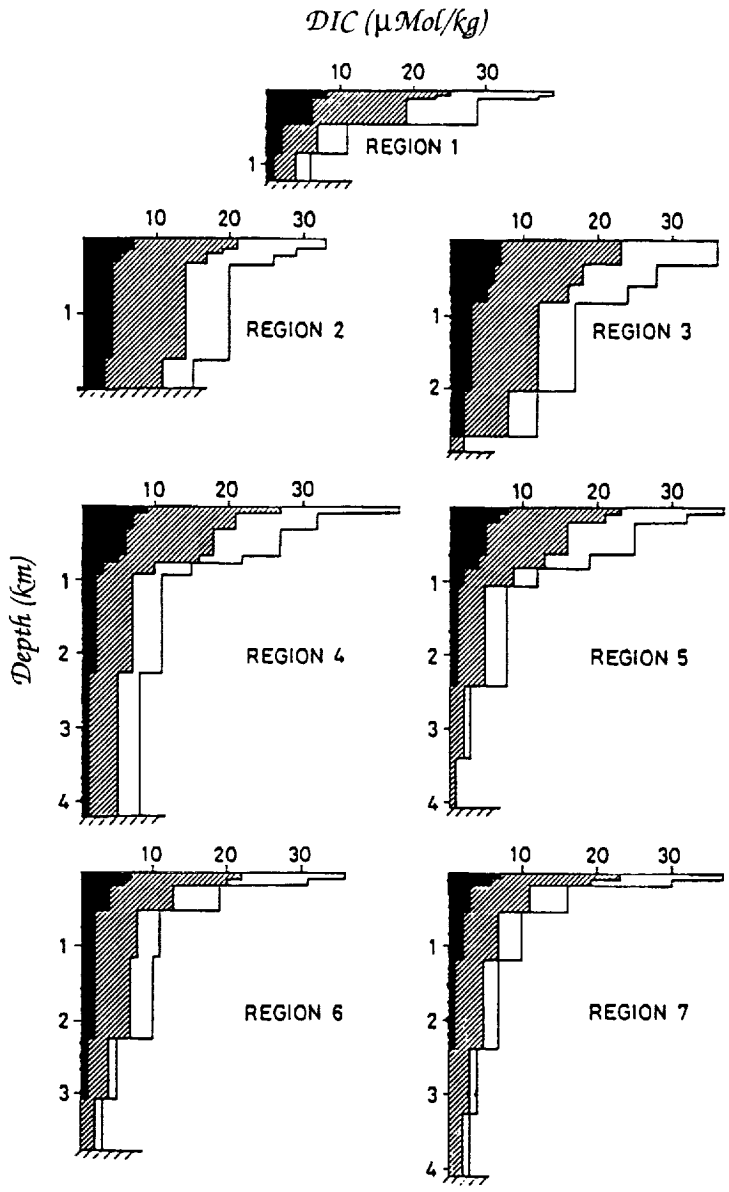

Figure 4. Modeled accumulation of carbon (in the form of DIC) in the Atlantic Ocean as a result of increasing atmospheric CO_2 concentrations. For selected regions, vertical profiles of CO_2 concentrations are shown for 1880 (black), 1955 (stippled), and 1983 (white), resulting from a transient calculation using the steady-state circulation. Note the greater concentration in the western basin (regions 2, 4, 6), reflecting transport of carbon into the interior by the formation of North Atlantic deep water (from Bolin et al., 1989).

tion for the importance of nonlinear interactions between physical and biological processes that are varying in time.

Mixed-layer models are generally one-dimensional; lateral advection and mixing are ignored. The depth and properties of the mixed layer depend on atmospheric forcing (wind stress, heat flux, freshwater flux), turbulent vertical mixing, and in situ absorption of solar radiation. The concentrations of dissolved gases, such as oxygen or carbon dioxide, depend on surface gas exchange as well. The mixed-layer models of interest here also include a biologically active component (e.g., phytoplankton or nutrient concentrations). The biological component is passively advected and diffused in the same manner as temperature and salinity, but has additional source/sink terms due to biological or chemical activity.

Kiefer and Kremer (1981) used a mixed-layer model to explain the origin of the subsurface chlorophyll maximum near the base of the euphotic zone. They employed a model of phytoplankton growth based on following flows of nitrogen between three pools: nitrate, nitrite, and phytoplankton. They concluded that the chlorophyll maximum resulted from the formation of the seasonal thermocline by the warming of the surface layers in the late spring. The thermocline stabilized the lower portion of the euphotic zone and isolated the layer in an environment favorable to growth.

While Kiefer and Kremer underscored the importance of *seasonal* changes in the depth of the mixed layer, Woods and Onken (1982) focused on the effect of *diurnal* variation on primary production. The "Lagrangian-ensemble" model of Woods and Onken is very different from the more commonly used "Eulerian-continuum" models, such as that of Kiefer and Kremer. The latter models treat phytoplankton concentration, for example, as a continuum property of the sea water that changes with time at fixed points. A Lagrangian model of phytoplankton, on the other hand, follows the trajectory of individual phytoplankters as they move through a variable environment (e.g., changing light levels or nutrient concentrations). Forming the ensemble average of the individual trajectories has the effect of averaging after integrating the nonlinear equations describing phytoplankton growth. Woods and Onken point out that this is particularly important at diurnal scales, because the physical environment and the physiological responses of the plankton to changing conditions vary on similar time scales.

Woods and Onken were interested in describing the initiation of the spring bloom, and they neglected the effects of zooplankton grazing, nutrient limitation, and self-shading, as well as lateral advection or diffusion, all of which would tend to increase the nonlinearity and further justify the use of Lagrangian methods. How-

ever, even the present simplified system is complex and uses a time step of three minutes for the phytoplankton equations. The prospect of scaling up such a model to large scales is intimidating. On the other hand, both the Kiefer and Kremer and Woods and Onken models result in similar behavior on seasonal time scales, perhaps indicating that we can get away with not resolving the nonlinearities on the scale of individual cells.

Klein and Coste (1984) emphasized a different type of nonlinear interaction in the mixed layer. They were particularly concerned with the effect of variable surface forcing (wind stress) on nutrient transport into the mixed layer. Klein and Coste concluded that the entrainment of nutrients was dominated by the interaction between time-varying wind stress and near-surface currents. In particular, a resonance between the wind stress and wind-generated inertial currents at the inertial frequency (about one day at 30° latitude) resulted in pulses of nutrients entering the mixed layer (Figure 5). This nonlinear interaction affects both instantaneous and mean values of the nutrient flux.

Klein and Coste did not include any active biology within the mixed layer. They focused on the net input of nitrate into the mixed layer, which is (by definition) equal to the new or export production. A different approach to estimating the new production using a mixed layer model has been taken by Musgrave et al. (1988). They have focused on simulating the seasonal cycle of oxygen in the upper ocean. The seasonal buildup of a subsurface oxygen maximum in the subtropical ocean can be used to estimate the amount of new production, since the recycled production loop has no net effect on oxygen concentrations (Shulenberger and Reid, 1981; Jenkins and Goldman, 1985). Moreover, since the oxygen produced during photosynthesis remains after the "new" organic matter has sunk out of the mixed layer, the oxygen concentration tends to average over a series of episodic production pulses (resulting, for example, from the pulses of nitrate input described by Klein and Coste).

The physical model employed by Musgrave et al. is based on that of Price et al. (1986). The equations include terms expressing the dependence of temperature, salinity, and horizontal velocity on entrainment of water from below; surface fluxes of heat, salt, and momentum; vertical advection; vertical diffusion; in situ absorption of solar radiation; and inertial rotation of the horizontal velocity due to the Coriolis force.

The rate of change of mixed-layer depth is needed to close the set of equations. Musgrave et al. express the entrainment rate as a function of convection forced by surface cooling and evaporation, wind mixing, and shear instability at the base of the mixed layer.

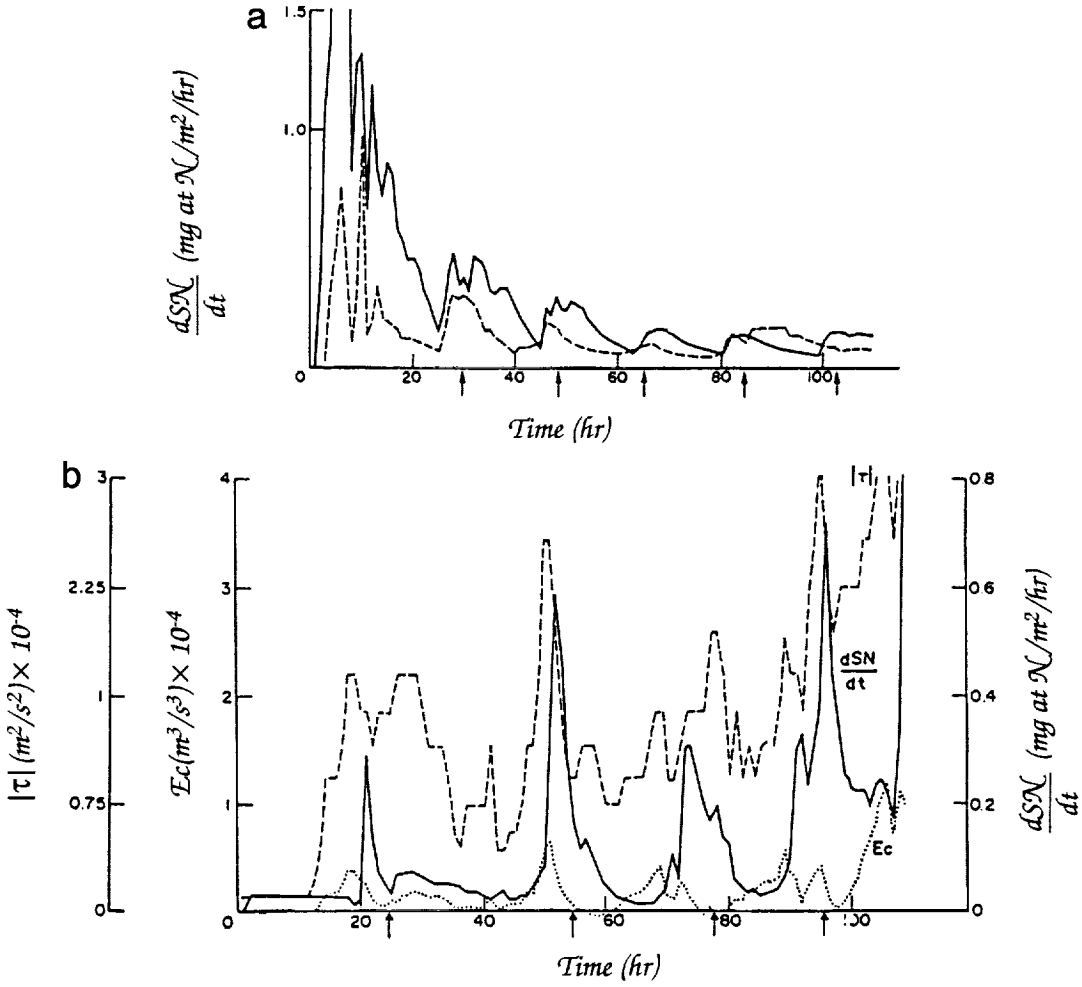

Figure 5. (a) Time variation of the nitrate flux (dSN/dt) into the mixed layer in response to constant wind stress. Solid line: wind stress = 4×10^{-4} m^2/s^2; dashed line: 2×10^{-4} m^2/s^2. (b) Time variation of nitrate flux (dSN/dt, solid) in the case of varying wind stress (|τ|, dashed). Ec (dotted) is the energy supplied to the sea surface by the wind stress (from Klein and Coste, 1984).

The model thus requires specified surface fluxes (wind stress, heat, fresh water) as well as boundary conditions at 300 m for temperature, salinity, diatomic oxygen, and velocity. Monthly averages were used for the surface fluxes other than wind stress. Wind stress is proportional to the square of the wind speed, so high winds, which are not properly represented by monthly averages, can contribute significantly to the surface momentum budget. To simulate the effect of periodic storms, Musgrave et al. superimposed a stochastic wind spectrum on the monthly averaged wind speeds.

Musgrave et al. reached the following conclusions:

- The resonant interaction between the wind stress and inertial currents noted by Klein and Coste (1984) was a crucial part of the model physics, implying that resolving the inertial period was important.
- Using the thermal cycle for calibration limited the vertical mixing coefficient to a fairly narrow range.
- The vertical mixing was still sensitive to the surface fluxes and the parameterization of the penetration of solar radiation. Therefore, the optical properties of sea water at a given location (which may change in time) must be known to determine the vertical mixing there.
- Reproduction of the seasonal oxygen signal required representation of storms using a stochastic wind field.

All of the models discussed above are one-dimensional and neglect lateral processes. Woods and Barkmann (1986) have pointed out that advection of water columns through regions of varying surface forcing may have a large impact on mixed-layer properties, and hence primary production. Recent measurements of a larger-than-expected pool of dissolved organic matter also suggest that lateral transport may be a critical link in basin-scale carbon and nutrient cycles.

A further example of the importance of spatial variations in determining the net export from the euphotic zone was given by Nelson et al. (1989). They showed that the shoaling of the main thermocline due to the frictional decay in a Gulf Stream warm core ring led to upwelling in the ring interior. The upwelling did not itself provide an input of nitrate to the euphotic zone; rather, the nitracline shoaled within the ring so that less energetic wind-mixing events were capable of breaking through the nitracline and entraining nutrient-rich water. Thus, lateral variations in the upwelling rate can "warp" the nutricline sufficiently that the nutrient supply is increased, even if the strength of vertical mixing does not change. Moreover, Nelson et al. found that the episodic injection of nitrate led to elevated levels of nitrate uptake by the phytoplankton, so that the ratio of new to regenerated production (the f ratio) was very high (about 0.6). The global significance of locally enhanced new production in mesoscale features is unknown.

Each of the models discussed above underscores the importance of nonlinear interactions between physical and biological processes, even with the simple proxies for the biological system used to date. As yet we do not know how important it is to reproduce these inter-

actions if we are to model, for example, basin-scale patterns of new production and their evolution in time. Parameterization in terms of bulk or mean values may be difficult, if not impossible. Progress is likely to come from detailed observational and numerical studies on small scales, which will develop the understanding of the fundamental mechanisms that is the first step in the development of appropriate parameterizations.

Three-Dimensional Models

Wroblewski et al. (1988) took the next step from one-dimensional toward three-dimensional simulations by considering an $n \times 1$-D model, consisting of multiple applications of a one-dimensional mixed-layer model at each point of a $1° \times 1°$ grid. Using this model, they were able to reveal some of the space and time scales of the spring bloom in the North Atlantic. To include the effect of lateral advection and mixing, however, a three-dimensional circulation model is required.

The first attempts at including a biological model in an oceanic general circulation model have recently begun (Sarmiento et al., 1989; Bacastow and Maier-Reimer, 1990). Sarmiento and co-workers set out to model the seasonal progression of the spring bloom in the North Atlantic. The circulation model is the $2° \times 2°$ "robust diagnostic" primitive equation model of Sarmiento and Bryan (1982), with increased vertical resolution in the upper ocean. Interior and surface values of temperature and salinity are restored to observed climatological values using a Newtonian damping term.

Embedded within the circulation model is a food web model of upper ocean ecology (Fasham et al., 1990). The food web model follows flows of nitrogen between various pools: phytoplankton, zooplankton, bacteria, nitrate, ammonium, DON, and detritus. Each of these pools is advected and diffused, in addition to the biologically mediated transfers from one pool to another. The ecological model requires estimates of a large number of coefficients that express the efficiency with which organic matter is transferred within trophic levels, the photosynthetic response to light, the relative preference for nitrate or ammonium as a substrate, the fraction of production that enters the DON pool, etc. The parameter values have been selected by calibrating a one-dimensional version of the food web model to a time series of observations at Bermuda.

The time step in the model is limited by the need to resolve the sinking of detritus from the euphotic zone. As a result it is not possible to integrate the model long enough for the deep ocean to reach equilibrium. Currently the model is integrated for three years in each experiment.

The food web model will ultimately include carbon as well as nitrogen, and additional pools such as different size classes of plankton. A model of particle cycling in the water column and a sediment-diagenesis model of $CaCO_3$ dissolution and organic carbon oxidation will be incorporated.

Several important lessons have already been learned from the preliminary experiments. First, lateral transport has a major impact on the results, supporting the need for full three-dimensional models. Furthermore, the greatest discrepancies between the model results and the observations are due to the deficiencies of the *physical* model. In particular, the mixed-layer depths are unrealistic in some areas, which has a large impact on the biology, and the equatorial upwelling is poorly reproduced, perhaps due to errors in the wind data. Second, a major constraint is the lack of observations: The only time series measurements of the sizes of the various pools in the food web are from a single site. It is not clear that the parameter values that give the best fit to observations at Bermuda can apply to different oceanic regimes. At the large scale, satellite observations of ocean color provide time series observations to which the model can be compared. However, it is not obvious which model quantity is most appropriate to compare to the satellite measurements. Third, there is some indication that even the present ecosystem model, which is fairly complex, is too simplified to capture the essential dynamics. In particular, additional compartments, including different plankton size classes and detritivores, may be necessary.

Bacastow and Maier-Reimer (1990) have taken a somewhat different approach. The model equations are a filtered version of the full primitive equations, which is appropriate for long period integrations. Using a one-month time step, Bacastow and Maier-Reimer can integrate the model for 5000 years in prognostic mode (i.e., there is no restoring to data to accelerate convergence as in the model of Sarmiento et al.). The biology component of the model is much simpler than that of Sarmiento et al. Rather than model the marine food web explicitly, Bacastow and Maier-Reimer specify the new production as a function of the nutrient concentration in the mixed layer using Michaelis-Menten kinetics. Particles leaving the mixed layer are regenerated in the same grid box. The carbon model is run with a seasonal time step.

Bacastow and Maier-Reimer used their model to explore the differences between the model carbon cycle with and without biota. The patterns of sources and sinks of atmospheric CO_2 were similar in the two cases, but the magnitudes were changed. In particular, with no biota the difference between DIC concentrations in surface water and deep water was 25% of the surface to deep water contrast

in the model with biology. In the case with no biota, the difference is solely due to the solubility pump. With biology, the carbonate and soft-tissue pumps act to increase the downward flux of carbon. When the circulation is decreased in strength, all three carbon pumps increase in efficiency, decreasing surface water carbon and hence atmospheric pCO_2.

Exchange with the Continental Margins

The relative productivity of the coastal ocean vs. the open ocean is the most dramatic feature of satellite maps of ocean color (e.g., Esaias et al., 1986). Upwelling along eastern boundaries and mixing due to energetic eddies near western boundaries provide a source of nutrients supporting the high levels of productivity observed. Higher productivity and a shallower water column near continental boundaries imply a higher probability that organic matter sinking out of the euphotic zone will be buried on the sea floor rather than remineralized within the water column. Several investigators (e.g., Walsh et al., 1981) have therefore concluded that burial of organic matter formed on the continental shelves provides a major oceanic sink of carbon. Rowe et al. (1986), on the other hand, showed that if pelagic microbial consumption and the lag in coupling between seasonal production and consumption were taken into account, then no net export of organic matter from the shelf occurred in the northwest Atlantic. Emerson (1985) has also argued that rates of organic matter degradation are too rapid for significant burial on the continental slope to occur. However, the net flux between the continental margins and the open ocean largely remains an open question. The fluxes are difficult to measure directly, due to the nonlinear interaction of transport and biological processes and the potential importance of rare, but extreme, events such as hurricanes or storm-induced turbidity currents.

If exchange between the coastal ocean and the deep ocean plays a significant role in biogeochemical cycles, how can these processes be included in models? Interdisciplinary modeling of coastal systems has received more attention than that of the open ocean (see the recent review by Wroblewski and Hoffman, 1989). These models have tended to focus on the local effects of a particular physical phenomenon. By limiting the spatial and temporal extent of the models, it is possible to resolve very small scales and to explicitly calculate the effect of nonlinear physical-biological interactions.

As was the case for the mixed-layer models, it is difficult to see how to scale up the detailed coastal models to larger scales. One possibility may be to use the results of a high-resolution coastal margin model to derive flux boundary conditions for a larger scale model.

A second approach is to paramaterize the effect of continental boundaries in some way. The primary productivity maps of Berger et al. (1987), for example, provide some reassuring evidence that the main distinction between the continental margins and the open ocean can be represented in a simple manner. Berger et al. constructed their map by assuming that primary production was a function of only three variables: phosphate concentration at 100 m, latitude, and distance from land. The resulting map looks very similar to a map based on direct productivity observations (Figure 6).

Particle Cycling in the Water Column

Relatively little work has been done on explicitly modeling the dynamics of particulate organic matter as it sinks through the water column. More commonly, the rate of decomposition is expressed as an empirical relation derived from sediment trap results. These rules generally express the decrease in organic carbon flux as an exponential or power law function of depth (e.g., Suess, 1980; Berger et al., 1987; Martin et al., 1987). However, the depth exponent varies over a wide range in different formulations. Bishop (1989) has suggested that the large spread may be due to differences in zooplankton feeding in different environments.

As mentioned in the first section, calcium carbonate dissolves at a greater depth than that at which organic matter decomposes. As a result, changes in the species of the organisms contributing the bulk of the particle flux out of the euphotic zone can affect the vertical distribution of carbon in the ocean. In models it is frequently assumed that all calcium carbonate dissolution occurs on the sea floor, but the extent to which dissolution may occur in the water column is unknown.

Models of particle cycling have also been constructed based on thorium isotope distributions. Thorium is very effectively scavenged by particles, and the disequilibrium between ^{234}Th and its parent ^{238}U gives a measure of the particle flux (e.g., Coale and Bruland, 1985). The isotope-based particle models have not yet been coupled to carbon cycle models.

Benthic Processes

A small fraction (1–2%) of the export production escapes being regenerated in the water column and reaches the sea floor. Most of this organic matter is oxidized at the surface of the sediments, providing an energy source for benthic organisms, as well as a source of dissolved carbon and a sink for oxygen. Berger et al. (1989) estimate that about 30% of the increase in apparent oxygen utilization

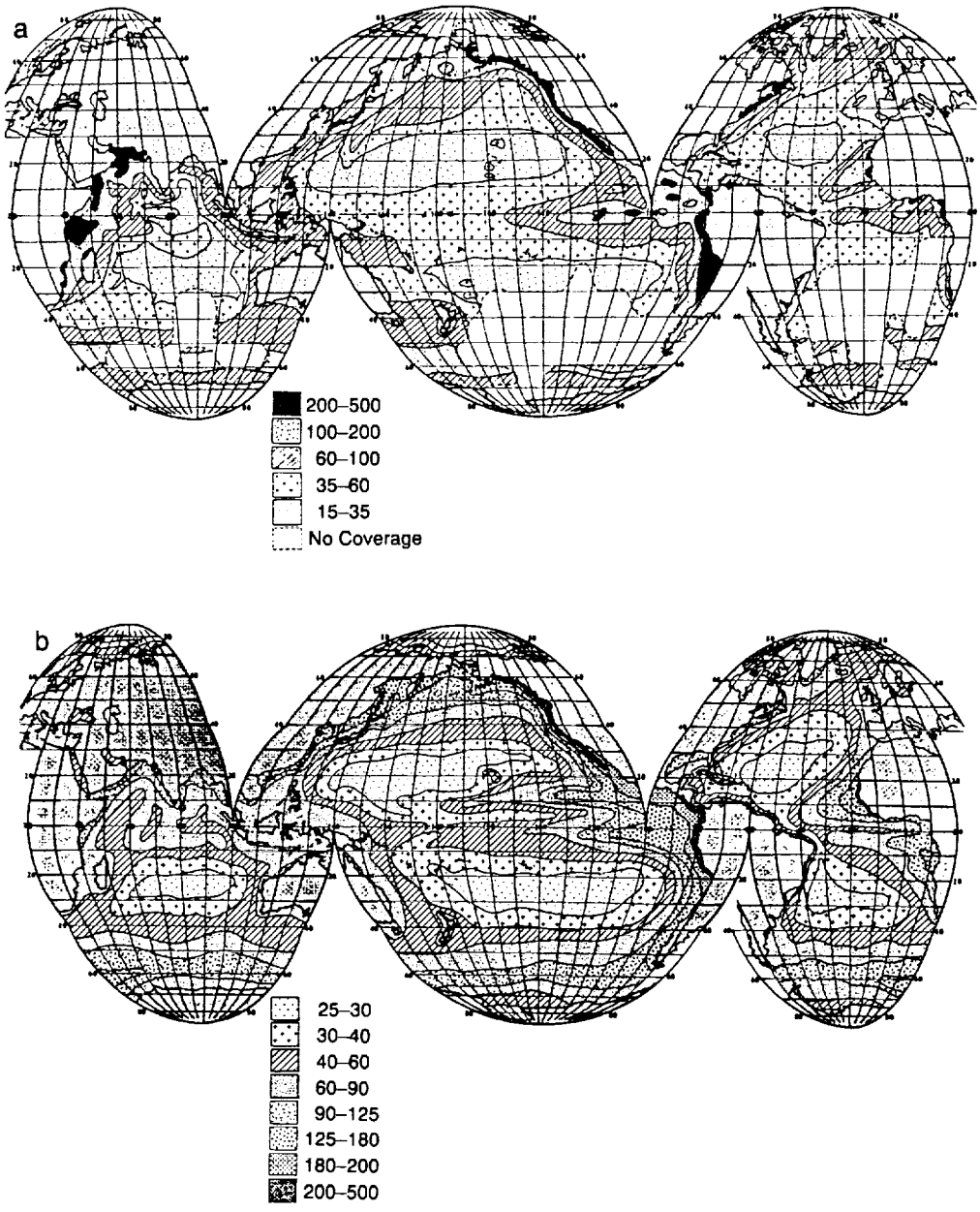

Figure 6. Annual primary production (PP) of the world's ocean, in g C/m^2/yr: (a) based on integrated productivity measurements compiled from the literature and (b) modeled using phosphate distributions, latitude, and distance from shore (adapted from Berger, 1989).

(AOU) with depth is the result of bottom respiration. The dynamics of the bottom boundary layer control the flux of regenerated carbon and nutrients from the sea floor back into the interior. Thus far this aspect of biogeochemical cycling in the ocean has received little attention in models.

Recommendations for Improved Coupled Physical-Biogeochemical Models

The models discussed above have displayed a wide range of complexity and scale, from the two-box model in which the physics and the biology are each parameterized by a single term, to detailed mixed-layer models in which the trajectories of individual phytoplankton are resolved. The main difficulty in designing coupled physical-biogeochemical models that can be used to predict the system response to changing external forcing is determining the right compromises to make: We need a model that reproduces the essential interactions, and yet is simple enough to be feasible with finite computational resources. By "feasible" in this case I mean cheap enough to run that a variety of experiments and sensitivity tests can be performed.

The first problem we face is identifying these "essential interactions." The mixed-layer models have demonstrated the sensitivity of new production to physical-biological interactions occurring on small space and time scales (e.g., resonant interactions between variable winds and inertial currents, or adaptation of photosynthetic efficiency to variable light levels). These models suggest that the essential nature of the processes depends on the nonlinear interactions between physical and biological fields varying in space and time. On the other hand, simple empirical relations seem to capture the net effect of these small-scale effects with some success. The maps of Berger et al. (1987), for example, suggest that there is a simpler underlying structure to the coupled system we are trying to model.

Clearly, empirical relations are not enough if we are to construct a predictive model that can describe how the system changes in response to changing forcing. The trick to finding parameterizations that reflect the essence of the active mechanisms is to understand the system well enough to say which pieces are important and which are not. At present we can do this for few, if any, of the processes involved in oceanic biogeochemical cycles.

It is unusual for a modeler to step back from a calculation and ask: How much can I simplify my model and still reproduce the essential results? Such an exercise, however, could be a fruitful way to derive appropriate parameterizations. At present we too fre-

quently choose a particular simplification because it is "sensible" and feasible, rather than by demonstrating that the parameterization retains the important features of the complex system.

The terrestrial ecosystem models discussed by Running in this volume provide an example of the type of "devolutionary" model development I have in mind. The natural tendency in making models is to gradually increase their complexity in an effort to make the simulation more closely resemble the observations. In the terrestrial context, this tendency led to ecosystem models based on individual trees, whose physiology was modeled explicitly. As interest shifted to regional scales, it became apparent that this level of detail was unnecessary. In particular, Running has found that climate, leaf area index, and soil water capacity are sufficient to define the regional ecosystem. For the evergreen forests he considered, the time steps could be increased from one hour to one day for hydrologic processes, and to one year for carbon and nutrient cycling. In this case, the simplifications introduced could be justified by comparing the results to those of the more detailed model. Such a comparison, for example, showed that if the time step for hydrologic processes was increased beyond one day, the simulation was no longer adequate.

A similar exercise is necessary in the ocean if we are to have confidence in the results of coupled physical-biogeochemical models, which will of necessity be highly parameterized. A major stumbling block has been the lack of observations. The nonlinear nature of the interactions causes difficulties for the observationalist as well as the modeler; physical and biogeochemical variables are rarely measured at the same time and place, with the necessary resolution and duration. Focused mesoscale studies involving close collaboration between observers and modelers, physicists and biologists, in a variety of regions are needed to develop high-resolution models for the individual regions. These detailed models can then be used to calibrate the simpler models appropriate for coupling to global ocean and atmosphere models.

The lack of observations also causes problems for the modeler, who needs data to calibrate the model parameters and to validate the model. In this regard it is important that the model produce as output an analog of something that is measurable. Satellite observations of ocean color, for example, provide a global, synoptic data set of some quantity related to primary productivity, but this is related to typical model output such as net export production in a complicated and unknown way.

Given the variety of evidence, from both models and observational studies, of the importance of episodic events in the biogeochemical

system, more work is required on including a stochastic element in our models.

We need a different sort of physical model as well. Of primary importance is a more realistic treatment of the upper ocean. While an accurate prediction of the properties of the mixed layer is of obvious importance to the biology, it is also a necessity for improved modeling of the ventilation processes responsible for the physically mediated transport of carbon into the ocean interior. A better representation of the upper ocean is also necessary to allow direct coupling of atmospheric and oceanic GCMs without the introduction of ad hoc "flux corrections" (see Rintoul, this volume).

At the moment, ocean models used for climate studies lie at one of two extremes: simple box models, in which the dynamics are reduced to a small number of exchange coefficients; and GCMs, which are computationally intensive but still do not resolve the mixed layer very well. There is a need for a model of intermediate complexity, particularly for consideration of climate change on decadal time scales. Such a model should include a well-resolved mixed layer and thermocline, with coarser resolution in the deep sea. In addition, the mixing parameterization used should more accurately reflect the nature of the physical processes responsible for mixing in the ocean (e.g., internal mixing along isopycnals, vertical mixing dependent on vertical shear or stability). This type of model would more accurately represent ocean ventilation processes than present GCMs. It would also be more appropriate for coupling to biological models.

Ideally, we would like a model that is consistent with everything we know from past observations and physical reasoning, and that can be integrated forward in time to predict how things change. Thus, we would like a model that is capable of assimilating a wide variety of data: satellite measurements of ocean color, sea surface temperature and sea surface height, observations of f-ratio or community structure, an estimate of the meridional heat flux, a float trajectory or current meter measurement, etc. We would also like the model to determine the things we know least well from information on the things we do know well. For example, one might use interior observations of temperature and salinity to constrain estimates of the heat and fresh water flux at the sea surface (e.g., see Tziperman, this volume). Much progress is currently being made in the field of data assimilation or optimal estimation in meteorology and oceanography. These methods are in a sense a marriage of the prognostic and diagnostic methods, and may hold promise for the biogeochemical problem as well, although there is a long way to go in the development of such models.

Acknowledgments

I would like to thank the organizers of the Global Change Institute for a stimulating and enjoyable conference. Part of this paper was prepared while I was a visiting scientist in the Atmospheric and Oceanic Sciences Program at Princeton University. I thank the AOS program for its hospitality and, in particular, J. Sarmiento, R. Toggweiler, and K. Bryan for many interesting discussions during my stay.

References

Bacastow, R., and E. Maier-Reimer. 1990. Ocean-circulation model of the carbon cycle. *Climate Dynamics 4*, 95–126.

Berger, W.H. 1989. Global maps of ocean productivity. In *Productivity of the Ocean: Present and Past* (W.H. Berger, V.S. Smetacek, and G. Wefer, eds.), Dahlem Conference, John Wiley and Sons, Chichester, England, 429–456.

Berger, W.H., V.S. Smetacek, and G. Wefer. 1989. Ocean productivity and paleoproductivity—an overview. In *Productivity of the Ocean: Present and Past* (W.H. Berger, V.S. Smetacek, and G. Wefer, eds.), Dahlem Conference, John Wiley and Sons, Chichester, England, 1–34.

Berger, W.H., K. Fisher, C. Laai, and G. Wu. 1987. Ocean productivity and organic carbon flux. Part I. Overview and maps of primary productivity and export production. SIO Reference 87–30, University of California, San Diego.

Bishop, J.K.B. 1989. Regional extremes in particulate matter composition and flux: Effects on the chemistry of the ocean interior. In *Productivity of the Ocean: Present and Past* (W.H. Berger, V.S. Smetacek, and G. Wefer, eds.), Dahlem Conference, John Wiley and Sons, Chichester, England, 117–138.

Bolin, B., A. Björkstrom, and B. Moore. 1989. Uptake by the Atlantic Ocean of excess atmospheric carbon dioxide and radiocarbon. In *Understanding Climate Change* (A. Berger, R.E. Dickinson, and J.W. Kidson, eds.), Geophysical Monograph 52, American Geophysical Union, Washington, D.C., 57–78.

Boyle, E.A. 1988. The role of vertical chemical fractionation in controlling late quaternary atmospheric carbon dioxide. *Journal of Geophysical Research 93*, 15701–15714.

Brewer, P.G. 1986. What controls the variability of carbon dioxide in the surface ocean? A plea for complete information. In *Dynamic Processes in the Chemistry of the Upper Ocean* (J.D. Burton, P.G. Brewer, and R. Chesselet, eds.), Plenum Press, New York, 215–231.

Broecker, W.S. 1982. Ocean chemistry during glacial time. *Geochimica et Cosmochimica Acta 46*, 1689–1705.

Broecker, W.S., and T.-H. Peng. 1982. *Tracers in the Sea.* Eldigio Press, Lamont-Doherty Geophysical Observatory, Palisades, New York, 690 pp.

Broecker, W.S., and T.-H. Peng. 1986. Global carbon cycle, 1985: Glacial to interglacial changes in the operation of the carbon cycle. *Radiocarbon 28,* 309–327.

Broecker, W.S., and T. Takahashi. 1984. Is there a tie between atmospheric CO_2 content and ocean circulation? In *Climate Processes and Climate Sensitivity* (J.E. Hansen and T. Takahashi, eds.), Geophysical Monograph 29, American Geophysical Union, Washington, D.C., 314–326.

Bryan, F. 1987. Parameter sensitivity of primitive equation ocean circulation models. *Journal of Physical Oceanography 17,* 970–985.

Bryan, K. 1979. Models of the world ocean. *Dynamics of the Atmosphere and Oceans 3,* 327–338.

Coale, K.H., and K.W. Bruland. 1985. Th-234/U-238 disequilibria within the California Coastal Current. *Limnology and Oceanography 30(1),* 22–33.

Codispoti, L.A., G.E. Friederick, R.L. Iverson, and D.W. Hood. 1982. Temporal changes in the inorganic carbon system of the southeastern Bering Sea during spring 1980. *Nature 296,* 242–244.

Craig, H. 1957. The natural distribution of radiocarbon and the exchange time of carbon dioxide between atmosphere and sea. *Tellus 9,* 1–17.

Dymond, J., and M. Lyle. 1985. Flux comparisons between sediments and sediment traps in the eastern tropical Pacific: Implications for atmospheric CO_2 variations during the Pleistocene. *Limnology and Oceanography 30,* 699–712.

Emerson, S. 1985. Organic carbon preservation in marine sediments. In *Carbon Dioxide and the Carbon Cycle: Natural Variations Archean to Present* (E.T. Sundquist and W.S. Broecker, eds.), Geophysical Monograph 32, American Geophysical Union, Washington, D.C., 78–88.

Esaias, W.E., G.C. Feldman, C.R. McClain, and J.A. Elrod. 1986. Monthly satellite-derived phytoplankton pigment distribution for the North Atlantic Ocean basin. *Eos 67,* 835–837.

Fasham, M.J.R. 1985. Flow analysis of materials in the marine euphotic zone. *Canadian Bulletin of Fisheries and Aquatic Science 213,* 139–162.

Fasham, M.J.R., H.W. Ducklow, and S.M. McKelvie. 1990. A nitrogen-based model of plankton dynamics in the oceanic mixed layer. *Journal of Marine Research 48(3),* 591–639.

Garcon, V., and J.F. Minster. 1988. Heat, carbon and water fluxes in a 12-box model of the world ocean. *Tellus 40B*, 161–177.

Houghton, J.T., G.J. Jenkins, and J.J. Ephraums (eds.). 1990. *Climate Change: The IPCC Scientific Assessment*, Intergovernmental Panel on Climate Change and Cambridge University Press, Cambridge, 365 pp.

Jenkins, W.J., and J.C. Goldman. 1985. Seasonal oxygen cycling and primary production in the Sargasso Sea. *Journal of Marine Research 43*, 465–491.

Keeling, C.D. 1968. Carbon dioxide in surface ocean waters, 4: Global distribution. *Journal of Geophysical Research 73*, 4,543–4,553.

Keir, R. 1988. On the late Pleistocene ocean geochemistry and circulation. *Paleoceanography 3*, 443–445.

Kiefer, D.A., and J.N. Kremer. 1981. Origins of vertical patterns of phytoplankton and nutrients in the temperate, open ocean: A stratigraphic hypothesis. *Deep Sea Research 28*, 1087–1105.

Klein, P., and B. Coste. 1984. Effects of wind-stress variability on nutrient transport into the mixed layer. *Deep Sea Research 31*, 21–37.

Knox, F., and M. McElroy. 1984. Changes in atmospheric CO_2: Influence of biota at high latitudes. *Journal of Geophysical Research 89*, 4629–4637.

Lin, C.A. 1988. A mechanistic model of isopycnal diffusion in the ocean. *Climate Dynamics 2*, 165–172.

Liss, P.S., and L. Merlivat. 1986. Air-sea gas exchange rates: Introduction and synthesis. In *The Role of Air-Sea Exchange in Geochemical Cycling* (P. Buat-Menard, ed.), D. Reidel, Hingham, Massachusetts, 113–127.

Martin, J.H., G.A. Knauer, D.M. Karl, and W.H. Broenkow. 1987. VERTEX: Carbon cycling in the northeast Pacific. *Deep Sea Research 34*, 267–285.

Martin, J.H., and S.E. Fitzwater. 1988. Iron deficiency limits phytoplankton growth in the north-east Pacific subarctic. *Nature 331*, 341–343.

Martin, J.H., and R.M. Gordon. 1988. Northeast Pacific iron distribution in relation to phytoplankton productivity. *Deep Sea Research 34*, 267–285.

Martin, J.H., R.M. Gordon, and S.E. Fitzwater. 1990. Iron in Antarctic waters. *Nature 345*, 156–158.

Metzl, N., B. Moore, and A. Poisson. 1990. Resolving the intermediate and deep advective flows in the Indian Ocean by using temperature, salinity, oxygen and phosphate data: The interplay of biogeochemical and geophysical tracers. *Palaeogeography, Palaeoclimatology, Palaeoecology (Global and Planetary Change Section) 89*, 81–111.

Michaels, A.F., and M.W. Silver. 1988. Primary production, sinking fluxes and the microbial foodweb. *Deep Sea Research 35*, 473–490.

Musgrave, D.L., J. Chou, and W.J. Jenkins. 1988. Application of a model of upper-ocean physics for studying seasonal cycles of oxygen. *Journal of Geophysical Research 93*, 15679–15700.

Neftel, A, H. Oeschger, J. Schwander, B. Stauffer, and R. Zumbrum. 1982. Ice core measurements give atmospheric CO_2 content during the past 40,000 years. *Nature 295*, 222–223.

Nelson, D.M., J.J. McCarthy, T.M. Joyce, and H.W. Ducklow. 1989. Enhanced near-surface nutrient availability and new production resulting from the frictional decay of a Gulf Stream warm-core ring. *Deep Sea Research 36*, 705–714.

Nydal, R. 1968. Further investigation on the transfer of radiocarbon in nature. *Journal of Geophysical Research 75*, 2271–2278.

Oeschger, H., U. Siegenthaler, U. Schotterer, and A. Gugelmann. 1975. A box diffusion model to study the carbon dioxide exchange in nature. *Tellus 27*, 168–192.

Price, J.R., R. A. Weller, and R. Pinkel. 1986. Diurnal cycling: Observations and models of the upper ocean response to diurnal heating, cooling, and wind mixing. *Journal of Geophysical Research 91*, 8411–8427.

Redfield, A.C., B.H. Ketchum, and F.A. Richards. 1963. The influence of organisms on the composition of sea-water. In *The Sea, Volume 2: The Composition of Sea Water: Comparative and Descriptive Oceanography* (M.N. Hill, ed.), Interscience Publishers, New York, 26–77.

Revelle, R., and H. E. Suess. 1957. Carbon dioxide exchange between atmosphere and ocean and the question of an increase of atmospheric CO_2 during the past decade. *Tellus 9*, 18–27.

Riley, G.A. 1951. Oxygen, phosphate and nitrate in the Atlantic Ocean. *Bulletin of the Bingham Oceanographic Collection 12(3)*, 169 pp.

Rintoul, S.R., and C. Wunsch. 1991. Mass, heat, oxygen, and nutrient fluxes and budgets in the North Atlantic Ocean. *Deep Sea Research 38(1A)*, S355–S377.

Rowe, G.T., S. Smith, P. Falkowski, T. Whitledge, R. Theroux, W. Phoel, and H. Ducklow. 1986. Do continental shelves export organic matter? *Nature 324*, 559–561.

Sarmiento, J.L., and K. Bryan. 1982. An ocean transport model for the North Atlantic. *Journal of Geophysical Research 87*, 394–408.

Sarmiento, J.L., and J.R. Toggweiler. 1984. A new model for the role of the oceans in determining atmospheric pCO_2. *Nature 308*, 621–624.

Sarmiento, J.L., J.R. Toggweiler, and R. Najjar. 1988. Ocean carbon cycle dynamics and atmospheric pCO_2. *Philosophical Transactions of the Royal Society of London A 325*, 3–21.

Sarmiento, J.L., M.J.R. Fasham, U. Siegenthaler, R. Najjar, and R. Toggweiler. 1989. *Models of Chemical Cycling in the Oceans: Progress Report II.* Ocean Tracers Laboratory Technical Report No. 6, Princeton University, Princeton, New Jersey.

Sarmiento, J.L., J.C. Orr, and U. Siegenthaler. 1990. A perturbation simulation of CO_2 uptake in an ocean general circulation model. *Journal of Geophysical Research.*

Schlitzer, R. 1988. Modeling the nutrient and carbon cycles of the North Atlantic. Part I: Circulation, mixing coefficients and heat fluxes. *Journal of Geophysical Research 93*, 699–723.

Shackleton, N.J., and N.G. Pisias. 1985. Atmospheric carbon dioxide, orbital forcing and climate. In *Carbon Dioxide and the Carbon Cycle, Archean to Present* (E.T. Sundquist and W.S. Broecker, eds.), American Geophysical Union, Washington, D.C., 313–318.

Shulenberger, E., and J.L. Reid. The Pacific shallow oxygen maximum, deep chlorophyl maximum and primary productivity, reconsidered. *Deep Sea Research 28*, 901–920.

Siegenthaler, U., and T. Wenk. 1984. Rapid atmospheric CO_2 variations and ocean circulation. *Nature 308*, 624–625.

Suess, E. 1980. Particulate organic carbon flux in the oceans—surface productivity and oxygen utilization. *Nature 288*, 260–263.

Sugimura, Y., and Y. Suzuki. 1988. A high-temperature catalytic oxidation method for the determination of non-volatile dissolved organic carbon in seawater by direct injection of liquid samples. *Marine Chemistry 24*, 105–131.

Sundquist, E.T. 1985. Geological perspectives on carbon dioxide and the carbon cycle. In *Productivity of the Ocean: Present and Past* (W.H. Berger, V.S. Smetacek, and G. Wefer, eds.), Dahlem Conference, John Wiley and Sons, Chichester, England, 99–110.

Tans, P.P., I.Y. Fung, and T. Takahashi. 1990. Observational constraints on the global atmospheric carbon budget. *Science 247*, 1431–1438.

Toggweiler, J.R. 1989. Is the downward dissolved organic matter (DOM) flux important in carbon transport? In *Productivity of the Ocean: Present and Past* (W.H. Berger, V.S. Smetacek, and G. Wefer, eds.), Dahlem Conference, John Wiley and Sons, Chichester, England, 65–85.

Vezina, A.F., and T. Platt. 1987. Small-scale variability of new production and particulate fluxes in the ocean. *Canadian Journal of Fisheries and Aquatic Science 44*, 198–205.

Volk, T. 1989. The changing patters of pCO_2 between ocean and atmosphere. *Global Biogeochemical Cycles 3*, 179–189.

Volk, T., and M.J. Hoffert. 1985. Ocean carbon pumps: Analysis of relative strengths and efficiencies in ocean-driven atmospheric CO_2 changes. In *Carbon Dioxide and the Carbon Cycle, Archean to Present* (E.T. Sundquist and W.S. Broecker, eds.), American Geophysical Union, Washington, D.C., 313–318.

Walsh, J.J., G.T. Rowe, R.L. Iverson, and C.P. McRoy. 1981. Biological export of shelf carbon is a sink of the global CO_2 cycle. *Nature 291*, 196–201.

Williams, P.J.leB., and B. von Bodungen. 1989. Export productivity from the photic zone. In *Productivity of the Ocean: Present and Past* (W.H. Berger, V.S. Smetacek, and G. Wefer, eds.), Dahlem Conference, John Wiley and Sons, Chichester, England, 99–115.

Woods, J.D., and W. Barkmann. 1986. A Lagrangian mixed layer model of Atlantic 18°C water formation. *Nature 391*, 574–576.

Woods, J.D., and R. Onken. 1982. Diurnal variation and primary production in the ocean—preliminary results of a Lagrangian ensemble model. *Journal of Plankton Research 4*, 735–756.

Wroblewski, J. S., and E.E. Hoffman. 1989. U.S. interdisciplinary modeling studies of coastal-offshore exchange processes: Past and future. *Progress in Oceanography 23*, 65–100.

Wroblewski, J.S., J.L. Sarmiento, and G.R. Flierl, 1988. An ocean basin scale model of plankton dynamics in the North Atlantic. 1. Solutions for the climatological oceanographic conditions in May. *Global Biogeochemical Cycles 2(3)*, 199–218.

Dynamic Constraints on CO_2 Uptake by an Iron-Fertilized Antarctic

Tsung-Hung Peng, W.S. Broecker, and H.G. Östlund[1]

Introduction

Because of the concern regarding the impacts of greenhouse warming caused by rising atmospheric CO_2 content, consideration is being given to the possibility that the power of the ocean's biological carbon pump could be artificially strengthened. The linkage between atmospheric CO_2 and marine biological activity is the gas exchange across the sea-air interface and photosynthesis in the photic zone of the surface waters. The organic material formed in surface water would take up about 130 carbon atoms per phosphorus atom. Thus the effect of biological activity is to reduce the total CO_2 (ΣCO_2) content in the surface water. The CO_2 partial pressure (pCO_2) in surface ocean water is influenced, in turn, by the extent to which photosynthesis reduces the ΣCO_2 content of the water. The magnitude of this reduction is controlled by the efficiency with which the limiting nutrients phosphorus tetroxide or phosphate (PO_4) and nitrogen trioxide or nitrate (NO_3) are utilized. In temperate and tropical oceans the utilization efficiency is high, and hence pCO_2 reduction is close to maximum. By contrast, in the polar oceans the utilization efficiency is low, leaving plenty of nutrients unused. Therefore, if a way can be found to increase the efficiency of

[1]This chapter has been authorized by a contractor of the U.S. government under contract DE-AC05-84OR21400. Accordingly, the U.S. government retains a nonexclusive, royalty-free license to publish or reproduce the published form of this contribution, or allow others to do so, for U.S. government purposes.

nutrient utilization in these waters, their pCO_2 and in turn that for the atmosphere could be reduced.

Recently (Martin, 1990; Martin et al., 1990b; Baum, 1990), iron fertilization in the Antarctic has been proposed as a potential means to enhance the biological carbon pump for drawing down pCO_2 in this region and hence to absorb more CO_2 from the atmosphere to reduce the rising atmospheric CO_2. Martin and his co-workers (Martin and Fitzwater, 1988; Martin and Gordon, 1988; Martin et al., 1989, 1990a, 1990b; Martin, 1990) have shown in incubation experiments that plant growth rates in waters from polar regions can be accelerated through the addition of trace amounts of dissolved iron. Iron is an essential micronutrient required for the metabolism of all forms of life. Its primary function is in cytochrome formation. Because iron is one of the most particle-reactive elements, its concentration in the sea is very low, with the lowest values occurring in regions like the Antarctic which are most remote from the continental sources.

Extensive discussion and consideration have been given to the biological aspects of Martin's iron fertilization hypothesis. However, very little attention has been directed to the potential dynamic constraints on CO_2 uptake resulting from the enhanced biological carbon pump in the Antarctic. Through discussion with J. Sarmiento, we became interested in studying the response of atmospheric CO_2 to a successful iron fertilization in the Antarctic. Our major concern is the limitation by ocean dynamics of the potential for CO_2 removal. We present here a tracer-calibrated advection-diffusion box model which incorporates the rate at which surface waters in the Antarctic Ocean are replaced by vertical mixing and advection. This replacement process governs the rate of CO_2 removal from the atmosphere.

In a hypothetical case where water circulation does not exist in the Antarctic ocean, only an amount of CO_2 equivalent to that removed as a result of the initial iron fertilization would be sequestered from the atmosphere. In such a situation the atmosphere and surface oceans of Antarctic and non-Antarctic regions would rapidly reach a new equilibrium, leaving the atmosphere with a CO_2 content only slightly lower than it had before iron fertilization was instituted. In order to achieve a significant reduction of the atmosphere's CO_2 content, the surface waters of the Antarctic must be replaced frequently from below. Thus, the critical issue is the rate of vertical mixing in the Antarctic ocean.

Tracer Distribution and Dynamics in the Antarctic Ocean

The distribution of anthropogenic tracers in the Antarctic provides important constraints regarding the surface water replacement

rate. Measurements made as part of the Geochemical Ocean Sections Survey (GEOSECS) program (see Figure 1 for station locations) provided the basic data. The first piece of information these results supply is geographic domain in which surface waters contain appreciable amounts of unused NO_3 and PO_4. As can be seen from the map in Figure 1, the ambient PO_4 level for Antarctic surface water (during the summer months) of 1.6 μmol drops off rapidly between 50°S and 40°S. We adopted 45°S to be the northern boundary of the region where iron fertilization has potential. Table 1 shows the area of the ocean in 5° latitude belts south of this boundary. The total represents 16.8% of the global ocean.

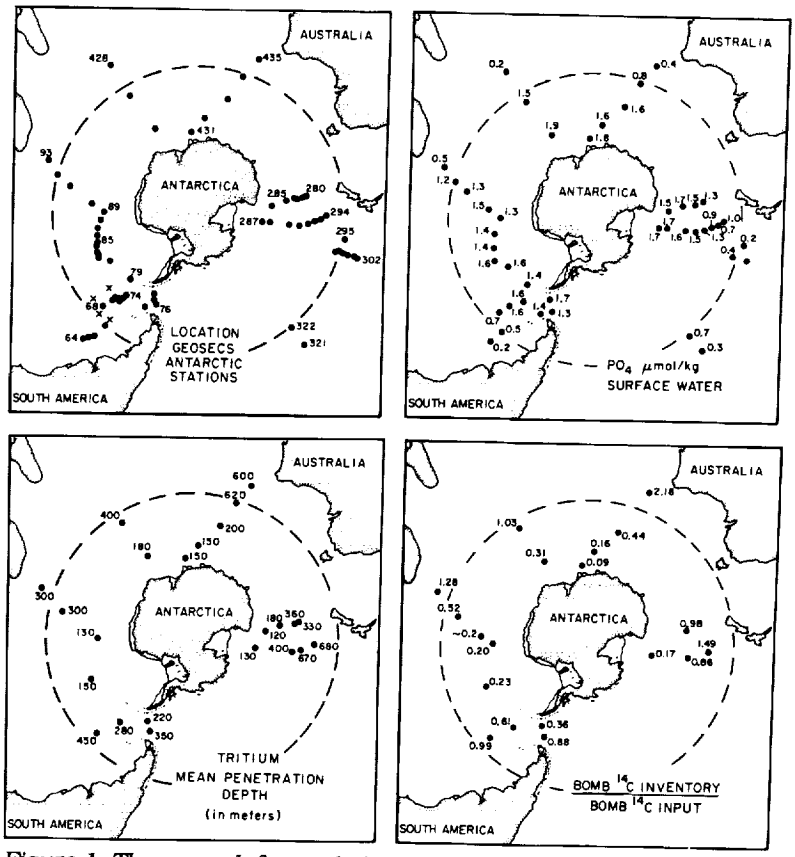

Figure 1. The upper left panel shows the location of the GEOSECS Antarctic stations (black dots) and of four SAVE stations (crosses). The other three maps show the surface water PO_4 concentrations at these stations, the mean penetration depth of tritium at the time of the GEOSECS surveys (see Broecker et al., 1986), and the ratio of the water column inventory of nuclear testing radiocarbon to the input of nuclear testing radiocarbon (see Broecker et al., 1985). The dashed circle at 45°S marks the latitude where, on the average, surface PO_4 reaches one-half its ambient Antarctic concentration.

Table 1: Ocean areas in 5° latitude belts for the Antarctic region

Latitude Range	Area (10^6 km^2)	% of Global Ocean Area
80°S–75°S	0.52	0.1
75°S–70°S	2.60	0.7
70°S–65°S	6.82	1.9
65°S–60°S	10.30	2.9
60°S–55°S	12.01	3.3
55°S–50°S	13.89	3.8
50°S–45°S	14.69	4.1
Total	60.83	16.8

From Sverdrup et al., 1942.

The results of the tritium (^{3}H), carbon-14 (^{14}C), and silica (SiO_2) measurements for Southern Ocean stations are summarized in Figure 2. Two aspects are important. First, the tritium results allow an estimate to be made of the extent of downward mixing into the thermocline on the time scale of one decade (i.e., the time between the tritium delivery and the GEOSECS surveys). As can be seen from the summary in Figure 1, this depth ranges from as little as 150 m in the deep Antarctic to as much as 600 m at 45°S. Second, as the tritium profile at any given station is the mirror image of the dissolved silica profile, the far more complete silica data set can be used to portray the upper ocean volume available for the uptake of

(text continues on p. 84)

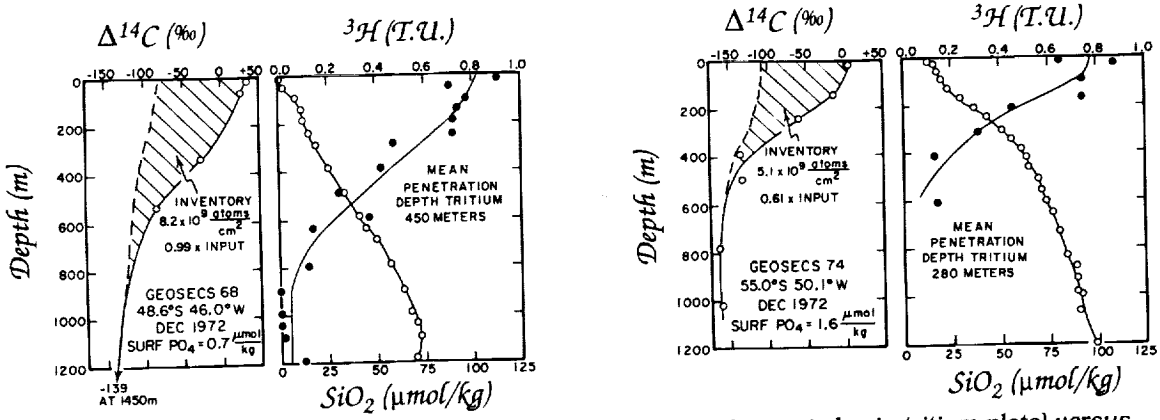

Figure 2. Plots of radiocarbon, tritium (solid circles), and silica (open circles in tritium plots) versus depth for 24 stations occupied during the GEOSECS program. Following Broecker et al. (1985), an estimate of the prenuclear radiocarbon profile is reconstructed, allowing the inventory of bomb ^{14}C (cross-hatched sections) to be calculated. The error of individual tritium measurements ranges from 0.5 T.U. for the Indian Ocean stations to 0.9 T.U. for the Atlantic and Pacific stations. The data are from Östlund and Stuiver, 1980; Stuiver and Östlund, 1980; Stuiver and Östlund, 1983; and the GEOSECS atlas series.

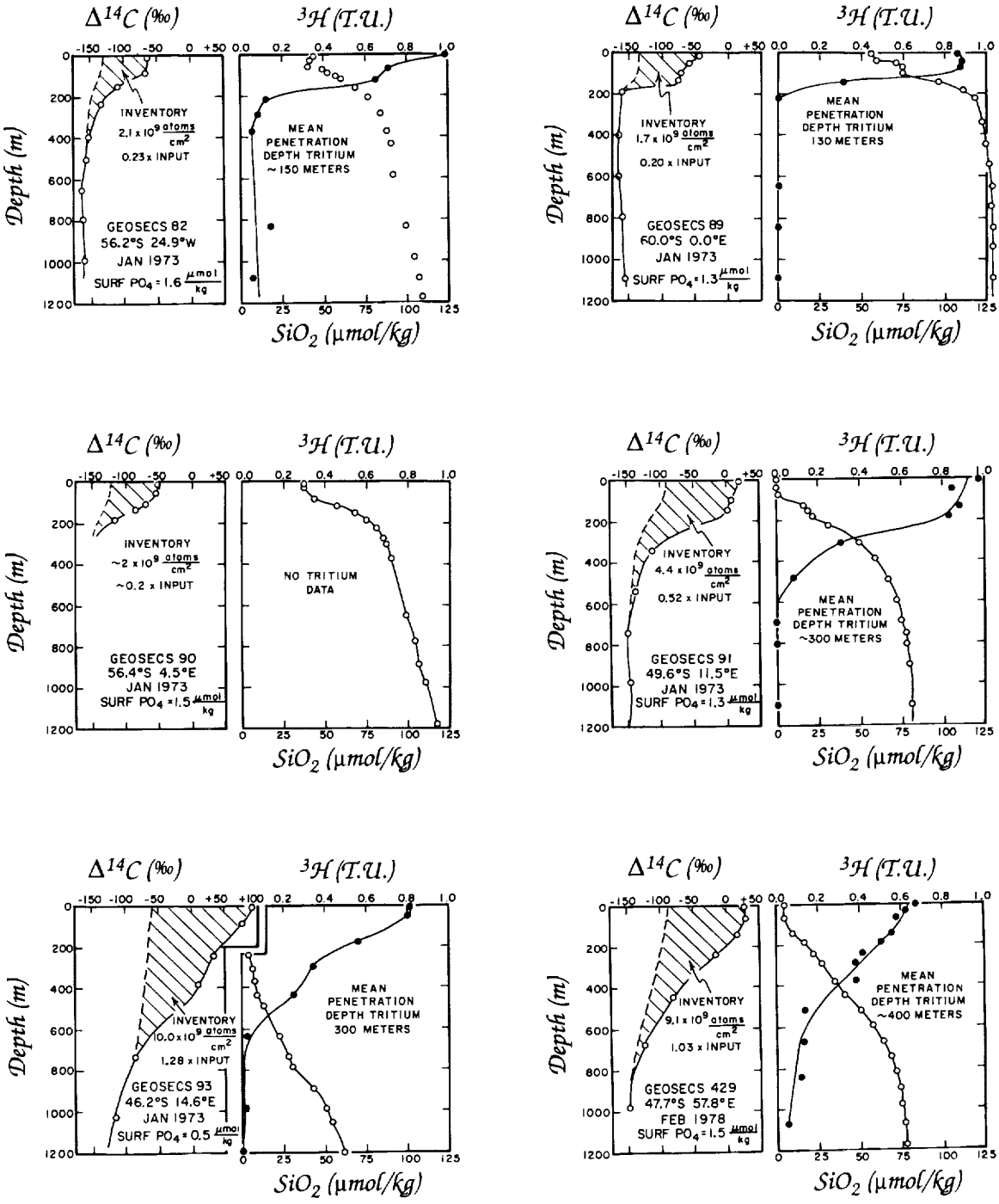

Figure 2, continued.

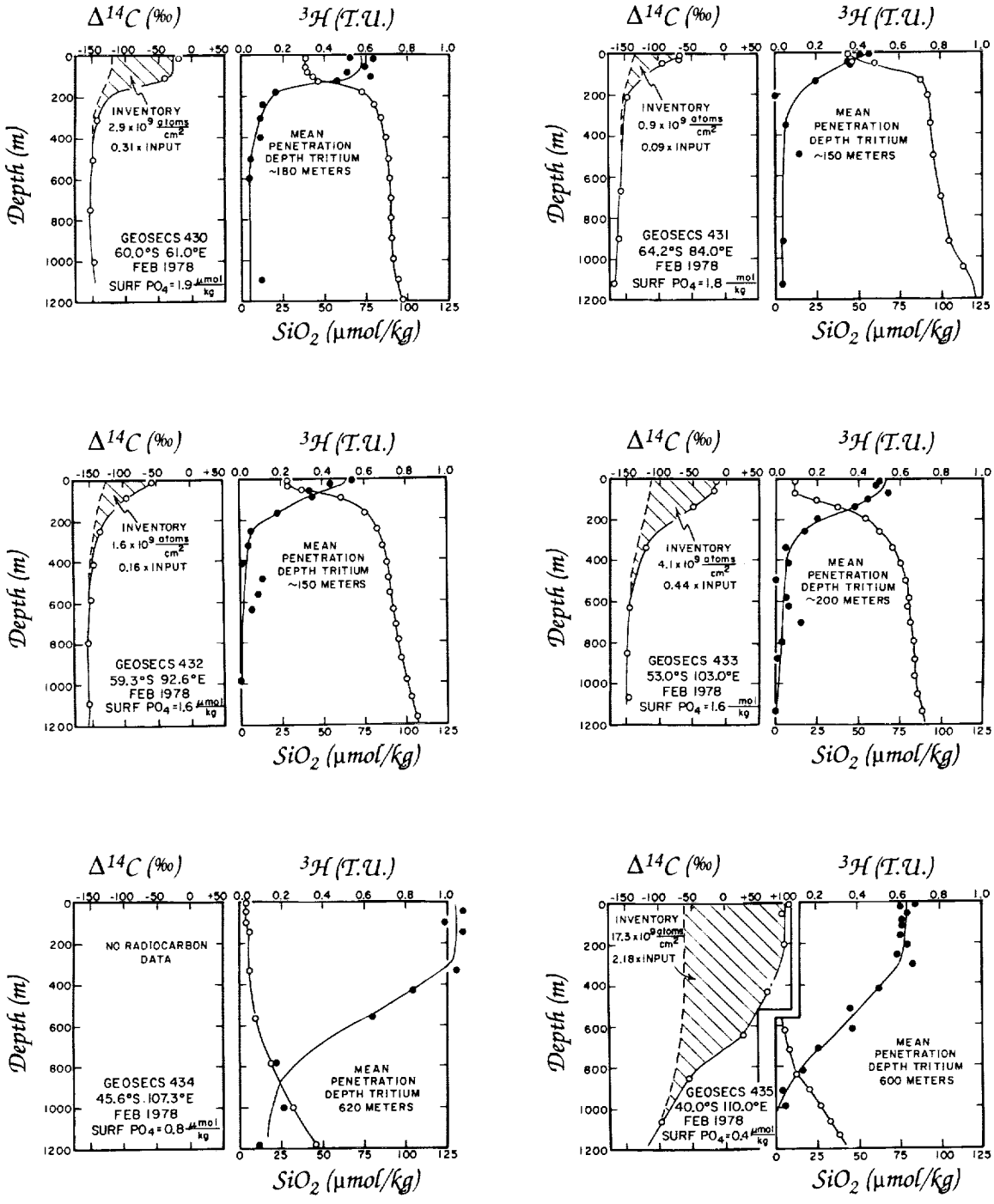

Figure 2, continued.

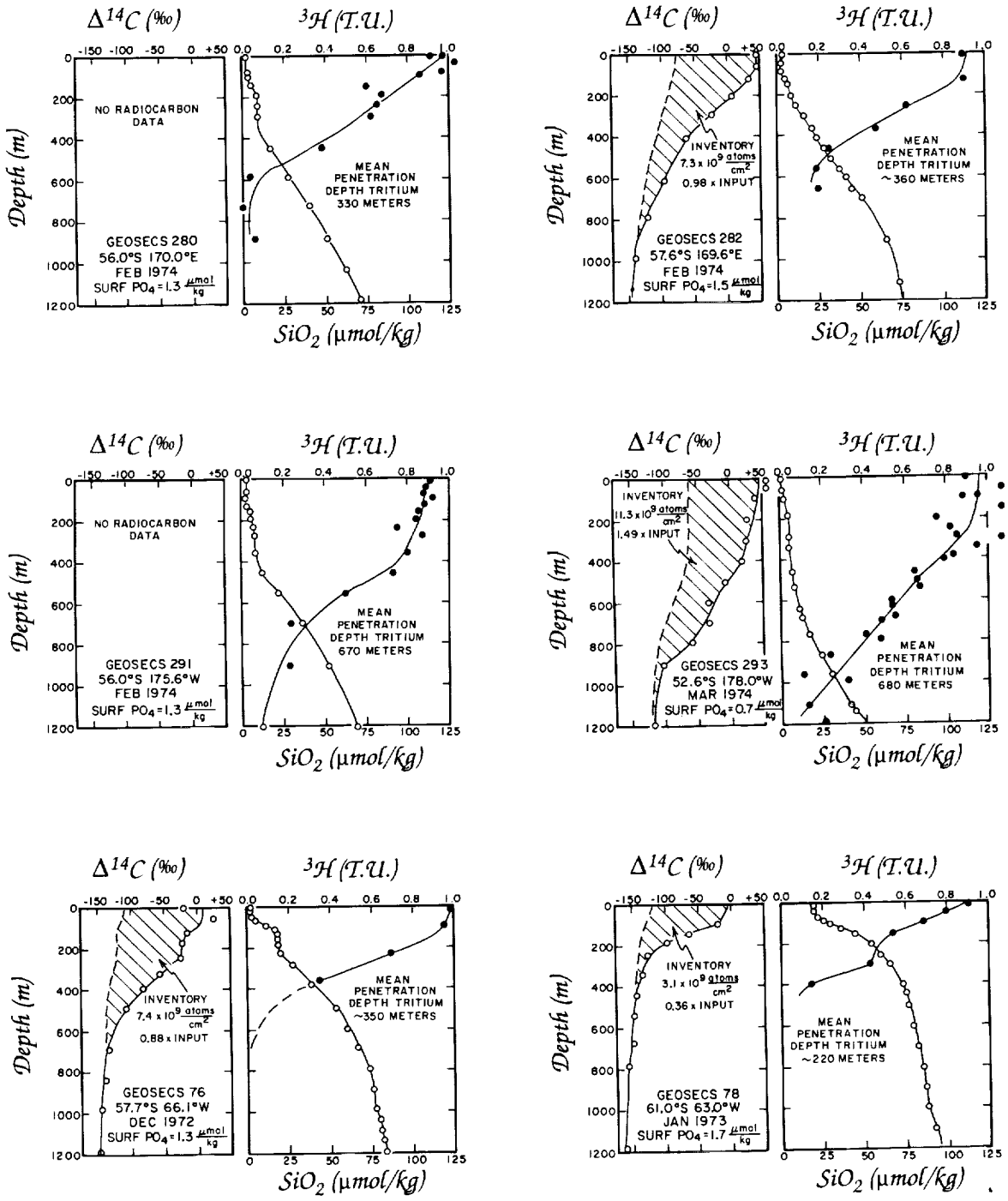

Figure 2, continued.

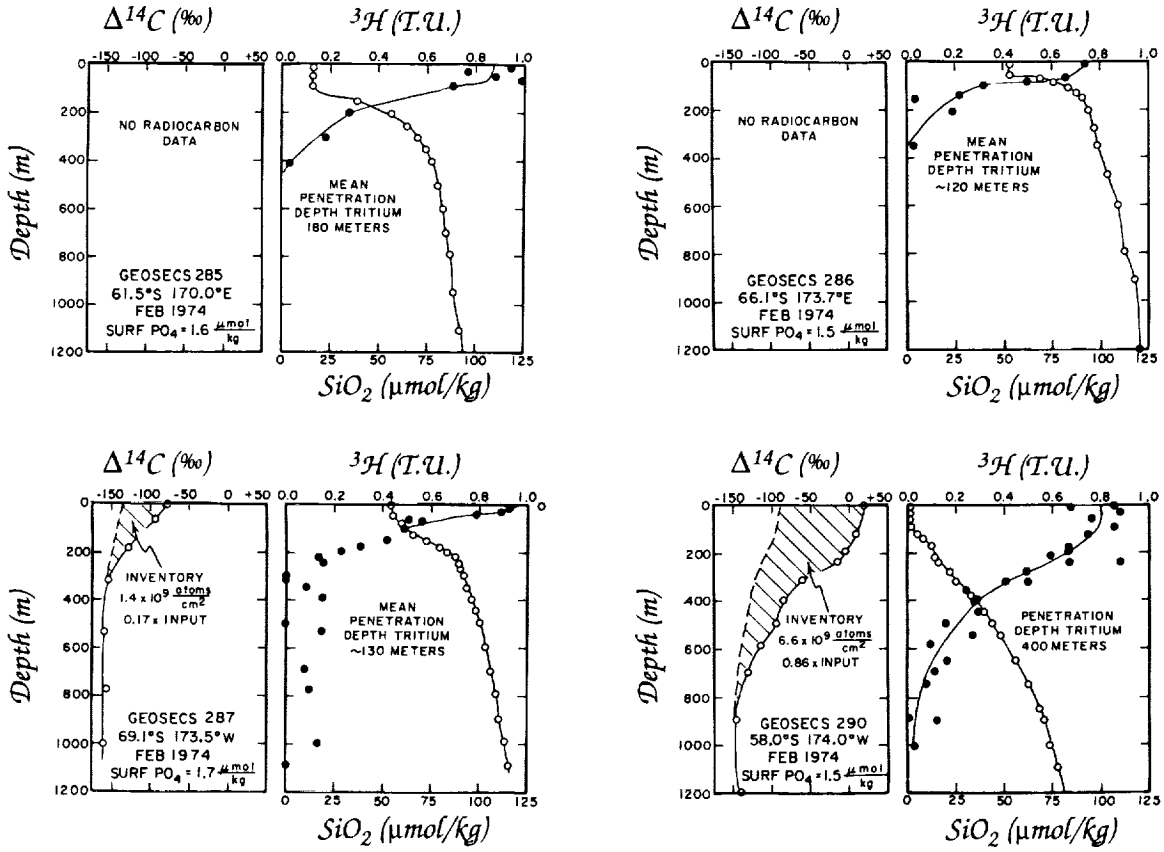

Figure 2, continued.

excess CO_2 on the time scale of one decade. Figure 3 summarizes meridional sections of dissolved silica for the Antarctic.

The other important source of information comes from the ^{14}C results. Broecker et al. (1985) used measurements on samples taken before the above-ground nuclear testing of the 1950s to estimate the prenuclear $\Delta^{14}C$ values for surface waters at the GEOSECS stations at which ^{14}C measurements were made. The ^{3}H measurements allowed an estimate to be made of the depth to which significant amounts of bomb-produced ^{14}C had penetrated at the time of the GEOSECS surveys. With these two end points and a knowledge of the shape of the ^{3}H profile, the prenuclear ^{14}C profile for each station could be established. The area between the measured profile and the prenuclear profile provided an estimate of the water column burden of excess ^{14}C. Broecker et al. (1985) showed that these excesses have a distinct geographic pattern (see Figure 4). Higher-than-average inventories are found in the temperate regions of the ocean and in the northern Atlantic. Lower-than-aver-

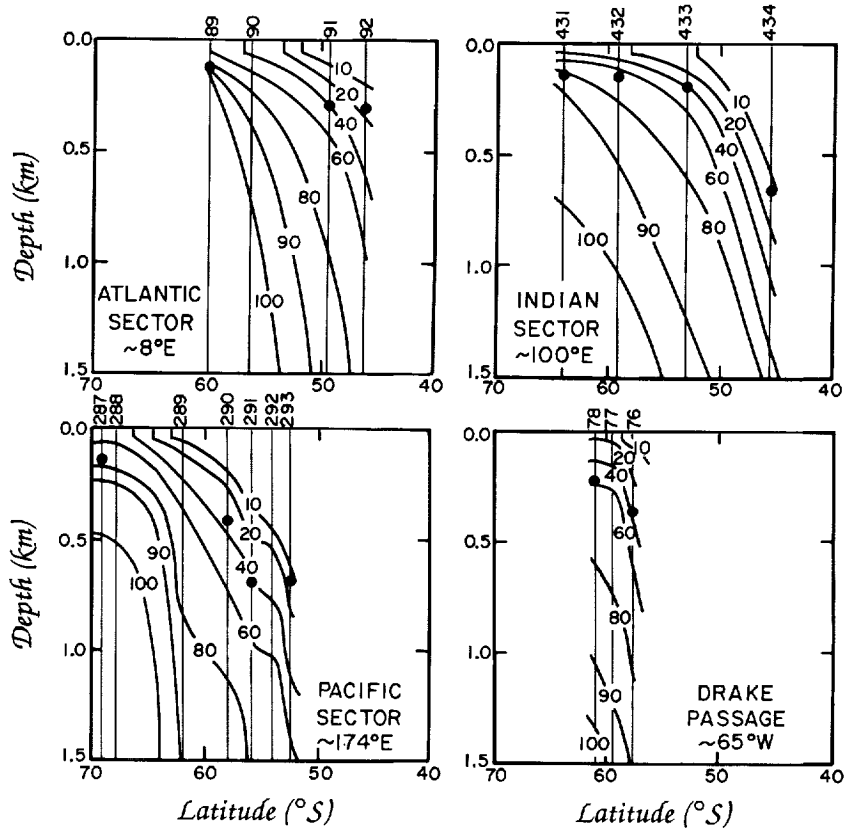

Figure 3. Meridional sections of dissolved silica (μmol/kg) for the Antarctic. At the time of the GEOSECS survey an excellent anticorrelation existed between tritium and silica for each station (see Figure 2). The large dots show the mean penetration depth of tritium for those stations (numbers on top axis) where tritium measurements were made. This diagram provides a feeling for the geometry of the volume available for excess CO_2 storage.

age inventories are found in the equatorial zone, in the northern Pacific, and in the Southern Ocean. These authors pointed out that the areas of high inventory correspond to regions of downwelling and the areas of low inventory to regions of upwelling. Further, they attributed this correspondence to lateral transport of bomb-produced ^{14}C from regions of upwelling to regions of downwelling. Experiments conducted with the Geophysical Fluid Dynamics Laboratory ocean model confirmed that such transports can explain the inventory pattern (Toggweiler et al., 1989).

Broecker et al. (1985) went a step further and compared the inventory at any given station to the net amount of bomb-produced ^{14}C invading that station from the atmosphere. This allowed the magnitude of the excess or deficiency to be quantified (see Figure 5). Their

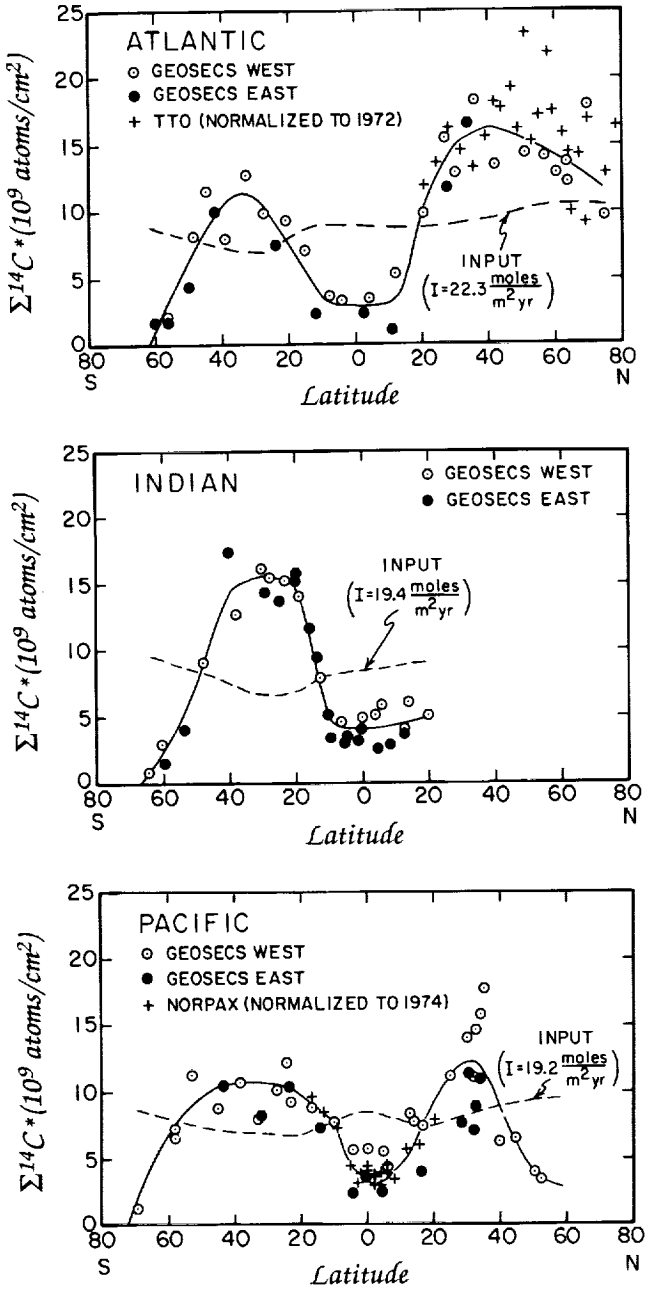

Figure 4. Bomb-produced ^{14}C inventories as measured during the GEOSECS, NORPAX, and TTO programs (as summarized by Broecker et al., 1985). The dashed lines show the amount expected at the time of the GEOSECS program were there no lateral transport from one zone to another. "I" represents CO_2 invasion rate.

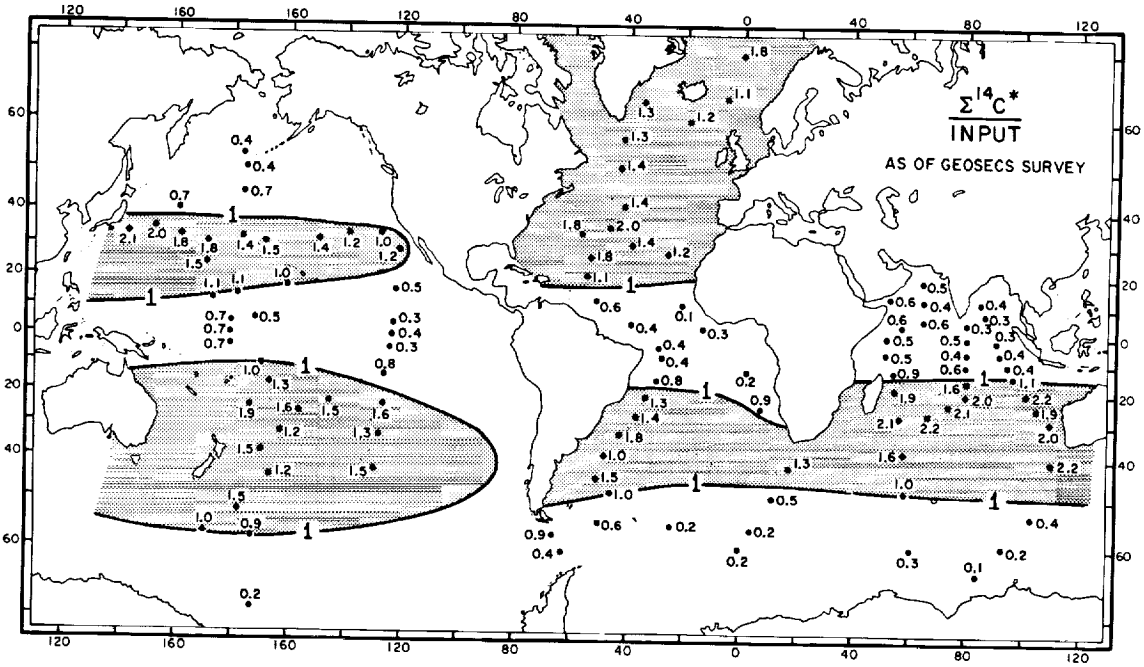

Figure 5. Map showing the ratios of observed bomb-testing radiocarbon inventories to those calculated were there no lateral transport (from Broecker et al., 1985).

calculations neglected the dependence of CO_2 exchange rate on wind speed. Were wind speed to be taken into account, the magnitude of the deficiencies for the Antarctic stations would be increased. The reason is that the wind speed and hence the CO_2 exchange rate over the Antarctic is higher than the global average. At all latitudes in the Antarctic, less bomb-produced ^{14}C is present than entered the ocean. The deficiencies range from very small at 45°S to as much as 90% of the total input closer to the Antarctic continent.

Together the ^{3}H penetration depths and the bomb-produced ^{14}C deficiencies allowed Broecker et al. (1985) to obtain estimates of the average upwelling and downwelling velocities for various regions of the ocean. The values they obtained are summarized in Table 2. For the Antarctic they require an average vertical eddy diffusivity of 3 cm^2/s and upwelling velocities ranging from 9 m/yr (for the Indian sector) to 31 m/yr (for the Atlantic sector).

Model of Antarctic and Non-Antarctic Oceans

Based on these tracer distributions and lateral transport mechanism of Broecker et al. (1985), we devised a box model of Antarctic and non-Antarctic oceans (Peng and Broecker, 1991a). It involves two, side-by-side, Oeschger et al. (1975) box-diffusion columns

Table 2: Comparison of surface water $\Delta^{14}C$ excesses and water column inventories of bomb-produced radiocarbon generated by the model of Broecker et al., 1985, with those observed GEOSECS.

Latitude Belt	Area (10^{12} m^2)	W[a] (m/yr)	Flux (Sv)	K[b] (cm^2/s)	z[c] (m)	$\Delta^{14}C - \Delta^{14}C^0$ (Modeled) (‰)	$\Delta^{14}C - \Delta^{14}C^0$ (Observed) (‰)	Bomb ^{14}C Input (10^{26} atoms)	Bomb ^{14}C Inventory (Modeled) (10^{26} atoms)	Bomb ^{14}C Inventory (Observed) (10^{26} atoms)
Atlantic (I[d] = 22.3 mol/m^2/yr)										
80°N–40°N	18.6	–8.5	5	9.9	710	130	120	20	26	26
40°N–20°N	15.8	–30.0	15	0.5	470	215	195	14	24	23
20°N–20°S	26.7	+21.2	18	1.0	190	146	150	25	11	10
20°S–45°S	18.4	–22.3	13	1.0	400	185	170	14	20	18
45°S–80°S	15.1	+31.2	15	3.0	270	100	100	14	6	7
Indian (I = 19.4 mol/m^2/yr)										
25°N–15°S	27.0	+15.2	13	1.0	215	130	160	26	11	12
15°S–45°S	29.8	–20.1	19	1.0	510	190	180	23	43	42
45°S–70°S	20.7	+9.1	6	3.0	410	115	100	19	14	13
Pacific (I = 19.2 mol/m^2/yr)										
65°N–40°N	15.1	+10.4	5	1.5	260	152	145	13	9	8
40°N–15°N	35.0	–10.8	12	1.0	365	206	210	30	39	37
15°N–10°S	50.0	+16.4	26	1.0	255	134	150	44	25	25
10°S–55°S	63.0	–12.5	25	2.0	410	166	170	48	64	60
55°S–80°S	13.8	+13.7	6	3.0	335	111	100	11	8	7

[a]W = upwelling rate
[b]K = vertical eddy diffusivity
[c]z = mean penetration depth, i.e., K/W
[d]I = CO_2 invasion rate
From Broecker et al., 1985

linked together by an overlying atmosphere and underlying deep sea (see Figure 6). One column represents the Antarctic and the other the non-Antarctic region of the ocean. Each column is capped by a 75-m-thick mixed layer. These mixed layers are underlain by 2000-

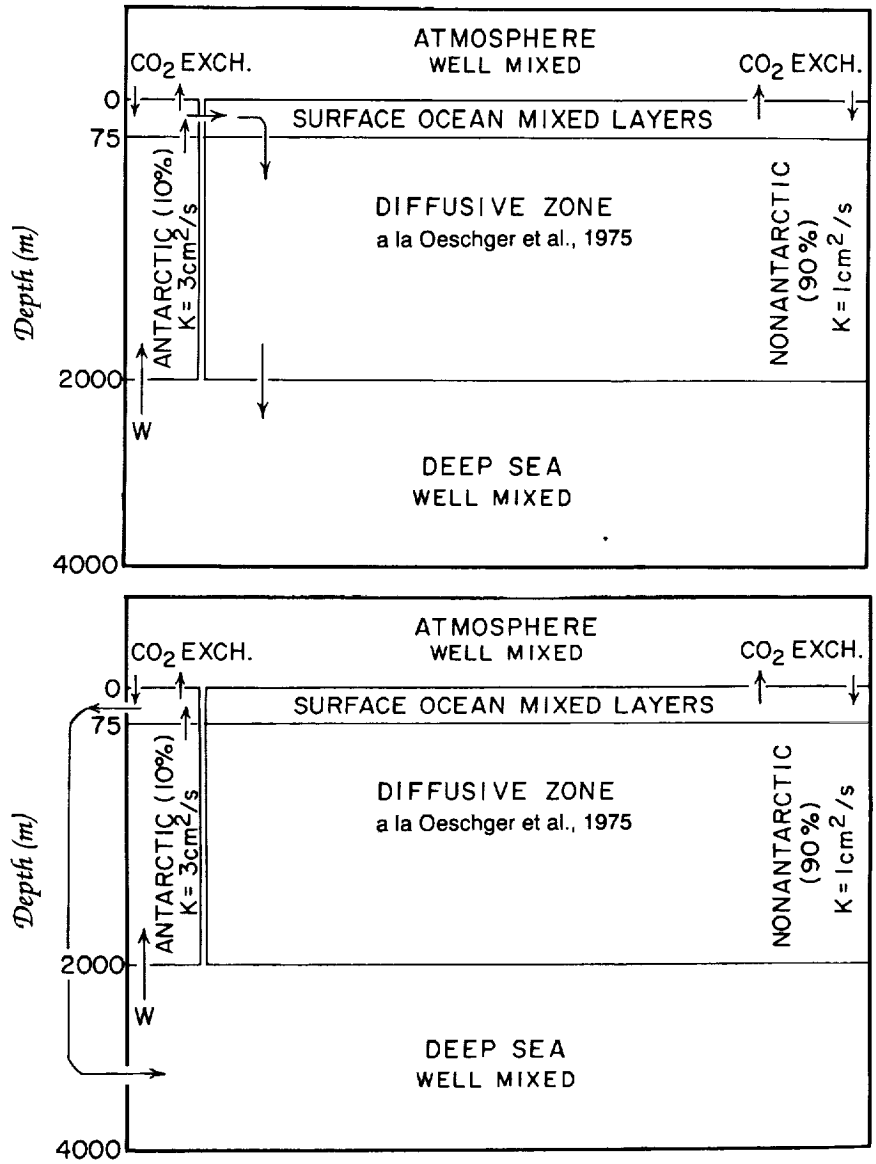

Figure 6. Linked vertical advection-diffusion model used to evaluate the response to iron fertilization of Antarctic surface waters. The upper panel shows the case where the water upwelled in the Antarctic is transferred laterally to the non-Antarctic surface ocean. The lower panel shows the case where this upwelled water is converted to deep water and transferred directly to the model's deep reservoir.

m-thick diffusive zones. Beneath the diffusive zone is a single well-mixed deep reservoir. The area and volume of the Antarctic column are taken to be 10% of the ocean total. We did not set the area of the Antarctic at 17% because iron fertilization could draw the surface water pCO_2 only during those months when sunlight is plentiful. In the light-poor austral winter months the pCO_2 would be driven back toward its prefertilization value by vertical mixing in the upper 100 m or so of the water column.

Consistent with the distribution of bomb radiocarbon, we set the vertical eddy diffusivity in the Antarctic column at 3 cm^2/s and that in the non Antarctic column at 1 cm^2/s. The upwelling flux in the Antarctic column was set at 17.4 Sverdrups (i.e., an upwelling rate of 15.2 m/yr). Because we had no firm means to determine the fate of the upwelled water, we adopted two limiting scenarios. In the first, all of the water is transferred entirely to the surface of the non-Antarctic column. In the second, it is transferred entirely to the deep reservoir.

We started our calculation with a steady state. The residence times for PO_4 with respect to biological removal from the surface reservoirs were set so as to yield 1.6 μmol PO_4 in the surface water above the Antarctic column and close to zero PO_4 in the surface waters of the non-Antarctic column. The regeneration function for falling organic debris was set to yield PO_4 vs. depth profiles similar to the observed (we hasten to point out that the choice of this respiration function has no influence on the result of the calculation of the atmospheric CO_2 response to iron fertilization). The atom ratio of carbon to phosphorus in the organic matter falling from the surface mixed layer is 130. We then adjusted the ΣCO_2/alkalinity ratio in the model ocean to yield an atmospheric pCO_2 pressure of 280 μatm.

To simulate a totally successful iron fertilization, we perturbed this steady state by greatly decreasing the residence time with respect to biological removal of PO_4 from Antarctic surface water, bringing its PO_4 content to near zero. In this simulation we continued the iron fertilization for 100 years, holding the PO_4 content of the surface Antarctic water at zero over this entire period. The evolutions of the vertical distributions of PO_4 and ΣCO_2 in the Antarctic column are shown in Figure 7. As can be seen, while the water column integral of PO_4 remains unchanged, a bulge of excess ΣCO_2 appears. This bulge represents the CO_2 transferred from the atmosphere and the non-Antarctic column to the Antarctic column (Peng and Broecker, 1991a). The time trends for the pCO_2 in the two ocean surface layers and in the atmosphere are shown in Figure 8. In the lateral transfer scenario, the atmospheric CO_2 content drops ever more slowly as the century progresses, reaching an asymptote about 15 μatm lower than the initial value. In the deep transfer sce-

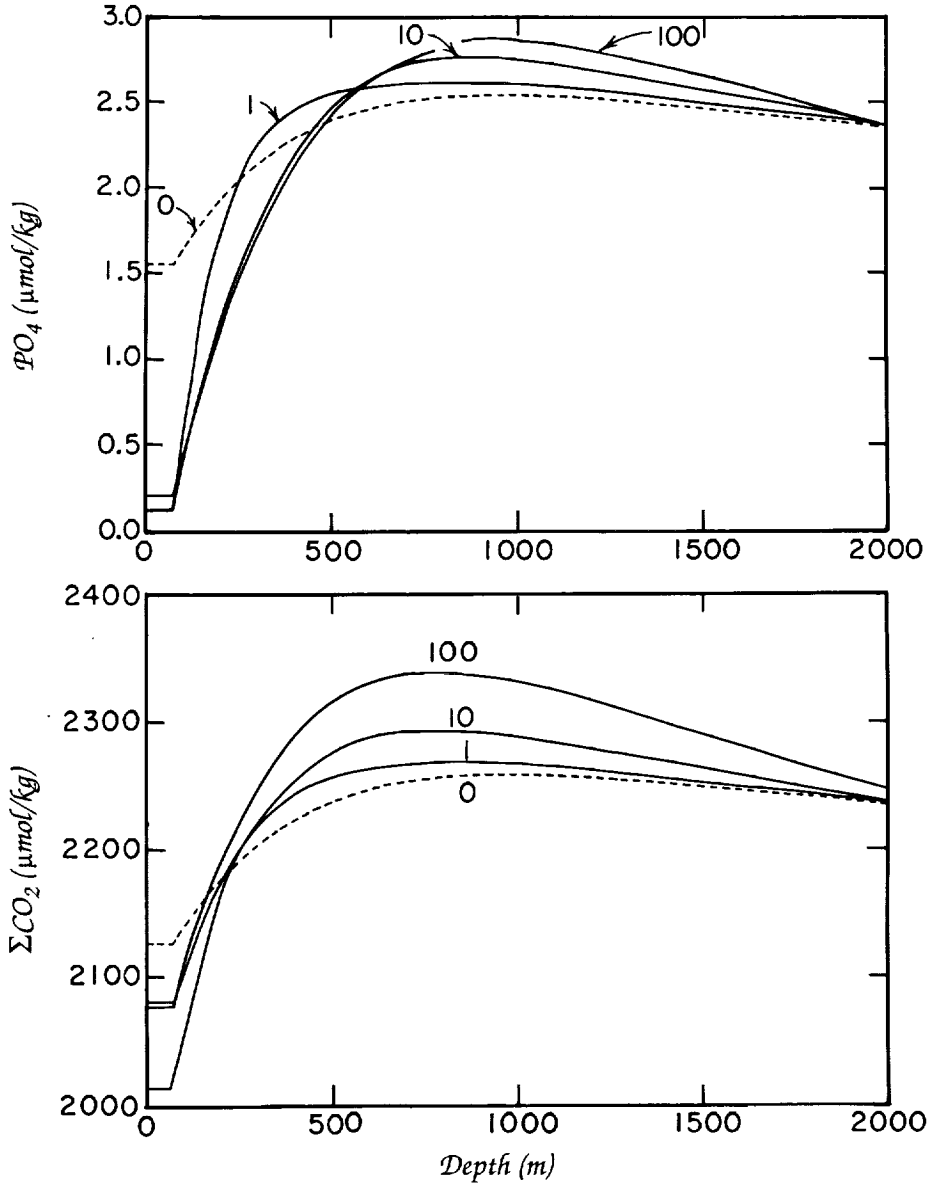

Figure 7. Vertical distribution of PO_4 and ΣCO_2 in the Antarctic column before the onset of fertilization (dashed line) and 1, 10, and 100 years after the onset of fertilization for the scenario where water is upwelled at the rate of 17.4 Sverdrups and transferred to the deep sea.

nario the decrease continues, reaching about 34 μatm after one century (Peng and Broecker, 1991a). The reason for the difference is that in one case the surface water from the Antarctic is transferred to the surface of the non-Antarctic region, allowing the excess CO_2

to reenter the atmosphere, while in the other this water is removed to the deep sea, isolating it from the atmosphere.

The question naturally arises as to what would happen if at some point iron fertilization were terminated. As shown in Figure 8, the answer is that any reduction in atmospheric CO_2 content accom-

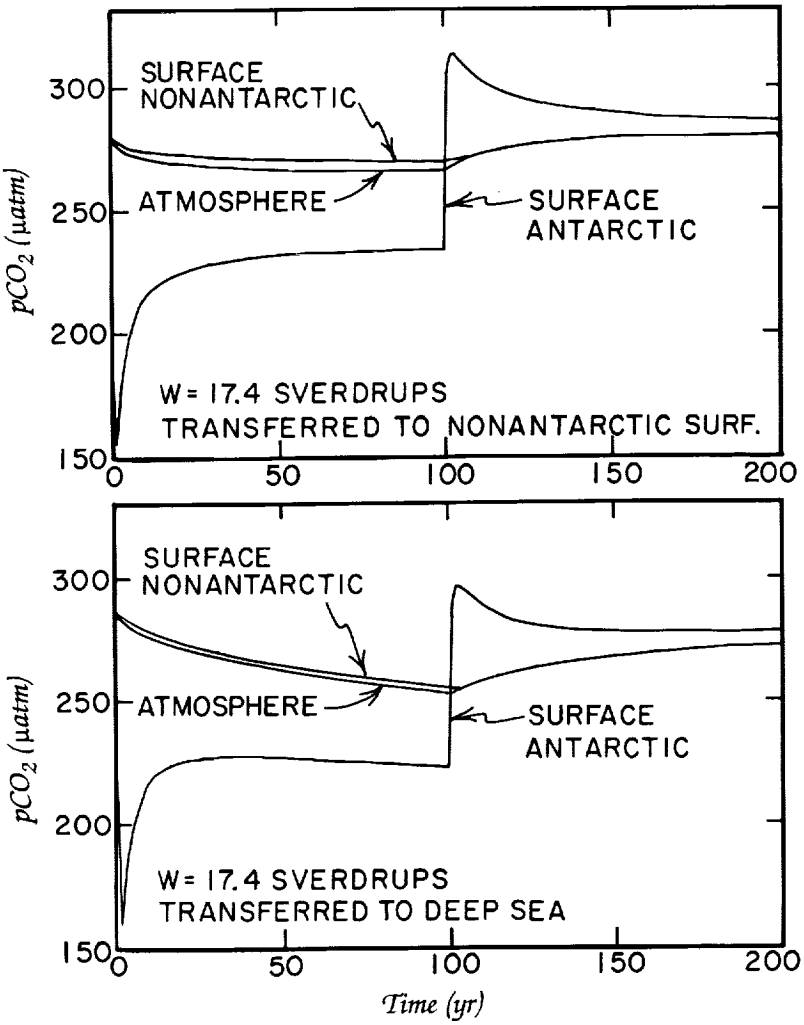

Figure 8. Model runs for an Antarctic upwelling flux of 17.4 Sverdrups. The upper panel shows the case where the upwelled water is transferred to the surface of the non-Antarctic Ocean; the lower panel shows the case where the upwelled water is transferred to the deep sea. In each case totally successful iron fertilization is conducted for 100 years and then stopped. For the steady state conditions which precede the onset of fertilization, the pCO_2 for Antarctic surface waters is nearly identical to that for the atmosphere.

C-2

plished by the fertilization would be lost on more or less the same time scale as it was gained.

As a sensitivity test, we have made runs for upwelling fluxes of twice and half the 17.4 Sverdrups value for our best case scenario and also for no advection. As summarized in Table 3, changes in upwelling flux have little effect on the results for the lateral transport endmember model. However, in the case of the deep transfer endmember model, the greater the upwelling flux, the greater the reduction of the atmospheric CO_2 content brought about by iron fertilization. Clearly, the key question to be answered in the evaluation of the dynamic constraints on the iron fertilization scheme is the rate and extent of vertical transport in the Antarctic.

Effects on an Anthropogenically Affected Atmosphere

To test the effects of iron fertilization on an anthropogenically affected atmosphere, we introduced excess CO_2 into the atmosphere starting in 1800 and continuing through 1990. The input function of fossil fuel production was based on a recent estimate (Marland, 1990). The release of CO_2 from the perturbed terrestrial ecosystem was derived from deconvolution (Peng, 1991) of the time history of atmospheric pCO_2 based on pCO_2 measurements of air bubbles in ice cores (Neftel et al., 1985) and of air samples (Keeling et al., 1989). The release scenario of the business-as-usual case for the next century was taken from a report of the Intergovernmental Panel on Climate Change (IPCC; Houghton et al., 1990). The CO_2 emission between 1800 and 2100 is shown in Figure 9. Before introducing anthropogenic CO_2, the steady state of our ocean-atmosphere model with pCO_2 of 280 μatm was the same as described earlier. Shown in Figure 10 is the atmospheric pCO_2 for the next century resulting from the

Table 3: Summary of pCO_2 after 100 years of iron fertilizaiton

Experiment No.	Upwell Rate (sv)	pCO_2 initial Atm. (μatm)	pCO_2 final Atm. (μatm)	pCO_2 final non-Ant. (μatm)	pCO_2 final Ant. (μatm)	ΔpCO_2 Atm. (μatm)
1	34.8	280.5	265.5	270.8	215.2	-15.0
2	17.4	279.7	265.0	268.5	232.2	-14.7
3	8.7	280.0	263.2	265.6	240.1	-16.8
4	0.0	284.3	262.2	263.2	248.2	-22.1
5	8.7*	283.1	255.2	256.8	233.4	-27.9
6	17.4*	286.0	251.6	253.7	221.7	-34.4
7	34.7*	291.0	244.0	246.8	200.7	-47.0

*The water upwelled in the Antarctic is converted to deep water.

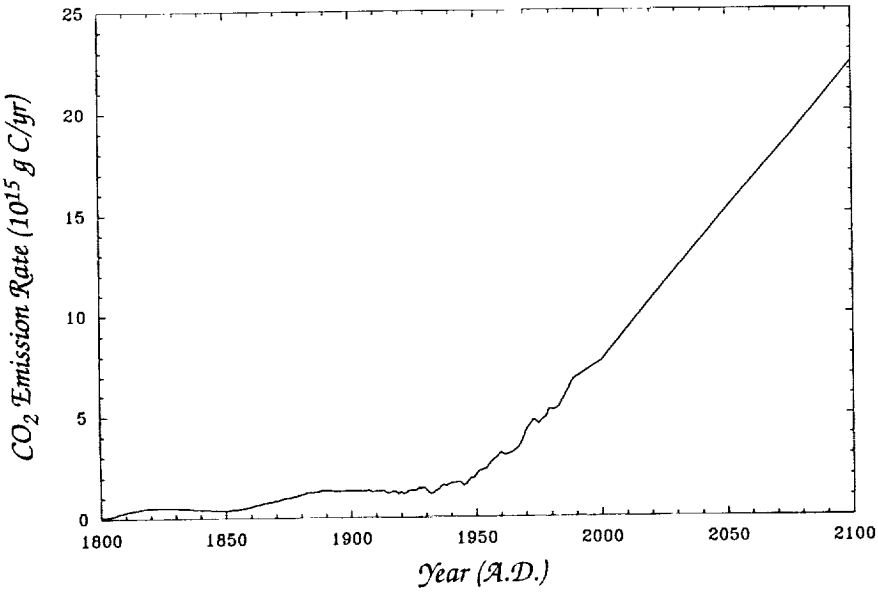

Figure 9. Time history of CO_2 emission for the period between 1800 and 1990 combined with the IPCC business-as-usual CO_2 release scenario for the period between 1991 and 2100.

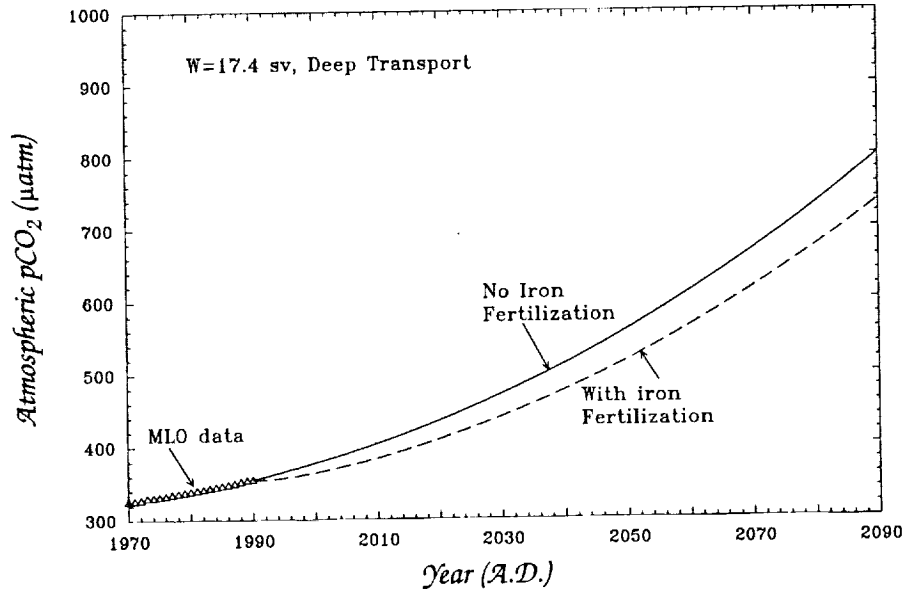

Figure 10. Atmospheric pCO_2 from Mauna Loa Observatory measurements (1970–1990) combined with the IPCC business-as-usual CO_2 emission scenario (1991–2090). The solid curve is the predicted atmospheric pCO_2 without iron fertilization, and the dashed curve is the one with iron fertilization in the Antarctic Ocean. Standard dynamic conditions of 17.4 sv upwelling flux and deep transport of upwelled water are used for simulation.

IPCC CO_2 release scenario without iron fertilization in the Antarctic Ocean. An upwelling flux of 17.4 sv is used, and the upwelled water is transferred to the deep reservoir. The result of a successful iron fertilization to reduce the atmospheric pCO_2 under such dynamic conditions is also shown in the same figure for comparison. The difference between these two curves represents the net effect of iron fertilization.

We made a series of sensitivity calculations with various upwelling fluxes to estimate the amount of reduction in atmospheric pCO_2 with 100% successful iron fertilization in the Antarctic. As shown in Figure 11, the lateral transport scenario is not sensitive to upwelling fluxes, with reductions in the range of 20 to 30 μatm for the time in the next century when the atmospheric pCO_2 reaches 800 μatm. This reduction corresponds to only about 3% of the atmospheric CO_2 content. But, in the case of deep transport, the reduction is very sensitive to upwelling fluxes. The reduction ranges from 6% of the atmospheric pCO_2 for an 8.7-sv upwelling flux to 12% for a 34.8-sv upwelling flux, with the best case of 8% reduction (or 64 μatm) for a 17.4-sv upwelling flux.

Similar model simulations of the possible effects of iron fertilization in the Southern Ocean on atmospheric pCO_2 have been made by Joos et al. (1991a, 1991b). Their model is a high-latitude exchange and low-latitude interior diffusion advection four-box model calibrated with bomb ^{14}C distribution. The Antarctic Ocean is represented by two well-mixed boxes, one for the surface and one for deep water. They obtained a reduction of 107 μatm for the IPCC business-as-usual release scenario under their standard dynamic condition after 100 years of successful iron fertilization in the Antarctic. Their sensitivity tests showed that the most important factors affecting the magnitude of CO_2 reduction are the area of fertilization and the amount of future CO_2 emissions.

The lower estimates of atmospheric pCO_2 reduction in our simulations as compared with those of Joos et al. (1991a, 1991b) have been criticized as resulting from the failure of our model to use a larger surface area for fertilization (i.e., 16%, instead of 10%). However, as reported by Peng and Broecker (1991b), a reduction of 71 μatm after 100 years of successful iron fertilization is estimated if the total Antarctic surface area is taken to be 16% of the global ocean area. This estimate is not significantly different from a reduction of 64 μatm in the standard case. The reason for such a small difference is that the upwelling flux of 17.4 sv is kept constant in spite of increased surface area. It was the upwelling flux rather than an upwelling rate that was constrained by Broecker et al. (1985) in their analysis of the bomb ^{14}C data. The increase in surface area causes the upwelling rate to drop from 15.2 to 9.5 m/yr.

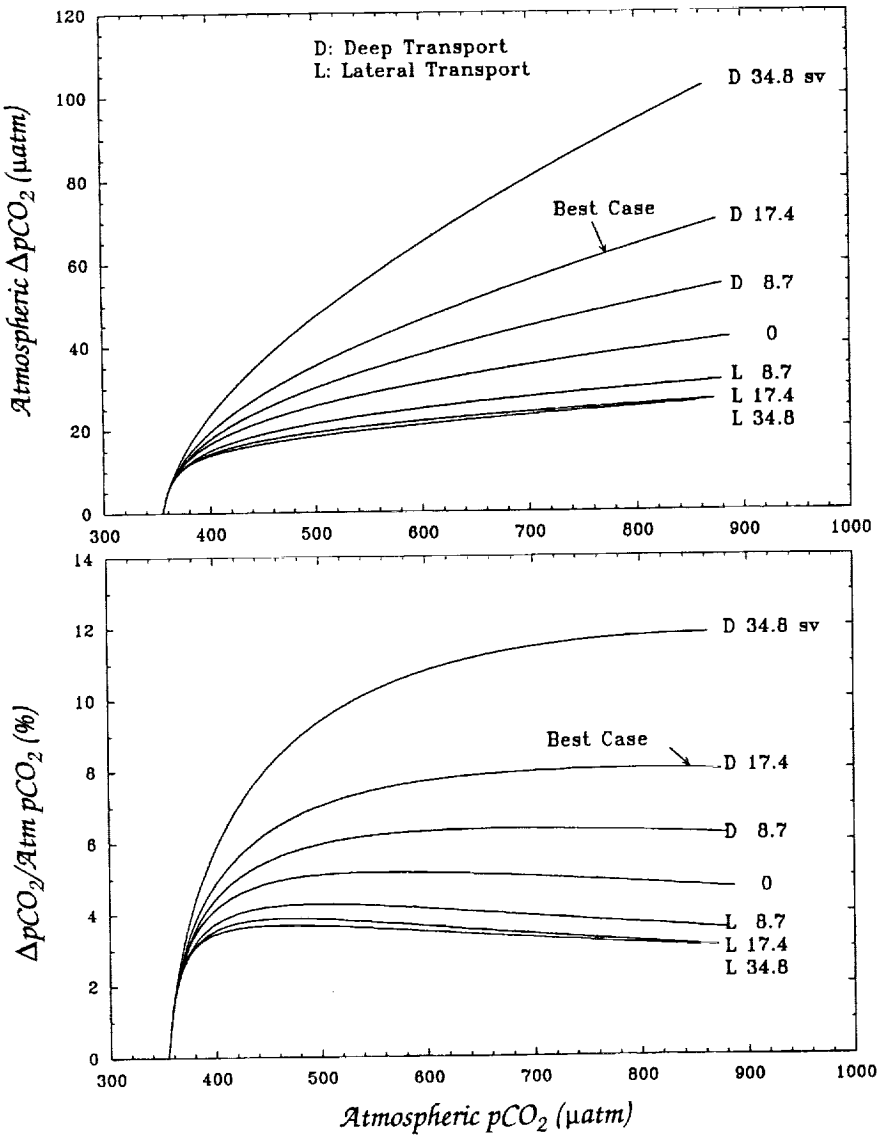

Figure 11. Reduction in pCO_2 in the atmosphere with iron fertilization in the Antarctic ocean for the period between 1991 and 2100 when the release of anthropogenic CO_2 into the atmosphere is taken from the IPCC business-as-usual case. Magnitude of reduction is plotted against the atmospheric pCO_2 in the upper panel, while the percentage of reduction is plotted in the lower panel.

More elaborate model simulations were made by Sarmiento and Orr (in press) using a three-dimensional ocean carbon cycle model based on a general circulation model (GCM). A reduction of 72 μatm in the next 100 years was obtained for a successful iron fertilization in the Southern Ocean (with 16% surface area) when the anthropogenic CO_2 emission followed the IPCC business-as-usual scenario. It is interesting to note that our estimate is comparable with theirs, although there are large differences in the modeling approaches.

Effects of Seasonal Iron Fertilization

Light availability certainly limits photosynthesis in the Antarctic, especially during the winter months. To gain some idea regarding the impact of this limitation, we have introduced seasonality into our model. It involves turning off the impact of iron fertilization for a number of months each year. We do this without changing the model's dynamics: i.e., upwelling and vertical mixing continue unchanged throughout the year. Shown in Figure 12 are the resulting surface water PO_4 and pCO_2 cycles for the first four years after the onset of fertilization for the scenario involving 17.4 sv upwelling coupled with transport to the deep sea. The period of totally successful fertilization is set at eight, four, and two months. These results depend strongly on our choice of PO_4 residence time in the mixed layer during the period of fertilization and on the choice of vertical eddy diffusivity. Our choices lead to a rapid drawdown of phosphate content of the mixed layer after the onset of fertilization, but much slower rise when fertilization ceases. Under these circumstances four winter months of no productivity caused only a small reduction in the long-term CO_2 drawdown (see Figure 13). Even when the period of fertilization was reduced to only two months per year, two-thirds of the atmospheric CO_2 drawdown achieved for the full-year scenario occurred (see Figure 13).

It is tempting to conclude from this that were iron added for only two months of the year, two-thirds of the maximum possible atmospheric drawdown would be achieved. We urge caution in this regard; our result depends very strongly on the ratio of the PO_4 drawdown time to the water replacement time for the mixed layer. Were a less favorable ratio to be adopted, the turnoff of iron fertilization would have more nearly a proportional impact. Our choice of one month for the phosphate drawdown time is just a guess. As our surface water replacement time is chosen to match the vertical distribution of tritium about one decade after the cessation of large-scale bomb testing, it has little bearing on the actual rate of water exchange

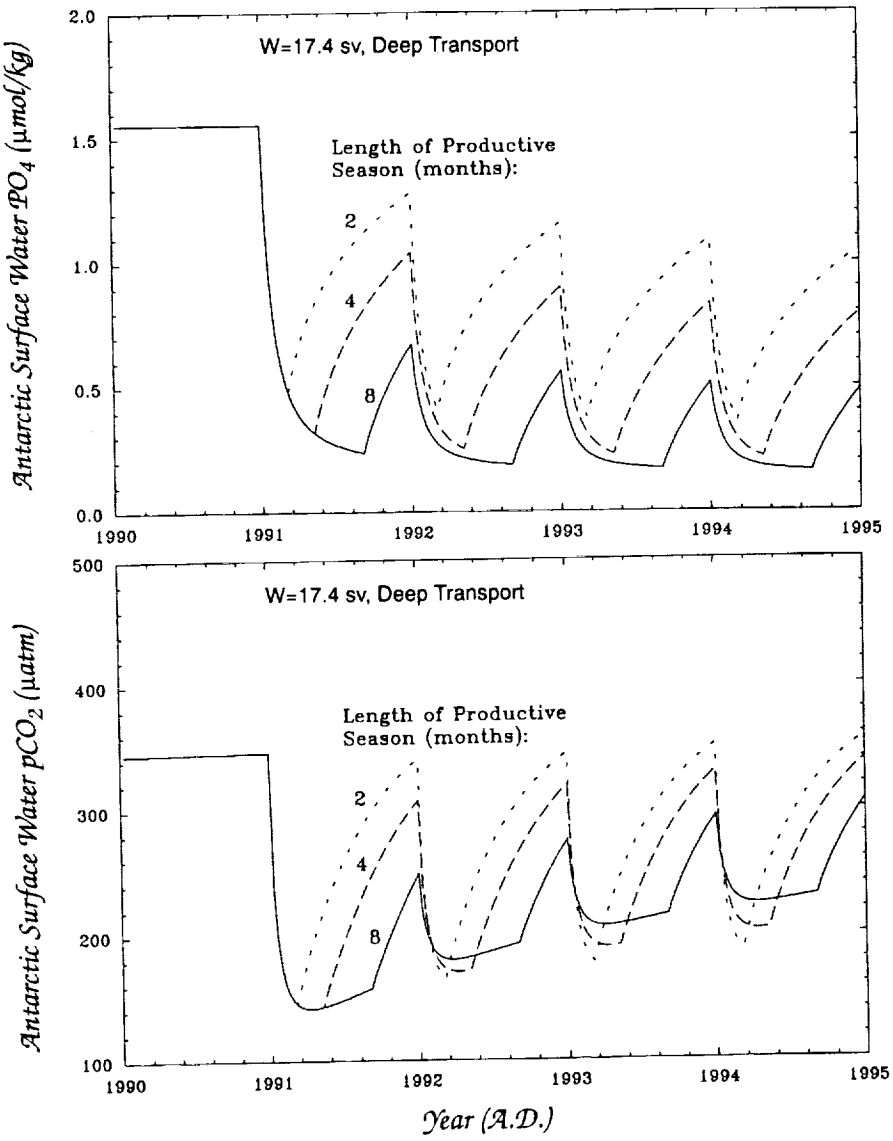

Figure 12. Seasonal cycles of surface water pCO_2 and PO_4 in the Antarctic with a productive season of eight months (solid line), four months (long dashed line), and two months (short dashed line). Iron fertilization is assumed to work successfully during the productive season. The PO_4 cycle is plotted in the upper panel for the first four years after the fertilization, and the pCO_2 cycle is plotted in the lower panel.

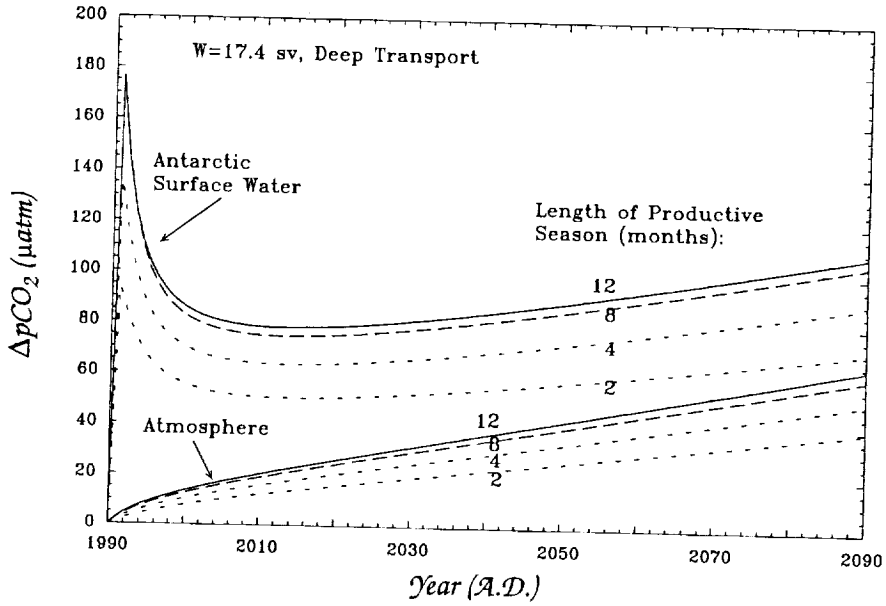

Figure 13. Reduction of pCO_2 in the atmosphere and in the Antarctic surface water resulting from seasonal iron fertilization. A two-thirds total reduction in the atmosphere can be achieved by two-twelfths yearly fertilization with iron in the Antarctic Ocean.

between the mixed layer and the underlying thermocline. Further, the actual vertical exchange has a strong seasonality. Winter cooling thickens the mixed layer, while summer warming and sea ice melting thin it. The only valid conclusion to be drawn from our seasonality exercise is that careful attention should be given to seasonality in any plan for iron fertilization. The interplay of changing light availability and vertical mixing with the timing of iron addition could be used to optimize the amount of atmospheric CO_2 drawdown per unit fertilization cost.

Implications of SAVE ^{14}C Results

The real power of transient tracer data is seen when the spatial distribution is used in combination with temporal evolution. Unfortunately, no more recent tritium and ^{14}C data sets are available. However, ^{14}C data have recently become available from four stations occupied during the South Atlantic Ventilation Experiment (SAVE) survey of the South Atlantic (see Figure 1 for locations). Two of these stations are close to GEOSECS station 68 at the northern fringe of the Antarctic in the Argentine Basin. While the depth profiles of ^{14}C at these stations are quite different than that at station 68, when ^{14}C is plotted against silica absolutely no difference is seen (Figure 14). This is puzzling because the silica distribution is at steady state

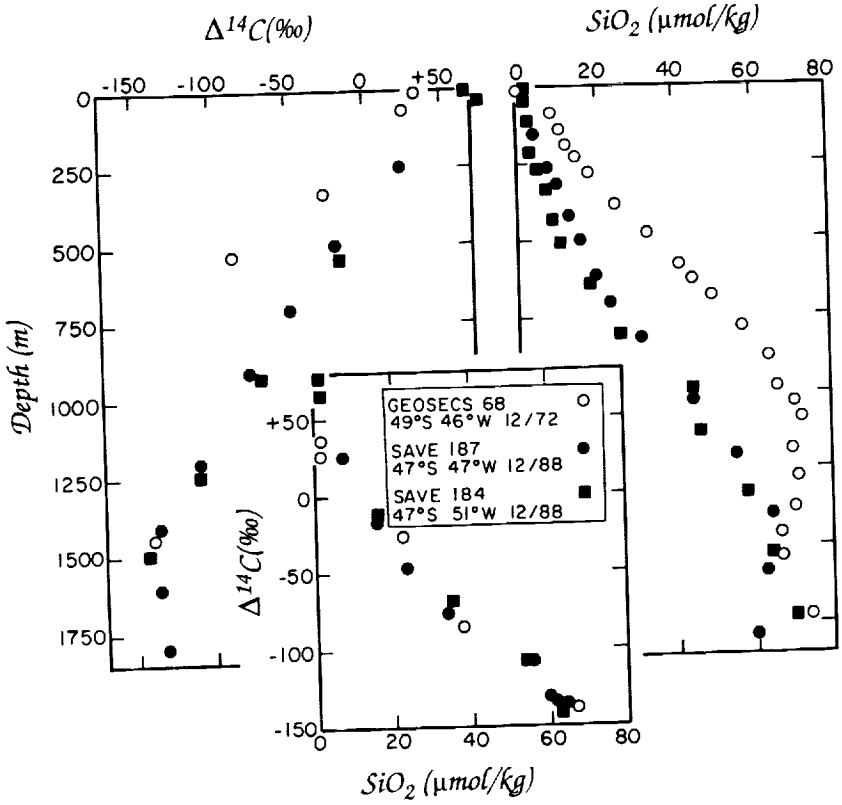

Figure 14. Comparison of depth profiles for silica and radiocarbon and of silica vs. radiocarbon trends for GEOSECS station 68 (December 1972) and nearby SAVE stations 184 and 187 (December 1988). As can be seen, the relationship between radiocarbon (a transient) and silica (at steady state) shows no change over this period of time. The 1988 silica results are from the SAVE preliminary data report series and the 1988 radiocarbon results are from Östlund, 1990.

while the ^{14}C distribution is evolving. The other two recent stations lie within the Antarctic. As can be seen in Figure 15, again no change in the ^{14}C-silica trend is seen over a 16-year period. One gets the idea that the vertical distribution of bomb-produced ^{14}C adjusted to a transient steady state on a time scale of a decade and that as the surface water $\Delta^{14}C$ value went up and then came back down again (see Figure 16) in response to the changing atmospheric $\Delta^{14}C$, the Antarctic $\Delta^{14}C$-silica trend rotated first toward a higher $\Delta^{14}C$ value and then back down again, reaching by chance its December 1972 value once again in December 1988 during SAVE survey.

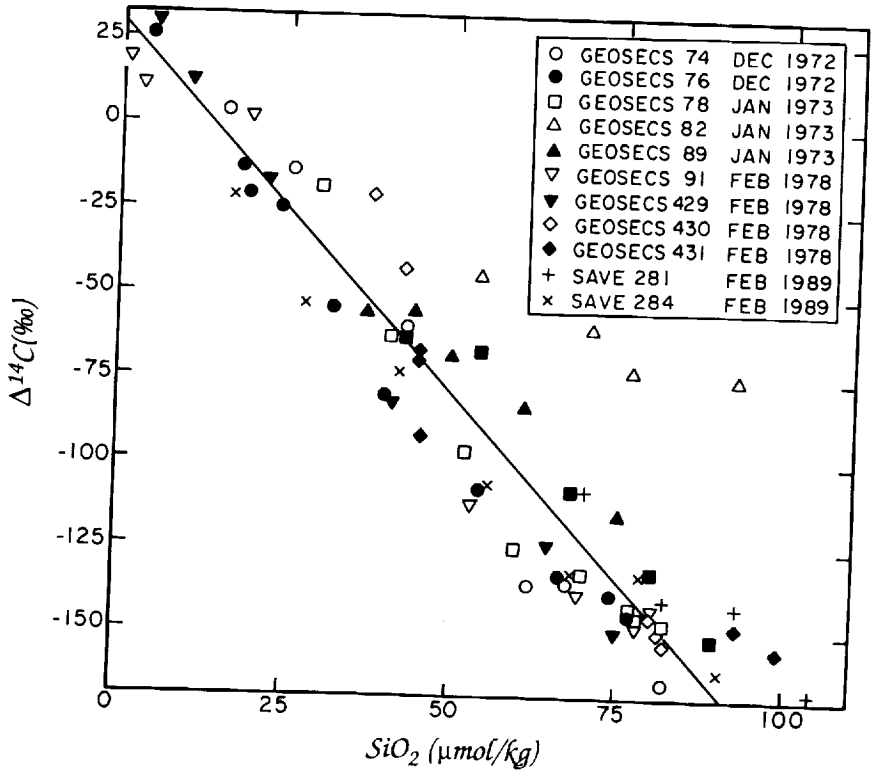

Figure 15. Relationship in the Antarctic between radiocarbon and silica for the GEOSECS Atlantic stations, three of the GEOSECS Indian stations, and two SAVE stations. Despite the passage of 16 years from late 1972, when the GEOSECS Atlantic samples were taken, to early 1989, when the SAVE samples were taken, no evidence exists for a change in the radiocarbon-silica relationship. Only the GEOSECS station (82) which is the nearest to the Weddell Sea departs from the ambient trend. It should be kept in mind that prior to bomb testing no waters in the Antarctic had ^{14}C values above −75‰. The GEOSECS data are from sources mentioned above and the SAVE data are from the preliminary shipboard measurement report and from Östlund, 1990.

As can be seen in both Figures 14 and 15, no evidence exists for a buildup of bomb ^{14}C in waters with more than about 80 µmol of silica. The ^{14}C content of these waters lies close to the average (see Figure 17) obtained by GEOSECS for deep waters of the Antarctic (potential temperatures in the range of 0 to 1°C). Hence, little excess CO_2 entering the Antarctic as the result of iron fertilization can be expected to reach waters with more than 80 µmol of silica on a time scale of 25 years. A sense of magnitude of the volume of water lying above this silica horizon is shown in Figure 3.

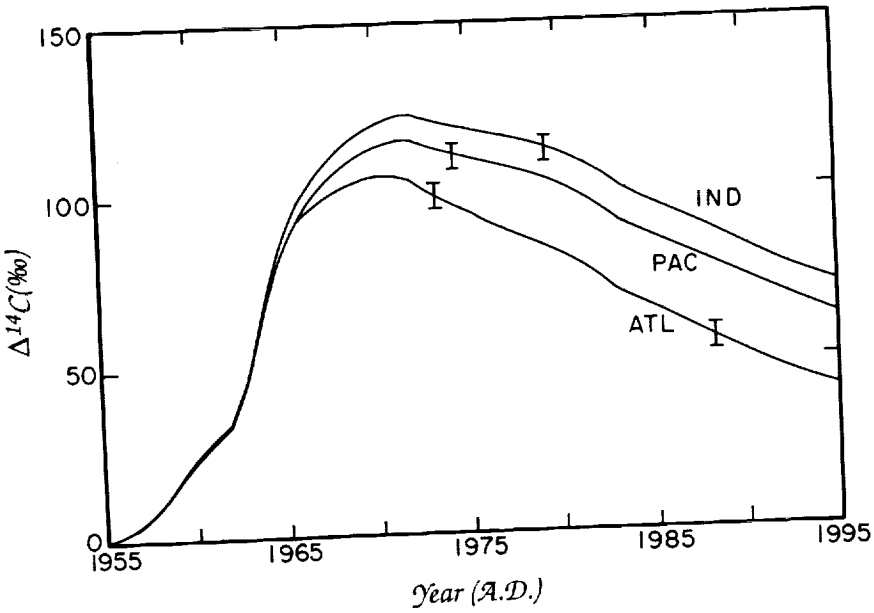

Figure 16. Time trends for the surface water ^{14}C computed using the Broecker et al. (1985) column models for three sectors of the Antarctic. The times for the GEOSECS and SAVE sampling are marked with hashes.

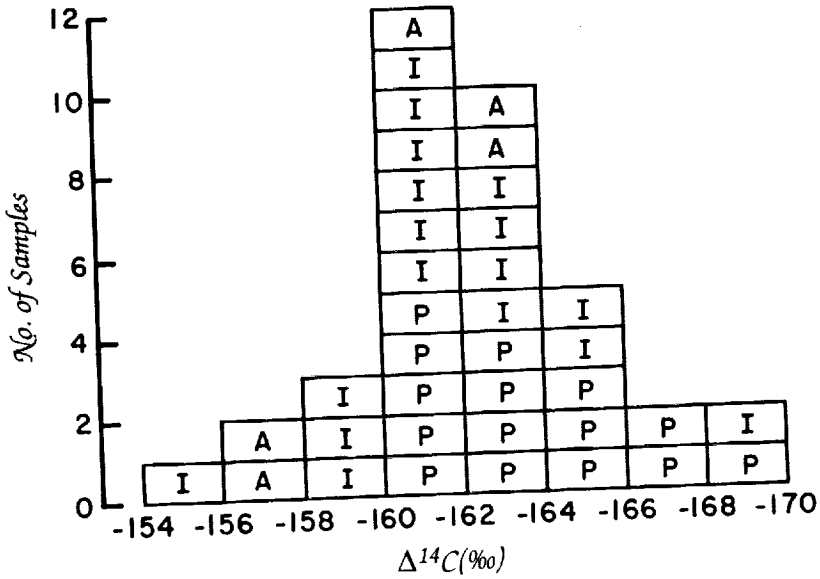

Figure 17. Summary of GEOSECS results on deep water samples from the Antarctic (Östlund and Stuiver, 1980; Stuiver and Östlund, 1980; Stuiver and Östlund, 1983). A represents Atlantic, P represents Pacific, and I represents Indian.

Conclusion

While our ability to model what goes on in the Antarctic remains in a primitive state, the evidence we have certainly waves a red flag with regard to optimistic claims (see Baum, 1990) that iron fertilization of the Antarctic, even if biologically successful, will significantly draw down the CO_2 content of the atmosphere. Interest in this possible intervention scenario clearly adds yet another item to an already long list of reasons why we should redouble our efforts to obtain extensive transient tracer data for the Antarctic.

Acknowledgments

Discussion with J. Sarmiento prompted this study. Modeling of bomb radiocarbon transient in an ocean GCM by R. Toggweiler rekindled our thinking about tracers in the Antarctic. Financial support was provided by grants from the Exxon Corporation and the Carbon Dioxide Research Program, Environmental Sciences Division, Office of Health and Environmental Research, U.S. Department of Energy, under contract DE-AC05-84OR21400 with Martin Marietta Energy Systems, Inc. This chapter is publication No. 3744, Environmental Sciences Division, Oak Ridge National Laboratory, and contribution No. 4828, Lamont-Doherty Geological Observatory of Columbia University.

References

Baum, R. 1990. Adding iron to ocean makes waves as way to cut greenhouse CO_2. *Chemical & Engineering News*, July 2, 1990, 21–24.

Broecker, W.S., T.-H. Peng, G. Östlund, and M. Stuiver. 1985. The Distribution of bomb radiocarbon in the ocean. *Journal of Geophysical Research 90*, 6953–6970.

Broecker, W.S., T.-H. Peng, and G. Östlund, 1986. The distribution of bomb tritium in the ocean. *Journal of Geophysical Research 91*, 14331–14344.

Houghton, J.T., G.J. Jenkins, and J.J. Ephraums (eds.). 1990. *Climate Change: The IPCC Scientific Assessment.* Intergovernmental Panel on Climate Change and Cambridge University Press, Cambridge, 329–341.

Joos, F., J.L. Sarmiento, and U. Siegenthaler. 1991a. Potential enhancement of oceanic CO_2 uptake by iron fertilization of the Southern Ocean. *Nature 349*, 772–775.

Joos, F., U. Siegenthaler, and J.L. Sarmiento. 1991b. Possible effects of iron fertilization in the Southern Ocean on atmospheric CO_2 concentration. *Global Biogeochemical Cycles 5*, 135–150.

Keeling, C.D., R.B. Bacastow, A.F. Carter, S.C. Piper, T.P. Whorf, M. Heimann, W.G. Mook, and H. Roeloffzen. 1989. A three-dimensional model of atmospheric CO_2 transport based on observed winds: 1. Analysis of observational data. In *Climate Change in the Eastern Pacific and Western Americas* (D. Peterson, ed.), Geophysical Monographs 55, American Geophysical Union, Washington, D.C., 165–231.

Marland, G. 1990. Global CO_2 emissions. In *Trends '90: A Compendium of Data on Global Change* (T.A. Boden, P. Kanciruk, and M.P. Farrell, eds.), ORNL/CDIAC-36, Carbon Dioxide Information Analysis Center, Oak Ridge National Laboratory, Oak Ridge, Tennessee, 92.

Martin, J.H. 1990. Glacial-interglacial CO_2 change: The iron hypothesis. *Paleoceanography 5*, 1–13.

Martin, J.H., and S.E. Fitzwater. 1988. Iron deficiency limits phytoplankton growth in the northeast Pacific subarctic. *Nature 331*, 341–343.

Martin, J.H., and R.M. Gordon. 1988. Northeast Pacific iron distributions in relation to phytoplankton productivity. *Deep Sea Research 35*, 177–196.

Martin, J.H., R.M. Gordon, S. Fitzwater, and W.W. Broenkow. 1989. VERTEX: Phytoplankton/iron studies in the Gulf of Alaska. *Deep-Sea Research 36*, 649–680.

Martin, J.H., R.M. Gordon, and S. Fitzwater. 1990a. Iron in Antarctic waters. *Nature 345*, 156–158.

Martin, J.H., S.E. Fitzwater, and R.M. Gordon. 1990b. Iron deficiency limits phytoplankton growth in Antarctic waters. *Global Biogeochemical Cycles 4*, 5–12.

Neftel, A., E. Moor, H. Oeschger, and B. Stauffer. 1985. Evidence from polar ice cores for the increase in atmospheric CO_2 in the past two centuries. *Nature 315*, 45–47.

Östlund, H.G. 1990. South Atlantic Ventilation Experiment (SAVE) Radiocarbon results, Legs 4,5 and Hyrdos Leg 4. University of Miami Report.

Östlund, H.G., and M. Stuiver. 1980. GEOSECS Pacific radiocarbon. *Radiocarbon 22*, 25–53.

Oeschger, H., U. Siegenthaler, U. Schotterer, and A. Gugelman. 1975. A box diffusion model to study the carbon dioxide exchange in nature. *Tellus 27*, 168–192.

Peng, T-H. 1991. Oceanic CO_2 uptake and future atmospheric CO_2 concentrations. In *Air-Water Mass Transfer: Selected Papers from the Second International Symposium on Gas Transfer at the Water Surfaces* (S.C. Wilhelms and A.J. S. Gulliver, eds.). American Society of Chemical Engineers, New York, 618–636.

Peng, T.-H., and W.S. Broecker. 1991a. Dynamic limitations on the Antarctic iron fertilization strategy. *Nature 349*, 227–229.

Peng, T.-H., and W.S. Broecker. 1991b. Factors limiting the reduction of atmospheric CO_2 by iron fertilization. *Limnology and Oceanography 36(8)*, 1919–1928.

Sarmiento, J.L., and J.C. Orr. Three dimensional ocean model simulations of the impact of Southern Ocean nutrient depletion on atmospheric CO_2 and ocean chemistry. *Limnology and Oceanography*, in press.

Stuiver, M., and H.G. Östlund. 1980. GEOSECS Atlantic radiocarbon. *Radiocarbon 22*, 1–24.

Stuiver, M., and H.G. Östlund. 1983. GEOSECS Indian Ocean and Mediterranean radiocarbon. *Radiocarbon 25*, 1–29.

Sverdrup, H.U., M.W. Johnson, and R.H. Fleming. 1942. *The Oceans, Their Physics, Chemistry and Biology*, Prentice-Hall, Englewood Cliffs, New Jersey.

Toggweiler, J.R., K. Dixon, and K. Bryan. 1989. Simulations of radiocarbon in a coarse-resolution world ocean model: 2. Distributions of bomb-produced carbon 14. *Journal of Geophysical Research 94*, 8243–8264.

The Role of Sea Ice Dynamics in Global Climate Change

W. D. Hibler, III

Introduction

The response of the polar regions to climatic change is significantly affected by the presence of sea ice. This sea ice cover is very dynamic and hence contains a variety of thicknesses, ranging from open water to pressure ridges tens of meters thick. In addition to undergoing deformation, the ice pack is typically transported from one region to another, with melting and freezing occurring at different locations. This transport tends to create net imbalances in salt fluxes into the ocean. On the large scale, an important factor here is the amount of ice drifting out of the Arctic Basin through the Fram Strait. Information on the variability of this export can be estimated from satellite data on ice drift. However, estimates of the thickness distribution of the ice are difficult to obtain. Moreover the spatial and temporal variability of the transport is substantial. There is also the issue that the mechanical characteristics of the ice cover, which dictate the amount of ice flowing out of the Arctic Basin, may vary in response to climate change, and hence may cause feedback effects that could affect the response of the system.

As a consequence it seems clear that while statistical models and observations of present-day ice extent are important for validating physically based models of sea ice growth, drift, and decay, relying solely on such observations to ascertain the sensitivity of the high latitudes to climatic variations may result in leaving out important feedbacks that could affect the response. Instead, it appears important to develop physically based models to successfully explain observed features of sea ice growth drift and decay and then to

make use of some version of these models in numerically based climate studies.

In this regard it is important to develop models that include ice drift and dynamics in climate studies and begin to examine the response of such models to simulated rather than observed atmospheric forcing. These comments need to be viewed in light of the fact that present climatic studies usually only include thermodynamic sea ice models which do not even come close to including the major sea ice processes relevant to climatic change. As a consequence, inclusion of any level of data-verified ice dynamics would appear to be an improvement provided the forcing wind fields of the atmospheric circulation models have an acceptable level of correctness. Some simple, robust sea ice dynamic models developed by the author and co-workers are discussed below.

Overall, it appears that there are three broad areas where determining the physical mechanisms is important for developing a physically based understanding of the response of the high latitudes to climate change. They are, broadly, sea ice dynamics and thermodynamics, the thickness distribution of sea ice and its evolution, and the coupling of sea ice with the ocean. Aspects of these features relevant to climatic change are discussed below. A more detailed pedagogical discussion of this material is given in Hibler and Flato (in press).

Sea Ice Dynamics

General Characteristics of Sea Ice Drift

The overall characteristic of ice drift is that on short time scales, it tends to follow the wind, with the drift approximately following the geostrophic wind with about one-fiftieth of the magnitude. This general feature of ice drift has been known for many years, beginning with Fridtjof Nansen's expeditions to the Arctic at the end of the 19th century. Since wind variations are larger than those of currents on a short time scale, this also means that, except for shallow regions, fluctuations in ice drift will be dominated more by wind than by currents. However, on a long time scale, the more steady currents can play a significant role.

These characteristics are illustrated in Figure 1, which shows short-term and long-term drift rates using a linear ice drift model. As can be seen, including current effects has only a minor effect on short-term variations. In examining cumulative drift over several years, however, significant differences occur if currents and ocean tilt are neglected. Basically, while smaller, current effects are steady. On the other hand, wind effects, while large, tend to fluctuate out over a long time period, leaving a smaller constant value.

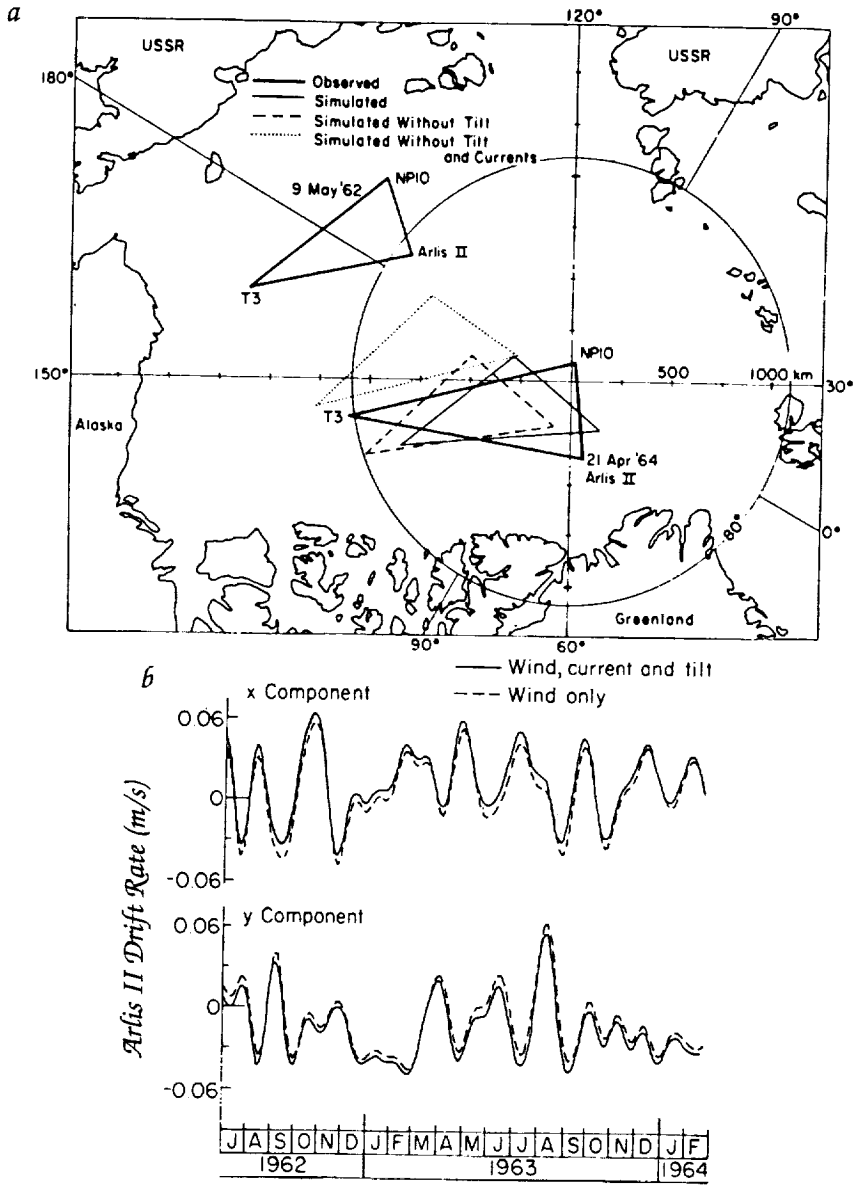

Figure 1. (a) Predicted and observed net drift of three drift stations, with and without current and ocean tilt effects; (b) effect of currents and ocean tilt on the 25-day smoothed predicted drift rate of the Arlis II ice island (from Hibler and Tucker, 1979; reproduced by courtesy of the International Glaciological Society).

Sea Ice Rheology

Sea ice motion results from a balance of forces that include wind and water drag, sea surface tilt, and ice interaction. The latter is a consequence of the large-scale mechanical properties of sea ice which include shear and compressive strengths but little tensile resistance.

In many cases the net effect of the ice interaction is to cause a force opposing the wind stress roughly in the manner shown in Figure 2. As a consequence, to achieve the same ice velocity under these circumstances, a larger wind stress more nearly parallel to the ice velocity is required. This feature is consistent with observations by Thorndike and Colony (1982), which show ice motion to be very highly correlated with geostrophic winds, with the ice drift rate decreasing somewhat in winter for the same geostrophic wind. However, examination of drift statistics shows higher winds producing an almost discontinuous shear near the coast. Moreover, observations show that while ice drift against the shore increases the ice thickness, the buildup is not unlimited.

As noted by Hibler (1979), both of these characteristics of discontinuous ice drift and a limit on near-shore ice buildup may be explained by nonlinear plastic ice rheologies. These rheologies have yield stresses that are relatively independent of strain rate. Hence far from shore, even though the ice is interacting strongly, there may be very low stress gradients since the stresses are relatively

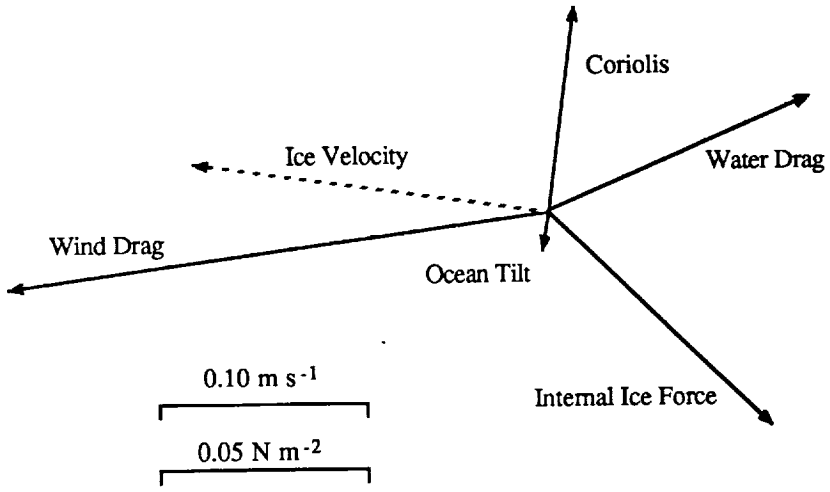

Figure 2. An estimate of the force balance on sea ice for winter conditions based on wind and water stress measurements (from Hunkins, 1975). In this balance the force due to internal ice stress is determined as a residual and the dashed line shows the ice velocity.

constant. Also this fixed yield stress will cause a discontinuous slippage at coastal points and prevent the ice from building up without bound. Without such a nonlinear rheology it is very difficult to obtain these features.

For climatic purposes probably the most important feature of the ice interaction is some type of resistance to ice buildup that does not drastically affect the ice drift. While this can be accomplished by a nonlinear plastic rheology including a shear strength, reasonable results may also be obtained by considering the ice to have only resistance to compression and no resistance to dilation or shearing. This "cavitating fluid" model has been compared by Flato and Hibler (1990) to a more complete plastic rheology with good success. The ice interaction term for the cavitating fluid model is characterized by the following stress tensor:

$$\sigma_{ij} = -P\,\delta_{ij} \tag{1}$$

where σ_{ij} represents the i and j components of the two-dimensional Cartesian stress tensor, P is ice pressure, and δ_{ij} is the Kronecker delta vehicle is equal to 1 if i = j and 0 otherwise.

This rheology can be simulated using the viscous-plastic scheme of Hibler (1979) or an iterative method, in which the free drift velocity field is calculated (i.e., by a simple analytic solution of the momentum equation neglecting the ice interaction term) and then this estimated field is corrected in an iterative manner to account for the compressive strength of ice. This correction can be accomplished by adding a small outward velocity component to each computational grid cell such that after correction all convergence is removed. After a number of interactions all convergence will be removed from the velocity field, simulating an incompressible ice cover. This correction procedure can also be formulated in terms of an internal ice pressure field, allowing specification of a failure strength beyond which plastic flow ensues. A particularly simple approximate solution to the cavitating fluid applicable to climate modeling was presented earlier by Flato and Hibler (1990).

The appropriate yield stress depends on how one is characterizing the ice thickness distribution as discussed below. However, if one is using a simple two-level sea ice model where H is the mean thickness and A is the compactness (i.e., fraction of area covered by ice), a reasonable yield stress P is given by

$$P = P^* H e^{-K(1-A)} \tag{2}$$

where K is 20, P^* is a fixed strength constant (say 2.75×10^4 N/m^2), and e is the exponential function. This strength formulation was originally proposed by Hibler (1979) and has been utilized by Flato

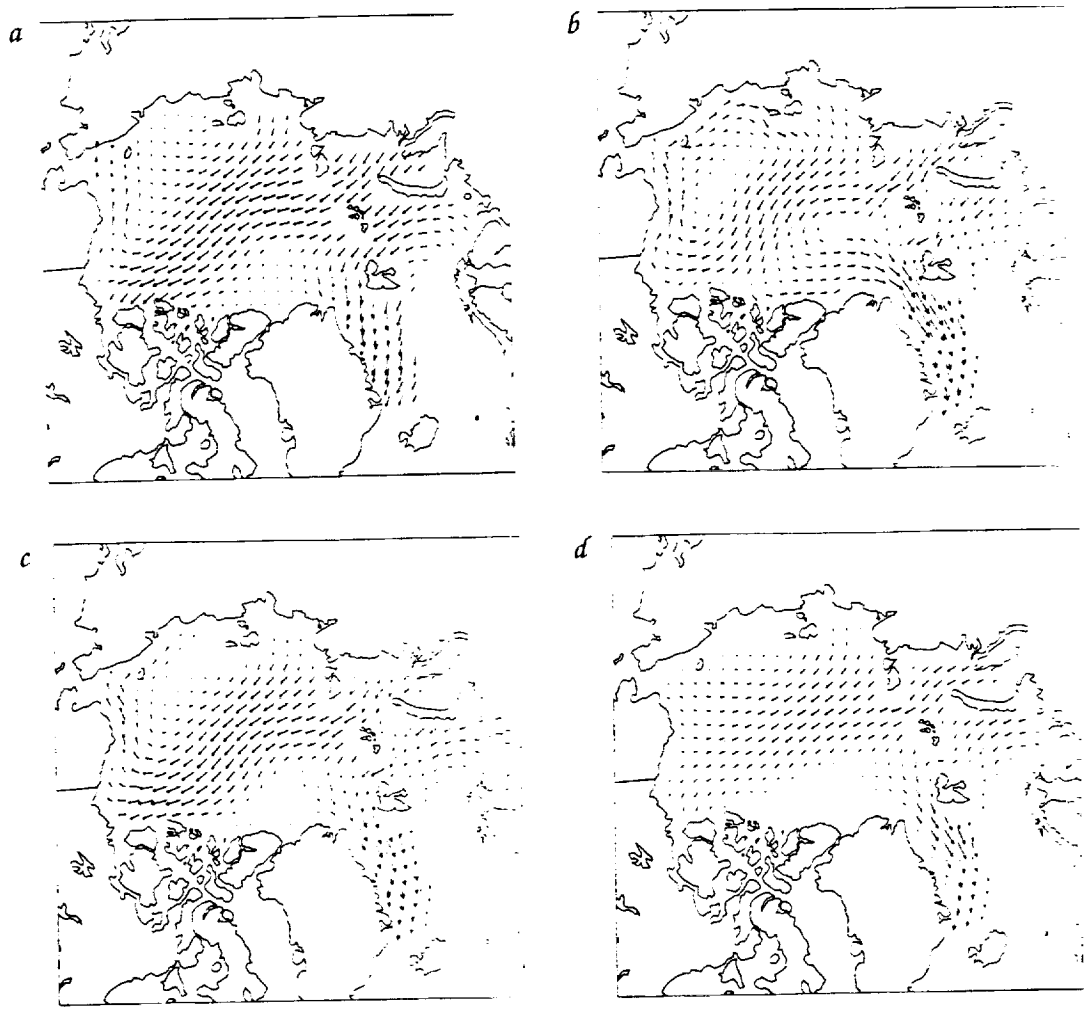

Figure 3. Average ice velocity fields calculated using forcing from March 1983: (a) free drift, (b) incompressible cavitating fluid, (c) cavitating fluid model with realistic compressive strength, (d) viscous-plastic, elliptical yield curve model with shear and compressive strength.

and Hibler (1990, in press). This procedure is easily extended to spherical coordinates as discussed by Flato and Hibler (in press).

An example of the use of the cavitating fluid model is shown in Figure 3, where we have applied the cavitating fluid correction to the free drift velocity field shown in Figure 3a. Two types of corrections are applied: In Figure 3b a totally incompressible sea ice drift field is shown, while in 3c we have assumed a constant 3-m-thick ice everywhere with a 2% fraction of open water. This, together with a yield strength constant P^* of 2.75×10^4 N/m^2, gives a maximum allowable two-dimensional pressure of 5.53×10^4 N/m. As can be seen,

including a maximum yield pressure modifies the velocity field somewhat inasmuch as some convergence is allowed. The main characteristic of both fields, however, is that the cavitating fluid approximation does not damp out the ice velocity field but rather simply modifies it to prevent convergence.

A more complete sea ice rheology, the viscous-plastic elliptical yield curve rheology, was presented by Hibler (1979). In this scheme plastic failure and rate-independent flow are assumed when the stresses reach the yield curve values represented by an ellipse in principal stress space. Here the compressive strength is given by the length of the ellipse while the shear strength is given by its width. Stress states inside the yield curve correspond to slow viscous creep deformation. This model has been widely used and produces realistic thickness and velocity patterns; however, its relative complexity and the dramatic slowdown in ice drift it produces when the wind fields are temporally smoothed (Flato and Hibler, 1990) make it somewhat less desirable for long-term climate studies. As a comparison, the velocity field calculated using this model with a constant ice strength of 5.53×10^4 N/m is shown in Figure 3d. Readily apparent here is the less robust velocity field that results from the increased resistance afforded by the shear strength. For a more complete comparison of a variety of plastic rheologies for the Arctic Basin, the interested reader is referred to Ipp et al. (in press), where a variety of nonlinear rheologies are compared, including a more exact solution to the cavitating fluid than presented above. It should be noted that the approximate solution discussed here compares very closely with exact, but less computationally efficient, solution methods (see, e.g., Flato and Hibler, in press).

It should be emphasized that the main reason for using some model such as the cavitating fluid in ice drift is to ensure that realistic ice transport occurs. When ice forms, heat is transferred to the atmosphere (i.e., by the latent heat of fusion). When the ice melts later at a different location, it absorbs this latent heat. Consequently, in some sense, the net effect of ice transport is to transfer heat from one location in the atmosphere to a different location. Ice transport effects are even more pronounced for the oceanic circulation in that where the ice freezes, most of the salt is expelled into the ocean. The ice is then transported to a different location, where it melts and produces a surface fresh water flux. These flux imbalances play a critical role in the salt budget and circulation of the Arctic Basin and may affect the global-scale ocean circulation by producing fluctuations in effective surface precipitation in the North Atlantic. Because of such considerations, climate studies must include ice motion as well as ice thermodynamics.

Ice Thickness Distribution

A key coupling between sea ice thermodynamics and ice dynamics is the ice thickness distribution. Ice thickness is an important factor in controlling deformation, which causes pressure ridging and creates open water. When combined with ice transport, these factors change the spatial and temporal growth patterns of the sea ice and, when coupled with mechanical properties of ice, can modify its response to climatic change.

Many features of the thickness distribution may be approximated by a two-level sea ice model (Hibler, 1979) where the ice thickness distribution is approximated by two categories: thick and thin. In this two-level approach the ice cover is broken down into an area A (often called the compactness), which is covered by ice with mean thickness H, and a remaining area 1 – A, which is covered by thin ice, which, for computational convenience, is always taken to be of zero thickness (i.e., open water).

For the mean thickness H and compactness A the following continuity equations are used:

$$\partial H/\partial t = -\partial(uH)/\partial x - \partial(vH)/\partial y + S_h \tag{3}$$

$$\partial A/\partial t = -\partial(uA)/\partial x - \partial(vA)/\partial y + S_A \tag{4}$$

where $A < 1$, u is the x component of the ice velocity vector, v the y component of the ice velocity vector, and S_h and S_A are thermodynamic terms and are described in Hibler (1979).

The thermodynamic terms in Equations (3) and (4) represent the total ice growth (S_h) and the rate at which ice-covered area is created by melting or freezing (S_A). The parameterization of the S_A term is particularly difficult to do precisely within the two-level model and generally represents one of the weaknesses of the model.

To allow this model to be integrated over a seasonal cycle, it is necessary to include some type of oceanic boundary layer or ocean model. The simplest approach (used for example by Hibler and Walsh, 1982) is to include a motionless fixed depth mixed layer (usually 30 m in depth). With this model, any heat remaining after all the ice is melted is used to warm the mixed layer above freezing. Under ice growth conditions, on the other hand, the mixed layer is cooled to freezing before the ice forms. Another approach that treats vertical penetrative convection processes much better is to include some type of one-dimensional mixed layer. Such an approach, using a Kraus-Turner-like mixed layer, was carried out by Lemke et. al (1990) for the Weddell Sea. Another approach is to utilize a complete oceanic circulation model which also allows lateral heat transport in the ocean. The latter approach was used by Hibler and Bryan (1987)

in a numerical investigation of the circulation of an ice-covered Arctic Ocean. In this study, a two-level dynamic-thermodynamic sea ice model was coupled to a fixed-level baroclinic ocean circulation model. In this ice-ocean model the upper level was taken to be 30 m thick and, as in the motionless case, was not allowed to drop below freezing if ice was present. Inclusion of some type of penetrative convection in a similar ice-ocean circulation model is an item of high priority for future research and is presently being pursued.

A more precise theory of ice thickness distribution may be formulated by postulating an areal ice thickness distribution function and developing equations for the dynamic and thermodynamic evolution of this distribution. In this case, a probability density g(H)dH is defined to be the fraction of area (in a region centered at position x at time t) covered by ice with thickness between H and H + dH. This distribution evolves in response to deformation, advection, growth, and decay. Neglecting lateral melting effects, Thorndike et al. (1975) derived the following governing equation for the thickness distribution:

$$\frac{\partial g(H)}{\partial t} + \nabla \bullet \left[\underline{u} g(H)\right] + \frac{\partial \left[f_g g(H)\right]}{\partial H} = \psi \qquad (5)$$

where $\underline{u}$ is the vector ice velocity with x and y components u and v, ∇ is the gradient operator, f_g is the vertical growth (or decay) rate of ice of thickness H, and ψ is a redistribution function (depending on H and g) that describes the creation of open water and the transfer of ice from one thickness to another by rafting and ridging. Except for the last term on the left-hand side and ψ on the right-hand side, Equation (5) is a normal continuity equation for g(H). The last term on the left-hand side can also be considered a continuity requirement in thickness space since it represents a transfer of ice from one thickness category to another by the growth rates. An important feature of this theory is that it presents an "Eulerian" description in thickness space. In particular, growth occurs by rearranging the relative areal magnitudes of different thickness categories.

This multilevel ice thickness distribution theory represents a very precise way of handling the thermodynamic evolution of a continuum composed of a number of ice thicknesses. However, the price paid for this precision is the introduction of a complex mechanical redistributor. In particular, to describe the redistribution one must specify what portion of the ice distribution is removed by ridging, how the ridged ice is redistributed over the thick end of the thickness distribution, and how much ridging and open water creation occur for an arbitrary two-dimensional strain field, including shearing as well as convergence or divergence. In selecting a redistributor

one can be guided by the conservation conditions that ψ renormalizes the g distribution to unity due to changes in area and that ψ does not create or destroy ice but merely changes its distribution. An additional consistency condition can be imposed if one asserts that all the energy lost in deformation goes into pressure ridging and that the energy dissipated in pressure ridges is proportional to the gravitational energy.

A redistribution function that satisfies these constraints may be constructed (for an explicit form see Hibler, 1980) by allowing open water to be created under divergence and ridging to occur under convergence. Within this formalism ridging occurs by the transfer of thin ice to thicker categories, assuming a certain amount of ridging and hence open water created under pure shear or more generally under an arbitrary deformation state. This "energetic consistency" condition will affect the thermodynamic growth via open water fractions and hence the total ice created.

The main relevance of the variable thickness distribution to climate modeling is its more precise treatment of the growth of ice. A comparison of the two-level and multilevel approaches to modeling the dynamic-thermodynamic evolution of an ice cover will be presented below. However, here we note that the ice thickness is considerably greater with the multilevel model due to its more realistic treatment of the thickness distribution.

Sea Ice Thermodynamic Models

Sea ice grows and decays in response to long- and shortwave radiation forcing, to air temperature and humidity via turbulent sensible and latent heat exchanges, and to heat conduction through the ice. The heat conduction is significantly affected by the amount of snow cover on the ice and by the brine remaining in the ice after it has frozen. These internal brine pockets cause the thermodynamic characteristics of sea ice to be very much different than those of fresh water ice of the same thickness.

Many features of the thermal processes responsible for sea ice growth and decay can be identified from semiempirical studies of ice breakup and formation of relatively motionless lake ice and sea ice (e.g., Langleben, 1971, 1972; Zubov, 1943). Overall, the two dominant components of the surface heat budget relevant to sea ice growth and freezing are the shortwave radiation during melting conditions and sensible and radiative heat losses during freezing. Observations of fast ice (relatively motionless ice attached to land) at the border of the Arctic Ocean indicate that once the initial stages of breakup (snow cover melt and formation of melt ponds) have

passed, the remaining decay of a stationary ice cover is almost entirely due to the shortwave radiation incident on the ice surface (Langleben, 1972). However, at the initial stages of breakup and decay, the sensible heat flux plays an important role (when the air temperature rises to ~ 0°C) in causing rapid melting of the surface snow cover. This melting forms melt ponds (Langleben, 1971), which reduce the albedo and greatly enhance the rate of ice melt. After only a few weeks, drainage canals and vertical melt holes develop, and the characteristic appearance of a summer ice cover evolves, with melt ponds and surrounding smooth hummocks. Once these melt ponds have formed, the remaining decay is dominated by the radiation absorbed by open water.

As is clear from this discussion, the decay of sea ice in nature is rather critically affected by the amount of open water, which, because of its low albedo, can absorb much more radiation than the ice. On motionless ice sheets, the open water is present only through melt ponds or holes. However, in an actual dynamic variable-thickness ice cover, as occurs almost everywhere in the polar regions, the growth and decay of sea ice can be substantially affected by spatial thickness variations. Perhaps the most obvious example is the effect of open water on the adjacent pack ice. During melting conditions the radiation absorbed by leads can contribute to lateral melting by ablation at the edges of ice floes.

A number of sea ice thermodynamic models have been used in the past, ranging from the simple empirical models of Zubov (1943) and Anderson (1961) to complex numerical models that compute the surface heat budget (Parkinson and Washington, 1979) and the conduction through an inhomogeneous ice sheet (Maykut and Untersteiner, 1971).

Equilibrium Thermodynamic Models

While it is possible to construct simpler thermodynamic models that capture the essence of sea ice growth and decay (see Thorndike, this volume), what is usually done in climate modeling is to make use of an equilibrium ice/snow system in conjunction with a complete surface heat budget. One can solve this system iteratively and come up with an ice growth rate. The basic idea is illustrated in Figure 4, in which the steady state temperature profile is shown. Assuming no melting at the snow ice interface, the amount of heat going through this interface must be the same in the snow and the ice so that

$$(T_i - T_0)\frac{\kappa_s}{H_s} = \frac{\kappa_i}{H_i}(T_B - T_i) \qquad (6)$$

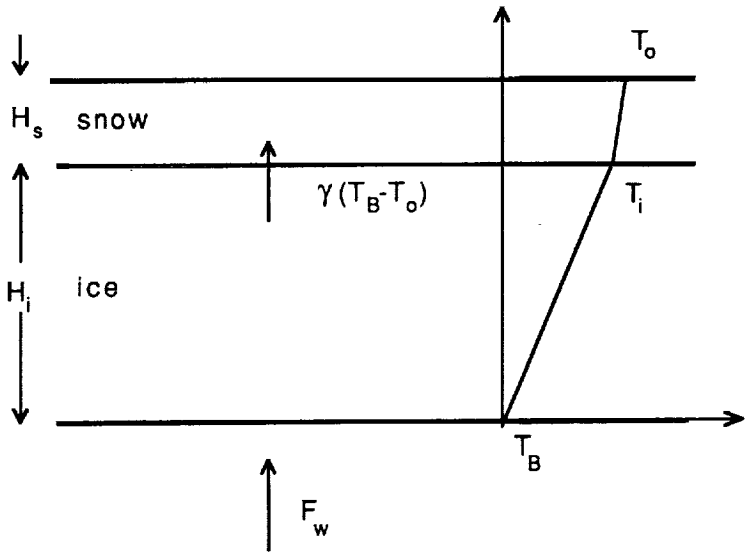

Figure 4. Sketch of combined snow and ice system used in equilibrium thermodynamic sea ice model. F_w is oceanic heat flux; other terms are defined in the text.

where T_i is the temperature of the ice at the snow-ice interface, T_0 is the surface temperature of the snow, T_B is the water temperature, κ_i and κ_s are the thermal conductivities of ice and snow, and H_i and H_s are the thicknesses of the ice and snow.

This equation allows us to solve for T_i in terms of T_B and T_0. Substituting the resulting expression into the conductive flux through the ice, we obtain

$$(T_i - T_0)\frac{\kappa_s}{H_s} = \gamma(T_B - T_0) \tag{7}$$

where $\gamma = \dfrac{\kappa_i \kappa_s}{[\kappa_s H_i + \kappa_i H_s]}$ is the effective conductivity.

The complete surface heat budget equation, with a sign convection such that fluxes *into* the surface are considered positive, then becomes

$$(1-\alpha)F_s + F_l + D_1 V_g(T_a - T_0) + D_2 V_g[q_a(T_a) - q_s(T_0)] - D_3 T_0^4 + (\gamma)(T_B - T_0) = 0 \tag{8}$$

where α is the surface albedo, T_a is the air temperature, γ is the effective conductivity, V_g is the wind speed, q_a is the specific humidity of the air, q_s is the specific humidity of the ice surface, and F_s

and F_l are the incoming shortwave and longwave radiation terms. The constants D_1 and D_2 are bulk sensible and latent heat transfer coefficients, and D_3 is the Stefan-Boltzmann constant times the surface emissivity. The equation is usually solved iteratively (see, e.g., Appendix B of Hibler, 1980, for details and numerical values of various constants) for the ice surface temperature. The conduction of heat through the ice is used to estimate ice growth using

$$\gamma(T_b - T_0) + F_w = \rho_i H \frac{dH_i}{dt} \tag{9}$$

where F_w is the oceanic heat flux, ρ_i is the ice density, H_i is the ice thickness, and dH_i/dt is the rate of change of ice thickness. When the calculated surface temperature of the ice is above melting, it is then set equal to melting, and the imbalance of surface flux is used to melt ice.

Effect of Internal Brine Pockets and Snow Cover

Apart from the absence of dynamics, the global thermodynamic models mentioned above are still somewhat simplified in nature, the main simplification being that no internal melting due to brine pockets in the ice has been considered. In particular, in sea ice the density, specific heat, and thermal conductivity are all functions of salinity and temperature (the dependence on temperature is indirectly also due to the salinity). These dependencies are caused by salt trapped in brine pockets that are in phase equilibrium with the surrounding ice. The equilibrium is maintained by volume changes in the brine pockets. A rise in temperature causes the ice surrounding the pocket to melt, diluting the brine and raising its freezing point to the new temperature. Because of the latent heat involved in this internal melting, the brine pockets act as a thermal reservoir, retarding the heating and cooling of the ice. Since the brine has a smaller conductivity and a greater specific heat than the ice, these parameters change with temperature.

Maykut and Untersteiner (1971) developed a time-dependent thermodynamic model for level multiyear sea ice and carried out a variety of calculations that yielded considerable insight into the growth and decay of sea ice. A simplified model that reproduced most of the Maykut-Untersteiner results was proposed by Semtner (1976). The Semtner model assumed that sea ice could be represented as a matrix of brine pockets surrounded by ice where melting can be accomplished internally by enlarging the brine pockets rather than externally by decreasing the thickness. As a consequence, for the same forcing sea ice can have a substantially greater equilibrium thickness than fresh water ice.

Based on this "brine damping" concept, Semtner (1976) proposed a simple model in which the snow and ice conductivities were fixed. In this model the salinity profile does not have to be specified. To account for internal melting, an amount of penetrating radiation was stored in a heat reservoir without causing ablation. Energy from this reservoir was used to keep the temperature near the top of the ice from dropping below freezing in the fall. Using this simplified model, Semtner was able to reproduce many aspects of Maykut and Untersteiner's model results within a few percent.

For an even simpler diagnostic model, Semtner proposed that a portion of the penetrating radiation I_0 be reflected away. The remainder of I_0 was applied as a surface energy flux. In addition, to compensate for the lack of internal melting, the conductivity was increased to allow greater winter freezing. In the simplest model, linear equilibrium temperature gradients are assumed in both the snow and ice. Since no heat is lost at the snow-ice interface, the heat flux is uniform in both snow and ice.

The results of Semtner's prognostic and diagnostic models are compared to Maykut and Untersteiner's results in Figure 5. This figure also shows the importance of the assumed penetration of radiation which causes internal melting. By allowing no radiation to penetrate, the internal melting is mitigated and the radiation instead is used to melt the ice, causing a reduced thickness. Note that while the 0-layer diagnostic model reproduces the mean thickness well, the amplitude and phase of the seasonal variation of thickness are somewhat different from those of the 3-layer prognostic model. This simplest diagnostic model has taken on special significance for numerical simulations of sea ice because almost continual ridging and deformation make it difficult to record the thermal history of a fixed ice thickness. Selected thermodynamic-only simulations using this model will be discussed in the next section.

Finally, because of the problems with an excessive seasonal cycle in the simplest Semtner model, it may be useful to employ some type of brine damping in sea ice models that are used in climate studies. However, the difficulty here is that when a full dynamic model is used, the advection of ice makes it difficult to record the internal temperature characteristics of the ice. An approach that improves the summer thermodynamic response of the ice cover is to include a brine pocket heat storage term in an equilibrium one-level model. Such an approach was carried out by Flato (1991) in a numerical investigation of a variable-thickness sea ice model. While his approach does not take into account the heat capacity of the ice, it does create a much more realistic summer cycle in that it retards spring melting and fall freezing.

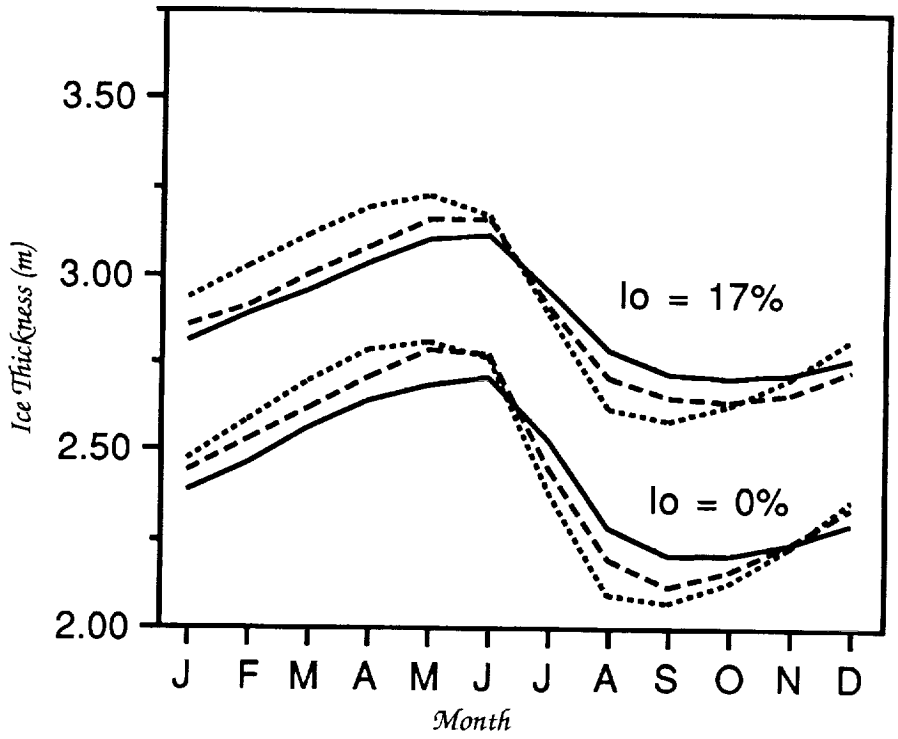

Figure 5. Annual thickness cycles of three thermodynamic sea ice models for the cases of 0 and 17% penetrating radiation. Solid line, Maykut-Untersteiner model; dashed line, Semtner 3-layer model; dotted line, Semtner 0-layer model.

The role of snow cover in modifying the thermodynamic growth of sea ice was also investigated by Maykut and Untersteiner (1971) and Semtner (1976). The thermal conductivity of snow is considerably less than that of ice; however, the albedo of snow is much higher than that of ice. Lower conductivity implies less ice growth, whereas higher albedo implies less summer melt. These conflicting processes combine to produce little change in mean annual ice thickness for snowfall rates less than about 80 cm/yr. Since this is much higher than the snowfall rate for most of the Arctic, snow cover can be expected to have little effect on the amount and distribution of sea ice. This notion is confirmed by recent dynamic-thermodynamic simulations with a multilevel sea ice model that included the effect of snowfall (Flato, 1991).

Model Simulations of Arctic Sea Ice

Sea ice in climate models has generally been included simply as a motionless sheet, in some cases using a thermodynamic growth model to calculate the surface temperature and ice thickness. As

discussed above, neglecting ice dynamics not only removes the lateral heat and salt transport capabilities of the ice pack, it also leads to unrealistic spatial patterns of thickness buildup and air-sea heat fluxes. In this section we will discuss some numerical model results to illustrate a few of these effects. In particular we will compare free drift (no ice interaction), the cavitating fluid rheology, and the elliptical yield curve, viscous-plastic rheology in simulations employing climatological wind and thermodynamic forcing (Flato and Hibler, 1990). For comparison we will also show the result of a thermodynamics-only simulation in which the ice cover is assumed to be a motionless, unbroken sheet.

Perhaps the most illustrative comparison of these simulations is provided by the seasonal equilibrium thickness contours (Figure 6) shown here for the end of March. The lack of ice interaction in the free drift case leads to unreasonable thickness buildup near the coasts after only a couple of months and is thus clearly undesirable for climate studies. Both the cavitating fluid and viscous-plastic models produce thickness buildup patterns which are roughly similar to observations (e.g., Bourke and Garrett, 1987), with the thickest ice (4–6 m) off the Canadian Archipelago and North Greenland coast. The similarity here reinforces the notion that, to lowest order, the role of ice interaction is to prevent excessive convergence when ice is driven against a coast. Shear strength in the viscous-plastic case acts primarily to slow the ice drift and impede outflow through the Fram Strait (Flato and Hibler, 1990), although it does modify the thickness buildup pattern somewhat. We might note, however, that including shear strength in the ice cover modifies the curl of the wind stress applied to the ocean and thus influences the barotropic ocean circulation, a modification which may be important in long-term ice-ocean simulations. It is also interesting that the net ice growth patterns (contours of net ice growth at a point over a year) are almost unaffected by shear strength in the ice cover (Figure 7), and, since net growth corresponds to a net source of salt at the ocean surface, the baroclinic ocean circulation should be impacted little. In addition to the unrealistic thickness patterns, it is this last issue which makes the thermodynamics-only model unsuitable for long-term climate studies with a coupled ice-ocean model. The problem here is that in a thermodynamics-only model the ice grows and melts in place, and hence, over an annual cycle, there is no net salt flux to the ocean. Atmospheric general circulation models can tolerate coupling to a thermodynamics-only sea ice model since the principal bottom boundary condition is temperature; however, some parameterization of leads is necessary if the fluxes of heat and water vapor are to be at least crudely included.

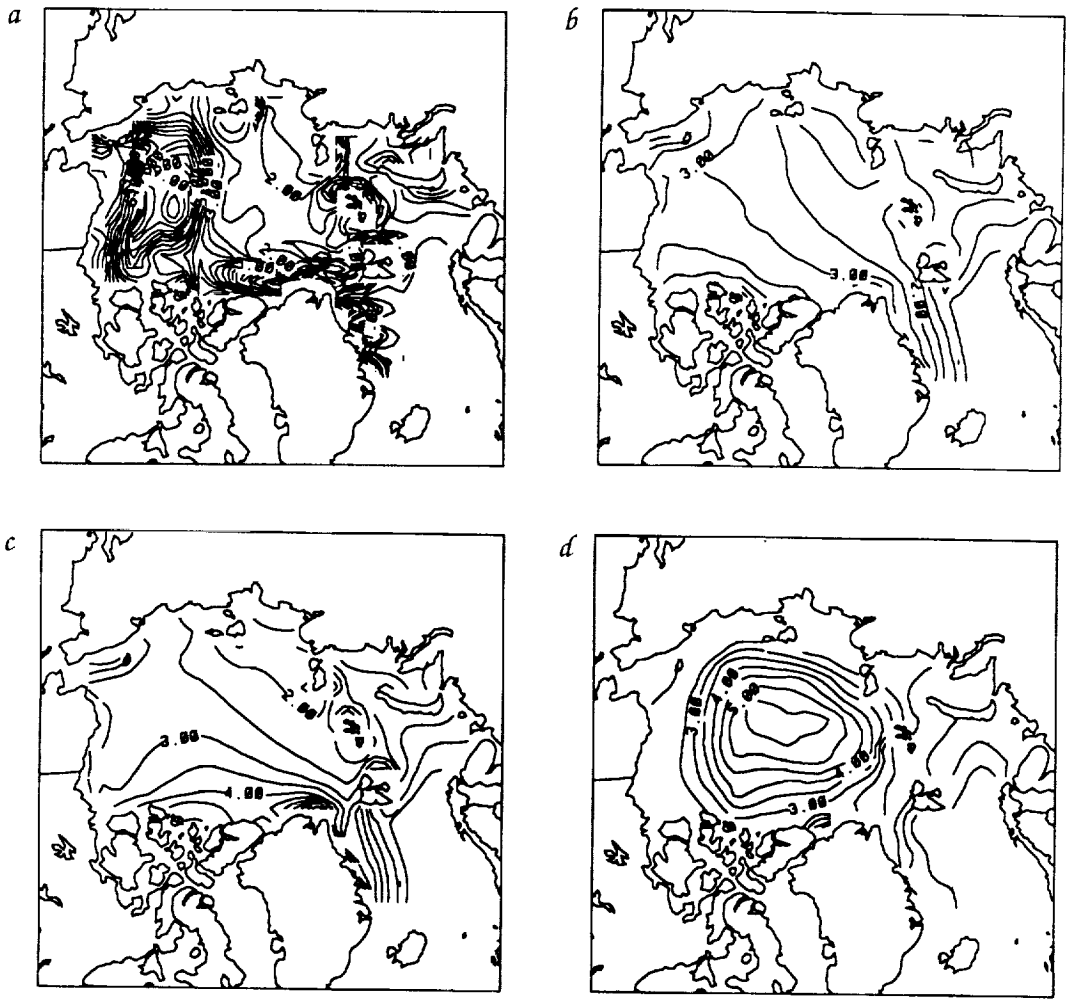

Figure 6. Equilibrium March thickness fields in the Arctic calculated using climatological forcing: (a) free drift model, (b) cavitating fluid model, (c) viscous-plastic, elliptical yield curve model, (d) thermodynamic-only model. Contours are in meters with a half-meter contour interval.

The multilevel model approach represents an improvement over the two-level model since the proportion of ice in a number of thickness categories is kept track of and the thermodynamic growth rate of each category is calculated separately. Furthermore, the multilevel case allows the ice strength to be parameterized in terms of the deformational work done during ridging (Rothrock, 1975). The effect of the improved representation of thermodynamic growth is illustrated in Figure 8, which shows the thickness field calculated by the multilevel model using the same strength parameterization as the two-level model. The increase in overall thickness here is due in part to the improved resolution of thin ice and open water, for which the

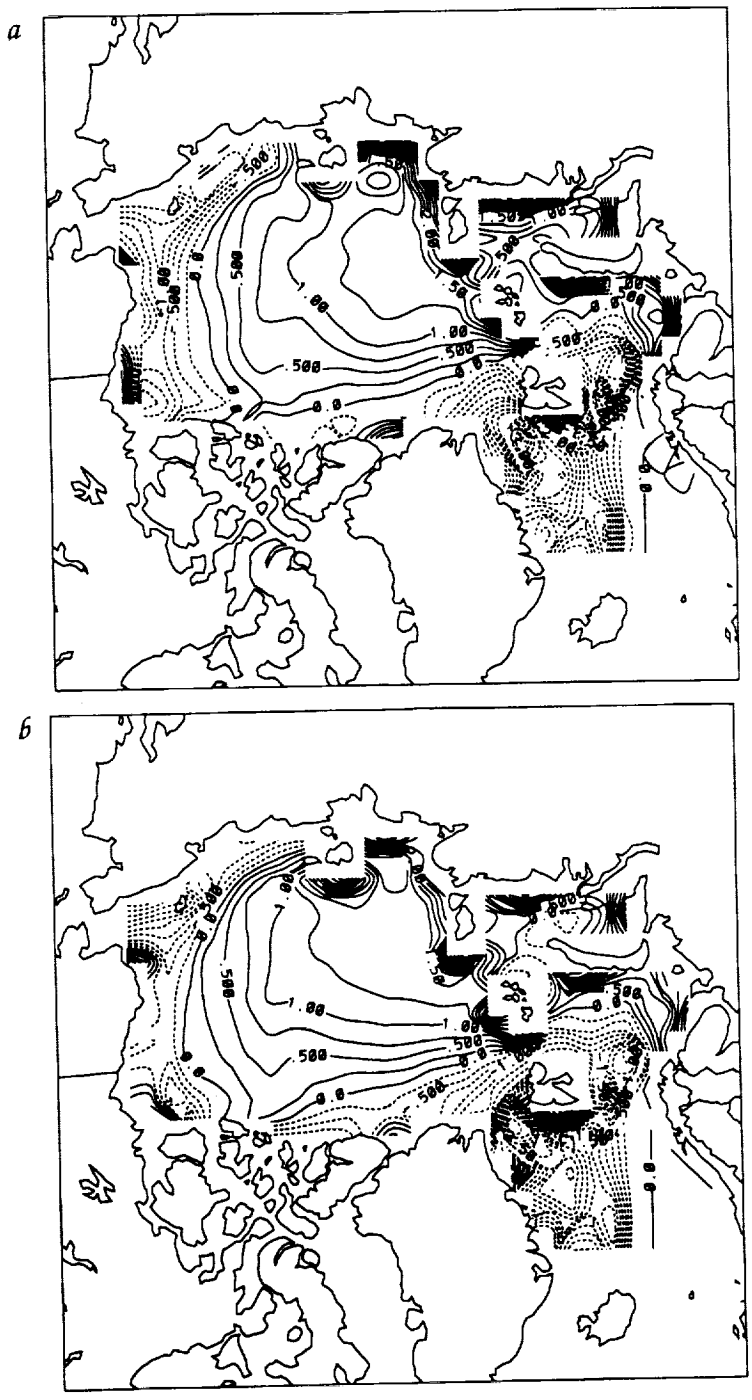

Figure 7. Net annual ice growth fields (in meters of ice per year) calculated using climatological forcing: (a) viscous-plastic, elliptical yield curve model, (b) cavitating fluid model. The contour interval is 0.25 m of ice per year.

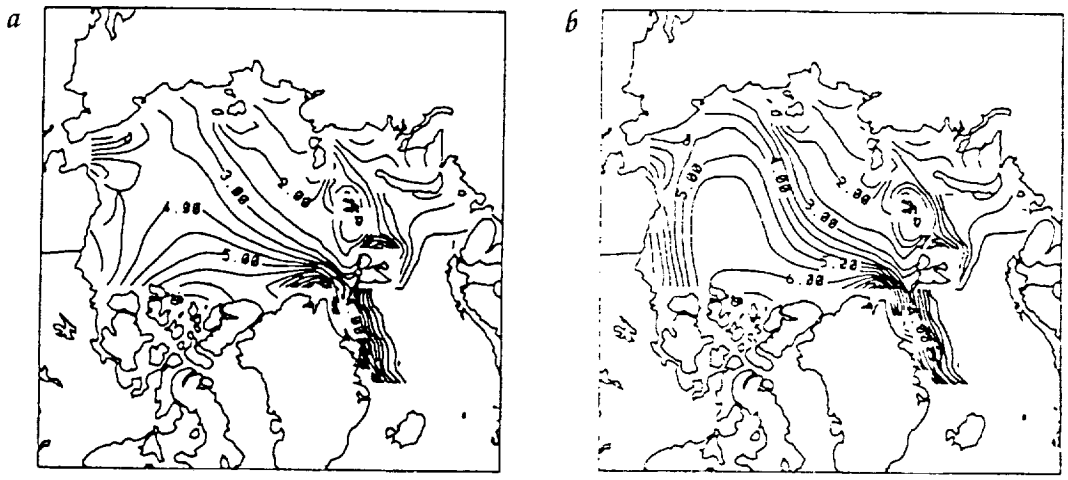

Figure 8. Equilibrium March thickness fields calculated using (a) climatological forcing, together with (b) a multilevel sea ice model with two-level model strength parameterization. Contours are in meters with a half-meter contour interval.

growth rate is very high, and redistribution from thin to thick ice representing the formation of ridges during deformation. It is likely that the complexity and computational demands of the multilevel model are unjustified for climate studies at this point, although a simpler three- or four-level model (currently under development) would be a significant improvement over the two-level scheme.

Sensitivity of Sea Ice Models to Climate Change

In this section we will demonstrate the sensitivity of the modeled sea ice cover to changes in atmospheric forcing which might accompany changes in global climate. Aside from dramatic alterations in atmospheric circulation patterns, the most significant impact on the ice cover will likely be due to changes in air temperature and cloud cover. An increase in air temperature results in greater sensible and latent heat fluxes and incident longwave radiation, all of which inhibit ice growth. An increase in the cloud cover, on the other hand, reduces the incoming shortwave radiation while increasing the longwave flux. These effects will be investigated here by examining several simulations of the Arctic ice cover using the two-level dynamic-thermodynamic sea ice model with forcing fields covering the period 1981–83.

The four simulations we will discuss here are the standard or unperturbed run, runs in which the cloud cover was increased or decreased by 20%, and a run in which the air temperature was increased by 1°C. Time series of total ice volume and ice extent (the

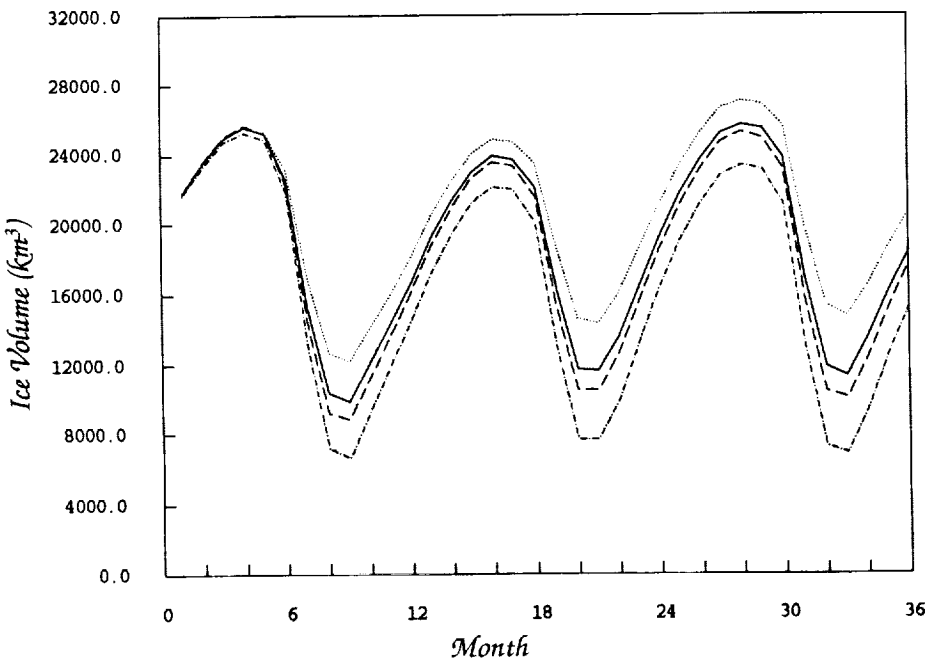

Figure 9. Total ice volume and ice extent (area enclosed by 15% compactness contour) time series calculated using two-level viscous-plastic model and forcing fields from 1981–83. Results are shown for (solid line) a standard simulation, (dotted line) a case with cloud cover increased by 20%, (dashed line) a case with cloud cover decreased by 20%, and (dot-dashed line) a case with a 1°C increase in air temperature.

area enclosed by the 15% compactness contour) are plotted in Figure 9 and show the sensitivity to each of these changes. The increase in total ice volume and summer ice extent in the increased cloud cover case points out that the dominant role of clouds is to control the incoming shortwave radiation—their contribution to longwave radiation being secondary. It is also apparent from the asymmetry of the response to increasing and decreasing the cloud cover that this effect is rather nonlinear. A significant decrease in both ice volume and summer ice extent is seen to accompany a 1°C rise in air temperature; in fact, the summer ice volume is reduced by almost a third. An increase in air temperature of about 4°C (a value obtained by Manabe and Stouffer, 1980, for a doubling of CO_2) is sufficient to almost eliminate the summer ice cover. What is missing here, of course, is the feedback between the increase in open water area and the amount of cloud cover. The increase in open water area, not only in the peripheral seas but also in the central pack, is illustrated by the August 1983 compactness fields for the four simulations (Figure 10). A general increase in cloud

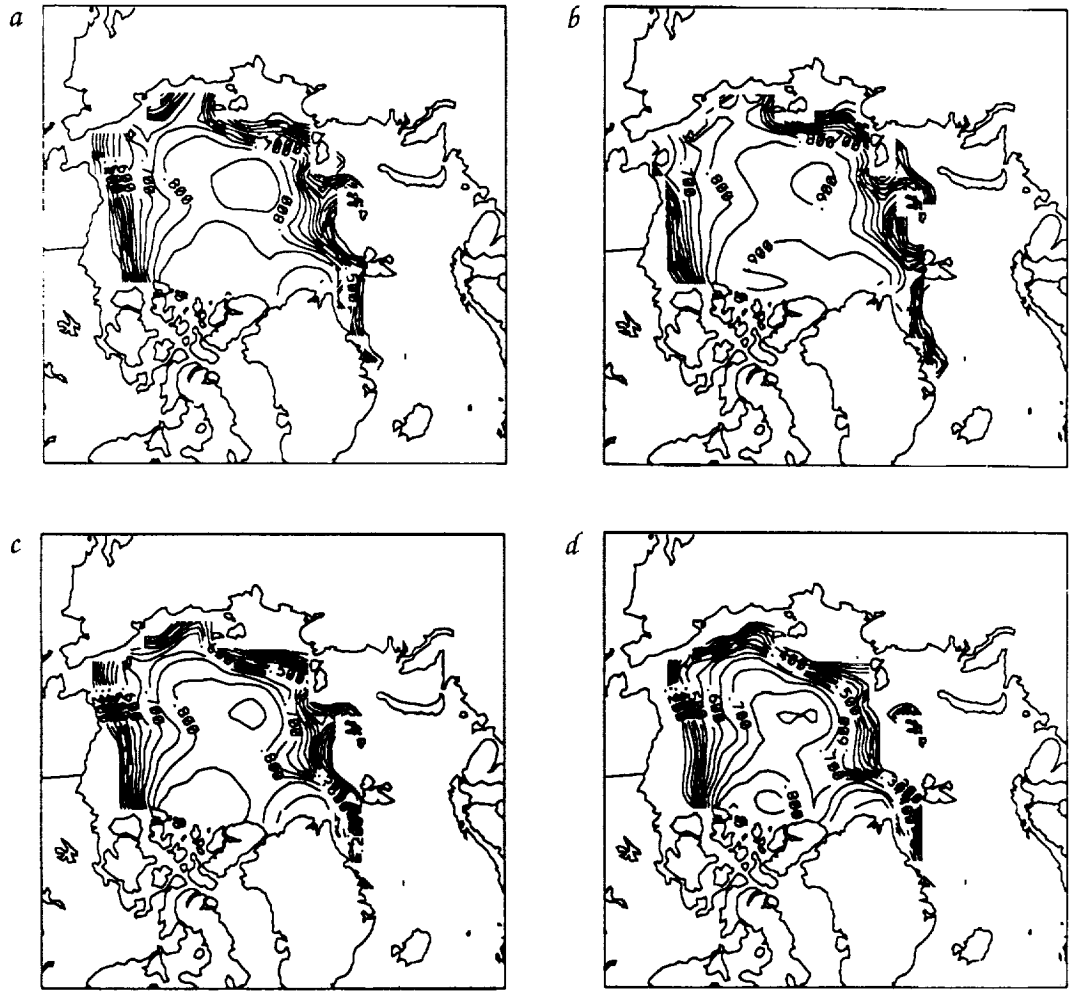

Figure 10. Compactness fields calculated by the two-level model for August 1983: (a) standard simulation, (b) 20% increase in cloud cover, (c) 20% decrease in cloud cover, (d) 1°C increase in air temperature.

cover would be expected in the warming case due to the increased availability of water vapour from leads, and this, based on the cloud sensitivity results, may counteract the effect of increased air temperature.

We might note here that the ice edge location, particularly in the eastern Arctic, is somewhat too far north in these simulations—a shortcoming of the two-level model. The ice edge position is somewhat better in the multilevel model case; however, the sensitivity to clouds and warming is about the same. We should also point out here that the shape and interannual variability of the ice edge in the

Barents and Greenland seas is controlled primarily by upwelling of heat from the ocean. To properly simulate the ice cover in this climatically important region requires a coupled ice-ocean model which not only provides realistic ocean currents (to properly represent the lateral transport of heat) but also includes a sufficiently detailed parameterization of the vertical processes to bring the heat from the deeper ocean to the surface at the correct location.

Concluding Remarks

Because of almost constant motion and deformation, the dynamics and thermodynamics of sea ice are intrinsically coupled. In addition, the ice and ocean circulation are tied together by the freezing and melting of ice, which causes salt and fresh water fluxes into the ocean, and ice transport, which yields unbalanced fluxes. As a consequence, understanding the response of the high latitudes to climatic change requires considering the coupled ice-ocean system (including ice interaction) in the polar regions. Results and theory reviewed here have indicated the complexity of different thermodynamic and dynamic effects and the role they can play in air-sea interaction. This complexity makes it difficult to guess the correct ad hoc treatment of sea ice to use in climate models. Instead, the results emphasize the importance of including a more realistic treatment of sea ice vis-á-vis a fully coupled, ice interaction–based, dynamic-thermodynamic sea ice model. These models at least contain the main first-order aspects of the sea ice system, whereas simple thermodynamics-only models clearly do not.

By coupling such models with treatments of the ocean, we may obtain quantitative insights. It also appears that due to the variety of complex dynamic processes, specifying ice fluxes and transport for use in ocean circulation modeling will leave out many major feedbacks that affect climatic change.

References

Anderson, D.L. 1961. Growth rate of sea ice. *Journal of Glaciology 3*, 1170–1172.

Bourke, R.H., and R.P. Garrett. 1987. Sea ice thickness distribution in the Arctic Ocean. *Cold Region Science and Technology 13*, 259–280.

Flato, G.M. 1991. *Numerical Investigation of the Dynamics of a Variable Thickness Arctic Ice Cover.* Ph.D. thesis, Thayer School of Engineering, Dartmouth College, Hanover, New Hampshire.

Flato, G.M., and W.D. Hibler, III. 1990. On a simple sea ice dynamics model for climate studies. *Annals of Glaciology 14*, 72–77.

Flato, G.M., and W.D. Hibler, III. On modeling pack ice as a cavitating fluid. *Journal of Physical Oceanography*, in press.

Hibler, W.D., III. 1979. A dynamic thermodynamic sea ice model. *Journal of Physical Oceanography 9*, 815–846.

Hibler, W.D., III. 1980. Modeling a variable thickness sea ice cover. *Monthly Weather Review 108*, 1942–1973.

Hibler, W.D., III, and K. Bryan. 1987. Ocean circulation: Its effect on seasonal sea ice simulations. *Science 224*, 489–492.

Hibler, W.D., III, and G.M. Flato. Sea ice models. In *Climate Systems Modeling* (K. Trenberth, ed.), Cambridge University Press, Cambridge, England, in press.

Hibler, W.D., III, and W.B. Tucker. 1979. Some results from a linear viscous model of the Arctic ice cover. *Journal of Glaciology 4*, 110.

Hibler, W.D., III, and J.E. Walsh. 1982. On modeling seasonal and interannual fluctuations of arctic sea ice. *Journal of Physical Oceanography 12*, 1514–1523.

Hunkins, K. 1975. The oceanic boundary layer and stress beneath a drifting ice floe. *Journal of Geophysical Research 80*, 3425–3433.

Ip, C.F., W.D. Hibler, III, and G.M. Flato. On the effect of rheology on seasonal sea ice simulations. *Annals of Glaciology*, in press.

Langleben, M.P. 1971. Albedo of melting sea ice bottomside features in the Denmark Strait. *Journal of Geophysical Research 79*, 4505–4511.

Langleben, M.P. 1972. Decay of an annual cover of sea ice. *Journal of Glaciology 11*, 337–344.

Lemke, P., W.B. Owens, and W.D. Hibler, III. 1990. A coupled sea ice–mixed layer–pycnocline model for the Weddell Sea. *Journal of Geophysical Research 95*, 9513–9526.

Manabe, S., and R. Stouffer. 1980. Sensitivity of a global climate model to an increase of CO_2 concentration in the atmosphere. *Journal of Geophysical Research 85*, 5529–5554.

Maykut, G.A., and N. Untersteiner. 1971. Some results from a time dependent, thermodynamic model of sea ice. *Journal of Geophysical Research 76*, 1550–1575.

Parkinson, C.L., and W.M. Washington. 1979. A large-scale numerical model of sea ice. *Journal of Geophysical Research 84*, 311–337.

Rothrock, D.A. 1975. The energetics of the plastic deformation of pack ice by ridging. *Journal of Geophysical Research 80*, 4514–4519.

Semtner, A.J., Jr. 1976. A model for the thermodynamic growth of sea ice in numerical investigations of climate. *Journal of Physical Oceanography 6*, 379–389.

Thorndike, A.S., and R. Colony. 1982. Sea ice motion in response to geostrophic winds. *Journal of Geophysical Research 87*, 5845–5852.

Thorndike, A.S., D.A. Rothrock, G.A. Maykut, and R. Colony. 1975. The thickness distribution of sea ice. *Journal of Geophysical Research 80*, 4501–4513.

Zubov, N.N. 1943. *Arctic Ice*. Translation, National Technical Information Service (AD426972), Washington, D.C., 491 pp.

Land Surface Interaction

Robert E. Dickinson

Land and Climate Modeling

Historically, climate models have evolved out of general circulation models (GCMs) of the atmosphere, developed by meteorologists, and radiative convective models, developed by atmospheric physicists. These areas are my background. Land was thought of simply as a lower boundary condition to be put in as simply as possible. This was an implicit message in all of my academic training and was the basis for my first attempts to be involved in climate modeling. Conversely, many other disciplines have studied the role of soils and vegetation over land in great detail but traditionally with a very local focus, and with the atmosphere and radiation prescribed from observations rather than as part of the model.

When GCMs were originally developed, requirements for accuracy and realism in the physical descriptions were much lower than they have become today. I recall conversations two decades ago where a model simulation of the tropical tropopause 40 degrees warmer than reality was regarded as satisfactory. Now only a few degrees is of considerable concern, a discrepancy small enough that it could result as readily from errors in the data themselves or their interpolation or the model layer structure as from errors in the model treatment of radiation. Except for the basic fluid equations, physical treatments in the original GCMs were all generally quite simple, represented by a single equation and/or describable in one or two sentences. Land has been no exception. S. Manabe in 1969 first moved from the viewpoint of land as a boundary condition to land as an interactive part of the system with his "bucket" hydrology model; all

land points had a water-holding capacity with any surplus going into runoff, and otherwise the storage was determined by the balance between precipitation or snowmelt and evapotranspiration. Surface albedos have been simply specified numerical values, often the same value for all land points, and the aerodynamic drag coefficients (determined in principle by surface roughness) have had one value for land and one for ocean.

Demands for better answers and increasing maturity of the science are driving climate models to much more detailed treatments of physical processes, much greater emphasis on validation of the assumed process physics, and in general greater complexity. These demands are shifting the requirements for training and the research emphases of individual scientists. Initial work with GCMs required a state-of-the-art knowledge of available methods for solving the model fluid equations and procedures for handling the large data sets generated by the models. Other than that, modelers needed only the ability to copy and implement the one-line descriptions of the various model physical processes. There was no urgent requirement to validate or improve upon these descriptions, or to obtain observational data for model input or validation. Thus, it was possible for a single highly skilled individual with the help of a couple of programmers to develop a GCM and carry out a research program with it. This traditional approach is still viable for programs emphasizing improved understanding of atmospheric processes. However, the task of developing models with adequate realism and validation to meet the challenge of global change requires scientists to specialize in particular aspects of a model, although still retaining at least some familiarity with the overall model structure and behavior. Indeed, we now need to develop teams or other collaborative groupings of scientists to focus on the development of critical and still poorly developed aspects of climate models. Two particular examples that come to mind are the treatment of cloud-radiative interactions and land processes within models.

Suppose you have decided to participate in a team effort to improve the treatments of land in climate system models with both the objective of relating this effort to development of this area as part of global change models and the immediate task of improving model projections of climate change. What must you know to get started? The issue is primarily the treatment of energy and water fluxes, since these have strong direct interactions with climate models. At the same time, you must develop a framework for treatment of fluxes of carbon dioxide and other trace gases from the land surface. Currently, climate modelers start with scenarios of trace gas increases and do not attempt to make them interactive with the cli-

mate model. Practically, at present the future human contributions and natural feedbacks are too poorly known for there to be any practical improvement possible in model projections with inclusion of these feedbacks, but from a viewpoint of better understanding the system, they must be explored. These notes are an attempt to provide the appropriate background material for someone who would like to start research in the treatment by climate models of surface water and energy fluxes.

Our past knowledge base consists of two distinct threads of effort: (1) model sensitivity studies that give us better insight into the role of land processes and help sort out the relative importance of various factors, and (2) consideration of the detailed processes that must be modeled to represent land in climate models. To the extent that we are guided by the requirements of modeling the overall system, these two threads must proceed in parallel. In practice, we are working with a system of infinite complexity, and the level of abstraction vs. details required must be guided by overall modeling experience. For example, a decade ago we did not know enough about the treatment of land processes in climate models to be able to argue that we had to consider soils and vegetation as separate components. While there is still not general agreement as to this claim, a good case can be made that it is true. We can also show that the distinction between a forest and a grassland has a noticeable impact on a climate model, at least in the tropics. However, we are a long way from being able to distinguish through modeling the implications of switching between a maple and an oak forest, or pine and spruce, as might be provided by ecological modeling of response to climate change. Thus current research on feedbacks of surface fluxes with vegetation is emphasizing primarily short and intermediate scales, that is, from model time steps of a few tens of minutes to the annual and interannual time scales.

Sensitivity Studies

A climate model with an atmospheric hydrologic cycle must on the average evaporate as much water from the surface as it precipitates from the atmosphere in order to conserve water and energy. However, the presence of runoff precludes such a balance over land alone. That is, the evaporative cooling that is a major determinant of summertime land temperatures depends not only on precipitation but also on how the surface apportions this input into evapotranspiration and runoff. This apportioning in turn depends on how net radiative energy is divided between latent and sensible heat fluxes. Past conventional wisdom has largely ignored potential feedbacks of

land on the atmosphere, but with increasing understanding from modeling simulations of these exchanges, we can begin to appreciate what might happen. The most common approach has been to study the effect of an arbitrary, though perhaps physically motivated, change in surface energy or hydrological processes. The study of the effect of postulated large increases in surface albedo became popular following the suggestion of Charney et al. (1977) that this might represent a positive biophysical feedback. A large number of other such studies has been reviewed by Mintz (1984). Of these I mention only that of Shukla and Mintz (1982). They considered two scenarios, an earth with either perfectly wet or completely dry continents. Their July simulations showed that the latter would have continental surfaces on the order of 10°C warmer than if they were wet, and that large reductions in continental rainfall might occur. Physical changes of continental land surfaces disrupt global energy flows by relatively small amounts compared to increasing trace gases (Dickinson, 1986). Therefore, their effects on climate are likely to be most pronounced on a regional scale.

Current studies are attempting to formulate more realistic change scenarios, though perhaps still hypothetical. I now consider the three kinds of such scenarios.

The climate effects of tropical deforestation have long been a source of speculation. However, now that land surface models are beginning to plausibly address the role of vegetation in determining the surface fluxes of moisture and energy in GCM climate models, there is some hope of establishing at least qualitatively reasonable conclusions. The Amazon region contains about half of the world's tropical forests, and in the last decade humans have been rapidly removing these forests. Thus it is useful to focus the question of climate effects of tropical deforestation on this region. Water budget studies have established that about half of the precipitation in the Amazon is supplied by evapotranspiration from the forest. How might removal of the forest reduce the evapotranspiration? Would this reduction, in turn, reduce the amount of precipitation? What effects might changing surface fluxes and precipitation have on global circulation patterns by analogy with the more thoroughly studied effects of anomalies over the tropical oceans? Several studies in the last few years have established that large decreases in evapotranspiration would result from forest removal. The most recent studies are also indicating comparable decreases in precipitation, possibly even greater in amount than the reduction in evapotranspiration.

Another important role of land surface models is in the exploration of the contribution of land to year-to-year variations in precipitation and temperature anomalies. The continental-scale

drought of 1988 and the current long-term drought in California are practical examples, dependent to some extent on feedbacks between atmosphere and surface. The currently most popular hypothesis is that such anomalies are initially related to anomalies in patterns of rainfall over the tropical oceans related to the El Niño phenomenon. Studies are addressing the role of land interactions in this question, but it is too early for definitive results.

The third scenario currently being studied in which land interactions have an important role is that of global warming in response to increasing greenhouse gases. Model simulations that have produced midcontinental drying during the summer have found that the consequent feedbacks (lack of evapotranspiration) further amplified the warming. Interactive clouds have been found to have a yet further amplification effect: that is, the surface is further warmed by more solar radiation reaching the surface because of fewer clouds.

The Process of a Land Model

The atmospheric components of a GCM (Figure 1) provide the surface with fluxes of solar and thermal infrared radiation and precipitation in the form of rain or snow, and with near-surface values of wind vector, air temperature, and humidity. Water conservation is imposed by transferring the water applied to the surface either into storage by soil reservoirs or into loss by evapotranspiration or by runoff. The total radiation absorbed by the surface is balanced by emission of thermal infrared radiation, by the latent heat loss associated with the evapotranspiration or by fluxes of sensible heat, and by diffusion of thermal energy into the soil.

The original Manabe bucket model for the above processes was supposed to evaporate at the same rate as a wet surface (zero canopy resistance) during well-watered conditions, and to hold a maximum water level of typically 0.15 m, which corresponds to the available soil water, that is, the water in the rooting zone at some average field capacity minus that still present at some average wilting point. However, since it did not include the process of diffusion of water in soils or canopy resistance, its evaporation rates were unrealistic both for bare soil (after a very brief period at the rate of atmospheric demand) and for vegetated areas. Evaporation from most bare soils, in reality, is greatly reduced after the loss from the surface layer of about 1 cm of water.

Vegetation acts as a completely wet surface only during and immediately following precipitation when its foliage is wet. Otherwise, it has two important controls: (1) It can extract soil water from a greater depth than would evaporation from bare ground, and (2) it

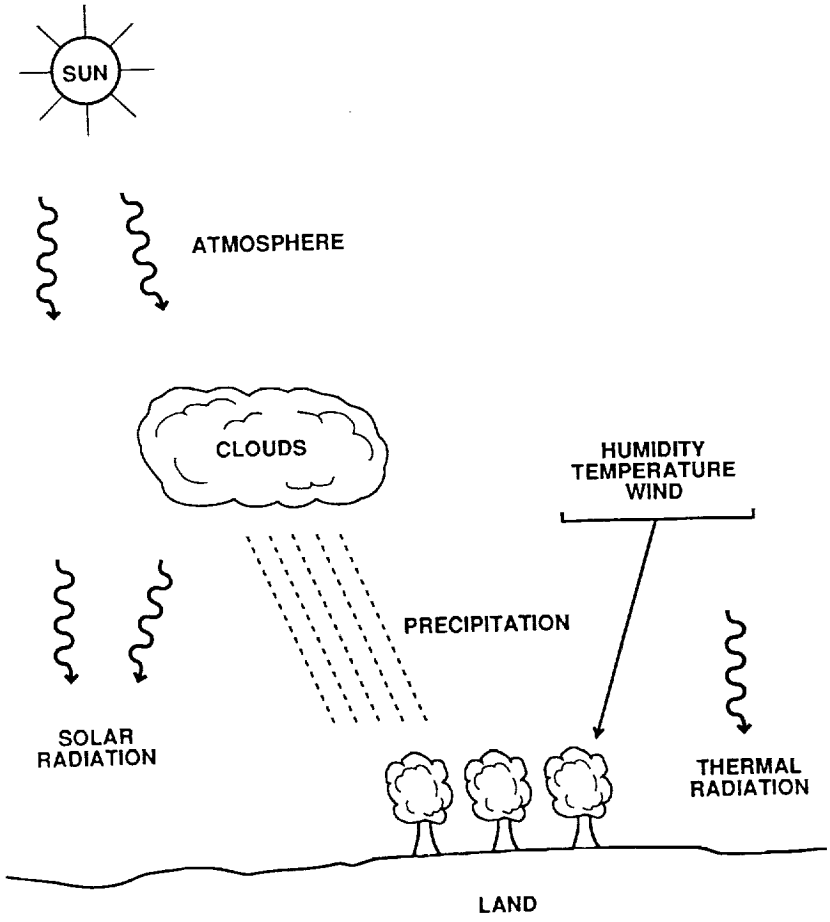

Figure 1. Sketch of the inputs needed at the surface from the atmospheric model (Dickinson et al., 1991).

retards the rate of evapotranspiration from the potential rate through resistance by the stomates to molecular diffusion of water.

The initial bucket model formulation, neglecting any reference to canopy resistance, is still widely used in GCMs for studies of climate change, and in particular has been used to address the question of effects of increasing carbon dioxide and other trace gases (e.g., Manabe and Stouffer, 1980; Washington and Meehl, 1984). The standard Goddard Institute for Space Studies (GISS) GCM has a more detailed but otherwise similar bucket model with an additional layer and water storage capacities depending on ecosystem type, and includes a rough approximation of the vegetative removal of deeper soil water by allowing infinite upward diffusion during the growing season in vegetated regions (Hansen et al., 1983).

Inclusion of geographic distributions of soil and vegetation properties in a model as shown in Table 1 allows increased realism. In particular the aerodynamic resistance of a shortgrass vegetation is over an order of magnitude less than that of forest vegetation, and this difference can have major effects on the nature of evapotranspiration in model simulations. Smooth surfaces have higher temperatures for the same atmospheric conditions because larger temperature and moisture differentials are needed to drive the fluxes required by the energy balance (Figure 2). These warmer temperatures reduce net radiation (by increasing longwave emission) by up to several tens of W/m^2. A comparable additional reduction in net radiation is implied by the higher albedo that usually applies to shorter vegetation.

For fixed net radiation and atmospheric conditions, the differences in evapotranspiration between tall and short vegetation can be obtained from the Penman-Monteith equation. For dry conditions, the relative effect of changing surface roughness depends on

Table 1a: Vegetation/land cover parameters used for South America

Parameter	Land Cover/Vegetation Type*								
	1	2	5	6	7	11	17	18	19
Maximum fractional vegetation cover	0.85	0.80	0.80	0.90	0.80	0.10	0.80	0.80	0.80
Difference between maximum fractional vegetation cover and cover at temperature of 269 K	0.6	0.1	0.3	0.5	0.3	0.1	0.3	0.2	0.3
Roughness length (m) of vegetation	0.06	0.02	0.8	2.0	0.1	0.1	0.1	0.8	0.05
Depth of the total soil layer (m)	1.0	1.0	2.0	1.5	1.0	1.0	1.0	2.0	1.0
Depth of upper soil layer (m)	0.1	0.1	0.1	0.1	0.1	0.1	0.1	0.1	0.1
Rooting ratio (upper to total soil layers)	3	8	10	12	8	8	5	10	10
Vegetation albedo for wavelengths <0.7 μm	0.10	0.10	0.08	0.04	0.08	0.17	0.08	0.06	0.08
Vegetation albedo for wavelengths >0.7 μm	0.30	0.30	0.28	0.20	0.30	0.34	0.28	0.24	0.30
Minimum stomatal resistance (s/m)	150	250	250	250	250	250	250	250	250
Maximum LAI	6	2	6	6	6	6	6	6	6
Minimum LAI	0.5	0.5	1.0	5.0	0.5	0.5	1.0	3.0	0.5
Stem (and dead matter) area index	0.5	4.0	2.0	2.0	2.0	2.0	2.0	2.0	2.0
Inverse square root of leaf dimension ($m^{-1/2}$)	10	5	5	5	5	5	5	5	5
Light sensitivity factor (W/m^2)	0.01	0.01	0.03	0.03	0.01	0.01	0.01	0.03	0.01

*See definitions in Table 1b.
From Dickinson and Henderson-Sellers, 1988.

Table 1b: Vegetation/land cover types used in the CCM

1. Crop
2. Short grass
3. Evergreen needleleaf tree
4. Deciduous needleleaf tree
5. Deciduous broadleaf tree
6. Evergreen broadleaf tree
7. Tall grass
8. Desert
9. Tundra
10. Irrigated crop
11. Semi-desert
12. Ice-cap/glacier
13. Bog or marsh
14. Inland water
15. Ocean
16. Evergreen shrub
17. Deciduous shrub
18. Mixed woodland
19. Impoverished scrub-grassland*

*Land type 19 was introduced especially for a deforestation study and is not part of the CCM land data set.

the magnitudes of the net radiation flux and the vapor pressure deficit. Under wet conditions the greater surface roughness of forests tends to enhance the evaporation loss resulting from interception, but how much depends on the spatial distribution of rainfall and on the interception model in use. In the limit of sparse or absent vegetation, evaporation will be determined by the treatment of diffusion of water through the soil.

To help summarize the common content of two canopy models developed for application in GCMs (i.e., the biosphere-atmosphere transfer scheme—BATS—Dickinson et al., 1986, and the simple biosphere model—SiB—Sellers et al., 1986), I consider the "lowest common denominator" that they both contain, then describe why various models introduce further complexity in various features. The following derivations (Dickinson et al., 1991) capture the essence of all the model treatments under full canopy conditions while leaving out many details such as treatment of fluxes into the ground and through leaf boundary layers.

In meteorological models, the upward flux F_x of a quantity X is generally represented with the aerodynamic expression

$$F_x = \rho_a C_D u (X_s - X_a) \tag{1}$$

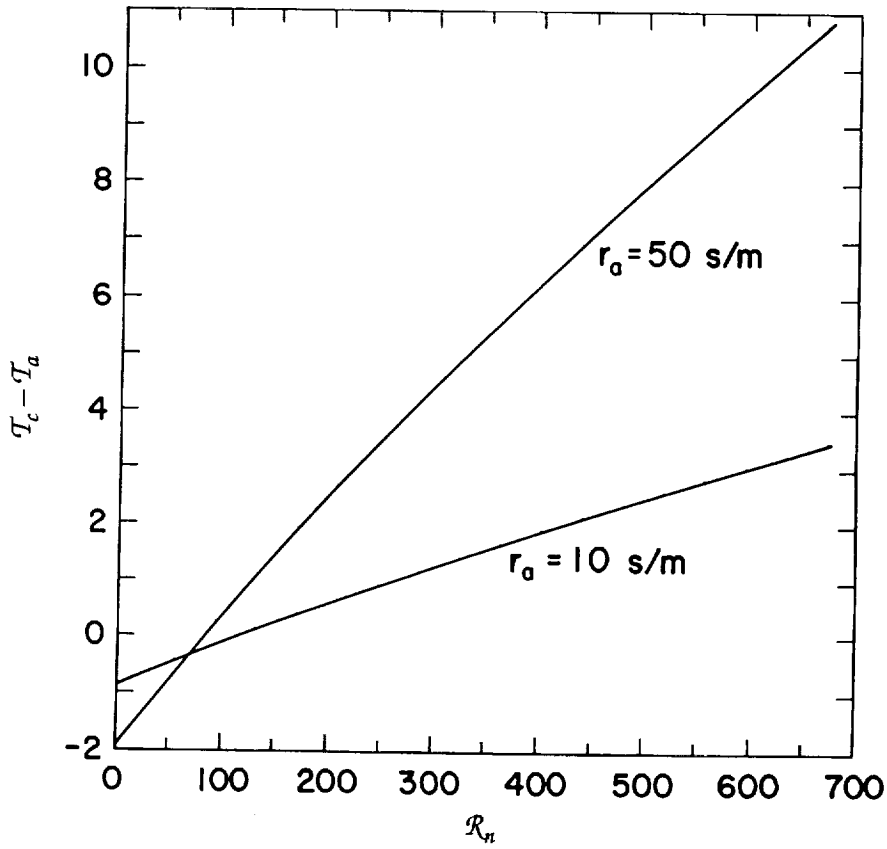

Figure 2. Difference between canopy (T_c) and atmospheric (T_a) temperature vs. net radiation (R_n) for two different surface resistances (r_a) calculated using the simple model described in this paper. Both net radiation and surface resistance are defined for isothermal conditions, that is, canopy and air temperature the same. Hence radiative and stability feedbacks are not included. A relative humidity of 0.7 and air temperature of 22°C are assumed; canopy resistance is 100 s/m (Dickinson et al., 1991).

Subscripts s and a refer to surface and overlying air concentrations of X, u is the magnitude of wind, ρ_a the air density, and C_D a nondimensional transfer coefficient. The factor C_D is from Monin-Obukhov similarity theory for the surface mixed layer of the atmosphere.

For better semblance to the current notation of micrometeorology, we introduce surface resistance $r_a = (C_D u)^{-1}$. Then the flux H of sensible heat is given by

$$H = \rho_a C_p (T_a - T_c)/r_a \tag{2}$$

where T refers to temperature, C_p the specific heat of air, and the subscript c refers to the surface being a canopy. For vegetated sur-

faces, inclusion of the diffusive resistance by stomates to evapotranspiration E is crucial and so must be included. The integrated effect of the resistances of individual leaves is the canopy resistance r_c such that

$$E = \frac{\rho_a (q_a - q_c)}{r_a + r_c} \tag{3}$$

where q refers to water vapor mixing ratio and q_c is determined for the internal leaf tissues, i.e., for saturated conditions. The fluxes defined by Equations (2) and (3) are illustrated in terms of resistances in Figure 3.

Equations (2) and (3) are constrained by the requirement that sensible plus latent energy flux be balanced by net radiation R_n given by

$$R_n = S_{\downarrow}(1 - \text{albedo}) + R_{l\downarrow} - \varepsilon\sigma T_c^4 \tag{4}$$

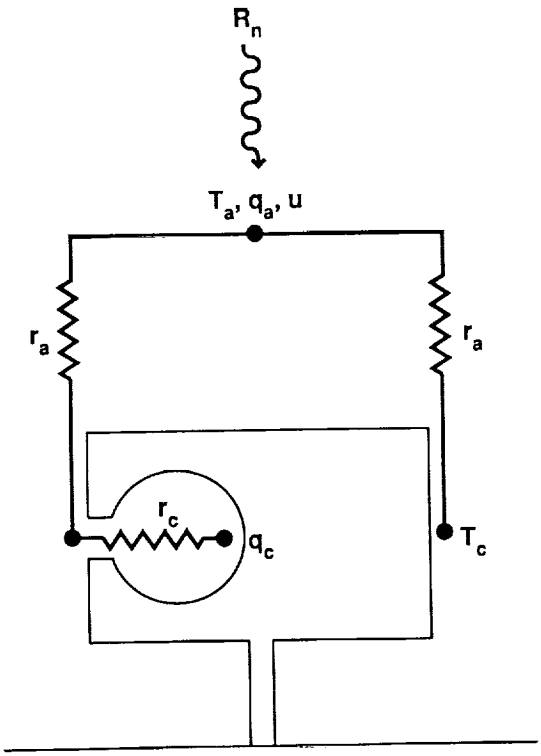

Figure 3. Schematic resistance diagram for the simple generic canopy model described here. See text for definitions of terms (Dickinson et al., 1991).

where $S_{\downarrow}$ = the incident solar energy, $R_{I\downarrow}$ = the downward thermal infrared energy minus any that is reflected, ε = surface emissivity, and σ = the Stefan-Boltzmann constant. The surface energy balance with soil heat flux neglected is written

$$H + \lambda E = R_n \tag{5}$$

where λ = latent heat of evaporation. More realistic models add to Equation (5) a soil heat flux term.

Observational data are conveniently analyzed by the Penman-Monteith approach of combining Equations (2) and (3) with (5), expressing q_c in terms of $T_a - T_c$ and saturated q_a (= q_a^{sat}). The resulting expression relates E to R_n, $q_a - q_c^{sat}$, r_a, and r_c. If all but one of these are measured, the remaining quantity, usually either r_c or E, can be inferred. The main difference between applying these principles to analysis of observational data and applying them to climate modeling is that for the latter none of these quantities can be assumed measured. Rather they must be determined from more basic data and model processes.

Net radiation as described by Equation (4) is conceptually relatively simple. The atmospheric model provides $S_{\downarrow}$ and $R_{I\downarrow}$ and the canopy model provides albedo (according to some combination of specified parameters and a canopy radiative model) and T_c, the latter of which is unknown until Equations (2) through (5) have been solved. As already mentioned, r_a is obtained from boundary-layer theory. The difference $q_a - q_c^{sat}$ is known from the atmospheric model, so the only real complexity is in the specification of r_c and the determination of T_c.

The leaves are assumed to contribute in parallel so conductances $1/r_s$ are averaged, i.e.,

$$r_c = < r_s > /\mathrm{LAI} \tag{6}$$

where the wedge brackets denote an inverse average over the range of the canopy leaf area index (LAI), that is, equivalently, the resistances are summed in parallel.

We represent the dependence of r_s on model variables and for different ecosystems by a minimum value r_{smin} and a product of limiting factors, i.e.,

$$r_s = r_{smin}\, f_1(T) f_2(vpd) f_3(PAR) \ldots \tag{7}$$

where each of the fs has a minimum value of 1; f_1 gives a dependence on some characteristic temperature, the most obvious being that of canopy or root zone soil; f_2 a dependence on vapor pressure deficit $vpd = (q_c - q_{ca})p_s/0.622$ where q_{ca} is the water mixing ratio in the air outside the leaves and p_s the surface pressure; f_3 a depen-

dence on the photosynthetically active radiation flux density (*PAR*). Additional dependences include water stress (crucial but implemented differently in different models) and nutrient stress (not yet included in existing models).

Water loss and CO_2 uptake by plants are obviously linked by their sharing of the stomates as their path of dominant diffusion resistance. Physiologists indicate that this linkage is active; that is, stomates act to maintain a constant ratio between water loss and carbon assimilation. Such an active linkage between transpiration and carbon assimilation would provide a basis for understanding the functional dependences in Equation (7). The calculation of carbon assimilation may be required to determine stomatal resistance, or at least may be feasible with little or no additional computation. Such a computation would couple the components of the carbon cycle with fast time scales to the climate model.

There is little guidance for current treatments of the temperature dependence term, beyond the recognition that optimality will generally be achieved in the range of 20–30°C and that stomates will cease functioning at temperatures of freezing, 0°C, and of rapid protein denaturation, ~50°C. Hence BATS makes a quadratic fit to these limits for f_1^{-1} (Figure 4a).

There is also no systematic basis for specifying a *vpd* dependence for r_s. However, many observations indicate a near linear dependence of f_2^{-1} on *vpd*, with stomatal closure in the range 0.03 to 0.05 p_s. Hence, SiB and the latent version of BATS assume $f_2^{-1} = 1 - vpd/c$ where $c \cong 0.04\ p_s$ (Figure 4b).

In SiB and BATS, a canopy light model is used to provide light levels at a given depth in the canopy, and hence average or integrate the f_3 component of r_s as indicated in Equation (6). This term differs superficially between BATS and SiB but is functionally the same (Figure 4c). In SiB, it is written

$$f_3 = 1 + \frac{a_2/c_2}{b_2 + PAR} \tag{8}$$

where a_2, b_2, c_2 are adjustable constants. BATS uses

$$f_3 = \frac{1 + PAR/PAR_c}{r_{smin}/r_{smax} + PAR/PAR_c} \tag{9}$$

where r_{smax} is the maximum (cuticular) resistance of green leaves, and PAR_c chosen as the light level where $r_s = 2r_{smin}$. Equations (8) and (9) are equivalent, provided

$$r_{smin} = c_2$$

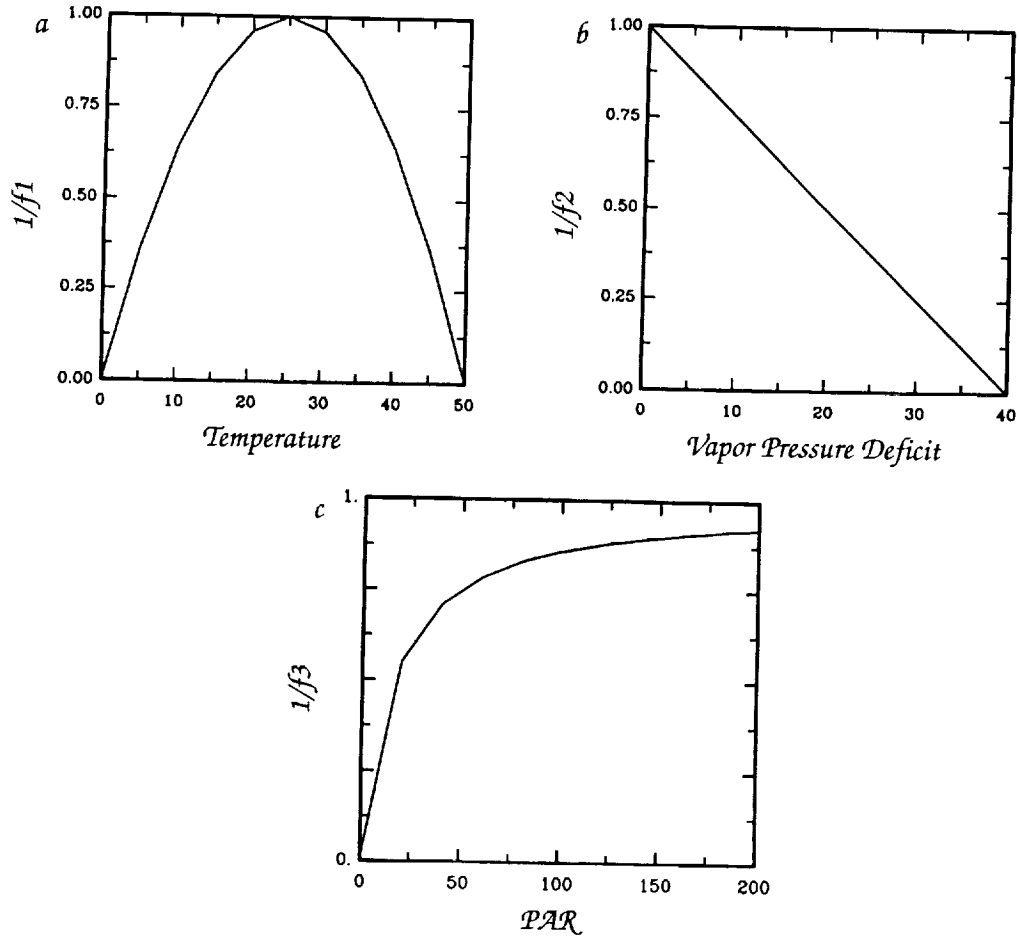

Figure 4. Environmental dependences of inverse of stomatal resistances (i.e., conductance) in BATS model: (a) dependence of conductance on temperature; (b) dependence of conductance on vapor pressure deficit, (c) dependence of conductance on photosynthetically active radiation flux density, or PAR (Dickinson et al., 1991).

$$r_{smax} = c_2 + \frac{a_2}{b_2}$$

$$PAR_c = b_2 + \frac{a_2}{c_2}$$

In W/m^2 of visible radiation, $PAR_c \approx$ 10–50. Precise specification of this parameter is neither necessary nor practical. However, factor-of-two variations change r_c significantly, so ideally, an accuracy of better than ±20% is desirable.

For canopies with random leaf angle distributions exposed to direct radiation, the average *PAR* on a leaf surface is determined from

$$PAR = GrS_{\downarrow} \exp(-GD/\mu) \tag{10}$$

where D is the depth into the canopy in units of LAI, μ = cosine of solar zenith angle, $G \sim 0.5$ is the average leaf projection in the direction of the sun, and r = ratio of *PAR* to total incident solar radiation. BATS uses Equation (10) with diffuse sky radiation accounted for through an additional term which assumes $\mu = 0.5$. SiB does likewise but allows in addition for effects of leaf orientation. Neither model attempts to account in detail for radiation scattered by the foliage, which for *PAR* has about 0.1 the intensity of the incident solar radiation. SiB uses elegant analytic solutions to Equation (9), whereas BATS uses somewhat simpler and probably equally effective numerical solutions.

Interception, the water from precipitation that evaporates from the canopy without reaching the soil, has similar one-layer parameterizations in all models. The interception parameterizations also provide dew or frost formation when the water vapor gradient from foliage to air reverses. The fraction of canopy surface covered by water has zero resistance r_c and hence, especially in forests, can rapidly evaporate back into the atmosphere. The parameterization choices are the water-holding capacity of the foliage W_{sc}, the fraction of the incident precipitation that is intercepted, and the fraction of the foliage that is covered by water when it has less water than full capacity. After the canopy reaches capacity, all additional precipitation is put into throughfall.

BATS and SiB now use W_{sc} = 0.1 LAI (in mm) for water capacity. This quantity is tuned to give observed canopy interception losses and is somewhat lower than the observed storage of water by leaves. BATS has a "stem area index" surface, as well as LAI, that is also wetted. SiB determines a cross section for interception depending on LAI, similar to that for radiation, whereas BATS assumes all precipitation over vegetation is first captured by foliage. SiB assumes the fraction of canopy surface wetted is the ratio of canopy water to W_{sc}, whereas BATS and a new model being developed at GISS use a 2/3 power. In reality, the fractional wetting is very dependent on the hydrophilic properties of the leaves. Some leaves are partially wetted with smooth water films, while on others, water droplets form. Thus, for application to specific sites and vegetation, the present models may be unrealistic. The values of W_{sc} in SiB and BATS are inferred from two years of Amazon measurements (Shuttleworth, 1988).

Model-Specific Parameterizations

The components of vegetation resistance summarized in the previous section either are treated similarly in essentially all of the veg-

etation resistance models or else are assumed constant. While details are debatable, we can agree that there is an appropriate functional form consistent with observational information, and that the prescribed constants in the different models are not drastically different. In this section I discuss those components that diverge more drastically in the different land parameterizations.

Water Stress

The models differ in their treatment of the effect of water stress on stomatal resistance, in part because of the lack of reliable quantitative information on the subject. SiB assumes that this contribution to r_s depends on leaf water potential, with the leaf water potential being related to soil water potential through the effect of soil and root diffusion resistance to the water movement. These processes have been represented through more detailed mechanistic models, and some observational information is available for individual sites. However, there is little or no basis for specifying the necessary parameters over large areas.

BATS uses a simplified version of the approach illustrated in Figure 5. Each ecosystem is characterized by a maximum transpiration rate under well-watered conditions, presumed to be determined by root and soil resistance. This maximum rate is reduced below field capacity according to the difference between the soil water suction (negative potential) for wilting and that computed for existing soil moisture. The latter is obtained as an average over the model soil layers, where the average is weighted with the root surface density in each layer. This averaging requires only an estimate of the relative distribution of roots because their absolute contribution is subsumed in the assumed maximum transpiration rate. The most crucial parameter in the BATS treatment of root resistance is this maximum rate, which in principle could be specified from remote sensing.

A similar but even simpler concept is used in the new GISS model being developed, i.e., the contribution to transpiration is reduced in each soil layer from that computed by the unstressed canopy model by the ratio of the total water potential to that for wilting.

Within-Canopy Resistances

SiB and BATS attempt to include the bulk effect of boundary-layer resistances across leaf surfaces. Given a local wind in the canopy, this resistance for heat and moisture can be inferred from laboratory studies. Its accurate specification is limited by the knowledge of the wind distribution within the canopy. BATS simply esti-

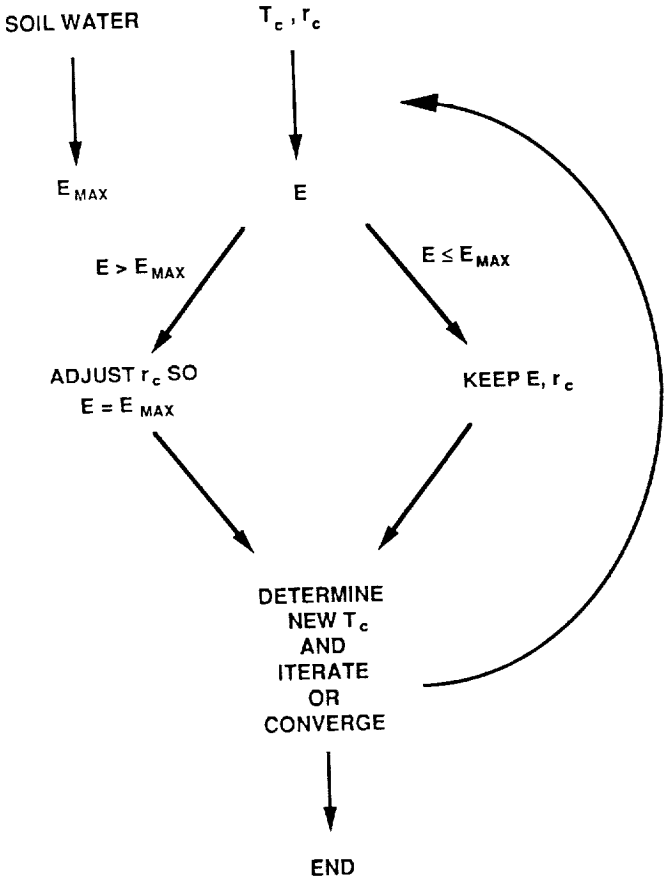

Figure 5. Schematic of the approach used by BATS to determine dependence on stomatal resistance on soil water. Atmospheric demand is determined and compared with the maximum that can be supplied by roots for given soil water. If the former exceeds the later, stomatal resistance is increased to reduce the demand to match supply (Dickinson et al., 1991).

mates this wind from the frictional velocity, whereas SiB bases it on a solution for eddy diffusion within the canopy.

Partial Vegetation

The treatment of partial vegetation in BATS helps illustrate some of the questions that must be faced in treating this issue. The fraction of vegetation covered by a model grid square is prescribed, with a seasonal variation determined from soil temperature. No specification is given as to the spatial scales to be associated with the bare soil fraction. Land classes range from desert (that is, all bare soil)

and semidesert (that is, mostly bare soil) to various forest types that are mostly vegetation cover. Sensible and latent fluxes are computed separately for the bare ground and for the fraction of soil under vegetation. Both soil fractions are assumed to have the same temperature and moisture content but to differ in values of overlying wind and transfer coefficients, i.e., different values of r_a are determined for these two fractions. The details of these prescriptions are guided by their reasonableness in the limits of bare soil and full canopy. A more realistic treatment might determine separate soil temperatures and moisture for shade vs. sun and require information on the spatial scales of the vegetation and exposed soil areas.

In SiB, the effects of partial vegetation are incorporated directly into the radiation, momentum (turbulent), and energy transfer submodel. However, no account is taken of larger-scale heterogeneities. The new GISS model separates the grid box into vegetation-covered and bare soil components. Fluxes and soil temperatures are calculated for each of these surface types, and then area-weighted to interface to the first layer of the atmosphere.

Canopy Temperature

Calculation of canopy temperature has been the most difficult aspect of vegetation resistance models in GCMs, because implementing the calculation of surface temperatures can lead to worrisome inaccuracies and, at worst, to severe computational instabilities. Without a successful approach to this question, much greater errors in determination of evapotranspiration can be made than might result from inaccuracies in canopy resistance. In general, we must distinguish between two or more temperatures that are coupled through energy fluxes and must separately satisfy energy balance requirements. For example, SiB and BATS have separate soil and canopy temperatures, and the GISS model in addition distinguishes between bare ground and under-vegetation soil temperatures. These surfaces each have heat capacities, some of which may be zero.

Let T be the vector representing all the model surface temperatures and C a diagonal matrix where elements are individual surface heat capacities. To determine T, knowing its value at a previous time step, we must solve numerically an equation of the form

$$C\frac{\delta T}{\delta t} - F(T) = 0 \qquad (11)$$

where F(T) is a vector whose individual elements represent the sum of energy fluxes into a given surface and t is time. Let superscript n refer to the value of T at the nth model time step. Time steps are Δt. We could first try the simplest solution to Equation (11), i.e.,

$$T^n = T^{n-1} + C^{-1}F\left(T^{n-1}\right)\Delta t \tag{12}$$

This may work with short enough time steps, a few minutes or less, and large enough heat capacities (i.e., provided Δt is small compared to the inverse of the largest eigenvalue of $C^{-1}\ \delta F/\delta T$), but otherwise it can be a prescription for numerical disaster giving wild and growing oscillations from one time step to the next. In the limit of small heat capacities, Equation (11) should approach a statement of energy balance at the present time level. An alternative solution likely to be more accurate and stable is hence

$$T^n = T^{n-1} + C^{-1}F\left(T^n\right)\Delta t \tag{13}$$

but this form appears to require already knowing the solution to use. However, its solution may be possible using a Newton iteration, i.e., by writing the ith component of $F = F_j$ as

$$F_j\left(T^{n,n+1}\right) = F_j\left(T^{n,i}\right) + \frac{\delta F_j\left(T^{n,i}\right)}{\delta T_k}\left(T_k^{n,i+1} - T_k^{n,i}\right) \tag{14}$$

where the second, ith, superscript refers to the number of the iteration, there is a summation over the kth subscripts, and T_k is the kth temperature. Equation (14) is substituted into Equation (13) for $F(T^n)$ and Equation (13) is solved for $T^{n,i+1}$, taking as a first guess the value of T at the previous time step, that is, $T^{n,1} = T^{n-1}$.

The SiB model specifies soil and canopy heat capacities and uses only the first-guess form of Equation (14). BATS, on the other hand, assumes zero heat capacity for the canopy and first iterates Equation (14) for canopy temperature to convergence, taking soil temperature as that from the previous time step. It then solves Equation (13) as a scalar equation for soil temperature, using the first derived canopy temperature and only the first guess from Equation (14). A further simplification, sometimes used, e.g., at the European Centre for Medium Range Weather Forecasts (ECMWF), is to assume all surfaces have the same temperature, so that Equation (13) is applied as a scalar to derive joint soil and canopy temperatures.

Preliminary examination of the errors from the SiB and BATS solutions for canopy temperature, including lack of conservation of energy, suggests that both approaches can reasonably control errors; SiB conserves energy even if its first iteration is inaccurate, whereas BATS only does so with convergence of the temperature iteration. The BATS solution may be more accurate for canopy-dominated transpiration, but the SiB approach requires less numerical computation and so may be preferable, considering all of the other uncertainties in the parameterizations.

Present Experience with a Land Model Coupled to a GCM

Here we will report on the latest simulation studies with the community climate model version 1 (CCM1) of the National Center for Atmospheric Research (NCAR) coupled to the BATS land surface treatment. Shortcomings are emphasized more than successes to point to where further progress is needed.

Over the last year, we have developed two slightly different versions of the CCM1 tuned to give top-of-the-atmosphere fluxes of solar and longwave radiation that match those observed by satellite. Both start with the standard CCM1 with a diurnal cycle added and the solar radiation calculation done with a treatment developed by A. Slingo of NCAR and the British Meteorological Office. One version in addition calculates clouds with a scheme developed by A. Slingo, initially for the ECMWF model. During these studies, we discovered that previous models which assumed a diurnal average sun would absorb globally about 10 W/m^2 additional solar radiation when a diurnal cycle was added, hence requiring us to adjust the solar cloud treatment to reflect about that much more radiation to get the match with data from the Earth Radiation Budget Experiment (ERBE) satellite (since the treatment had previously been tuned for an average sum).

The bulk of our simulations have been done with the standard CCM1 clouds, and we have not noticed any major differences over land with the other code. The integration includes an eight-year control simulation with a lower boundary over ocean as the new sea surface climatology developed by K. Trenberth and collaborators. The first four years of this integration are used to specify monthly average ocean heat transport (flux correction) needed to balance net surface energy fluxes at each ocean grid point. Otherwise, we treat the ocean at each grid point as a 60-m slab of water for its temperature calculation.

Together with a thermodynamic sea ice model, we have begun to integrate this CCM1/BATS/flux-corrected slab-ocean model for 330 and 660 ppm of CO_2. In both cases we used a 30-m slab for one year to speed up convergence and, for the doubled CO_2, initialized with a uniform 3°C warming over all the ocean points.

The purpose of these integrations is to explore the behavior and feedbacks of a detailed land model (BATS) in a global climate change scenario, comparable to those that have been used previously with simple bucket models.

Acknowledgment

The National Center for Atmospheric Research is sponsored by the National Science Foundation.

References

Charney, J.G., W.J. Quirk, S.-H. Chow, and J. Kornfield. 1977. A comparative study of the effects of albedo change on drought in semiarid regions. *Journal of the Atmospheric Sciences 34*, 1366–1385.

Dickinson, R.E. 1986. How will climate change? The climate system and modelling of future climate. In *The Greenhouse Effect, Climate Change, and Ecosystems* (B. Bolin, B.R. Döös, J. Jäger, and R.A. Warrick, eds.), John Wiley and Sons, Chichester, England, 207–270.

Dickinson, R.E., and A. Henderson-Sellers. 1988. Modeling tropical deforestation: A study of GCM land-surface parameterizations. *Quarterly Journal of Research of the Meteorology Society 114*, 439–462.

Dickinson, R.E., A. Henderson-Sellers, P.J. Kennedy, and M.F. Wilson. 1986. *Biosphere-Atmosphere Transfer Scheme (BATS) for the NCAR Community Climate Model.* Technical Note TN-275, National Center for Atmospheric Research, Boulder, Colorado.

Dickinson, R.E., A. Henderson-Sellers, C. Rosenzweig, and P.J. Sellers. 1991 Evapotranspiration models with canopy resistance for use in climate models: A review. *Agricultural and Forest M* 373–388.

Hansen, J., G. Russell, D. Rind [illegible] and L. Travis. 1983. [illegible] climate studies: Model 609–662.

Manabe, S., and R.J. Stouffer. 19[illegible] an increase of CO_2 conc *Geophysical Research 85*,

Mintz, Y. 1984. The sensitivity of [illegible] surface boundary condition ed.), Cambridge University P.

Sellers, P.J., Y. Mintz, Y.C. Sud, and [illegible] ple biosphere model (SiB) for [illegible] *Journal of the Atmospheric Scie*

Shukla, J., and Y. Mintz. 1982. Influe[illegible] spira- tion on the earth's climate. *Scien*

Shuttleworth, W.J. 1988. Evaporation from Amazonian rainforest. *Proceedings of the Royal Society of London B 233*, 321–346.

Washington, W.M., and G.A. Meehl. 1984. Seasonal cycle experiment on the climate sensitivity due to a doubling of CO_2 with an atmospheric general circulation model coupled to a simple mixed layer ocean model. *Journal of Geophysical Research 89*, 9475–9503.

Report: The Carbon Cycle Revisited

Bert Bolin and Inez Fung

Introduction

In developing an integrated perspective on the earth system, it has been essential to use simplified conceptual models representing the pool sizes and flux rates between major earth system components. The carbon cycle, because of the integral role it plays in the earth system, has served as a focal point for developing these models. From carbon-based models, new models have been developed, studies have been initiated, and insights have been gained. To achieve greater understanding of the controls and dynamics of the earth system as represented by the conceptual model of the carbon cycle, it is beneficial to review our current state of knowledge regarding the carbon cycle to identify critical gaps in our understanding of the earth system.

Discussions during the Global Change Institute indicated a need to present, in some detail and as accurately as possible, our present knowledge about the carbon cycle, the uncertainties in this knowledge, and the reasons for these uncertainties. Figure 1 provides an overview of the carbon cycle. By its very nature, a diagram of this sort understates key assumptions and oversimplifies the interlinking processes, so it may be misleading without rather precise annotations. Figure 1 is based on extensive research over a number of years and is not merely a rough qualitative overview, but all aspects of this research are not apparent from the condensed information in the figure. The extensive comments below offer a fuller appreciation of our present knowledge. Following these comments, we discuss basic issues of internal consistency within the carbon cycle, and end by summarizing the key unknowns.

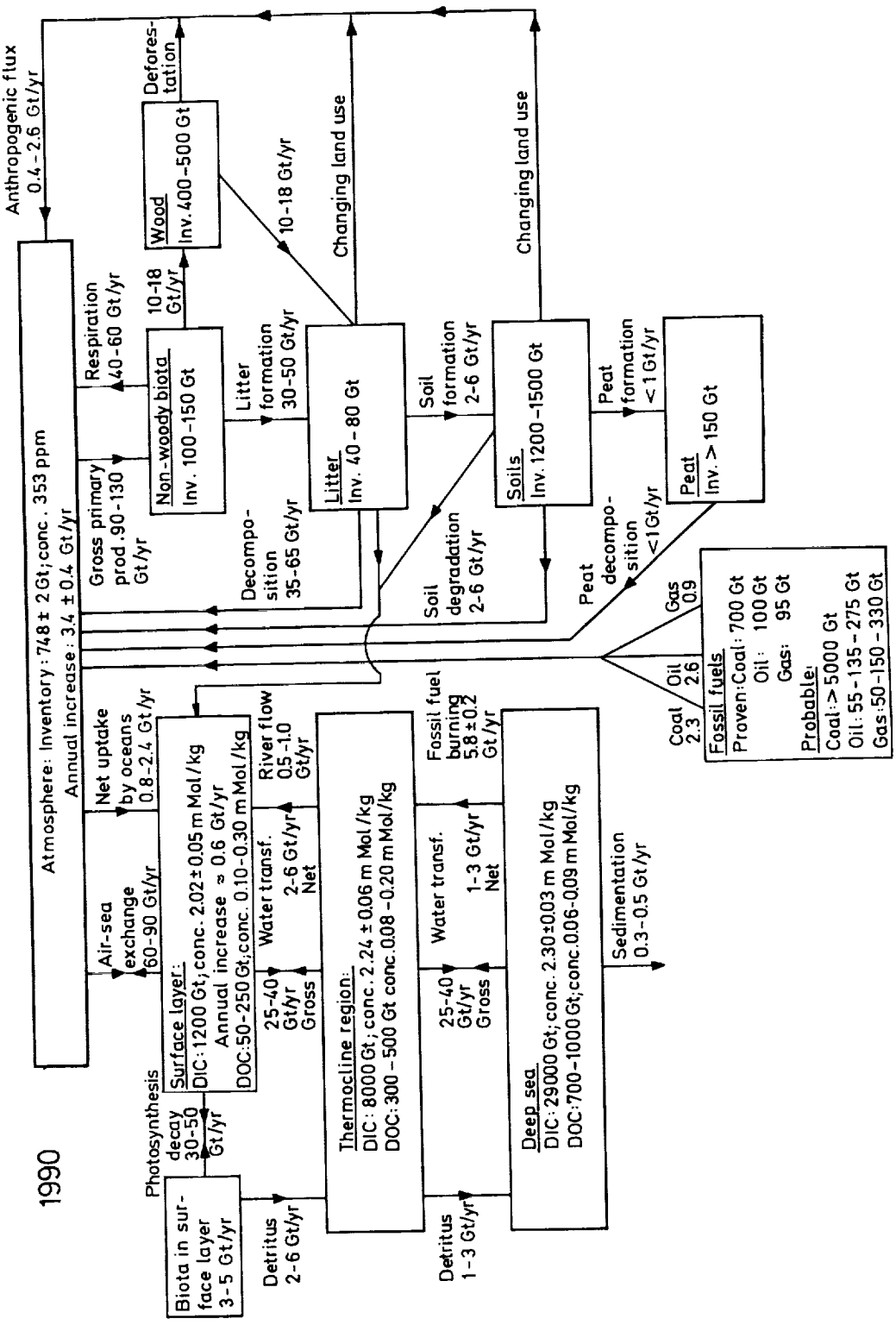

Figure 1. The carbon cycle. The magnitudes of the carbon compartments are given in gigatons (Gt: 10^9 ton) C, which are equal to pentagrams (Pg: 10^{15} g). The fluxes between these are expressed in Gt C/yr = Pg C/yr.

Compartments

Atmosphere

Inventory: 748 ± 2 Gt C, based on the present (i.e., A.D. 1990) annual mean concentration of 353 ± 1 ppmv (1 ppmv CO_2 = 2.12 Gt C).

Annual increase: Rate of 3.4 ± 0.4 Gt C corresponds to 1.6 ± 0.2 ppmv/yr (cf. Watson et al., 1990; Tans et al., 1990).

Oceans

Total ocean volume: 1370 x 10^{15} m^3. The best estimate of the total amount of dissolved inorganic carbon (DIC) in the ocean is 38,000 ± 700 Gt C, based on this volume and an average DIC concentration of 2.27 ± 0.04 mMol/kg.

Surface layer: Usually defined as the top 100 m of warm surface water and about 200 m (sometimes more) of cold surface water. Volume: ca. 50 x 10^{15} m^3; the precise volume is somewhat arbitrary.

Surface layer DIC: 1200 Gt; average concentration assumed to be 2.02 ± 0.05 mMol/kg (Takahashi et al., 1981); the uncertainty is partly dependent on the thickness of the layer. An annual increase of ocean surface carbon concentrations of about 0.05%/yr is taking place due to transfer of CO_2 from the atmosphere to the sea (assuming that quasi-equilibrium between the atmosphere and the sea is approximately being maintained and that the average Revelle factor is 10; see Rintoul report, this volume). Model calculations suggest that since preindustrial time an increase of this reservoir by 2–2.5%, i.e., 24–30 Gt C, has occurred (cf. Maier-Reimer and Hasselmann, 1987; Bacastow and Maier-Reimer, 1990).

Surface layer dissolved organic carbon (DOC): 50–250 Gt C; uncertainty due to few data available. Those available, if globally representative, show concentrations of about 0.2 mMol/kg, corresponding to a total amount of 120 Gt C.

Surface layer biota: 3–5 Gt C, estimated indirectly by assuming that the amount present at any time is about 10% of the annual net primary production (NPP), i.e., the turnover time for biota in the surface layer is assumed to be about one month (de Vooys, 1979).

Thermocline: On the average extending to about 1000 m in tropical and midlatitude regions, absent in polar regions. Volume 300 x 10^{15} m^3.

Thermocline DIC: 8000 Gt C; average concentration assumed to be 2.24 ± 0.06 mMol/kg (Takahashi et al., 1981); uncertainty is partly dependent on the definition of the size of the reservoir. This reservoir is estimated to have increased by 75–125 Gt C since early last century due to transfer of excess carbon dioxide from the atmos-

phere directly or via the ocean surface layer (cf. Maier-Reimer and Hasselmann, 1987; Moore et al., 1989).

Thermocline DOC: 300–500 Gt C, primarily in the upper half of the region; uncertainty due to very few data. The concentration seems to decline from the surface values given above to about 0.08 mMol/kg in the lower part of the region.

Deep sea (including the outcrop regions in the polar seas): Volume 1020×10^{15} m^3.

Deep sea DIC: 29,000 Gt C; average concentration assumed to be 2.30 ± 0.03 mMol/kg (Takahashi et al., 1981); uncertainty is partly dependent on the definition of the size of the reservoir.

Deep sea DOC: 700–1000 Gt C; average concentration assumed to be 0.06–0.09 mMol/kg; less relative uncertainty than for the surface layers because of a more homogeneous distribution as revealed by ^{14}C values of about 0.65, implying a radiocarbon age of 3000–4000 years (cf. Williams, 1975).

Terrestrial System

Biota (nonwoody plus wood): 500–650 Gt C; assessment by direct inventory estimate. About 80% is judged to reside in wood (cf. Ajtay et al., 1979; Olson et al., 1983).

Litter: 40–80 Gt C (cf. Ajtay et al., 1979; Olson et al., 1983); dead roots may not have been adequately accounted for.

Soils: 1200–1500 Gt C (cf. Ajtay et al., 1979; Schlesinger, 1984); this estimate may to some extent include dead roots. It generally represents organic matter above about 50 cm depth.

Peat: >150 Gt C (cf. Ajtay et al., 1979); this is probably an underestimate, since peat often extends far below 50 cm, which usually is used for soil sample analysis.

Fossil fuels: Estimates of fossil fuel resources are given in Table 1.

Fluxes

Atmosphere–Ocean

This flux is 60–90 Gt C/yr. In steady state there is a mutual molecular exchange maintained by the partial pressure of carbon dioxide (pCO_2), preindustrially about 280 ppmv, in the atmosphere and the ocean. Given the 1973 pCO_2 of 328 ppmv, this yields an estimated average residence time for a CO_2 molecule in the atmosphere of 8–12 years and an estimated exchange rate of 15–21 mol $CO_2/yr/m^2$. These estimates (cf. Bolin et al., 1981) are based on (1) determination of rate of radon evasion from the sea (Peng et al., 1979), (2) balance between ^{14}C radiocarbon invasion into the sea

Table 1: Fossil fuel reserves

	Coal (10^9 ton)	Oil (10^9 m^3)	Gas (10^{12} m^3)
Used until 1988	150	100	40
Proven reserves (1985)	700	100	95
Probable reserves, low/mean/high*	>5000	55/135/275	55/150/330

*95/50/5% probability
Energy content: 1000 m^3 gas = 1.03 tons of oil equivalent; 1 ton coal = 0.65 tons of oil equivalent.
Carbon content: Coal and lignite, 69%; oil, 84%; gas, 540 g/m^3
Relative CO_2 emission per unit of energy: gas, 1.0; oil, 1.5; coal, 1.8
From Schilling and Wiegand, 1987; White, 1987; cf. also Goldemberg et al., 1988.

and radioactive decay in the sea, and (3) rate of invasion of ^{14}C produced by nuclear bomb testing (Stuiver, 1980).

During preindustrial times a net evasion of CO_2 from the oceans in tropical latitudes was approximately balanced by a net invasion into the oceans in polar and subpolar latitudes, which were associated with poleward transfer in the atmosphere and equatorward transfer in the oceans. The net circulation is estimated to have been 2–4 Gt C/yr (Pearman and Hyson, 1986; Keeling et al., 1989a, 1989b). The derivation of this transfer rate is based on an evaluation of the transport capability of the atmosphere between tropical latitudes and polar regions and an assessment of differences between the average atmospheric concentrations of CO_2 in these regions of 1–1.5 ppmv, as evaluated from data taken around 1960 (cf. Keeling et al., 1989a, 1989b). This pattern has been markedly disturbed due to anthropogenic CO_2 emissions, primarily in the Northern Hemisphere. Fossil fuel burning, deforestation, and changing land use have created a mean excess of 5–10 ppmv of CO_2 in the atmosphere relative to the oceans. As a result, a net flux of CO_2 into the oceans takes place at present, which is estimated to be 08–2.4 Gt C/yr (cf. Bolin, 1986; Siegenthaler and Oeschger, 1987; Tans et al., 1990; Watson et al., 1990).

Within the Oceans

The following estimates are based both on direct measurements and on assessments with the aid of carbon cycle models (cf. Oeschger et al., 1975; Siegenthaler, 1983; Bolin, 1986; Maier-Reimer and Hasselmann, 1987; Sarmiento et al., 1992).

DIC in surface water used for marine biota production: 30–50 Gt C/yr; estimated from a large number of measurements of NPP.

Marine biota transferred into dead organic matter, detritus, and DOC, and partly mineralized in the surface layers within a month to a year: 30–50 Gt C/yr. This flux is, however, less than the total NPP referred to above because a part is transferred into the thermocline region (see below).

Detritus settling into the thermocline region: 2–6 Gt C/yr. Mineralization of detritus and DOC in the thermocline region: 2–6 Gt C/yr as estimated from the oxygen deficit (AOU, apparent oxygen utilization) in the layer.

Transfer of detritus and DOC into the deep sea and mineralization into DIC: 1–3 Gt C/yr; estimated on the basis of radiocarbon age of DIC in the deep sea (see below).

DIC (gross) exchange between the surface layer, thermocline region, and deep sea due to ocean circulation and turbulence: 25–40 Gt C/yr, estimated with the aid of present knowledge of ocean circulation; of turbulent transfer, including penetrative convection in polar regions; and of the radiocarbon age of DIC in the deep sea. Due to a DIC gradient between the deep sea and the surface layer, this leads to:

Net upward transfer of DIC to the thermocline region: 1–3 Gt C/yr, and to the surface layer: 2–6 Gt C/yr. Because of increased DIC in the surface layer during the 20th century caused by the transfer of excess carbon from the atmosphere to the sea, this upward transfer has decreased by 1–2.5 Gt C/yr, primarily from the thermocline region to the surface layer, which enhances the uptake by the oceans of excess atmospheric CO_2 (cf. above). Mineralization of detritus and/or DOC in the deep sea: 1–3 Gt C/yr, balancing the net upward transfer due to water motions (see above).

The fluxes as given above constitute the biological pump, which maintains a higher pCO_2 (400–700 ppmv) in the thermocline region and the deep sea than would be expected otherwise.

Atmosphere–Terrestrial Exchange (Preindustrial Estimates)

The following are direct estimates of undisturbed preindustrial conditions as obtained from field data gathered in major biomes (cf. Ajtay et al., 1979; Olson et al., 1983; Bolin, 1986).

- Gross primary production: 90–130 Gt C/yr
- Respiration: 40–60 Gt C/yr, i.e., NPP: 40–70 Gt/yr, of which about 25% is stored in wood

- Formation of dead organic matter, litter: 40–70 Gt C/yr
- Litter decay within a few years: 35–65 Gt C/yr
- Litter to organic carbon in soil: 2–6 Gt C/yr
- Soil decomposition: 2–6 Gt C/yr
- Peat formation as well as peat decomposition: <1 Gt C/yr.

Erosion of the Continents and Flux to the Ocean (Preindustrial Estimates)

The following estimates of preindustrial river loads have been calculated (cf. Kempe, 1979):

- HCO_3-C: 0.4 Gt C/yr
- DOC: 0.1 Gt C/yr
- Particulate organic carbon (POC): 0.1 Gt C/yr
- Inorganic, suspended C: 0.2 Gt C/yr
- Total: 0.8 Gt C/yr.

It is likely that the flux of carbon to the sea has increased due to anthropogenic activities, this being particularly so for the flux of DOC and POC.

Other Fluxes

Carbon flux from the ocean to the sea floor: Sediments of carbonates: 0.1–0.2 Gt C/yr; organic carbon, open sea: about 0.05 Gt C/yr; shallow seas, partially anthropogenic: 0.3–0.5 Gt C/yr (cf Kempe, 1979).

Deforestation and changing land use: Release of CO_2 into the atmosphere: 0.4–2.6 Gt C/yr; accumulated release from about 1750 to 1980: 80–140 Gt C. These direct estimates have been made by using information from national forest services, calibrated against field measurements from present activities as well as satellite observations (Houghton et al., 1987; Detweiler and Hall, 1988).

Fossil fuel combustion: At present 5.6–6.0 Gt C/yr; accumulated emissions since the beginning of the industrial revolution (about 1840) until 1985: 190–210 Gt C. At present, the respective contributions from burning coal, oil, and gas are approximately 40%, 44%, and 16%.

Constraints on the System

Due to a number of constraints on the system, it is not permissible to combine any numbers given for reservoir sizes and fluxes within the uncertainty ranges that have been assigned. These constraints are listed below.

- It should be noted that variations of atmospheric CO_2, during the period from A.D. 1000 until anthropogenic influences became significant, have been less than 3–5 ppmv for any period of a decade or two. Therefore, the mean net exchange between the atmosphere, on the one hand, and the oceans and the terrestrial system, on the other, must have been less than 1 Gt C/yr and probably less than 0.5 Gt C/yr. This close balance is remarkable in the light of the sizes of the different reservoirs and the gross exchanges that take place between them.

- This balance has been disturbed by emissions of CO_2 from the burning of fossil fuels, deforestation, and changing land use. The average fossil fuel input during 1980–1987 was 5.1–5.5 Gt C/yr, while that from deforestation and changing land use was 0.4–2.6 Gt C/yr, i.e., the total anthropogenic emissions were 5.9–8.1 Gt C/yr. The atmospheric increase during this same period was 2.8–3.4 Gt C/yr, while the oceanic uptake is computed to have been 1.6–3.0 Gt C/yr, i.e., the total sinks are 4.4–6.4 Gt C/yr. Although there is a slight overlap between the estimated ranges for the total sources and the total sinks, it seems likely that there is an additional unknown sink, the "missing sink."

- In addition to showing an upward trend, the atmospheric CO_2 data from the globally distributed network of monitoring sites also show that CO_2 concentrations are higher in the Northern Hemisphere than in the south, reflecting the dominance of the Northern Hemisphere midlatitude fossil fuel sources. In 1980–87 the average concentration difference between 82°N (Alert) and the South Pole was 3.0 ppmv. Tans et al. (1990) attempted to simulated the north-south CO_2 gradient in a three-dimensional atmospheric tracer transport model. If we accept the geographic distribution of the fossil fuel sources and an approximate distribution of land sources, a major sink is required in the Northern Hemisphere rather than in the Southern Hemisphere to match the atmospheric observations.

- The difference in CO_2 concentrations between the hemispheres during the preindustrial era is unknown and is a source of uncertainty in the above inference about the hemispheric distribution

of the sinks. Keeling et al. (1989a, 1989b) have extrapolated the concentrations back in time and estimated that the CO_2 concentration at the South Pole may have been about 2 ppmv higher than in the Northern Hemisphere in the 1700s. Even when this estimate is included in the calculations, the requirement of a comparatively large contemporary northern sink remains.

- The data from the Northern Hemisphere further indicate that the magnitude of the sinks in the North Atlantic and the North Pacific was significantly less than what is required to balance the carbon budget and that a land sink for anthropogenic CO_2 must be assumed. The mechanism of this missing sink is unknown.

- A major uncertainty remains, however, in that the estimate of the uptake by the oceans critically depends on the determination of the global distribution of pCO_2 in ocean surface water. Observations, particularly from the southern seas, are still few.

- Carbon cycles should be tested against data on total carbon, as well as against the distributions of $\delta^{13}C$ and $\Delta^{14}C$. The transient changes of the latter due to anthropogenic activities also put some constraints on the behavior of the system as a whole. The decrease of $\Delta^{14}C$ from the middle of last century until 1954 (the Suess effect) is thus consistent with the estimated past emissions of fossil carbon (free of ^{14}C), although the associated decrease of the concentrations in the surface water of the oceans has not been verified by measurements.

- M. Heimann and R. Keeling have carried out simulations using a three-dimensional ocean model, similar to those reported by Tans et al. (1990), including a simulation of the ^{13}C distribution in the 1980s. They found that a large land sink in the Northern Hemisphere does not match the observed $\delta^{13}C$ gradient. They confirm, however, that uptake by the Northern Hemisphere oceans would require a partial pressure difference between the atmosphere and the ocean far in excess of what is observed. A small land sink, approximately proportional to the net primary production, is in any case required to match available observations.

- It is further important to consider the history of the CO_2 balance since the 1700s and, in particular, to assess the integrated changes during this period. Houghton (1989) estimated both the total magnitude and the distribution with time of a missing sink for the period 1860–1985. Although such a residual is necessarily quite uncertain, it appears that there was no missing sink before about 1940. It was largest in the 1970s and has decreased since

then. A careful analysis of such modeling results with gradually improved models might reveal the nature of this sink or the inadequacy of other features of present carbon cycle models.

Key Questions and Suggestions for Further Research

The global carbon cycle remains a puzzle. The enigma is caused by the difficulty of making direct measurements and the paucity of such measurements. Increasingly complex models can be developed in order to estimate the relative importance of difference processes and interactions and to assess the sensitivity of atmospheric CO_2 concentrations to assumed changes in these processes. Critical areas with remaining questions and important research needs are listed below.

- What is the current distribution of pCO_2 in the oceans? What are the seasonal variations of oceanic pCO_2? What is the magnitude of the errors introduced by inadequate seasonal sampling in current estimates of the annual mean pCO_2, especially in the North Pacific and North Atlantic? What is the role of the marginal seas?
- What are the rate-limiting processes that determine the magnitude of the ocean uptake of anthropogenic CO_2? How can we improve our modeling of these processes? How can we improve the model calculations on time scales important for anthropogenic CO_2? Currently, various tracers whose input histories differ from that of fossil fuel CO_2 are used to calibrate/validate transport characteristics of various time scales in ocean models. The magnitude of the CO_2 uptake by the oceans in these models is very sensitive to the calibration procedure (e.g., Joos and Siegenthaler, 1989).
- What was the preindustrial distribution of CO_2 in the atmosphere and in the oceans? Was the Southern Hemisphere concentration higher than in the north, as suggested by Keeling's extrapolation of the Mauna Loa and South Pole records? If so, what processes were responsible for the elevated pCO_2 (relative to the atmosphere) in the southern oceans? Simulation of preindustrial ^{14}C distribution (Levin et al., 1987) may help test hypotheses of air-sea CO_2 exchange.
- Seasonal transport in atmospheric models of the global carbon cycle should be tested by the simulation of inert tracers. The validation has only been done in the annual mean.
- Establishment of a calibration standard for ^{13}C measurements and expansion of the network for monitoring atmospheric ^{13}C

must receive high priority, so that latitudinal gradients and long-term trends can be interpreted with confidence. Likewise, carbon cycle models must include ^{13}C together with CO_2 to constrain the partitioning between land and ocean sources and sinks.

- The interannual variations of CO_2 in the atmosphere provide clues to the carbon cycle's responses to perturbations. What transient shifts in the CO_2 balance between photosynthesis and decomposition have resulted from increasing CO_2 concentration and fluctuations in surface air temperature and precipitation? Similarly, the upper ocean temperature is known to have fluctuated in the past 30 years. How might these fluctuations in thermodynamics and associated dynamics affect the oceanic carbon cycle and be manifested in the atmospheric CO_2 record?

- How have the numerous carbon pools in the terrestrial biosphere been altered by deforestation, afforestation, and changing agricultural practices? How can we narrow the uncertainties in our estimates of the CO_2 sources that result from land use modification?

- The size of the different carbon pools and the dominant controls and turnover rates of each pool need to be determined. How would climate change and anthropogenic perturbations change substrate properties (such as pH and soil fertility) and alter photosynthesis, allocation, decomposition, and other dynamical properties of terrestrial ecosystems? What controls the geographic variations in these processes? Can the uncertainties of C flux into various pools be reduced to determine whether a Northern Hemisphere terrestrial sink for C exists?

References

Ajtay, G.L, P. Ketner, and P. Duvigneaud. 1979. Terrestrial primary production and phytomass. In *The Global Carbon Cycle* (B. Bolin, E. Degens, S. Kempe, and P. Ketner, eds.), SCOPE 13, John Wiley and Sons, Chichester, England.

Bacastow, R.B., and E. Maier-Reimer. 1990. Ocean-circulation model of the carbon cycle. *Climate Dynamics* 4, 95–126.

Bolin, B. 1986. How much CO_2 will remain in the atmosphere? The carbon cycle and projections for the future. In *The Greenhouse Effect, Climate Change and Ecosystems* (B. Bolön, B. Döös, J. Jäger, and R.A. Warrick, eds.), SCOPE 29, John Wiley and Sons, Chichester, England.

Bolin, B., C.D. Keeling, R.B. Bacastow, A. Björkström, and U. Siegenthaler. 1981. Carbon cycle modelling. In *Carbon Cycle Modeling* (B. Bolin, ed.), SCOPE 16, John Wiley and Sons, Chichester, England.

Broecker, W.S., T.-H. Peng, and R. Engh. 1980. Modeling the carbon system. *Radiocarbon 22*, 565–598.

Codispoti, L.A., G.E. Friederick, R.L. Iverson, and D.W. Hood. 1982. Temporal changes in the inorganic carbon system of the southeastern Bering Sea during spring 1980. *Nature 296*, 242–244.

Detweiler, R.P., and C.A.S. Hall. 1988. Tropical forest and the global carbon cycle. *Science 239*, 42–47.

de Vooys, C.G.N. 1979. Primary production in aquatic environments. In *The Global Carbon Cycle* (B. Bolin, E. Degens, S. Kempe, and P. Ketner, eds.), SCOPE 13, John Wiley and Sons, Chichester, England, 259–282.

Enting, I.G., and J.V. Mansbridge. 1989. Seasonal sources and sinks of atmospheric CO_2: Direct inversion of filtered data. *Tellus 41B*, 111–126.

Goldemberg, J., T.B. Johansson, A.K.N. Reddy, and R.H. Williams. 1988. *Energy for a Sustainable World.* Wiley Eastern, New Delhi, India.

Houghton, R.A. 1989. The long-term flux of carbon to the atmosphere from changes in land use. In *Proceedings of the Third International Conference on Analysis and Evaluation of CO_2 Data, Present and Past.* Hinterzarten, 16–20 October 1989. Publication No. 59, WMO Environmental Pollution Research Programme, Geneva, Switzerland.

Houghton, R.A., R.D. Bone, J.R. Fruci, J.E. Hobby, J.M. Melillo, C.A. Palm, B.J. Peterson, G.R. Shaver, G.M. Woodwell, B. Moore, D.L. Skole, and N. Myers. 1987. The flux of carbon from terrestrial ecosystems to the atmosphere in 1980 due to changes in land use: Geographic distribution of the global flux. *Tellus 29B*, 122–139.

Joos, F., and U. Siegenthaler. 1989. Study of the oceanic uptake of anthropogenic CO_2 and C-14 using a High-latitude Exchange/Iterior Diffusion-Advection (HILDA) model. In *Proceedings of the Third International Conference on Analysis and Evaluation of CO_2 Data, Present and Past.* Hinterzarten, 16–20 October 1989. Publication No. 59, WMO Environmental Pollution Research Programme, Geneva, Switzerland.

Keeling, C.D., R.B. Bacastow, A.F. Carter, S.C. Piper, T.P. Whorf, M. Heimann, W.G. Mook, and H. Roeloffzen. 1989a. A three dimensional model of atmospheric CO_2 transport based on observed winds: 1. Analysis of observational data. In *Aspects of Climate Variability in the Pacific and the Western Americas* (D.H. Peterson, ed.), Geophysical Monograph 55, American Geophysical Union, Washington, D.C., 165–236.

Keeling, C.D., S.C. Piper, and M. Heimann. 1989b. A three dimensional model of atmospheric CO_2 transport based on observed winds: 4. Mean annual gradients and interannual variations. In *Aspects of Climate Variability in the Pacific and the Western Americas* (D.H. Peterson, ed.), Geophysical Monograph 55, American Geophysical Union, Washington, D.C., 305–363.

Kempe, S. 1979. Carbon in the rock cycle. In *Carbon Cycle Modeling* (B. Bolin, ed.), SCOPE 16, John Wiley and Sons, Chichester, England, 343–377.

Levin, I., B. Kromer, D. Wagenbach, and K.O. Münnich. 1987. Carbon isotope measurements of atmospheric CO at a coastal station in Antarctica. *Tellus 39B*, 89–95.

Maier-Reimer, E., and K. Hasselmann. 1987. Transport and storage of carbon dioxide in the ocean, and in organic ocean-circulation carbon cycle model. *Climate Dynamics 2*, 63–90.

Moore, B., B. Bolin, A. Björkström, K. Holmén, and C. Ringo. 1989. Ocean carbon models and inverse methods. In *Ocean Circulation Models: Combining Data and Dynamics* (D.L.T. Anderson and J. Willebrand, eds.), Kluwer Academic Publishers, Dordrecht, The Netherlands, 409–449.

Oeschger, H., U. Siegenthaler, U. Schotterer, and A. Gugelmann. 1975. A box diffusion model to study the carbon dioxide exchange in nature. *Tellus 27*, 168–192.

Olson, J.S., J.A. Watts, and L.J. Allison. 1983. *Carbon in Live Vegetation of Major World Ecosystems*. Publication TROO4, U.S. Department of Energy, Washington, D.C.

Pearman, G.I., and P. Hyson. 1986. Global transfer and inter-reservoir exchange of carbon dioxide with particular reference to stable isotopic distributions. *Journal of Atmospheric Chemistry 4*, 81–124.

Peng, T.-H., W.S. Broecker, G. Mathieu, and Y.-H. Li. 1979. Radon evasion rates in the Atlantic and Pacific Oceans as determined during the GEOSECS Program. *Journal of Geophysical Research 84*, 2471–2486.

Sarmiento, J.L., J.C. Orr, and U. Siegenthaler. 1992. A perturbation simulation of CO_2 uptake in an ocean circulation model. *Journal of Geophysical Research 97(3)*, 3621–3647.

Schilling, H.-D., and D. Wiegand. 1987. Coal resources. In *Resources and World Development* (D.J. McLaren, and B.J. Skinner, eds.), Dahlem Workshop, John Wiley and Sons, Chichester, England, 129–156.

Schlesinger, W.H. 1984. Soil organic matter: A source of atmospheric carbon dioxide. In *The Role of Terrestrial Vegetation in the Global Carbon Cycle* (G.M. Woodwell, ed.), SCOPE 23, John Wiley and Sons, Chichester, England, 111–127.

Schlosser, P., G. Bonisch, M. Rhein, and R. Bayer. 1991. Reduction of deep water formation in the Greenland Sea during the 1980s: Evidence from tracer data. *Science 251*, 1054–1056.

Siegenthaler, U. 1983. Uptake of excess CO_2 by an outcrop-diffussion model of the ocean. *Journal of Geophysical Research 88(C6)*, 3599–3608.

Siegenthaler, U., and H. Oeschger. 1987. Biospheric CO_2 emissions during the past 200 years reconstructed by deconvolution of ice core data. *Tellus 39B*, 140–154.

Stuiver, M. 1980. ^{14}C distribution in the Atlantic Ocean. *Journal of Geophysical Research 85*, 2711–2718.

Takahashi, T., W.S. Broecker, and A.E. Bainbridge. 1981. The alkalinity and total carbon dioxide concentration in the world oceans. In *Carbon Cycle Modelling* (B. Bolin, ed.), SCOPE 16, John Wiley and Sons, Chichester, England.

Tans, P.P., I.Y. Fung, and T. Takahashi. 1990. Observational constraints on the global atmospheric CO_2 budget. *Science 247*, 1421–1438.

Toggweiler, J.R. 1989. Is the downward dissolved organic matter (DOM) flux important in carbon transport? In *Productivity of the Ocean: Present and Past* (W.H. Berger, V.S. Smetacek, and G. Wefer, eds.), John Wiley and Sons, New York, 65–83.

Watson, R.T., H. Rodhe, H. Oeschger, and U. Siegenthaler. 1990. Greenhouse gases and aerosols. In *Climate Change: The IPCC Scientific Assessment.* Intergovernmental Panel on Climate Change and Cambridge University Press, Cambridge, England, 1–40.

White, D.A. 1987. Conventional oil and gas resources. In *Resources and World Development* (D.J. McLaren, and B.J. Skinner, eds.), Dahlem Workshop, John Wiley and Sons, Chichester, England, 113–128.

Williams, P.J.LeB. 1975. Biological and chemical aspects of dissolved organic matter in sea water. In *Chemical Oceanography* (J.P. Riley and G. Skirrow, eds.), Academic Press, London, 301–363.

Report: Ocean-Atmospheric Linkages

Stephen R. Rintoul

This chapter focuses on the role of the ocean in the global carbon cycle on the time scale of decades to centuries. The input rate of CO_2 to the atmosphere due to fossil fuel burning and deforestation has continued to increase over the last century. To balance the global carbon budget, a sink is required whose magnitude is changing on similar time scales. We have sought to identify aspects of the ocean system that are capable of responding on decadal time scales, to examine our present ability to model such changes, and to pinpoint ways in which this ability could be improved. Many other important aspects of the ocean's role in global change are not addressed, including the importance of oceanic heat transport and thermal inertia to the climate system, biogeochemical cycling of elements other than carbon, and the importance of the ocean as a source or sink of trace gases.

Estimates of Present Oceanic Uptake of CO_2

The chemical buffering of the ocean carbon system and the large size of the oceanic carbon reservoir relative to that of the atmosphere place a fundamental limit on the uptake of CO_2 by the ocean. The Revelle factor is a measure of the change in ocean pCO_2 required for a given change in atmospheric pCO_2 to establish a new equilibrium. This number is around 10 for most of the surface ocean, expressing the fact that for a given change in atmospheric CO_2 the expected change in oceanic pCO_2 is an order of magnitude smaller.

A second constraint on the extent to which the ocean can be a net sink of atmospheric CO_2 is due to the inherent negative feedback of

the ocean-atmosphere system. In a system in equilibrium, the net oceanic sources and sinks of CO_2 will be in balance. If the equilibrium is disturbed, for example, by circulation changes at high latitude resulting in more efficient CO_2 uptake by the ocean, atmospheric pCO_2 will decrease. In turn, the oceanic source regions will become more effective and the sinks less so, tending to restore atmospheric pCO_2 toward its equilibrium value.

The flux of CO_2 across the air-sea interface is equal to the product of the gas transfer coefficient and the difference in pCO_2 between the atmosphere and the surface ocean. Direct estimates of the air-sea exchange of CO_2 based on observed δpCO_2 suggest that the ocean is taking up 1.6 Gt/yr (Tans et al., 1990); however, the uncertainty in this estimate is large (range of 0.8–2.4 Gt/yr; see Bolin and Fung, this volume). Expressions for the dependence of the gas transfer coefficient on wind speed vary by a factor of two. A more serious problem is the lack of pCO_2 measurements in the surface ocean. Over large portions of the globe, particularly in the Southern Hemisphere, there are no observations at all. Compounding the sampling problem is the fact that oceanic pCO_2 is highly variable, both in space and in time. Accurate direct estimates of the net exchange of CO_2 across the air-sea interface will require at a minimum seasonal data at all latitudes.

A variety of models, ranging in complexity from relatively simple box-diffusion models to three-dimensional general circulation models (GCMs), have been employed to simulate the uptake of CO_2 by the ocean (Oeschger et al., 1975; Bolin, 1981; Siegenthaler, 1983; Peng and Broecker, 1985; Maier-Reimer and Hasselmann, 1987; Sarmiento et al., 1992). The model calculations suggest that the ocean is taking up 26–44% of the fossil fuel CO_2 input to the atmosphere. However, this range of values probably does not reflect the true uncertainty in the CO_2 uptake by the ocean. The ocean circulation in the models used so far to estimate the oceanic sink of CO_2 has been in steady state and much more diffusive in nature than that of the real ocean. In addition, the circulation and mixing have generally been calibrated by fitting to the same "clock," based on ^{14}C observations. In the simpler models, there are usually insufficient degrees of freedom to simultaneously fit more than one tracer distribution (Bolin, 1986). Given these similarities, it is not surprising that all of the models result in a similar uptake of the CO_2 transient. However, in box models in which geostrophy is included, imposing on the system a different "clock" that is based on ocean dynamics, the uptake of CO_2 is considerably more efficient (Moore, this volume).

Thus there remains a large uncertainty in both direct and model-based estimates of the amount of fossil fuel CO_2 presently entering

the ocean. Additional observations that resolve the seasonal cycle are critically needed, especially in the Southern Hemisphere. Accurate estimates based on observations would provide a critical test of the models we hope to use to predict the climatic response to increasing atmospheric CO_2 concentrations. The atmosphere and the upper ocean equilibrate with respect to CO_2 on a time scale of about one year (Broecker and Peng, 1982). The rate-limiting step in the oceanic uptake of CO_2 is thus the exchange between the surface ocean and the ocean interior (Oeschger et al., 1975; Broecker et al., 1980; Sarmiento et al., 1992). Reliable predictions of the future oceanic sink therefore depend critically on accurate treatment of the physical and biological mechanisms that transport carbon from the sea surface to the deep ocean.

Physical Transport of Carbon into the Ocean Interior

As mentioned above, the models so far used to estimate the oceanic uptake of CO_2, whether box models or coarse-resolution GCMs, are heavily diffusive. The penetration of tracers into the ocean interior thus goes as the square root of time. In reality, we believe the pathways between the upper ocean and the interior are primarily advective. Sites of strong mixing are sparse and of limited extent, with the end products of active vertical exchange at these sites carried into the interior by flow along isopycnals. The penetration of the tracer in this case is linear in time. Either type of model can be calibrated to a transient tracer such as ^{14}C at a particular time, but the time evolution in each case will be very different. Recent simulations of tritium penetration into the subtropical gyre of the North Atlantic confirm that higher-resolution models with less diffusive circulations result in more efficient tracer injection into the interior (F. Bryan, personal communication).

A variety of vertical mixing processes act to transfer physical and chemical properties between the mixed layer and the ocean interior. Each vertical exchange mechanism is characterized by different time and space scales. The mixing processes which represent the exchange between the thermocline and deeper layers of the ocean play the greatest role in oceanic uptake on decadal time scales. In particular, we are interested in the potential for variability in the vertical exchange mechanisms on this time scale.

The Thermohaline Circulation

The global thermohaline circulation, or "conveyor belt," plays a major role in carrying CO_2 and tracers from the sea surface to the deep interior. Wust (1935), for example, concluded from deep oxygen measurements that North Atlantic deep water was the primary

agent responsible for the ventilation of the deep ocean. More recent observations of tracers such as tritium and freon confirm that the formation and export of intermediate and deep water masses provide an efficient conduit from the sea surface to the deep ocean (Jenkins and Rhines, 1980; Weiss et al., 1985).

Although the importance of the thermohaline circulation in ventilating the deep ocean has been recognized for many years, fundamental aspects of its operation are still not well understood. We do not have a good conceptual model of the forces driving the conveyor belt or the factors determining the transport of the overturning cell. We know even less about how the global thermohaline circulation is closed. Consequently, we are unable to predict how the conveyor belt will change in response to changes in atmospheric forcing.

Model studies have suggested that the thermohaline circulation is delicately balanced, and may be characterized by significant variability. Stommel (1961) and Bryan (1986) demonstrated the possibility of multiple solutions for the thermohaline circulation in simplified ocean models. Coupled ocean-atmosphere models can also lead to nonunique solutions. For example, Manabe and Stouffer (1988) showed that for the same external forcing a coupled model exhibited two possible climates, one with an active thermohaline circulation in the North Atlantic and another with almost no Atlantic thermohaline overturning.

If an atmospheric GCM is forced by the observed sea surface temperature distribution, it is possible to determine from the solution the surface fluxes of heat and moisture over the ocean required for a balanced equilibrium. If an ocean model is forced by the observed sea surface temperature and salinity fields, another set of surface fluxes of heat and moisture is required for equilibrium. At present, the fluxes derived from atmospheric and oceanic models do not agree with each other. As a result, when such models are coupled, the model climate is apt to drift rapidly away from the observed climate toward another equilibrium state with a very different ocean circulation and sea surface temperature distribution. In order to make progress in the face of this inconsistency, ad hoc constant corrections to the surface fluxes have been used to prevent the model climate from drifting away from that observed (Sausen et al., 1988; Manabe and Stouffer, 1988). This approach has been applied by Stouffer et al. (1989) in a coupled model simulation of greenhouse warming. In a control experiment, the coupled model oscillates about a climate with a sea surface temperature distribution close to what is observed for an extended integration of 150 years.

A weakness of this approach is that it is not clear that it can be used to simulate climates that are very different from the present

one, excluding many interesting applications to paleoclimate or to extreme greenhouse warming scenarios. Most of the flux corrections required in the Stouffer et al. (1989) calculation appear to be due to inadequacies in the cloud model used and to the poor resolution of heat and salinity transport by ocean currents. These are both areas where active efforts are being made to improve the models.

The major shifts in the thermohaline circulation (e.g., reversal of the overturning cell in the North Atlantic) seen in some of the model results require approximately 1000 years to occur. However, the transport or properties of the thermohaline circulation may be modulated on shorter time scales. There is some observational evidence that such changes may have occurred in recent decades. A layer of anomalously fresh water capped the subpolar North Atlantic in the 1970s and may have prevented the convective formation of deep water (Schlosser et al., 1991). Roemmich and Wunsch (1985) observed a shift in the depth of the deep branch of the North Atlantic thermohaline circulation between 1959 and 1981, but no change in the volume transport.

The deep variability noted by Roemmich and Wunsch may be due to changes in the thermohaline characteristics of the upper ocean such as the salinity anomaly observed in the 1970s. However, our models of the thermohaline circulation are inadequate to predict the change in properties or transport of deep water in response to a change in atmospheric forcing. More realistic modeling of deep convection will require a more detailed treatment of the upper ocean than currently appears in oceanic GCMs. Suggestions for such a model are discussed below.

Thermocline Ventilation

The thermohaline conveyor belt is not the only mechanism of vertical exchange that plays a role in the oceanic uptake of CO_2 on decadal time scales. Both convective formation of intermediate waters and Ekman pumping by the wind inject water masses from the sea surface into the thermocline. The relative importance of deep and intermediate water mass formation in supplying tracers to the ocean interior is not well known. However, several studies suggest that the major input is through ventilation of the thermocline. Stuiver (1978), for example, concluded at the time of the Geochemical Ocean Sections Study (GEOSECS) expedition that 80% of the bomb-produced radiocarbon was found in the thermoclines of the subtropical gyres. Atmospheric inverse calculations that calculate the sources and sinks of CO_2 implied by the atmospheric distribution also suggest that the primary oceanic sink is at midlatitudes (Enting and Mansbridge, 1989). Coupled model studies show that the ocean warming resulting

from a doubling of atmospheric CO_2 is concentrated in the subtropical gyres at midlatitude (Schlesinger et al., 1988).

The volume and physical and chemical properties of the water transferred from the sea surface to the interior depend on the fluxes of heat and moisture and the wind stress at the sea surface. Variability in the forcing thus leads to variability in the net uptake of tracers by the ocean. We know that the forcing varies on the time scale of years to centuries, but we do not have observations of the resulting changes in the vertical exchange driven by these processes, except in a few instances.

To model such changes, we need to improve the treatment of the upper ocean in GCMs. No existing ocean model, for example, does a good job of reproducing the large-scale sea surface temperature distributions. An ocean model that is appropriate to couple to an atmospheric GCM will require higher vertical resolution in the upper ocean and must be able to reproduce the observed temperature and salinity when driven with realistic heat and moisture fluxes at the sea surface. In addition, the model should include a physically based mixing parameterization (e.g., shear- or stability-dependent vertical mixing, lateral mixing along isopycnals). For short-term climate predictions (approximately 10–100 years), resolving the deep ocean is not necessary. A climate model that includes a highly resolved mixed layer and thermocline patched to a coarse-resolution deep ocean would be most appropriate for studying the uptake of CO_2 on decadal time scales. Such models are now being developed.

A critical test of improved models of the upper ocean will be how well they reproduce the seasonal cycle and interannual variability of temperature and salinity in the upper several hundred meters. However, the existing observations are inadequate for verifying models on the basin scale. The primary source for measurements of these properties is ships of opportunity, supplemented by moored and drifting buoy systems away from shipping routes. The observational network must be substantially expanded to supply the global data sets needed. Satellite measurements of sea ice and sea surface temperature provide valuable complements to the in situ measurements.

Biologically Mediated Carbon Transport to the Ocean Interior

The export of organic matter from the euphotic zone and its regeneration at depth play a major role in determining the large-scale nutrient and carbon distributions (Broecker and Peng, 1982). Changes in ocean productivity at high latitude may have contributed to the large changes in atmospheric CO_2 that accompanied

the glacial-to-interglacial transition (Siegenthaler and Wenk, 1984; Knox and McElroy, 1984; Sarmiento and Toggweiler, 1984). However, the capacity of the biological system to change on decadal time scales is limited. Carbon, nitrogen, and phosphorus occur in marine organic matter in fixed ratios (i.e., Redfield ratios; Redfield et al., 1963). Export of organic carbon is thus accompanied by an export of nitrogen and phosphorus. When organic matter is decomposed at depth, the nutrients and carbon are remineralized, again in the same ratio. Mixing of the regenerated nutrients into the euphotic zone can support the formation of more organic matter, but the regenerated carbon is mixed up as well. Thus, in the equilibrium case the biological cycling results in no net flux of carbon into the ocean interior. For the biological pump to transfer carbon from the surface ocean to the interior, the stoichiometric constraint imposed by the Redfield ratios must be broken.

Dissolved Organic Matter

Recent observations of a much larger pool of dissolved organic carbon (DOC) than was previously believed to exist challenge several long-held assumptions of biological and chemical oceanography (Sugimura and Suzuki, 1988; Toggweiler, 1989). If the measurements so far obtained in the North Pacific and North Atlantic are representative, the DOC reservoir in the ocean is comparable in magnitude to the terrestrial carbon reservoir. Small changes in the residence time of such a large carbon reservoir, perhaps in response to changes in temperature, might have a significant impact on atmospheric pCO_2. DOC can be transported laterally for long distances between its formation and decomposition, so that the traditional one-dimensional view of particle formation in the euphotic zone, rapid sinking, and regeneration at depth may not be applicable (Toggweiler, 1989). If the C:N:P ratio of DOC is not in the Redfield proportion, then our understanding of the biological pump needs to be substantially revised.

However, very little is known at this point about the nature of the "new" DOC. In particular, we do not know the mechanisms responsible for the formation and destruction of this material, or how rapidly these processes operate. The ratio of nitrogen and phosphorus to carbon in the pool of dissolved organic matter (DOM) is also unknown. Some measurements suggest that most of the oxygen consumption occurring in the ocean is due to the oxidation of DOM (Sugimura and Suzuki, 1988), which seems to conflict with the observed decrease in organic particle flux with depth, and which also seems roughly consistent with observed AOU (Martin et al., 1987). Until these issues are resolved it is difficult to evaluate the

role of DOM in the ocean's biogeochemical cycles. The analogy to the terrestrial DOC pool (e.g., humic and fulvic acids) should be explored more thoroughly to see whether additional insight can be gained into the character of the oceanic DOC reservoir. For example, it is known that aromatics in terrestrial DOC are resistant to ultraviolet oxidation but can be oxidized by high-temperature methods such as those used by Sugimura and Suzuki (1988).

Iron Limitation

Over large regions of the ocean, in particular the Southern Ocean, there are significant concentrations of the major nutrients nitrate and phosphate in the mixed layer, suggesting that some other factor is limiting growth. Traditionally the limiting factor has been assumed to be either light, temperature, or grazing by zooplankton. An alternative hypothesis, that the absence of the trace nutrient iron is limiting plankton growth, has been put forward by Martin and co-workers (Martin and Fitzwater, 1988; Martin et al., 1989, 1990). This has led to the suggestion that iron fertilization of the high-latitude ocean could lead to an increase in productivity and a net uptake of CO_2 from the atmosphere.

The effectiveness of such a strategy is a topic of active debate (Peng and Broecker, 1991; Peng et al., this volume; Joos et al., 1991; Keir, 1991). The species that dominate in incubation studies that have been spiked with iron are not the same as those that tend to dominate in the natural system. In the open ocean, aspects of the marine ecosystem that are not well represented in closed incubations, such as herbivory, may limit the net fertilization effect. The effect may also be constrained by limitations imposed by other nutrients, such as phosphorus. Perhaps more important is the inherent negative feedback of the coupled ocean-atmosphere system mentioned above. Experiments with a simple box-diffusion model (see Peng et al., this volume) suggest that as atmospheric CO_2 decreases, the low-latitude oceanic sources of CO_2 become more effective, acting to damp the initial response. The equilibrium atmospheric pCO_2 is only slightly lower than the initial value. Further experiments with more sophisticated models are needed before the effectiveness of iron fertilization can be evaluated.

Role of Calcareous Organisms

Organisms forming calcium carbonate structures or tests lead to vertical fractionation of carbon and nutrients in the water column. Soft organic tissue is decomposed rapidly in the upper ocean, regenerating both carbon and nutrients. The calcium carbonate shells, on the other hand, sink to the deep sea before dissolving, carrying car-

bon but not nitrogen or phosphorus to the deep ocean. Therefore an increase in the relative abundance of calcareous organisms, such as coccoliths, could result in increased sequestering of carbon at depth. An increase in the formation and export of calcium carbonate from the upper ocean also decreases surface alkalinity and thus increases oceanic pCO_2. If the climatic changes associated with an increase in atmospheric CO_2 favored calcareous organisms for some reason, there would be a potential for a positive feedback. However, we do not understand the factors controlling community structure well enough to predict what environmental changes could lead to a relative increase in the population of calcareous organisms.

Changes in Community Structure and Bloom Frequency

More general changes in the community structure of marine ecosystems in response to changing environmental conditions may affect the uptake of CO_2 by the ocean. A general feature of ocean ecosystems is that stable environmental conditions lead to a community of multiple, coadapted species which is effective at recycling nutrients, while episodic environments are dominated by blooms of one or a few species followed by large export of organic matter from the euphotic zone (Williams and von Bodungen, 1989). Therefore, changes in the variability of environmental variables relevant to the biological system (e.g., mixed-layer depth or nutrient supply) can lead to changes in the export of organic carbon.

A net increase in the sequestering of carbon in the deep sea would result if changes in the circulation or mixing occurred in regions of the ocean where unutilized nutrients exist in the surface layers, allowing for production of new biomass. We know that the physical environment can change on decadal time scales, but we are not yet able to predict how such changes may lead to changes in community structure and thus net export.

Perhaps the best evidence for a biological response to physical forcing is at the mesoscale (e.g., Nelson et al., 1989). Satellite observations and field campaigns in the 1980s showed that the cores of eddies associated with western boundary currents evolve differently from the waters of origin and the waters surrounding the eddy. The fundamental explanation for this lies in the different conditions for convection and restratification that exist within the eddy. These result both from the change in air-sea interaction occurring as the core of the eddy is displaced from the region of origin, and from the vertical motion of density surfaces as the eddy spins down. Studies within the cores of such eddies have also provided the opportunity to observe the direct biological response to storm-induced mixing. The net effect of all of these processes is to enhance the upward flux of nutrients into

the euphotic zone of the eddy, leading to increased rates of production and a shift in community composition to large diatoms, which tend to export a larger fraction of the total production.

Marine Productivity and Variability in Surface Ocean pCO_2

One way in which marine biology does affect the uptake of CO_2 on short time scales is in modifying the chemical properties of the surface waters introduced to the interior by physical processes. High productivity at the start of the spring bloom can draw down surface pCO_2 by more than 100 ppm in a few weeks (Codispoti et al., 1982). The physical processes exchanging surface water with deeper layers, such as deep convection or Ekman pumping, also vary on seasonal and shorter time scales. Therefore it is essential to account for the interaction between physical transport and biologically induced variability in pCO_2 in models and observational studies.

Sources and Sinks of Trace Gases

The ocean plays an important role as a source or sink of various trace gases that have an impact on the radiative or chemical properties of the atmosphere (Table 1). Both the production and exchange of these species across the air-sea interface are in many cases mediated by biological processes. Although this chapter cannot discuss this issue in detail, we feel it is important to mention some of the climatically important trace gases in the present context, since it may be that changes in the strengths of the sources or sinks of these species are the most important way in which ocean biology can affect climate. To date there have been no attempts to model the biologically mediated sources or sinks of these gases, or their potential variability in response to changes in ocean circulation or atmospheric forcing.

Improved Coupled Physical-Biological Models

Most coupled physical-biological ocean models have focused on a particular small-scale phenomenon (Rintoul, this volume). Recently, work has begun to couple simple food web models to basin-scale ocean GCMs (Sarmiento et al., 1989). However, ocean GCMs perform most poorly in the regions of most relevance to the biology: the mixed layer and the ocean margins. The mixed-layer–thermocline climate model discussed in the previous section would also be well suited to coupling to a biological model.

The biological component of these coupled models needs refinement so that climatically relevant changes in community structure can be simulated. A promising approach may be to focus on func-

Table 1: Important trace gas species with a marine source or sink

Species	Atmospheric Lifetime	Importance	Controls
Sources			
CH_3Cl	Long	Natural source of stratospheric chlorine	Surface bio source (?), monolayer/gas exchange
DMS	Short	Source of CCN, sulfate aerosols, sulfonic acids	Surface bio source, monolayer/gas exchange
Hydrocarbons	Short	"Remote" source of reactive hydrocarbons	Surface bio source, monolayer/gas exchange
N_2O	Long	Possibly 10-20% of global budget	Rapid upwelling, denitrification
Chloroforms, Bromoforms	Short	Reactive halogens in boundary layer	Surface bio source, monolayer/gas exchange
Sinks			
CH_3CCl_3	Long	Uptake and loss may be 25% of total	Exchange, solubility, hydrolysis (loss)
CFCs	Long	Long-term reservoir (100-yr time scale)	Exchange, solubility, deep circulation

tional groups defined by biogeographic provinces or some other descriptor of the physical environment. Such a model requires observations of the physical and biological characteristics as a function of time so that the functional groups and the rules governing transitions between them can be defined. Mesoscale observational and modeling studies at representative sites are necessary to develop the understanding of the essential processes required to design realistic parameterizations for large-scale models. On the global scale, the ship-of-opportunity observations should be expanded to include measurements of optical depth and fluorescence, pH, total CO_2 (TCO_2), alkalinity, pCO_2, nitrate, and silicate. These measurements can now be done continuously while the ship is under way or on stored samples. Optical instruments on moored or drifting buoys and satellite measurements of ocean color would be valuable in filling the gaps between shipping routes.

Summary and Recommendations

This chapter has focused on the role of the ocean in the uptake of CO_2 on decadal time scales. Direct estimates of the oceanic CO_2

sink are very uncertain due to the lack of surface ocean pCO_2 measurements. Simple models predict that the ocean is taking up 26–44% of the fossil fuel input (Tans et al., 1990). However, all of the models are excessively diffusive and are calibrated by the same tracer, ^{14}C. The small range of present estimates probably reflects the similarity of the models used rather than the true uncertainty in the magnitude of the oceanic sink.

Several factors combine to determine the magnitude and timing of oceanic uptake of CO_2. The coupled air-sea system has an inherent negative feedback: If atmospheric pCO_2 decreases, perhaps due to an increase in high-latitude biological production, the oceanic source regions will become more effective and the oceanic sinks less so, tending to restore the system toward equilibrium. The Revelle factor also imposes a fundamental limitation on the capacity of the ocean to respond to atmospheric pCO_2 changes.

The ultimate factor determining the rate of oceanic uptake of CO_2 is the transfer of carbon to the interior by physical and biological processes. The physical transport pathways are primarily advective, connecting sparse sites of active "vertical" exchange. Both the exchange processes and the circulation between them have the capacity to change substantially on the 10–100-year time scale. However, present models do not treat the upper ocean well enough to predict how the vertical exchange processes will change in response to changes in atmospheric forcing.

The potential for changes in the biology to lead to significant changes in the oceanic sink of CO_2 on decadal time scales is probably small. Possible exceptions include changes in the size or residence time of the dissolved organic matter pool, an increase in the relative importance of calcareous organisms, and changes in the community structure in regions of high surface nutrient concentrations. Our present understanding of the dynamics of these pools or processes is so poor that we do not know whether changes in them can lead to changes in the oceanic uptake of carbon on these time scales.

Present models are not able to predict how the ocean circulation or biology will change in response to changes in the atmospheric forcing, or the impact of such changes on climate or the carbon cycle. We recommend that the following steps be taken in the design of more realistic models:

- Ocean circulation models must do a better job of simulating the primarily advective nature of the pathways between the mixed layer and the ocean interior. This will require higher-resolution models with physically based mixing parameterizations (e.g., shear- or stability-dependent mixing, isopycnal mixing).

- Ocean models must be forced with surface fluxes of heat and moisture, rather than restoring sea surface temperature and salinity to observed climatology, if they are to be used for predicting the response to changing atmospheric forcing.

- For coupling ocean circulation models to atmospheric GCMs or to marine ecosystem models, model treatment of the upper ocean must be improved. A model with a highly resolved mixed layer and thermocline and a coarsely resolved deep ocean would be appropriate for climate studies on decadal time scales. A critical test of such a model will be reproducing the observed seasonal cycle and interannual variability of upper ocean temperature, salinity, and biological properties.

- Improved upper ocean models therefore require basin-scale, long-term observations of the seasonal cycle of temperature and salinity in the upper several hundred meters. For ocean biology models, measurements of nitrate, silicate, carbon species (pH, TCO_2, alkalinity, pCO_2), and optical depth/fluorescence (as a measure of biomass) are required. These observations could be obtained under way from ships of opportunity. Satellite measurements of sea surface temperature, sea ice extent, and ocean color would also be useful for verifying such models. The use of moored or drifting buoys with temperature and salinity chains and optical instruments would help fill the data gaps away from shipping routes.

- Marine ecosystem models appropriate for basin scales need to be developed. In particular, the model must be able to simulate climatically relevant changes in community structure or functional groups in response to changes in the physical environment. Progress is most likely to come from building on the experience gained from mesoscale observational and modeling studies.

- More observational work is urgently needed on the role of the ocean as a source/sink of radiatively or chemically active trace gases.

References

Bolin, B. (ed.). 1981. *Carbon Cycle Modeling.* SCOPE 16, John Wiley and Sons, Chichester, England.

Bolin, B. 1986. Requirements for a satisfactory model of the global carbon cycle and current status of modeling efforts. In *The Changing Carbon Cycle: A Global Analysis* (J.R. Trabalka and D.E. Reichle, eds.), Springer-Verlag, New York, 403-424.

Broecker, W.S., and T.-H. Peng. 1982. *Tracers in the Sea*. Eldigio Press, Lamont-Doherty Geological Observatory, Palisades, New York.

Broecker, W.S., T.-H. Peng, and R. Engh. 1980. Modeling the carbon system. *Radiocarbon 22*, 565–598.

Codispoti, L.A., G.E. Friederick, R.L. Iverson, and D.W. Hood. 1982. Temporal changes in the inorganic carbon system of the southeastern Bering Sea during spring 1980. *Nature 296*, 242–244.

Enting, I.G., and J.V. Mansbridge. 1989. Seasonal sources and sinks of atmospheric CO_2: Direct inversion of filtered data. *Tellus 41B*, 111–126.

Jenkins, W.J., and P.B. Rhines. 1980. Tritium in the deep North Atlantic Ocean. *Nature 286*, 877–880.

Joos, F., J. Sarmiento, and U. Siegenthaler. 1991. Estimates of the effect of Southern Ocean iron fertilization on atmospheric CO_2 concentrations. *Nature 349*, 772–775.

Keir, R.S. 1991. Ironing out greenhouse effects. *Nature 349*, 198.

Kempe, S. 1979. Carbon in the rock cycle. In *Carbon Cycle Modeling* (B. Bolin, ed.), SCOPE 16, John Wiley and Sons, Chichester, England, 343–377.

Knox, F., and M. McElroy. 1984. Changes in atmospheric CO_2: Influence of biota at high latitudes. *Journal of Geophysical Research 89*, 4629–4637.

Maier-Reimer, E., and K. Hasselmann. 1987. Transport and storage of carbon dioxide in the ocean, and in organic ocean-circulation carbon cycle model. *Climate Dynamics 2*, 63–90.

Manabe, S., and R. Stouffer. 1988. Two stable equilibria of a coupled ocean-atmosphere model. *Journal of Climate*, 841–866.

Martin, J.H., and S.E. Fitzwater. 1988. Iron deficiency limits phytoplankton growth in the north-east Pacific subarctic. *Nature 331*, 341–343.

Martin, J.H., G.A. Knauer, D.M. Karl, and W.W. Broenkow. 1987. VERTEX: Carbon cycling in the northeast Pacific. *Deep Sea Research 34*, 267–285.

Martin, J.H., R.M. Gordon, S. Fitzwater, and W.W. Broenkow. 1989. VERTEX: Phytoplankton/iron studies in the Gulf of Alaska. *Deep Sea Research 36*, 649–680.

Martin, J.H., R.M. Gordon, and S. Fitzwater. 1990. Iron in Antarctic waters. *Nature 345*, 156–158.

Oeschger, H., U. Siegenthaler, U. Schotterer, and A. Gugelmann. 1975. A box diffusion model to study the carbon dioxide exchange in nature. *Tellus 27*, 168–192.

Pearman, G.I., and P. Hyson. 1986. Global transfer and inter-reservoir exchange of carbon dioxide with particular reference to stable isotopic distributions. *Journal of Atmospheric Chemistry 4*, 81–124.

Peng, T.-H., and W.S. Broecker. 1985. The utility of multiple-tracer distributions in calibrating models for uptake of anthropogenic CO_2 by the ocean thermocline. *Journal of Geophysical Research 90*, 7023–7035.

Peng, T.-H., and W.S. Broecker. 1991. Dynamical limitations on the Antarctic iron fertilization strategy. *Nature 349*, 227–229.

Redfield, A.C., B.H. Ketchum, and F.A. Richards. 1963. The influence of organisms on the composition of sea water. In *The Composition of Sea Water: Comparative and Descriptive Oceanography* (M.N. Hill, ed.), The Sea, Vol. 2, Interscience Publishers, New York, 26–77.

Roemmich, D., and C. Wunsch. 1985. Two transatlantic sections: Meridional circulation and heat flux in the subtropical North Atlantic Ocean. *Deep Sea Research, 32*, 619–664.

Sarmiento, J.L., and J.R. Toggweiler. 1984. A new model for the role of the oceans in determining atmospheric pCO_2. *Nature 308*, 621–624.

Sarmiento, J.L., J.C. Orr, and U. Siegenthaler. 1992. A perturbation simulation of CO_2 uptake in an ocean circulation model. *Journal of Geophysical Research 97(3)*, 3621–3647.

Sausen, R., K. Barthel, and K. Hasselmann. 1988. Coupled ocean-atmosphere models with flux correction. *Climate Dynamics 2*, 145–163.

Schlesinger, M.E., W.L. Gates, and Y.-J. Han. 1988. The role of the ocean in CO_2-induced climate change: Preliminary results from the OSU coupled atmosphere-ocean general circulation model. In *Coupled Ocean-Atmosphere Models* (J.C. Nihoul, ed.), Elsevier, Amsterdam, 447–478.

Schlosser, P., G. Bonisch, M. Rhein, and R. Bayer. 1991. Reduction of deep water formation in the Greenland Sea during the 1980s: Evidence from tracer data. *Science 251*, 1054–1056.

Siegenthaler, U. 1983. Uptake of excess CO_2 by an outcrop-diffussion model of the ocean. *Journal of Geophysical Research 88(C6)*, 3599–3608.

Siegenthaler, U., and T. Wenk. 1984. Rapid atmospheric CO_2 variations and ocean circulation. *Nature 308*, 624–625.

Stommel, H. 1961. Thermohaline convection with two stable regimes of flow. *Tellus 13*, 224–230.

Stouffer, R.J., S. Manabe, and K. Bryan. 1989. Interhemispheric asymmetry in climate response to a gradual increase of atmospheric carbon dioxide. *Nature 342*, 660–662.

Stuiver, M. 1978. Atmospheric carbon dioxide and carbon reservoir changes. *Science 199*, 253–258.

Sugimura, Y., and Y. Suzuki. 1988. A high-temperature catalytic oxidation method for the determination of non-volatile dissolved organic carbon in seawater by direct injection of liquid samples. *Marine Chemistry 24*, 105–131.

Tans, P.P., I.Y. Fung, and T. Takahashi. 1990. Observational constraints on the global atmospheric CO_2 budget. *Science 247*, 1421–1438.

Toggweiler, J.R. 1989. Is the downward dissolved organic matter (DOM) flux important in carbon transport? In *Productivity of the Ocean: Present and Past* (W.H. Berger, V.S. Smetacek, and G. Wefer, eds.), John Wiley and Sons, New York, 65–83.

Weiss, R.F., W.S. Bullister, R.H. Gammon, and M.J. Warner. 1985. Atmospheric chlorofluoromethanes in the deep equatorial Atlantic. *Nature 314*, 608–610.

Williams, P.J.leB., and B. von Bodungen. 1989. Export productivity from the photic zone. In *Productivity of the Ocean: Present and Past* (W.H. Berger, V.S. Smetacek, and G. Wefer, eds.), Dahlem Conference, John Wiley and Sons, Chichester, England, 99–115.

Wust, G. 1935. Schichtung und Zirkulation des Atlantischen Ozeans: Die Stratosphäre. Reprinted in *The Stratosphere of the Atlantic Ocean*, W.J. Emery, ed. Amerind, New Delhi, 1978, 112 pp.

Report: Linkages between Terrestrial Ecosystems and the Atmosphere

Francis Bretherton, Robert E. Dickinson, Inez Fung, Berrien Moore III, Michael Prather, Steven Running, and Holm Tiessen

Introduction

The possibility of major changes in the global environment presents a difficult task to the scientific research community: to devise ways of analyzing the causes and projecting the courses of these shifts as they are occurring. Purely observational approaches are inadequate for providing the needed predictive or anticipatory information because response times of many terrestrial ecosystems are slow, and there is a great deal of variation from place to place. Furthermore, many important processes, such as soil processes, cannot be measured directly over large areas. We need models to express our understanding of the complex subsystems of the earth, how they interact, and how they respond to and control changes in climate and biogeochemical cycles.

The primary research issue in understanding the role of terrestrial ecosystems in global change is analyzing the coupling between processes with vastly differing rates of change, from photosynthesis to community change. Representing this coupling in models is the central challenge to modeling the terrestrial biosphere as part of the earth system.

Terrestrial ecosystems participate in climate and in the biogeochemical cycles on several temporal scales. Examples of processes that operate on short time scales (i.e., less than days) are the metabolic processes responsible for plant growth and maintenance, and certain microbial processes associated with dead organic matter decomposition. The associated energy balance is also affected at short time scales.

CONT →

Some of the carbon fixed by photosynthesis is incorporated into plant tissue and is delayed from returning to the atmosphere until it is oxidized by decomposition or fire. This slower (i.e., days to months) carbon loop through the terrestrial component of the carbon cycle, which is matched by cycles of nutrients required by plants and decomposers, affects the increasing trend in atmospheric CO_2 concentration and imposes a seasonal cycle on that trend. Moreover, this cycle includes key controls over biogenic trace gas production. The structure of terrestrial ecosystems, which responds on even longer time scales (annual to century), is the integrated response to the biogeochemical and environmental constraints that develop over the intermediate time scale. The loop is closed back to the climate system since it is the structure of ecosystems, including species composition, that sets the terrestrial boundary condition in the climate system through modification of surface roughness, albedo, and, to a great extent, latent heat exchange.

These separate temporal scales contain explicit feedback loops which may modify ecosystem dynamics and linkages between ecosystems and the atmosphere. Consider again the coupling of long-term climate change with vegetation change. Climate change will affect vegetation dynamics, but as the vegetation changes in quantity or type of structure, this may feed back to the atmosphere by changing water, energy, and gas exchange. Biogeochemical cycling will also change, altering the exchange of trace gas species and nutrient availability. The long-term change in climate, resulting from increased atmospheric concentrations of greenhouse gases (e.g., CO_2, CH_4, and nitrous oxide [N_2O]) will further modify the global environment and potentially induce further ecosystem change. Modeling these interactions requires coupling successional models to biogeochemical models to physiological models that describe the exchange of water, energy, and biogenic trace gases between the vegetation and the atmosphere at fine time scales. There does not appear to be any obvious way to allow direct reciprocal coupling of atmospheric general circulation models (GCMs), which inherently run with fine time steps, to ecosystem or successional models, which have coarse temporal resolution, without the interposition of physiological canopy models. This is equally true for biogeochemical models of the exchange of carbon dioxide and trace gases. This coupling across time scales is nontrivial and sets the focus for the modeling strategy.

Scales of Interactions

Based on current model structures, atmosphere-biosphere interactions can be captured with simulations operating with three char-

acteristic time constants (Figure 1). The first level represents rapid (seconds-day) biophysical interactions between the climate and the biosphere. The dynamics at this level result from changes in water, radiation, and wind and accompanying physiological responses of organisms. Dynamics at this level occur rapidly relative to plant growth and nutrient uptake, and far more rapidly than species replacement can occur. Simulations at this level are required to provide information to climate models on the exchange of energy, water, and CO_2. Tests of this level of model can be accomplished using experimental methods including leaf cuvettes, micrometeorological observations, and eddy correlation flux measurements.

The second level captures important biogeochemical interactions. This level captures weekly to seasonal dynamics of plant phenology, carbon accumulation, and nutrient uptake and allocation (Figure 1). Most existing models at this level use integrative measures of climate such as monthly statistics and degree-day sums. Changes in soil solution chemistry and microbial processes can be captured at this level for calculation of trace gas fluxes. Primary outputs from

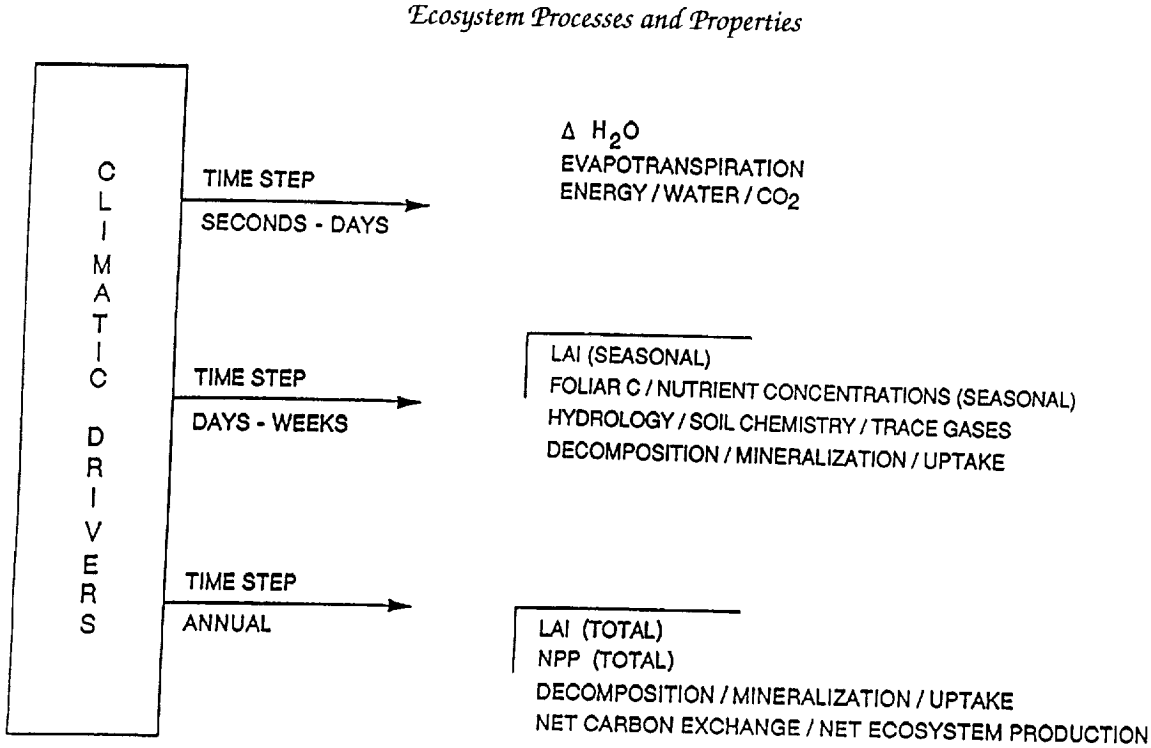

Figure 1. Scales of interaction between climatic interactions and ecosystem properties.

this level of model are carbon and nutrient fluxes, biomass, leaf area index (LAI), and canopy height or roughness. This level of model is usually tested in field studies with direct measurements of biomass, canopy attributes, and nutrient pools or fluxes.

A third level of model represents annual to decadal changes in biomass and soil carbon (net ecosystem productivity, carbon storage) and in ecosystem structure and composition (Figure 1). Inputs are statistical distributions of climate variables and calculated indices summarizing the effects of climatic conditions on biomass accumulation and decomposition. The outputs include ecosystem element storage, allocation of carbon and other elements among tissue types, and community composition and structure. Such models are currently based either on individual organisms or on species correlations with environment. The former are difficult to apply at large scales because of computational and data requirements, and considerable work will be required to develop large area implementations. This type of model is validated using a combination of process studies, as described above. These processes need to be integrated and validated in comparative studies to derive annual fluxes. The community composition and population dynamics aspects of these models are often validated using paleodata.

There are two scales of spatial resolution. At fine resolution, climate model results are used to drive regional-scale ecosystem process models, which are rather mechanistic. Much higher spatial resolution than currently available is needed for terrestrial climate variables, particularly for complex terrain (e.g., mountain ranges). Next-generation GCMs, such as the community climate model version 2 (CCM2) from the National Center for Atmospheric Research (NCAR) (with 250 x 250 km resolution), will improve on this problem, but only in a modest fashion, and will not satisfy all needs of terrestrial modeling. Development of nested model techniques and greater computing power will be needed to produce climate-related results in the range of resolution (10–20 km) required by ecosystem process models. Spatial distribution of precipitation is most critical, and improved surface topographic definition (as done in CCM2) is a critical step in improving orographically related precipitation.

At the coarser scale required for the operation of global terrestrial vegetation models, GCM grid scale is nearly adequate, although improvements are highly desirable. However, any dynamic process model of global vegetation can be linked to key satellite-derived variables, such as advanced very high resolution radiometer (AVHRR) vegetation index data and the normalized difference vegetation index (NDVI), that provide reference characteristics of the land surface. Current global NDVI-based land cover maps have a resolution of

about 4 x 4 km; however, for many global applications these data could be aggregated to near GCM cell scales. It is important that future GCMs be able to interactively incorporate satellite data for regular redefinition of surface albedo and of vegetation characteristics related to evapotranspiration (ET), such as LAI. Additionally, regular monitoring of changing land cover and land use will be important.

Atmospheric GCMs tend to simulate mean atmospheric conditions. However, many terrestrial processes, such as biome replacement, are triggered by occasional extreme events. Although these events do not have global significance, they are of unsurpassed importance regionally. The meteorological conditions that triggered the 1988 fires at Yellowstone National Park will have regional consequences for the next century. Spring frosts, which occur early in the growing season; multiple years of successive drought; floods; and hurricanes are other examples of extreme meteorological events that have potentially significant ecological ramifications. Some lakes in central Australia only contain water a few times per century, when extreme precipitation events occur. The utility of augmenting GCM results with regional climatological statistics, as suggested by F. Bretherton in the appendix to this chapter, may be the most reasonable way of providing this data.

Specific Variables Linking the Atmosphere with the Terrestrial Ecosystem

Precipitation

Simulation of precipitation requires high spatial resolution (10–50 km), particularly in complex terrain. Minimum event resolution is around 3 mm for regional process simulations. At least daily time resolution is essential to differentiate between precipitation that is intercepted by vegetation canopies and evaporated immediately and precipitation that enters the soil rooting zone, with a subsequent residence time of days to months. Also, interception and evaporation have only physical controls; the dynamics of soil water uptake are controlled by plant physiology in concert with physical drivers.

There are several ways to reduce uncertainties of local precipitation from coarse-resolution models:

- Empirical relationships can be developed between mean precipitation and other large-scale circulation statistics for the region defined by a GCM grid cell and precipitation data at individual stations within the grid cell (see appendix to this chapter, "A Regression of Atmospheric Circulation to Local Weather"). Such relationships can then be used to extract subgrid-scale precipi-

C-3.

tation variations from GCM simulations. This is the approach used in standard numerical weather forecasts. However, it is not clear whether such empirical relationships will hold in a changing climate.

- The planned Tropical Rainfall Measuring Mission (TRMM) will allow precipitation to be derived from satellite observations (in the microwave). Limiting its value, TRMM is planned to be an exploratory mission, i.e., of limited lifetime, and it will be focused on the tropics.

- Algorithms are being developed to extract intensities of convective precipitation in the tropics from satellite measurements of outgoing longwave radiation (OLR) at the top of the atmosphere. They employ the fact that colder brightness temperature is correlated with higher convection and more intense rainfall. The approach looks promising, and it should be extended to the rest of the globe. High-resolution (15-minute, ≈20-km) OLR data are in the archives, as are high-resolution precipitation data at river gauge stations (U.S. Geological Survey network); these data are useful for testing the algorithms. If global algorithms can be developed, they offer the possibility of gaining a self-consistent data set for expressing subgrid-scale precipitation in terms of larger-scale variables such as mean precipitation or OLR. It is not known whether the relationships will hold in a changing climate. Looking at year-to-year variations in the relationships may provide a clue, depending on the quality and availability of data sets for regional verification.

- Mesoscale models nested in GCMs (e.g., Dickinson et al., 1989) promise predictive capability for local precipitation. A GCM is run at coarse resolution, and then a high-resolution mesoscale model for a region such as the western United States uses the GCM output as boundary conditions or driving functions and simulates the climate within each grid cell of the region. The usefulness of this approach depends, of course, on whether cloud physics and precipitation dynamics are properly incorporated in the models. For global applications, precipitation with a precision of 10 mm may be acceptable.

Temperature

Canopy-level temperatures are needed to drive evapotranspiration, photosynthesis, and respiration computations, preferably at daily time scales. Various growing season definitions, ecosystem phenology, etc., are best defined either by integrated daily temperatures

(i.e., growing degree day crop forecasts) or by thresholds, e.g., last frost–first frost growing periods. The needed accuracy is about 1°C. Substantial spatial variability within GCM cells is caused by topography (slope, aspect and elevation) and by variability in land surfaces, such as forest vs. cropland, irrigated land vs. desert, and upland vs. wetland. Variability in topography and land cover can be described statistically, rather than by geographically explicit treatments.

Monthly or yearly average temperatures are used to drive models of soil processes, such as decomposition and N mineralization. For these models, soil temperatures at a depth of 10–20 cm are needed, as well as surface or canopy temperatures. Additionally, simplified primary production models, once they have been "calibrated" by daily canopy models, can be used for general global estimates with minimal data requirements. GCM grid cell output of daily maximum and minimum temperatures is very useful for defining continental-scale vegetation phenology and growing seasons.

Atmospheric Deposition of Nutrients

A subset of required precipitation data for terrestrial ecosystems is wet and dry deposition of atmospherically transported chemicals, including nutrients such as the nitrate, ammonium, sulfate, and phosphate radicals (NO_3^-, NH_4^+, $SO_4^=$, and $PO_4^{\equiv}$). Acid rain and air pollutant deposition effects on terrestrial ecosystems have been widely studied. GCMs simulate the physical mechanism of transport of these aerosols, particulate matter, etc., but they do not couple the compounds to measured source fields, and they do not include any of the atmospheric chemistry involved in their transformations. Future versions of GCMs should be able to provide deposition estimates globally.

NO_3^- is deposited from the atmosphere both as nitrate in rainfall and directly as nitric acid (HNO_3). The fractional input from both sources appears to be about equal, as some recent studies of HNO_3 downward fluxes over grasslands have shown. Dry deposition of nitrogen dioxide (NO_2) is less important because of the smaller relative atmospheric abundance. The atmospheric budget of NO_x, which consists of nitric oxide (NO) plus NO_2, is approximately 18.5–89.5 Tg N/yr, as shown in Table 1.

In remote areas, the abundance of HNO_3 is typically 0.1 ppbv or 0.2 Tg N, with an average atmospheric lifetime against rainout of five days. This gives a budget of 50 Tg N/yr (with an uncertainty of at least a factor of two). The lightning source may be dependent on latitude and can be regionally important (Liaw et al., 1990), but will be dispersed since the NO it produces must be oxidized to HNO_3 before deposition. Most of the large emissions associated with urban pollution are observed to decay rapidly (presumably to the nearby areas).

Table 1: Global budget for NO_x

Source	Tg N/yr
Stratospheric input (from N_2O)	0.5–1.5
Lightning	8 (2–20)* [81 ± 65.7]**
Soil sources	8 (1–16)
Fossil fuel burning	21 (14–28)
Biomass burning	12 (1–24)
Total	**18.5–89.5** excluding large lightning values

Logan, 1983; Liu and Cicerone, 1984
*Liaw et al., 1990

Accurate global modeling of the nitrate system is difficult and has only recently been attempted in global chemical transport models (CTMs). The current models cannot be used to predict nitrate input accurately, but in the next few years they are expected to produce a good but incomplete global picture of the NO_x budget. Anthropogenic inputs are expected to dominate near industrial regions.

Ammonia (NH_3) deposition from the atmosphere is most likely to come in the form of ammonium nitrate (NH_4NO_3) or some other neutralized ammonium aerosol. Although elevated concentrations of NH_3 gas have been measured above biologically active "hot spots" (e.g., animal feedlots), concentrations are difficult to detect in the free troposphere. The implication (consistent with the observed abundances of HNO_3 and acidic aerosols) is that NH_3 is removed from the atmosphere in aerosols. (The lifetime against oxidation of the hydroxyl free radical, OH, is greater than 30 days, even in the tropics.) If NH_3 forms aerosols in the boundary layer in the immediate vicinity of where it is emitted, then the most likely effect of ammonia volatilization is the horizontal dispersion of nitrogen.

Ammonia releases are deposited within a few hundred to a thousand km (generally downwind) of their source. Global models for atmospheric NH_3 are not available.

The sources of sulfates deposited to the ecosystem include marine sea salt, photochemically oxidized marine sulfides, and anthropogenic sulfates. (We exclude here volcanic emissions.) In regions where marine sulfide-to-sulfate sources may be important, it is likely that deposition of sea salt sulfates provides adequate fertiliza-

tion. These regions are thus independent of the atmospheric chemistry. Large perturbations to sulfate-limited ecosystems will probably occur only if they are downwind from industrial sources, such as areas with considerable combustion of sulfur-containing fuel or smelting.

For ecosystems that are limited by phosphorus, the only atmospheric source is associated with large dust storms. Such storms are not regular, annual processes, but rather extreme events that cannot be predicted from current atmospheric CTMs. Changes in inputs of phosphorus are likely to be the result of extreme climatic events.

The potential impact of acid rain is proportional to the total flux of hydrogen ions (H^+) both in rainfall and in dry deposition (e.g., HNO_3). Normal rain is acidic: pH's of about 5.5 are due to the solubility of 350 ppm of CO_2 in water. Even in remote regions, organic acids such as formic acid (the result of oxidation of CH_4 and other hydrocarbons) reduce the pH of rainfall to 5 or less. In regions perturbed by large anthropogenic sources of acid precursors (e.g., NO and sulfur dioxide, or SO_2), the acidity of the rain is likely to be below a pH of 4. However, in regions with alkaline soils, the natural dust can neutralize the acidity of rain (pH > 6). Regional acid deposition models have been used to predict H^+ fluxes for part of the United States, but the deposition of H^+ is difficult to predict on a global scale. Significant amounts of acid rain (and deposition) are expected a few thousand km downwind of large anthropogenic sources of NO and SO_2.

Ozone

The interaction between ozone and vegetation is an important link in modeling both the ecosystem and the atmosphere. High local ozone concentrations can be deleterious to vegetation, damaging stomata and affecting evapotranspiration. Currently there are regional models for air quality that predict tropospheric ozone over part of the United States. Many research groups are developing CTMs for global tropospheric ozone, and we may expect such models to contribute to these regional atmospheric-ecosystem models in the next few years. The occurrence of extreme ozone events will still be difficult to predict in the global models.

The destruction of ozone at the earth's surface is an important part of the global budget for tropospheric ozone. Observations show that ozone is removed with high efficiency above regions with active plants. Emissions of NO, N_2O, CH_4, isoprene (C_5H_8), and other hydrocarbons from vegetation and soils play a major role in global atmospheric chemistry.

Humidity

GCMs provide a water mixing ratio in the lowest layer of the model (900–1000 mb, depending on the model). In some boundary-layer models, this can be translated into dewpoint at the canopy surface. Humidity is critical for modeling ET and stomatal response models, but less so for soil carbon or nitrogen cycling except as a component of hydrologic balance. If a spatially and diurnally conservative measure of humidity is used, such as dewpoint or mixing ratio, fairly broad regional average conditions may be adequate. The needed accuracy is $\approx 1°$. However, canopy- or surface-level estimates are needed, as a bulk tropospheric mixing ratio probably underrepresents the near-surface humidity over vegetated surfaces.

Solar Radiation

Incoming shortwave or photosynthetically active radiation (PAR) is very critical for photosynthesis and ET models, although less so for modeling soil processes. Incoming solar radiation is well modeled by GCMs for a molecular atmosphere, but inadequate simulation of clouds and aerosols in current climate models makes this a feature of questionable value. Hourly or daily resolution is needed for photosynthesis and ET models; monthly or annual totals are used in ecosystem dynamics models. It is not critical to partition between direct and diffuse radiation or between total radiation and PAR. Subgrid-scale topographic variability can easily be handled with corrections for slope and aspect. However, subgrid-scale clouds and optical variability are problems.

Wind and Dust

Extreme storms, hurricanes, etc., are important ecosystem disturbance triggers. The recurrence of extreme climatic events determines ecosystem structure to a certain extent. There really is no satisfactory way to simulate extreme winds with a coarse-resolution model. Parameters such as minimal surface pressure may be useful for defining storm existence and perhaps storm tracks. However, an operational diagnostic of maximum winds may not be readily available in GCMs. Average wind velocity is also an important component of evaporation, and daily averages may be adequate for ET estimates. This parameter, average wind velocity, is highly variable and unpredictable in complex topography that is below grid-scale resolution.

Extreme wind conditions are of high importance for dust plumes and soil erosion calculations (which also require soil texture and moisture information). Dust affects soil properties, incident solar radiation, and terrestrial productivity. All of the necessary atmos-

pheric parameters are available in principle in GCMs. However, the current capabilities of the GCMs and our understanding of source functions need significant improvements before useful applications can be made.

Snowpack

Snowpack is a critical available output from GCMs. Snowpack is a major albedo and hydrologic balance determinant and is an important output variable of most GCMs. Obviously there is much subgrid-scale, topographically induced variability in snowpack dynamics. However, even grid-scale snowpack information, as provided currently by GCMs, is useful. Subgrid-scale modeling is possible from higher-resolution topographic and topoclimatological models, and the U.S. Soil Conservation Service operates a national Snow Survey Network (used for summer irrigation scheduling) of ground measurements for model development/validation.

Snowpack is a critical mechanism for water storage, providing summer water in arid regions and controlling flood potential in many wetter areas. Snowmelt is an important trigger of growing season, causing an intense burst of trace gases from the spring soil and hydrologic flushing of dissolved elements. Spring snowmelt initializes calculations of seasonal soil water depletion and ecosystem stress and produces primary annual hydrologic discharge in semiarid lands. Snowpack insulates soils from extreme temperatures, and is important in vegetation/crop survival.

Variables Linking Terrestrial Ecosystems to Atmospheric GCMs

Evapotranspiration

The single most important feedback from the land to the climate models is the partitioning of incident solar radiation (H) to sensible or latent heat (LE), the Bowen ratio (H/LE). This partitioning is controlled by the surface evapotranspiration in a complex fashion and is computed with soil-vegetation-atmosphere models. Major decreases in seasonal Bowen ratio occur as vegetation develops, increasing ET and latent energy. Later in the growing season, as vegetation either senesces or endures soil water deficits, physiological water stress and stomatal closure can cause Bowen ratios to increase by an order of magnitude as progressively more of the incoming energy produces sensible heat. This cannot be effectively simulated by meteorological measures alone, but can be calculated (interactively) in models of ecosystem water balance that determine

seasonal LAI, soil moisture, and water use efficiency as a function of climate, CO_2 concentrations, plant physiology, and other perturbations and stresses. Ecosystem water balances are typically executed on hourly or daily time scales.

Albedo

At minimum, ecosystem models predict seasonal phenology and assume some ecosystem structure and soils. A look-up table translation scheme can be used to yield broadband albedos for each of these ecosystem compartments, which can then be weighted to give the mean albedo for a GCM grid cell as a function of time. There are sophisticated models (e.g., ray tracing models) that calculate spectral reflectivities as a function of, among other things, leaf shape, orientation, and distribution. However, significant generalization of these models is needed before they are useful for GCM-scale applications. Inversion of satellite-derived surface reflectance can now provide global maps of surface albedo.

A major uncertainty in GCMs is the highly dynamic albedo changes caused by the delivery and melting of snow. Albedo varies with age (and depth) of snow and with the masking depth of vegetation. This introduces a large degree of uncertainty to the energy balance of high latitudes. Either mechanistic submodels of snowpack dynamics or regular reparameterizations of the GCM during simulations by satellite data are probably required to meaningfully improve this situation.

Roughness Length

Topographic roughness and vegetation height affect momentum dissipation at the surface. In general, topographic roughness dominates the momentum exchange. The improved spatial resolution of the NCAR CCM2 allows higher definition of grid-cell topography. However, additional improvement may be possible by using subgrid-scale information on topographic variation.

Typically, a roughness length is assigned to each vegetation type, ranging from around 0.02 to 6.0 m, small relative to topography. Models that simulate ecosystem transitions can, in principle, output roughness length as a function of time. How important this is for altering GCM circulation has not been established.

Greenhouse Gases

Models of canopy photosynthesis-respiration balances and soil carbon cycle dynamics in ecosystems by definition keep track of surface CO_2 uptake from the atmosphere by simulating the produc-

tion and return of CO_2 to the atmosphere through soil organic matter turnover. When applied to scenarios of climate change, these models project changes in the net fluxes of CO_2 that are useful for studies of the carbon cycle. A daily or longer surface CO_2 balance could in principle be entered into a GCM. Again, the primary problem is the spatial aggregation of the ecosystem model outputs to the GCM cell size. Alternatively, simple satellite-driven AVHRR/NDVI-based models have been highly correlated with CO_2 balance and could be implemented globally (Running and Nemani, 1988).

Carbon dynamics models can be adapted to the study of other trace gases. We envisage that a separate treatment would be required for each gas. N_2O and NO fluxes require elaboration in soil compartments and explicit treatment of soil moisture regimes. Isoprenes, terpenes, and other nonmethane hydrocarbons require some scaling to the metabolic function of certain vegetation species. Modeling of carbon monoxide must be linked to a fire model, and CH_4 requires a detailed hydrology model. Because of the many linkages required, global-scale modeling of trace gas fluxes is not currently possible.

Unmodeled Land Parameters Needed by GCMs

A number of soil and vegetation characteristics are needed for GCM surface parameterization, as exemplified by the biosphere-atmosphere transfer scheme (BATS; see Tables 2 and 3 in Dickinson et al., 1986). Many of these characteristics are not outputs of ecosystem models but are surface parameterizations also needed by them. Some of these parameters can be estimated globally, but many are impossible to do accurately. Satellite-derived estimates of vegetation cover and seasonal variation are available from weekly composite global AVHRR/NDVI maps. These can be translated reasonably well to maximum-minimum LAI for different biome types. Physiological parameters like minimum stomatal resistance or leaf light sensitivity cannot be directly inferred. Global albedo is now being monitored weekly by satellite and could be entered into the GCMs. Soil physical and hydraulic parameters cannot be monitored by satellite, and existing global soils maps are taxonomically based and of questionable accuracy. It is not clear how this problem can be improved (see Parton et al. report, this volume).

References

Dickinson, R.E., A. Henderson-Sellers, P.J. Kennedy, and M.F. Wilson. 1986. *Biosphere-Atmosphere Transfer Scheme (BATS) for the NCAR Community Climate Model.* Technical Note NCAR/TN-275, National Center for Atmospheric Research, Boulder, Colorado.

Dickinson, R.E., R.M. Errico, F. Giorgi, and G. Bates. 1989. A regional climate model for the western United States. *Climatic Change 15*, 383–422.

Liaw, Y.P., D.L. Sisterson, and N.L. Miller. 1990. Comparison of field, laboratory, and theoretical estimates of global nitrogen fixation by lightning. *Journal of Geophysical Research 95*, 22489–22494.

Liu, S., and R.J. Cicerone. 1984. Fixed nitrogen cycle. In *Global Tropospheric Chemistry: A Plan for Action*, National Academy Press, Washington, D.C., 113–116.

Logan, J.A. 1983. Nitrogen oxides in the troposphere: Global and regional budgets. *Journal of Geophysical Research 88*, 10785–10807.

Running, S.W., and R.R. Nemani. 1988. Relating seasonal patterns of the AVHRR vegetation index to simulated photosynthesis and transpiration of forests in different climates. *Remote Sensing of Environment 24*, 347–367.

Appendix: A Regression of Atmospheric Circulation to Local Weather

A critical gap in connecting atmospheric climate models to ecosystem models of the land surface lies in the provision of local estimates of surface precipitation and daily weather statistics. Atmospheric climate models are designed to operate on spatial resolutions of several hundred kilometers horizontally and 1000–300 millibars vertically, whereas ecosystem models are developed and tested on data relevant to a small watershed, typically of 1–10 km. The variables predicted explicitly in GCMs (pressure, temperature, moisture, and wind in the free atmosphere) relate to the atmospheric circulation on regional scales. The lowest atmospheric cell may be between 1000 and 950 mb and will not be representative of surface conditions without a boundary-layer submodel. Subgrid-scale topography, land cover, and lake effects can all have a major impact on local temperature and precipitation, particularly the daily maximum and minimum temperatures, the incidence of solar radiation, and the probabilities of rainfalls of different intensities, which are the variables needed to run ecosystem models. Although for biogeochemical purposes monthly averages are adequate, to simulate the hydrologic balance, daily data and a knowledge of the diurnal cycle are imperative. Successional models are sensitive not only to seasonal averages but also to disturbances such as unseasonal frosts and fires. Giving a general definition of disturbance is difficult, but the meteorological factors involved can all be derived from a good daily weather record. Though surface temperature, solar radiation, and rainfall are all computed hourly in a GCM as part of the treatment of the atmospheric boundary layer,

these are highly parameterized estimates on a scale of the GCM grid, and it is not obvious how to derive locally valid values.

A similar problem is encountered in weather prediction, in which model simulations of the atmospheric circulation have to be translated on a daily basis into specific local forecasts for transmission to the public. It is believed that changes in local weather are largely controlled, at least in a statistical sense, by the regional atmospheric circulation, so a widely used technique is to correlate over several years the values of a selected subset of variables in the weather prediction model with the daily record from a local weather station. The correlation table is then used, in conjunction with future values from the prediction model, to predict the local station's weather. This technique, known as model output statistics, has proved as skillful as most human forecasters using more subjective methods.

This approach could easily be adapted to translate the output of climate models into equivalent local climates. Running a climate model in forecast mode for many years is normally not practical; instead, the observed values of the regional-scale circulation variables required for the correlation may be taken from actual observations rather than from a forecast, using a daily weather analysis. Of course, it is not to be expected that subsequent application of this correlation table to the output of a climate GCM will automatically produce a good simulation of local climate if the GCM produces inadequate statistics of the regional circulation patterns. However, the exercise will certainly focus attention on which aspects of the GCM circulation are incorrect, and, in conjunction with a local ecosystem model, could lead to a figure of merit by which improvements in simulations of present climate and the significance of projected changes could be assessed.

An issue that at once arises in applying this approach is the availability of suitable data. In most regions of the world there are many weather stations recording daily maximum and minimum temperature, total rainfall, and hours of sunshine. However, long records of hourly precipitation are less readily available, and intensity of solar radiation (as opposed to the more qualitative surrogates of cloudiness and hours of sunshine) is measured at only a few stations. However, surface solar radiation can be inferred fairly directly from geostationary satellite measurements of solar reflectance. Corrections must be made for variations in viewing angle, for surface albedo, and for absorption of solar radiation within clouds and other aerosols, and the results must be calibrated against the available surface radiation measurements. Once this is done, the data required are widely available over most, though not all, of the world.

Another issue is whether the structural relations between a given regional circulation pattern and local weather are likely to be stable under conditions of changing climate. To the extent that these connections are controlled by the interactions of topography, wind direction, and temperature through the troposphere, changes are indeed likely to be caused by changes in frequency of a regional-scale pattern and allowed for in this methodology. To the extent that they depend upon changes in aerosol or cloud condensation nuclei, which are not discussed in routine weather analyses, the correlation tables would change over decades. Indeed, systematic trends observed in such correlation tables might be the best indicators of this type of climate change.

It is also clearly inadequate to be able to estimate local climates only at points where there are weather station records. Modeling of the effects of topography and other causes specific to the local weather station is clearly an integral part of any application. This modeling may be empirical or may be based on more sophisticated local process studies using dynamical mesoscale models for phenomena such as lake effects and mountain drainage. In some locations such studies are already going on for reasons other than climate change, but it is important to generalize this experience to a global scale.

There are also extreme events of great importance to certain ecosystems, such as hurricanes and tornados, of which the frequency may well change with climate regime. Yet these events are not predicted within present climate models. Because of their rarity, such events are unlikely to appear in daily correlation tables, though special studies might well reveal the regional circumstances under which they are most likely to occur. GCM simulations should then be examined for changes in hurricane and tornado potential, which would be fed off line into ecosystem models.

If applied to a suitable sample of weather stations within a region, the correlation technique would also provide data sets to test and validate the physically based parameterizations of the surface variables predicted in the climate model for the purpose of keeping track of the surface energy and moisture balance. Indirectly, these parameterizations depend on the same regional atmospheric variables. It is, of course, straightforward to produce similar correlation tables within the climate model itself. It could be argued that it is inconsistent to maintain within the same framework two distinct connections between regional circulation variables and surface climatology and water balance, one empirical and site-specific, the other physically based but highly parameterized. In the long run this argument is probably correct, but until more experience has been gained the dualism is likely to be a source of strength.

Four Simple Ocean Carbon Models

Berrien Moore III

The change in atmospheric carbon dioxide concentration resulting from fossil fuel combustion, land management activities, and other human-induced disturbances of the global carbon cycle (Figure 1) is strongly governed by the CO_2 exchange between the atmosphere and ocean. The ocean is believed generally to be the largest sink for atmospheric CO_2; however, there is evidence, though quite controversial, that the temperate biosphere may have been a comparable net annual sink during the last decade (Tans et al., 1990).

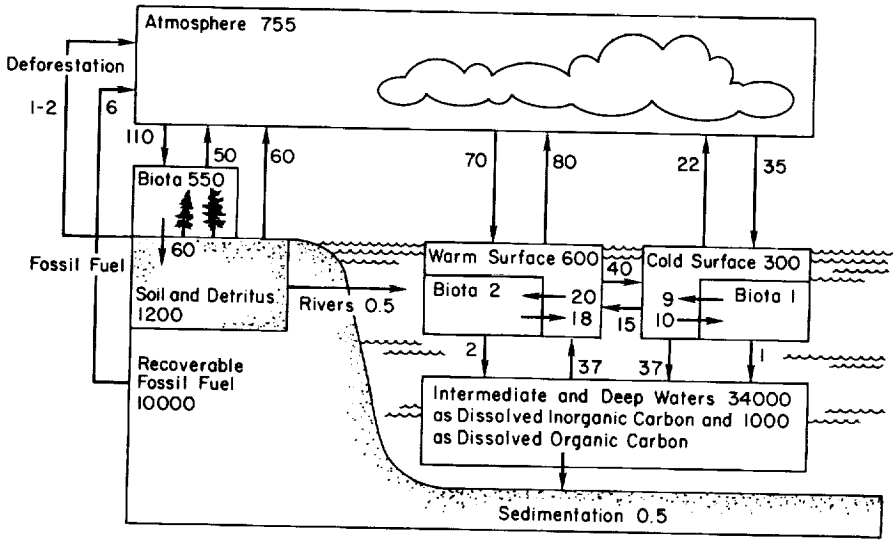

Figure 1. The global carbon cycle. The boxes are in Pg C, and the fluxes (arrows) are in Pg C/yr as CO_2.

Granting this and other uncertainties about the carbon cycle, future atmospheric concentrations of CO_2 will depend on the rate of industrial CO_2 emissions, the net exchanges between the atmosphere and the terrestrial biosphere, and the rate of uptake by the oceans.

This paper briefly reviews the key processes that determine oceanic CO_2 uptake and sets this description within the context of four simple ocean carbon models. These models capture, in varying degrees, these key processes and establish a clear foundation for more realistic models that incorporate more directly the underlying physics and biology of the ocean rather than relying on simple parametric schemes.

The purpose of this paper is more pedagogical than purely scientific. The problems encountered by current attempts to understand the global carbon cycle not only require our efforts but set a demand for a new generation of scientist, and it is hoped that this paper and the text in which it appears will help in this development. The student reader might also want to study SCOPE Reports 13 (Bolin et al., 1979) and 16 (Bolin, 1981); a review of the carbon cycle is given by Moore (1984); and finally, Moore and Schimel (1992) provide an extremely useful context for these discussions.

Ocean Modeling

The oceanographic community already has a rich history that parallels the atmospheric modelers' advances in seeking the development of ocean general circulation models (GCMs), in which the steady state circulation of the oceans may be deduced in response to a given external forcing, i.e., specification of sources and sinks at the ocean surface of momentum, energy, and water. The efforts and accomplishments are significant, but the ocean models lag behind atmospheric GCMs, primarily because the data for the oceans are far more sparse and the turnover constants span a much greater range. In addition, to employ ocean GCMs for studies of the carbon cycle, one needs to incorporate biological and chemical processes that occur within the fluid medium being modeled (i.e., the ocean).

From a long-term perspective, the development of ocean GCMs is undoubtedly the most rational approach not only for improving our understanding of the general circulation of the oceans but also for dealing with the issue of atmosphere-ocean carbon exchanges. However, these models have only recently begun to incorporate carbon dynamics; they demand significant computing resources; and they are rather complicated, employing a number of subroutines (and people). Thus, they may not yet be sufficiently well developed or sufficiently well understood to serve as the appropriate introductory

scientific tool for gaining insight into the ocean uptake of CO_2. Simpler models are perhaps more appropriate to this pedagogical requirement; furthermore, simple models may be useful in the policy process.

An approach to studying the general circulation of the ocean, including carbon exchanges, that has been taken by chemical oceanographers offers a particularly useful framework for describing and understanding the basic outline for ocean-atmosphere carbon exchanges. For quite some time, they have been exploring several questions: What transfer processes due to water motions and biological activity are needed to explain the quasi-steady distribution of chemical compounds in the ocean? What can we learn about the biochemistry of the sea by the simultaneous use of several tracers? How can we extract information about the ocean from the observed transient tracers, particularly tritium, ^{14}C, and chlorofluorocarbons, that are now invading the world ocean due to human-caused emissions into the atmosphere?

The basic idea of this approach is to make use of the fact that the distributions of chemical and physical properties (e.g., concentrations of inorganic carbon or the varying pattern of temperature) are a reflection of the water motions (advective and turbulent) and perhaps of biological activities (e.g., new production, decomposition, carbonate formation, and dissolution) as well as the result of different distributions of sources and sinks.

For example, Craig (1957) recognized that the distribution of ^{14}C in the sea could be used to determine the rate of renewal of the deep waters of the oceans, and this led to the development of simple ocean models to interpret available ^{14}C data. The simultaneous use of ^{14}C and more traditional marine tracers was first attempted by Bolin and Stommel (1961) and further developed by Keeling and Bolin (1967). These early developments were based on very simple (usually two-box) ocean models. Oeschger et al. (1975) recognized the need to resolve the vertical structure of the oceans in more detail to depict reality better, and thereby formulated the box-diffusion model (Figure 2). Siegenthaler (1983) further elaborated on this same idea by considering the isopycnal ventilation of the deep sea through the cold polar regions (the outcrop model) (Figure 3). Björkström (1979) also incorporated cold polar regions which communicated directly with deep layers as distinct from warmer regions which did not. This simple low-dimensional box model of the global ocean (Figure 4) also distinguished intermediate waters from deeper ones and included advection as well as eddy diffusion. It also contained biological processes (organic and carbonate) as well as a full treatment of ocean surface carbon chemistry.

Box-Diffusion Model
(Oeschger et al., 1975)

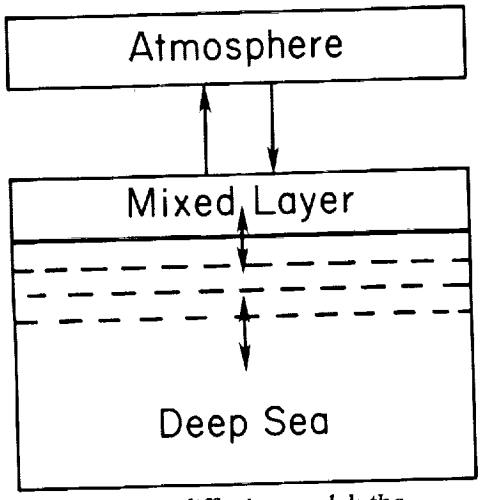

Figure 2. Box-diffusion model: the turnover of carbon below 75 m is represented by a diffusion equation. A constant coefficient of diffusivity is estimated to match an idealized profile of natural ^{14}C (Oeschger et al., 1975).

Box-Diffusion Model with Polar Outcrops
(Siegenthaler, 1983)

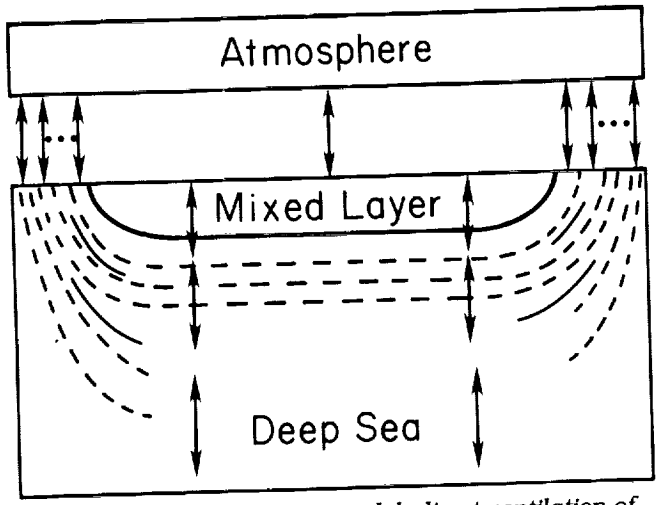

Figure 3. Outcrop-diffusion model: direct ventilation of the intermediate and deep oceans at high latitudes is allowed by incorporating outcrops for all sublayers into the box-diffusion formulation (Siegenthaler, 1983).

Advection-Diffusion Model
(Björkström, 1979)

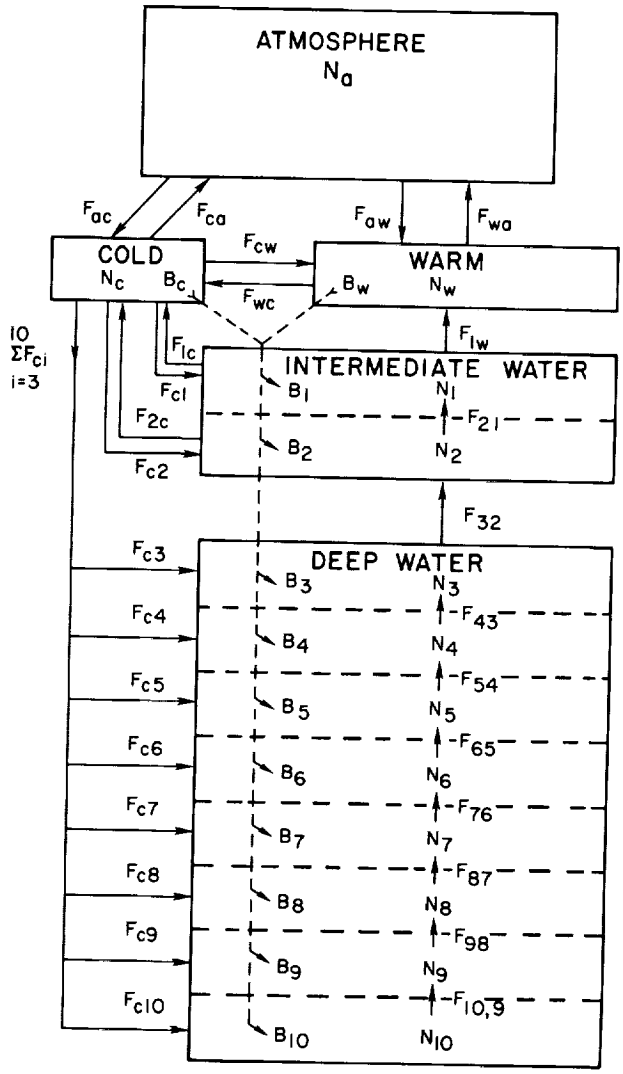

Figure 4. Advection-diffusion model: the first of a number of models whose structures are meant to be more realistic than the simple diffusive assumption. Boxes are labeled with an N with subscript, water mass fluxes are labeled by an F with subscript (some are in both directions and act as mixing terms); the biotic flux from the surface boxes to deeper layers (the biological pump) is denoted by B with the dashed vertical line, and the dissolution or decomposition within a nonsurface box is indicated by the solid arrow (Björkström, 1979).

Broecker and colleagues have made extensive use of tracers in the study of the biogeochemistry of the oceans, particularly by applying the concept of large-scale mixing of major water masses ("endmembers") with particular chemical signatures (e.g., Broecker, 1974; Broecker and Peng, 1982). When these formulations are expressed as continuity equations, the resulting matrical system is often mathematically indeterminate (i.e., there are an infinite number of solutions), and it is not generally clear how to select a single solution out of the many that are possible, particularly in light of the fact that one of the researcher's interests is the time-dependent aspects of the solution. Simply stated, it is difficult to know which of these indeterminate solutions to select or how to evaluate the response to a given forcing of the entire class of solutions.

In a deterministic setting, Bolin et al. (1983) have employed five tracers—total dissolved inorganic carbon, alkalinity, radiocarbon, oxygen, and dissolved inorganic phosphorus—in a constrained inverse methodology to parameterize a coarse-resolution (12 boxes) ocean model (Figure 5) in their study of the role of the ocean in the global carbon cycle. The fluxes of organic and inorganic detrital matter from the surface layers into the thermocline region and the deep sea were considered, and these fluxes became additional unknowns. The source and sink terms for the biologically important tracers were interrelated by assuming constant values for the Redfield ratios (the ratios of carbon to nitrogen to phosphorus to oxygen in organic matter). No deposition of detrital matter on the sea bottom was permitted. The inverse problem was formally overdetermined, and a condition of minimizing the errors of the conservation equations was employed, as well as a set of inequality constraints requiring that turbulent transfer be along the concentration gradient of the tracers and that detrital matter form in surface reservoirs and be dissolved or decomposed in deeper layers of the ocean. The deduced circulation pattern generally agreed with the current view of the gross features of the global ocean circulation. These same techniques were used to develop a more detailed model of the Atlantic Ocean (Bolin et al., 1987; Moore et al., 1989).

We should note that the choice of an indeterminant system, for example the Broecker and Peng models, or a determinant (often called incompatible) system, for example the 12-box model of Bolin and colleagues, is not a choice between bad and good models, but rather a more complicated issue of how much information can be extracted from a given set of observations. The issue goes beyond the scope of this paper and is addressed more fully in Fiadeiro and Veronis (1984), Wunsch (1985), Bolin et al. (1987), and Moore et al. (1989).

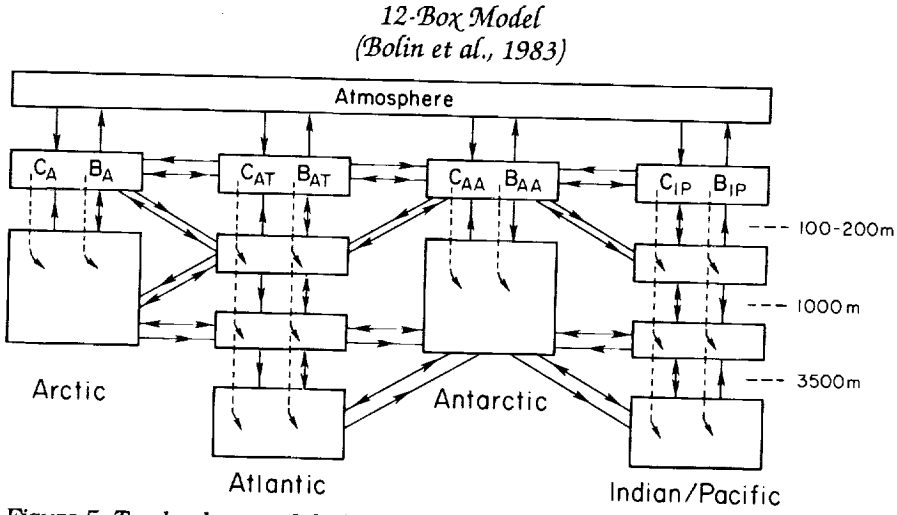

Figure 5. Twelve-box model: the Atlantic and Pacific–Indian oceans are each divided into surface, intermediate, deep, and bottom water components. The Arctic and Antarctic oceans are divided into surface and deep water components. The soft tissue and carbonate formation in surface boxes is indicated by B and C, with appropriate subscripts for region, and the fluxes to and decomposition in deeper layers are indicated by the vertical dashed line and the branching solid arrow, respectively. The model is calibrated against multiple tracer distributions (Bolin et al., 1983).

In considering the overall collection of simple, low-dimensional box models of the ocean carbon system, it appears that these models do provide insight into the processes, and their relative roles, controlling the ocean-atmosphere exchange of CO_2.

Key Ocean Processes Controlling CO_2 Exchange

The oceans are a large sink (2–3 Pg C/yr; Pg = 10^{15} g) for the additional CO_2 that is being added to the atmosphere by human activities; however, the rate of carbon uptake by the oceans is limited by surface ocean chemistry and biology, and by the various patterns of mixing and circulation that determine the amount of carbon transported from surface waters to the deep ocean, where long-term carbon storage occurs.

The exchange of CO_2 between the ocean and the atmosphere is controlled primarily through gas transfer at the air-sea interface and hence is governed by the difference in partial presssure of CO_2 between the atmosphere and the sea surface and the rate of air-sea exchange. One way to view this exchange is to consider the two components separately: (1) the flux of CO_2 from the atmosphere to

the sea (F_{am}), and (2) the flux of CO_2 from the sea surface to the atmosphere (F_{ma}) (see Björkström; 1979).

The flux F_{am} can be represented as a first-order process dependent only upon the atmospheric residence time (T_a) of CO_2 (note that this is different from the atmospheric lifetime for CO_2 in the atmosphere, since a given molecule may move several times back and forth between the atmosphere and the ocean before being "sequestered" in the ocean or perhaps in theh biosphere) and the mass of carbon as atmospheric CO_2 (N_a). This expression, and in particular the assumption about residence time, is an implicit statement about the globally averaged rate of air-sea exchange. The values of T_a and N_a are reasonably well established as global averages; however, the actual distribution of the air-sea exchange rates is quite complicated, depending on sea surface winds and sea surface state, and is not well established.

For the flux F_{ma}, let us consider a unit area (A) of ocean. Then the flux from the ocean to the atmosphere across A can be expressed as:

$$F_{ma} = (A/A_m)(N_{ao}/P_{ao})(P_A/T_a) \qquad (1)$$

where A_m is the surface area of the oceans (3.6×10^{14} m^2), and N_{ao} is the mass of carbon in the atmosphere as CO_2 at some initial point in time with partial pressure P_{ao}; the established value for N_{ao}/P_{ao} is 2.1314921×10^{15} g C $(ppmv)^{-1}$. The key unknown is P_A, the partial pressure of CO_2 in the surface area A. Thus, the essential uncertainties are the distribution of the partial pressure of CO_2 in the surface of the ocean and the factors controlling this distribution.

From the perspective of the global carbon cycle one might consider the partial pressure of CO_2 in sea water as a linear function of the concentration of CO_2 in sea water (Broecker, 1974; Björkström, 1979); however, CO_2 dissociates in sea water at a rate that is itself a function of CO_2 concentration. Further complicating this chemical phenomenon are the dynamics of biological and physical processes. Primary production consumes CO_2; respiration and decay processes produce CO_2. Each process affects the chemical equilibrium. Additionally, carbonate formation and dissolution alter alkalinity, which affects the partial pressure of CO_2 in sea water. The physical processes of advection and eddy diffusion continually alter not only the concentration of dissolved CO_2 in surface waters but the concentration of total inorganic carbon through the ocean, and thereby continually alter the CO_2 partial pressure distribution.

Although chemical, biological, and physical processes are combined in the marine environment, we shall discuss separately (and briefly) the principal attributes of each process.

Chemical Processes

Since CO_2 is not conservative in sea water, a more practical conceptual construct for determining the partial pressure of CO_2 in the ocean surface water is the concentration of total dissolved inorganic carbon (ΣC). This is defined as

$$\Sigma C = [CO_2] + [HCO_3^-] + [CO_3^=] \tag{2}$$

where "[ ]" indicates molar concentration. The difficulty with this construct is that the functional relationship between ΣC and the partial pressure P is only locally linear (depending not only on ΣC but on temperature salinity, and alkalinity as well), whereas P is essentially a globally linear function of $[CO_2]$. However, the conservative character of ΣC more than justifies the increase in complexity in calculating P and ΣC. In fact, one can treat the exploration as the answer to two questions: (1) What is the current relationship between ΣC and P? and (2) How does this relationship change with future and perhaps far greater changes in ΣC?

At a constant temperature, salinity, and alkalinity, and for relatively small changes in ΣC, the major aspects of the current relationship are captured by the linear function:

$$P = (10P_0/\Sigma C_0)\Sigma C - 9P_0 \tag{3}$$

where P_0 is the preindustrial partial pressure exerted by surface water and ΣC_0 is the sum of the concentrations of CO_2, HCO_3^-, and $CO_3^=$ at an initial preindustrial point. Rewriting this linear expression as a normalized ratio of the change in P against the change in ΣC yields a more familiar expression:

$$\{(P - P_0)/P_0\}/\{(\Sigma C - \Sigma C_0)/\Sigma C_0\} = 10 \tag{4}$$

This ratio, usually denoted R and termed the Revelle factor, was measured as part of the Geochemical Ocean Sections Study (GEOSECS) (see Takakashi, 1977), with a range from 8 for the warmest surface waters to 15 for the coldest. Considering the surface area of these waters, 10 is a good weighted average value. This expression, with a Revelle factor of 10, is used in the Oeschger et al. (1975) model (Figure 2) at the air-sea interface.

A direct calculation may clarify further the locally linear relationship expressed by Equation (4) and the essentially nonlinear behavior of P against ΣC, which is important in carbon cycling as CO_2 increases. Also, we need to consider formally the role of chemical solubility because it is temperature dependent. This calculation explicitly exploits ionic equilibria, and hence it describes more precisely the underlying relations between the partial pressure of CO_2 in the surface waters and its solubility at different temperatures,

ΣC, the concentration of hydrogen ions, and total alkalinity. A more thorough and yet easily grasped picture of carbonate-borate chemistry is given by Baes (1982).

The ionic composition of CO_2 in sea water is determined largely by the carbonate system and secondarily by the borate system. The underlying carbonate of sea water is expressed through the following equilibria reactions:

$$CO_2(g) \leftrightarrow CO_2(aq) \tag{5}$$

$$CO_2(aq) + H_2O \leftrightarrow H_2CO_3 \tag{6}$$

$$H_2CO_3 \leftrightarrow H^+ + HCO_3^- \tag{7}$$

$$HCO_3^- \leftrightarrow H^+ + CO_3^= \tag{8}$$

$$H_2O \leftrightarrow H^+ + OH^- \tag{9}$$

and the borate system is expressed by

$$H_3BO_3 \leftrightarrow H^+ + H_2BO_3^- \tag{10}$$

If P denotes the partial pressure of CO_2 in sea water, then the ratio of the concentration of $CO_2(aq)$ ($[CO_2]$) to P is the solubility, K_0, of CO_2. Similarly,

$$K_1 = [H^+][HCO_3^-]/[CO_2] \tag{11}$$

and

$$K_2 = [H^+][CO_3^=]/[HCO_3^-] \tag{12}$$

are the first and second dissociation constants of carbonic acid (H_2CO_3), respectively. [Actually, $K_1$is the apparent first dissociation constant for H_2CO_3. In other words, it is the product of the inverse of the equilibrium constant for the hydration process of $CO_2(aq)$ and the first dissociation coefficient of H_2CO_3].

A direct calculation yields the relationship between ΣC and $[CO_2]$:

$$[CO_2] = [H^+]\Sigma C / \left\{[H^+]^2 + [H^+]K_1 + K_1K_2\right\} \tag{13}$$

Consequently, if one knows ΣC and $[H^+]$ then it is possible to calculate $[CO_2]$, P, and hence F_{ma}. However, with changes in $[CO_2]$ and hence ΣC, $[H^+]$ is altered through the carbonate reactions; furthermore, the production of carbonic acid and its dissociation perturbs the boric acid speciation in seawater, and hence $[H^+]$, since the carbonate ions compete with the borate ions for the available hydrogen ions. If one assumes that the carbonate-borate alkalinity, denoted by A, remains constant (Keeling, 1973), where A is defined by

$$A = [HCO_3^-] + 2[CO_3^=] + [H_2BO_3^-] + [OH] - [H^+] \quad (14)$$

it is then possible to use the dissociation coefficients of H_2CO_3, boric acid (H_3BO_3), and water to determine $[H^+]$, given only ΣC. In fact, given any two of the following four variables—P, ΣC, $[H^+]$, and A—the remaining two terms are determined.

In closing this section, let us return to Equation (4), the simple linear expression for the relationship between total dissolved inorganic carbon and the associated partial pressure—the Revelle factor. The importance of this factor is best expressed by an example that uses current data. Since the atmospheric concentration of CO_2 has increased by approximately 25% over the last 125 years since 1860, then in light of Equation (4), the increase in surface concentration of total dissolved inorganic carbon would be only 2.5% (assuming the surface layer remains in equilibrium with the atmosphere). Since this surface mixed layer is about the same size, with respect to total inorganic carbon, as the atmosphere (the 900 Pg C in Figure 1 reflects a somewhat deeper mixed layer than is generally accepted), this small increase would imply, for an abiotic, physically static ocean, much less carbon uptake than is generally associated with the role of the ocean in the global carbon cycle. Consequently, the biological and mixing processes must have removed from surface waters whatever additional CO_2 entered the ocean.

Biological Processes

Although the oceans are the largest active reservoir of carbon and cover almost 70% of the globe, the total marine biomass contains only about 3 Pg of carbon or just about 0.5% of the carbon stored in terrestrial vegetation. On the other hand, total primary production of marine organisms is 30–40 Pg/yr, corresponding to 30–40% of the total primary production of terrestrial vegetation. However, only a relatively small portion of this production results in a sink for atmospheric carbon, primarily through the sinking of particulate organic carbon, which decomposes in deeper layers or is incorporated into sediments. There is, in addition, a very large pool of dissolved organic carbon. The size of this pool is uncertain, but it appears to be on the order of the pool of carbon stored in terrestrial soils, approximately 1000–1500 Pg C.

The consumption of CO_2 in primary production in biologically active surface water, and the enrichment of the deep water in ΣC as the result of the decomposition and dissolution of detrital matter that originates from biological processes in the surface waters, taken together, are often referred to as the biological pump; the biology "pumps" carbon to the bottom. The most obvious pumping

is the incorporation into living organisms of ΣC that is dissolved in surface waters, either in tissue or as carbonate in shells. This lowers the partial pressure of CO_2, followed by the "shipping" of some of the ΣC to the bottom, "packed" in the remains of dead marine organisms.

So, as a consequence of the biological pump, the concentration of total dissolved inorganic carbon is not uniform with depth; the concentration in surface waters is 10–15% less than deeper waters. There is a corresponding depletion of phosphorus (and nitrogen) in surface water, even in areas of intense upwelling, as the result of biological uptake and the loss of the detrital material, which also contains phosphorus (and nitrogen) as well as carbon.

The fate of the carbon that falls from the surface waters depends, in part, upon its characteristics. If it is organic material, then it is oxidized at intermediate depths, which results in an oxygen minimum and a carbon and phosphorus maximum. If the material is carbonate, it dissolves, raising both alkalinity and the concentration of carbon, primarily at great depths where the high pressure (and the effect of the increased "corrosiveness" of the sea water because of increased concentrations of ΣC) increases the solubility of calcium carbonate.

Thus, the biological pump lowers the partial pressure of CO_2 in surface waters and increases it in deep water not in contact with the atmosphere. It is as if the biological pump moves the partial pressure around in a way that allows CO_2 to work its way into the ocean. However, since the preindustrial carbon cycle was in quasi-steady state and since there is little reason to believe that the biological pump has changed over the last 300 years, its direct role in the perturbation problem that has been induced by human activities may be minimal. There is the possibility of an increase in the importance of the biological pump as the result of human-induced nutrient fluxes, but the low carbon-to-nutrient ratios in marine organic matter mitigate against this possibility; see Smith and Mackenzie, 1991, and Revelle, 1991. However, in a changing climate the role of the biological pump, including issues like ecosystem and alkalinity change, is open to question. The interested reader should also see Broecker, 1991; Smith and Mackenzie, 1991; Banes, 1991; Sarmiento, 1991; Revelle, 1991; Rintoul, this volume; and Longhurst, 1991, for a lively discussion of the biological pump and other carbon-related issues.

Physical Processes

The role of the oceans in the carbon cycle is much dependent on their rate of overturning (the meridional circulation) and mixing. In

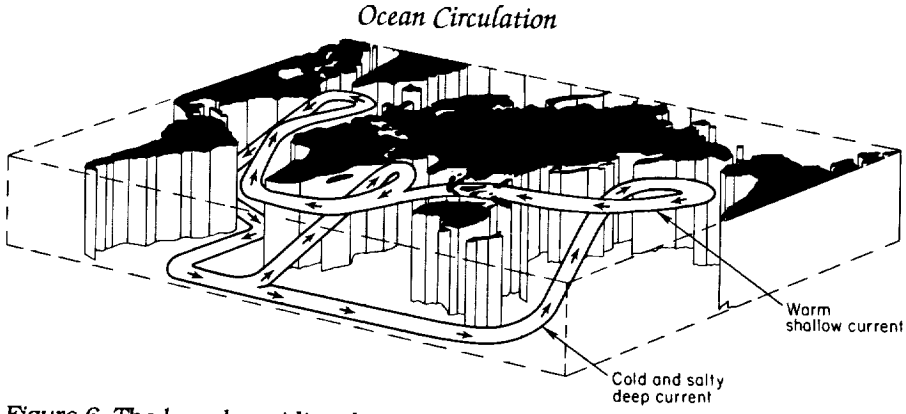

Figure 6. The broad meridional circulation of the ocean (adapted from Broecker and Peng, 1982).

polar regions, ice formation leaves much of the salt "behind," still in solution. The result is an increase in salinity in these already cold waters and hence an increase in density; furthermore, in the North Atlantic, evaporation exceeds precipitation. As a consequence, these cold, saline, and hence dense North Atlantic surface waters sink, and thereby they have the potential to form, in effect, a pipeline or conveyor belt (Figure 6; this concept was developed by Broecker; see Broecker and Peng, 1982) for transferring atmospheric CO_2 to the large reservoirs of abyssal waters which have long residence times. This downward convection of surface waters in polar regions of the North Atlantic during "bottom water formation" creates a sink for CO_2 in high latitudes, but the balancing upwelling of carbon-rich waters in low latitudes creates a source. In other words, what goes down (cold polar water with CO_2) must come up (warm equatorial water with excess CO_2). In addition to the bottom water formation in polar regions, there is water exchange between surface waters and intermediate waters due to vertical exchange in association with the surface ocean currents, like the Gulf Stream. These different exchange processes maintained by water motions renew the abyssal part of the oceans in a matter of a few hundred years in the Atlantic Ocean and up to about 1500 years in the Pacific. Intuitively we realize that this rather slow rate of oceanic turnover limits the oceans as a sink for CO_2.

In order to sort out the effects of these many processes that govern the exchange of CO_2 between the atmosphere and the sea, it is necessary to use models. Such models range from complex formulations of the oceanic general circulation to simpler box models that seek to capture net effects of the processes.

Simple Ocean Carbon Models

Models are required to capture the net effect of these interwoven chemical, biological, and physical processes. As discussed above, GCMs that incorporate carbon dynamics are still under development and are rather demanding. In this paper, we shall explore briefly the four classical box models mentioned in the first section, which treat the oceanic uptake of CO_2. We note in passing that one of these, the box-diffusion model, was used by the Intergovernmental Panel on Climate Change (IPCC) as the basis for determining future oceanic intake. The four models are:

- Box-diffusion model (BD; Figure 2): The turnover of carbon below 75 m is represented by a diffusion equation. A constant coefficient of diffusivity is estimated to match an idealized profile of natural ^{14}C.
- Advection-diffusion model (AD; Figure 4): The surface ocean is divided into cold and warm compartments. Water downwells directly from the cold surface compartment into intermediate and deep layers.
- 12-box model (12B; Figure 5): The Atlantic and Pacific–Indian Oceans are each divided into surface, intermediate, deep, and bottom water compartments. The Arctic and Antarctic Oceans are divided into surface and deep water compartments. The model is calibrated against multiple tracer distributions.
- Outcrop-diffusion model (OD; Figure 3): The intermediate and deep oceans at high latitudes are allowed direct ventilation by the incorporation of outcrops for all sublayers into the box-diffusion formulation.

The four models have, naturally, much in common: They are all diagnostic rather than prognostic, each uses ^{14}C in the parameterization process (in fact, ^{14}C is the basic clock for all of the models and hence controls much of their response), and each includes ocean carbon chemistry (buffer or Revelle factor) and some form of ocean mixing. There are, however, major differences: Ocean biology is explicitly included only in two (AD, 12B), whereas it is simply "part of" the diffusive process in both the BD and OD models; deep water formation is not explicitly considered in the box-diffusion model; the treatment of ocean chemistry varies in complexity; in the BD and OD models all of the physics is captured by a single constant eddy diffusivity term, whereas in the AD model the system is primarily advective (eddy diffusivities can be incorporated); the 12B model has both advection and eddy diffusivities; and, perhaps most impor-

tantly, the geometrical configurations are quite different. In addition, there are a host of smaller differences: ocean volume and surface area, parameterization procedures, ^{14}C profiles, initial conditions, and atmospheric residence time.

As a result of these large and small differences, we find (as described in the next section) a range of responses. Briefly, the OD model is the most efficient in taking up CO_2; the BD, AD, and 12B models all tend toward less carbon uptake. The reason the OD model is more efficient is because of the infinitely rapid connection of the atmosphere to the deeper layers; the reason the three other models are so similar is the overarching importance of ^{14}C in setting the basic rates within the models, but without a direct link to deeper layers.

We should note (again, see the next section) that their relative responses are in part a function of the forcing term, and in this study we consider only past and various future fossil fuel emission scenarios without any terrestrial release. Rapidly increasing emissions generally lead to a decreasing percentage going into the ocean model, whereas decreasing emissions have the opposite effect. Because they capture these changes, models are preferable to a constant multiplier or percentage for varying emission scenarios.

Basic Results

The change in atmospheric carbon dioxide is due primarily to two forcings: the combustion of fossil fuels and the net CO_2 flux to the atmosphere generated by changing land use patterns (Figure 7). The former is certainly greater today than in the past. There are significant uncertainties associated with the latter. For more discussion on calculating directly the biotic source, see Moore et al., 1981; Houghton et al., 1983, 1985, 1987, 1990, 1991; Palm et al., 1986; Detwiler and Hall, 1988; Melillo et al., 1988; Houghton and Skole, 1990; and Skole, 1990. We should also mention that perhaps the most careful analyses of the current characteristics of the carbon cycle that can be deduced from atmospheric data and models are provided by Keeling et al., 1989a, 1989b; Heinmann and Keeling, 1989; and Heinmann et al., 1989.

For the purposes of this paper, a more simplistic and direct consideration is appropriate. Consequently, we shall not consider the biotic flux in Figure 7, but simply the behavior of the four atmosphere-ocean systems when forced by the historic fossil fuel flux alone, except in one test case. In order to further simplify the comparison, we set all initial conditions at the 1860 ice core value for atmospheric CO_2. The four ocean-atmosphere systems show

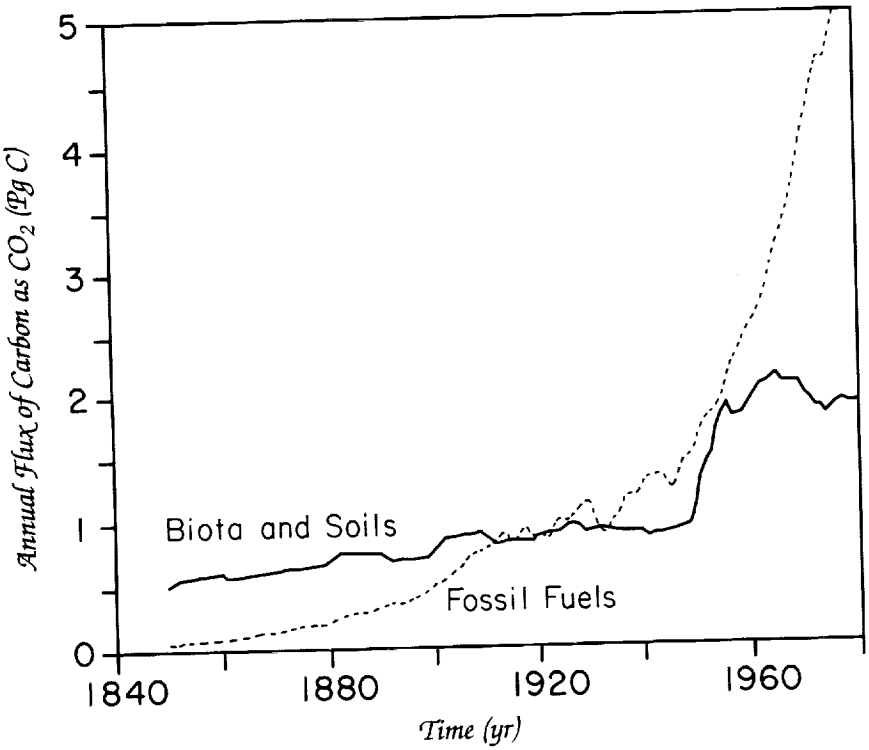

Figure 7. The fossil fuel emissions record (dashed line) and an estimate of the biotic release due to land use change (solid line). The fossil fuel record is from R. Rotty and G. Marland, cited in Moore et al. (1981). The biotic release is from Houghton et al., 1983.

remarkable agreement when compared to the ice core record for atmospheric CO_2 (Figure 8). One notes that if we had initialized the models at the 1740 ice core value, it would be possible to add additional CO_2 to the atmosphere during the early part of the record; but little, if any, additional CO_2 could be added to the current fossil fuel forcing term without exceeding atmospheric measurements (or introducing a new sink). We explore this in a highly simplified fashion simply to illustrate this point by defining an additional nonfossil fuel release (a "biotic" release; Figure 9), and then examine the response of the four ocean-atmosphere systems to the combined forcing of the historic fossil fuel record plus the "created" additional release (Figure 10). Obviously, the combined flux of fossil fuel with the calculated CO_2 flux associated with land use change (Figure 7) would take the response well above the observed increase in the atmosphere.

We now consider three future records simply to capture the general characteristics of the response of the ocean-atmosphere to dif-

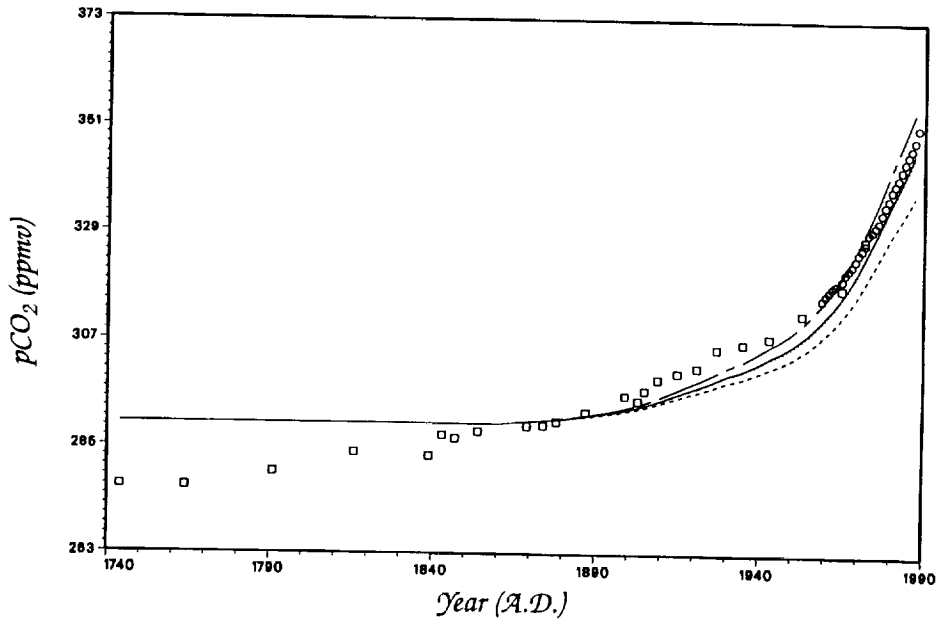

Figure 8. The responses of the four ocean-atmosphere models to the historic fossil fuel forcing. All models were initialized at the 1860 ice core value for CO_2. Open boxes represent the CO_2 values from the ice core record at Siple Station, Antarctica, and the open circles at right are annual averaged atmospheric measurements from Mauna Loa Observatory (the Keeling record). The short dashed line represents the OD model results, the dotted line (just below the solid line) the AD model, the solid line the 12B model, and the short-long dashed line the BD model.

ferent CO_2 forcing; later, we will consider another slightly more policy-oriented forcing term. These initial three emission scenarios do not reflect any particular energy future; rather, they are chosen to reflect a broad range of responses. The two forcing functions are:

- The actual fossil fuel record (i.e., Rotty record; see Figure 7) to 1986 and then the best fit straight line to the 1977–86 data for the period 1987–2000 (Figure 11).
- A Gaussian-like fit (see Bacastow and Björkström, 1981) to the Rotty record such that (1) it has the same total input for the period 1860–1986, (2) it passes through the 1986 data point, and (3) the total integral is eight times the amount of CO_2 as in the preindustrial atmosphere (Figure 12).

We use the four models discussed earlier and actually include two parameterizations for the OD model. One uses steady-state ^{14}C to parameterize the dynamic processes in the model, and the other uses ^{14}C produced by nuclear bomb testing (see Siegenthaler, 1983). Hence, for each forcing term, there are actually five

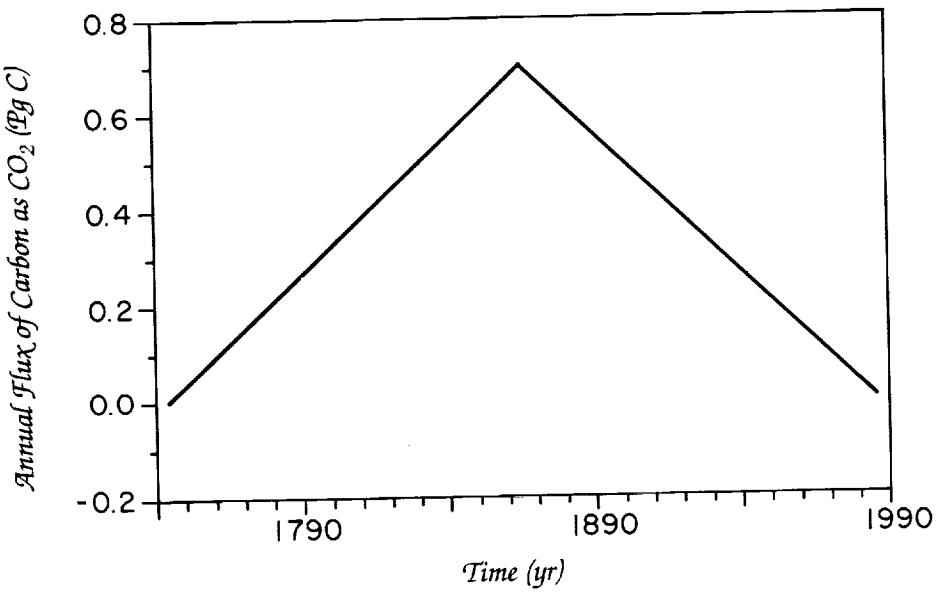

Figure 9. A highly artificial net biotic source flux of CO_2.

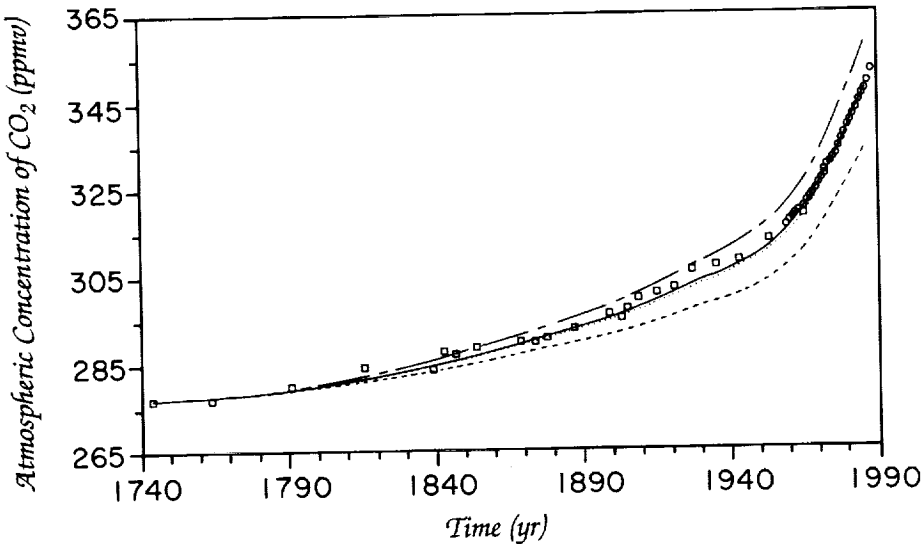

Figure 10. The response of the four ocean-atmosphere models to the historic fossil fuel forcing plus the source term shown in Figure 9. The models were initialized at the 1740 ice core value for CO_2. Open boxes and open circles represent the Siple Station and Mauna Loa records, as in Figure 8. The short dashed line represents the OD model results, the dotted line (just below the sold line) the AD model, the solid line the 12B model, and the short-long dashed line the BD model.

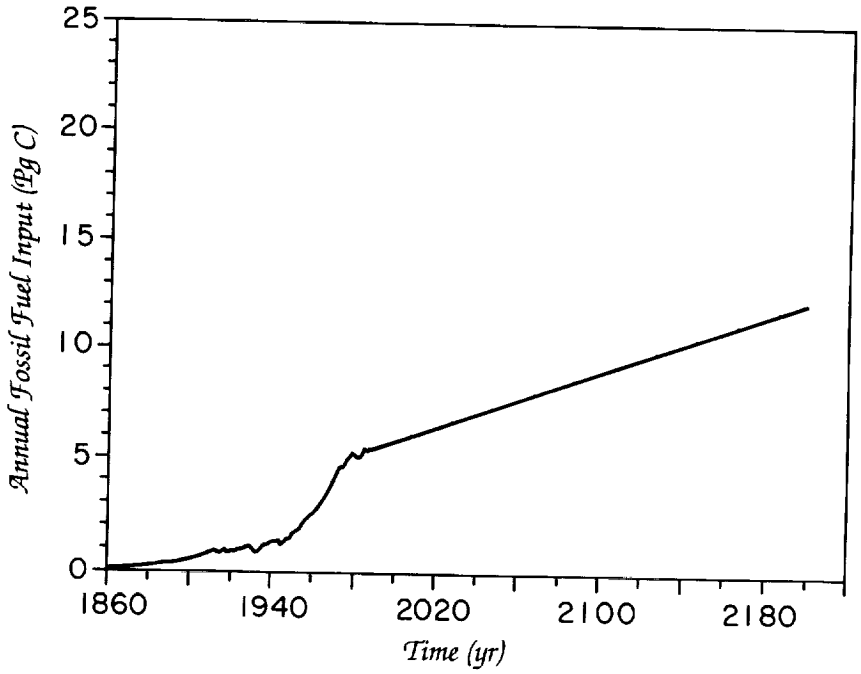

Figure 11. The fossil fuel record to 1986 and then the best fit straight line to the 1977–86 data for the period 1987–2000.

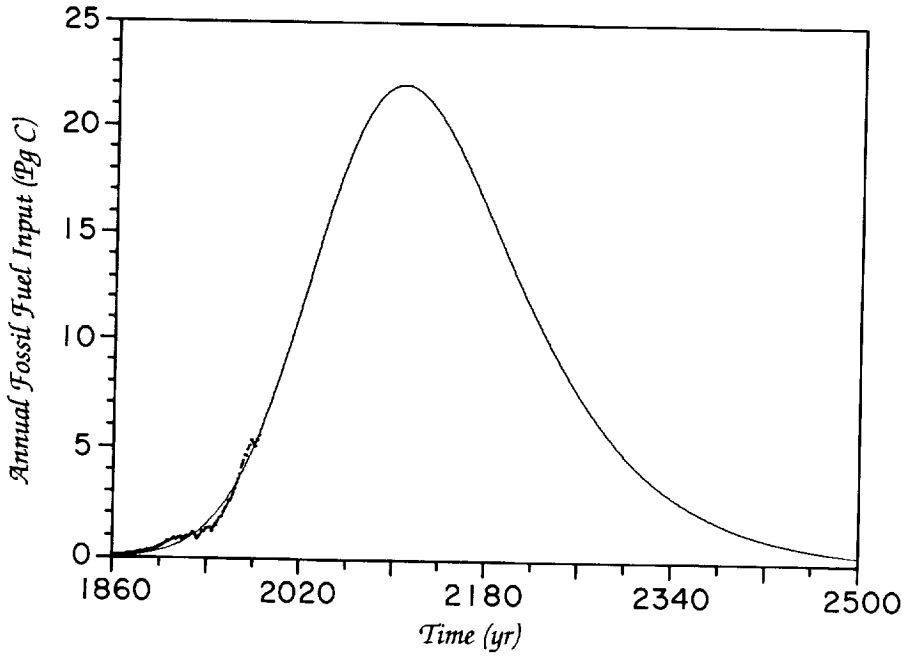

Figure 12. A Gaussian-like fit to the fossil fuel record.

responses. The results are shown in Figures 13–14. In using the Gaussian-like input functions, we extend the time frame to 2500 in order to show how the atmosphere-ocean system begins to relax as the forcing term (Figure 12) goes to zero. In all cases, the OD model, in either parameterization, is by far the most efficient in taking up CO_2. The primary reason is that the structure of the OD model allows, as mentioned, an infinitely fast (and perhaps unreasonable) transfer of some of the atmospheric CO_2 to deep layers.

This range of models certainly includes what is the currently accepted role of the ocean in the global carbon cycle; however, it does not include a model that is efficient enough to allow for the uptake of the currently accepted deforestation-produced CO_2, though the OD model comes the closest. Therefore, either (1) the current understanding of the oceans is insufficient, (2) the current estimates of land use–derived CO_2 are in error, or (3) there are important missing processes. It is likely that all three are true. One intermediate approach in testing the sensitivity of CO_2 projections is to include the mismatch as a "donor-controlled" sink in atmospheric concentrations when one includes as a forcing term the deforestation-produced CO_2 with the fossil fuel–derived CO_2.

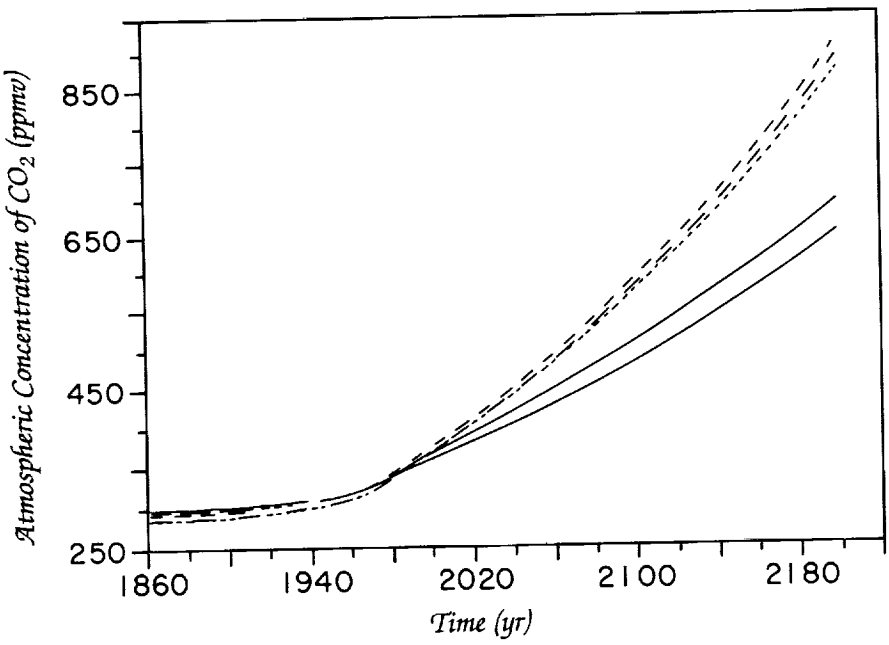

Figure 13. The responses of the ocean-atmosphere models to the fossil fuel forcing followed by the linear forcing (Figure 11). The solid lines represent two versions of the OD model, the short dashed line the AD model, the medium dashed line the BD model, and the long dashed line the 12B model.

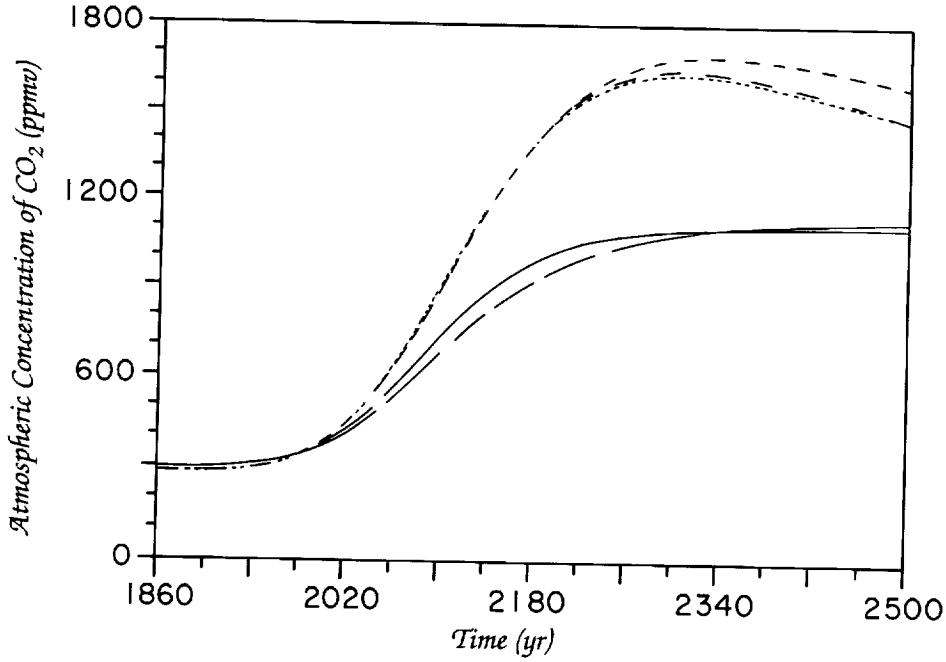

Figure 14. The responses of the ocean-atmosphere models to the Gaussian forcing (see Figure 12). The solid and dashed-solid lines represent two versions of the OD model, the short dashed line the AD model, the medium dashed line the BD model, and the long dashed line the 12B model.

Finally, in light of a recent editorial by Firor (1988), we tested the four models using an emission scenario investigated by Maier-Reimer and Hasselman (1987), the results of which are referenced by Firor. In this scenario, fossil fuel use decreases at 2% per year until it reaches half the current (1986) level of 5.56 BMT/yr; a graph of this forcing function is given in Figure 15. In his editorial, Firor suggests that society may be able to "come close to stabilizing the atmospheric burden of CO_2 with a 50% reduction in fossil fuel use."

The responses of the four models to this emissions scenario are given in Figure 16, and although there is an initial stabilization of atmospheric CO_2, we find that after the input function becomes constant, the rise in atmospheric CO_2 concentration averages between 0.4 ppm/yr (for the OD model) and 0.5 ppm/yr (for the BD model). Admittedly, this rise is considerably less than the approximately 1 ppm/yr rise that is presently occurring, but it does not constitute a stable atmosphere. Tests of the responses of the four models to similar emissions scenarios indicate that emissions would have to be cut to approximately one-tenth of the present level to bring about something close to stabilization (a 0.05 ppm/yr rise).

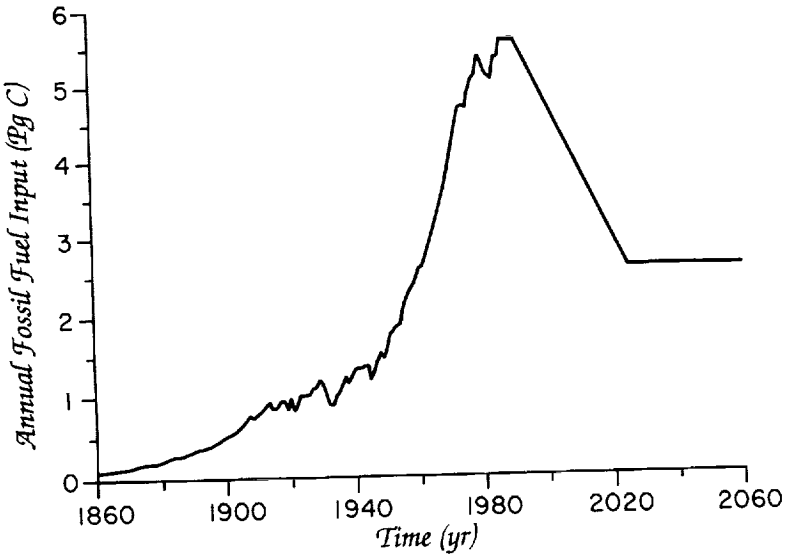

Figure 15. A plot of fossil fuel CO_2 emission to 1986 followed by a five-year period at the 1986 level, and then decreasing at 2% per year until it reaches half of the 1986 level of 5.56 Pg C/yr.

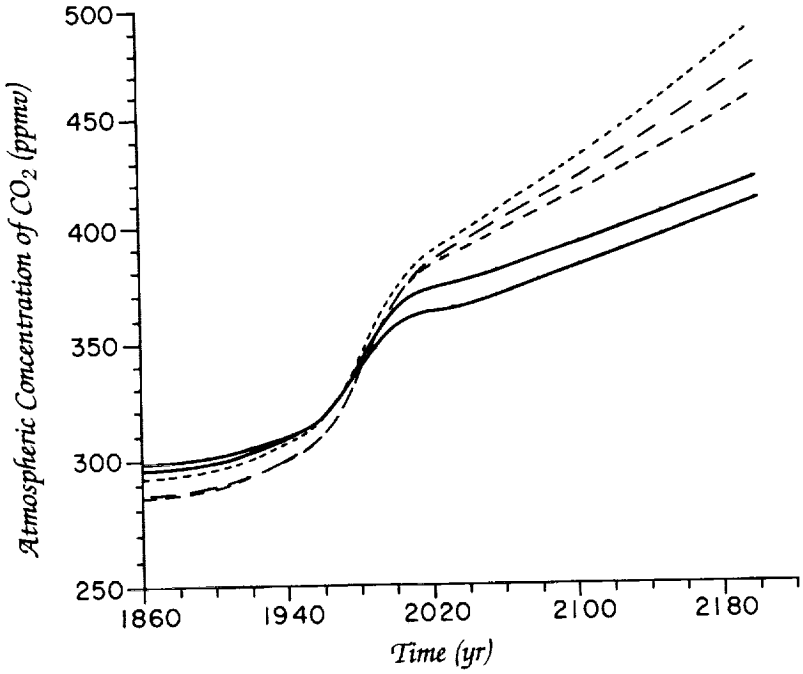

Figure 16. The responses of the four atmosphere-ocean models to the historic fossil fuel forcing, followed by a declining forcing as shown in Figure 15. The solid lines represent two versions of the OD model, the short dashed line the AD model, the medium dashed line the BD model, and the long dashed line the 12B model.

This topic and other related questions raised by Firor (1988) have been the subject of additional investigations (Harvey, 1989), and the differences between these studies in which atmospheric stabilization is achieved and the current findings need further investigation. This is but one area where simple models of the ocean-atmosphere carbon system might continue to prove useful. Other interesting issues relate to defining better the character of the terrestrial sink that would be required given an ocean-atmosphere model, a set of anthropogenic release terms, and the historical record for either CO_2 or ^{13}C.

References

Bacastow, R.B., and A. Björkström. 1981. Comparison of ocean models for the carbon cycle. In *Carbon Cycle Modeling* (B. Bolin, ed.), John Wiley and Sons, Chichester, England, 29–79.

Baes, C.F. 1982. Effects of ocean chemistry and biology on atmospheric carbon dioxide. In *Carbon Dioxide Review: 1983* (W.C. Clark, ed.), Oxford University Press, New York, 189–204.

Banes, K. 1991. False advertising in the greenhouse? *Global Biogeochemical Cycles 5*, 305–307.

Björkström, A. 1979. A model for CO_2 interaction between atmosphere, oceans, and land biota. In *The Global Carbon Cycle* (B. Bolin, E.T. Degens, S. Kempe, and P. Ketner, eds.), SCOPE 13, John Wiley and Sons, Chichester, England, 403–458.

Bolin, B. 1970. The carbon cycle. *Scientific American 223*, 124–132.

Bolin, B. (ed.). 1981. *Carbon Cycle Modeling.* SCOPE 16, John Wiley and Sons, Chichester, England.

Bolin, B. 1983. Changing global biogeochemistry. In *The Future of Oceanography* (P. Brewer, ed.), 50th Anniversary Volume, Woods Hole Oceanographic Institution, Springer-Verlag, Berlin, Germany, 305–326.

Bolin, B. 1986. How much CO_2 will remain in the atmosphere? In *The Greenhouse Effect, Climate Change, and Ecosystems* (B. Bolin, B. Döös, J. Jäger, and R. Warrick, eds.), John Wiley and Sons, Chichester, England, 93–155.

Bolin, B., and H. Stommell. 1961. On the abyssal circulation of the world ocean-IV. *Deep-Sea Research 8*, 95–110.

Bolin, B., E.T. Degens, S. Kempe, and P. Ketner (eds.). 1979. *The Global Carbon Cycle.* SCOPE 13, John Wiley and Sons, Chichester, England.

Bolin, B., A. Björkström, K. Holmen, and B. Moore. 1983. The simultaneous use of tracers for ocean circulation studies. *Tellus 35B*, 206–236.

Bolin, B., A. Björkström, K. Holmen, and B. Moore. 1987. *On Inverse Methods for Combining Chemical and Physical Oceanographic Data: A Steady State Analysis of the Atlantic Ocean*. Technical Report, Meteorological Institute (MISU), Arrhenius Laboratory, Stockholm University, Sweden.

Broecker, W.S. 1974. *Chemical Oceanography*, Harcourt Brace Jovanonich, New York, 214 pp.

Broecker, W.S. 1991. Keeping global change honest. *Global Biogeochemical Cycles 5(3)*, 191–192.

Broecker, W.S., and T.-H. Peng. 1982. *Tracers in the Sea*. Lamont-Doherty Geological Observatory, Columbia University, Palisades, New York, 690.

Craig, H. 1957. The natural distribution of radiocarbon and the exchange time of carbon dioxide between atmosphere and sea. *Tellus 9*, 1–17.

Detwiler, R.P., and C.A.S. Hall. 1988. Tropical forests and the global carbon cycle. *Science 239*, 42–47.

Fiadeiro, M.E., and G. Veronis. 1984. Obtaining velocities from tracer distributions. *Journal of Physical Oceanography 14*, 1734–1746.

Firor, J. 1988. Public policy and the airborne fraction (guest editorial). *Climatic Change 12*, 103–105.

Harvey, D. 1989. Managing atmospheric CO_2. *Climatic Change 15*, 343–381.

Heinmann, M., and C.D. Keeling. 1989. A three-dimensional model of atmospheric CO_2 transport based on observed winds: 2. Model description and simulated tracer experiments. In *Aspects of Climate Variability in the Pacific and Western Americas* (D.H. Peterson, ed.), Geophysical Monograph 55, American Geophysical Union, Washington, D.C., 237–276.

Heinmann, M., C.D. Keeling, and C.J. Tucker. 1989. A three-dimensional model of atmospheric CO_2 transport based on observed winds: 3. Model description and simulated tracer experiments. In *Aspects of Climate Variability in the Pacific and Western Americas* (D.H. Peterson, ed.), Geophysical Monograph 55, American Geophysical Union, Washington, D.C., 277–304.

Houghton, R.A. 1990. The future role of tropical forests in affecting the carbon dioxide concentration of the atmosphere. *Ambio 19*, 204–209.

Houghton, R.A., and D.L. Skole. 1990. Carbon. In *The Earth as Transformed by Human Action* (B.L. Turner, W.C. Clark, R.W. Kates, J.F. Richards, J.T. Mathews, and W.B. Meyer, eds.), Cambridge University Press, Cambridge, England, 393–408.

Houghton, R.A., and D.L. Skole. 1990. Changes in the global carbon cycle between 1700 and 1985. In *The Earth as Transformed by Human Action* (B.L. Turner II, ed.), Cambridge University Press, New York.

Houghton, R.A., J.E. Hobbie, J.M. Melillo, B. Moore, B.J. Peterson, G.R. Shaver, and G.M. Woodwell. 1983. Changes in the carbon content of terrestrial biota and soils between 1860 and 1980: A net release of CO_2 to the atmosphere. *Ecological Monographs 53*, 235–262.

Houghton, R.A., R.D. Boone, J.M. Melillo, C.A. Palm, G.M. Woodwell, N. Myers, B. Moore, and D.L. Skole. 1985. Net flux of carbon dioxide from tropical forests in 1980. *Nature 316*, 617–620.

Houghton, R.A., R.D. Boone, J.R. Fruci, J.E. Hobbie, J.M. Melillo, C.A. Palm, B.J. Peterson, G.R. Shaver, G.M. Woodwell, B. Moore, D.L. Skole, and N. Myers. 1987. The flux of carbon from terrestrial ecosystems to the atmosphere in 1980 due to changes in land use: Geographic distribution of the global flux. *Tellus 39B*, 122–139.

Houghton, R.A., D.L. Skole, and D.S. Lefkowitz. 1991. Changes in the landscape of Latin America between 1850 and 1980. II. A net release of CO_2 to the atmosphere. *Forest Ecology and Management 38*, 173–199.

Keeling, C.D. 1973. The carbon dioxide cycle: Reservoir models to depict the exchange of atmospheric carbon dioxide with the oceans and land plants. In *Chemistry of Lower Atmosphere* (S.I. Rasool, ed.), Plenum Press, New York, 251–329.

Keeling, C.D. 1982. The oceans and the terrestrial biosphere as future sinks for fossil fuel CO_2. In *Interpretation of Climate and Photochemical Models, Ozone and Temperature Measurements*, American Institute of Physics, New York.

Keeling, C.D., and B. Bolin. 1967. The simultaneous use of chemical tracers in oceanic studies. I: General theory of reservoir models. *Tellus 19*, 566–581.

Keeling, C.D., R.B. Bacastow, A.F. Carter, S.C. Piper, T.P. Whorf, M. Heinmann, W.C. Mook, and H. Roeloffzen. 1989. A three-dimensional model of atmospheric CO_2 transport based on observed winds: 1. Analysis of observational data. In *Aspects of Climate Variability in the Pacific and Western Americas* (D.H. Peterson, ed.), Geophysical Monograph 55, American Geophysical Union, Washington, D.C.

Keeling, C.D., S.C. Piper, and M. Heinmann. 1989. A three-dimensional model of atmospheric CO_2 transport based on observed winds: 4. Mean annual gradients and interannual variability. In *Aspects of Climate Variability in the Pacific and Western Americas* (D.H. Peterson, ed.), Geophysical Monograph 55, American Geophysical Union, Washington, D.C.

Longhurst, A. 1991. A reply to Broecker's charges. *Global Biogeochemical Cycles 5(4)*, 315–316.

Maier-Reimer, E., and K. Hasselman. 1987. Transport and storage in the ocean—an inorganic ocean-circulation carbon cycle model. *Climate Dynamics 2*, 63–90.

Melillo, J.M., J.R. Fruci, R.A. Houghton, B. Moore, and D.L. Skole. 1988. Land-use changes in the Soviet Union between 1850 and 1980: Causes of a net release of CO_2 to the atmosphere. *Tellus 40B*, 116–128.

Moore, B. 1985. The oceanic sink for excess atmospheric carbon dioxide. In *Wastes in the Ocean, Volume IV: Energy Wastes in the Ocean* (I. Duedall, d.R. Kester, and P.K. Park, eds.), John Wiley and Sons, New York.

Moore, B., and D. Schimel (eds.). *Trace Gases in the Biosphere*. UCAR/Office for Interdisciplinary Earth Studies, Boulder, Colorado.

Moore, B., R.D. Boone, J.E. Hobbie, R.A. Houghton, J.M. Melillo, B.J. Peterson, G.R. Shaver, C.J. Vorosmarty, and G.M. Woodwell. 1981. A simple model for analysis of the role of terrestrial ecosystems in the global carbon budget. In *Carbon Cycle Modeling* (B. Bolin, ed.), SCOPE 16, John Wiley and Sons, Chichester, England, 365–385.

Moore, B., B. Bolin, A. Björkström, K. Holmen, and C. Ringo. 1989. Ocean carbon models and inverse methods. In *Ocean Circulation Models: Combining Data and Dynamics* (D.L.T. Anderson and J. Willebrand, eds.), Kluwer Academic Publishing, Dordrecht, The Netherlands, 409–449.

Nordhaus, W.D., and G.W. Yohe. 1983. Future carbon dioxide emissions from fossil fuel. In *Climate Change*, Carbon Dioxide Assessment Committee, National Academy of Sciences, Washington, D.C., 87–153.

Oeschger, H., U. Siegenthaler, and A. Gugelman. 1975. A box diffusion model to study the carbon dioxide exchange in nature. *Tellus 27*, 168–192.

Palm, C.A., R.A. Houghton, J.M. Melillo, and D.L. Skole. 1986. Atmospheric carbon from deforestation in Southeast Asia. *Biotropica 18(3)*, 177–188.

Peng, T.-H., and W.S. Broecker. 1985. The utility of multiple tracer distributions in calibrating models for uptake of anthropogenic CO_2 by the ocean thermocline. *Journal of Geophysical Research 90*, 7023–7035.

Revelle, R. 1991. Response to the comment by S.V. Smith and F.T. Mackenzie. *Global Biogeochemical Cycles 5(4)*, 317.

Sarmiento, J. 1991. Oceanic uptake of CO_2: The major uncertainties. *Global Biogeochemical Cycles 5(4)*, 309–314.

Siegenthaler, U. 1983. Uptake of excess CO_2 by an outcrop-diffusion model of the ocean. *Journal of Geophysical Research 88*, 3599–3608.

Skole, D.L. Acquiring global data on land cover change. In *Land Cover and Land Use Change* (W. Meyer and B.L. Turner, eds.), UCAR/Office for Interdisciplinary Earth Studies, Boulder, Colorado, in press.

Smith, S.V., and F. Mackenzie. 1991. Comments on the role of oceanic biota as a sink for anthropogenic CO_2 emissions. *Global Biogeochemical Cycles 5(3)*, 189–190.

Takahashi, T. 1977. Carbon dioxide chemistry in ocean water. In *Proceedings of the Workshop on the Global Effects of Carbon Dioxide from Fossil Fuels* (W.P. Elliot and L. Machta, eds.), Conference Publication 770385-UC-11, U.S. Department of Energy, Washington, D.C., 63–71.

Tans, P.P., I. Fung, and T. Takahashi. 1990. Observational constraints on the global atmospheric CO_2 budget. *Science 247*, 1431–1438.

Wunsch, C. 1985. Can a tracer field be inverted for velocity? *Journal of Physical Oceanography 15*, 1521–1531.

A Toy Model of Sea Ice Growth

A.S. Thorndike

My purpose here is to present a simplified treatment of the growth of sea ice. By ignoring many details, it is possible to obtain several results that help to clarify the ways in which the sea ice cover will respond to climate change. Three models are discussed. The first deals with the growth of sea ice during the cold season. The second describes the cycle of growth and melting for perennial ice. The third model extends the second to account for the possibility that the ice melts away entirely in the summer. In each case, the objective is to understand what physical processes are most important, what ice properties determine the ice behavior, and to which climate variables the system is most sensitive.

Climate

Divide the year into a cold and a warm season, each of duration Y. During the cold season, the average downwelling longwave radiation is f_{lwc} which equals 180 W/m^2 in today's climate. In the warm season, the downwelling radiation is f_{lww} = 270 W/m^2, and there is shortwave radiation f_{sw} = 200 W/m^2. (These values are from Maykut and Untersteiner, 1971.) A fourth climate variable is the heat supplied to the ice from the ocean, f_w. Its value is not known, and it surely varies in space and time. We will regard it as constant throughout the year, and expect it to have a value in the range 0 to 10 W/m^2 in the central Arctic. The four parameters f_{lwc}, f_{lww}, f_{sw}, and f_w specify the climate.

To examine the response of the ice to changes in climate, we will have in mind perturbations to the longwave fluxes, such as might

accompany tropospheric warming or changes in atmospheric composition:

$$f_{lwc} \rightarrow f_{lwc} + \delta$$

$$f_{lww} \rightarrow f_{lww} + \delta$$

Sea Ice Parameters

The ice will be described by two variables, its thickness h and surface temperature T. Other ice properties and their values used in this paper are:

longwave emissivity	ε	1
thermal conductivity	k	2 W/m/K
specific heat	c	2×10^6 J/m^3/K
latent heat	L	3×10^8 J/m^3
albedo	α	0.65.

In taking these parameters to be constant, we ignore the strong dependence some have on temperature and salinity. In effect, we replace the thermal properties of sea ice with those of fresh ice. In so doing, we give up the possibility of resolving the sea ice behavior within a few degrees of the freezing point.

Ice Growth

The black body radiation from the ice surface can be expressed as a linear approximation to the Stefan-Boltzmann law, in the form A + BT. Here A = 320 W/m^2 and B = 4 ε σ $(271.2)^3$ = 4.6 W/m^2/K. Here σ is the Stefan-Boltzmann constant, 5.7×10^{-8} J/m^2/s/K^4, and 271.2 K is the freezing point of sea water.

In the cold season, and in the absence of upward heat flux from below, the radiation from the ice surface must balance the downwelling longwave radiation. This implies

$$T = -(A - f_{lwc})/B = -D/B = -29°C \qquad (1)$$

The quantity $D \equiv A - f_{lwc}$ is a convenient scale for the radiative fluxes. It is the net radiation balance over a surface at the freezing point. Similarly, the quantity -D/B is a natural scale for the surface temperature. It is the minimum temperature the ice surface can attain.

For ice of thickness h, having a linear temperature profile, heat is conducted upward at the rate -kT/h, and this flux must be included in the surface energy balance:

$$A + BT = f_{lwc} - kT/h \tag{2}$$

It follows that the surface temperature and the ice thickness are related as

$$T = -Dh/(k + Bh), \text{ and } h = -kT/(D + BT) \tag{3}$$

These relations hold when the ice is growing, because then the temperature profile through the ice is approximately linear, and the expression for the conductive heat flux is justified.

At the bottom of the ice, the rate at which heat can be conducted through the ice determines the rate of ice growth:

$$L\, dh/dt = -kT/h - f_w \tag{4}$$

After substituting for T, the equation can be integrated to give the relationship between the thickness h, after time t, and the initial thickness h_o:

$$tB/L + kDf_w^{-2} \log\left(\frac{k(D - f_w) - f_w Bh}{k(D - f_w) - f_w Bh_o}\right) + B(h - h_o)f_w^{-1} = 0 \tag{5}$$

In the special case $h_o = 0$, the logarithm can be expanded in the form $\log(1 - \beta) \simeq -\beta - \beta^2/2$, provided $f_w \ll D$, leading to

$$L\, dh/dt = -kT/h - f_w \tag{6}$$

This result establishes k/B as a natural scale of ice thickness. B determines how much the surface must cool to maintain radiative equilibrium. Together with k, this fixes the conductive heat flux, and therefore the ice growth. The value of k/B is about 0.4 m. It also appears from this result that kL/BD is a natural time scale, having the value of about 11 days. It is worth noting that the ocean heat flux decreases the thickness through the linear factor $(1 - f_w/D)$. With $D \simeq 140$ W/m^2 and $f_w \simeq 1$ W/m^2, the ocean heat flux has a small effect on the ice produced in one year, but we will see below that it can have a large effect on the equilibrium thickness.

It can also be noted that a steady state solution to Equations (2) and (4) is possible. The ice must grow to a thickness where the conductive heat flux equals f_w. This occurs when $h = (k/B)(D/f_w - 1)$, which is about 50 m. However, the time required to approach this equilibrium is much longer than a single growing season, so the model needs to be extended to account for the seasonal cycle of growing and melting (see "A Model of the Perennial Ice Cover").

For very thin ice, $t \ll kL/BD \approx 11$ days, we have the further approximation that

$$h \simeq (D - f_w)t/L \qquad \text{(small t)} \tag{7}$$

In this case, the conduction through the ice is not important. The ice growth is determined completely by the net heat balance for the slab, and the latent heat, and therefore grows at a constant rate.

For large t, $t \gg kL/BD$, we obtain

$$h \simeq (k/B)(1 - f_w/D)\sqrt{2BDt/kL} \qquad \text{(large t)} \tag{8}$$

which shows that h grows as $t^{1/2}$. The thicker the ice gets, the slower it grows. Here the growth is regulated by the conduction of heat through the slab. With time, the ice both cools and thickens, but the combined effect is that the temperature gradient decreases, which controls the rate at which heat can be removed from the bottom surface, and thus the rate of ice growth.

The ice thickness depends on the climate through the variables $D = A - f_{lwc}$ and f_w. It is interesting to note that in the coldest climate possible, f_{lwc} and $f_w = 0$, the ice would only grow to $h = (k/B)(2kAY/BL)^{1/2} \simeq 4$ m in a single growing season, where Y = one-half year.

Now consider the case $h_o > 0$, as for ice which has survived the summer. During the subsequent growing season, the ice will reach a thickness h after time t. In the case where the new growth $h - h_o$ is small compared to h_o, we obtain

$$h - h_o \simeq \left(\frac{kD}{k + Bh_o} - f_w\right)\frac{t}{L} \qquad (h - h_o \ll h_o) \tag{9}$$

This implies that the ice cannot grow thicker than $(k/B)(D/f_w - 1)$, a quantity that is sensitive to the ocean heat flux f_w. Compare this result with Equation (25), below, which accounts for the annual cycle of ice growth and melting.

Equation (5) can be solved for h numerically. Thus we can express

$$h = H(h_o t) \tag{10}$$

though we cannot write the function H explicitly.

The assumption of a linear temperature profile through the ice has been essential in obtaining these results. As the ice grows, it also cools, according to Equation (3). There is an internal inconsistency here. An element of ice cannot cool if the temperature profile is linear there. The only way to avoid this kind of inconsistency is to formulate the ice growth as a heat diffusion problem, as Maykut and Untersteiner did. To estimate how large an error the assumption introduces, note that the model properly accounts for the heat released by the new ice growth, Ldh, but it does not account for the heat which must be removed to cool the ice, dQ, where $Q = chT/2$. For ice that grows one meter in the winter, Ldh is 3×10^8 J/m^2. The

heat storage term is $(2 \times 10^6$ J/m/K)(1 m)(–21 K)/2 = 2×10^7 J/m^2. So we may expect errors of about 5 to 10% to arise because we have not properly accounted for the heat storage (although in the next section it is shown that a large part of the heat storage can easily be accounted for).

A Model of the Perennial Ice Cover

Since the ice is characterized by its thickness and surface temperature, it is useful to plot its behavior as a trajectory in (h,T) space. Figure 1 displays the results of the Maykut and Untersteiner model this way. We will approximate the annual cycle as follows. Imagine a slab of ice at the end of the melt season, having thickness h and temperature T = 0 throughout. When the weather turns cold, the ice cools until its surface temperature reaches the temperature appropriate for its thickness, Equation (3). Then it grows for the remain-

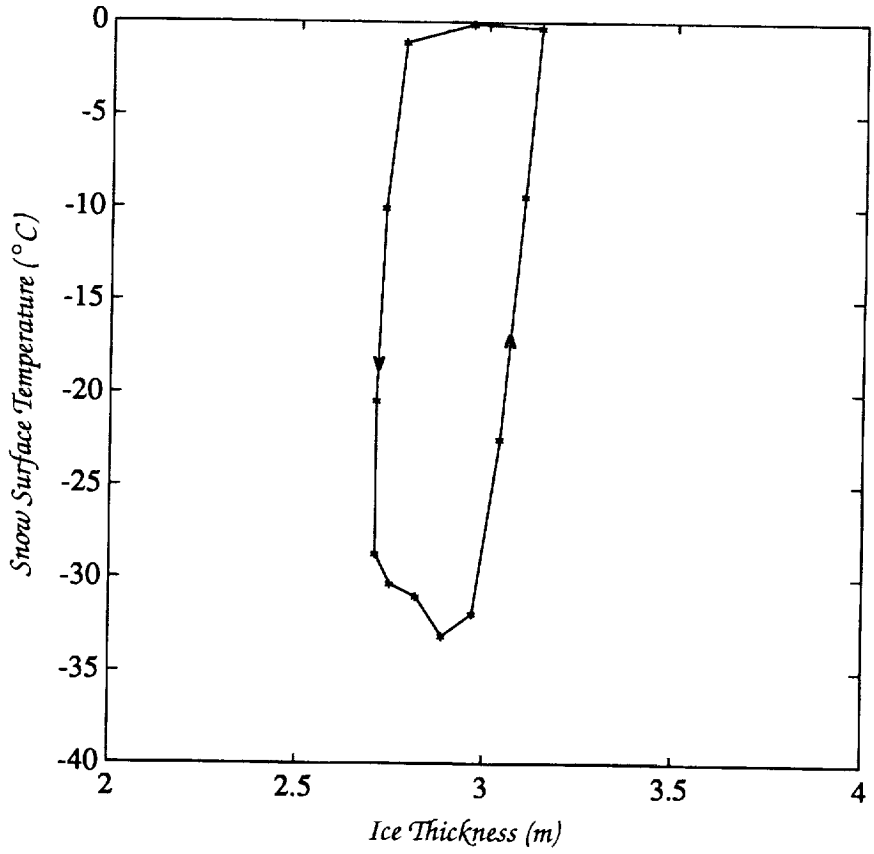

Figure 1. The equilibrium cycle for the standard case of the Maykut and Untersteiner model, plotted in (h,T) space.

ing part of the cold season, according to the ice growth model of the previous section. In the warm season, the ice first warms up to the freezing point, and then melts. The cooling and warming processes take place with no change in thickness. They account for the storage of heat by the ice. The equations governing this four-process cycle of cooling, growing, warming, and melting are

Cooling

$$D = A - f_{lwc} \tag{11}$$
$$T = -Dh/(k + Bh)$$
$$Q = -chT/2$$
$$\tau_c = Q/(A + BT/2 - f_{lwc} - f_w)$$

Growing

$$\tau_g = Y - \tau_c \tag{12}$$
$$h_g = H(h, \tau_g) \qquad \text{(Equations 5 and 10)}$$
$$T_g = -Dh_g/(k + Bh_g)$$

Warming

$$Q = -ch_g T_g/2 \tag{13}$$
$$D = f_{lww} + (1-\alpha)f_{sw} + f_w - A - BT_g/2$$
$$\tau_w = Q/D$$

Melting

$$\tau_m = Y - \tau_w \tag{14}$$
$$h = h_g - \tau_w[f_{lww} + (1-\alpha)f_{sw} + f_w - A]/L$$

where τ is duration with subscripts c, g, w, and m indicating the four processes.

A short program can be written to do these calculations. The results (see Table 1) show that for the present climate, the ice is attracted to a periodic orbit, as sketched in Figure 2. The ice is saved from the two alternatives, melting completely or growing without bound, by the negative feedback provided by the ice thickness. If the ice is too thin in the fall, it will grow more in the winter than it melts in the summer. If it is too thick in the fall, it grows less than it melts. In either case, it approaches the equilibrium orbit.

For other climates, the orbit changes. For large enough perturbations to the climate, the equilibrium cycle cannot be maintained. If the climate is too warm, the ice melts completely in the summer; the

Table 1: Results of model simulations

Perennial Ice Cover

δ (W/m^2)	f_w (W/m^2)	τ_c (d)	h_g (m)	T_g (°C)	τ_w (d)	h_m (m)
−15	1	43	9.4	−32	44	9.1
−10	1	21	5.3	−30	23	4.8
0	1	7	2.9	−26	11	1.9
5	1	3	2.5	−25	8	1.1
10	1	1	2.2	−24	7	0.6
15	1	0.1	2.0	−22	6	0.2
0	2	5	2.7	−26	10	1.6
0	5	3	2.3	−26	8	1.0
0	10	0.5	1.8	−25	6	0.3

Seasonal Ice Cover

δ (W/m^2)	f_w (W/m^2)	T_{ml} (°C)	τ_{ml} (d)	h_g (m)	T_g (°C)	τ_w (d)	τ_h (d)
20	1	2	37	1.7	−21	5	36
30	1	6	117	1.0	−16	2	115
37	1	9	170	0.3	−9	0.4	165
20	5	4	82	1.3	−19	3	82
20	10	6	119	0.9	−18	2	119

h_g and T_g are the ice thickness and temperature at the end of the growing season. h_m is the thickness at the end of the melting season. τ_c, τ_w, τ_{ml}, and τ_h are the durations of the processes which cool and warm the ice, and cool and heat the mixed layer. δ is the perturbation to the longwave radiation fluxes. f_w is the upward flux of heat from the ocean. T_{ml} is the temperature of model's upper ocean layer.

model is patched up to treat this case below. If the climate is too cold, the ice grows without bound. The behavior of the model as a function of the perturbation δ is sketched in Figure 3. The longwave fluxes can vary up to about ± 20 W/m^2 from the present climate and still support an annual equilibrium cycle.

A Seasonal Ice Model

If the ice melts away before the end of the summer, the positive heat balance at the surface must cause the upper ocean to warm. The model of the preceding section can be modified to account for this heat by including an upper ocean layer. The thickness of the layer h_{ml} is assumed to be fixed at 50 m, and its temperature is allowed to change. The layer is assumed to be well mixed, so that a single temperature describes its state. Begin the annual cycle at the end of summer with the mixed layer having temperature T_{ml}. We calculate how long it takes for the mixed layer to cool, and then how much ice will grow during the remainder of the cold season. During the warm season, the ice must warm up to the freezing point, and

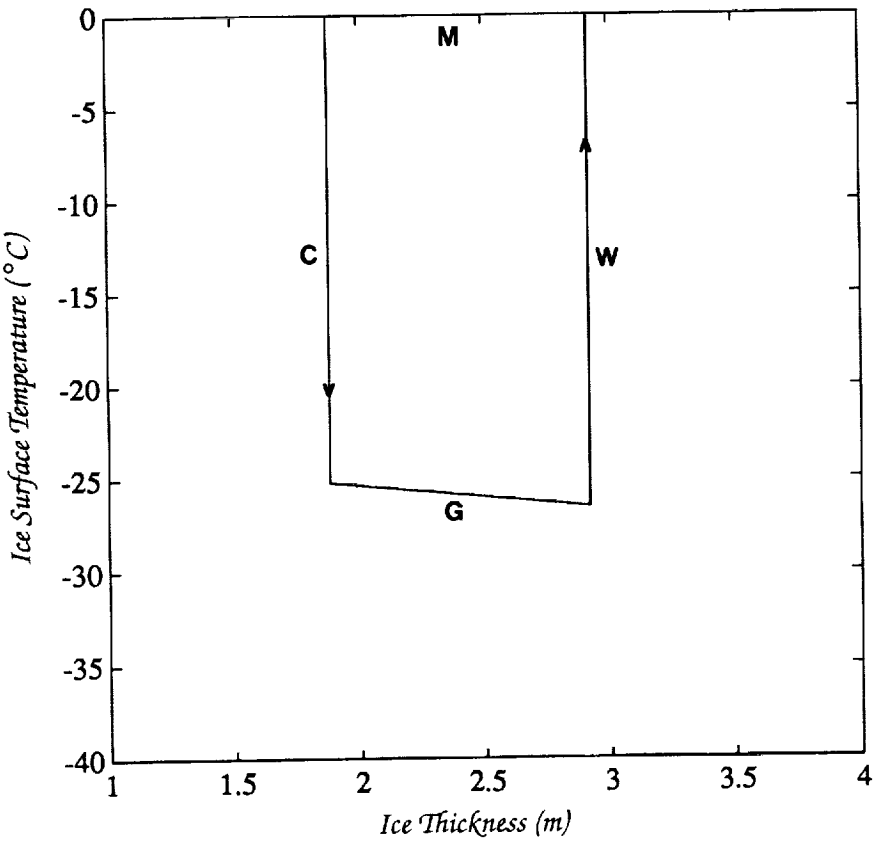

Figure 2. The equilibrium cycle for the perennial ice model, under the present climate; C is cooling, G is growing, W is warming, M is melting.

then melt, requiring times τ_w and τ_m. The remainder of the warm season is spent heating the mixed layer. The model equations are:

Cooling the mixed layer:

$$Q = c_w h_{ml} T_{ml} \tag{15}$$
$$\tau_{ml} = Q/(A + BT_{ml}/2 - f_{lwc} - f_w)$$

Ice growth:

$$\tau_g = Y - \tau_{ml} \tag{16}$$
$$h = H(0, \tau_g)$$
$$T = -(A - f_{lwc})h/(k + Bh)$$

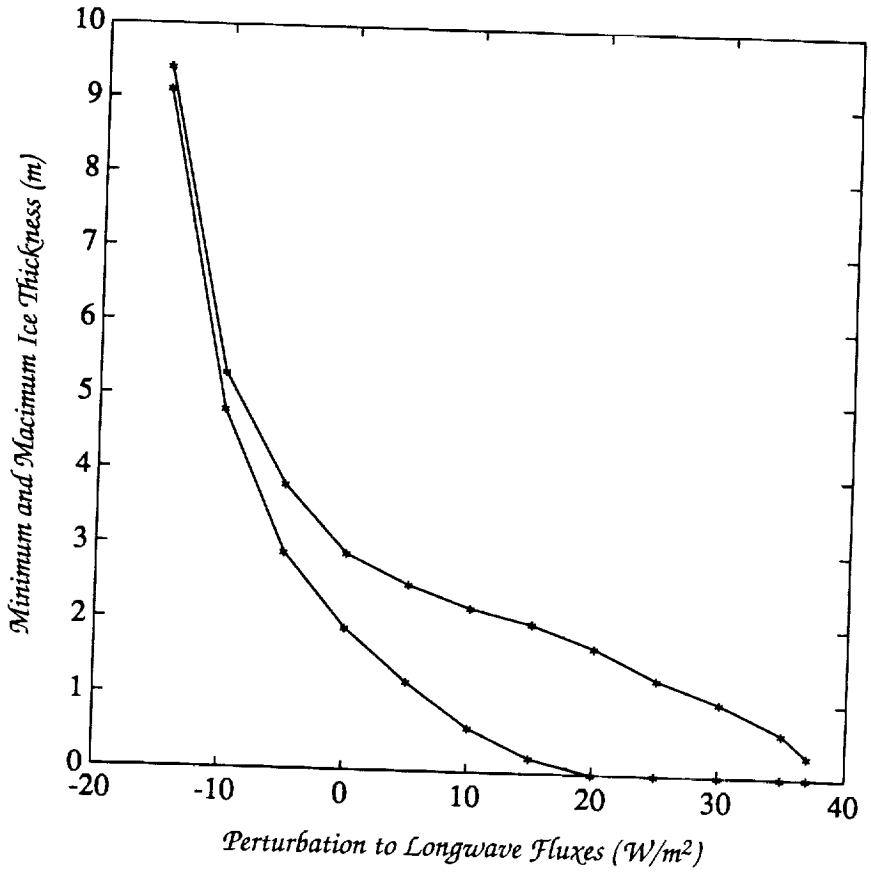

Figure 3. The maximum and minimum thicknesses in the annual cycle for the perennial and seasonal ice models, as functions of the perturbation δ to the longwave fluxes.

Warming:

$$\begin{aligned} Q &= -chT/2 \\ D &= f_{lww} + (1-\alpha)f_{sw} + f_w - A - BT/2 \\ \tau_w &= Q/D \end{aligned} \tag{17}$$

Melting:

$$\tau_m = hL/\left[f_{lww} + (1-\alpha)f_{sw} + f_w - A\right] \tag{18}$$

Heating the mixed layer:

$$\begin{aligned} \tau_h &= Y - \tau_w - \tau_m \\ D &= f_{lww} + (1-\alpha_w)f_{sw} + f_w - A \\ T_{ml} &= (D/B)\left[1 - \exp(-B\tau_h/c_w h_{ml})\right] \end{aligned} \tag{19}$$

For sea water the specific heat is $c_w = 4 \times 10^6$ J/m^3/K and the albedo is taken to be 0.2. The last equation is the result of integrating the heat balance for the mixed layer:

$$d(c_w h_{ml} T_{ml})/dt = D - BT_{ml} \tag{20}$$

For positive perturbations to the longwave fluxes in the range 17 W/m^2 < δ < 40 W/m^2, a seasonal ice pack is possible (see Figure 3). For example, with δ = 30 W/m^2, the mixed layer reaches 6°C. It requires 117 days to cool off in the fall. In the remaining 65 days of cold weather, the ice grows to 1 m, reaching a surface temperature of -16°C. In the warm season, it takes 2 days to warm the ice to the freezing point, 65 days to melt it, and 115 days to warm the mixed layer.

For climates warmer than δ = 40 W/m^2, the mixed layer gets so warm that it cannot cool completely in half a year, so ice never forms.

The Annual Energy Balance

The coldest surface temperature and the thickest ice occur at the end of the freezing season. A simple energy argument leads to estimates of these quantities. Since the temperature varies between T = 0 and T = T_g during the cold season and during the warm season, the radiated energy for the entire year must be approximately

$$2Y(A + BT_g/2)$$

In an equilibrium cycle, this must equal the energy reaching the ice, which is

$$Y(f_{lwc} + f_w) + Y[f_{lww} + (1-\alpha)f_{sw} + f_w]$$

Equating these, and neglecting f_w for the moment, leads to

$$T_g = (D_m - D_g)/B \tag{21}$$

in which D_g and D_m are the net radiation balances over an ice surface at the freezing point during the growing and melting seasons. Using this expression in the surface heat balance, Equation (3), gives the maximum thickness as

$$h_g = (k/B)(D_g - D_m)/D_m \tag{22}$$

With $D_m = f_{lww} + (1 - \alpha)f_{sw} - A$ = 20 W/m^2, and $D_g = A - f_{lwc}$ = 140 W/m^2, we obtain T_g = -26°C, and h_g = 2.6 m. The expression for h_g underlines the sensitivity to the heat balance in the melting season. As D_m approaches zero, the ice grows without bound.

The simulations in "A Model of the Perennial Ice Cover" showed that the perennial ice cover gives way to a seasonal ice cover for a

positive perturbation of 18 W/m^2 to the longwave fluxes. To see why this is, we develop a condition on D_g and D_m which just causes the ice to melt completely at the end of the melting season. If h = 0 at the beginning of the cold season, the thickness at the end of the season will be, Equation (6),

$$h = (k/B)\left[\left(1 + 2BYD_g/kL\right)^{1/2} - 1\right] \tag{23}$$

In an equilibrium cycle, this must equal the ice melted in the warm season, which is approximately YD_m/L. Combining these results gives the constraint

$$\left(1 + BYD_m/L\right)^2 = 1 + 2BYD_g/kL \tag{24}$$

which is plotted in Figure 4. For climates having (D_g, D_m) below this line, the ice will melt away completely during the summer. If we set $D_m = 20 + \delta$ and $D_g = 140 + \delta$ the equation requires $\delta = 17$ W/m^2, in good agreement with the simulations.

Sensitivity to the Ocean Heat Flux

One result of the Maykut and Untersteiner simulations is a strong dependence on the ocean heat flux. They showed that increasing f_w from 0 to 7 W/m^2 caused the equilibrium thickness to decrease from about 6 m to zero. When one considers how poorly the ocean heat flux is known, and the uncertainties in the other heat fluxes, this sensitivity is unsettling.

The present models have been run using different values of f_w, with results that support the Maykut and Untersteiner results. In particular, holding other climate variables fixed, f_w = 1 W/m^2 produced ice of thickness 1.9 m at the end of summer. With f_w = 12 W/m^2 that thickness is reduced to 0.1 m.

We can appreciate how this works by restoring f_w to the expressions for T_g and h_g, Equations (21) and (22):

$$T_g = \left(D_m - D_g + 2f_w\right)/B \tag{25}$$

$$h_g = \frac{k}{B}\,\frac{\left(D_g - D_m + 2f_w\right)}{\left(D_m + 2f_w\right)}$$

From the first expression, we see that the surface temperature responds to the ocean heat flux exactly as it responds to the radiative fluxes. If an increment of heat Δ is added to the ice, in any way, the ice must respond by warming its surface Δ/B to maintain the overall energy balance. However, the response of the ice thickness is

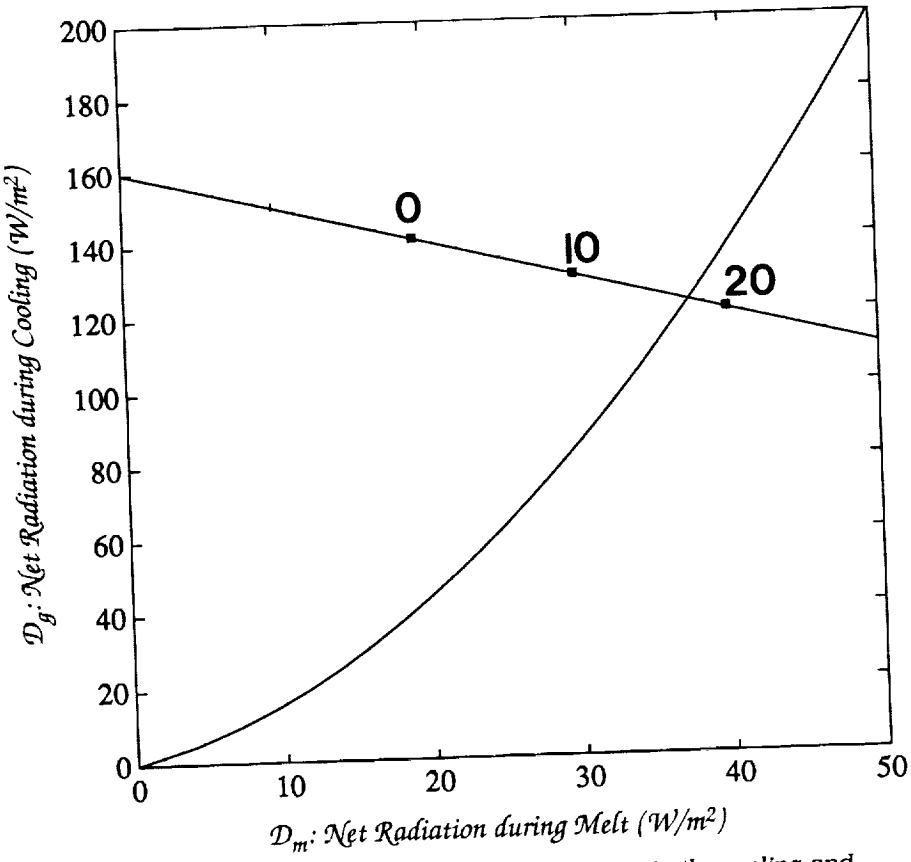

Figure 4. The condition on the net radiation balances in the cooling and melting seasons, D_g and D_m, which causes the ice just to vanish at the end of the summer. The straight line represents climates in which the longwave fluxes differ by δ from the present climate.

more subtle. An increase to f_w decreases the numerator and increases the denominator, and therefore has a larger effect on the thickness than one might expect.

The Time Scale for the Ice Response

By combining the ice grown in the cold season and the ice melted in the warm, we obtain the ice thickness after one year, beginning with initial thickness h_n,

$$h_{n+1} = F(h_n) = h_n + YL^{-1}\left(\frac{kD}{k + Bh_n} - 2f_w - D_m\right) \qquad (26)$$

Now the time scale for the ice to reach its equilibrium cycle is

$$\Gamma = h_n - h_{eq}/(h_n - h_{n+1}) \qquad \text{(years)} \qquad (27)$$

If we also write

$$h_{n+1} = h_{eq} + (h_n - h_{eq})dF/dt \tag{28}$$

and substitute for h_{n+1} in (27), we find

$$\Gamma = (1 - dF/dh_n)^{-1} \tag{29}$$

where the derivative is evaluated at the equilibrium thickness

$$h_{eq} = (k/B)\left(\frac{D}{D_m + 2f_w} - 1\right) \tag{30}$$

This gives the time scale

$$\Gamma = (kL/YB)\frac{D}{(D_m + 2f_w)^2} \cong 3 \text{ yr} \tag{31}$$

Discussion

The essential mechanism at work is that the ice adjusts its surface temperature to maintain the energy balance at the surface. In the present climate, the annual energy balance over a surface at the melting point is $D_m - D_g = -120$ W/m^2, meaning that a surface at T = 0°C would lose 120 W/m^2 more than it receives. The surface adjusts by cooling to about -26°C.

The second important idea is that during ice growth, the ice thickness is related to its surface temperature; the colder the temperature, the thicker the ice. Therefore we can assess the response of the ice thickness to a climate perturbation, in the form of a change dE in the energy reaching the surface, by evaluating

$$dT/dE \quad \text{and}$$

$$dh/dE = dh/dT \bullet dT/dE = -\left[(k + Bh)^2/DBk\right] \tag{32}$$

For h = 3 m, the sensitivity is about -0.2 m for 1 W/m^2 increase in incoming energy. Note that the sensitivity is a strong function of thickness.

Thus the thickness is rather sensitive to the energy fluxes. Perturbations of 10 W/m^2 can mean several meters of ice thickness. Nevertheless, the system can adjust to perturbations of this magnitude.

However, for larger fluctuations, the system cannot adjust. A cooler climate in which the longwave fluxes were 20 W/m^2 less than present (about 5°C of tropospheric cooling) would allow the ice to grow without bound. A positive perturbation of the same magnitude would cause the ice to melt away completely in the summer, so that the entire Arctic would support only a seasonal ice cover. With a positive perturbation of about 40 W/m^2, enough heat is stored in

the upper ocean during the warm season to prevent ice from forming during the winter.

Of course, with a model that ignores many physical processes and treats others badly, one cannot have great confidence in the numerical results. Still, I expect the relationships between quantities in these models to have a qualitative validity, in the sense that in a more careful model, the signs and powers in the expressions would survive, while different numerical factors, of order unity, might appear.

These ideas have implications for climate models that attempt to simulate the Arctic ice cover. First, the level of detail in the perennial and seasonal models discussed here may be about right for use in a climate model. The models surely allow an interactive ice cover without a heavy computational burden. A second point is that we have found limits on errors that can be tolerated in the energy fluxes supplied by the climate model to the ice. Fluxes in error by ± 10 W/m^2 will not destroy the ice, but errors of ± 20 W/m^2 will lead to a qualitatively wrong ice pack. Finally, given the sensitivity of the ice thickness and temperature to perturbations on the order of 10 W/m^2, and the likelihood that climate models will have this much uncertainty for some time to come, it is not realistic to expect a climate model to reproduce the observed ice thickness, or to predict how much the thickness will change. It is enough to ask that a climate model distinguish between a perennial ice cover and a seasonal ice cover, or between an ice cover and no ice at all.

Of course, the actual Arctic ice cover is too complicated for a toy model. There is in fact a great range of thicknesses, all growing and melting at different rates, and all responding to mechanical as well as thermal forcing. I do not want to leave the impression that these processes are unimportant.

Acknowledgments

I wish to thank G.A. Maykut and N. Untersteiner for pointing out a blunder in an early draft of this paper, and K. Bryan for a helpful comment regarding the time response of the system, when the paper was presented at Snowmass. The work was supported in part by the National Aeronautics and Space Administration, Cryospheric Interactions, managed by Bob Thomas.

References

Maykut, G.A., and N. Untersteiner. 1971. Some results from a time dependent, thermodynamic model of sea ice. *Journal of Geophysical Research 76*, 1550–1575.

A Toy Model for Estimating N_2O Emissions from Natural Soils

Inez Fung

Introduction

Nitrous oxide is present in the atmosphere in minute quantities. Its concentration in 1988 was ~307 parts per billion by volume (ppbv), about a thousand times less than that of CO_2, and it is increasing at the rate of ~0.8 ppbv/yr (Elkins et al., in press). The seemingly small growth rate, ~0.25%/yr, is the result of a large imbalance (~30%) between the sources and sinks.

Despite its low abundance in the atmosphere, N_2O plays an important role in the radiative and chemical balance of the atmosphere. The extremely long lifetime of N_2O, ~150 years, means the system has a very long memory of its emission history. The radiative forcing of N_2O, molecule for molecule, is ~200 times that of CO_2 (Houghton et al., 1990). N_2O is destroyed in the stratosphere by photolysis and by reaction with electronically excited oxygen atoms [$O(^1D)$], making it the dominant precursor of odd nitrogen (NO_x) in the stratosphere. Thus an increase in N_2O would lead to an increase in stratospheric NO_x, which would catalyze the destruction of stratospheric ozone.

The sources of N_2O are not well known. Of the ~15 Tg N (1 Tg = 10^9 kg) produced annually, by far the largest source seems to be emissions from natural soils, 6 ± 3 Tg/yr, followed by emissions from the oceans, 2 ± 1 Tg/yr (Seiler and Conrad, 1987). The strength of these natural sources is estimated from only a handful of flux measurements. Other sources include emission from combustion, biomass burning, and agricultural fields amended with nitrogenous fertilizers. For some time, it was thought that, like CO_2, the primary cause for the increasing trend was combustion of fossil

fuels, in particular, coal-burning power plants producing electricity (Hao et al., 1987). However, recent identification of an artifact in the flask sampling procedure ruled out combustion (including biomass burning) as the major cause of the N_2O trend (Muzio and Kramlich, 1988). We do not know why N_2O is increasing in the atmosphere.

Global models of the N_2O cycle (e.g., Prinn et al., 1990) use variations in the concentrations of N_2O in the atmosphere to infer the location and magnitude of the N_2O sources and sinks. The results point to large source(s) located in the tropics that contribute significantly to the latitudinal gradient and secular trend of N_2O in the atmosphere. Such an approach, however, cannot distinguish among individual sources without direct information about at least some of the sources and sinks themselves.

In a separate paper (Bouwman et al., in preparation), we focused, not on the N_2O budget itself, but on the largest single source term in the budget, i.e., emissions from natural soils. The effects of fertilizer application and other human perturbations on the N_2O emissions from soils were not considered. A very simplistic model was developed for estimating directly the geographic and seasonal variations of N_2O emissions from natural soils. We hope that the model, and the sensitivity studies using it, will provide guidance for measurement strategies to reduce systematically uncertainties about this single source. The source distribution may also be a useful input to two-dimensional and three-dimensional models to test hypotheses about the N_2O budget. The reader is referred to Bouwman et al. for a detailed description of the data, model, and sensitivity analyses. Here, we present an account of the assumptions and decisions involved in the construction of the model.

A Conceptual Model of N_2O Production

N_2O is produced by both nitrification and denitrification. Denitrification occurs under oxygen limiting conditions. Nitrogenous oxides, principally nitrate (NO_3^-) and nitrite (NO_2^-), are reduced to dinitrogen gases (N_2), nitrous oxide, and nitric oxide (Firestone and Davidson, 1989). Under strictly anaerobic conditions nitrous oxide and nitric oxide (NO) may also be used as electron acceptors. In nitrification, ammonia (NH_4^+) is oxidized to NO_2^- or NO_3^-. In natural soil ecosystems, the NH_4^+ comes from decomposition and mineralization of organic matter only. The reader is referred to Bowden (1986) for a review of the biogeochemistry and measurements of N_2O production in undisturbed ecosystems.

Consider a conceptual model of N_2O production in a unit area of unperturbed land with a given vegetation/soil complex. Litterfall

associated with vegetation cycles supplies fresh organic matter to the soils. The organic matter is decomposed and mineralized by microbial activity, thus delivering N for nitrification and denitrification. The decomposition rate is regulated by soil temperature and other parameters of the soil environment. Under most soil conditions, both nitrifying and denitrifying bacteria are active. The relative contribution of N_2O produced via the nitrification and denitrification pathways is determined largely by the degree of water saturation and aerobicity of the soils. The wetter the soil, the lower the oxygen content and the more likely denitrification processes are to dominate. Soil water and oxygen status are, in turn, governed by the net water supply at the surface, soil water-holding capacity, and drainage properties. Other inherent soil properties, such as pH and fertility, also modulate the microbial activity and N_2O production.

The controls on N_2O production from natural soils can be summarized as (1) carbon and nitrogen availability, (2) temperature, (3) soil moisture, (4) soil oxygen status, (5) soil fertility, and (6) soil pH. Because global data on soil pH are of questionable quality, this factor was not included in our analysis.

Global Data for the Toy Model of N_2O Production

We now present a synthesis of our conceptual understanding of the controls on N_2O fluxes into a quantitative framework, i.e., into a model. The ultimate objective of the model is to evaluate what contribution natural ecosystems make to the global N_2O budget and how the contribution would change with global change. Given the paucity of measurements, our immediate goal is to test the conceptual model of N_2O fluxes and identify gaps where measurements and analyses are needed.

The focus of the model requires data or inputs that must be global in domain and span at least a year. The primary gridded data sets available are described below:

- *Soils:* The 1:5M FAO/Unesco soil maps (1971–1982, 1974, 1988) include information on dominant soil units, associated soils (when they cover at least 20% of the area) and inclusions, texture of the dominant soil, and slope. We used information on the major soil units (106) and texture of the topsoil (upper 30 cm) from the data digitized at $1° \times 1°$ resolution for the globe by Zobler (1986). The spatially dominant soil units in the 1° grid cell were recorded.

Texture reflects the relative proportions of clay (particles less than 2 μm in size), silt (2–50 μm), and sand (50–2000 μm). Three tex-

ture classes for the topsoil are distinguished in the FAO soil maps: coarse, medium, and fine. At 1° resolution, a spatially dominant texture cannot always be established. And so, four other texture classes were included in the digital data base: coarse/medium, coarse/fine, medium/fine, and coarse/medium/fine. Furthermore, texture information was not available everywhere in the FAO soil maps, in particular for some of the organic soils, e.g., Histosols. A separate class, "organic," was added to the texture description. These additional five classes composed <10% of the land surface.

The soil type information is used to translate directly into fertility and drainage, while the type and texture information are used to derive soil storage capacity. These are described briefly below and in detail in Bouwman et al. (in preparation). Figure 1 shows the global distribution of soil texture, grouped into six classes.

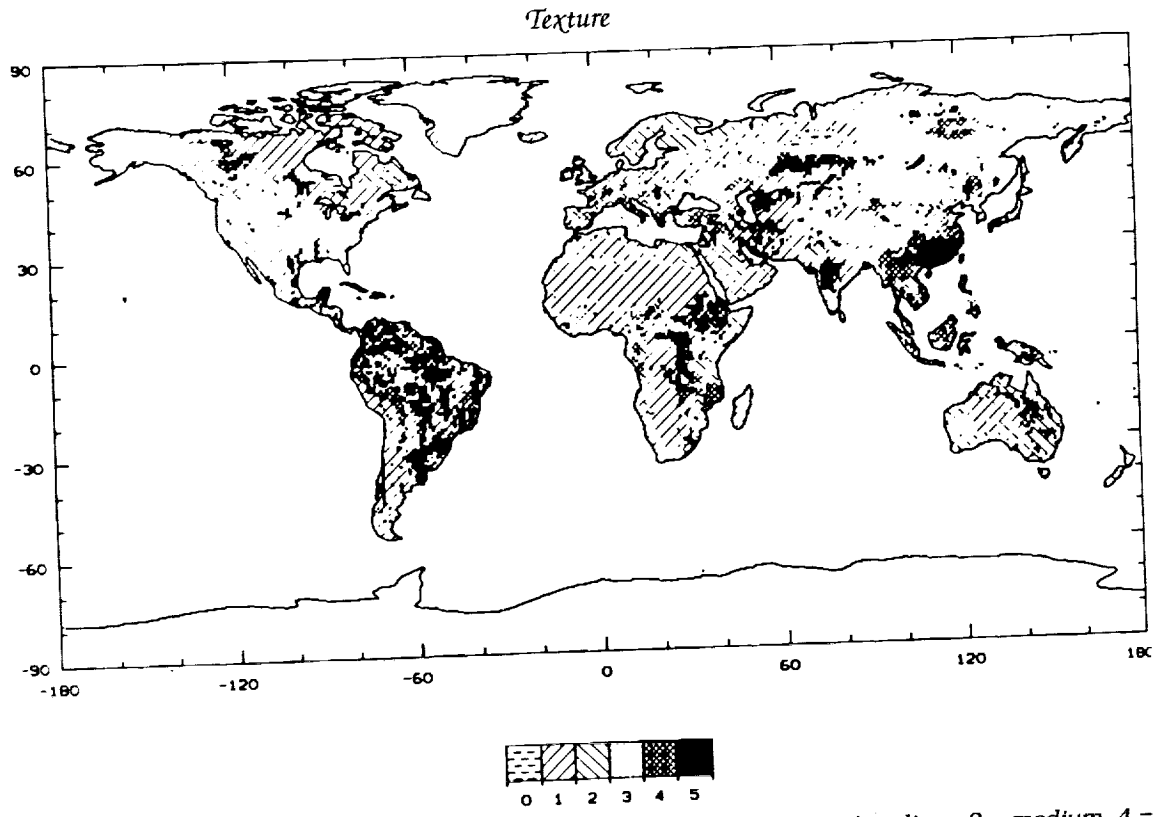

Figure 1. Distribution of soil texture: 0 = organics, 1 = coarse, 2 = coarse/medium, 3 = medium, 4 = medium/fine, 5 = fine. Spatial resolution is 1° × 1°.

- *Vegetation:* The satellite-derived normalized difference vegetation index (NDVI) is a measure of primary productivity of the vegetation. The NDVI is the difference between the radiances in the visible (0.58–0.68 μm) and near-infrared (0.725–1.1 μm) wavelengths, normalized by the sum of the radiances. The radiances are measured by the advanced very high resolution radiometer (AVHRR) on board the NOAA series of polar-orbiting satellites (Tarpley et al., 1984). In this study, monthly NDVI composites for 1984 were gridded at 1° × 1° resolution for the globe, and then summed to produce the annual total. Although a digital data base of vegetation types exists (Matthews, 1983), vegetation information is used only for verifying measurement site characteristics and for analysis of model results.
- *Climate:* Shea (1986) has produced climatologies of monthly mean surface air temperature and precipitation, at 2° × 2° resolution for the globe, from the available station observations. In the conceptual model, the climate parameter important for N_2O production is soil temperature. Lacking a global climatology for soil temperature, we used surface air temperatures instead. This would introduce phase errors, of up to a season in middle and high latitudes, in the seasonality of N_2O production.

The finest spatial resolution of these data sets is 1° latitude by 1° longitude, so that there are ~15,000 grid cells for the ice-free land surface. The climate data are monthly means. With this resolution, the model cannot resolve episodic effluxes of N_2O after rainstorms and spatial "hot spots" which are often reported. The importance of such high-frequency, local events in the global budget has not been established. The model must parameterize, in some way, their integrated effect, and evaluate their contribution to the global annual flux.

A Toy Model for N_2O Production

Fluxes of N_2O from temperate grasslands have been extensively modeled based on the comprehensive measurements there (e.g., Parton et al., 1987, 1988). For the other soil types around the globe, there is a dire lack of N_2O flux measurements, let alone quantitative relationships between N_2O fluxes and the various controlling parameters. We do not know if the relationships established for grasslands can be extrapolated elsewhere.

Our strategy for the toy model for N_2O production is to first translate ideas about relative importance of each of the controlling parameters into ranked nondimensional indices. The indices are scaled

from 0 to 10, or from 0 to 5, with high numbers signifying importance for N_2O production and 0 signifying no production. Our choice of a scale of 5 or 10 depends on the number of levels we think we can discriminate within the scale.

Using nondimensional variables to denote relative importance is not a new concept. It was employed, for example, to represent temperature and moisture controls in the N_2O model of Mosier and Parton (1985). Such a translation is straightforward for numeric data such as temperature. In this toy model, we also created nondimensional scales for ordinal data such as fertility and drainage by carrying out a subjective ranking of soil units and texture information. The control indices are then combined to form the index for N_2O fluxes. Comparison of the scaled nondimensional N_2O fluxes with field measurements provides an evaluation of the validity of the model and, one hopes, an algorithm for calculating N_2O fluxes from the scaled variables.

The model is illustrated schematically in Figure 2. A central part of the problem is to model how soil water regulates the degree of nitrification/denitrification and hence N_2O production. A bucket model of water balance is used. The bucket model takes into account differences in soil drainage and topsoil texture and determines the water and oxygen status of the topsoil. For both nitrification and denitrification, N_2O flux is also proportional to the amounts of carbon and nitrogen available in the soil, the rate of mineralization of the carbon and nitrogen, and soil fertility.

With this approach, we need to derive the global distribution of the five major regulators of N_2O production. Three of them vary monthly: decomposition of soil organic matter (SOD), water availability (WATER), and oxygen limitation (OXYGEN); the remaining two, soil fertility (FERT) and carbon and nitrogen availability (CARBON), are constant through the year. Below, we describe in detail the derivation of each of the regulators and their synthesis to yield the nondimensional N_2O flux.

Soil Carbon and Nitrogen Available

Litterfall and root decay are the major sources of carbon and nitrogen to the soil. For most ecosystems, there is an abundance of litter on the ground throughout the year. Hence the seasonal variation of C and N mobilization in the litter is generally governed by decomposition rates rather than by seasonal variations in litterfall. Here we assumed that geographic pattern of annual litterfall is the same as that of annual net primary productivity of the ecosystems, for which the satellite-derived NDVI has been shown to be a good correlate (Goward et al., 1986; Box et al., 1989). Because litterfall is

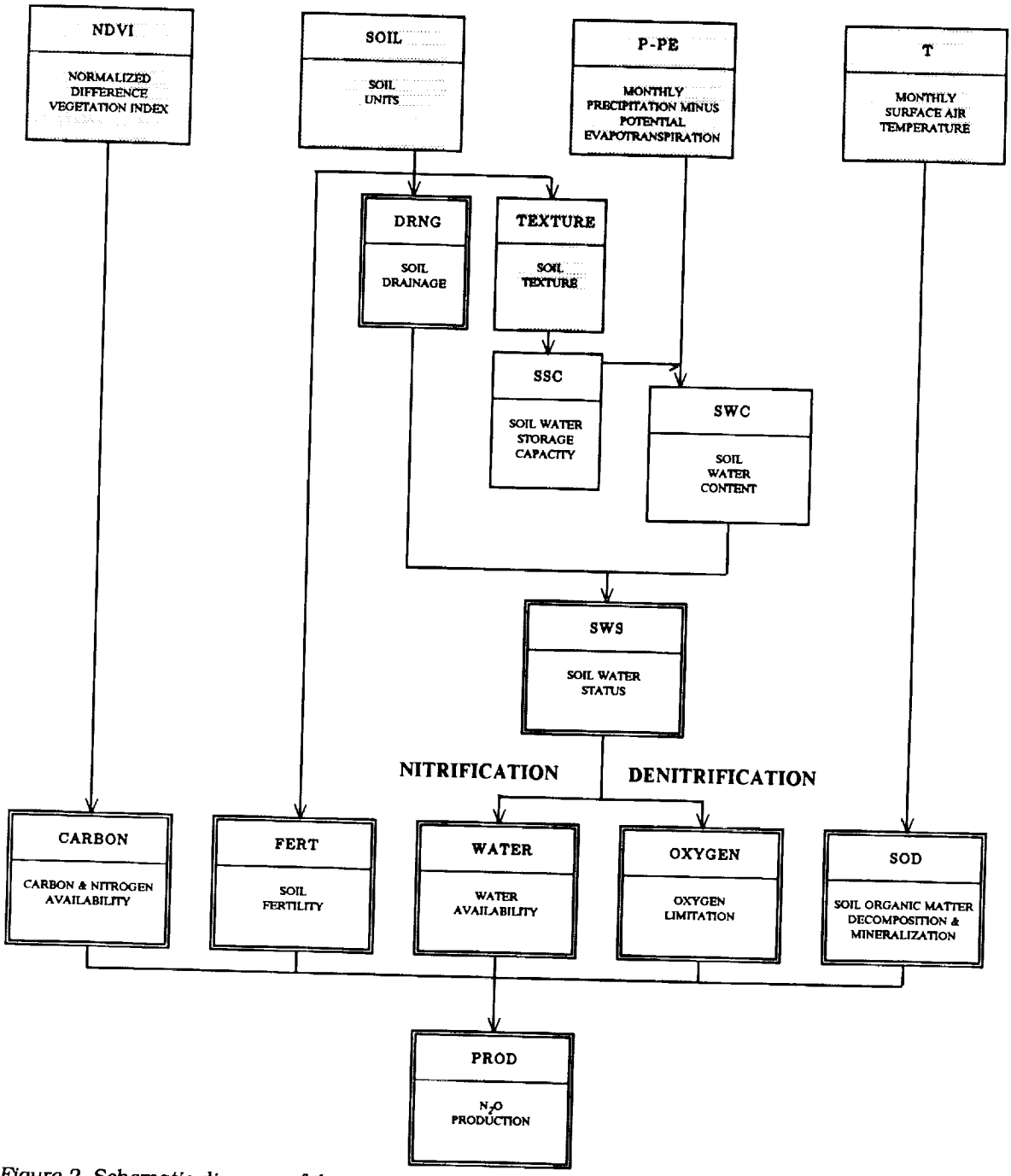

Figure 2. Schematic diagram of the toy model of N_2O production. Shaded boxes denote input data and double-bordered boxes denote nondimensional indices.

not in phase with productivity, the annual NDVI totals, rather than NDVI for individual months, were used.

Monthly NDVI values range from –0.1 to 0.5, and the annual totals range from –0.1 to 4. To be consistent with the other factors used in the study, these NDVI totals were, in turn, rescaled to range from 0 to 10 to obtain the index CARBON (Figure 3). We note that we could have used, instead of the NDVI, a global distribution of net primary production (NPP) obtained by assigning literature values of annual NPP to the digital data base of vegetation. The use of the NDVI captures the variability of NPP within each vegetation type, at the same resolution as the soil data.

Delivery of Nitrifiable N

The rate of carbon and nitrogen delivery is governed by the rate of decomposition and mineralization of soil organic matter, which are regulated by soil temperature, soil moisture, soil fertility, and soil texture. Here, we introduced a factor in the model to represent the

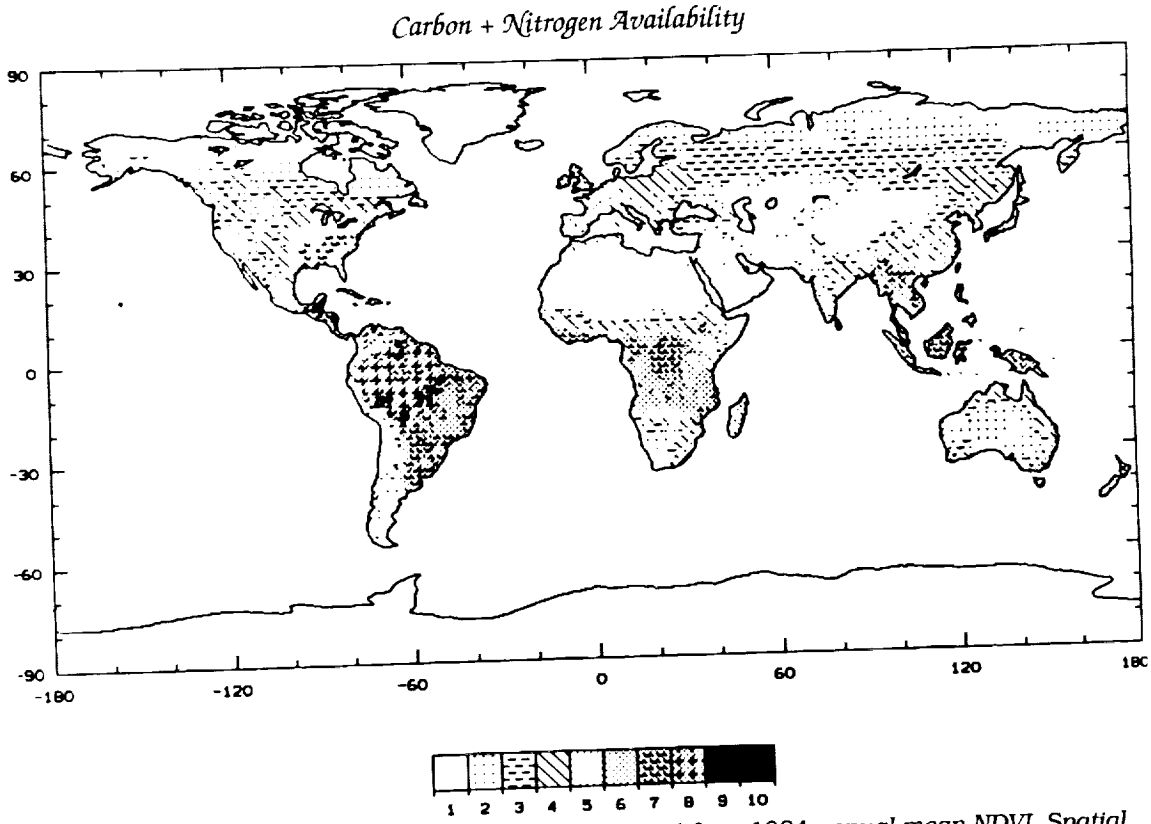

Figure 3. Global distribution of the index CARBON, scaled from 1984 annual mean NDVI. Spatial resolution is 1° × 1°.

temperature effect on the supply of nitrogen and carbon through decomposition of organic matter (SOD).

Three temperature dependencies for the factor SOD were investigated (Figure 4). The first (referred to as SOD1) is an exponential function describing the temperature effect on N_2O fluxes obtained for semiarid grasslands (Mosier and Parton, 1985; Parton et al., 1988). SOD1 = 10 at T = 50°C, and SOD1 = 0 for T ≤ 0°C, with a rapid increase between 10 and 30°C. The second equation (referred to as SOD2) is a quadratic function adapted from Parton et al.'s (1988) equation for N_2O fluxes from grasslands. The optimum (SOD2 = 10) is at T = 35°C. To avoid negative values, SOD2 was set to zero at T < 7°C and T > 50°C. The third relationship tested (referred to as SOD3) is a set of linear functions for four broad ecosystem groups: broad-leaved vegetation, needle-leaved vegetation, grasslands, and tropical vegetation. The functions were derived from observations of CO_2 evolution from soils (Fung et al., 1987). They were set to SOD3 = 10 at T = 50°C. The different slopes of the four functions reflect the differences in litter composition for the broad biome groups. For comparable temperature ranges, grasslands, having a higher fraction of easily decomposed material in its detritus than needle-leaved woody vegetation, would have a faster relative decomposition rate. The maximum

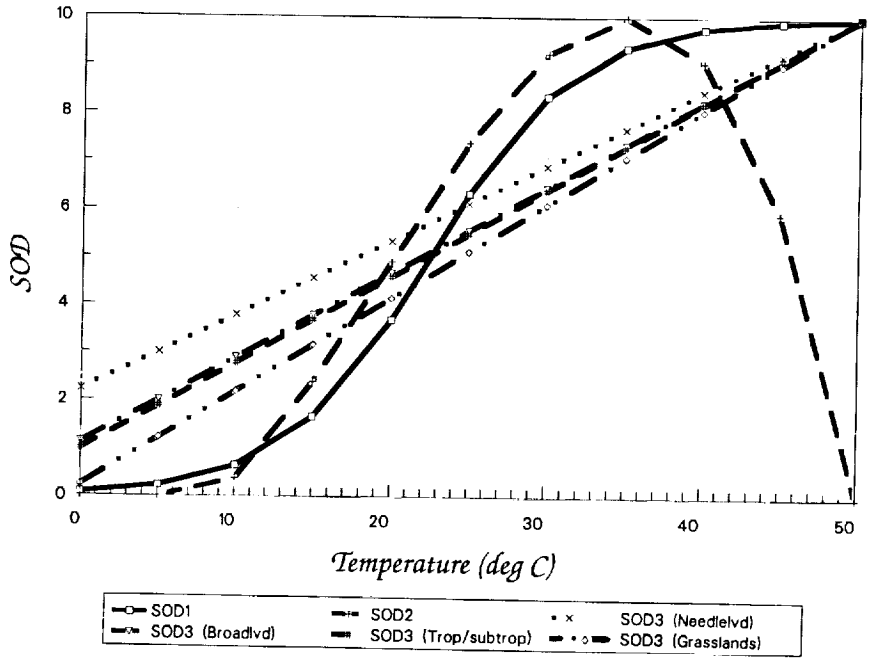

Figure 4. Index of the rates of soil matter decomposition (SOD) as a function of temperature.

values at T = 50°C do not capture the adaptation of microbes to their environmental conditions.

We used the exponential curve (SOD1) in the reference formulation for N_2O production (see "N_2O Production" below).

Soil Water and Oxygen Status

A key to distinguishing the pathways of nitrification vs. denitrification is the degree of saturation and aerobicity of the soil, which is, in turn, determined by the soil drainage properties, as well as by the amount of water present in the topsoil vs. the maximum amount of water allowed in the topsoil, i.e., the soil water storage capacity (SSC).

A first step in modeling the water balance of the topsoil is the determination of the soil water storage capacity. SSC is the total amount of water held in the upper 30 cm of the soil profile at field capacity (soil water potential of 10 kPa), after internal drainage and redistribution have ceased. Global distributions of SSC are used in general circulation models (GCMs); recent hydrology schemes assign SSC based on vegetation and/or soil characteristics. We prescribed SSC based on soil texture for most soils. SSC is 120 mm, 80 mm, and 40 mm for fine-, medium-, and coarse-textured soils, respectively. For a number of soils, covering about 30% of the ice-free land surface, properties other than texture exert the primary influence on water retention; their SSCs were assigned without regard for texture. Generally, these are fine-textured Ferralsols and Vertisols whose aggregates and swell-shrink properties, respectively, reduce their water-holding capacity to that of medium-textured soils. The global distribution of SSC is shown in Figure 5.

Soil Water Budget Model

The change in soil water content (SWC) is the difference between the supply and demand of moisture at the surface. Supply is governed to a large extent by precipitation, while demand is governed by evaporation through soils and transpiration through plants. Runoff (on sloping land) or ponding (on level land) occurs when the net input of water plus the initial amount of soil water exceed soil water storage capacity after drainage has been accounted for.

There are several soil moisture models used in general circulation models, ranging from the simple bucket model of Manabe (1969), where SSC was uniformly 15 cm, to the simple biosphere model (SiB) of Sellers et al. (1986) and the complex biosphere-atmosphere transfer scheme (BATS) of Dickinson (1984) and Dickinson et al. (1986), which take into account the effects of biome differences on soil water balance. Not only do these recent models distinguish among soil evaporation and plant evaporation and transpiration,

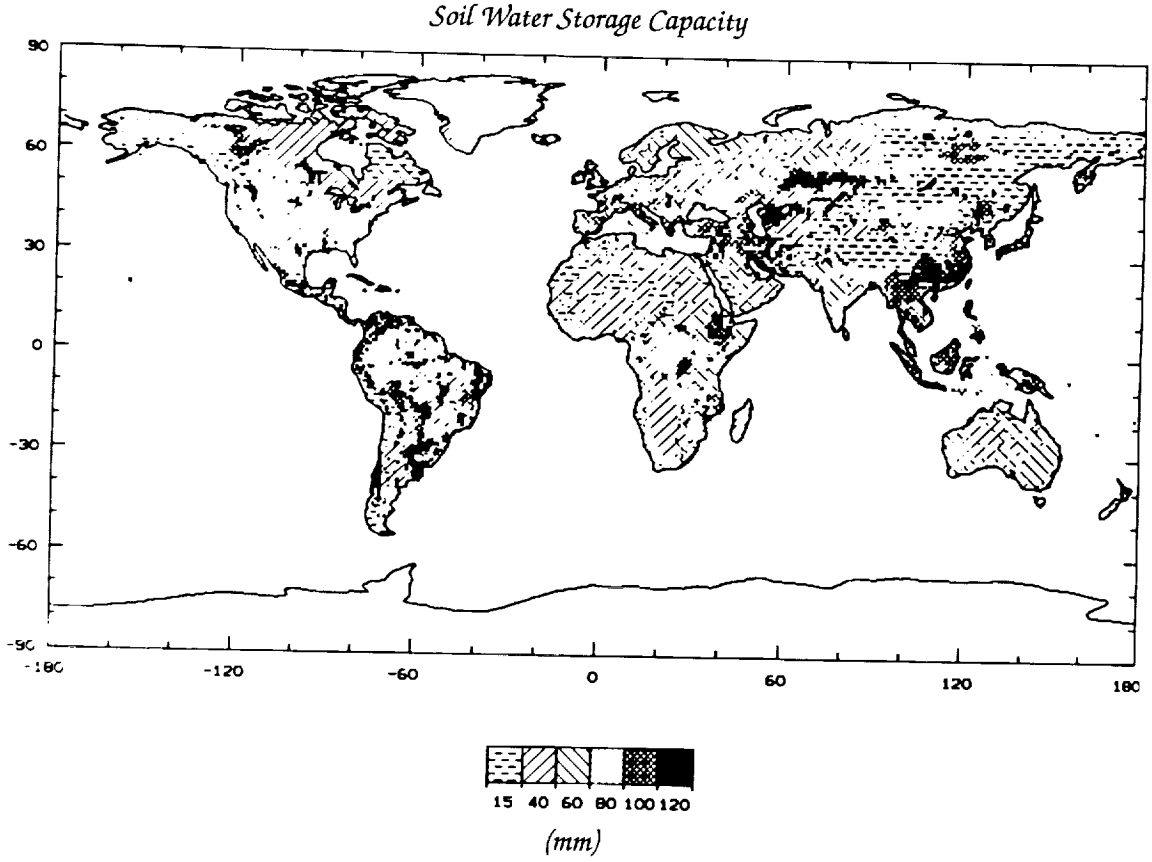

Figure 5. Distribution of SSC.

they also model explicitly vertical profiles of moisture in the soil. These recent models are not yet fully validated in GCMs and are too complicated for the toy model at hand. However, in a simple bucket model where supply and demand are independent of soil moisture itself, the solution to the soil moisture equation is not uniquely determined; it is dependent on the initial SWC assumed, unless the SWC = 0 or SWC = SSC (runoff) sometime during the year.

In this study, we chose a soil moisture model that is simple in design, and whose solution is not dependent on an arbitrarily chosen initial condition. We adapted the Mintz and Serafini (1981) model for the calculation of the monthly soil water content (SWC_m). In this model, net supply is the difference between monthly precipitation (P_m) and evaporation from wet canopies (EI_m), while demand is the sum of transpiration through plants and evaporation from soils (ETS_m). The time step of a month corresponds to the time resolution of the global precipitation climatology used.

$$SWC_m = SWC_{m-1} + (P_m - EI_m) - ETS_m$$

Potential evaporation (PE_m), a measure of the maximum demand for moisture by the atmosphere, was calculated from the surface air temperature according to Thornthwaite (1948). Mean monthly surface air temperatures (T_m) and precipitation (P_m) were obtained from the climatologies compiled by Shea (1986). For simplification, precipitation in the form of snow was treated as rainfall. Three moisture regimes were considered, dependent on the relation between P_m and PE_m:

$P_m = 0$

$$EI_m = 0$$
$$ETS_m = PE_m \times \beta_m \times \alpha$$

$P_m < PE_m$

$$EI_m = P_m$$
$$ETS_m = (PE_m - P_m) \times \beta_m \times \alpha$$

$P_m \geq PE_m$

$$EI_m = PE_m$$
$$ETS_m = 0$$

where

$$\alpha = 0.4$$

and

$$\beta_m = 1 - e^{-\gamma\left[\{SWC_{m-1} + (P_m - EI_m)/2\}/SSC - \delta\right]}$$

The coefficient α expresses the ratio of the amount of water extracted from the topsoil to the extraction from the full rooting zone (as noted before, we consider only the topsoils). The function β describes the maximum water extraction as a function of soil water content and soil characteristics. Its parameter γ depends on topsoil texture and mineralogy, while δ represents the water unavailable to plants, i.e., the intercept of the water extraction curve β. The values of δ and γ are dependent on soil texture (see Bouwman et al., in preparation). For fine textured soils, $\gamma = 6$, resulting in a strong decrease in water extraction below SWC/SSC $\approx$ 50%. Due to the selected value of δ for clays, water extraction at SWC/SSC < 10% is reduced. In sands and medium-textured soils β sharply declines at values of SWC/SSC of about 40% and 20%, respectively. Because SWC is a function of β, the monthly equilibrium SWC is achieved independently of the initial water content at the start of the simulation.

Effects of Drainage

In the calculation of the soil water content of the topsoil described above, drainage properties of the soil were not considered. Drainage

determines how excess water is removed from the soil, and it is also an indicator of the soil aeration. We ranked the soil drainage index DRNG based on soil texture and other soil properties, with a high rank favoring N_2O production. The very poorly drained soils (DRNG = 5) include those soil groups strongly influenced by groundwater, i.e., Gleysols and Histosols, as well as soils with permafrost within 200 cm of the soil surface (gelic soil units). Freely drained soils, such as Xerosols and Yermosols, occurring in deserts, were assigned a drainage rank of 1. The distribution is shown in Figure 6.

We are uncertain how to model quantitatively the effects of drainage on soil water content. Adding diffusion at the base of the "bucket" may be an appropriate approach, but the values of the diffusion coefficients for different drainages are not well known. Here, we introduced the factor soil water status (SWS), an index of the soil water saturation when drainage effects are considered (Table 1). It is clear that the highest SWS rank of 10 would be assigned to a poorly drained soil when the monthly soil water content SWC is close to the storage capacity SSC of the soil. It is not clear how to rank the intermediate values of drainage and SWC/SSC. We noted several points: (1) Distinguishing saturation levels <20% is not important, so that the SWC/SSC scale can be divided into ten levels as shown. (2) We linearly increased the SWS scale up the saturation scale. (3) We filled in the rest of the table by assuming that N_2O production would likely be asymptotic at high saturation and poor drainage. There is thus much arbitrariness in the SWS scale. It nevertheless represents a first attempt at quantifying our descriptive understanding of the effects of soil drainage characteristics on soil moisture.

Nitrification and Denitrification Potentials

It remains to describe the effects of soil water status on oxygen supply in the soils, i.e., on nitrification and denitrification. Two factors, water availability (WATER) and oxygen limitation (OXYGEN), were derived as indices for nitrification and denitrification potentials, respectively. These two indices are based on the two moisture indices derived by Parton et al. (1988) for the two processes.

The influence of soil water status on nitrification and denitrification has been documented by many authors (Mosier and Parton, 1985; Klemedtsson et al., 1988; Groffman and Tiedje, 1988). Aerobic microbial activity increases with soil water content until a point is reached where water displaces air and restricts oxygen diffusion. Maximum rates of nitrification occur at the highest water content at which soil aeration remains nonlimiting, with SWC ~60–80% of SSC. And so we assigned maximum nitrification potential WATER at SWS around 6–8 (Table 2).

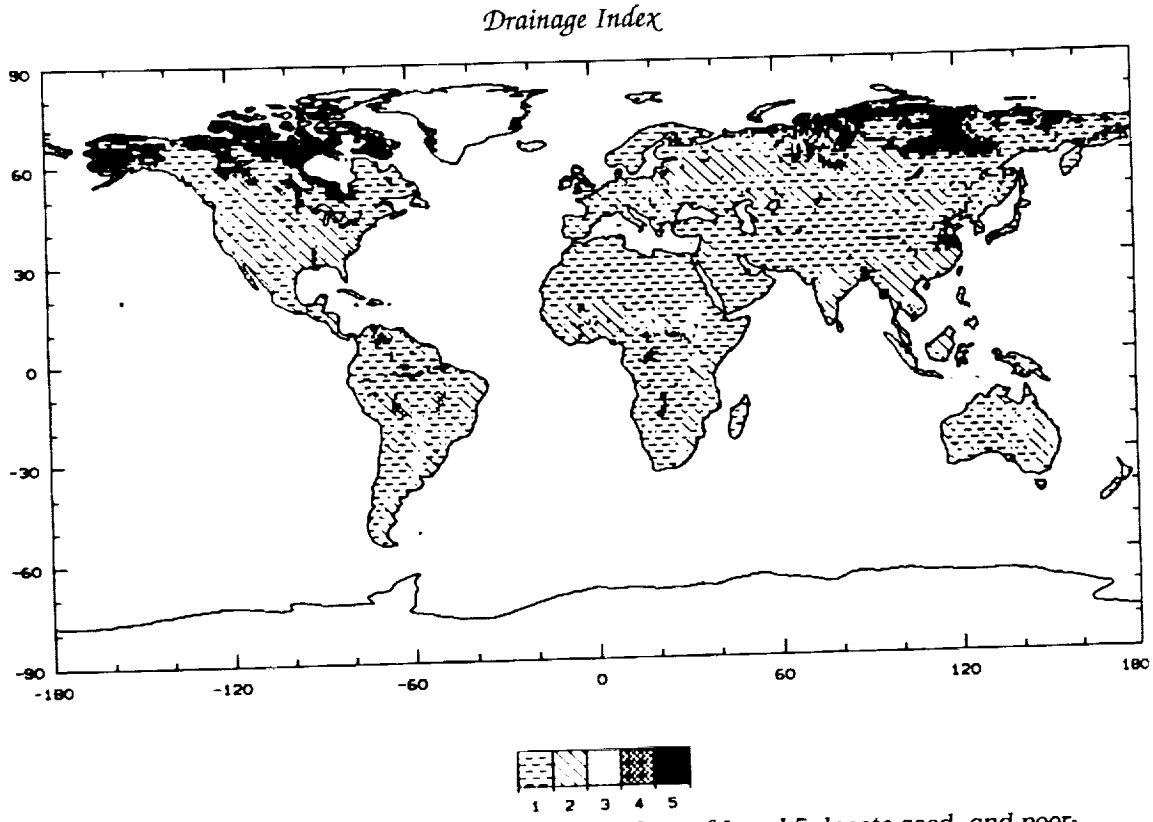

Figure 6. Distribution of the drainage index DRNG. Values of 1 and 5 denote good- and poor-drainage soils, respectively.

Table 1: Soil water status, as a function of the soil drainage scale and calculated soil water content/soil water storage capacity

SWC/SSC (%)	Drainage Scale				
	1	2	3	4	5
0 - 20	1	1	1	1	2
20 - 30	2	2	2	2	3
30 - 40	3	3	3	4	5
40 - 50	4	4	4	5	7
50 - 60	5	5	5	6	8
60 - 70	6	6	6	7	9
70 - 80	6	7	7	8	9
80 - 90	7	7	8	9	10
90 -100	7	8	9	10	10
>100%	8	9	10	10	10

Table 2: Water availability as a function of soil water status in current and preceding months

SWS, preceding month	SWS, current month									
	1	2	3	4	5	6	7	8	9	10
1	1	2	4	6	9	10	10	10	6	1
2	1	1	3	5	8	9	10	10	6	1
3	1	1	2	4	7	8	9	10	5	1
4	1	1	2	4	7	8	8	8	4	1
5	1	1	2	4	6	7	7	7	3	1
6	1	1	2	4	6	7	7	6	2	1
7	1	1	2	4	6	7	7	6	2	1
8	1	1	2	4	5	6	6	5	2	1
9	1	1	2	3	4	6	6	4	2	1
10	1	1	2	3	4	5	6	4	2	1
No dependence*		1	2	3	5	7	10	10	5	21

*Scalars depend only on the SWS in the current month.

The maximum N_2O production by nitrifier denitrification is between 80 and 100% water-holding capacity, while the peak for respiratory denitrifier N_2O production may be at water contents exceeding 100% water-holding capacity (Klemedtsson et al., 1988). Hence OXYGEN, the index of oxygen limitation and denitrification potential, was assigned a maximum value for SWS = 10 (Table 3).

Field measurements generally show high pulses of N_2O efflux from the soils after rainfall. Lacking any statistics, we do not know how significant these episodic pulses are in the global N_2O budget. Furthermore, there are presently no gridded climatologies of daily rainfall even for a continent. To test the importance of wetting and drying using the data available, we made the nitrification and denitrification indices dependent on the soil water status of the previous month in addition to the current month (see Tables 2 and 3). We hypothesized that dry soils that are wetted (large difference in SWS between previous and current months) are more favorable for N_2O production than soils with constant SWS. In this way, pulses of N_2O at the onset of a wet season would give a higher average monthly N_2O flux than in wet months preceded by moist conditions. The hysteresis effect observed (Groffman and Tiedje, 1988) is included by making the indices under drying conditions lower than those under equal amounts of wetting. This procedure imposes a one-month memory on the system, and the memory is probably much longer than that represented in the episodic pulses observed. This is thus one of the most uncertain aspects of the toy model, but an aspect that can be tested with long time-series measurements such as that of Parton et al. (1988).

Table 3: Oxygen limitation as a function of soil water status in current and preceding months

SWS, preceding month	SWS, current month 1	2	3	4	5	6	7	8	9	10
1	1	1	1	4	6	8	10	10	10	10
2	1	1	1	4	6	8	10	10	10	10
3	1	1	1	3	5	7	9	10	10	10
4	1	1	1	3	4	6	8	9	10	10
5	1	1	1	2	3	5	7	8	9	10
6	1	1	1	1	2	4	6	7	8	9
7	1	1	1	1	2	3	5	6	7	8
8	1	1	1	1	2	3	4	5	6	7
9	1	1	1	1	2	3	4	5	6	7
10	1	1	1	1	2	3	4	5	6	7
No dependence*	1	2	2	3	3	4	5	6	8	10

*Scalars depend only on the SWS in the current month.

In the reference case for N_2O production (see "N_2O Production"), we included the WATER and OXYGEN dependence on the water status of the previous month.

Soil Fertility

The last control on N_2O production we need to quantify is soil fertility. Matson and Vitousek (1987, 1990) have shown a strong relationship between N_2O flux and soil fertility in the tropics and subtropics, and that relationship is useful for regional estimation of N_2O emission. In this study, soil fertility for each of the 106 soil units was ranked subjectively based on general understanding of the cation exchange capacity and other soil properties. Because we did not feel that we were capable of distinguishing as many as ten levels of soil fertility, five ranks were used. A high value denotes a fertile soil, conducive to high levels of N_2O production. For example, Ferralsols, occurring mainly in the tropics, are strongly leached soils and their fertility is low because of their low cation exchange capacity, presence of alumina on the exchange complex, low content of weatherable minerals, and phosphorus fixation. A rank of 1–2 was assigned. In contrast, Chernozems and Kastanozems, underlying much of the agricultural lands in midlatitudes, are fertile soils to which a rank of 5 is assigned. The global distribution of the index FERT is shown in Figure 7.

N_2O Production

With the controls on N_2O fluxes quantified, it remains to combine them to yield PROD, the nondimensional index of N_2O production.

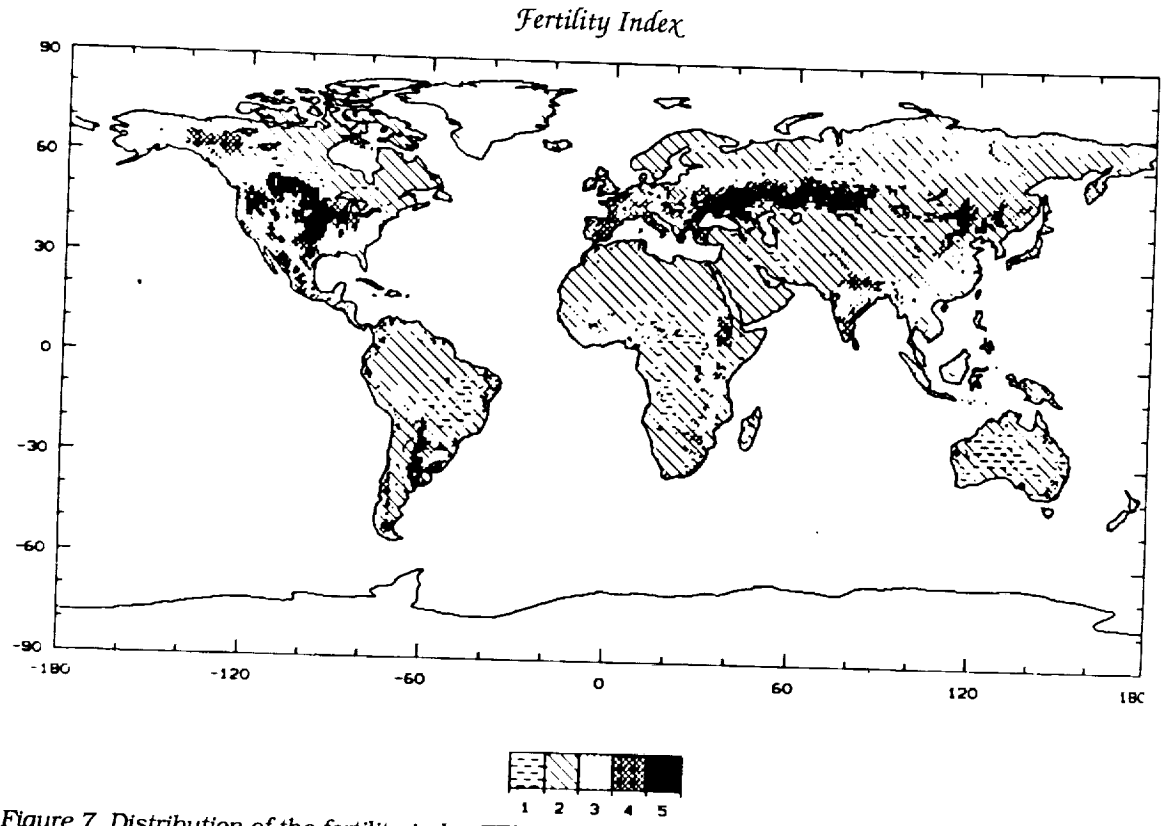

Figure 7. Distribution of the fertility index FERT. High values denote fertile soils, conducive to N_2O production.

We note that the five factors chosen are not independent. In particular, CARBON, scaled from the annual NDVI integral, captures geographic variations in temperature and soil moisture, as well as variations in soil fertility. While it may be argued that annual N_2O production may be proportional to CARBON alone, we still need to obtain seasonal variations in the production.

There are many ways to combine the factors. Lacking any global information, we first assumed that all five controlling factors are of equal importance, i.e., the maximum fertility factor has the same effect as the maximum oxygen limitation factor as far as N_2O production is concerned. Hence, although FERT was scaled from 1 to 5 because of our inability to discriminate further, FERT was multiplied by two to normalize to the other factors. The effects of the five factors may not be equal and can be analyzed in sensitivity analyses.

We then modeled the nondimensional N_2O production every month as the geometric mean of all five controlling factors. We

chose a geometric mean rather than an arithmetic mean because a factor of zero, such as when temperature falls below 0°C, automatically shuts down N_2O production. Also, a low value for one of the factors would lower the N_2O production index. For example, values of 1 and 9 for two factors are given less weight than 5 and 5, which yield the same arithmetic mean.

The degrees of nitrification and denitrification are both governed by the water and oxygen supply in the soil, and the products of nitrification provide the substrate for denitrification. However, the processes themselves are carried out by different microbial populations and are, to a large extent, independent of each other. It is thus not correct to multiply the denitrification and nitrification indices OXYGEN and WATER. In their model of N_2O production in the Colorado grasslands amended with urine, Parton et al. (1988) summed the contribution of the two processes to obtain the total N_2O production. There, sufficient data allowed the relative contributions of the processes to be obtained as a constant in the regression equation between the model and the flux measurements. Parton et al. found that nitrification contributed 60–80% of the total flux. This is in sharp contrast to tropical soils where denitrification dominates (e.g., Matson and Vitousek, 1990). We do not have information on the relative importance of nitrification and denitrification for all ecosystems, nor do we have sufficient N_2O flux measurements to carry out a regression analysis similar to that of Parton et al. (1988). Thus, this version of the toy model cannot discriminate between N_2O produced via the different processes, and the product of OXYGEN and WATER can only be viewed as an index of the total production.

The monthly N_2O production index, PROD, is calculated as follows in the reference case:

$$\mathrm{PROD} = [\mathrm{OXYGEN} \times \mathrm{WATER} \times \mathrm{SOD} \times \mathrm{FERT}^* \times \mathrm{CARBON}]^{1/5}$$

where PROD, OXYGEN, WATER and SOD are indices calculated monthly; FERT* = 2 × FERT; and CARBON has a fixed value for all months.

Model Evaluation

The model was applied at each of the 1° × 1° grid boxes for the globe, to yield, every month, the global variation of N_2O production. A series of sensitivity experiments was carried out. Instead of the reference exponential temperature dependence (SOD1), the quadratic (SOD2) and linear (SOD3) curves were used separately. Other sensitivity experiments selectively excluded each of the controlling factors.

Our next step is to compare our modeled indices for N_2O production from the reference case and each of the sensitivity experiments

with fluxes directly measured in the field. With the comparison, we hope to establish that the geographic and seasonal variations in the nondimensional N_2O indices capture those found in the field. We carried out a literature survey of measurements of N_2O fluxes from natural systems. Only six different ecosystems (wetlands, temperate forests, steppes, tropical savannas, tropical dry forests, and tropical rain forests) are represented. Some of the measurements spanned less than a month.

Where measurement conditions corresponded with the vegetation/soil/climate conditions in the digital data bases used as inputs to our toy model, we compared the measured N_2O flux and the modeled PROD, both averaged over the period of the measurements. For measurement sites where discrepancies exist between field conditions and model inputs, we recomputed PROD using the conditions of the measurement sites.

By averaging the data and model results over the period of measurements, we hope to ameliorate the impact of the phase errors associated with using surface air rather than soil temperatures in our analysis. Small-scale variability may still confound the comparison between point measurements and model calculations at 1° resolution. Ideally, we would average measurements in the 1° grid box for comparison. This being impossible, we averaged the modeled indices over a few grid boxes adjacent to the measurement sites, in hopes that variability within a grid box is reflected in variability among several grid boxes. A total of 30 data points resulted for the comparison.

Of all the sensitivity experiments, the standard model as presented above yielded the highest correlation coefficient. This is shown in Figure 8 together with the best line fit to the data. A quadratic fit

$$y = 78.9 - 52.3x + 12.4x^2$$

was found to produce the highest $r^2 = 0.57$ between the model and observations. Here x represents the modeled monthly averaged index PROD, and y the monthly averaged N_2O flux measured (g N/ha/mo).

Figure 9 shows the global distribution of PROD, summed over a year. The highest N_2O production is found in the equatorial regions where both temperature and NDVI exhibit their maximum values. In the reference case, the equatorial regions (30°N–30°S) account for 80% of the global production. While midlatitude Chernozems and Kastanozems have the highest fertility, and permafrost regions have highest oxygen limitation, their inclusion only reduces the latitudinal gradient in N_2O production.

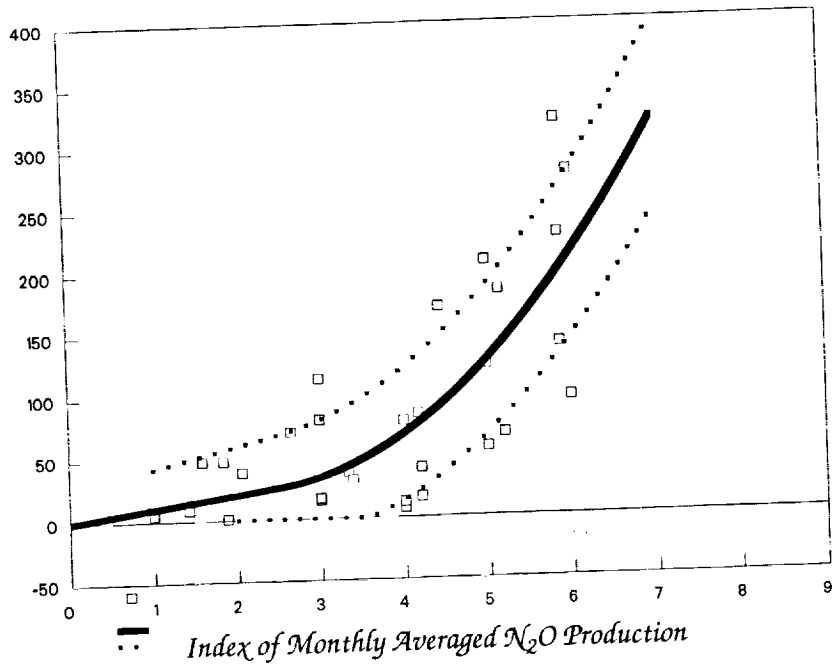

Figure 8. Comparison of PROD, the modeled N_2O index, with measured N_2O fluxes (boxes). The thick and dotted lines represent the best line fit ± 1 standard deviation.

Conclusion

The regression equation provides the transformation of the modeled nondimensional N_2O indices into dimensional N_2O fluxes. The global N_2O emission from natural soils obtained is 7 Tg N/yr (with a confidence interval of 3.1 to 13.4 Tg/yr). That our modeled estimate is within previous estimates for this source should be no surprise, as all extrapolation schemes are based on the same limited set of measurements of N_2O fluxes. Of the ~15,000 1° × 1° ice-free land cells, only 30 are represented with measurements. Thus the toy model, while more elaborate, does not provide a more accurate estimate of the global N_2O emission than other extrapolation schemes. However, the model and the sensitivity experiments do present a framework for analyzing how different controls affect N_2O production in different regions and for identifying the gaps in our understanding of N_2O emissions from natural soils, as well as a strategy for measurements.

A major implication of the toy model is that the tropics account for >80% of the global emission, within the range inferred by Prinn et al. (1990) from the atmospheric N_2O distribution. The large tropical source, in our model, is a result of the equal weighting given to

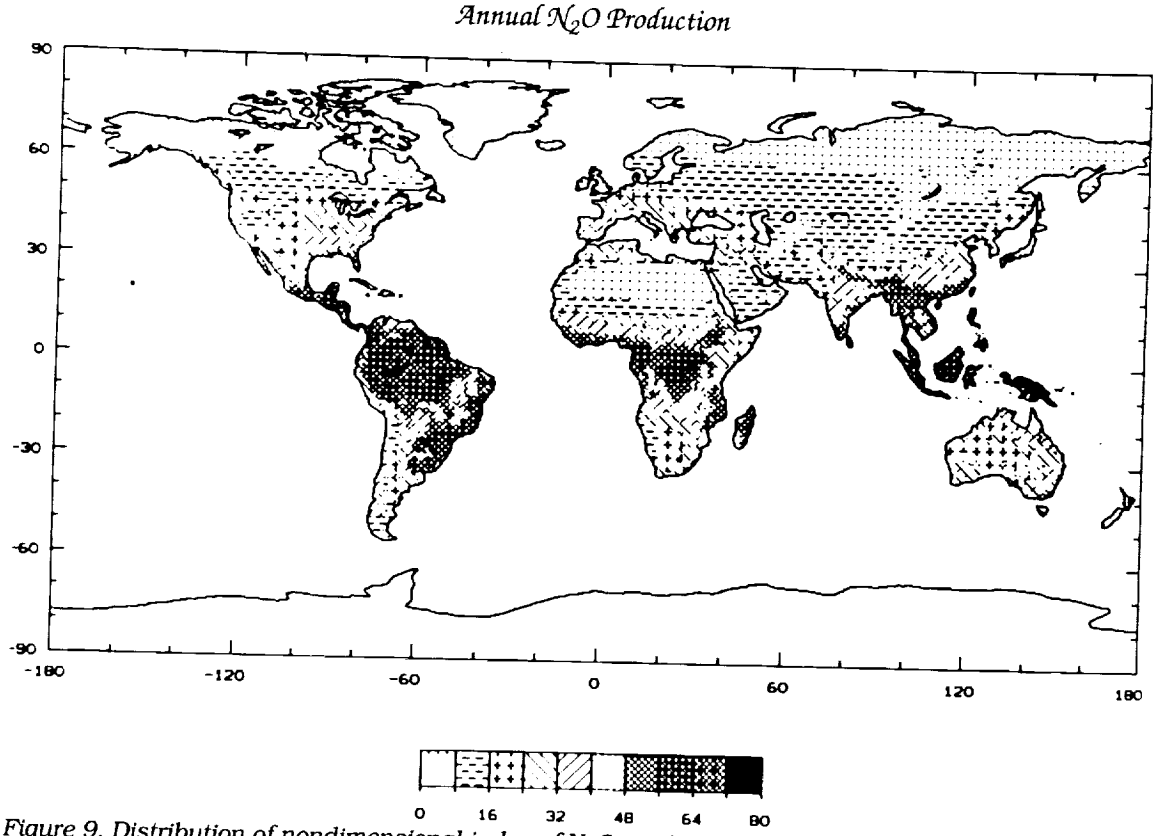

Figure 9. Distribution of nondimensional index of N_2O production, summed over the year.

the control factors. The latitudinal gradient in N_2O production is dominated by the controlling factors CARBON (carbon and nitrogen availability, proportional to NDVI) and SOD (decomposition rates, proportional to temperature). The two moisture indices for nitrification (WATER) and denitrification (OXYGEN) show no distinctive latitudinal gradients, while soil fertility peaks in the Chernozems and Kastenozems of midlatitudes. Whether the latitudinal gradient of N_2O production is as steep as that estimated by the toy model can be assessed by a detailed comparison and analysis of flux measurements from different locations.

We note Matson and Vitousek (1990) appear to have a significantly lower emission from the tropics than that estimated by the toy model. The difference may not be real, but may lie in the choices of areas or soil types included in the two calculations or in land use effects not included in this study. With the series of geographic data bases used in the toy model, it is straightforward to carry out parallel analyses so that the discrepancies can be evaluated and understood.

Improvement of the global estimate of N_2O emission from natural soils clearly requires more flux measurements. The toy model suggests that measurements should span at least a complete annual cycle, and should be carried out along several transects that cover different gradients in temperature, precipitation, soil texture and fertility, and vegetation productivity. It is also clear that complete site description, with soil, vegetation, and climatic data, is crucial for understanding the controls on N_2O production.

References

Bouwman, L., I. Fung, E. Matthews, and J. John. On the global distribution of N_2O emission from natural soils (in preparation).

Bowden, W.B. 1986. Gaseous nitrogen emissions from undisturbed terrestrial ecosystems: An assessment of their impacts on local and global nitrogen budgets. *Biogeochemistry 2*, 249–279.

Box, E.O., B.N. Holben, and V. Kalb. 1989. Accuracy of the AVHRR vegetation index as a predictor of biomass, primary productivity and net CO_2 flux. *Vegetatio 80*, 71–89.

Dickinson, R.E. 1984. Modeling evapotranspiration for three-dimensional global climate models. In *Climate Processes and Climate Sensitivity* (J.E. Hansen and T. Takahashi, eds.), Geophysical Monograph 29, American Geophysical Union, Washington, D.C., 58–72.

Dickinson, R.E., A. Henderson-Sellers, P.J. Kennedy, and M.F. Wilson. 1986. *Biosphere-Atmosphere Transfer Scheme (BATS) for the NCAR Community Climate Model.* Technical Note TN-275+STR, National Center for Atmospheric Research, Boulder, Colorado, 69 pp.

Elkins, J.W., T.M. Thompson, B.D. Hall, K.B. Egan, and J.H. Butler. NOAA/GMCC halocarbons and nitrous oxide measurements at the South Pole. *Antarctic Journal of the United States*, in press.

FAO-Unesco. 1971–1982. *Soil Map of the World*, 1:5000000, Vol. II-X, FAO, Rome, Italy.

FAO-Unesco. 1974. *Soil Map of the World*, Volume I, Legend. FAO, Rome, Italy.

FAO-Unesco. 1988. *Soil Map of the World. Revised Legend.* World Resources Report 60, FAO, Rome, Italy.

Firestone, M.K., and E.A. Davidson. 1989. Microbiological basis of NO and N_2O production and consumption in soil. In *Exchange of Trace Gases between Terrestrial Ecosystems and the Atmosphere* (M.O. Andreae and D.S. Schimel, eds.), John Wiley and Sons, Chichester, England, 7–21.

Fung, I.Y., C.J. Tucker, and K.C. Prentice. 1987. Application of Advanced Very High Resolution Radiometer Vegetation Index to study atmosphere-biosphere exchange of CO_2. *Journal of Geophysical Research 92*, 2999–3015.

Goward, S.N., C.J. Tucker, and D.G. Dye. 1986. North American vegetation patterns observed with the NOAA-7 advanced very high resolution radiometer. *Vegetatio 64*, 3–14.

Groffman, P.M., and J.M. Tiedje. 1988. Denitrification hysteresis during wetting and drying cycles in soil. *Soil Science Society of America Journal 52*, 1626–1629.

Hao, W.M., S.C. Wofsy, M.B. McElroy, J.M. Beer, and M.A. Toqan. 1987. Sources of atmospheric nitrous oxide from combustion. *Journal of Geophysical Research 92*, 13345–13372.

Houghton, J.T., G.J. Jenkins, and J.J. Ephraums (eds.). 1990. *Climate Change: The IPCC Scientific Assessment.* Intergovernmental Panel on Climate Change and Cambridge University Press, Cambridge, 329–341.

Klemedtsson, L., B.H. Svensson, and T. Rosswall. 1988. Relationships between soil moisture content and nitrous oxide production during nitrification and denitrification. *Biology and Fertility of Soils 6*, 106–111.

Manabe, S. 1969. Climate and ocean circulation. Part I: The atmospheric radiation and the hydrology of the earth's surface. *Monthly Weather Review 93*, 739–774.

Matson, P.A., and P.M. Vitousek. 1987. Cross-ecosystem comparisons of soil nitrogen and nitrous oxide flux in tropical ecosystems. *Global Biogeochemical Cycles 1*, 163–170.

Matson, P.A., and P.M. Vitousek. 1990. Ecosystem approach to a global nitrous oxide budget. *Bioscience 40*, 667–672.

Matthews, E. 1983. Global vegetation and land use: New high-resolution data bases for climate studies. *Journal of Climate and Applied Meteorology 22*, 474–487.

Mintz, Y., and Y. Serafini. 1981. *Global Fields of Soil Moisture and Land Surface Evapotranspiration.* Technical Memorandum 83907, Research Review 1980/81, NASA Goddard Flight Center, 178–180.

Mosier, A.R., and W.J. Parton. 1985. Denitrification in a shortgrass prairie: A modeling approach. In *Planetary Ecology* (D.E. Caldwell, J.A. Brierley, and C.L. Brierley, eds.), Van Nostrand Reinhold Co., New York, 441–451.

Muzio, L.J., and J.C. Kramlich. 1988. An artifact in the measurement of N_2O from combustion sources. *Geophysical Research Letters 15*, 1369–1372.

Parton, W.J., A.R. Mosier, and D.S. Schimel. 1988. Rates and pathways of nitrous oxide production in a shortgrass steppe. *Biogeochemistry 6*, 45–48.

Parton, W.J., D.S. Schimel, C.V. Cole, and D.S. Ojima. 1987. Analysis of factors controlling soil organic matter levels in Great Plains grasslands. *Soil Science Society of America Journal 51*, 1173–1179.

Prinn, R.G., D. Cunnold, R. Rasmussen, O. Simmonds, F. Alyea, A. Crawford, P. Fraser, and R. Rosen. 1990. Atmospheric trends and emissions of nitrous oxide deduced from ten years of ALE-GAGE data. *Journal of Geophysical Research 95*, 18369–18385.

Seiler, W., and R. Conrad. 1987. Contribution of tropical ecosystems to the global budgets of trace gases, especially CH_4, H_2, CO and N_2O. In *Geophysiology of Amazonia* (R.E. Dickinson, ed.), John Wiley & Sons, New York, 133–162.

Sellers, P.J., Y. Mintz, Y.C. Sud, and A. Dalcher. 1986. A simple biosphere model (SiB) for use within general circulation models. *Journal of the Atmospheric Sciences 43*, 505–531.

Shea, D.J. 1986. *Climatological Atlas 1950–1979: Surface Air Temperature, Precipitation, Sea-Level Pressure and Sea Surface Temperature (45°S–90°N)*. Technical Note NCAR/TN-269+STR, National Center for Atmospheric Research, Boulder, Colorado.

Tarpley, J.D., S.R. Schneider, and R.L. Money. 1984. Global vegetation indices from the NOAA-7 meteorological satellite. *Journal of Climate and Applied Meteorology 23*, 491–494.

Thornthwaite, C.W. 1948. An approach toward a rational classification of climate. *Geographical Review 38*, 55–74.

Zobler, L. 1986. *A World Soil File for Global Climate Modeling*. NASA Technical Memorandum 87802, NASA, New York, 32 pp.

A Bottom-Up Evolution of Terrestrial Ecosystem Modeling Theory, and Ideas toward Global Vegetation Modeling

Steven W. Running

Introduction

A primary purpose of this review is to convey the lessons I have learned in the development of our current forest ecosystem modeling approach, from its origins in 1973 as a single-tree water-balance model to our current regional applications. This is not an exhaustive literature review, but an opportunity for me to share past successes and failures, and ideas on future terrestrial modeling appropriate to earth systems modeling.

My interests in 1973 as a physiological ecologist were to use computer simulation to explore the system significance of the canopy transpiration measurements I was taking in the field, and to understand the importance of stomatal closure in maintaining a tree's water balance under the severely water-limited conditions of western forests. My introduction to mountain climatology in 1977, and remote sensing in 1982, has resulted in our present modeling logic that incorporates ecological, meteorological, and remote sensing theory and measurements into an integrated framework for calculating ecosystem process rates over large areas.

My second intent here is to use this accumulated bottom-up experience to offer ideas of how terrestrial ecosystem modeling can be taken to the global scale, earth systems modeling. I will suggest a logic where rather mechanistic ecosystem models are not themselves operated globally, but are used to "calibrate" much simplified models, primarily driven by remote sensing, that could be implemented in a semiautomated way globally, and in principle could interface with atmospheric general circulation models (GCMs).

At the outset, I acknowledge the leadership of R.E. Dickinson and P.J. Sellers in developing first-generation models of biospheric processes operated within the GCMs. To me, it is not an accident that physical scientists, not biologists, developed the first GCM-connected biospheric models. It seems that most biologists of my generation were trained from the beginning as reductionists, attempting to dissect and understand what they observed. The fundamental unit of biology is the individual organism, which automatically defines a very restricted spatial domain of interest, and makes global scaling rather untenable. Finally, much of classical biology was descriptive and revolved around taxonomy, the classification of species (which now total something like 100,000 vascular plants worldwide), and attention was focused on the unique characteristics defining each species. The search for common general principles of biological activity, for simple definition of structural and functional attributes of organisms, and for intraorganismal activity (i.e., ecosystem activity) has been a rather recent emphasis of "ecosystem analysis" or systems ecology, a branch of biology that still is in its infancy.

Current Problems of Global Biosphere Models

I believe that the GCMs with integrated biospheric models, such as the biosphere-atmosphere transfer scheme (BATS; Dickinson et al., 1986; Wilson et al., 1987) and the simple biosphere model (SiB; Sellers et al., 1986), are the best point of departure for future earth system models. I will not discuss some other biologically based global models, particularly the global carbon models (Emanuel et al., 1984), because they do not incorporate a direct interface with global atmospheric and hydrospheric models, which is essential. It seems to me that the core deficiencies of BATS and SiB are in two areas. First, the original BATS and SiB treated only energy, water, and momentum variables of the land surface because those are the core flux variables active in the GCMs, so their purpose was to provide surface boundary conditions for the climate models, not represent complete biospheric systems. Ideally a general earth system model will also want a rather sophisticated carbon cycle (including methane and nonmethane hydrocarbons, or NMHCs), nitrogen, phosphorus, sulfur, and possibly other elemental cycles. Additionally, some level of surface disturbance–biome replacement and succession must be treated.

Second, current GCMs define the landscape at a scale that is coarse (≈20,000 km^2) and rather static over time. The spatial coarseness means that a cell that actually incorporates a wide variety of biomes and mesoclimates is aggregated to a single defined

surface type and activity. It also stretches the measurement and modeling capabilities of ecology beyond the size that we have ever worked with before. Without seasonal dynamics in the GCM surface parameterizations linked to the climate simulations, the feedback ability for the surface biological responses to influence the atmosphere is lost, and the ability to realistically model events like the 1988 drought of North America is also lost.

Lessons from the Regional Ecosystem Simulation System

Defining Key Processes, Variables, and Classifications

To begin the evolution of "point-scale" ecological models to GCM scales, my colleagues and I have developed a Regional Ecosystem Simulation System (RESSys) over the last six years (Figure 1). RESSys has three core models, which use four additional core data sets. A topographic model from Band (1986) inputs digital elevation data and outputs effectively a terrain map. This provides a template for the definition of the rest of the system, which can be defined to differing levels of topographic complexity and spatial resolution. Hence, it allows us to zoom in on a small 10-km^2 watershed or pan out to a whole 10,000-km^2 region. A mountain climatological model uses this topographic file to extrapolate point-measured meteorological data across the region two-dimensionally for slope, aspect, and elevation. The output file of this model generates the input file of daily meteorological conditions, across the landscape for Forest-BGC (Forest Biogeochemical Cycle), the ecosystem process model. Forest-BGC then simulates the ecosystem processes of importance, which are then mapped back to the region on the topographic template. TOPMODEL then allows topographically defined hydrologic routing. A new project, HYBRID, is connecting the carbon balance of Forest-BGC with the population succession dynamics of a FORET-type model (Shugart, 1984) to give the most realistic forest stand simulator possible.

Agreement on the key processes required for a global terrestrial ecosystem model will be important when defining the essential classification logic for global partitioning. From the origins as a water balance model, Forest-BGC emphasizes canopy gas exchange processes and system water storages in snow and soil. Currently in RESSys we require definition of only leaf area index (LAI) and soil water holding capacity (SWC) of the landscape, with defaults for all other parameters. The Forest-BGC model was specifically designed to be sensitive to the parameterization of canopy processes by LAI and soil processes by SWC. These choices of one key vegetation and

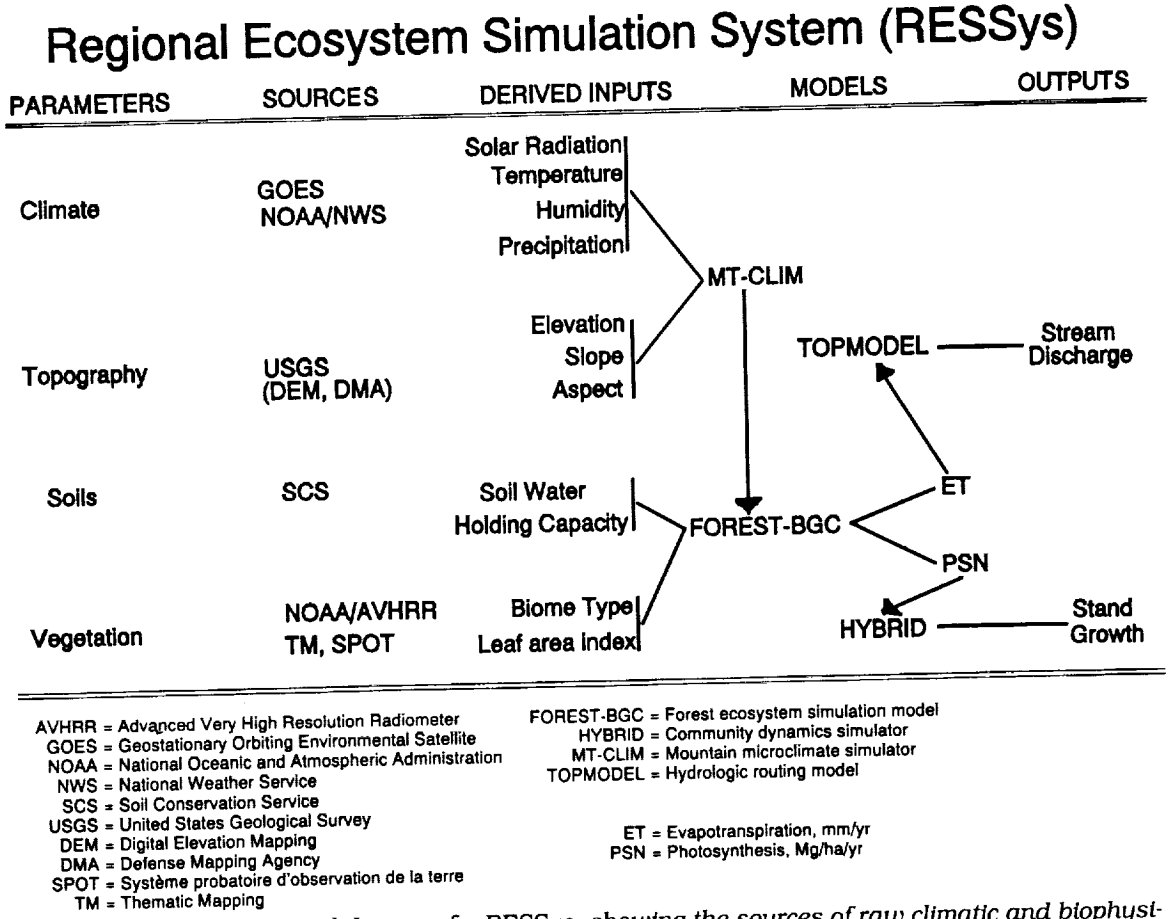

Figure 1. An organizational diagram for RESSys, showing the sources of raw climatic and biophysical data, the derived variables produced, and their incorporation into the topoclimate (MT-CLIM, Running et al., 1987) and ecosystem simulation (Forest-BGC, Running and Coughlan, 1988) models.

one edaphic variable then direct our landscape classification, which otherwise could have near-endless layers of variables (quite fashionable when showing off geographical information system, or GIS, capabilities). We have recently added total canopy nitrogen as a similar, simplifying definition of forest nutrient status.

The other control on landscape definition is the topographically induced microclimate variability. Sensitivity of the ecosystem model to climate then helps to define what resolution of elevational and topographic detail need be defined. For example, we have found temperature resolution of ± 1°C and precipitation of ± 2mm to be adequate for driving the ecosystem model.

In simplifying earlier ecosystem models, I eliminated a number of seemingly important details. No internal physiology is represented (of cellular water stress, phloem carbohydrate transport, etc.). No canopy

structure, leaf age class, or leaf angular distribution is defined, only simple LAI. No below-ground details of rooting processes, root water, or nutrient uptake capacity are explicitly defined. Some of these variables are virtually unmeasurable in the field even for small intensive study sites; how would we estimate them at regional or global scales? What we really want is to relate below-ground activity to canopy responses that can be more directly measured.

The following processes are calculated by Forest-BGC:

- Hydrologic:
  precipitation, snow vs. rain partitioning
  snowmelt
  canopy/litter interception and evaporation
  surface runoff vs. soil storage
  transpiration physiological water stress and surface resistance
  subsurface outflow
- Carbon:
  photosynthesis
  maintenance respiration
  growth respiration
  carbon allocation (leaf/stem/root)
  net primary production
  litterfall decomposition (trace gas emissions, CH_4, NMHC)
- Nitrogen:
  mineralization
  allocation (leaf/stem/root/available)

Although the resulting model, neglecting many ecosystem attributes and relating most key variables to LAI and climate, will seem oversimplified to many ecologists, it provides the only means we see to bring ecosystem modeling to regional scales.

I emphasize that an optimal global vegetation classification scheme cannot be devised until a modeling logic has been defined, so that the classification can be based on the variables, such as LAI in our case, that the model has been designed to be particularly sensitive to.

Spatial Scale Definition

GCMs define the land surface in only a spatially coarse (cells of ≈20,000 km^2) and static way. Each cell is defined initially as a single vegetation type, and no dynamic interaction occurs between the resulting climate and surface vegetation definition, a limitation that is particularly unfortunate for long time simulations of 10–100 years. We have found in RESSys development that the limiting fac-

tor is *not* the accuracy of our "point" models, but the accuracy with which we can define key parameters across the landscape. First, one must decide upon the key variables, such as LAI; then one must devise ways to map them across the region. A breakthrough in our regional logic was the demonstration that LAI could be defined by satellite (Peterson et al., 1987).

By far our greatest difficulty in landscape definition has been in soils data. The soil reservoirs of water, carbon, and nitrogen are significant components of the ecosystem cycles, and have fundamentally different (usually 10–100 times slower) time constants than canopy processes. Historically, soil science has emphasized the taxonomic classification of soils into a system that *qualitatively* defines the temperature and moisture conditions of soil development. However, standard soils maps, such as those of the U.S. Soil Conservation Service, do not define soil physical structure, depth, water potential release curves, or chemistry *quantitatively*. At global scales the problem of nonquantitative, spatially coarse soils data is even more acute. We are working on a hydrologic equilibrium theory that integrates climate, LAI, and soil water holding capacity, and allows one to infer the soil characteristics from observable climate and maximum LAI (Nemani and Running, 1989a). For global-scale work, we suspect some type of similar logic will be necessary.

Time Scale Definition

The ecosystem process model Forest-BGC has a dual time resolution. Key hydrologic processes (e.g., interception and evapotranspiration), and carbon process variables (e.g., photosynthesis and maintenance respiration) are calculated daily. The carbon allocation to biomass is calculated annually, as are the litterfall, decomposition, and nitrogen budget processes. We found the dual time step essential for adequately and efficiently simulating these ecosystem processes. The hydrologic partitioning of precipitation into instantaneous interception and evaporation vs. longer-term snow or soil water storage and transpiration or hydrologic outflow proved to be the key process that demands daily timing. Accurate hydrologic partitioning is essential in arid areas for simulating seasonal soil drought and plant water stress, and is essential for producing correct timing on stream discharge hydrographs. In areas of frequent showers, even higher time resolution is useful. However, we have compromised on a daily time step for our models after many years of modeling at hourly time steps (see Knight et al., 1985). Because, on average, diurnal climatology is very predictable, we found that going from hourly to daily meteorological drivers cut the climate files to 1/24 size, yet we could simulate the diurnal conditions well enough

to predict seasonal canopy process rates from a daily model to within 3% of the hourly simulations (Running, 1984). However, given that GCMs require high time resolution, nothing precludes our ecosystem model from matching their time step except computational load.

The carbon growth and decomposition processes and the nitrogen budgets do not require daily time scales. In temperate evergreen ecosystems, yearly calculations match the timing of field measurements, making initial model development and validation convenient. In more seasonal biomes, such as grasslands, the carbon/nitrogen computations need to be done monthly or even weekly to describe certain processes.

The commonly stated principle relating small space to short time resolution and progressively larger spatial scale to longer time resolution makes a nice graph, but has many exceptions. GCMs define a huge spatial scale at a very fine temporal scale, on the order of 12–30 minutes. For atmospheric dynamics, this is an appropriate space-time definition for the processes being represented. Likewise in ecology, events that are large in spatial scale can occur in a very short time. Ecosystem processes that are driven by meteorological conditions, notably the canopy gas exchange processes, are just as dynamic temporally as climate is. A critical problem of ecological representation, though, is that while a canopy process such as photosynthesis occurs over a large region, the absolute control is still exerted within the physiology of the individual organism. However, this does not argue that we then must represent those individual organisms explicitly.

Many important ecosystem processes are triggered by episodic extreme events. Major freezes can alter regional vegetation cover and activity in one night, and the vegetation may take years to recover. The meteorological conditions that triggered the Yellowstone fires of 1988 were of a short time scale, yet the results will be felt for a century. Both our ecosystem models and our climate models tend to be central tendency simulators, representing mean conditions and mean responses and missing important extreme events.

Standardized Meteorological Data

Ecological modeling has typically been developed around intensive study sites, where a central meteorological station was a first priority. Because one cannot install custom meteorological stations everywhere, the logic of using a routine weather data base with extrapolations was necessary for RESSys. It became clear that daily meteorological data were routinely available from standard sources like the U.S. National Weather Service or the World Meteorological Organization, but hourly, weekly, or any other time were not. Use of

standard available meteorological data became a critical design criterion for RESSys, even if the data were not exactly what was wanted. Part of the purpose of the mountain climate (MT-CLIM; Running et al., 1987) simulator was to calculate humidity and insolation from the daily maximum-minimum temperature and precipitation records that are the standard "weather" data recorded at the greatest number of stations. Humidity and radiation data are available from only about 5% of the reporting weather stations in the U.S.

An alternative to this point meteorological data might be satellite observations that have an areal average of around 100 km^2. We did not find satellite surface meteorology routinely available, and surface conditions are often obscured by clouds. Areally averaged data would also invert our problem from extrapolation of point data to interpolation of areal averages, problems that both require similar climatology. It should be noted that our mountain climatology out of necessity ignored wind speed and direction, both because of the unpredictability and because forest canopies tend to have high inherent aerodynamic mixing, so exchange processes are not very sensitive to wind. Secondly, our mountain climatology ignores nocturnal, topographically induced cold air drainage.

It appears that the next step of coupling dynamic meteorology to regional-scale ecology should be pursued with mesoscale models run embedded in a GCM (Dickinson et al., 1989). Mesoscale models such as the National Center for Atmospheric Research's MM4 have a spatial resolution much more compatible with RESSys, and variable vegetation dynamics produce important feedbacks to local meteorology (Segal et al., 1988).

Regional Measurements and Validations

For many years the only "ecological" data that could be directly measured at regional scales were occasional land cover classifications from Landsat. Because of the expense and computer requirements needed, these regional maps were produced as one-time static products, much like vegetation maps in atlases. The development of the advanced very high resolution radiometer/normalized difference vegetation index (AVHRR/NDVI) products, produced weekly, began to add some temporal dynamics to our regional view of ecosystems. The observable continental-scale dynamics were dramatic, following the seasonal "green wave" northward in the spring and then back south in the fall (Justice et al., 1985; Goward et al., 1985, 1987). However, the NDVI was still one long step removed from the ecosystem process rates of greatest interest: carbon, water, and nutrient cycling by the surface. More recently, our first- generation RESSys products (Running et al., 1989) have developed the

computational ability to calculate these process rates over progressively larger areas.

We are now finding that there is no established methodology for *validating* these regional ecosystem process maps, particularly from the classical field measurements that ecologists consider "hard" validation. The point samples of 0.1 ha that field ecologists have worked on only represent 0.00001% of the land area of a single GCM cell, and rules for extrapolation are casual. Only remote sensing, a tool foreign to most ecologists, has the capability for repetitive, standardized measurements of regional-scale processes. Yet, with remote sensing we are back to observing optical phenomena, such as the NDVI.

One notable exception is some of the global-scale atmospheric CO_2 concentration analyses (Houghton, 1987; Tans et al., 1990; Fung et al., 1987). These CO_2 data coupled with the seasonal NDVI satellite data are the closest thing to observing a global biospheric "heartbeat" I have yet seen. At a smaller scale, the CO_2 flux measurements taken from aircraft (Wofsy et al., 1988) or micrometeorological tower systems (Baldocchi, 1989) over multiple kilometer scales, if done repetitively, could provide an integrated regional measure of carbon cycle activity. The one other regional-scale data base we have for interpreting ecosystem processes is the hydrologic discharge and balances of gauged watersheds, providing a large spatial measurement of a key ecosystem variable, water cycling. Both these CO_2 and water balance data may provide an integrated spatial measurement for validation, but only at restricted, rather long monthly to yearly time scales. The aircraft and tower flux measurements are the only regional calculations that could provide daily validations.

Another potential source of validation for carbon cycle simulations is the variety of crop yield, forest growth, range forage production, etc., standard measurements taken by land management agencies. These again are point samples and not the exact variables needed, but are a huge network of data that could be used for validation of regional primary production simulations.

Applying Ecosystem Modeling Globally

We currently cannot envision taking RESSys-level mechanistic process modeling to the global scale. Alternatively, we see that these ecosystem process models could be used to "calibrate" highly simplified global models in a variety of different biome/climate situations. Many of the following ideas are incorporated in our research plan for the Moderate Resolution Imaging Spectrometer (MODIS), an instrument in the Earth Observing System (EOS) program of the National Aeronautics and Space Administration. EOS is the observational cor-

nerstone of the U.S. Global Change Research Program, and MODIS is the sensor planned for regular global land surface monitoring.

The best current candidate for this global modeling logic is the NDVI, time integrated through the year (annual ΣNDVI). Due to the fact that the NDVI integrates both surface characteristics (vegetation greenness, soil, and LAI) and key meteorological factors such as solar intensity to the surface, the ΣNDVI provides a simple yet surprisingly versatile global measure (Tucker et al., 1985). We tested the correlation between seasonal NDVI and ecosystem process rates for seven locations around North America (Running and Nemani, 1988). For continental-scale dynamics, we found amazingly good correlations between annual ΣNDVI and seasonal photosynthesis, transpiration, and net primary production (r^2 = 0.72–0.87; see Figure 2a). Even weekly ecosystem activity was fairly well described by the seasonal NDVI trace. However, we also found that the NDVI does not change in evergreen forests that are drought or temperature stressed, indicating that the NDVI alone may be able to define structure, but only fortuitously correlates with canopy function (Figure 2b).

We have also found the NDVI to correlate well against LAI of natural forests across Montana (Figure 3a). To provide some satellite-based definition of canopy stress, we combined in a ratio the NDVI and surface temperature, producing an algorithm that represents the partitioning of absorbed solar energy into sensible and latent heat, or Bowen ratio, and mimicking a surface resistance quite well (Figure 3b).

While details of these ideas are available in the references, the general conclusion we have drawn is that the time-integrated NDVI can be a very robust global measure of vegetation activity, if calibrated well to varying conditions and biomes. We are planning to do precisely that for our ten-year MODIS project, as summarized on Figures 4 and 5. We plan to first define a very limited number of biome types based on very simplified structural and functional characteristics. The global vegetation would then be preclassified by these characteristics, illustrating why we feel the model logic must come before the classification scheme. Next we will build a mechanistic ecosystem process model for each of these biomes, designated collectively BIOME-BGC (Running and Hunt, in press), which then would be used to calibrate the simple global NDVI, biome-specific conversion factors, and surface temperature data. After the launch of EOS, this global simulation of biome processes would be done weekly from MODIS data.

Because a prototype of this logic is already fairly complete for western coniferous forests, we feel reasonably confident in this overall idea. However, at this point not all ecosystem processes have

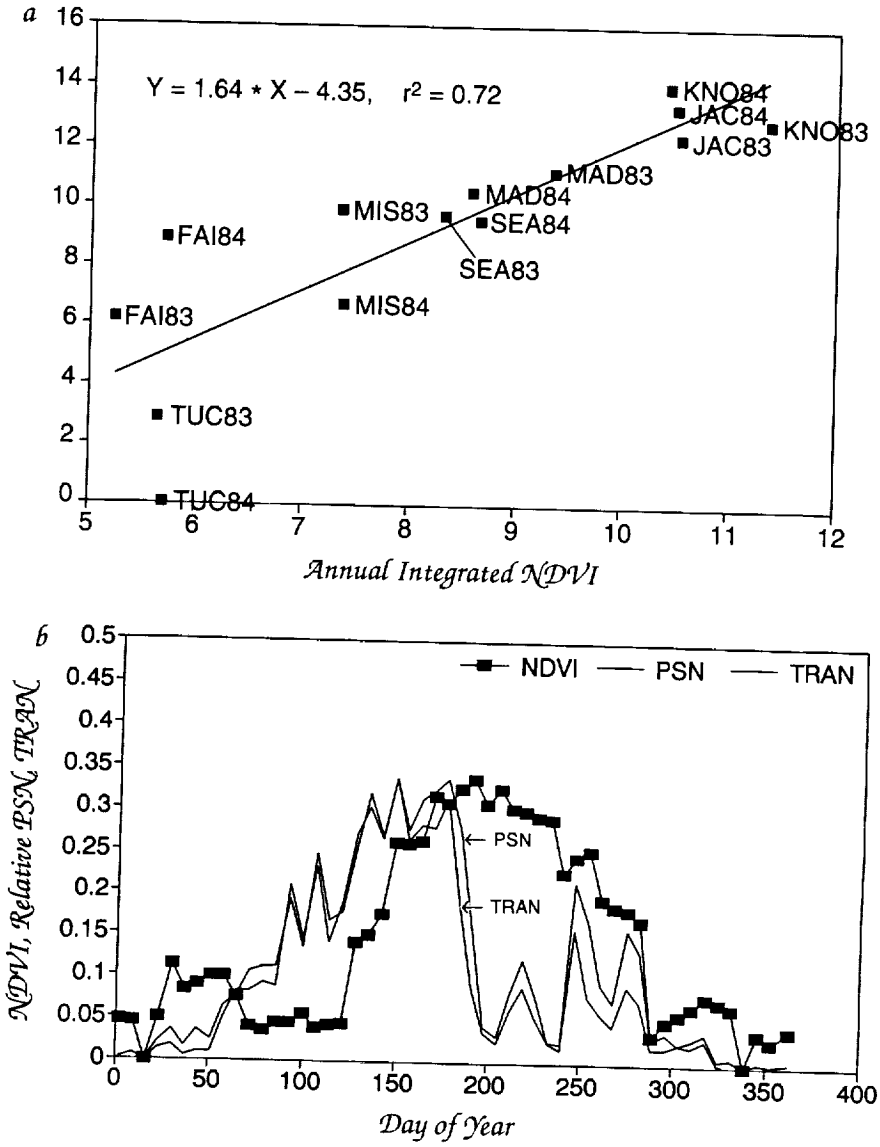

Figure 2. (a) The correlation found between the annual time-integrated NDVI and annual net primary production (NPP) simulated for forests from seven contrasting sites around North America in 1983 and 1984. The sites are Fairbanks, Alaska (FAI); Jacksonville, Florida (JAC); Knoxville, Tennessee (KNO); Madison, Wisconsin (MAD); Missoula, Montana (MIS); Seattle, Washington (SEA); and Tucson, Arizona (TUC). (b) The seasonal trend of weekly composited NDVI compared to scaled weekly photosynthesis (PSN) and transpiration (TRAN) simulated for a cold, dry climate conifer forest in 1984. The absolute units are PSN = 1.78 MG C/ha/week/NDVI and TRAN = 48.1 mm/ha/week/NDVI (reprinted by permission of the publisher from Running and Nemani, 1988; ©1988 by Elsevier Science Publishing Co., Inc.).

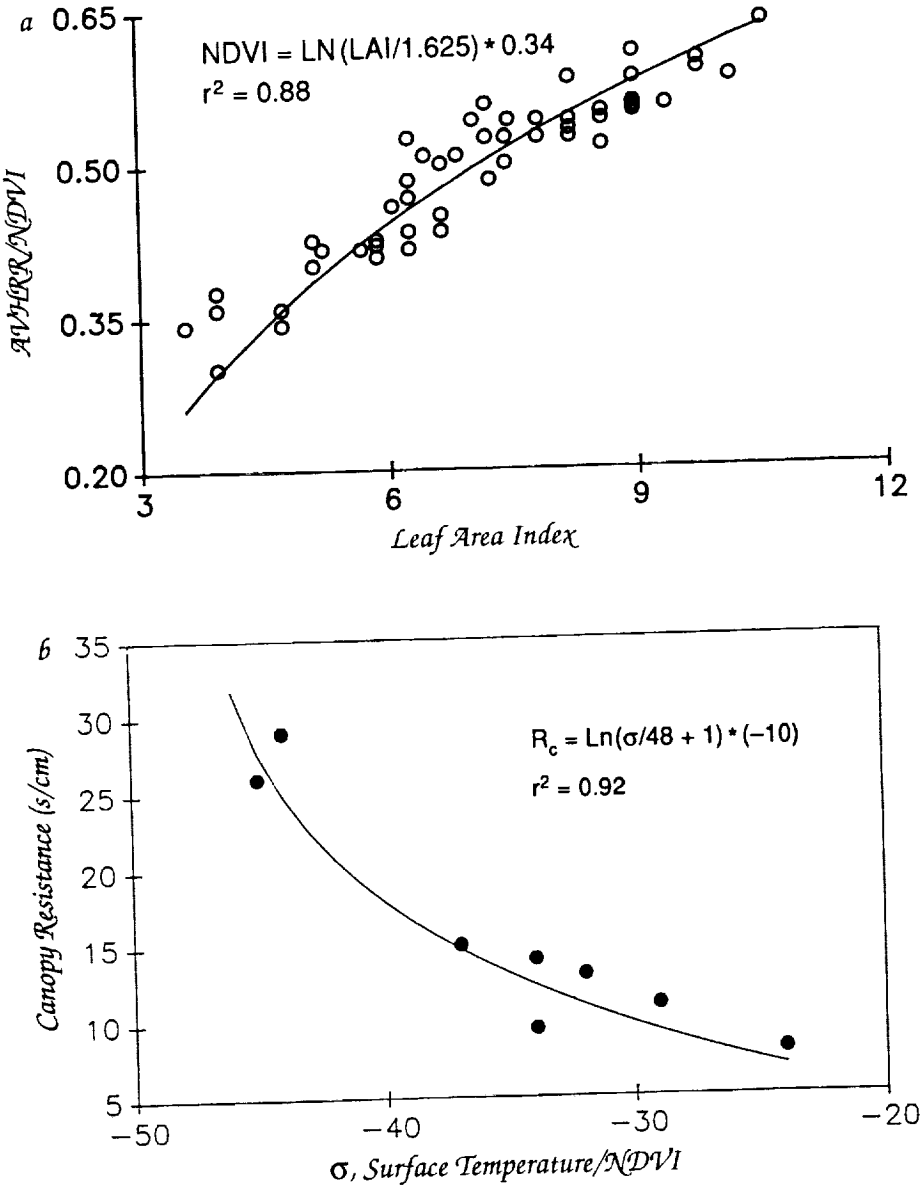

Figure 3. (a) The relationship between AVHRR/NDVI for September 25, 1985, and an estimated LAI for 53 mature conifer forest stands across Montana (Nemani and Running, 1989a). (b) The relationship between simulated canopy resistance (R_c; from Forest-BGC) and the slope of the surface temperature/NDVI, σ, for eight days during the summer of 1985, for a 20 x 25 km forested area of Montana. We hypothesize that this σ factor approximates a Bowen ratio of latent/sensible heat partitioning at a regional scale (Nemani and Running, 1989b).

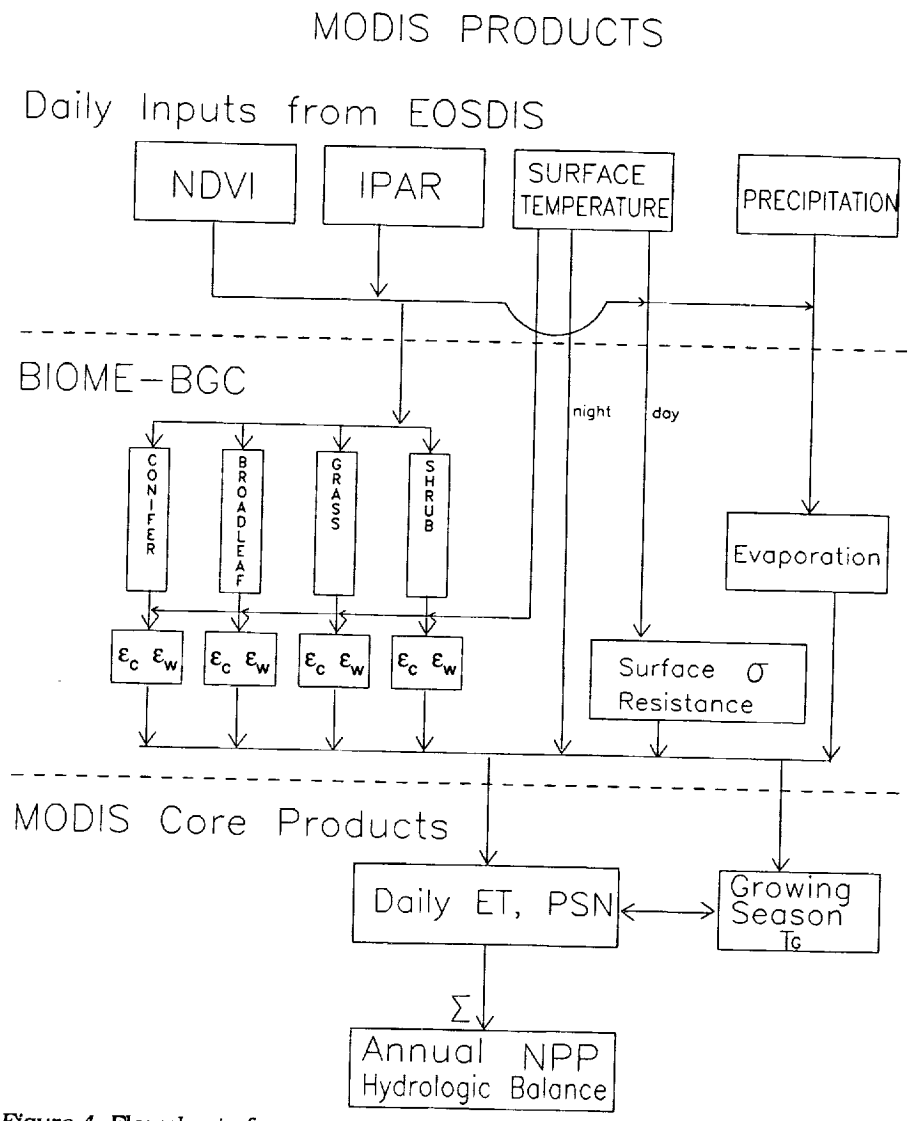

Figure 4. Flowchart of representative biome types we are defining, the input data required for simulating ecosystem processes at local to regional scales, and the output variables required for MODIS algorithm development.

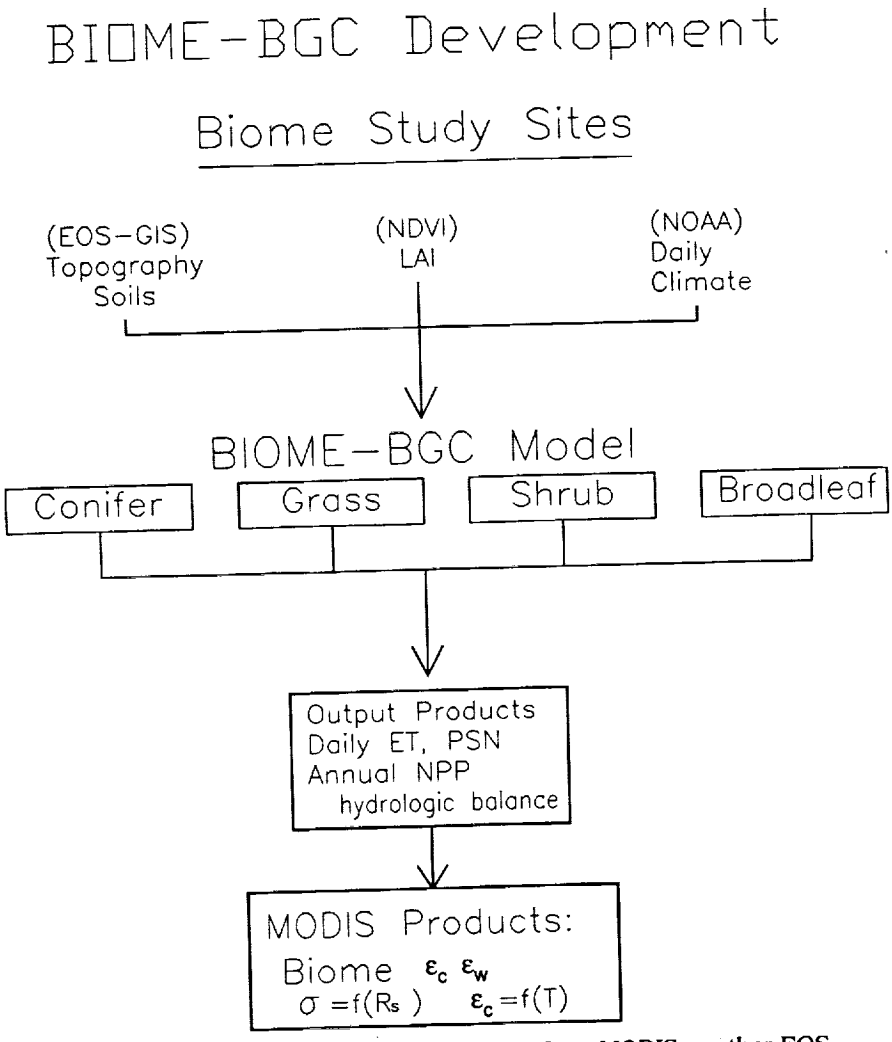

Figure 5. Flowchart of the global-scale inputs from MODIS or other EOS sources, the computational organization, and our planned outputs of MODIS-derived ecosystem process simulations to be executed globally by 1998 as part of EOS.

been tested against NDVI. For example, some of the trace gas and nutrient fluxes may not be correlated with NDVI, which logically can be expected to represent canopy processes best. Hydrologic balances leading to river discharge, ocean coupling, etc., would not be represented here. So, we offer this not as a complete global terrestrial model, but as a dynamic global vegetation model that we know is attainable with current technology.

Connection of this modeling to a GCM would require at minimum a weekly redefinition of the surface characteristics of the GCM cells, which in principle should not be difficult. A more dynamic coupling that would allow real-time system feedbacks might require the NDVI model to be run within the atmospheric model so daily fluxes would enter the atmosphere, and responses would influence the vegetation. Then important responses like continental biome shifts resulting from climate change could be explicitly simulated. However, it is difficult to combine real-time global NDVI measurements interfaced to an internally self-sufficient simulation, unless for retrospective testing.

Conclusions

The following issues emerge as important considerations as we further develop earth system models:

- Global land classification logic must be developed in concert with the global modeling. We have found climate, LAI, and soil water capacity to be most fundamental for regional ecosystem definition.
- Vegetation must be defined simply and generically; basic biome types plus LAI seem best from our experience. This definition must then pervade the logic of the biome models.
- In the absence of a GCM with calculated surface meteorology, regional terrestrial models must be designed around a routinely available meteorological data base, which will undoubtedly require both climatological enhancement to fill in missing variables and spatial extrapolation/interpolation to produce a continuous representation of the landscape at scales equivalent to the terrestrial model.
- Any meaningful definition of the physical/chemical nature of the global soils will be a problem.
- Full mechanistic models of biome processes are probably not possible globally, especially at the higher spatial resolution we desire, so the biome models can be used to calibrate simple satellite-driven vegetation models such as weekly ΣNDVI that would then be surface drivers for the GCMs.

Acknowledgments

The "we" referred to frequently in this paper are David L. Peterson, NASA Ames Research Center; Larry Band, University of Toronto; and Ramakrishna Nemani, former Ph.D. student now at University of Toronto. More recent additions to this team include Joseph Coughlan, E. Raymond Hunt, and Lars Pierce, University of Montana. Funding has been provided primarily from NASA, grants NAGW-252 and NAS5-30920, and NSF grant BSR-8817965.

References

Baldocchi, D.D. 1989. Turbulent transfer in a deciduous forest. *Tree Physiology 5*, 357–377.

Band, L.E. 1986. Topographic partitioning of watersheds with digital elevation models. *Water Resources Research 22*, 15–24.

Dickinson, R.E., A. Henderson–Sellers, P.J. Kennedy, and M.F. Wilson. 1986. *Biosphere-Atmosphere Transfer Scheme for the NCAR Community Climate Model.* Technical Note NCAR/TN–275+STR, NCAR, Boulder, Colorado, 69 pp.

Dickinson, R.E., R.M. Errico, F. Giorgi, and G.T. Bates. 1989. A regional climate model for the western United States. *Climatic Change 15*, 383–422.

Emanuel, W.R., G.G. Killough, W.M. Post, and H.H. Shugart. 1984. Modeling terrestrial ecosystems in the global carbon cycle with shifts in carbon storage capacity by land–use change. *Ecology 65*, 970–983.

Fung, I., C.J. Tucker, and K.C. Prentice. 1987. Application of Advanced Very High Resolution Radiometer Vegetation Index to study atmosphere-biosphere exchange of CO_2. *Journal of Geophysical Research 92*, 2999–3015.

Goward, S.N., C.J. Tucker, and D.G. Dye. 1985. North American vegetation patterns observed with the NOAA-7 advanced very high resolution radiometer. *Vegetatio 64*, 3–14.

Goward, S.N., A. Kerber, D.G. Dye, and V. Kalb. 1987. Comparison of North and South American biomes from AVHRR observations. *Geocarto 2*, 27–40.

Houghton, R.A. 1987. Biotic changes consistent with the increased seasonal amplitude of atmospheric CO_2 concentrations. *Journal of Geophysical Research 92*, 4223–4230.

Justice, C., J. Townshend, B. Holben, and C. Tucker. 1985. Analysis of the phenology of global vegetation using meteorological satellite data. *International Journal of Remote Sensing 6*, 1271–1318.

Knight, D.H., T.J. Fahey, S.W. Running. 1985. Factors affecting water and nutrient outflow from lodgepole pine forests in Wyoming. *Ecological Monographs 55*, 29–48.

Nemani, R., and S.W. Running. 1989a. Testing a theoretical climate-soil-leaf area hydrologic equilibrium of forests using satellite data and ecosystem simulation. *Agricultural and Forest Meteorology 44*, 245–260.

Nemani, R., and S.W. Running. 1989b. Estimating regional surface resistance to evapotranspiration from NDVI and Thermal-IR AVHRR data. *Journal of Climate and Applied Meteorology 28*, 276–294.

Peterson, D.L., M.A. Spanner, S.W. Running, and K.B. Teuber. 1987. Relationship of Thematic Mapper Simulator data to leaf area index of temperate coniferous forests. *Remote Sensing of the Environment 22*, 323–341.

Running, S.W. 1984. Microclimate control of forest productivity: Analysis by computer simulation of annual photosynthesis/transpiration balance in different environments. *Agricultural and Forest Meteorology 32*, 267–288.

Running, S.W., and J.C. Coughlan. 1988. A general model of forest ecosystem processes for regional applications. I. Hydrologic balance, canopy gas exchange and primary production processes. *Ecological Modeling 42*, 125–154.

Running, S.W., and E.R. Hunt, Jr. Generalization of a forest ecosystem process model for other biomes, BIOME-BGC, and an application for global-scale models. In *Scaling Processes Between Leaf and Landscape Levels* (J.R. Ehleringer, and C. Field, eds.), Springer-Verlag, New York, in press.

Running, S.W, and R.R. Nemani. 1988. Relating seasonal patterns of the AVHRR vegetation index to simulated photosynthesis and transpiration of forests in different climates. *Remote Sensing of the Environment 24*, 347–367.

Running, S.W., R.R. Nemani, and R.D. Hungerford. 1987. Extrapolation of synoptic meteorological data in mountainous terrain, and its use for simulating forest evapotranspiration and photo- synthesis. *Canadian Journal of Forest Research 17*, 472–483.

Running, S.W., R.R. Nemani, D.L. Peterson, L.E. Band, D.F. Potts, L.L. Pierce, and M.A. Spanner. 1989. Mapping regional forest evapotranspiration and photosynthesis by coupling satellite data with ecosystem simulation. *Ecology 70*, 1090–1101.

Segal, M., R. Avissar, M.C. McCumber, and R.A. Pielke. 1988. Evaluation of vegetation effects on the generation and modification of mesoscale circulations. *Journal of the Atmospheric Sciences 45*, 2268–2292.

C-4.

Sellers, P.J., Y. Mintz, Y.C. Sud, and A. Dalcher. 1986. A simple biosphere model (SiB) for use within general circulation models. *Journal of the Atmospheric Sciences 43*, 505–531.

Shugart, H.H. 1984. *A Theory of Forest Dynamics*. Springer-Verlag, New York, 278 pp.

Tans, P.P., I.Y. Fung, and T. Takahashi. 1990. Observational constraints on the global atmospheric CO_2 budget. *Science 247*, 1431–1438.

Tucker, C.J., J.R.G. Townshend, and T.E. Goff. 1985. African land cover classification using satellite data. *Science 227*, 369–374.

Wilson, M.F., A. Henderson-Sellers, and R.E. Dickinson. 1987. Sensitivity of Biosphere-Atmosphere-Transfer-Scheme (BATS) to the inclusion of variable soil characteristics. *Journal of Climate and Applied Meteorology 26*, 341–363.

Wofsy, S.C., R.C. Harriss, and W.A. Kaplan. 1988. Carbon dioxide in the atmosphere over the Amazon Basin. *Journal of Geophysical Research 93*, 1377–1388.

Development of Simplified Ecosystem Models for Applications in Earth System Studies: The Century Experience

William J. Parton, Dennis S. Ojima, David S. Schimel, and Timothy G. F. Kittel

Introduction

During the past decade, a growing need to conduct regional assessments of long-term trends of ecosystem behavior and the technology to meet this need have converged. The Century model is the product of research efforts initially intended to develop a general model of plant-soil ecosystem dynamics for the North American Central Grasslands (Parton et al., 1983, 1987, 1988). This model is now being used to simulate plant production, nutrient cycling, and soil organic matter dynamics for grassland, crop, forest, and shrub ecosystems in various regions of the world, including temperate and tropical ecosystems (Parton et al., 1987; Sanford et al., 1991). This paper will focus on the philosophical approach used to develop the structure of Century. The steps included were model simplification, parameterization, and testing. In addition, we will discuss the importance of acquiring regional data bases for model testing and the present regional applications of Century in the Great Plains, which focus on regional ecosystem dynamics and the effect of altering environmental conditions.

The overall objective of this modeling activity was to develop a generalized ecosystem model that could simulate long-term (50 to 1000 years) changes in plant production, nutrient cycling, and organic matter caused by different management practices under actual or altered climatic conditions. The original goal was to simulate long-term trends of ecosystem processes and components over a large region. However, in recent years we have refined the model in order to simulate year-to-year variability of annual plant production and the seasonal dynamics of plant biomass.

To achieve the overall objective, it was necessary that the input variables be readily available and constitute a minimally sufficient data set to drive ecosystem processes. Given these conditions, the input variables that drive Century are monthly precipitation, average monthly daily maximum and minimum air temperature, soil texture, plant nutrient and lignin content, N inputs, and land management. The model was developed with these input variables specifically in mind, relative to temporal resolution; therefore, parameterizations of processes were made to accommodate these inputs. By achieving these conditions, the model lends itself to regional simulations including a large number of sites and has the potential to be linked to atmospheric mesoscale circulation and general circulation models (GCMs).

The Century model has been used extensively to simulate regional ecosystem dynamics for natural grassland (Parton et al., 1989; Burke et al., 1990) and agroecosystems (Cole et al., 1989) in the North American Central Grassland. The model simulates the spatial variability in the storage and fluxes of C and N within these systems and has recently been used to simulate the response of grasslands to potential climatic change scenarios (Schimel et al., 1990). In this paper we will describe the hierarchical approach used to simulate regional ecosystem dynamics and suggest how this type of model can be linked directly to GCMs.

Philosophical Approach

The philosophy used in developing Century was to use a minimal approach, that is, to use the simplest formulations of essential ecosystem processes. Thus, the model quantifies hypotheses based on our current understanding of these essential processes, which can then be objectively tested against observed data. We used those formulations of biological processes appropriate for the model time step (i.e., monthly) and input driving variables (monthly temperature and precipitation).

Model Description

Century is a general model for plant-soil ecosystems (Figure 1) and has been used to represent grasslands, forests, croplands, and shrublands. The grassland, crop, and forest systems have different plant production submodels that are linked to a common soil organic matter (SOM) submodel. The simplified flow diagram for the model shows that soil organic matter is separated into three fractions (active, slow, and passive) and that plant residue (dead shoots and roots) is split into structural and metabolic components. The

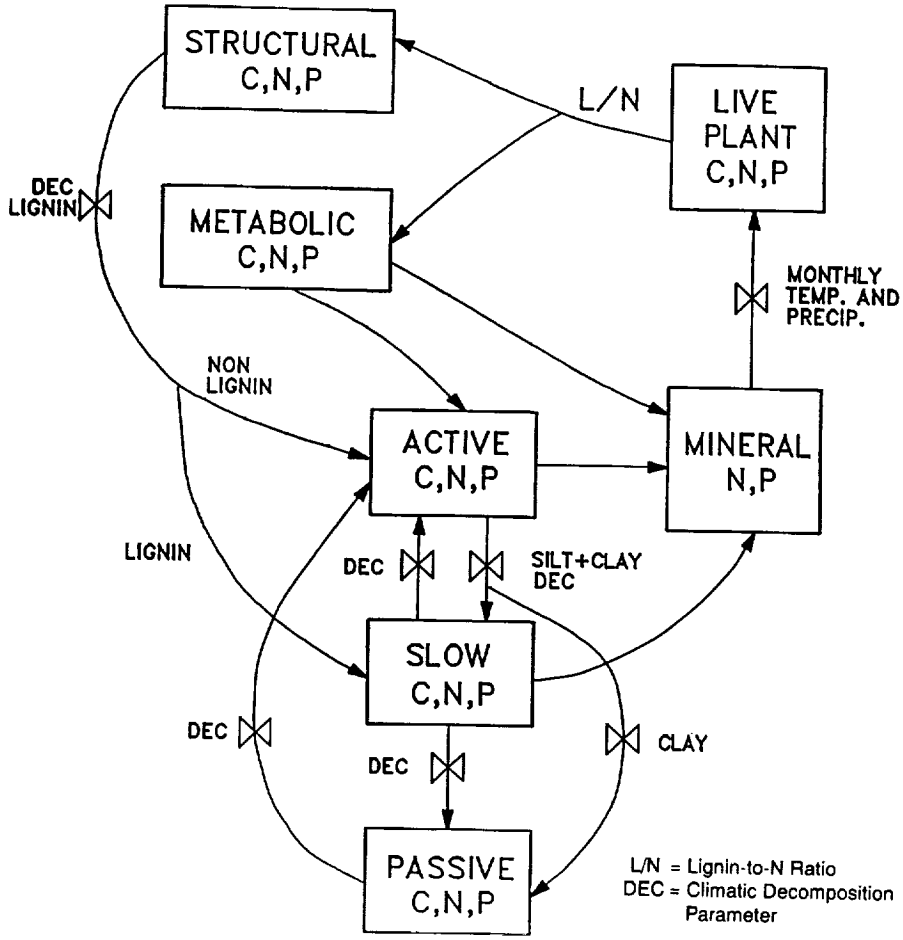

Figure 1. Flow diagram for the Century model.

turnover time of the SOM pools varies according to a soil abiotic decomposition parameter that is a function of monthly precipitation and temperature. Typical values for a temperate grassland site are 2, 20, and 1000 years, respectively, for active, slow, and passive SOM pools. Inputs of C to the soil are derived from plant residue (i.e., dead shoots and roots). The division of residue into structural (slow decomposition) and metabolic (fast decomposition) components is a function of the lignin-to-nitrogen (L:N) ratio of the material (i.e., a higher L:N ratio results in a greater partitioning of material into the structural fraction). The lignin fraction of the plant material does not go through the microbes (active SOM) and is assumed to cycle directly to the slow C pool. Soil texture influences the turnover rate of active SOM (higher rates for sandy soils), the stabilization of active SOM into slow SOM (lower for sandy soils), and the amount of passive SOM that is formed (higher for clay soils).

Plant production submodels simulate the dynamics of grasslands, agricultural crops, and woody (forest and shrubland) systems. The grassland model simulates grass growth and includes the effects of grazing and fire on plant production. The crop growth model simulates production for different crops (e.g., wheat and corn) and can simulate the effects of different fertilization levels, different cultivation practices, and the addition of plant residue on plant production. The forest model (Sanford et al., 1991) simulates forest growth and includes the effects of fire, large-scale disturbances (e.g., hurricanes), tree harvest practices, and fertilization on forest production. All of these plant production models assume that potential plant production is controlled by monthly temperature and precipitation and that plant production rates are decreased from these maximum rates if there are insufficient soil nutrients.

The grass (Figure 2) and crop growth submodels have the same structure and include live shoots and roots and standing dead material. In the grass model, allocation of C to shoots and roots changes as a function of the climate, grazing rate, and fire. The allocation pattern in the crop growth submodel is fixed for a specific crop. The forest growth model also uses a fixed allocation scheme, but in addition simulates the production of live shoots, fine roots,

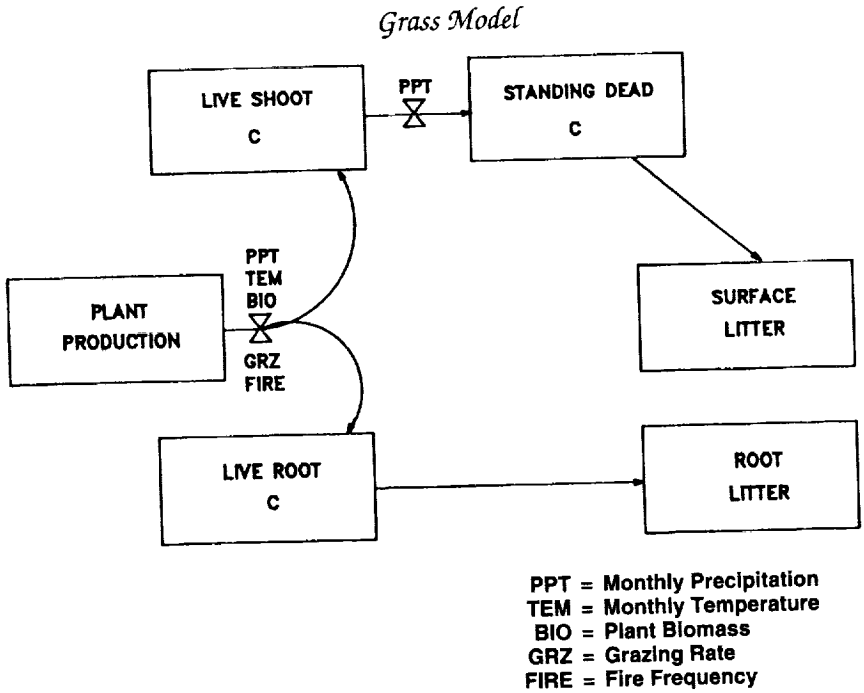

Figure 2. Plant production submodel flow diagram for grassland systems.

fine branches, large wood, and coarse roots. Wood decomposition is simulated in the forest model for three dead wood boxes (large wood, fine branches, and coarse roots). A detailed description of Century is presented in two papers (Parton et al., 1987, 1988) and in a user's manual for the PC version.

During the last few years, a number of simple ecosystem models have been developed that are amenable to regional studies over a long time period. Linkages (Pastor and Post, 1986) is a forest growth model that has been used extensively to simulate growth of different forest species and feedbacks between litter quality and plant growth. A comparison of the two models shows that soil texture, plant nitrogen and lignin contents, and climatic factors are the major controls over nutrient cycling in both models. A major difference is that Linkages uses a litter cohort approach, where the decomposition of each year's litter cohort is represented separately, while in Century new litter is aggregated into either the metabolic or the structural litter component (see Figure 3). Another major difference is that Linkages has one SOM pool while Century has three pools. We (J. Pastor and W. Parton) plan on making a formal comparison between Linkages and Century and anticipate that the utilization of the litter cohort approach will be more important for forest systems since litter quality (i.e., lignin and nitrogen content) is much more variable for forest species and litter types (e.g., large wood, fine wood, fine roots, and leaves) than for those observed in grassland ecosystems.

The model structure used in Century is similar to that used in some new simple ecosystem models such as the Vegie model (Aber et al., 1991) and the General Ecosystem Model (GEM) (Rastetter et al., in press). There are a substantial number of similarities between the Century, Vegie, and GEM models; however, decomposition of plant residue and plant production are calculated using different approaches. The importance of model differences is not clear, and we plan on making a formal comparison of these models.

Model Simplification and Parameter Determination

Century was developed by using a simple representation of biological processes to represent the dynamics of plant-soil systems. Two major model simplification processes were used: the hierarchical approach and the conceptual procedure.

Hierarchical Model Simplification Approach

The hierarchical approach is based on ideas presented by Kittel and Coughenour (1988) and Allen and Starr (1982). This approach takes advantage of high-resolution models with fine time and space

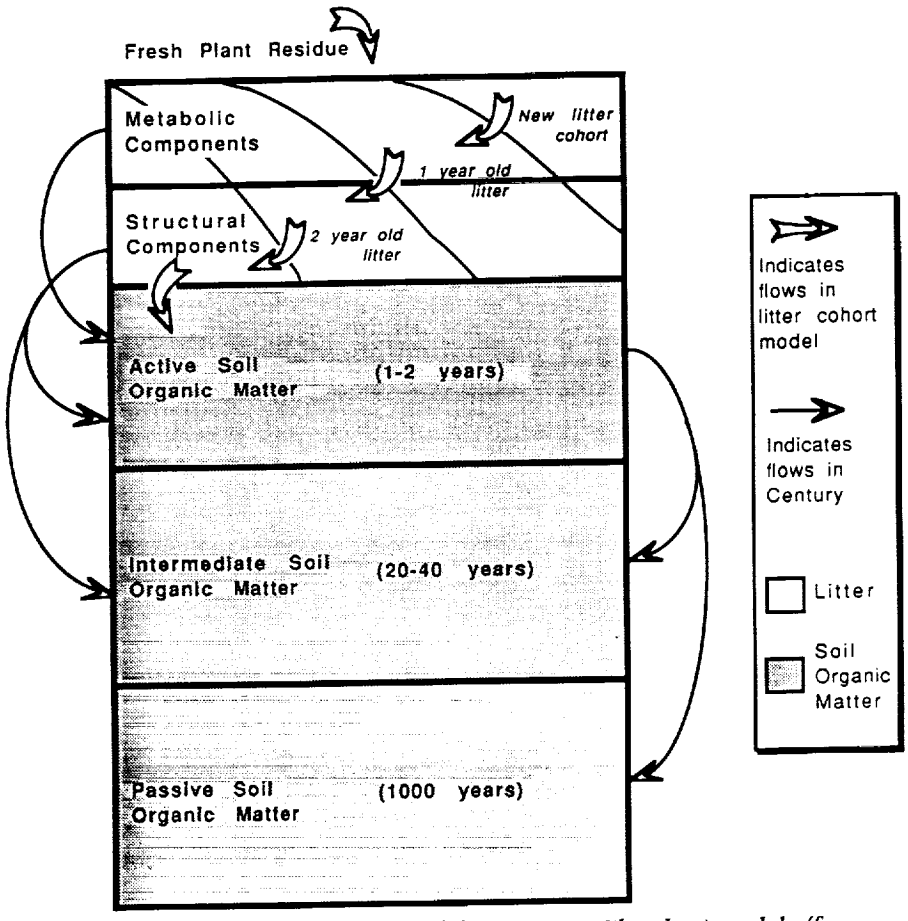

Figure 3. Comparison of Century model structure with cohort models (from Schimel et al., 1991).

scales to develop simplified relationships for coarser-scaled models. Model output from a fine-scaled model is transformed into an equation that is appropriate for a coarse model.

The hierarchical approach was used to derive the equation for the effect of monthly precipitation on the decomposition rate. A daily decomposition model and daily soil water and temperature models (Parton, 1978, 1984) were used to simulate daily decomposition rates for a 40-year time series using observed weather data to drive the models. These simulated daily decomposition rates were then aggregated on a monthly basis and used to develop a simplified equation for the effect of monthly precipitation on decomposition. A nonlinear least squares data-fitting procedure (Powell, 1965) was used to estimate the coefficients in the equation (Figure 4). This relationship is being refined in a new version of Century to include the effect of soil

texture on modifying the relationship shown in Figure 4. This hierarchical approach provides a methodology to determine the effect of precipitation on decomposition for a time step (monthly) that was not easily derived from existing decomposition data.

Conceptual Model Simplification Procedure

A conceptual procedure was used to develop the overall structure of Century (Figure 1). This process incorporates the essential concepts of more detailed nutrient cycling models that are needed to simulate the dynamics of the soil system for a monthly time step. Simplication of the model structure is based on extensive experience from field and laboratory studies in establishing these concepts and provides the basis to extend the concepts over longer time domains (decades to centuries) and over greater and more diverse geographic regions.

The structure of Century represents a simplification of concepts found in the process-oriented nutrient cycling models developed by

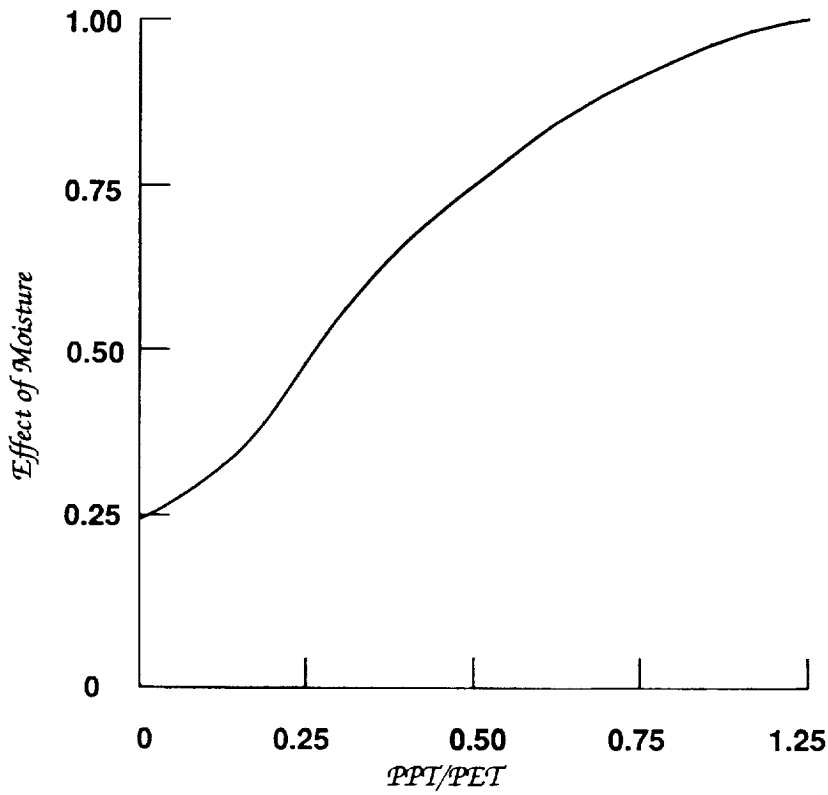

Figure 4. The effect of the ratio of precipitation (ppt) to potential evaporation (pet) on monthly decomposition rates (from Parton et al., 1987).

Hunt (1977) and McGill et al. (1981). McGill et al.'s model (Phoenix) is a detailed process-oriented nitrogen cycling and soil organic matter model (Figure 5) with a 0.2-day time step. The major structural simplification of the Phoenix model was accomplished by combining bacteria, fungi, and microbial products into a single state variable (active SOM). The specific effects of bacteria and fungi on the system were incorporated by using different microbial growth efficiencies for plant material decomposed at the soil surface and that decomposed in the soil. Surface litter is primarily decomposed by fungi, while soil litter is primarily decomposed by bacteria. This allowed us to simplify the model and still include the major role of bacteria and fungi. The conceptual simplification and aggregation of state variables in Century have resulted in the ability to test the potential role of microbial populations on SOM decomposition. In this case, the

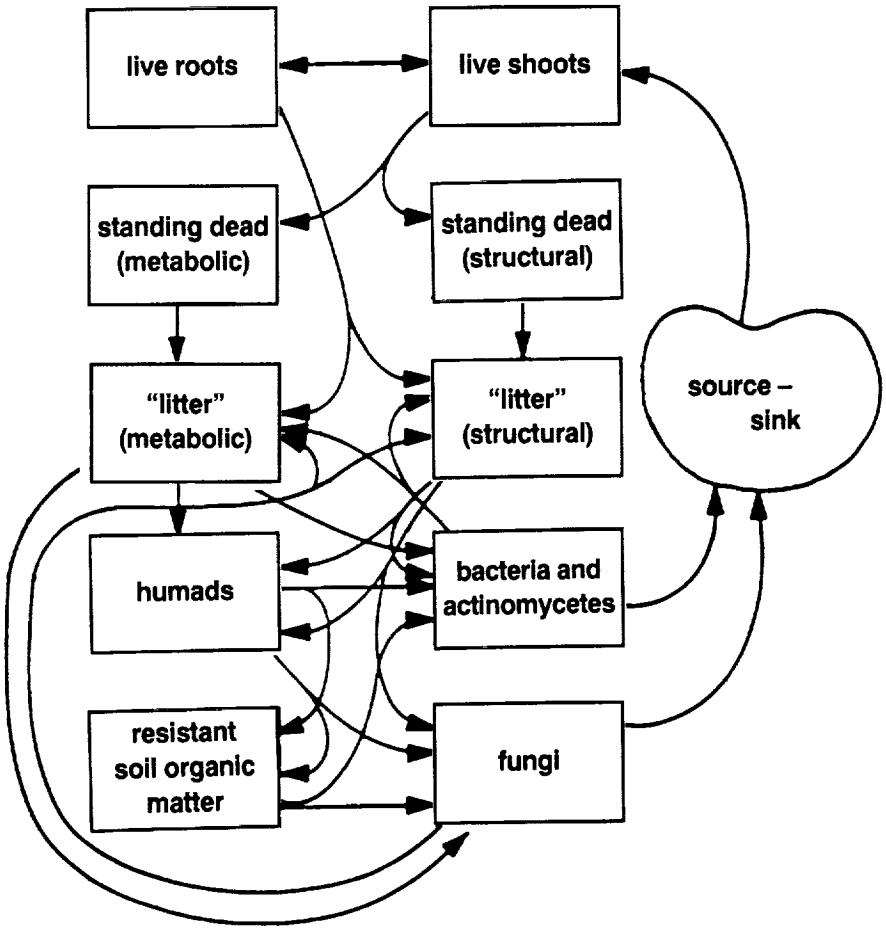

Figure 5. Carbon flow diagram for Phoenix soil organic matter model (from McGill et al., 1981).

model is testing a hypothesis that is based on literature data that is not definitive, and it could potentially be used to formulate a new hypothesis about the role of fungi and bacteria during decomposition. The Century model is also now being used to test the potential impact of earthworms on SOM dynamics. Some of the model parameters that are being modified include the decay rate for slow SOM and microbial growth efficiency for slow SOM.

Parameters Used

Most of the parameters in Century were determined by fitting the model to 15 long-term soil incubations where different types of plant material were added to the soil. A nonlinear data-fitting procedure (Powell, 1965) was used to determine the specific coefficients used in the model. A major contribution of the Century model was to include the effect of the soil texture on the stabilization of SOM. A comparison of the observed (Sorenson, 1981) and simulated effect of soil texture on soil C stabilization is shown in Figure 6. It is important to note that model coefficients determined during the original model fitting procedure have not been changed.

Model Testing and Development

The initial version of Century (Parton et al., 1987) was tested by comparing simulated long-term average plant production and steady state soil C and N levels with observed data from the U.S. Great Plains. The observed vs. simulated comparisons for soil C (Figure 7a) and plant production (Figure 7b) show that the model did an

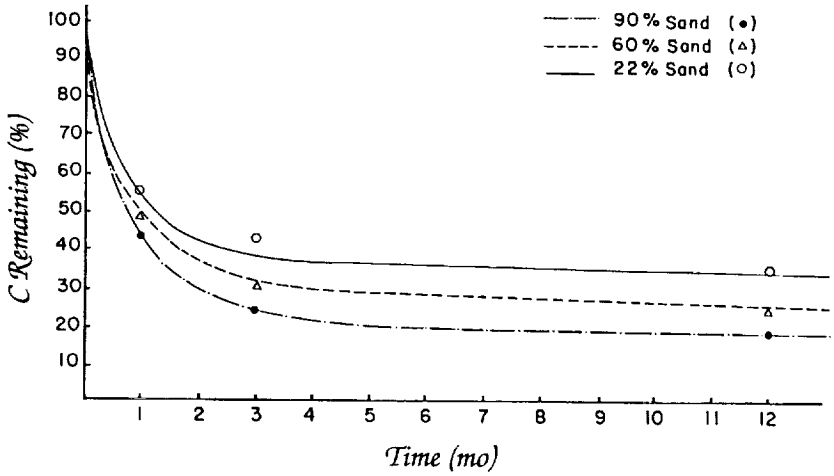

Figure 6. A comparison of observed and simulated effect of soil texture on soil C stabilization (from Parton et al., 1987).

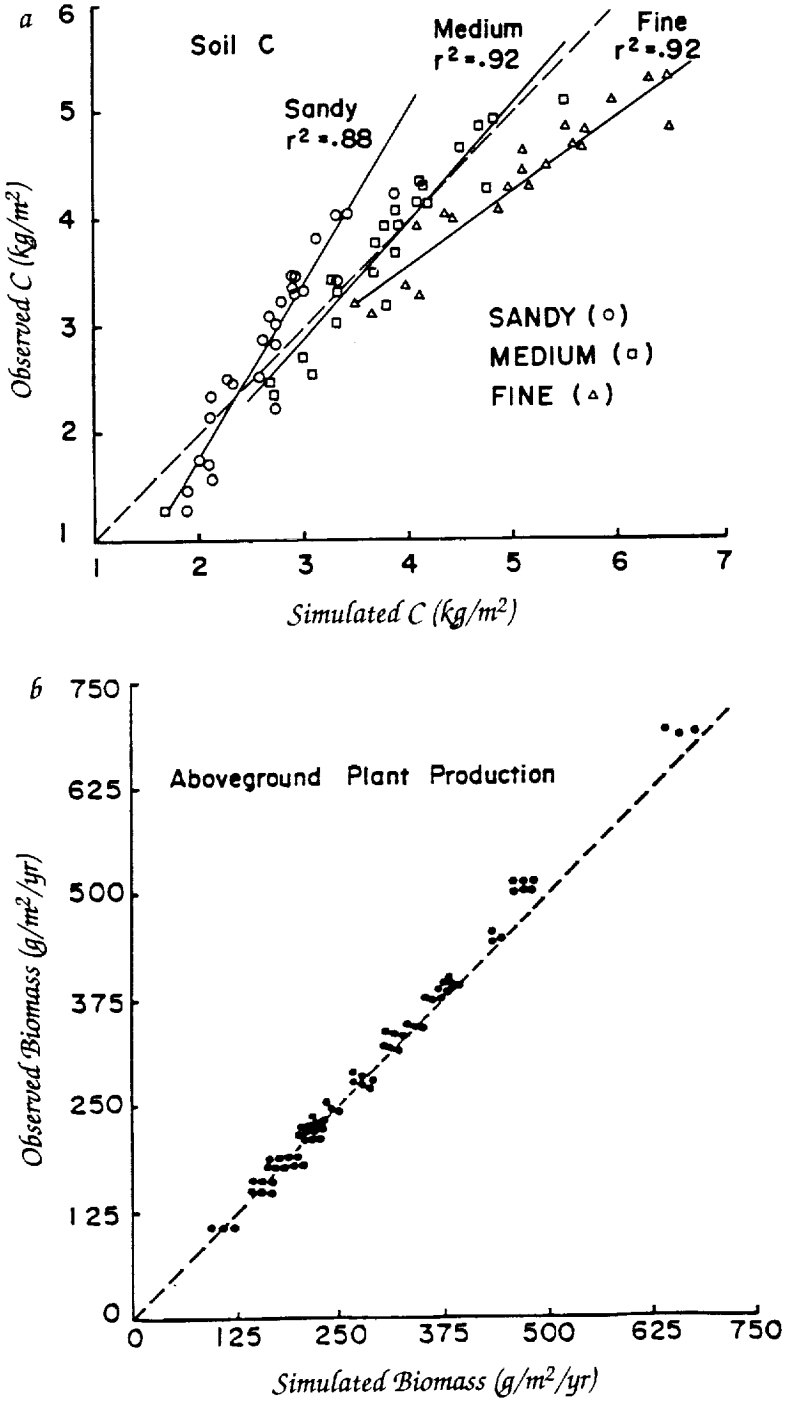

Figure 7. Comparison of observed and simulated (a) soil C levels and (b) plant production for different sites in the Great Plains (from Parton et al., 1987).

excellent job of simulating long-term grassland plant production for the Great Plains and did an adequate job of simulating soil C levels for different soil textures and abiotic environments in the region. One of the major parts of the model testing procedure was an analysis of observed regional plant production data (Sala et al., 1988) and soil C and N data (Burke et al., 1989) to develop a validation data set, since an adequate regional data set was not otherwise available for testing the model.

This regional soil data base for the Great Plains (Burke et al., 1989) was used to test and validate the ability of Century to simulate regional patterns of soil C and N for grassland soils (Parton et al., 1987). This data base is now being used to test new concepts about the formation of passive soil C (old soil C) and to test the ability of Century to simulate C and N losses due to cultivation. Recent data indicate that the slow SOM pool is not the primary source of passive soil C (the assumption made during the initial model development) and that the amount of passive soil C is higher for clay soils. The inability of Century to predict SOM dynamics for forest soils and to predict observed differences in C-to-N ratios of SOM for different soil textures (i.e., 13 to 14 for silty soils and 10 to 11 for clayey soils) has also helped to formulate these concepts. In the recent formulation, most of the passive soil C is derived from the turnover of active SOM, and passive SOM increases with clay content. By incorporating these concepts, the model correctly predicts observed differences in soil C-to-N ratios and predicts that the fraction of soil C in the passive pool will range from 30% for silty soils to 50% for clay soils. The regional soil data base is being used to test how well the model simulates soil textural differences in C-to-N ratios and steady state soil C and N levels. This demonstrates the importance of using regional data bases to test model performance and to help reformulate the model. Testing of general ecosystem models with a large number of sites is an essential part of the model development and testing procedure.

The original version of the model was tested by comparing simulated plant production and soil C and N levels with extensive data on plant production and soil organic matter (C and N) from the U.S. Great Plains (Parton et al., 1987). We are presently testing the model by using grassland plant production and soil organic matter data from 15 sites around the world. The testing of the model using data from many different grassland ecosystems has been an important part of the model development process and has suggested model changes which were necessary to formulate a truly general grassland ecosystem model.

During the last two years we have developed a more mechanistic version of the grassland plant production submodel with the objec-

tive of being able to simulate year-to-year variations in annual plant production and to simulate the seasonal dynamics of live plant biomass. The new model calculates maximum monthly plant production as a function of soil temperature, monthly precipitation, and the ratio of live shoots to dead shoots. The model also includes the effects of grazing and fire on plant root-to-shoot ratio and N content of the plant material (Holland et al., in press; Ojima et al., 1990). This new model was developed using long-term (1928–89) plant production data from a tallgrass prairie in eastern Kansas (Towne and Owensby, 1984; Owensby, unpublished data) and a seven-year time series of plant production data from a shortgrass prairie site in Colorado (Dodd and Lauenroth, 1978). Researchers measured plant production from 1970 to 1976 for control, irrigated (only), fertilized (only), and irrigated plus fertilized sites. Simulated annual plant production for the different treatments in the shortgrass prairie (Figure 8a) and a comparison of observed and simulated production (Figure 8b) show that the model reasonably simulates plant production for the different treatments ($r^2 = 0.85$). A comparison of observed and simulated annual aboveground plant production data from 1930 to 1968 for the tallgrass prairie site (Figure 9a) shows that the model has an observed and simulated r^2 of 0.60. Note that the observed plant production for these years is underestimated since the biomass measurements were made by clipping the biomass at a height of 5 cm, thereby omitting a portion of the grass biomass. Figure 9b shows the comparison of observed and simulated biomass data from 1970 to 1989 for the late-spring-burned and unburned sites. The model correctly estimated plant production for the very dry years (1981 and 1989) and correctly predicted the mean difference between the burned and unburned sites. Year-to-year variability was not as well predicted by the model; however, it is important to note that the standard deviation associated with the production estimates ranges from 100 to 200 $g/m^2/yr$ and makes it difficult to assess the significance of differences between modeled and observed data. In summary, Century reasonably simulated the impacts of fertilization, irrigation, and burning on plant production over an extended period of time, but further refinements may be needed to simulate smaller year-to-year variations in production.

The ability of the model to simulate seasonal biomass dynamics for live and standing dead biomass is now being tested by comparing the model results to monthly plant biomass data from four tropical grassland sites (Mexico, Kenya, Ivory Coast, and Thailand) and temperate grassland sites in the former USSR and Ireland. The results for the tropical sites are very promising and show that the model can correctly simulate the seasonal dynamics of live and dead

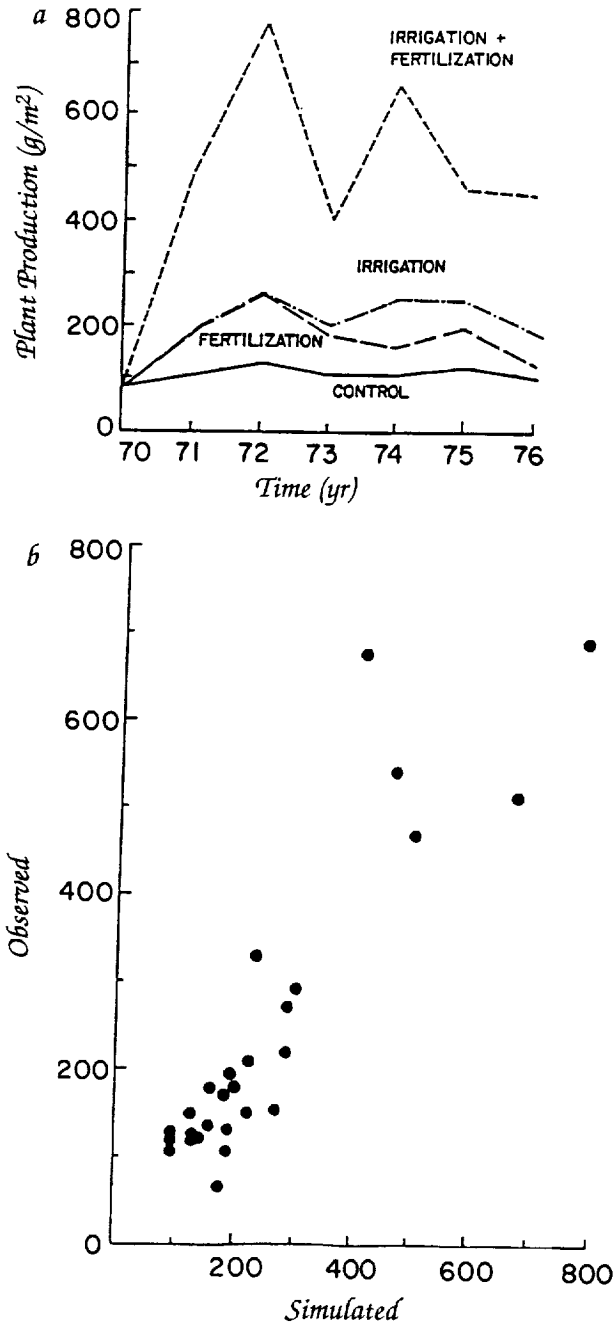

Figure 8. (a) Simulated patterns of plant production for control, fertilizer, irrigation, and irrigation plus fertilization treatments at a shortgrass prairie site and (b) comparison of observed and simulated plant production (g/m^2) for these treatments.

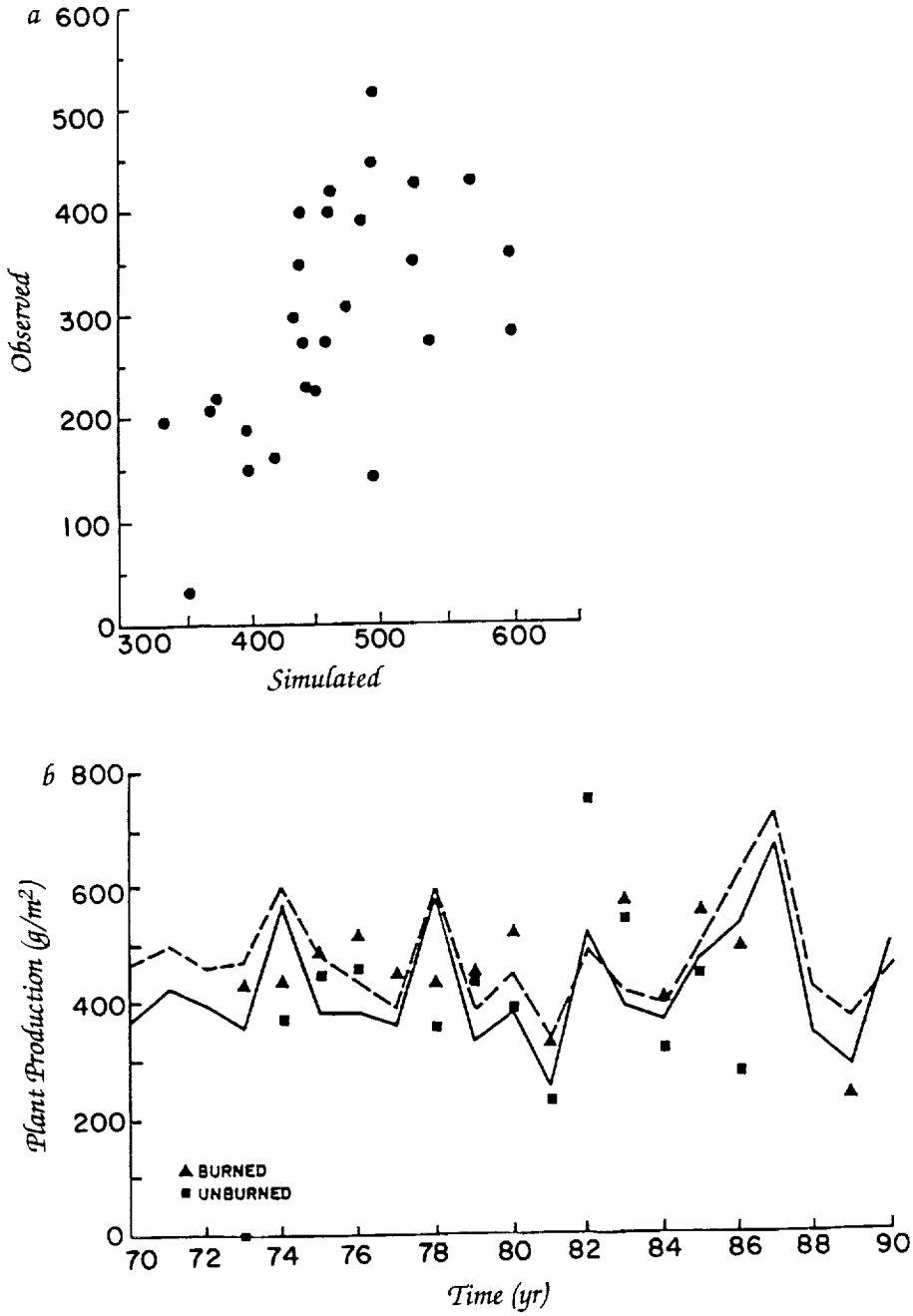

Figure 9. (a) Comparison of observed and simulated plant production (g/m^2) for a tallgrass site from 1930 to 1968. (b) Comparison of observed and simulated plant production from 1972 to 1989 for an unburned (squares = observed, solid line = simulated) site and a late-spring-burned (triangles = observed, dashed line = simulated) site.

biomass and respond appropriately to fire events. The turnover rate of live roots, the rate of transfer from standing dead biomass to litter, and the root-to-shoot ratio are parameters that vary considerably among the sites. These differences are caused by plant-specific differences and abiotic factors such as snow. The observed and simulated live biomass for the Lamto site in Ivory Coast agree reasonably well (Figure 10). The results for the Russian grassland sites indicate that the model underestimated plant production and soil N inputs to these systems and suggest that the equations for the effect of rainfall on plant production and soil N inputs need modification. Such testing of the model at sites with diverse climatic conditions is an important part of model testing and validation and has led to the development of a more accurate and general grassland model.

Regional Modeling

The Century model has been used to simulate regional patterns of grassland biogeochemistry (Burke et al., 1990; Parton et al., 1989). A hierarchical approach is used to simulate the regional ecosystem dynamics (Figure 11). Century is a patch model which represents plant production as an aggregate variable from a mixture of plant species. The external driving variables for the model are soil texture and monthly climatic data. In scaling up from patch to toposequence in a landscape or to a physiographic unit, the diversity of soil types tends to increase. In making a regional simulation with Century, soil variability is accounted for by identifying key soil types

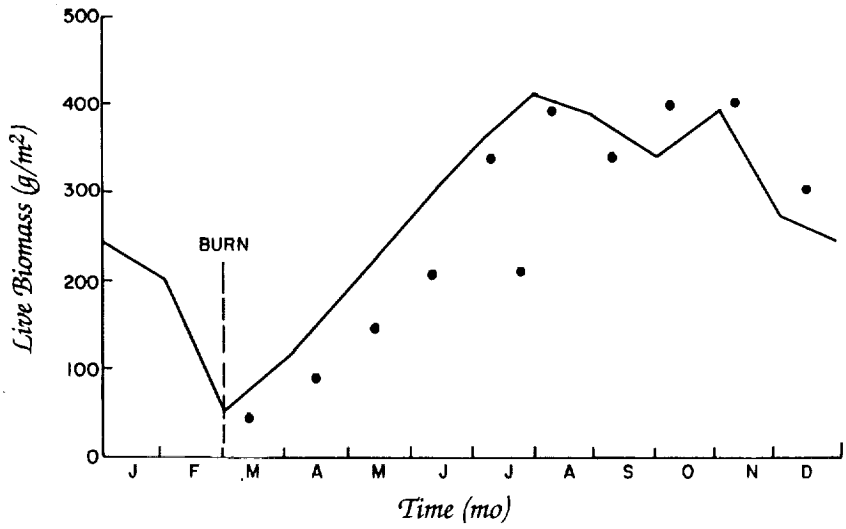

Figure 10. Comparison of observed and simulated live biomass for a burned grassland site in West Africa.

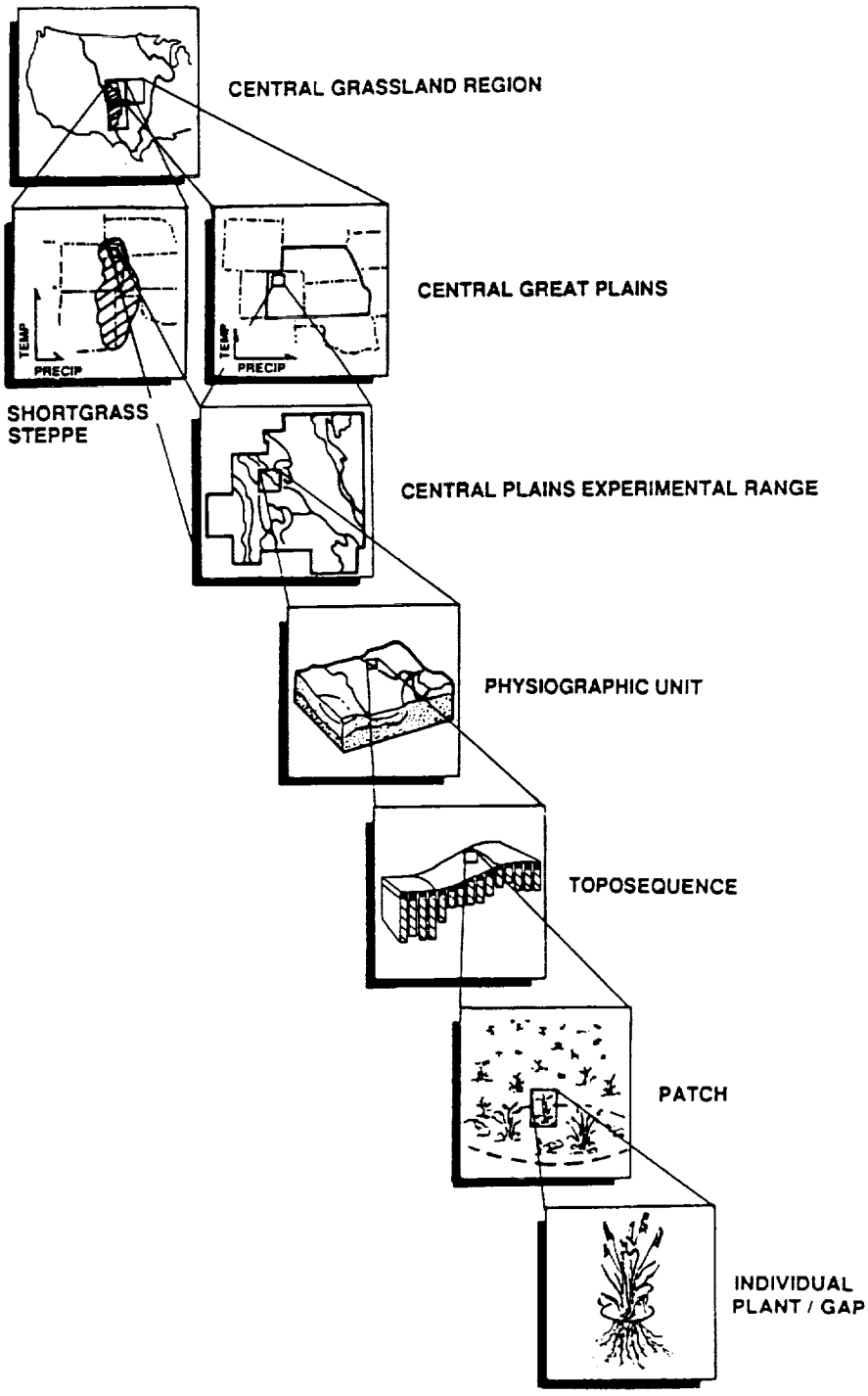

Figure 11. Hierarchical levels used in the regional modeling activity (from Kittel and Coughenour, 1988).

and parameterizing Century for each individual type. The results can then be aggregated as an areal average weighted mean. In addition, the range in climatic factors increases with the size of a region.

Overlaying regional soil variability on climatic variability within a region defines unique sets of driving variables for Century. This is facilitated by a geographic information system (GIS) that contains information on the spatial patterns of soil texture and monthly climatic data. A regional grassland simulation for northeastern Colorado (Burke et al., 1990) required 160 model runs to represent the unique combinations of soil texture and climate.

Across larger areas, dominant plant species changes may result in modifications to certain key ecosystem characteristics, such as the root-to-shoot ratio and plant lignin and nutrient content. For the Great Plains region we have developed equations which predict how the root-to-shoot ratio and plant lignin and nutrient contents change as a function of the annual precipitation. These equations work because plant communities change as a function of annual precipitation.

Simulated annual patterns for aboveground production, soil organic C, net N mineralization, and N gas flux (N_2O, NO_x, and NH_3) in northeastern Colorado (Figure 12) show that soil organic C is primarily controlled by soil texture, while regional patterns of the other variables correspond to annual precipitation (Burke et al., 1990). The effect of spatial resolution of input data indicates that regional estimates of the average plant production and N gas flux are relatively insensitive to changes in spatial resolution of inputs from 2.5 to 4000 km^2. In contrast, average soil C levels are substantially underestimated (14%) when the spatial resolution of inputs is decreased from 1500 to 4000 km^2. These results suggest that aggregation errors are noticeable for soil C levels when the spatial grid is coarse because of the nonlinear impact of soil texture on soil C levels.

Regional patterns for grassland ecosystem properties have been simulated for the North American Central Grasslands (Parton et al., 1989; Schimel et al., in press) based on regional variation in climate. While results are limited by the lack of detailed soil and land use data, the regional pattern of net primary production compares well with that of the annual integral of satellite-based vegetation index data (Schimel et al., 1991). At present, development of a regional GIS data base that includes climatic, land use, and soil data for the North American Central Grasslands is ongoing, and the data base will be used to more accurately simulate patterns of soil C and plant production.

Sensitivity of ecosystem processes and of fluxes of C and N to changes in climate and atmospheric CO_2 level has been evaluated

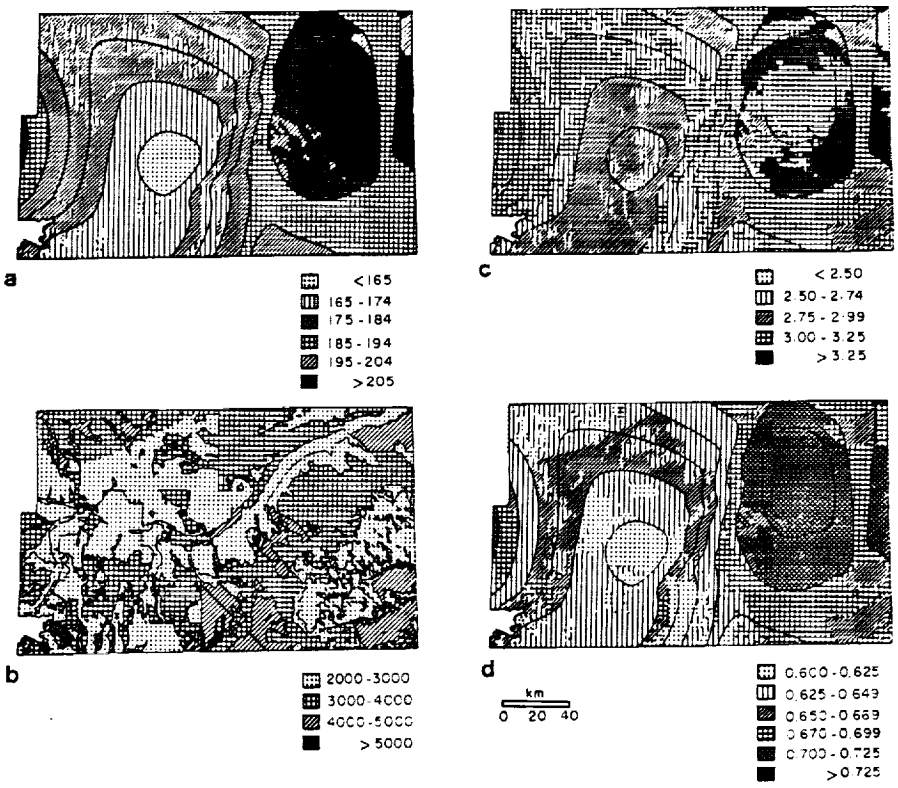

Figure 12. Simulated output from the Century ecosystem model for (a) net primary production in g C/m^2/yr, (b) soil organic carbon in g C/m^2 to 20 cm depth, (c) net annual N mineralization in g N/m^2/yr to 20 cm depth, and (d) net annual N gas flux in northeastern Colorado in g N/m^2/yr. Lines overlaid represent annual precipitation contours (a, c, d) and soil texture classes (b) (from Burke et al., 1990).

for Century. Results from simulating the effects of a GCM CO_2-doubling climate scenario (Hansen et al., 1988) suggest that plant production will generally increase in the northern portion of the North American Central Grasslands and decrease in the southern portion, largely in response to precipitation (Schimel et al., 1990; Kittel et al., in preparation). In addition, throughout the region there will be a net release of C from the soil and an increase in fluxes of nitrogenous gases (N_2, N_2O, and NH_3).

Conclusions

There has been substantial progress in the development of simplified ecosystem models which have the potential to be incorporated into earth system models and to address regional issues regarding changes in land use or climatic conditions. An essential part of the

development of these models is detailed comparison of models with data from a large number of sites having different climate and soil characteristics. These comparisons are critical for testing this class of models and have greatly enhanced our understanding of the complex interactions, leading to substantial improvements in their structure. These models are capable of simulating the impact of climatic change on different ecosystems and can provide insight to potential changes in carbon (e.g., CO_2) and nutrient (e.g., N_2O) fluxes from ecosystems that, as radiatively active gases, play a role in global climate. A significant problem with including simple ecosystem models in earth system models is that the spatial scale of the atmospheric GCM models is still too coarse to incorporate the spatial heterogeneity in surface climate and land surface properties (e.g., topography) needed to represent natural ecosystems. This is illustrated by the fact that the southern part of the Great Plains, which includes shortgrass, mid-grass, and tallgrass prairie ecosystems; montane systems; and agroecosystems that range from wheat-fallow to continuous corn systems, is covered by a single grid with 7.8° latitude × 10° longitude in the GCM at the Goddard Institute for Space Studies. Even with a very fine GCM grid network, it is anticipated that a need to consider subgrid diversity in agricultural land use and natural ecosystems must be explicitly addressed. This level of resolution will be necessary to represent the potential interactions between the atmosphere and the biosphere (Pielke and Avissar, in press; Avissar and Pielke, 1989; Avissar and Verstraete, 1990).

References

Aber, J.D., J.M. Melillo, K.J. Nadelhoffer, J. Pastor, and R.D. Boone. 1991. Factors controlling nitrogen cycling and nitrogen saturation in northern temperate forest ecosystems. *Ecological Applications 1*, 303–315.

Allen, T.F.H., and T.B. Starr. 1982. *Hierarchy: Perspectives for Ecological Complexity*. University of Chicago Press, Chicago, Illinois.

Avissar, R., and R.A. Pielke. 1989. A parameterization of heterogeneous land surfaces for atmospheric numerical models and its impact on regional meteorology. *Monthly Weather Review 117*, 2113–2136.

Avissar, R., and M.M. Verstraete. 1990. The representation of continental surface processes in atmospheric models. *Reviews of Geophysics 28(1)*, 35–52.

Burke, I.C., C.M. Yonker, W.J. Parton, C.V. Cole, K. Flach, and D.S. Schimel. 1989. Texture, climate, and cultivation effects on soil organic matter context in U.S. grassland soils. *Soil Science Society of America Journal 53(3)*, 800–805.

Burke, I.C., D.S. Schimel, C.M. Yonker, W.J. Parton, L.A. Joyce, and W.K. Lauenroth. 1990. Regional modeling of grassland biogeochemistry using GIS. *Landscape Ecology 4*, 45–54.

Cole, C.V., D.S. Ojima, W.J. Parton, J.W.B. Stewart, and D.S. Schimel. 1989. Modeling land use effect on soil organic matter dynamics in the central grassland region of the U.S. In *Ecology of Arable Land: Perspectives and Challenges* (M. Clarholm and L. Bergstrom, eds.), Kluwer Academic Publishers, Dordrecht, The Netherlands, 89–99.

Dodd, J.D., and W.K. Lauenroth. 1978. Analyses of the response of a grassland ecosystem to stress. In *Perspectives in Grassland Ecology* (N. R. French, ed.), Springer-Verlag, New York, 43–58.

Hansen, J., I. Fung, A. Lacis, D. Rind, G. Russel, S. Lebedeff, R. Ruedy, and P. Stone. 1988. Global climate changes as forecast by the GISS 3-D model. *Journal of Geophysical Research 93*, 9341–9364.

Holland, E.A., W.J. Parton, J.K. Detling, and D.L. Coppock. Physiological responses of plant populations to herbivory and their consequences for ecosystem nutrient. *American Naturalist*, in press.

Hunt, H.W. 1977. A simulation model for decomposition in grasslands. *Ecology 58*, 469–484.

Kittel, T.G.F., and M.B. Coughenour. 1988. Prediction of regional and local ecological change from global climate model results: A hierarchical modeling approach. In *Monitoring Climate for the Effects of Increasing Greenhouse Gas Concentrations* (R.A. Pielke and T.G.F. Kittel, eds.), Cooperative Institute for Research in the Atmosphere Workshop, Colorado State University, Fort Collins, 173–193.

Kittel, T.G.F., D.S. Schimel, and W.J. Parton. Sensitivity of the North American Central Grassland ecosystems to climate change (in preparation).

McGill, W.B., H.W. Hunt, R.G. Woodmansee, and J.O. Reuss. 1981. Dynamics of carbon and nitrogen in grassland soils. In *Terrestrial Nitrogen Cycles: Processes, Ecosystem Strategies and Management Impacts* (F.E. Clark and T. Rosswall, eds.), Ecological Bulletin, Stockholm, Sweden.

Ojima, D.S., W.J. Parton, D.S. Schimel, and C.E. Owensby. 1990. Simulated impacts of annual burning on prairie ecosystems. In *Fire in North American Prairies* (S.L. Collins and L. Wallace, eds.), University of Oklahoma Press, Norman, Oklahoma.

Parton, W.J. 1978. Abiotic section of ELM. In *Grassland Simulation Model* (G.S. Innis, ed.), Springer-Verlag, New York, 31–53.

Parton, W.J. 1984. Predicting soil temperature in a shortgrass steppe. *Soil Science 138*, 93–101.

Parton, W.J., J. Persson, and D.W. Anderson. 1983. Simulation of soil organic matter changes in Swedish soils. In *Analysis of Ecological Systems: State-of-the-Art in Ecological Systems* (W.K. Lauenroth, G.V. Skogerboe, and M. Flug, eds.), Elsevier, New York, 511–516.

Parton, W.J., D.S. Schimel, C.V. Cole, and D. Ojima. 1987. Analysis of factors controlling soil organic levels of grasslands in the Great Plains. *Soil Science Society of America Journal 51*, 1173–1179.

Parton, W.J., J.W.B. Stewart, and C.V. Cole. 1988. Dynamics of C, N, P, and S in grassland soils: A model. *Biogeochemistry 5*, 109–131.

Parton, W.J., C.V. Cole, J.W.B. Stewart, D.S. Ojima, and D.S. Schimel. 1989. Simulating regional patterns of soil C, N, and P dynamics in the U.S. central grassland region. In *Ecology of Arable Land: Perspectives and Challenges* (M. Clarholm and L. Bergstrom, eds.), Kluwer Academic Publishers, Dordrecht, The Netherlands, 99–108.

Pastor, J., and W.M. Post. 1986. Influence of climate, soil moisture and succession on forest carbon and nitrogen cycles. *Biogeochemistry 2*, 3–27.

Pielke, R.A., and R. Avissar. Influence of landscape structure on local and regional climate. *Landscape Ecology*, in press.

Powell, M.J.D. 1965. A method for minimizing a sum of squares of nonlinear function without calculating derivatives. *Computer Journal 7*, 303–307.

Rastetter, E.B., M.G. Ryan, G.R. Shaver, J.M. Melillo, K.J. Nadelhoffer, J.E. Hobbie, and J.D. Aber. A general biogeochemical model describing the responses of the C and N cycles in terrestrial ecosystems to changes in CO_2, climate and N deposition. *Tree Physiology*, in press.

Sala, O.E., W.J. Parton, L.A. Joyce, and W.K. Lauenroth. 1988. Primary production of the Central Grassland Region of the United States. *Ecology 69(1)*, 40–45.

Sanford, R.L., W.J. Parton, D.S. Ojima, and D.J. Lodge. 1991. Hurricane effects on soil organic matter dynamics and forest production in the Luquillo Experimental Forest, Puerto Rico: Results of simulation modeling. *Biotropica 23(4)*, 364–373.

Schimel, D.S., T.G.F. Kittel, and W.J. Parton. 1991. Terrestrial biogeochemical cycles: Global interactions with the atmosphere and hydrology. *Tellus 43(AB)*, 188–203.

Schimel, D.S., W.J. Parton, T.G.F. Kittel, D.S. Ojima, and C.V. Cole. Regional simulation of grassland biogeochemistry. *Climatic Change*, in press.

Sorensen, L.H. 1981. Carbon-nitrogen relationships during the humification of cellulose in soils containing different amounts of clay. *Soil Biology and Biochemistry 13*, 313–321.

Towne, G., and C. Owensby. 1984. Long-term effects of annual burning at different dates in ungrazed Kansas tallgrass prairie. *Journal of Range Management 37*, 392–397.

Report: A Toy Terrestrial Carbon Flow Model

William Parton, Steven Running, and Brian Walker

Background

Simplified or toy models have been commonly used to test specific hypotheses about complex systems. During the 1990 Global Change Institute (GCI), we attempted to propose the structure of various toy models of different earth system components from which we can eventually test hypotheses relevant to global change. These toy models have been pared down to incorporate only essential attributes of key components and processes.

The value of these toy models is derived from their relatively transparent nature. That is, processes connecting various components are easily discerned, and responses of these models to perturbations to their parameter environment can be more readily determined. The development and testing of these simplified models will quicken the rate at which we are able to unravel specific interlinkages of the earth system. Thus, these toy models can be viewed as an important step in building more complex and intricate earth models.

Scientists presented several toy models in discussions during the 1990 GCI. These were: ocean biogeochemistry (W. Broecker), global nitrous oxide (N_2O) flux (I. Fung), biosphere interaction with climate (F. Bretherton), ocean carbon (B. Moore), terrestrial biogeochemistry (W. Parton), forest carbon and water flux (S. Running), and sea ice growth (A. Thorndike).

Carbon Flow Model

At the GCI, a conceptual framework was developed for a generalized carbon flow model for the major terrestrial ecosystems of the

world. The model is a simplification of the Century model (Parton et al., 1987, this volume) and the Forest-Biogeochemical (BGC) model (Running and Coughlan, 1988). The C flow diagram (Figure 1) shows that live foliage, roots, and woody biomass are represented and that C flows from these compartments to the plant residue compartment. Plant residue then decomposes and forms soil organic matter. The soil organic matter is divided up into two compartments (slow and passive), with the slow pool having an approximate turnover time of 20 to 50 years and the passive pool having a long turnover time (1000 to 3000 years). The actual turnover times of these pools depend on abiotic decomposition factors (soil temperature and water), with shorter times in warm, humid environments and longer in cold, dry locations. This structure is a simplification of the Century soil organic matter model where the slow compartment of soil organic matter is further divided up into two boxes (active and slow with approximate turnover times of 2 and 20 years, respectively). The model also represents the dynamics of nutrients in the plants and soil. The nutrient flows are represented because either N or P limits plant production for most terrestrial ecosystems, and production can be constrained by the ratios of C:N or C:P in the various components. The nutrient flow model has the same structure as the C flow diagram and will represent the dynamics of the most limiting nutrient for plant production. Nitrogen limits most terrestrial systems; however, P limits production for many tropical forest systems.

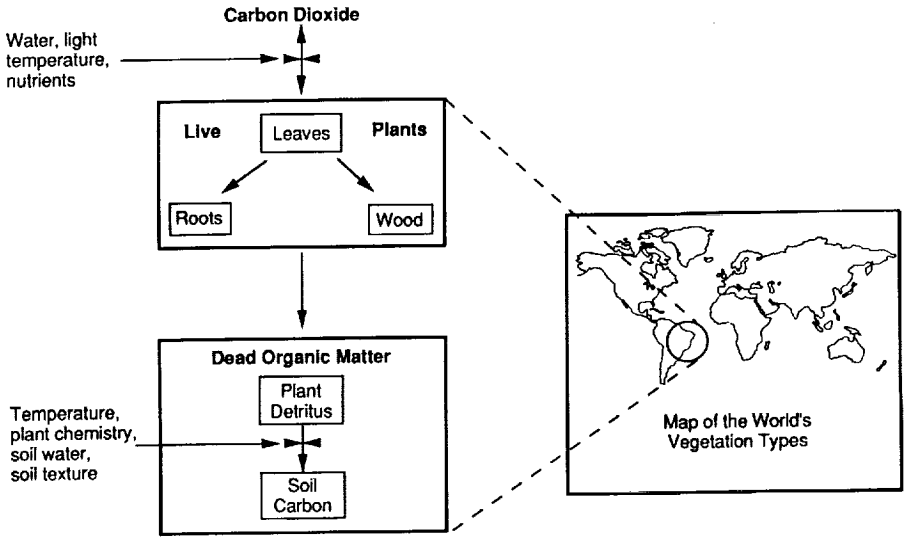

Figure 1. Conceptual framework for a global terrestrial C model.

Plant Production

Plant production is calculated using two different submodels. The model developed by Running and Coughlan (1988) is used to calculate net daily photosynthesis as a function of soil water content, solar radiation, air temperature, and leaf area index. The calculated net photosynthesis rate is the maximum potential plant production rate for the day; the actual plant production rate will be lower than the maximum rate if there is insufficient available inorganic N or P. The C fixed each day is then allocated into the live shoot, root, and wood biomass. The allocation of C is primarily a function of the type of ecosystem being represented; however, the allocation pattern is also a function of the annual rainfall, grazing level, and atmospheric CO_2 level.

The second submodel uses a less mechanistic approach where the controls on potential plant production are monthly rainfall and soil temperature. This type of model is currently being used in the Century plant production model. The effect of rainfall on plant production (Figure 2a) is calculated as a function of the ratio of monthly rainfall to potential evapotranspiration (increases linearly as the ratio increases). The potential evapotranspiration rate is calculated as a function of the maximum and minimum air temperature using the equations developed by Linacer (1977). Production increases rapidly as surface soil temperature increases from 5° to 15°C, then increases relatively slowly up to 20°C, followed by a decline in production above this temperature (Figure 2b). For certain specified plant communities adapted to cooler climates, a curve similar to the C3 curve of the Century model can be used, or for warmer climates the C4 curve can be specified. The potential plant production rate is calculated by multiplying the temperature effect times the rainfall term times the maximum plant production rate for a month. The actual plant production will be less than the potential rate if sufficient nutrients are not available. The allocation of C into the different plant parts is calculated using the same approach as in the high-resolution plant production model.

The live wood, foliage, and root biomass grow as a result of inputs of carbon from the plant production model. The different plant parts have different lignin contents and nutrient concentrations, which are a function of the plant community. We have tentatively identified eight ecosystems that need to be represented in the worldwide application of the model:

- Desert
- Arid and semiarid savannas and shrublands
- Humid savannas and woodlands

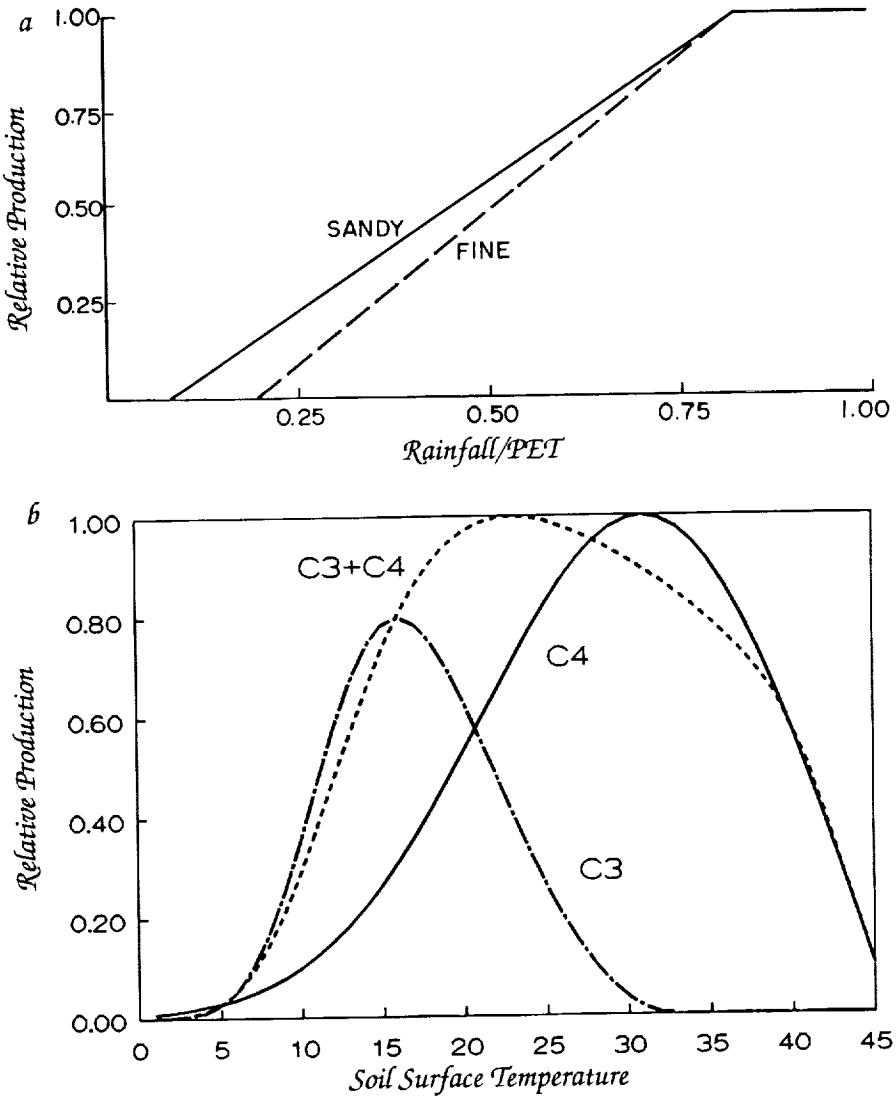

Figure 2. Climate controls on plant production. (a) Control of rainfall and potential ET on production as modified by soil texture. (b) Characteristic temperature response of terrestrial ecosystem dominated by C3, C4, or an even mixture of C3/C4 plants.

- Grasslands
- Temperate deciduous forests
- Temperate evergreen forests
- Arctic and subarctic tundra
- Tropical rainforests.

The live roots die at a constant rate that is a function of the ecosystem-specific annual fine root turnover rate. The large wood biomass includes the boles, large branches, and coarse roots. The model considers the effects of harvest and natural death of the live wood. Harvest of wood is an external driving variable, and wood death and decomposition are simulated. Wood death rates are ecosystem-specific and a function of the amount of wood biomass (higher for older and larger trees). Leaf death rates vary as function of the vegetation type, air temperature, and moisture stress. The ecosystem-specific patterns for leaf death (e.g., deciduous vs. coniferous) and the controls of air temperature and moisture stress are represented. Burning redistributes carbon and nutrients from live foliage and wood to litter and the atmosphere (as oxides of nitrogen and CO_2). The redistribution pattern needs to be modeled externally by a separate fire model, with the results being fed back into the carbon model.

Decomposition and Nutrient Cycling

Dead leaf and fine root material flow into the plant residue compartment (Figure 1), while dead wood goes into wood residue. Wood and plant residue decompose as a function of the lignin and N content of the material and the abiotic decomposition parameter. The abiotic decomposition rate is a function of soil temperature and rainfall, and the equations presented in the Century model are used for this model (Figure 3). The abiotic decomposition rate increases with increasing temperature and increasing values of the monthly ratio of rainfall to potential evapotranspiration rate. The effect of plant lignin and N content on decomposition is represented by the functions used in the Century model. Plant and wood residue decomposition rates decrease with increasing lignin content and decreasing N content. As plant residue decomposes, most (60 to 80%) of the C is lost to the atmosphere as respiration. The C lost as respiration is a function of soil texture and mineralogy and the plant lignin content of the vegetation. The effect of soil texture and lignin content on CO_2 respiration loss is represented using the equations presented in the Century model. CO_2 losses are higher for sandy soils and decrease as the lignin content of the vegetation decreases. Carbon not lost as CO_2 respiration flows into the two soil organic pools (slow and passive). The slow pool receives most of the carbon (98 to 99%). The fraction that goes to the passive pool is a function of the clay content of the soil, with higher values for clay soils. The slow and passive soil pools decompose at different rates (approximate turnover times of 20 and 1000 years) which are pool-specific and vary as a function of the abiotic decomposition rate (Figure 3).

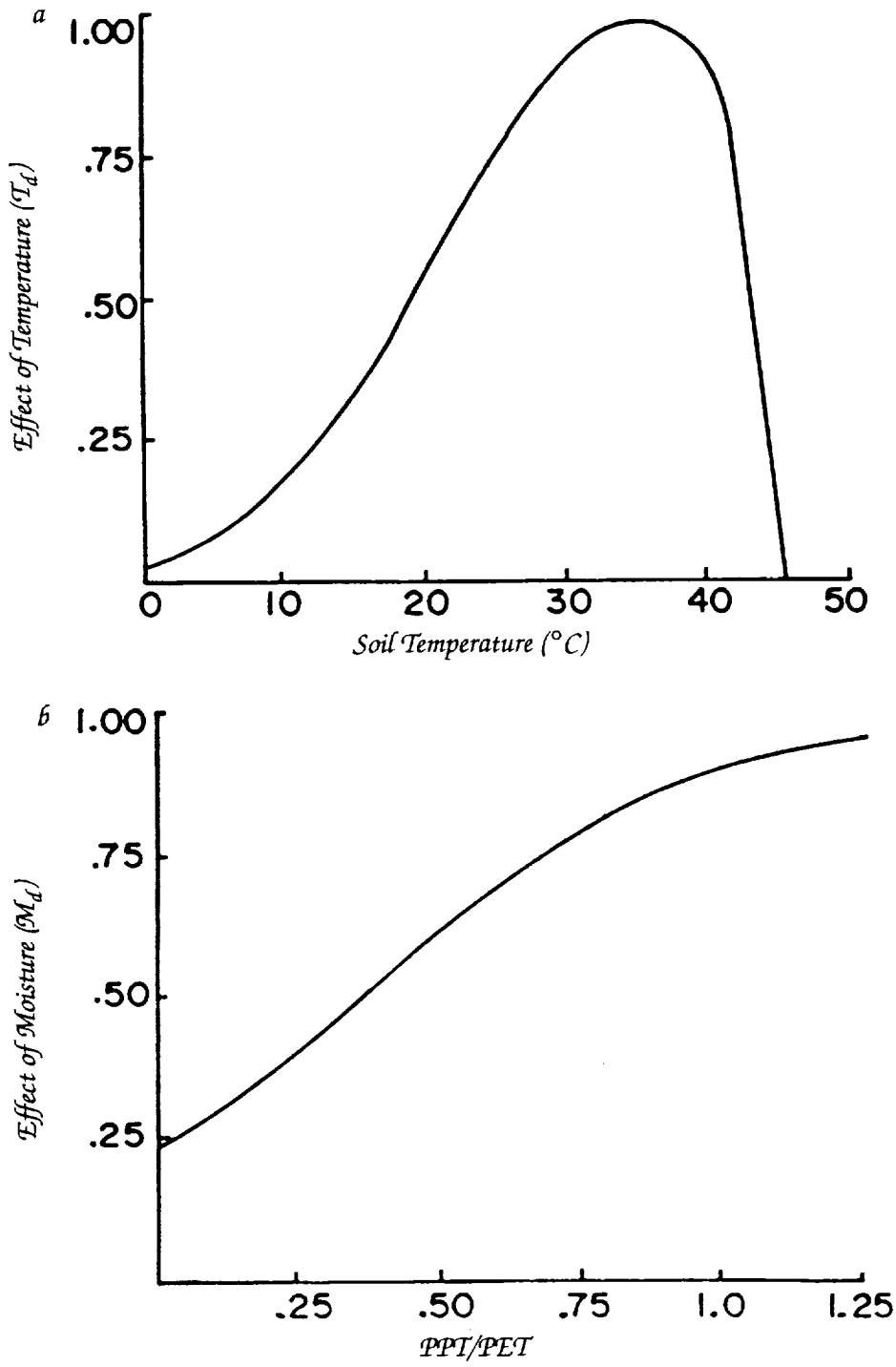

Figure 3. (a) The effect of soil temperature (T_d) on monthly deposition rates. (b) The effect of moisture (M_d) on monthly deposition rates.

When the soil organic pools decompose, the carbon is returned to the atmosphere as CO_2.

Nutrient cycling is modeled by using the same flow diagram as in the carbon model. The nutrient content of the vegetation is an ecosystem-specific input variable, and the plant nutrients flow along with the carbon. When soil C pools decompose they release C to the atmosphere, and nutrients associated with the decomposing soil C are assumed to be mineralized and flow into available mineral pools (nitrate, ammonium, and phosphate: NO_3^-, NH_4^+, and $PO_4^{\equiv}$).

When plant residue decomposes it immobilizes nutrients from the mineral pools at a rate that is a function of the nutrient and lignin content of the vegetation. The immobilization rate is higher for vegetation containing high lignin and low nutrients. The soil nutrient mineralization model uses the equations developed in the Century soil organic matter model. The nutrients remaining after immobilization into decomposing plant residue are then available for uptake into new plant production. Nutrients will be lost from the system by leaching, by erosion, and through gaseous emissions. Nutrient input to the system comes from the atmosphere and N fixation by the plants. Simple equations for these inputs and losses are included in the model.

A representative description of soils for the present modeling effort and for interactions with atmospheric models will need to specify both hydrologic and fertility parameters. These will likely include depth, texture, presence or absence of an impedance layer (for water or root penetration), active carbon content, sum of exchangeable bases, and an additional description of topography.

A combination of basic soil attributes such as parent material (from surface geological maps) and soil age, together with plant functional groups that grow on these soils (see below), may allow us to deduce both fertility and the hydrological cycle in an ecosystem without complex and detailed mapping of soil texture depth, infiltration, interflow, and runoff.

Biomes

The ability to model different processes in the carbon and nutrient cycles of terrestrial ecosystems needs to be tested in different biomes. On a precipitation and temperature plot, eight major biomes can be distinguished, as listed in the previous section. Within each of these, on a regional basis (i.e., by general circulation model grid cell), it is necessary to define the proportion that has been converted to dryland or irrigated arable land. Feasible land use systems can be superimposed upon these biomes, and the model should be tested under these combinations.

Since the C model describes productivity in several key plant components, and also allows for the incorporation of nutrient fluxes, it can be used with only minor additional algorithms to predict other important ecosystem variables such as leaf area index, albedo, and to some extent moisture.

A critical gap in this, as in most other models, is the inadequate representation of water use and storage within the ecosystem. Incoming precipitation controls primary production, but soil moisture storage and water uptake by roots from different soil layers at different times are not represented. The redistribution of precipitation into evaporation, soil moisture storage, transpiration, and drainage depends on such factors as relief, soil type, texture, rooting depth, and plant type. In sandy and loamy soils water will gradually penetrate the soil as successive layers become saturated. Water extraction (and loss to the atmosphere) subsequently depend on surface evaporation and root distribution. This is relatively simple to represent in a model. In heavier soils, cracks permit the rapid infiltration of incoming rainwater to depth without the complete saturation of upper soil layers. Subsequent water uptake and transpiration by plants from lower soil layers is an important factor for plant survival in dry climates, but is difficult to represent with simple models. The complex redistribution patterns of water on the individual ecosystem level will have to be simplified to provide water balances at a resolution appropriate at the general circulation model (GCM) grid scale. No satisfactory solution to this problem is yet available.

Scenarios

The utility of the carbon flow model for predicting C dynamics under global change depends on whether it can be applied to different scenarios of global change around the globe. The scenarios include different conditions and changes in atmospheric CO_2 levels; temperature; precipitation; atmospheric deposition of N, S, and others; land use, such as fertilization, irrigation, and cultivation; deforestation/afforestation; extraction of selected ecosystem products; grazing; and fire.

CO_2 levels are covered in the plant production portion of the model structure. In Running's model, photosynthesis depends on CO_2 gradients that inherently depend on atmospheric CO_2 levels. In the Century model, the slope of the relationship between available water and productivity is modified by atmospheric CO_2 levels.

Temperature and precipitation are controlling factors for both production and decomposition functions of the simplified Century models. In addition, the allocation of production to root and shoot

is controlled by moisture availability. Irrigation will have similar effects on production and decomposition through improved moisture availability.

Atmospheric deposition may affect the availabilities of nutrients for plant production. Productivity is modeled depending on C:nutrient ratios, which allows for the effects of such atmospheric deposition. Atmospheric deposition may also change acidity levels in the soil depending on the soil's buffering capacity. The potential productivity depression will lower the slope of the curve relating productivity to moisture availability of the simplified Century.

Levels of inorganic nutrients in the soil as affected by atmospheric deposition or land management (including fertilization) may need to be modeled separately from the C:nutrient function. Phosphorus, for instance, has several inorganic forms of differing solubility and availability, which interact with organic P forms and plant uptake. Transformations between these forms need to be modeled separately. This has been done successfully in the complete version of Century.

The effect of cultivation is to mix residues into the soil and speed up decomposition processes. This is successfully modeled by Century, and adequately represented in the present model.

The processes of deforestation and afforestation involve depletion and buildup of leaf, wood, and root components, which can be adequately modeled.

Extraction of selected products such as firewood, fruit, or animals in grazed systems without wholesale modification of the ecosystem can be represented by loss functions on the leaf or wood components. The partial return of materials through feces of grazing animals or accelerated litter production in extractive use may require additional simple models that provide new parameters to the simplified Century.

Similarly, fire causes a redistribution of model components, export of C and N, and generation of inorganic forms of nutrients in ashes that will need to be modeled in a separate fire model, which should account for the differential effects of burn intensities, fuel availability, and vegetation state.

Vegetation Change

The eight biomes listed above may be exchanged for a more appropriate classification of vegetation functional types once these have been developed using plant functional types (PFTs) and soil properties. The PFTs will be defined in terms of characteristics that determine their interaction with the atmosphere and other ecosystem components.

Thus far the terrestrial carbon model discussed here is applicable to a fixed vegetation cover within each of the eight biomes. As climate and atmospheric CO_2 change, however, the functioning of the terrestrial ecosystem will change, and this will eventually lead to global changes in the state of the ecosystem. To take these changes into account, fine-scale models of detailed changes in species composition are inappropriate. What is needed are a broad-scale data base of georeferenced characteristics of the earth's vegetation cover and a model that predicts changes that are significant in terms of their consequences for GCMs and atmospheric chemistry (i.e., carbon).

We propose the development of two complementary models for the changing ecosystem: a state-and-transition model and an environmentally driven global vegetation model.

State-and-Transition Model

This model should be based on a present-day land cover map of the world, classified into the eight biome types, with local and regional differences represented by:

- Separate descriptions of the vegetation functional types (woodland, grassland, etc.), with each vegetation type being defined by its proportional composition of plant functional types (evergreen vs. deciduous, annual vs. perennial, etc.)
- Differences in the amounts of the variables in the carbon model
- The proportion of the biome that has been converted to cultivated land.

The first requirement is that the model must apply to the entire land surface of the globe, and this puts a constraint on the scale. A grid cell or polygon size of about 100 x 100 km is tentatively proposed. For each grid (polygon) cell, the proportion of each biome type should be determined. It is necessary to determine the possible states in which each biome type can exist. The definition of these states should be guided by the interaction of the ecosystem with the atmosphere. Minor differences in species composition should not be considered as differences in state. Large differences in the proportions of different functional types of species (e.g., from evergreen to deciduous trees, or from trees to grass), which will lead to measurable differences in the atmosphere/climate models, are significant.

Transition from one state to another is driven by both endogenous (community) processes and exogenous (disturbance) effects. Both need to be taken into account. Change due to endogenous processes will be determined mostly as a function of the changes in levels of the C boxes and fluxes in the C model, but may also be

based on known successional processes in that type of ecosystem. In terms of environmental (precipitation and temperature) changes, present-day correlations between vegetation state and environment may be used to guide the degree of change in environment required to induce a "significant" change in state (with due recognition given to the various lag effects). In addition, there should be an attempt to derive relationships (within each biome) between the levels of C in each box of the model and the "state" of the vegetation. These relationships could then be used to drive the vegetation change model.

For ecosystems where change is predominantly a function of disturbance regime, the combinations and sequences of conditions for each transition need to be explicitly stated, based on what is currently known about the ecology of that region.

The two types of processes are then amalgamated into a set of rules which determines each transition.

Environmentally Driven Global Vegetation Model

We envisage this model as based on first principles, using fundamental processes of vegetation development, and having no recourse to existing maps. It is based on a set of plant functional types with defined environmental responses, and the proportional composition of the vegetation is determined by the individual and interactive dynamics of these PFTs in response to given climatic scenarios. The proposed model is a simplified FORET-type model (Shugart, 1984) of plant-by-plant replacement, with globally defined plant functional types replacing individual species.

Validation

Given our present understanding of global vegetation dynamics, and the existing data (or lack thereof), it will be particularly valuable to develop both of these vegetation change models. Discrepancies between them will focus attention on high-priority areas for reducing uncertainty. The vegetation model will be particularly valuable in setting bounds for the state-and-transition model and for checking on climate-driven changes to vegetation/environment combinations for which there are no current analogs. Other means of validation will include the use of advanced very high resolution radiometer (AVHRR) data and existing data sets on vegetation, soil, and climate for various regions within each biome.

References

Linacer. 1977. A simple formula for estimating evaporation rates in various climates, using temperature data above. *Agricultural Meteorology 18*, 409–424.

Parton, W.J., D.S. Schimel, C.V. Cole, and D. Ojima. 1987. Analysis of factors controlling soil organic levels of grasslands in the Great Plains. *Soil Science Society of America Journal 51*, 1173–1179.

Running, S.W., and J.C. Coughlan. 1988. A general model of forest ecosystem processes for regional applications. I. Hydrological balance, canopy gas exchange and primary production processes. *Ecological Modeling 42*, 125–154.

Shugart, H.H. 1984. *A Theory of Forest Dynamics*. Springer-Verlag, New York.

Report: Carbon Cycling in High-Latitude Ecosystems

Alan Townsend, Stephen Frolking, and Elizabeth Holland

The carbon-rich soils and peatlands of high-latitude ecosystems could substantially influence atmospheric concentrations of CO_2 and CH_4 in a changing climate. Currently, cold, often waterlogged conditions retard decomposition, and release of carbon back to the atmosphere may be further slowed by physical protection of organic matter in permafrost. As a result, many northern ecosystems accumulate carbon over time (Billings et al., 1982; Poole and Miller, 1982), and although such rates of accumulation are low, thousands of years of development have left Arctic ecosystems with an extremely high soil carbon content; Schlesinger's (1984) average value of 20.4 kg C/m^2 leads to a global estimate of 163 x 10^{15} g C.

All GCM simulations of a doubled CO_2 climate predict the greatest warming to occur in the polar regions (Dickinson, 1986; Mitchell, 1989). Given the extensive northern carbon pools and the strong sensitivity of decomposition processes to temperature, even a slight warming of the soil could dramatically alter the carbon balance of Arctic ecosystems. If warming accelerates rates of decomposition more than rates of primary production, a sizeable additional accumulation of CO_2 in the atmosphere could occur. Furthermore, CH_4 produced in anaerobic soils and peatlands of the Arctic already composes a good percentage of the global efflux (Cicerone and Oremlund, 1988); if northern soils become warmer and wetter as a whole, CH_4 emissions could dramatically rise. A robust understanding of the primary controls of carbon fluxes in Arctic ecosystems is critical.

As a framework for a systematic examination of these controls, we discussed a conceptual model of regional-scale Arctic carbon

turnover, including CH_4 production, proposed by E. Holland, and based upon an extension of the Century soil organic matter model (Parton et al., 1987, this volume). The details of Century will not be repeated here; rather, we will restrict our discussion to the specific modeling challenges posed by Arctic ecosystems.

Biophysical Model

Both soil temperature and soil moisture status are critical determinants of carbon dynamics in any ecosystem. Some unique features of the Arctic physical environment complicate the prediction of these variables:

- Permafrost, or permanently frozen subsurface soil, underlies much of the Arctic. It has a significant effect on regional hydrology by providing an impermeable barrier to vertical infiltration. Changes in permafrost will alter the size of the active carbon pool, regional hydrology, and perhaps topography through uneven settling. The extent to which the permafrost layer may change in a warmer climate is not well known, but recent evidence from oil wells in northern Alaska suggests a distinct warming trend in the permafrost over the 20th century.
- Snow, being a very effective insulator, can dramatically affect the soil thermal regime. In addition, snowmelt is a dominant source of water to Arctic ecosystems.
- Freeze/thaw processes in the soil are important to the regional hydrology (frozen soil is impermeable) and to the soil thermal regime due to delays at 0°C resulting from the energy requirements of a change in phase. The timing of the spring thaw is crucial, because it occurs when available sunlight is high (May-June). An earlier thaw would greatly enhance ecosystem productivity, and a deeper thaw in permafrost regions would thicken the active decomposition layer.

Due to high spatial variability of these factors in the Arctic, we believe a fairly comprehensive biophysical model of the soil environment that provides input to the carbon turnover model will be necessary for regional-scale simulations (Figure 1). The present conceptual structure of this model contains four distinct layers (Figure 2): unsaturated peat or soil at the surface; saturated peat or soil; deep, unfrozen, saturated mineral soil or extensively decomposed peat; and permafrost. Changes in the extent of the top two layers (that is, changes in the water table) may occur on time scales of days to weeks, while significant changes in permafrost are only likely to occur on decadal time scales.

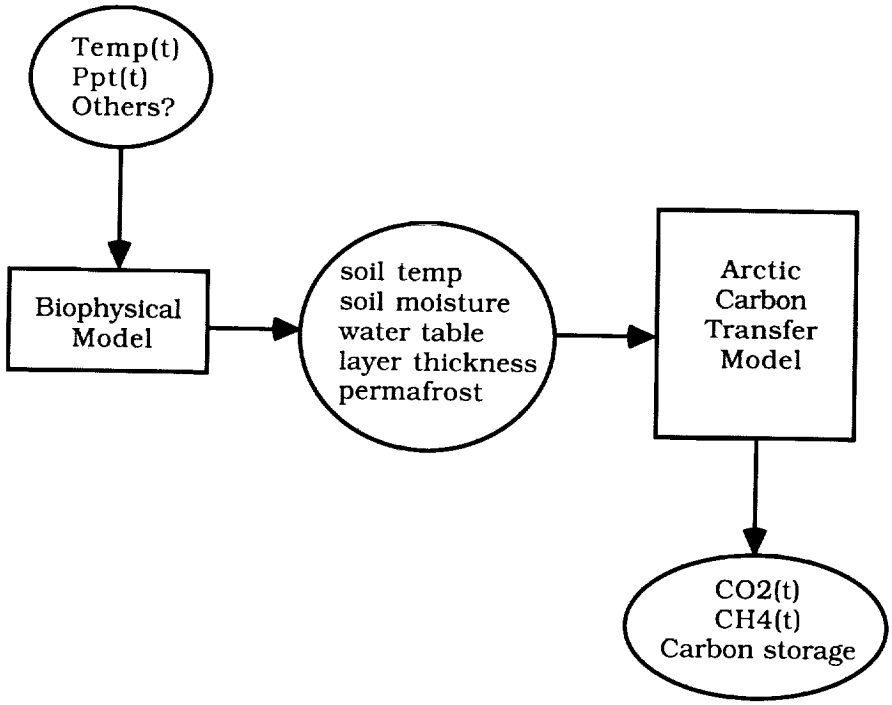

Figure 1. A diagram of the coupling of the Arctic carbon cycling model with the soil biophysical model. Inputs are climate variables, intermediate results are soil temperature and moisture profiles, and final outputs are CO_2 and CH_4 flux time series and the annual change in soil carbon storage.

Model inputs include the thermal and hydraulic properties of the surface vegetation and soil layers, and a parameterization of lateral surface water movement. The model will be driven by (at minimum) air temperature and precipitation, and will determine the temperature profile of each layer, the thickness of the aerobic vs. saturated layers, seasonal depth of thaw, and changes in permafrost. As well, the model will need to determine snow depth, extent of snow cover, and timing of snowmelt.

Carbon Turnover Model

Development of a good biophysical model is just one of a number of modeling challenges posed by Arctic ecosystems. While fluxes of carbon between the atmosphere and ecosystems are low, the stocks of available substrate in the soils are enormous. As a result, the initial response of Arctic systems to climate change will not be dramatic, but the cumulative effects and feedbacks to the climate system on longer time scales are potentially extreme. The most critical unknowns in predicting these dynamics concern the responses of

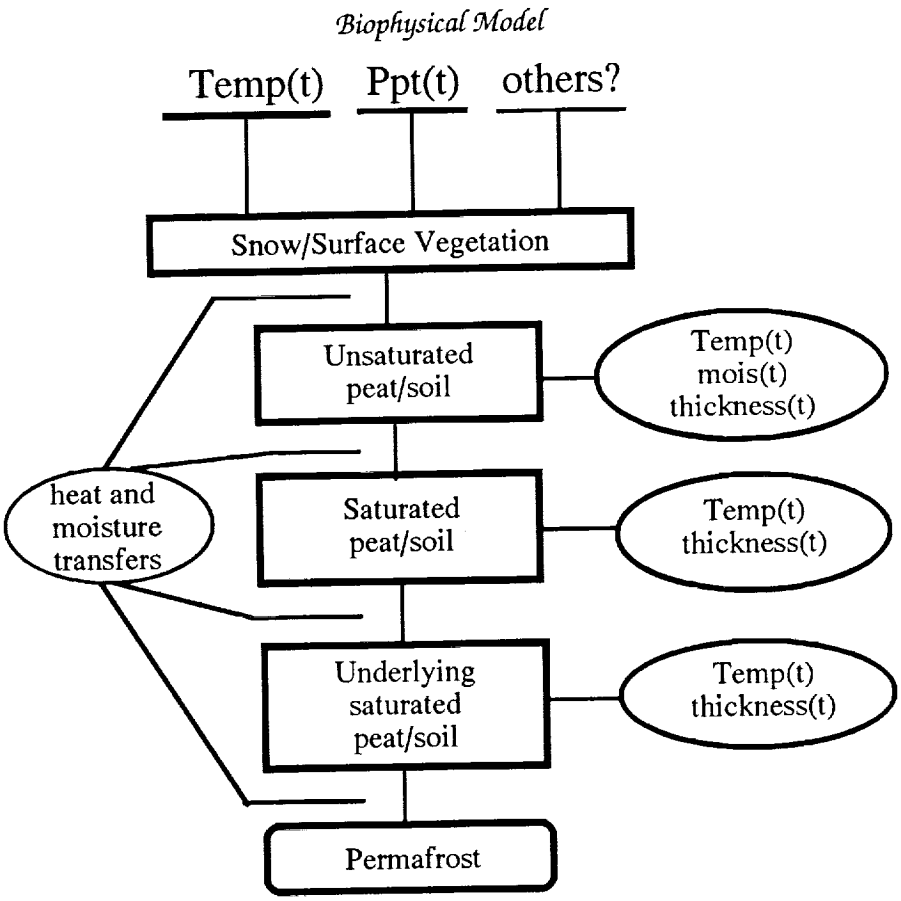

Figure 2. Schematic of biophysical model of soil heat transfer and moisture flux. Climate variables drive the model, and the output is the physical state of the modeled soil layers.

decomposition vs. production to changes in temperature and moisture. Whether any ecosystem produces a net release or uptake of carbon to or from the atmosphere in a given year depends on the ratio of primary production to decomposition. In the Arctic, this is a quotient of two relatively small numbers, so that the potential for a sizeable change in this ratio is high.

If inputs and effluxes of carbon varied in a similar fashion in response to climate-related perturbations, there would be less cause for concern, but most current evidence suggests that this is not the case. In a recent review of soil respiration (Raich and Schlesinger, in preparation), the authors point out that the vast majority of studies show soil CO_2 efflux to be related to temperature in an exponential fashion, with a mean Q_{10} of 2.4. Nadelhoffer et al. (1991) found essentially no change in soil respiration with temperatures between

2° and 10°C, but a large and rapid increase above 10°. Temperature effects on production of Arctic vegetation are poorly understood, but most existing evidence suggests a more linear relationship. If this is the case, warming in the northern latitudes could actually result in carbon accumulation in the soils, thus creating a negative feedback to further warming. The accumulation of carbon in tundra during warmer, interglacial periods lends some credence to this hypothesis. This potential sink of carbon could only exist, however, over a limited range; if temperatures increase enough to push the exponentially responding decomposition processes beyond those of production, the balance could shift to a net efflux, thereby generating a positive feedback leading to even higher temperatures (Townsend et al., in preparation). The actual responses of decomposition and production in Arctic environments to temperature changes and the current rates of these processes must be identified before accurate predictions of future dynamics are possible.

Temperature represents only one of many factors that can influence carbon balance. A similar analysis may be applied to moisture, whose controls and likely changes in a doubled-CO_2 climate are even less well understood. In general, both decomposition and production often increase in an exponential fashion with greater moisture availability over certain ranges, but excess moisture will render soils anaerobic and retard rates of production and decomposition. Due to the nonlinear nature of these processes, the responses and current conditions need to be worked out.

These challenges, however, do not preclude the design and preliminary application of a simulation model for carbon dynamics. Figure 3 is a diagram of the model's general structure, with total ecosystem carbon being divided into three vegetation compartments and three soil compartments. At present, Century calculates production as a function of temperature and moisture; we believe Arctic vegetation may also require an irradiance parameter. On shorter time scales and in the tundra, woody biomass should have little impact on the climate-induced responses; thus it is represented as an isolated pool. Both root and aboveground biomass create residue organic matter, which in turn feeds into the available soil carbon pool. The third soil pool, permafrost, is completely recalcitrant, but can feed into the other soil pools upon thawing. The details of this exchange will be determined by the biophysical model outlined earlier. Estimates of allocation between above- and below-ground material can be made from a variety of studies (cf. Chapin et al., 1986a, 1986b; Chapin and Shaver, 1988), as can estimates of lignin:N ratios. Since most of the tundra is highly organic, soil texture will not play as important a role as it does in other ecosystems. Signifi-

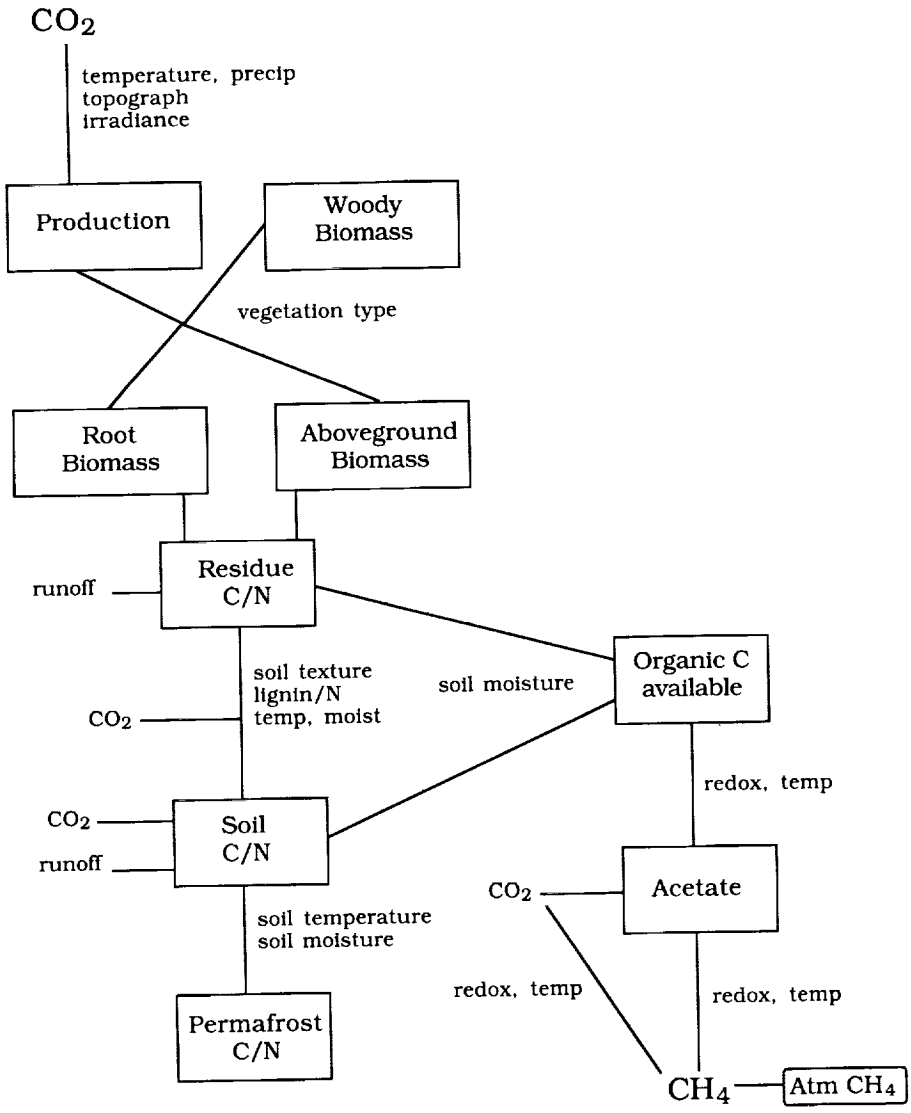

Figure 3. Conceptual model diagram for soil carbon, CO_2, and CH_4 cycling in Arctic ecosystems.

cant transport of organic acids through peat layers and into streams and groundwater could occur.

Waterlogged conditions may slow decomposition and the subsequent release of CO_2, but they do allow methanogenesis to occur; a warmer, wetter Arctic could also result in a positive feedback to further warming via accentuated CH_4 release from anaerobic peatlands and bogs. Work is currently under way to expand the Century struc-

ture to simulate CH_4 fluxes. Briefly, carbon in the soil and residue pools may become available for methanogenesis when anaerobic conditions arise. The proportion of this carbon that is converted to CH_4 is a function of soil temperature and redox status. Redox itself is a function of moisture and microbial activity, so that microbial utilization of oxygen in the previous time step will affect the redox state of the present time step. Oxidation of CH_4 produced to CO_2 is also determined by redox state, as well as by the speed at which CH_4 can escape to the atmosphere. A greater percentage of CH_4 produced will be released in vegetated areas, because plants provide effective conduits through the water/soil layer (Conrad, 1989; Schutz et al., 1989a, 1989b). Where vegetation does not supersede standing water, transport from source areas to the atmosphere is slower, relying on diffusion, ebullition, and wind-generated turbulence for escape. For this reason, vegetated and open-water areas should be treated differently in calculations of CH_4 flux. Finally, CH_4 is allowed to enter the soil/water environment from the atmosphere as a function of the concentration gradient. There is some suggestion (Steudler et al., 1989; Mosier et al., 1991) that CH_4 uptake by soils may be closely tied to N status, so that it may eventually be possible to tie this flux to the mineralization rates calculated by the central model.

Regional-Scale Modeling

Spatial heterogeneity can be extreme in Arctic regions (Miller, 1982). Therefore, extension of the model to regional scales will be challenging. As there is some evidence that Arctic vegetation can be tightly correlated with water status, some knowledge of topography (e.g., via digital elevation models) might also allow estimates of the vegetation parameters. This relationship is by no means certain; Miller (1982) states that vegetation zones in central Alaska are largely determined by nutrient availability rather than water status.

The best approach to spatial extrapolation of the local model may be that of King et al. (1989), which uses probability distributions and Monte Carlo sampling techniques to generate expected values throughout large regions to provide inputs to the ABISKO II (Bunnel and Scoullar, 1975) model. Estimates of the probability functions for the model inputs might be possible from a combination of regional vegetation maps, AVHRR data, and thematic mapper data bases. Using a probability function approach to calculate expected values in space may be critical in the Arctic, as many of the important dynamics respond in nonlinear fashion, and conventional averaging-in-space approaches could produce greatly erroneous results.

Critical Field Measurements

Complete data sets needed for model parameterization and validation are scarce, but some information is available from sites in Minnesota, Alaska, Scandinavia, and the Hudson's Bay region of Canada. Efforts to study carbon dynamics in northern latitudes are increasing (e.g., Svensson and Rosswall, 1984; Chapin et al., 1986a, 1986b; Sebacher et al., 1986; Crill et al., 1988; Whalen and Reeburgh, 1988; Nadelhoffer et al., 1991; and the National Aeronautics and Space Administration's Global Tropospheric Experiment/Arctic Boundary Layer–3 experiments). NASA, the National Environmental Research Centre (United Kingdom), and the Canadian Institute for Research in Atmospheric Chemistry are currently planning large-scale field campaigns in the boreal and tundra regions during the next few years. Nevertheless, we will have to know much more to test and direct regional-scale simulation models. A list of needed information follows:

- Production, decomposition, and CO_2 and CH_4 flux measurements coupled with soil moisture and temperature over at least a growing season, including freeze and thaw periods, and preferably for a full year in sites that span the general range of Arctic ecosystem types. This is the most critically needed information.
- Time series of winter snowpack, snowfall, air temperature, and the effects of topography on snowpack. Some such data exist (e.g., Woo et al., 1983).
- Depth profiles of organic carbon to the permafrost layer throughout the Arctic. Again, limited data are available, and Doolittle et al. (1990) suggest that ground-penetrating radar may provide a rapid and accurate means for determining the depth to frozen soil and thus the thickness of the active layer.
- Carbon-13, carbon-14, and deuterium isotope values for gas fluxes. The deuterium isotopic ratio can be used to determine whether methane was produced from acetate or carbon dioxide; the carbon isotopes allow differentiation among various types of substrate.
- Redox profiles (pH, pe) for various soil moisture conditions. One set of such data is available from northern Alaska.
- Soil texture (where applicable) and soil hydraulic and thermal properties for both organic and mineral soils.
- Root-shoot ratios and the lignin:N ratios for each vegetation component in different Arctic regions.

- Dissolved organic carbon and particulate organic carbon in rivers and streams. We need to determine how significant these are in the overall carbon balance.

- Atmospheric deposition rates of N and S compounds. Key questions here are whether N inputs fertilize these systems and whether S inputs provide significant alternative electron acceptors for microbial reduction.

Some Additional Questions

The model we outline here does not address the issue of methane hydrates or clathrates, that is, CH_4 trapped in ice lattices in permafrost and in the marine sediments of continental shelves. Kvenvolden (1988) reviews estimates of their extent (ranging from 1.7 to 4000 teratons of CH_4) and gives pressure-temperature phase diagrams for hydrate stability. If these hydrates are destabilized, the CH_4 can then be released. We believe that a separate modeling effort is needed to assess the time scale of hydrate destabilization by climate change and the subsequent movement of CH_4 to the land or sea surface.

The atmospheric CH_4 record reconstructed from ice-core data (Chappellaz et al., 1990; Rasmussen and Khalil, 1984; Craig and Chou, 1982) raises two questions:

- The high-latitude peatlands began forming about 9000 to 6000 years ago (Heinselman, 1975). Since these peatlands are a major natural source of CH_4 to the atmosphere, is there evidence in the ice-core record of the appearance and growth of such a significant source of methane?

- Is there evidence in the Vostok core CH_4 record of hydrate destabilization, and, if not, how sensitive are hydrate formations to climate perturbations?

References

Billings, W.D., J.O. Luken, D.A. Mortensen, and K.M. Petersen. 1982. Arctic tundra: A source or sink for atmospheric carbon dioxide in a changing environment? *Oecologia 53*, 7–11.

Bunnell, F.L., and K.A. Scoullar. 1975. ABISKO II: A computer simulation model of carbon flux in tundra ecosystems. In *Structure and Function of Tundra Ecosystems* (T. Rosswall and O.W. Heal, eds.), Ecological Bulletin 20, Swedish Natural Science Research Council, Stockholm, 425–448.

Chapin, F.S. III, J.D. McKendrick, and D.A. Johnson. 1986a. Seasonal changes in carbon fractions in Alaskan tundra plants of differing growth form: Implications for herbivory. *Journal of Ecology 74*, 707–732.

Chapin, F.S. III, G.R. Shaver, and R.A. Kedrowski. 1986b. Environmental controls over carbon, nitrogen, and phosphorus fractions in *Eriophorum vaginatum* in Alaskan tussock tundra. *Journal of Ecology 74*, 167–195.

Chapin, F.S. III, and G.R. Shaver. 1988. Differences in carbon and nutrient fractions among Arctic growth forms. *Oecologia 77*, 506–514.

Chappellaz, J., J. Barnola, D. Raynaud, Y. Korotkevich, and C. Lorius. 1990. Ice-core record of atmospheric methane over the past 160,000 years. *Nature 345*, 127–131.

Cicerone, R., and R. Oremlund. 1988. Biogeochemical aspects of atmospheric methane. *Global Biogeochemical Cycles 2*, 299–327.

Conrad, R. 1989. Control of methane production in terrestrial ecosystems. In *Exchange of Trace Gases between Terrestrial Ecosystems and the Atmosphere* (M.O. Andreae and D.S. Schimel, eds), Dahlem Conference, John Wiley and Sons, Chichester, England, 39–58.

Craig, H. and C. Chou. 1982. Methane: The record in polar ice cores. *Geophysical Research Letters 9*, 1221–1224.

Crill, P., K. Bartlett, R. Harriss, E. Gorham, E. Verry, D. Sebacher, L. Madzar, and W. Sanner. 1988. Methane flux from Minnesota peatlands. *Global Biogeochemical Cycles 2*, 371–384.

Dickinson, R.E., A. Henderson-Sellers, P.J. Kennedy, and M.F. Wilson. 1986. *Biosphere-Atmosphere Transfer Scheme for the NCAR Community Climate Model*. Technical Note NCAR/TN-275+STR, National Center for Atmospheric Research, Boulder, Colorado, 69 pp.

Doolittle, J.A., M.A. Hardisky, and M.F. Gross. 1990. A ground-penetrating radar study of active layer thicknesses in areas of moist sedge and wet sedge tundra near Bethel, Alaska, U.S.A. *Arctic and Alpine Research 22(2)*, 175–182.

Heinselman, M. 1975. Boreal peatlands in relation to environment. In *Coupling of Land and Water Ecosystems* (A. Hasler, ed.), Ecological Studies No. 10, Springer-Verlag, New York.

King, A.W., R.V. O'Neill, and D.L. DeAngelis. 1989. Using ecosystem models to predict regional CO_2 exchange between the atmosphere and the terrestrial biosphere. *Global Biogeochemical Cycles 3(4)*, 337–361.

Kvenvolden, K. 1988. Methane hydrates and global climate. *Global Biogeochemical Cycles 2*, 221–230.

Miller, P.C. 1982. Environmental and vegetational variation across a snow accumulation area in montane tundra in central Alaska. *Holocene Ecology 5*, 85–98.

Mitchell, J.F.B. 1989. The greenhouse effect and climate change. *Review of Geophysics 24*, 115–139.

Mosier, A., D. Schimel, D. Valentine, K. Bronson, and W. Parton. 1991. Methane and nitrous oxide fluxes in native, fertilized and cultivated grasslands. *Nature 350*, 330–332.

Nadelhoffer, K.J., A.E. Giblin, G.R. Shaver, and J.A. Laundre. 1991. Effects of temperature and substrate quality on element mineralization in six arctic soils. *Ecology 72(1)*, 242–253.

Parton, W.J., D.S. Schimel, C.V. Cole, and D. Ojima. 1987. Analysis of factors controlling soil organic levels of grasslands in the Great Plains. *Soil Science Society of America Journal 51*, 1173–1179.

Poole, D.K., and P.C. Miller. 1982. Carbon dioxide flux from three Arctic tundra types in north-central Alaska, U.S.A. *Arctic and Alpine Research 14(1)*, 27–32.

Raich, S.W., and W.Y. Schlesinger. Global CO_2 flux in soil respiration and its relationship to climate (in preparation).

Rasmussen, R., and M.A.K. Khalil. 1984. Atmospheric methane in the recent and ancient atmospheres: Concentrations, trends, and interhemispheric gradient. *Journal of Geophysical Research D7*, 11599–11605.

Schlesinger, W.H. 1984. Soil organic matter: A source of atmospheric carbon dioxide. In *The Role of Terrestrial Vegetation in the Global Carbon Cycle* (G.M. Woodwell, ed.), SCOPE 23, John Wiley and Sons, Chichester, England, 111–127.

Schutz, H., A. Holzapfel-Pschorn, R. Conrad, H. Rennenberg, and W. Seiler. 1989a. A 3-year continuous record on the influence of daytime, season, and fertilizer treatment on methane emission rates from an Italian rice paddy. *Journal of Geophysical Research D13*, 16405–16416.

Schutz, H., W. Seiler, and R. Conrad. 1989b. Processes involved in formation and emission of methane in rice paddies. *Biogeochemistry 7*, 33–53.

Sebacher, D., R. Harriss, K. Bartlett, S. Sebacher, and S. Grice. 1986. Atmospheric methane sources: Alaskan tundra bogs, and alpine fen, and a subarctic boreal marsh. *Tellus 3B*, 1–10.

Stauffer, B., E. Lochbronner, H. Oeschger, and J. Schwander. 1988. Methane concentration in the glacial atmosphere was only half that of the preindustrial Holocene. *Nature 332*, 812–814.

Steudler, P.A., R.D. Bowden, J.M. Melillo, and J.D. Aber. 1989. Influence of nitrogen fertilization on methane uptake in temperate forest soils. *Nature 341*, 314–316.

Svensson, B., and T. Rosswall. 1984. In situ methane production from acid peat in plant communities with different moisture regimes in a sub-arctic mire. *Oikos 43*, 341–350.

Townsend, A., P.V.M. Vitousek, and E.A. Holland. Tropical soils dominate the short term carbon cycle feedbacks to atmospheric CO_2 (in preparation).

Whalen, S., and W. Reeburgh. 1988. A methane flux time series for tundra environments. *Global Biogeochemical Cycles 2*, 399–409.

Woo, M., R. Heron, P. Marsh, and P. Steer. 1983. Comparison of weather station snowfall with snow accumulations in high arctic basins. *Atmosphere–Ocean 21*, 312–325.

Report: Cryosphere and Climate

W.D. Hibler, III, and A.S. Thorndike

This chapter will discuss two main issues related to the cryosphere and climate. One is the effect of sea ice and salinity gradients on ocean circulation, and in particular the possible role of sea ice transport on the ocean conveyer belt. The other is the effect of the cryosphere on climate, and in particular in high-latitude warming under increased CO_2.

In understanding the role of the cryosphere in both cases, it is useful to elucidate two types of toy sea ice models. Neither of these represents reality, but both are useful for illustrating the archetypal features of sea ice that control much of its large-scale behavior.

The first model is a simple slab thermodynamic sea ice model as presented by Thorndike (this volume). In this model there are no dynamical effects and the thickness of ice is determined by surface heat budget and oceanic heat flux considerations, with the thickness of the ice critically affecting the effective conductivity whereby heat is transferred from the bottom ice boundary to the upper ice boundary. In this model all of the sea ice characteristics are controlled by the vertical heat fluxes from the atmosphere and ocean into the ice. The thickness is controlled by the ice's becoming an effective insulator as it thickens, thus reducing conductive heat loss to the atmosphere.

A second model emphasizes the effects of dynamics (Hibler, this volume). It considers the ice pack to be a collection of floes moving in response to synoptic wind fields and ocean currents. These motions create semipermanent leads (open areas) over which ice can grow rapidly. Under the convergent phase the new ice is converted

into sea ice pressure ridges. In this idealized model, growth over the ice floes is neglected, and all of the ice production occurs over leads. The mean ice thickness of this system is determined by a balance between the ice growth over the leads and the removal of ice from a region by ice transport. An important facet of this model is that we can view a region, such as the Arctic Basin, as being a source of a river of ice. This river of ice leaves salt behind in the Arctic Basin as it freezes at its source, and delivers fresh water at its terminus somewhere in the Greenland or Labrador seas where the ice melts. Similarly, in the Antarctic this river of ice can aid in the outward expansion of the ice edge by virtue of ice's being formed near the coast and being transported outward to where it melts (see, e.g., Hibler and Ackley, 1983).

Influence of the Arctic Ocean on the North Atlantic

A caricature of the Arctic Ocean (as opposed to a toy model) is that it is an estuary receiving fresh water in the form of runoff from the large basin draining into it and from net precipitation over the ocean itself. It receives warm, salty Atlantic water from the West Spitzbergen Current. Also, it exports Arctic water in the East Greenland Current. The fresh water mixes with the salty water to form a thermocline capped by low-salinity surface water. The surface of the ocean is frozen, as a consequence of the strong negative radiation balance in the winter. The annual cycle of freezing and melting maintains a buoyant mixed layer, which limits any exchange of heat or salt with the deeper ocean. In summer, the ice shields the ocean from sunlight.

Because the ice transport out of the Arctic Basin is a major source of fresh water to the Greenland Sea, it may play a role in shutting off or maintaining that thermohaline circulation conveyer belt mechanism. The basic mechanism here is that the outward motion of ice from the Arctic Basin into the Greenland Sea, where it melts, causes a stable stratification in the Greenland Sea and hence a sealing off of the ocean and possibly a diminution of the conveyer belt. Whether the conveyer belt runs steadily or whether it is intermittently controlled by more detailed processes (most notably the various salt sources) in the North Atlantic and Greenland Sea is still unclear. In the latter hypothesis, the polar and subpolar portions of the Atlantic are believed to exert a strong influence on the conveyer belt. To clarify this point, there is a need to take a closer look at precipitation, the salt budget, and the ocean circulation-stratification problem for the Arctic and sub-Arctic regions.

In the North Atlantic, the Arctic Ocean is then a source of cold, low-salinity surface water. The fact that some of this water is frozen

may be of secondary importance. Having a large source of cold, buoyant water in a region where deep convection is supposed to occur is a potential embarrassment to theorists. Because of its low salinity and already low temperature, this water will not sink if it is cooled. It is the warm, salty Atlantic water that, after being cooled at the surface, may sink to the bottom. For deep convection to occur, the Arctic water must be shunted elsewhere. It is removed by forming the narrow East Greenland Current, which stays to the west of the regions of convection.

We can expect the Greenland Sea to be sensitive to climatic change. For one thing, it receives the ice exported from the Arctic Basin through the Fram Strait. The volume of this ice is determined by its thickness and motion, which in turn are determined by various energy fluxes and the winds and currents. All of these will change with a changing climate. About half of the ice in the Greenland Sea is formed locally in the winter and melts during the summer. As is the case with other regions of seasonal (not perennial) ice, the ice conditions are vulnerable to climate change.

The stability of the system that includes the East Greenland Current and the regions of deep convection in the Greenland, Iceland, and Norwegian seas is not known. Fluctuations that cause the buoyant Arctic water to spread out to the east might reduce or shut off the convection, with far-reaching implications for the thermohaline circulation of the world ocean.

An important issue is whether the conditions that regulate the deep convection are related to the limits of the ice extent. Thinking of the convection as part of the large-scale conveyor belt circulation, we may wonder whether the driving force is local or remote. If it is local, and related to sea ice extent in some way, the temperature of the sinking water may be fixed with respect to the freezing point, and therefore independent of global warming. In a changing climate, the location or the rate of the convection may change, but not the temperature of the downwelling water. This would be a powerful brake on global warming. On the other hand, if it is only a coincidence that the convection occurs in waters affected by the present ice edge, we should expect the deep ocean to be renewed with warmer water as the climate warms.

Another issue is the possibility of a hydrological-cycle oscillation. In this scenario, a reduction in ice extent causes greater precipitation, which in turn causes an increase in stratification, greater surface currents, and a gradual increase in ice export from the Arctic Basin, thus leading to greater ice extent. This in turn might decrease the precipitation.

The following work is needed:

- Improve our knowledge of the freshwater balance for the Arctic Ocean
- Monitor temperature, salinity, ice thickness, and ice velocity across the Fram Strait
- Model the upper Arctic Ocean, especially the role of sea ice processes in maintaining the ocean's vertical structure
- Model the Arctic Ocean circulation with the objective of learning the actual water, ice, and salt transports through Fram Strait.

Role of the Cryosphere in High-Latitude Warming under Increased CO_2

In this section, our focus is the role of sea ice (and, to a lesser extent, land snow) in the response of the high-latitude climate to atmospheric warming. The main mechanisms we will discuss are the feedback between ice extent and global albedo for both sea and land ice and increased sea-to-air heat transfer for a reduction of ice extent and thinning of ice that would occur under atmospheric warming.

Ice-Albedo Feedback and Climate

Most climate modelers include a positive ice-albedo feedback in their parameterizations. The reasoning hinges on the idea that increasing ice extent increases the global albedo. However, the extensive summer cloud cover at high latitudes means that the global albedo may not be sensitive to ice extent. That is, sunlight is now being reflected by clouds, so it cannot make much difference to the earth as a whole if sunlight is reflected by ice instead.

The relationship between sea ice extent and albedo is accessible to observations. The ice extent can be deduced from the 15-year satellite passive microwave record, because the microwave contrast between ice and water is much greater than the microwave contribution from clouds. The albedo can be determined from data collected by the Earth Radiation Budget Experiment (ERBE) satellite. A poor correlation between high albedo and ice extent would be interpreted to mean that the cloud cover remains more or less fixed despite variations in the underlying ice. On the other hand, a good correlation would mean either that the cloud cover is slaved to the ice extent or that the ice itself is contributing significantly to the albedo.

To understand the behavior of sea ice, we must know the albedo of the ice itself. Knowing the albedo at the top of the clouds is not enough. The ice albedo depends on the ice state, in particular, on the presence of snow or meltwater. The equilibrium thickness of the ice is sensitive to the albedo, because the albedo controls the sur-

face melt during the summer. Because of the persistent summer cloudiness, the ice albedo cannot be measured from space. A sequence of aircraft albedo surveys would substantially improve our knowledge of this sensitive parameter.

The working group felt that there are two additional reasons why the surface ice albedo effect cannot be discounted in any consideration of future high-latitude atmospheric warming. First, observational evidence in both the Arctic and the Antarctic shows that any modification of the surface albedo has major consequences for the summer ablation. Thus, the amount of shortwave radiation penetrating to the surface is certainly significant. Second, clouds over the pack in summer tend to be very low and foglike so that they may well act as a diffuser rather than a carrier of radiation.

High-latitude clouds are also important because of their impact on the surface energy balance. During summer, they reduce the shortwave radiation reaching the ice or sea surface. Throughout the year, they increase the downward longwave radiation. In existing model treatments of sea ice, the radiation balance is prescribed. It may now be an appropriate time to explore coupling between the ice surface conditions, such as temperature, ice concentration, and albedo, and the atmospheric conditions that determine the incoming radiation. Such a treatment would need to account for clouds.

These issues highlight the current lack of a high-latitude cloud climatology. Work within the International Satellite Cloud Climatology Project may lead to some improvement, but the difficulty in distinguishing ice from cloud has ruled out interpreting the data using algorithms that work well at lower latitudes. Effective high-latitude algorithms are sorely needed. Some progress has been reported using texture in AVHRR data to discriminate ice from cloud.

Sea Ice in the Arctic and Antarctic

Although the sea ice physics may be the same for the Arctic and Antarctic, there are considerable differences in the physical mechanisms controlling the sea ice extent in the Northern and Southern Hemispheres. In particular, in the Northern Hemisphere the northward transport of heat in the ocean plays a key role in the location of the ice edge (Hibler and Bryan, 1987), and in fact recent interannual coupled ice-ocean simulations suggest that variations in the ice margin may be affected more by changes in icean circulation than by atmospheric cooling. Also, the relatively large land mass in the Northern Hemisphere (except in the Arctic Ocean) suggests that albedo feedback effects may not be as pronounced until significant variations of the ice occur north of 70° latitude. In the Antarctic, there is only weak vertical stratification, and hence convective over-

turning plays a greater role in the ice edge and thickness. However, it was also noted in this regard that although Antarctic sea ice simulations based on thermodynamics considerations alone need to invoke large amounts of heat flux to explain the summer ice decay, simulations including full ice dynamics can yield a realistic ice decay without large amounts of oceanic heat flux. This is mainly due to the creation of leads by ice dynamics, which increases radiation absorption and accelerates the ice decay in the spring, as well as to ice transport, which moves large amounts of ice into open water to be melted (see, e.g., Hibler and Ackley, 1983).

For the Antarctic, we would expect the ice-albedo feedback to operate effectively as normally perceived, i.e., an increased warming leads to less ice extent and hence more radiation absorption. In the Arctic, on the other hand, the ice-albedo feedback effect is significantly constrained by the land geography and the ocean circulation. Atmospheric circulation models with only a mixed-layer ocean probably have too much ice in the control case and hence may well overestimate the effects of albedo feedback on enhanced high-latitude warming in the Arctic.

With regard to the geographical constraints on Arctic sea ice, the land snow albedo feedback may compensate for the reduced ocean area (until the Arctic Basin is reached), although the seasonal cycle of amplified warming may be different than that obtained with sea ice due to the high heat capacity of the land.

Treatment of Sea Ice

In modeling both the Arctic and the Antarctic, the timing of the maximum warming is likely to be affected by the treatment of sea ice employed. In particular, the use of a thermodynamics-only sea ice model will lead to positive feedback effects whereby there will be greater sea-to-air heat fluxes under warming due to thinner ice. However, if we replace a thermodynamics-only model with a model where the growth is mainly over leads (continually created by dynamical effects), then we would have a negative feedback effect with less sea-to-air heat exchange under an atmospheric warming. All warming effects may be modified by the presence of water vapor in the air, which will increase the downward longwave radiation. For a smaller warming, ocean circulation effects may constrain many of the feedback effects in the Arctic ice margin.

Needed Observations

A variety of observations could be made over the next several decades to detect CO_2 warming or verify some of the above theories.

In the Arctic, because of the critical control of the ocean on the ice margin, it may not be possible to deduce much from ice edge variations. However, it may be possible to get some indication of atmospheric warming from monitoring the ice thickness in the Arctic Basin. In this regard one of the most promising measurements would be moored, upward-looking sonar buoys at several locations in the basin (and possibly in the Fram Strait) that would supply a long time series of measurements of the thickness distribution of the sea ice. Regular oceanic measurements of temperature and salinity in the Greenland and Norwegian seas as well as oceanic transport characteristics through the Fram Strait would be most valuable with regard to the salt budget in the ocean.

In the case of the Antarctic ice cover it may be that ice extent variations obtained from passive microwave satellite observations can give us some insight into long-term atmospheric warming or cooling in the Southern Hemisphere.

The following work is needed:

- Develop cloud climatologies for the Arctic and Antarctic
- Correlate ice extent and planetary albedo
- Develop a toy model linking ice surface and clouds
- Study high-latitude behavior in current GCMs
- Improve the observational base for surface radiation balance.

References

Hibler, W.D. , III, and S.F. Ackley. 1983. Numerical simulation of the Weddell Sea pack ice. *Journal of Geophysical Research 88*, 2873–2887.

Hibler, W.D., III, and K. Bryan. 1987. A diagnostic ice-ocean model. *Journal of Physical Oceanography 17*, 987–1015.

Methods of Testing Parameterizations: Vertical Ocean Mixing

Eli Tziperman

Introduction

Because the ocean is stratified, water parcels move more easily horizontally along surfaces of constant potential density (isopycnals) than across these surfaces. Any movement across isopycnal surfaces must involve a change in gravitational energy, as well as a density change of the moving water parcel. This change occurs through vertical mixing with water of different potential density above or below. Vertical mixing in the ocean has an important role in maintaining the oceanic stratification at a steady state: The air-sea fluxes continuously cool and heat the surface water, thereby forming cold bottom water and warm surface water. The vertical mixing processes balance the air-sea fluxes by mixing the cold and warm water, to form the mid-density water found throughout the water column in the ocean. But the vertical mixing also presents a difficult challenge to the oceanographer interested in modeling the large-scale ocean circulation.

The ocean's velocity field is characterized by an exceptional variety of scales. While the small-scale oceanic turbulence responsible for the vertical mixing in the ocean is of scales a few centimeters and smaller, the oceanic general circulation is characterized by horizontal scales of thousands of kilometers. In oceanic general circulation models (GCMs) that are typically run today, the vertical structure of the ocean is represented by a few tens of discrete grid points, whose separation varies from a few meters near the surface of the ocean to hundreds of meters in the deep water. Such models cannot explicitly model the small-scale mixing processes, and must, there-

fore, find ways to parameterize them in terms of the larger-scale fields. Finding a parameterization that is both reliable and plausible to use in ocean models is not a simple task. Vertical mixing in the ocean is the combined result of many complex processes, and, in fact, mixing is one of the less known and less understood aspects of the oceanic circulation. In present models of the oceanic circulation, the many complex processes responsible for vertical mixing are often parameterized in an oversimplified manner. Yet, finding an adequate parameterization of vertical ocean mixing is crucial to the successful application of ocean models to climate studies. We will see below that the results of general circulation models for quantities that are of particular interest to climate studies, such as the meridional heat flux carried by the ocean, are quite sensitive to the strength of the vertical mixing.

Below we try to examine the difficulties in choosing an appropriate vertical mixing parameterization, and the methods that are available for validating different parameterizations by comparing model results to oceanographic data. First, some of the physical processes responsible for vertically mixing the ocean are briefly mentioned, and some possible approaches to the parameterization of these processes in oceanographic general circulation models are described in the following section. We then discuss the role of the vertical mixing in the physics of the large-scale ocean circulation, and examine methods of validating mixing parameterizations using large-scale ocean models.

Physical Processes Responsible for Oceanic Mixing/ Mixing Parameterizations for Large-Scale Models

Many physical processes participate in creating the small-scale turbulence (e.g., wave dynamics, shear flow, salinity gradients, and wind forces) responsible for vertical mixing in the ocean (Turner, 1981). Each of these processes may be dominant under different circumstances, at different times, and at different geographic locations. In addition, each of these small-scale vertical mixing mechanisms depends on the larger-scale fields in a different way, and may therefore require a different parameterization. In this section we briefly describe some of the vertical mixing mechanisms and discuss some of the commonly used parameterizations of vertical mixing in oceanic GCMs. Our purpose here is not to present an extensive review of vertical mixing parameterizations, but merely to demonstrate the difficulty in making a vertical mixing parameterization that accurately represents the variety of vertical mixing mechanisms. The terms "vertical mixing" and "cross-isopycnal mixing" are often used inter-

changeably, and we will do so below, but it is useful to keep in mind that what is meant in both cases is the mixing of water across surfaces of constant potential density. Although isopycnal surfaces in the ocean are nearly horizontal, and therefore the cross-isopycnal direction is nearly the same as the vertical direction in most places, the distinction is still important, as we will see below.

Constant Coefficient Parameterization

Simple scaling arguments based on the shape of the vertical temperature profile in the ocean immediately lead to the conclusion that mixing must be much larger than can be explained by molecular diffusivity, indicating the presence of small-scale turbulent mixing. Assuming that the small-scale turbulence in the ocean interior is of uniform intensity, it can be modeled with constant turbulent mixing coefficients, analogous to the molecular diffusion coefficients. Allowing for different vertical and horizontal mixing due to the preference of horizontal mixing in the ocean, we obtain the following advection diffusion equation for the temperature (T),

$$\frac{\partial T}{\partial t}+u\frac{\partial T}{\partial x}+v\frac{\partial T}{\partial y}+w\frac{\partial T}{\partial z}+K_v\frac{\partial^2 T}{\partial z^2}+K_h\left(\frac{\partial^2 T}{\partial x^2}+\frac{\partial^2 T}{\partial y^2}\right) \qquad (1)$$

where K_h and K_v are the horizontal and vertical mixing coefficients, and $K_h \gg K_v$; (u,v) and (x,y) are the horizontal velocity components and coordinates; w is the vertical velocity; z is the local vertical coordinate; and t denotes time. Such constant eddy coefficients, although clearly oversimplified, are still the most commonly used parameterization of oceanic mixing in general circulation models (K. Bryan, 1969; F. Bryan, 1987).

Tensor Diffusivities Parameterization

The strong horizontal mixing represented by the large horizontal mixing coefficient K_h in Equation (1) is due to oceanic mesoscale eddies, which are circulation features of horizontal scale of tens to hundreds of kilometers. These eddies do not mix water horizontally, but in fact along isopycnal surfaces that may be tilted relative to the horizon. The large horizontal mixing coefficient meant to represent these eddies in Equation (1) causes strong mixing in the horizontal direction and may therefore result in a much too strong cross-isopycnal mixing when the isopycnals are not exactly flat. In order to accurately separate long-isopycnal and cross-isopycnal mixing, and thus to better parameterize the cross-isopycnal mixing in which we are interested here, the mixing coefficients K_h and K_v in Equation (1) may be replaced by the more complex tensor diffusivities (Redi, 1982). These diffusivities guarantee that the mixing is stronger

along the direction of the isopycnals, and prevent the artificially strong cross-isopycnal mixing evident in models using the constant coefficient parameterization in Equation (1).

Stratification-Dependent Mixing Coefficients

An important source for turbulent energy in the interior of the ocean is the breaking of internal waves. Internal waves, expressed as the motion of the density layers in the ocean, are characterized by scales of kilometers and hours, and the amplitude of vertical movement of a given isopycnal layer due to these waves may be on the order of 10 m. These waves may break, like surface ocean waves, and produce patches of turbulence. The resulting small-scale turbulence is not uniform, but varies in intensity from place to place, and therefore cannot be represented by the simple constant mixing coefficient model. There are theoretical as well as experimental indications (Gargett and Holloway, 1984; Gargett, 1984) that when the small-scale turbulence comes mainly from internal wave breaking, the dependence of the vertical mixing coefficient on the vertical density stratification $\rho(z)$ may be written in terms of the buoyancy frequency, N, as

$$K_v = a_0 N^{-q} \qquad \text{where } q \approx 1, \text{ and } N^2 = -\frac{g}{\rho_0}\frac{\partial \rho}{\partial z} \tag{2}$$

a_0 is an empirical constant, g is the gravitational acceleration, and ρ_0 is a constant reference density. This parameterization is simple enough to use in a numerical general circulation model, and has more of a physical justification than the constant coefficient parameterization. This is a good example of the way in which work on the physics of small-scale mixing processes can benefit general circulation modeling. This form (and other possible ones) of the vertical mixing coefficient still needs to be validated using oceanographic data, as will be discussed below.

Richardson Number Parameterization

A vertically sheared flow (that is, a velocity in the horizontal direction whose magnitude changes with depth) in a stratified fluid may be unstable to small perturbations when the Richardson number, Ri, which is the ratio of the buoyancy frequency and the vertical velocity shear, is less than the critical value of 1/4. So when the Richardson number is near its critical value we may expect strong mixing to occur. In order to parameterize this instability, the following simple form of vertical mixing coefficient was suggested by Pacanowski and Philander (1981) and used by various researchers:

$$K_v = \frac{K_{max}}{(1+\alpha Ri)^n} + K_{background} \tag{3}$$

where K_{max} and $K_{background}$ are two values for the vertical mixing coefficient, with $K_{max} \gg K_{background}$, and α and n are adjustable empirical parameters. With an appropriate choice for α and n, the vertical mixing coefficient calculated by Equation (3) is small in most cases, near the "background" value. When the Richardson number approaches its critical value of 1/4, so that instability and strong vertical mixing may be expected to occur, the vertical mixing coefficient becomes large, of the size of K_{max}.

Different Eddy Coefficients for Temperature and Salinity

Salt fingering is an instability of the stratification caused by the different molecular diffusivities of heat and salt, and it may occur where warm, salty water lies above cold, fresh water. The instability results in finger-shaped intrusions at the interface of the different water masses, and eventually leads to strong mixing that is seen as vertical steps in the temperature and salinity profiles. There are some indications that the turbulent fluxes of heat and salt resulting from the occurrence of double diffusive salt fingers are not equal. This may justify using different values of eddy mixing coefficients for temperature and salinity in general circulation models. (There are also some more sophisticated parameterizations of mixing due to salt fingering, based on the relative magnitude of the local salinity and temperature gradients.)

Overturning Mixing Parameterization

A particularly important vertical mixing mechanism that occurs only in limited regions of the world ocean is that involved in water-mass formation. A statically unstable water column (heavy water above light water) may lead to strong vertical motion and mixing (convection). This typically happens in polar regions, where strong cooling of the surface water results in its sinking to the bottom. To represent such a process in oceanographic models, regions of unstable density profile are often simply vertically mixed together to uniform temperature and salinity at every time step (Cox, 1984). This mixing parameterization is based on the assumption that the strong vertical velocities due to the convection rapidly mix the parts of the water column where convection occurred.

Surface and Boundary Mixing Parameterization

A large portion of the mixing in the ocean occurs at the surface, and near the bottom and side boundaries. The wind forcing at the

surface of the ocean is an important energy source for mixing within the surface mixed layer. Similarly, the bottom boundary induces strong mixing in bottom boundary layers. To parameterize the wind mixing one could use one of the simpler models, such as the constant eddy coefficient parameterization, with a larger value for K_v near the surface, or some parameterizations of mechanical mixing depending on the wind stress strength are possible as well.

The side boundaries (i.e., continental slope, islands) are also a source of strong vertical mixing, through the breaking of internal waves incident on these boundaries, through upwelling or downwelling induced by the presence of the boundary, etc. It is not obvious what is the proportion of boundary mixing relative to interior mixing in the ocean, a question of obvious importance as far as mixing parameterizations for oceanographic models are concerned. Laboratory experiments have shown that a system where all the vertical mixing occurs near the boundaries, and where the vertically mixed water is rapidly advected from the boundaries into the interior by the velocity field or by the strong horizontal mixing, may seem very similar to a system where the vertical mixing occurs in the interior only. More work is required in order to improve our understanding of the boundary mixing mechanisms and in order to find ways to adequately parameterize them in general circulation models.

Turbulence Closure Models

Most of the above parameterizations are to some extent ad hoc solutions guided by the need to find a simple enough way of including the turbulent mixing in general circulation models. A more rigorous approach is that of turbulence closure models, which try to explicitly model the turbulent transports of heat and salt (and momentum) in terms of the larger-scale known fields (Mellor and Yamada, 1974). This approach was used mostly in upper ocean models, where it may be expected to improve the representation of the mixed layer dynamics.

There are various other instabilities and physical processes leading to vertical mixing, but for our purpose it is sufficient to note the large variety of processes leading to vertical mixing in the ocean. The variety of existing parameterizations indicates that the problem of finding an adequate parameterization for oceanic vertical mixing is far from being solved.

Role of Vertical Mixing in the General Circulation Dynamics

Before examining the efforts to validate mixing parameterizations using oceanographic data, it is instructive to first try and understand

the role of mixing in the dynamics of the oceanic general circulation. Consider, for example, the equation for the temperature in the ocean. Using simple scaling arguments it is easy to show that the effect of mixing on the temperature field is *locally* negligible compared to that of the advection by the oceanic horizontal velocity field. In terms of the simple advection diffusion model of Equation (1) this implies

$$\left(u\frac{\partial T}{\partial x}, v\frac{\partial T}{\partial y}\right) \gg \left[K_v\frac{\partial^2 T}{\partial z^2}, K_h\left(\frac{\partial^2 T}{\partial x^2}+\frac{\partial^2 T}{\partial y^2}\right)\right] \tag{4}$$

But this does not mean that mixing, and in particular vertical mixing, may be ignored in ocean models. In fact, when it is ignored for the purpose of modeling the wind-driven ocean circulation, the basic stratification of the ocean cannot be determined from the model but must be specified externally. Such ideal fluid models that do not include mixing in the dynamics (Luyten, et al., 1983; Rhines and Young, 1982) must specify the density stratification on, say, the eastern boundary of the ocean, and can only calculate the horizontal variation of the stratification relative to this basic stratification. In order to be able to calculate the basic stratification as well, one must include in the model both air-sea fluxes and interior vertical mixing processes.

The interior vertical mixing determines the oceanic stratification by balancing the water mass formation by air-sea heat fluxes. These fluxes cool the surface water in polar regions, and the resulting colder and denser water then sinks to the bottom of the ocean to form the bottom water masses. The air-sea heat fluxes also warm the surface water in the tropical and midlatitudes. This production of cold and warm water by the air-sea interaction is continuously balanced through the mixing of warm surface water and cold bottom water. Warm and cold water produced by the air-sea fluxes are turned by this mixing into mid-density water found in the ocean interior, and the stratification is thereby kept at a steady state. A similar picture applies to the modification of the oceanic salinity by precipitation and evaporation, and its balance by the mixing of water masses of different salinities.

In summary, vertical mixing is, locally, a second-order effect; yet, it is a process of major importance due to its role in the global budget of heat and salt in the oceans: Vertical mixing balances the water-mass formation by air-sea fluxes, and therefore is responsible for maintaining the ocean stratification at steady state.

It is important to note that in the context of global warming and models addressing the greenhouse problem, only some of the vertical mixing processes are significant. The time scales involved in the ther-

mocline problem and in the global heat and salt balances discussed above are of thousands of years, and the slow interior vertical mixing is therefore of major importance for these problems. The global warming problem is more concerned with the shorter time scales (10–100 years) required, for example, to mix atmospheric CO_2 into the upper ocean. For this purpose, faster mixing processes such as deep convection and mixing within the mixed layer and upper ocean are relevant and need to be carefully modeled and validated.

Validating Vertical Mixing Parameterizations Using Large-Scale Ocean Models

The variety of vertical mixing parameterizations mentioned above makes it obvious that no single satisfactory vertical mixing parameterization yet exists. New parameterizations and especially reliable methods for validating these parameterizations are clearly needed.

There are two main approaches to testing mixing parameterizations. The first involves laboratory or field experiments in order to compare the mixing predicted by a given parameterization with the mixing actually measured in the experiment. (See Gargett, 1984, for a review of such studies trying to deduce the dependence of the vertical mixing coefficient on the stratification.) But this approach does not directly test the effect of the different parameterizations on global ocean models, which are our main interest here. It is also not possible to examine in a single experiment the combined effect of the wide variety of mixing processes active in the ocean. We will, therefore, concentrate on efforts to validate vertical mixing parameterizations using general circulation data and the models themselves. We first discuss the sensitivity of general circulation models to vertical mixing parameterizations, and then describe the efforts to deduce mixing coefficients from general circulation data using inverse methods.

Sensitivity of Large-Scale General Circulation Models to Vertical Mixing

Before considering different parameterizations to be used in ocean models, it is sensible to try and find out the sensitivity of the model results to the choice of vertical mixing parameterization. Only if the results prove to be sensitive to the choice of parameterization, does it make sense to proceed and look for the optimal parameterization to use.

Sensitivity studies of ocean general circulation models involve running the model using a variety of choices for the model parameters. For this purpose, it is not possible to use the high-resolution (eddy resolving) ocean models, because the computational cost is forbid-

ding even when using the most powerful present-day computers. As a result, the common practice for sensitivity studies is to use low-resolution models that are relatively inexpensive to run. In such a study, Bryan (1987) used a primitive-equation general circulation model, within an idealized ocean basin, to examine model sensitivity to vertical mixing. He ran the model using a constant coefficient parameterization for the vertical mixing, and varying the magnitude of the vertical mixing coefficient. Bryan examined the dependence of the meridional heat flux carried by the ocean on the value of the vertical mixing coefficient (Figure 1). The maximum poleward flux varies from about 0.2 x 10^{15} W for K_v = 0.1 cm^2/s to 1 x 10^{15} W for K_v = 2.5 cm^2/s. Note that both values for the vertical mixing coefficients lie in the range of values suggested by observations, which further emphasizes the difficulty of finding a reliable parameterization for the vertical mixing. The ocean carries the poleward transport of heat through the meridional circulation cell: Warm surface water moves poleward, where it is cooled by the atmosphere, sinks to the bottom, and returns equatorward as cold bottom water. His results show that the strength of the meridional circulation is clearly sensitive to the vertical mixing coefficient, which results in the sensitivity of the meridional heat flux to this parameter (Figure 2). The depth of the oceanic

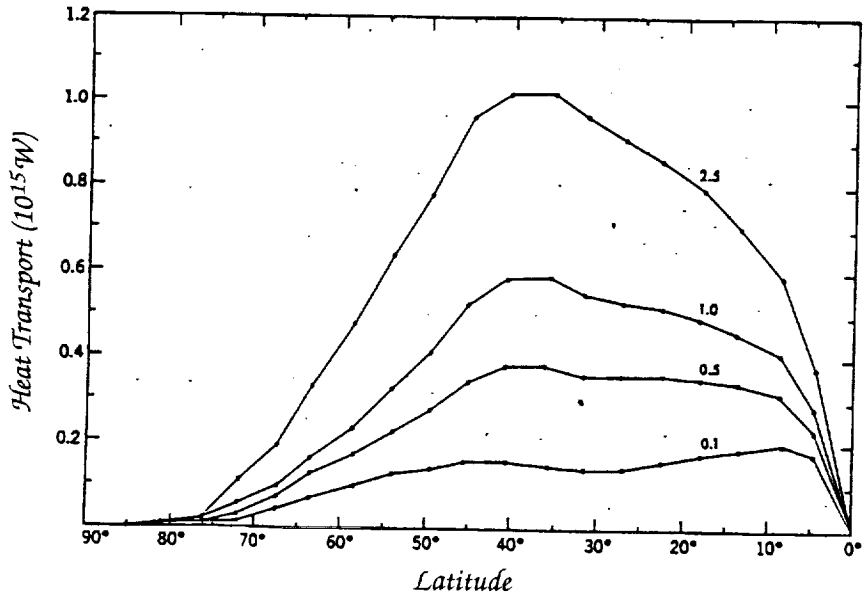

Figure 1. Dependence of the poleward heat transport in an oceanic primitive-equation model on vertical diffusivity (vertical mixing coefficient values vary from 0.1 to 2.5) (from Bryan, 1987; ©American Meteorological Society).

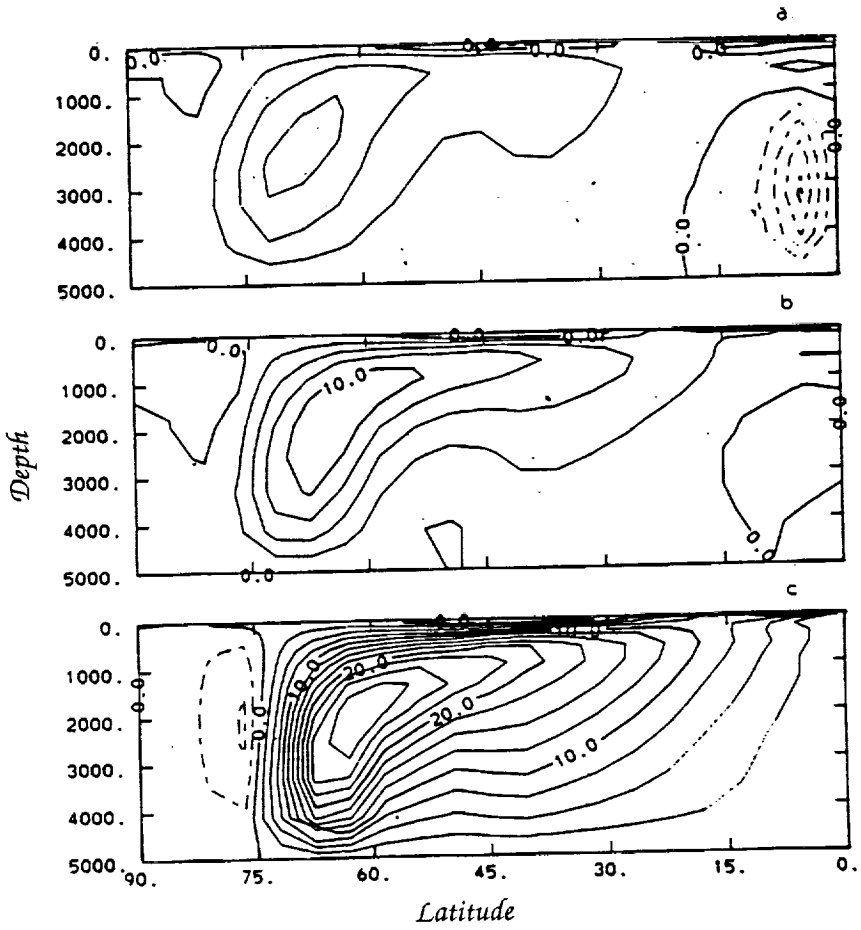

Figure 2. The meridional turning cell stream function calculated using a primitive-equation model, for three choices of the vertical mixing coefficient (from Bryan, 1987; ©American Meteorological Society).

main thermocline is another parameter of interest for climate studies, being relevant among other things to the total heat storage of the oceans. Figure 3 shows the zonally averaged thermocline structure calculated by Bryan for various choices of the vertical mixing coefficient. Again it is obvious that making the correct choice for the vertical mixing coefficient is critical for large-scale ocean modeling.

A similar sensitivity study was carried out by Colin de Verdiere (1988), using a simpler GCM that allows an even more extensive study of the sensitivity of the model results to various model parameters. He again found the meridional heat transport to be sensitive to the vertical mixing coefficient. Figure 4 summarizes his results, showing the sensitivity of various quantities of interest to the value of the vertical mixing coefficient.

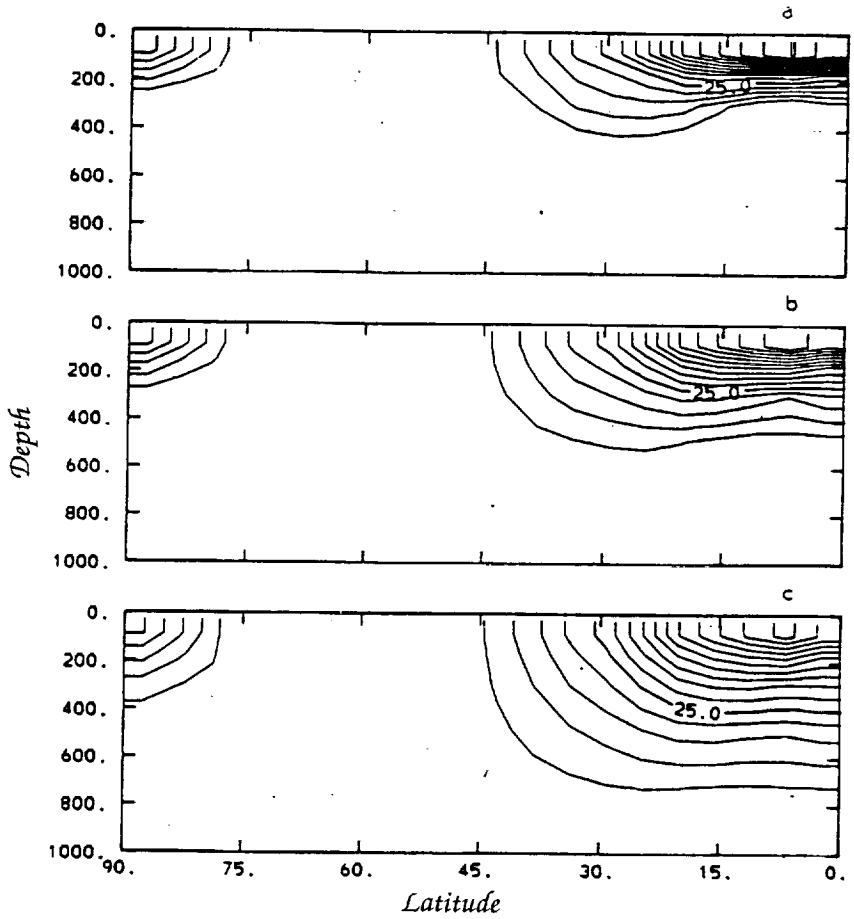

Figure 3. Zonally averaged thermocline in an oceanic primitive-equation model, for three choices of the vertical mixing coefficient (from Bryan, 1987; ©American Meteorological Society).

Validating Vertical Mixing Parameterizations Using Numerical GCMs

Having established that using the right value of the vertical mixing coefficient is crucial, and therefore more generally that using the right vertical mixing parameterization is important, we now consider the problem of choosing an appropriate parameterization for a numerical oceanic general circulation model from the many possible parameterizations presented above. The most straightforward method, which is often also the only one used, is to run the model with various possible parameterizations, and qualitatively compare the model results to the available observations for temperature, salinity, etc. By such a qualitative comparison of the main features of the data and model results, it is decided whether the parameteri-

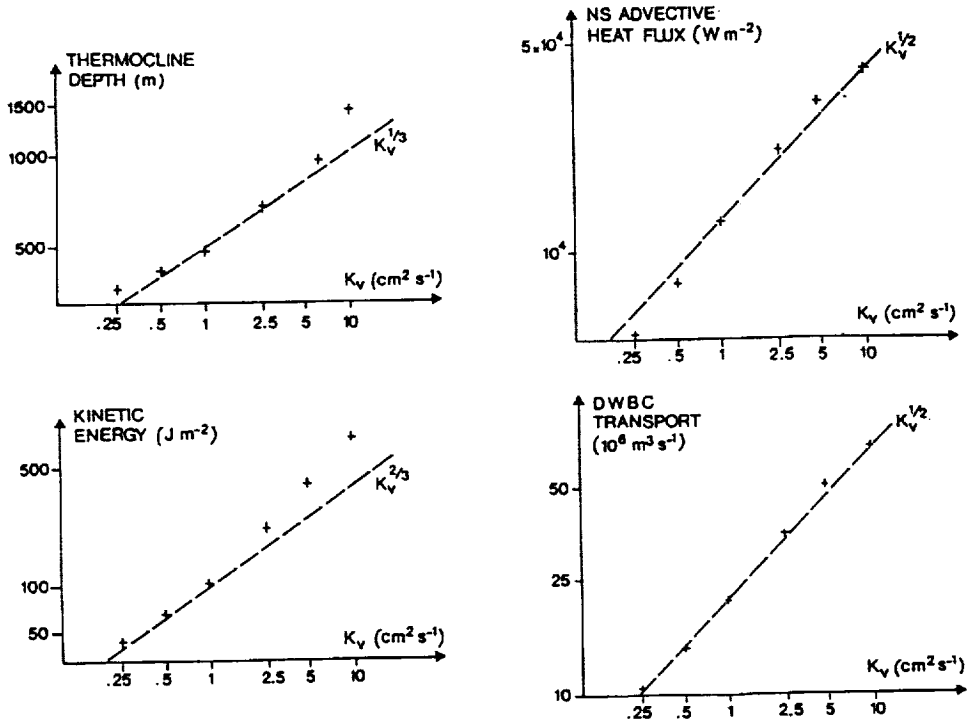

Figure 4. Mean thermocline depth, northward advective heat flux, kinetic energy, and deep western boundary current transport as function of the vertical mixing coefficient K_v, as calculated using a simple oceanic general circulation model (from Colin de Verdiere, 1988; used with permission).

zation is successful. Below are a few examples of validating vertical mixing parameterizations this way, and then a discussion of the limitations of this approach.

Richardson Number Parameterization

In an effort to develop an adequate vertical mixing parameterization for models of the tropical oceans, Pacanowski and Philander (1981) have demonstrated that using the Richardson number parameterization shown in Equation (3) results in a better fit to the data than using the constant coefficient vertical mixing parameterization. Figure 5 shows three temperature sections along the equatorial plane. The first is based on observations, the second is calculated by a general circulation model using constant vertical mixing parameterization, and the third is calculated using the Richardson number parameterization. It seems from these results that the Richardson number parameterization is indeed preferable, at least as far as equatorial ocean modeling is concerned.

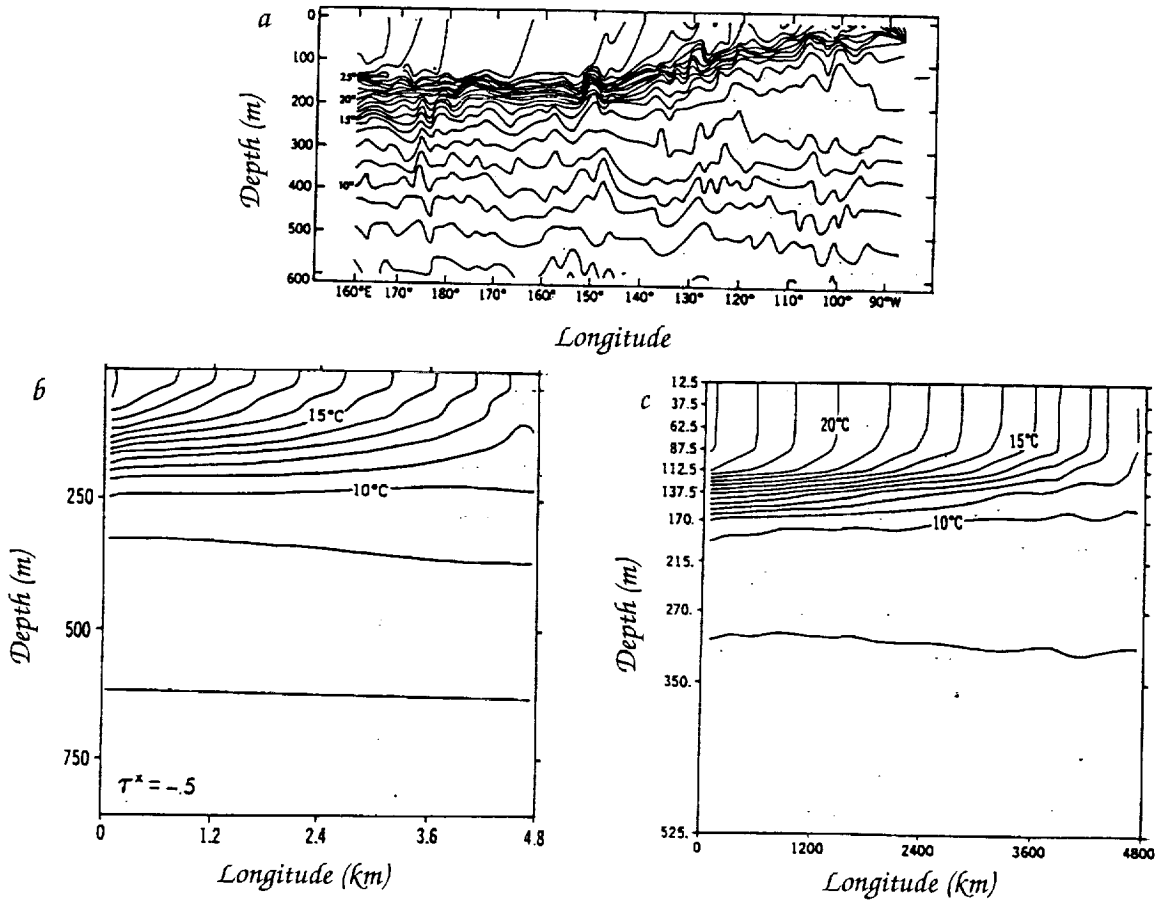

Figure 5. Three temperature sections along the equatorial plane: (a) based on observations, (b) from a model using constant vertical mixing, and (c) from a model using the Richardson number parameterization (from Pacanowski and Philander, 1981; ©American Meteorological Society).

Turbulence Closure Models

The closure model of Mellor and Yamada (1974) was applied to several upper ocean models and offers an alternative to the simple constant coefficient vertical mixing parameterization. Rosati and Miyakoda (1988) compared the performance of the constant coefficient parameterization with that based on a closure model and nonlinear viscosity. Figure 6 compares the observed Pacific Ocean sea surface temperature to that calculated by a variety of models, differing in mixing parameterizations as well as in atmospheric forcing frequency. Rosati and Miyakoda concluded that the more sophisticated closure parameterization works better than the one using constant mixing coefficients, although there are still misfits to the data whose sources are unclear.

Tensor Diffusivities

In the next few years coarse-resolution models, rather than high-resolution eddy resolving models, may still be expected to be used for climate studies because of the limits set by the available computational resources. For such coarse-resolution models it is most

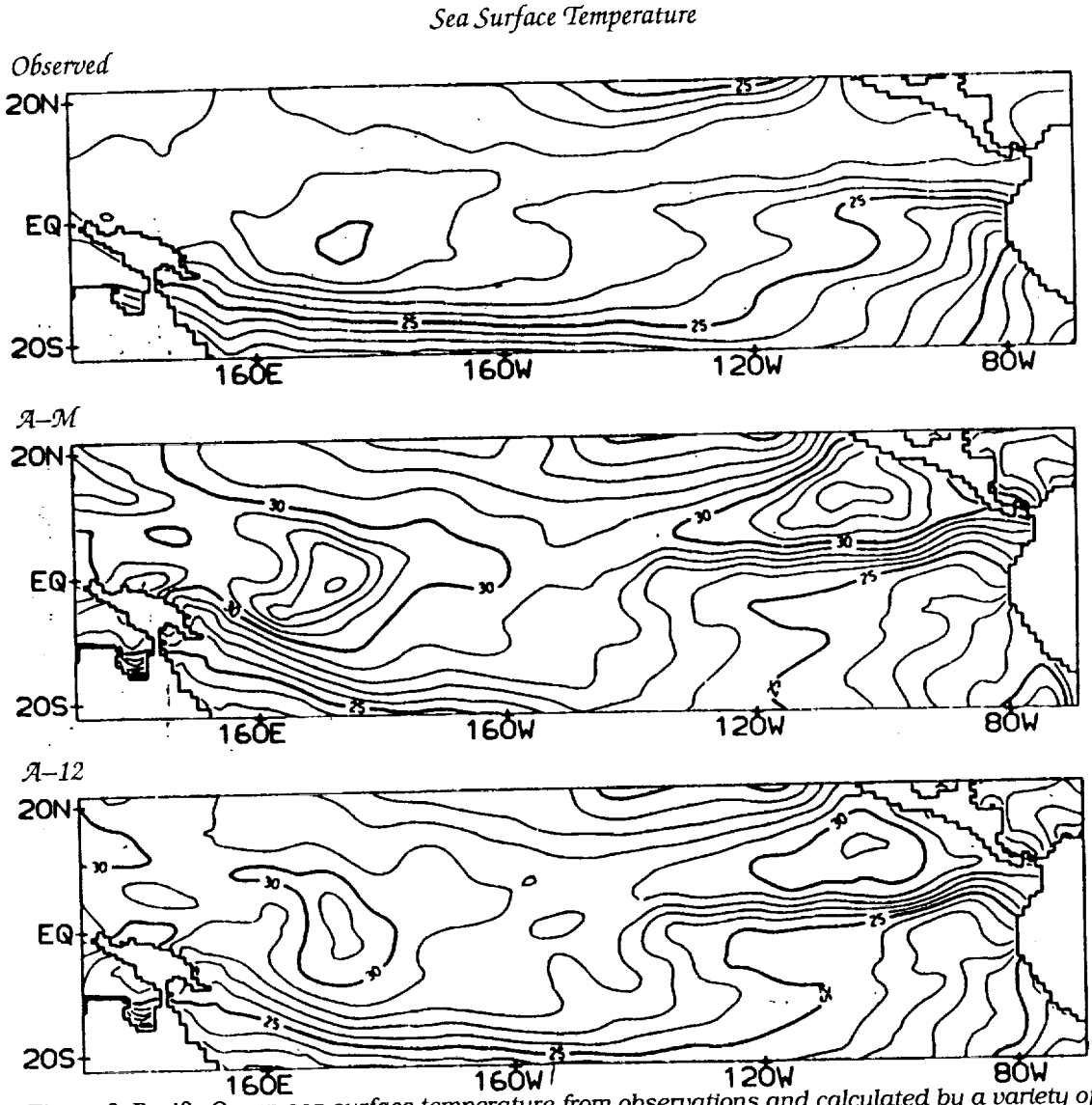

Figure 6. Pacific Ocean sea surface temperature from observations and calculated by a variety of models differing in the mixing parameterizations as well as atmospheric forcing frequency. A-M and A-12 are constant coefficient models. E-M and E-12 are models using a turbulence closure scheme. (M and 12 refer to monthly and 12-hour frequency of the atmospheric surface forcing used in the model) (from Rosati and Miyakoda, 1988; ©American Meteorological Society).

important to correctly parameterize the effect of mesoscale eddies. The mixing parameterization using tensor diffusivity, which can differentiate between long-isopycnal and cross-isopycnal mixing rather than between horizontal and vertical mixing, may be a reasonable substitute to using eddy resolving models in the near future. The tensor diffusivity prevents the artificially strong cross-isopycnal mixing created by the large horizontal mixing coefficients in regions where isopycnals are tilted relative to the horizon. Some long-term integrations with a coarse-resolution model using such tensor diffusivities were recently carried out by K. Bryan, resulting in an improved fit to some of the patterns of the oceanic stratification.

Discussion

The above common approach to validating parameterizations using GCMs suffers some obvious limitations. First, if there is a misfit between model results and data, it is not obvious which of the many model inputs is responsible. The problem could lie in using the wrong value for the vertical mixing coefficient, or in using the wrong model for the mixing process. But the problem could also be an error in the wind forcing at some location over the ocean, in the tracer boundary conditions that were not set correctly (e.g., in simulations

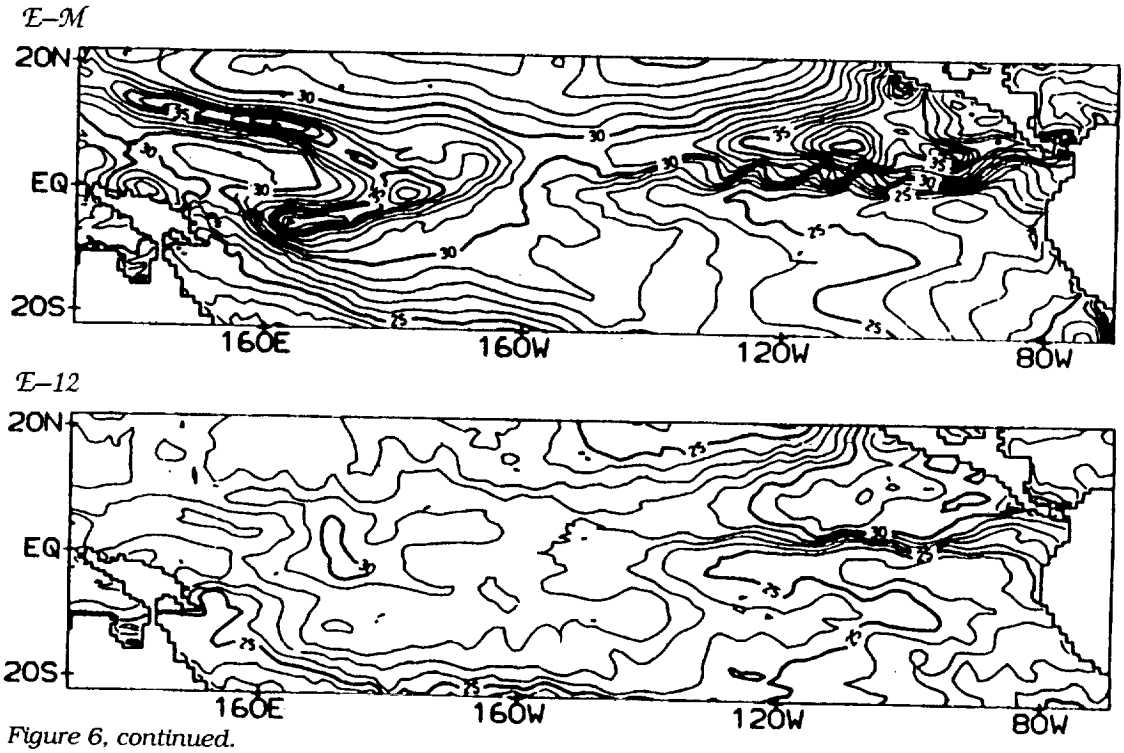

Figure 6, continued.

of tritium or ^{14}C), or in one of the many other different model inputs. Because of the large number of model inputs, it is not possible to vary each one separately in order to find its optimal value resulting in the best fit to observations. But changing only one of the inputs in order to improve the fit to observations may be misleading as well. By changing, for example, only the vertical mixing parameterization in order to better fit the data, we may be compensating for some completely different problem in another model input. Such a compensation will be an ad hoc solution only, and will most probably not work in another ocean basin, or under different physical conditions.

A second problem with the above approach to model validation is its inability to directly and quantitatively use the wealth of available oceanographic data to correct the model inputs or parameterizations. Model validation is mostly limited to a qualitative comparison of model results and data, and does not involve a quantitative comparison, use of error estimate for the data, etc. This inability to use the increasing number of oceanographic observations is in particular disturbing now that many new techniques of making oceanographic observations are becoming available, especially through remote sensing methods. A way must be found to use all of the available information in order to improve oceanic general circulation models.

An alternative to using general circulation models for validating model parameterizations that may overcome some of the above difficulties is the use of inverse methods. These methods use oceanographic data in order to calculate various unknown model parameters, and offer some advantages for model validation and parameter estimation, as discussed in the following subsection. Inverse methods are not meant to replace the general circulation models for the purpose of predicting the ocean's role in climate change, for example, but to quantitatively confront these models with the available data, in order to try and improve their less certain aspects.

Calculating Mixing Coefficients Using Inverse Methods

The original motivation for using the inverse methodology in oceanography was in trying to resolve the classical problem of level of no motion (Wunsch, 1978). The traditional dynamic method for calculating the oceanic circulation from temperature and salinity data used the simple geostrophic equations in order to calculate the horizontal velocity field in the ocean, relative to the velocity at some specified reference depth. In order to make that an absolute velocity estimate, one often assumed the velocity to vanish at some deep reference level—the level of no motion—and calculated the velocity relative to that level. The choice of this level was usually based on some subjective criteria, and the purpose of introducing the inverse

methodology to this problem was to use our knowledge of the ocean dynamics in order to quantitatively calculate the absolute velocity field. Later the method was also used to estimate mixing coefficients from oceanographic temperature and salinity data.

Using inverse methods, the velocity field and mixing coefficients are calculated by requiring the ocean to satisfy the conservation equations of mass, heat, and salt. Let us demonstrate this using the simple steady state temperature equation,

$$u\frac{\partial T}{\partial x}+v\frac{\partial T}{\partial y}+w\frac{\partial T}{\partial z}=K_v\frac{\partial^2 T}{\partial x^2}+K_h\left(\frac{\partial^2 T}{\partial x^2}+\frac{\partial^2 T}{\partial y^2}\right)\pm\varepsilon(x,y,z) \qquad (5)$$

where $\varepsilon(x,y,z)$ denotes the error in this equation due to measurement errors in the temperature field. Evaluating the temperature gradients appearing in Equation (5) from the data, we can obtain a linear system of equations for the velocity field and the mixing coefficients. (In fact the geostrophic equations are also used, to relate the three-dimensional velocity field to the known density and to an unknown reference velocity that is calculated together with the mixing coefficients.) In addition to solving for the unknown parameters, the inverse solution also provides the important resolution information and error estimates that together indicate which parameters can actually be solved for from the data, and what is the expected error for the estimated parameters.

Several variations on this approach have been used to try and calculate mixing coefficients from hydrographic data. Figure 7 shows the cross-isopycnal (vertical) mixing coefficient calculated by Olbers et al. (1985), using a beta spiral inverse method and sophisticated tensor diffusivities parameterization for the mixing processes. Olbers et al. found, however, that the mixing coefficients in general, and the vertical mixing coefficient in particular, are calculated with large error bars and cannot be distinguished from zero in most cases.

Hogg (1987) inverted the Levitus (1982) data for temperature, salinity, and oxygen in a region of the North Atlantic ocean. He fitted an advection diffusion equation to the data and calculated both the velocities and the mixing coefficients for various mixing models, including the vertical mixing low given in Equation (2). Hogg found that the velocities calculated by the inverse were not sensitive to the particular form of mixing parameterization used, but the mixing coefficients were very sensitive to the details of the mixing model used.

The difficulties found by these studies seem to be representative of a general problem concerning the calculation of mixing coefficients from data. It is often found that the coefficient could not be

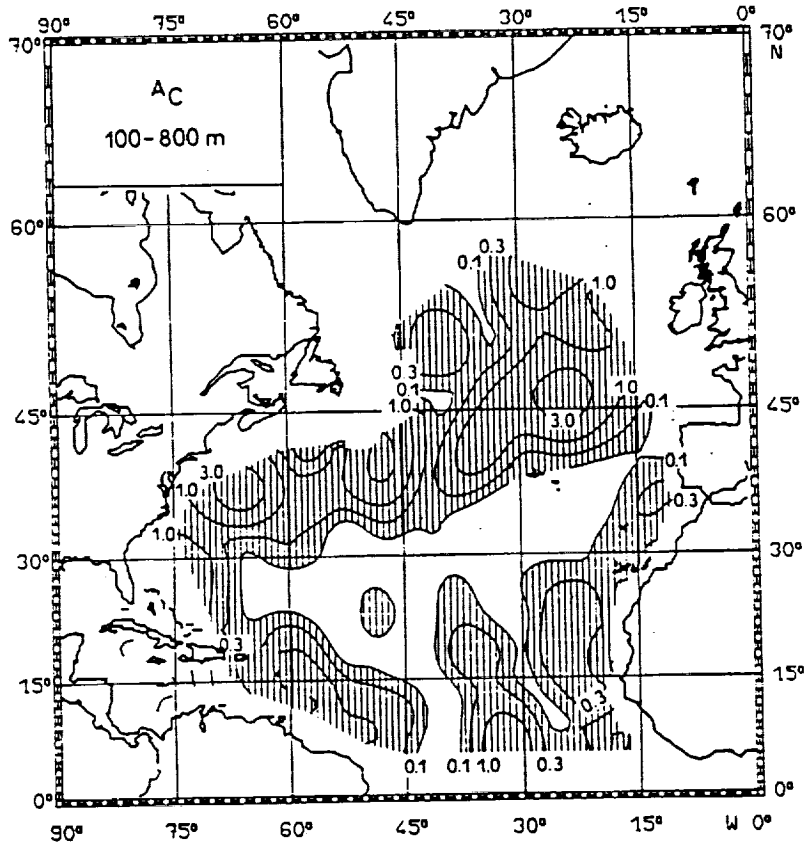

Figure 7. Cross-isopycnal mixing coefficient calculated for 100–800-m depths using a beta spiral inverse model of the North Atlantic (from Olbers et al., 1985).

resolved by the data, or that the large error estimates make them indistinguishable from zero, or that the values of the coefficients are too sensitive to the particular form of mixing model assumed.

The difficulty in calculating mixing coefficients can be explained using the fact that mixing is, locally, a second-order effect (Tziperman, 1988). As explained above, the mixing terms in the temperature equation are small compared to the advection terms. Figure 8 shows a vertical profile of the different terms in the temperature equation evaluated from data in the Mediterranean Sea where the velocities and mixing coefficients are calculated using an inverse model. The mixing terms are clearly smaller than the advection terms throughout the water column, and they can be as small as the noise in the equation [$\varepsilon(x,y,z)$ in Equation (5)]. The expected error in the horizontal advection terms [$u(\partial T/\partial x)+ v(\partial T/\partial y)$] is on the order of ε, which is much smaller than these terms. As a result, the error in the calcu-

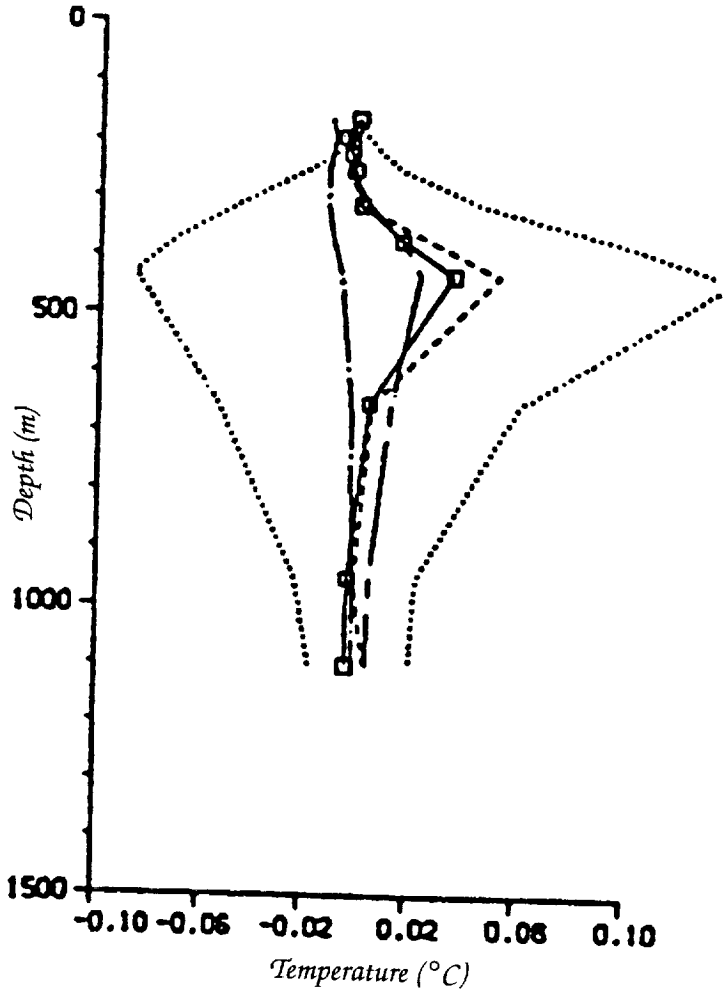

Figure 8. A vertical profile of the different terms in the temperature equation evaluated from data in the Mediterranean Sea where the velocities and mixing coefficients are calculated using an inverse model. Dotted lines are the horizontal advection terms, uT_x, vT_y; the dashed line is the sum of the horizontal advection terms, $uT_x + vT_y$; the chain–dotted line is the vertical advection term wT_z; and the chain–dashed line is the vertical diffusion term $[K_v(z)T_z]_z$ (from Tziperman, 1988; ©American Meteorological Society).

lated horizontal velocities (u,v) is relatively small. But because the mixing terms, and in particular the vertical mixing term $[K_v(\partial^2 T/\partial z^2)]$, are on the order of the noise ε, the error in the mixing coefficients could be on the order of the coefficients themselves.

In other words, the solution for the mixing coefficients is controlled by the noise level in the data. It is no surprise, therefore, that the coefficients calculated from hydrographic data are mostly statistically indistinguishable from zero, and that the solution for them is most sensitive to the exact parameterization used for the mixing processes. The problem clearly lies in our attempt to calculate the mixing coefficients from *local* balances, while they are physically significant only in determining the *global* balances in the ocean (and in the model). Furthermore, some of the inverse calculations, forced by the limitations on the number of equations that can be handled simultaneously, have not been able to calculate a mass conserving velocity field. It is difficult to justify the calculation of a second-order physical effect such as mixing, when the first-order requirement of mass conservation cannot be satisfied by the inverse solution.

In order to be able to obtain useful estimates for the mixing coefficients, it seems that an inverse model must have (at least) the following properties. First, its physics should include all second-order physical effects that may be of the same order as the vertical mixing we wish to estimate. This includes, for example, the nonlinear terms in the momentum equations that may be important in certain oceanic regions. In the absence of some second-order physical effects in the model, the inverse model may try to compensate for their lack by artificially modifying the mixing coefficients, resulting in a wrong solution for them. Next, the model should be of fairly high resolution in order to enable the estimation of various second-order terms in the model equations, which cannot be estimated in coarse-resolution box models. The inverse model should not be local in the sense that it needs to be mass conserving and satisfy all model boundary conditions for the velocity field. The above three requirements are equivalent to simply specifying that the physics and resolution of the inverse model should be similar to those used in oceanic general circulation models. Finally, although of high resolution, the inverse model should allow for global constraints such as requiring the total water-mass dissipation due to vertical mixing throughout the basin to exactly balance the water-mass formation by air-sea fluxes. Because vertical mixing has a dominant role in such global constraints, unlike its role in the local dynamics, using such constraints may enable us to obtain useful information about the vertical mixing.

But trying to formulate even a moderate-resolution inverse model that uses nonlocal constraints leads to a huge system of equations

(equations for the temperature, salinity, mass conservation, etc., at every grid point) that cannot be solved on any of the present-day computers. More sophisticated mathematical methods are needed for such large-scale optimization problems, and such a method has recently been introduced into the fields of meteorology and physical oceanography. This method, known as the optimal control or adjoint method, allows the efficient combination of a complex general circulation model and oceanographic data. The method has been suggested as an assimilation technique (Le Dimet and Talagrand, 1986; Long and Thacker, 1989), but can also serve as a powerful and efficient inverse procedure in oceanography (Tziperman and Thacker, 1989). Because a full numerical general circulation model is used in the inverse calculation, all second-order physical effects are included, and the resolution may be fairly high. Additional global balances may be added as constraints in the inverse calculation, as may be needed in order to resolve the mixing processes.

Given a numerical general circulation model, the adjoint method can be used to calculate the temperature, salinity, velocity, surface forcing by wind and air-sea heat fluxes, and mixing coefficients, all of which satisfy the model equations and boundary conditions, and at the same time fit the available data. A crucial component of the method is a numerical model composed of the adjoint equations of the GCM that is fitted to the data. The adjoint model is used, within an iterative procedure, to calculate the unknown parameters (surface forcing, mixing parameters, etc.) in an efficient and elegant way.

The use of the adjoint method in oceanography is still at a preliminary stage, but the method is most promising, and may be expected to serve as a useful tool for the purpose of model validation and parameter estimation. In particular, it should prove helpful in the effort to produce reliable vertical mixing parameterizations for large-scale oceanographic models. Given several vertical mixing parameterizations, they can all be included in a general circulation model, each with a weight factor determining its importance in the model equations. The weights may then be calculated by the adjoint method by requiring the inverse calculation to choose the parameterization that results in the best fit to the available data, thereby indicating which parameterization is the most appropriate.

Summary and Conclusions

Oceanic general circulation models have become quite sophisticated in recent years, and are now used with high eddy resolving resolution and realistic basin geometry and atmospheric forcing. Despite these improvements, these models are unlikely to be able to

directly resolve the small-scale physical processes responsible for vertical mixing in the ocean. Yet, some of the most basic elements of the oceanic circulation, such as the vertical structure of the main thermocline and the meridional transport of heat by the ocean, are quite sensitive to the vertical mixing parameterization. Models that are used for climate studies can greatly benefit, therefore, from an adequate parameterization of the vertical mixing processes in the ocean. (Note that models addressing the problem of greenhouse warming during the next 100 years or so will mostly benefit from improved parameterizations of only some of the mixing processes—in particular, those that are responsible for upper ocean mixing and that act on the tens of years time scale.) Because vertical mixing is the combined effect of many different and complex processes in the ocean, it is still not well understood, nor is there a single best parameterization that can represent this mixing in oceanographic models. More research is needed to both develop and validate vertical mixing parameterizations for large-scale ocean models.

Oceanic general circulation models are the main tool for investigating the role of the oceans in the climate system, but they are difficult to use at present for testing different vertical mixing parameterizations. These models are very expensive to run and are affected by quite a few input parameters and subgrid parameterizations for which no sufficient information is available, and of which vertical mixing is only one example. It is most difficult, therefore, to run the general circulation models for all possible combinations of unknown model inputs in order to choose the optimal inputs that best fit the oceanographic data. In addition, general circulation models cannot make a direct use of most of the available oceanographic data for calculating unknown input parameters. The large quantities of oceanographic data now available from classical measurements and through remote sensing methods can be used mostly for qualitative comparisons to model results. One would like to be able to use these data in order to quantitatively calculate unknown model inputs.

Inverse models may, in principle, be used for estimating unknown input model parameters from oceanographic data, but still may encounter serious difficulties in inferring mixing processes from the available data. These difficulties arise from the fact that mixing processes, although important in setting the global balances of heat and salt in the ocean, are locally negligible compared with other physical processes in the ocean. The small local effect of the mixing, on the tracer fields in particular, is near the noise level of the data. An inverse model that is to calculate useful estimates for the mixing processes needs to be able to handle the global constraints that may be able to constrain the mixing processes in the ocean. In addition,

such an inverse model should have both high resolution and the ability to handle second-order physical effects (such as nonlinear dynamics) that may have a comparable effect to that of vertical mixing. However, the limitations on the dynamics and resolution of inverse models set by the available computational resources have prevented so far the use of such inverse models for validating mixing parameterizations.

With new mathematical methods now becoming available, it may be possible to use the dynamics and resolution of general circulation models in inverse calculations, as well as to use global constraints for testing mixing parameterizations against oceanographic data. This must, of course, be accompanied by more work on the physics of the small-scale processes responsible for vertical mixing in the ocean, and the development of better parameterizations. The combination of better parameterizations and reliable validation procedures will, hopefully, result in useful vertical mixing parameterizations for oceanographic models, and therefore in better ocean models for climate studies.

References

Bryan, F. 1987. Parameter sensitivity of primitive equation ocean general circulation models. *Journal of Physical Oceanography 17*, 970–985.

Bryan, K. 1969. A numerical method for the study of the circulation of the world ocean. *Journal of Computational Physics 4*, 347–376.

Colin de Verdiere, A. 1988. Buoyancy driven planetary flows. *Journal of Marine Research 46*, 215–265.

Cox, M.D. 1984. *A Primitive eEquation 3 Dimensional Model of the Ocean.* GFDL Ocean Group Technical Report No 1, Princeton University, Princeton, New Jersey.

Gargett, A.E. 1984. Vertical eddy diffusivity in the ocean interior. *Journal of Marine Research 42*, 359–393.

Gargett, A.E., and G. Holloway. 1984. Dissipation and diffusion by internal waves breaking. *Journal of Marine Research 42*, 15–27.

Hogg, N.G. 1987. A least square fit of the advective diffusive equations to the Levitus atlas data. *Journal of Marine Research 45*, 347–375.

Le Dimet, F., and O. Talagrand. 1986. Variational algorithm for analysis and assimilation of meteorological observations: Theoretical aspects. *Tellus 38A*, 97–110.

Levitus, S. 1982. *Climatological Atlas of the World Ocean.* NOAA Technical Paper 3, 173 pp.

Long, R.B., and W.C. Thacker. 1989. Data assimilation into a numerical equatorial ocean model. I. The model and assimilation algorithm. *Dynamics of the Atmosphere and Oceans 13*, 379–412.

Luyten, J.L., J. Pedlosky, and H. Stommel. 1983. The ventilated thermocline. *Journal of Physical Oceanography 13*, 292–309.

Mellor, G.L., and T. Yamada. 1974. A hierarchy of turbulent closure models for planetary boundary layers. *Journal of the Atmospheric Sciences 31*, 1791–1806.

Olbers, D.J., M. Wenzel, and J. Willebrand. 1985. The inference of North Atlantic circulation patterns from climatological hydrographic data. *Reviews of Geophysics 23*, 313–356.

Pacanowski, R., and S.G.H. Philander. 1981. Parameterization of vertical mixing in numerical models of tropical oceans. *Journal of Physical Oceanography 11*, 1443–1451.

Redi, M.H. 1982. Oceanic isopycnal mixing by coordinate rotation. *Journal of Physical Oceanography 12*, 1154–1158.

Rhines, P.B., and W.R. Young. 1982. A theory of the wind-driven circulation. I. Mid ocean gyres. *Journal of Marine Research 40(Suppl.)*, 559–596.

Rosati, A., and K. Miyakoda. 1988. A general circulation model for upper ocean simulations. *Journal of Physical Oceanography 11*, 1601–1626.

Turner, J.S. 1981. Small scale mixing processes. In *Evolution of Physical Oceanography* (B.A. Warren and C. Wunsch, eds.) MIT Press, Cambridge, Massachusetts.

Tziperman, E. 1988. Calculating the time-mean oceanic general circulation and mixing coefficients from hydrographic data. *Journal of Physical Oceanography 18*, 519–525.

Tziperman, E., and W.C. Thacker. 1989. An optimal control/adjoint equations approach to studying the oceanic general circulation. *Journal of Physical Oceanography 19*, 1471–1485.

Wunsch, C. 1978. The general circulation of the North Atlantic west of 50°W determined from inverse methods. *Reviews of Geophysics 16*, 583–620.

The Challenge of Identifying Greenhouse Gas–Induced Climatic Change

Michael C. MacCracken

Introduction

Observations and diagnostic studies clearly indicate that the atmospheric concentrations of CO_2 and other trace gases have been rising steadily as a consequence of human activities. Laboratory experiments demonstrate that these increased concentrations will enhance the infrared absorptive capacity of the atmosphere, thereby intensifying the natural greenhouse effect that sustains the earth's climate well above freezing. Theoretical calculations suggest that the enhanced greenhouse effect since the 18th century should have measurably warmed the global climate, and indeed some warming has apparently occurred. Some environmentalists are suggesting that these results alone require that societal activities be substantially altered to prevent further climatic change. Critics may agree to cost-effective actions that also serve other purposes, but argue that the theoretical projections must be observationally confirmed before drastic steps are taken. This confirmation that greenhouse gas emissions are indeed causing significant climatic change has become a critical research challenge.

Successfully meeting this challenge is critical for several reasons. First, it would provide an affirmation of scientific understanding of the climate system, confirming that its behavior can be projected, at least within some limits to be identified. Second, being able to confirm that the enhanced greenhouse effect is occurring on a global scale will help in reducing uncertainties (i.e., constraining the range of possibilities suggested by models) and in enriching our understanding about how climate changes may be evidenced on a regional

scale. Third, being able to say with high statistical confidence that the initial stages of the changes have been identified and attributed to greenhouse gases will provide an incentive for enhanced efforts to improve understanding of potential impacts on societal resources and public and political appreciation of the need to consider societal responses to limit or adapt to future changes in climate.[1]

Meeting the challenge of identifying greenhouse gas–induced climatic change involves three steps. First, observations of critical variables must be assembled, evaluated, and analyzed to determine that there has been a statistically significant change. Second, reliable theoretical (model) calculations must be conducted to provide a definitive set of changes for which to search. Third, a quantitative and statistically significant association must be made between the projected and observed changes to exclude the possibility that the changes are due to natural variability or other factors. This paper provides a qualitative overview of scientific progress in successfully fulfilling these three steps.

Selecting Climatic Measures

Climate is a term that encompasses the mean and the higher statistical moments of all measures of the state of the atmosphere, the oceans, the cryosphere, and, in its broadest sense, at least some descriptors of the biosphere. For a number of reasons, the search for changes has been and must be narrowed to a limited set of variables.

Of primary importance, accurate observational records of the climatic parameters need to exist over a long enough time to determine whether a change has occurred. This requirement is not easily satisfied. First, the observations must be taken with sufficient precision that real changes can be distinguished from ones due to changes in instruments, in measurement protocol (e.g., time of day of measurement), and in or around the measurement location (e.g., station moves, urbanization, desertification, irrigation). Although there are a number of approaches to adjusting the observational record to account for such shortcomings, experience indicates that, because most observations are taken to aid in weather prediction rather than to document climatic change, the "corrections" are often nearly as large or larger than the greenhouse signal to be identified.

---

[1]It should be noted that detection of change will likely mean that an independent mathematician would be convinced that the present climate is different than that for some period in the 19th century, and not that a recent or sudden change has occurred, as so often seems to be implied by press accounts. Given the large range of paleoclimatic changes, being able to totally rule out natural variations as a cause may not be possible.

Second, the length of the record must be sufficiently complete (i.e., without long gaps) and long enough that the long-term changes associated with the changing greenhouse gas concentrations can be distinguished from fluctuations due to other factors. Natural fluctuations and variations can occur on scales from seasonal to interannual to decadal and longer and can result from inherent natural variability (e.g., atmosphere-ocean coupling) and radiative forcings other than those due to changes in greenhouse gas concentrations (e.g., volcanic activity, solar variability). Because the forcing-response patterns of these nongreenhouse variations are poorly understood, the requirement to have a long record is reinforced because of the need to establish a baseline climate to which to reference the greenhouse-induced change. Because the concentration changes (and presumably the induced climatic changes) have been occurring for more than 200 years and because climatic observations go back only about 100 years, even the longest sets of observations available allow examination only of trends (or changes in trends). These limits on the length of the record thus complicate identification of the greenhouse signal. (There are proxy or reconstructed records that extend further into the past, but these measures are less accurate due to the assumptions and transfer techniques that must be used to make them equivalent to presently observed climatic parameters.)

Because the temporal variability of the climate increases as the spatial scale decreases, having records of climatic variables over large areas allows averaging that tends to reduce the variability and more clearly shows the smaller, longer-term changes in climate. It is thus desirable to have records that can be used to generate hemispheric or global averages. This requirement, however, conflicts with the earlier requirements because spatial coverage generally decreases for older records (particularly over ocean areas and in the Southern Hemisphere). Ensuring consistency of instrument usage and the need to average records of different stations also can introduce difficulties. These difficulties include uneven spacing of stations, the differing baseline conditions at different stations (a factor that usually leads to averaging of deviations from a baseline value rather than averaging of the observations themselves), differing durations of the records at different stations, and different types of instruments and measurements in different regions (land vs. ocean, one country vs. another, etc.).

Given these many complications, the set of variables that might be analyzed to seek greenhouse gas–induced climatic change is not large. Table 1 lists parameters that might be analyzed. The entries are separated into those for which reasonable records exist and

Table 1: Parameters expected to be changed by greenhouse gas–induced climatic change

Parameters for which useful records exist
Near-surface air temperature
Sea surface temperature
Stratospheric temperature
Precipitation over land
Sea ice extent
Sea level
Parameters for which limited areal or temporal records currently exist
Tropospheric temperature
Upper ocean temperature*
Subsurface temperature (e.g., in permafrost)
Atmospheric water vapor
Snow cover/mountain glacier extent
Ocean circulation/salinity
Atmospheric chemistry
Ecological systems (extent and character)

*Over the next decade, a new acoustic measurement technique may elevate this parameter to the first category because the noise level of the technique is quite low.

those for which records may be developed in the future, but for which there are now overriding limitations in the areal extent of the measurements or the length and consistency of the record.

For those measures for which there is an extended record, there remains a range of problems in attempting to determine trends. None of the records is long enough to provide a baseline climate before greenhouse gas concentrations started to increase. Most statistical techniques assume the individual (e.g., annual) data points are independent and/or normally distributed, neither of which is true for climatic data; as a consequence, such techniques must be applied with caution. The limited length of the record, low-frequency variability, and changing spatial coverage of the measurements further complicate the analysis (Wigley et al., 1985).

Although the discussion here will cover only those parameters for which extended records now exist, there is great expectation that new techniques will make additional records available over the next decade. For example, Spencer and Christy (1990) are using satellite microwave radiance data to derive a precise, low-noise measure of midlevel tropospheric temperatures, and Munk (Gibbons, 1990) proposes to use acoustic signals to provide a temperature record of similar quality for the upper ocean. Permafrost temperature records will also become more abundant as measurements are made in the Eurasian Arctic.

At present, however, the set of measures now available to use in seeking to identify greenhouse gas–induced climatic change is

rather limited, consisting mainly of temperature, sea ice, and sea level. In addition, none of the records goes back in time before the start of significant increases in the concentration of greenhouse gases; as a result, we have no truly independent and highly resolved record of the natural variability of the climate.

Theoretical Estimates of Climatic Change

The concentrations of greenhouse gases have been increasing since the mid-1700s, with the CO_2 concentration having increased about 25% and the CH_4 concentration having more than doubled (Watson et al., 1990). These changes would imply that the climate has therefore been changing due to these emissions for more than 200 years, albeit at first quite slowly. If we are to be able to associate past changes in climate with these increasing concentrations, we must have available theoretical estimates of what the induced changes in climate were. Although climate models have been improving over their 30-year history, there has not yet been even one globally resolved model calculation attempting to simulate the last 200 years. There have been very few calculations attempting to realistically simulate the last 30 years (Hansen et al., 1988). That model had a simplified ocean and did not represent the residual effects of concentration changes earlier than its starting date of 1958, even though Hansen et al. (1988) estimate that the e-folding time of the oceanic response was of the order of 100 years.

Given the requirement for a theoretical estimate of the change to demonstrate identification (or detection), the lack of such an estimate obviously prevents attainment of the objective, at least without approximation. This failure to conduct the required simulation arises not primarily because of limitations in computer resources (although this is an important constraint). First, we do not have information about initial oceanic conditions, and about volcanic eruptions, solar variability, and other natural climate-forcing factors that would also be affecting the climate. Second, we do not yet have adequately verified, coupled atmosphere-ocean models capable of such simulations. Third, any such simulation experiment must be made in recognition of the confounding influence of natural variability, which is not yet either adequately understood or properly treated in the models. As a consequence, we are quite far from having the necessary model simulation(s) to permit accurate estimation of greenhouse gas–induced climatic change.

To sidestep this lack of the proper simulation, estimates of the greenhouse gas–induced climatic changes are commonly used, even though there are many simplifications and pitfalls involved in devel-

oping these approximations. The preferred technique for deriving estimates of the climatic change expected over the industrial period is to interpolate between equilibrium simulations of one and two times the 1950 (or thereabouts) concentration of CO_2, using the radiative forcing at the tropopause from the increasing concentrations of CO_2 and other trace gases as the interpolant. Account must also be taken of the role of the oceans in diminishing or postponing some fraction of the scaled equilibrium change, which requires that we understand how the oceans work. Modeling studies indicate that the instantaneous climatic effect may be reduced by 20–50% and that the oceanic response time may be from a few decades to much more than a century. Paleoclimatic studies suggest that the entire oceanic circulation can respond, which would further complicate the estimation of the expected change.

In addition to the uncertainties introduced because of limitations of and differences among models (which are extensive; see Grotch and MacCracken, 1991), this interpolative approach assumes that equivalent global radiative forcing by CO_2 and other trace gases will have the same climatic effect (see, however, Wang et al., in press, which suggests this may not be the case), that equilibrium climatic changes will look like time-dependent changes, and that climatic change is linear in radiative forcing. Each of these assumptions is known to be at least slightly incorrect. Different trace gases have different latitudinal and altitudinal effects on radiation. Model simulations of transient changes (e.g., Schneider and Thompson, 1981; the most recent general circulation model results are reviewed in Bretherton et al., 1990) indicate that changes are not equally proportional at all locations, and clearly the large temperature changes associated with the meltback of Arctic ice are not equal in all seasons, but occur initially in the transition seasons rather than in winter as doubled CO_2 simulations would suggest. Lorenz (1984) has pointed out that the climate may not be transitive; that is, the climate may have more than one stable state. As a consequence, it is conceivable that the climate may not change gradually, but rather may jump from one state to another, thereby nullifying the linear assumption. (The relatively rapid warmings centered around 1920 and 1980 would seem to support this proposition.) Theoretical calculations (Wigley and Schlesinger, 1985) also suggest that the climatic change at any time is dependent on the rate of change of forcing and the ultimate equilibrium change, thereby moderating the linear approximation. As other examples of nonlinearity, precipitation patterns shift (causing wetter and drier changes that cannot be linearly approximated), mountain glaciers eventually completely disappear, and sea level increase has a very long time constant because of the time for heat uptake in the deep ocean.

Brushing aside all of these approximations and uncertainties (and more), radiative model calculations (Shine et al., 1990) suggest that the greenhouse forcing at the tropopause has been 2.45 W/m^2 since 1765 (about 1.92 W/m^2 since 1900) in comparison to the 4.4 W/m^2 usually associated with a CO_2 doubling. If temperature changes are linear in forcing and the climatic sensitivity to a CO_2 doubling is 1.5 to 4.5°C, then, before accounting for ocean lag, the expected equilibrium temperature change since 1750 is about 0.8 to 2.5°C (about 0.65 to 1.95°C since 1900). Although not valid on a local basis, the realized temperature changes (i.e., estimates for which the effect of the ocean thermal inertia has been accounted) are about 50 to 80% of these equilibrium changes. Based on these techniques (invalid as they may be), temperature changes from 1765 to the present are expected to be about 0.4 to 2.0°C (0.35 to 1.6°C since 1900). If we also assume that the latitudinal pattern of the changes will be consistent with the equilibrium changes (probably a poor assumption, as indicated above), the present temperature changes are expected to be about twice the global average at high latitudes and one-third to one-half the global average at low latitudes.

Stratospheric temperatures at about 25 km, for which there would be somewhat less effect of the oceanic lag,[2] would be expected to have dropped about 2°C since 1765 and about 1°C since 1960, when a reasonably representative array of observations started to become available. Interpolation would suggest that global precipitation should have increased several percent, especially in high latitudes, although the high interannual and spatial variability would make these changes very difficult to identify (Bradley et al., 1987). Sea ice should have melted back, although models do not include processes such as sea ice advection that may obscure or compensate the meltback. Models of sea level increase are relatively limited, emphasizing the component due to thermal expansion, but not adequately treating changes in mountain glaciers or in the polar icecaps. Simplified ocean models suggest that a rise in sea level of 0.1 to 0.2 m might be expected based on predicted climatic changes of the last 150 years, but no comprehensive calculation has been done that treats all factors (and calibrated simulations with simplified models do not provide an independent check).

Thus, even allowing for approximations, the set of parameters that are expected to have changed in a manner that is detectable is

---

[2]Although the radiative time constant is short, stratospheric temperature changes will also depend on the tropospheric temperature change, which is delayed.

quite sparse and so uncertain that achieving definitive identification of the greenhouse signal is quite problematical.

Has the Climate Changed as Expected?

Not only are the observational data sets and the model estimates limited, but additional problems arise in attempting to associate changes with the increasing concentrations of greenhouse gases in a quantitative manner. The primary difficulty is that the climate has varied on many different time and space scales due to many factors in addition to changes in the concentrations of greenhouse gases. Examples of factors generally considered external to the climate system include volcanic eruptions and solar variations, although it appears that the flux changes caused by such factors are less than for trace gases (Hansen and Lacis, 1990). Paleoclimatic records suggest that, in addition to responding to cyclic variations in the earth's orbit and to changes in atmospheric composition, the climate has varied, even on relatively short time scales (decadal to centennial), by substantial amounts solely as the result of internal variability. These internal variations are also apparent in the historical record (the Medieval Warm Period, ca. A.D. 1100–1250, was probably somewhat warmer than present, and the Little Ice Age, ca. A.D. 1450–1850, somewhat cooler) and in year-to-year climate variations. Thus, in evaluating whether the climate has changed, the role of other factors in inducing climatic change must also be distinguished from the greenhouse gas–induced effects, even though we are even less certain of the types of climatic change that these other factors may have induced.

In spite of all of these limitations, it is nonetheless interesting to evaluate how well the observed changes in climate match the theoretically calculated changes. Changes in near-surface air temperature have been considered most often. (Changes in sea surface temperature give quite similar results.)

Figure 1 displays the estimates of Northern Hemisphere, Southern Hemisphere, and global changes in near-surface air temperature compiled by Jones et al. (1991) from land and marine records. Comparable data sets have been assembled by Hansen and Lebedeff (1988) and by Vinnikov et al. (1990), each making different adjustments to assure homogeneity and representativeness of the records. Problems remain with each set, particularly concerning spatial coverage and urbanization around stations, but these are steadily being reduced.

The records show significant year-to-year variability, especially in the 19th century, probably an artifact of the more limited spatial coverage of the observations. Although there is a general increase in

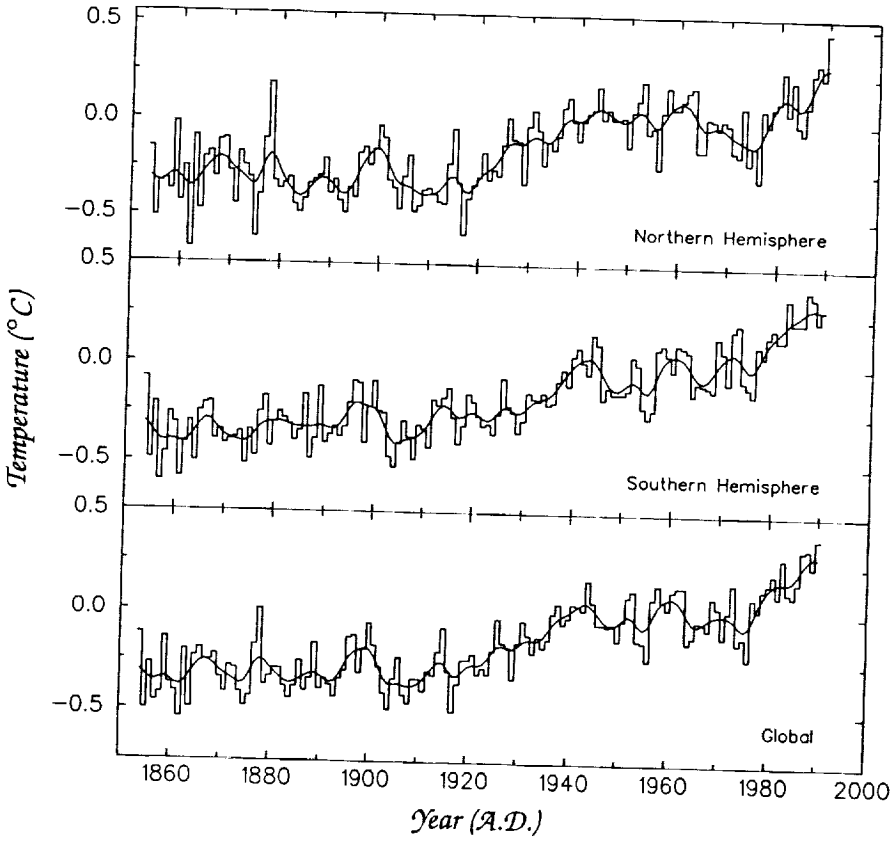

Figure 1. Area-weighted estimates of annual temperature departures from a reference normal for the Northern Hemisphere, Southern Hemisphere, and global land and ocean areas for the period since 1860 (Jones et al., 1991).

the temperature, the increase is less steady in the Northern than in the Southern Hemisphere, with a rapid rise in the early 20th century followed by a period of slight cooling from 1940 to the 1970s followed by a rapid rise. This uneven pattern of rise is most evident in the Northern Hemisphere land record, which is often cited as evidence that recent changes in climate are due at least in part to factors other than the greenhouse effect (e.g., natural variability, sulfate aerosols).

It is also important to understand that these curves are composited from values at many individual points. Although the year-to-year variation of the global mean is only about 0.5°C, the standard deviation of the set of individual grid-point values about the global average value was about 0.75–1°C prior to 1940, then decreasing to about 0.5°C (Grotch, 1987). Figure 2 presents a three-dimensional histogram of the distributions of individual grid-point values for

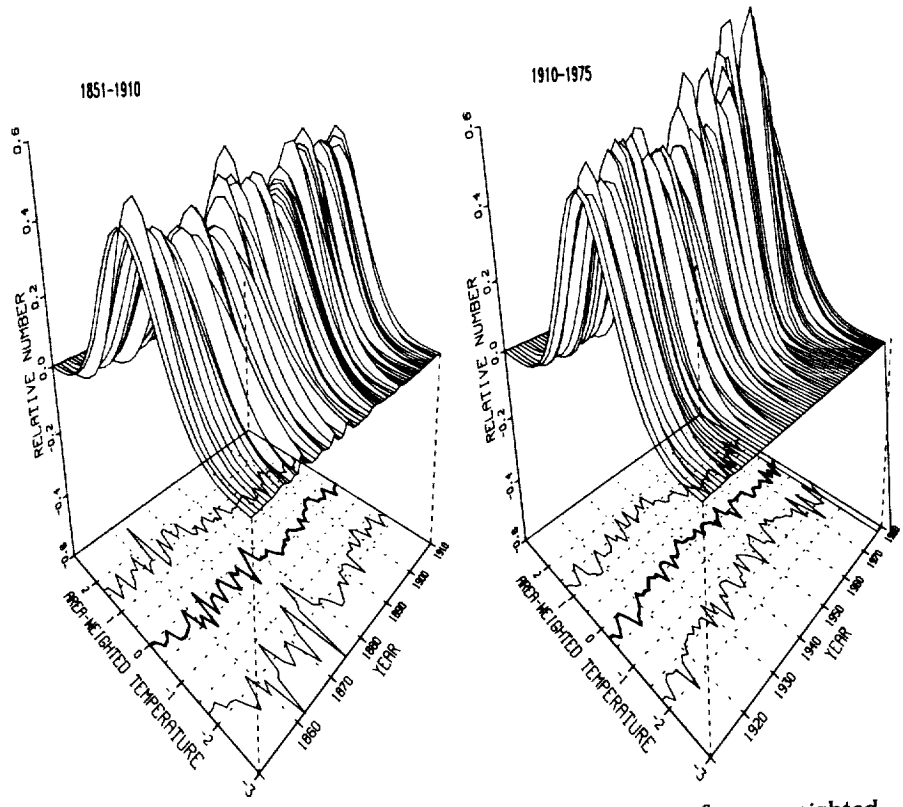

Figure 2. Three-dimensional histogram of the distribution of area-weighted temperature anomaly over time (CRU data 1850–1976). The values for each year are assumed to be normally distributed. On the lower surface, the estimated average anomaly is drawn as a heavy solid line and the ±2σ estimates are shown as lighter lines (Grotch, 1987).

each year of the record, illustrating that the changes in the mean are well within the bounds of past variations; that is, although the mean is increasing, particular locations can have quite different annual anomalies than the global mean. Grotch (1989) has shown that the correlation between changes at individual grid points and the global (or hemispheric) average value is positive, but low. Thus, it is interesting, but not surprising, that particular regions show patterns that are different than the global average. For example, the U.S. Historical Climate Network shows a relatively steady average temperature over the period of record (nighttime temperatures do rise and peaks tend to decline in time), which may be a consequence of natural variability, of an inadvertent but compensating increase in sulfate aerosol loadup, or of other factors, as well as possible problems with the models.

Deriving a linear temperature trend[3] from the available record is also difficult because it depends strongly on the period over which the trend is calculated. If the period is too short, interannual and other nongreenhouse variations in the temperature can unduly bias the estimate; if it is too long, the records are more subject to problems due to variations in spatial coverage, changes in instrument protocols, etc. Figure 3a shows estimates prepared by T. Karl (MacCracken et al., 1990) of the linear trend starting in years from 1880 to 1939 and ending in 1987. (If he had chosen earlier starting years, the trend would have decreased, and if he had chosen later starting years, it would have again increased.) He also prepared estimates of the trend when starting in 1880 and ending in years from 1930 to 1987 (Figure 3b). The trend is clearly very dependent on the starting and ending dates and does not seem to show an acceleration of the warming with the accelerating increase in greenhouse gas forcing.

If we, with some hesitation, accept that there has been a warming of about 0.5°C over the last 100 years due to the increasing concentration of greenhouse gases (and not amplified or diminished by other factors), this compares with an expectation from model simulations of about 0.4 to 1.6°C (as indicated earlier). In that the late 19th and early 20th centuries were probably somewhat cooler than average due to several large volcanic eruptions (and possibly due to persistence of the Little Ice Age), the warming to date is barely consistent with the lower bound of the theoretical estimates of warming (accepting, again with some hesitation, all of the approximations in deriving those estimates and assuming that no new cooling influences are active). Simplified ocean-atmosphere models also suggest that observations are near the lower bound of the model projections (Bretherton et al., 1990).

The temporal patterns of the observed and expected warmings are also not in accord, especially in the Northern Hemisphere. This may be due to problems with the observations (station moves, urbanization, etc.), with the linearity assumption (could the climate be slightly intransitive?), or with the possible counterbalancing effects of other forcing factors (sulfate aerosols, North Atlantic circulation changes). Over the past decade, several investigators have attempted to reconcile the simulated and observed behavior by accounting for solar and/or volcanic effects; each, however, has arrived at the conclusion that CO_2-induced warming is present, but

[3]The increase in radiative forcing since 1750 has actually been not linear, but gradually increasing. Nonetheless, a linear trend is most often sought in the absence of better estimates from models.

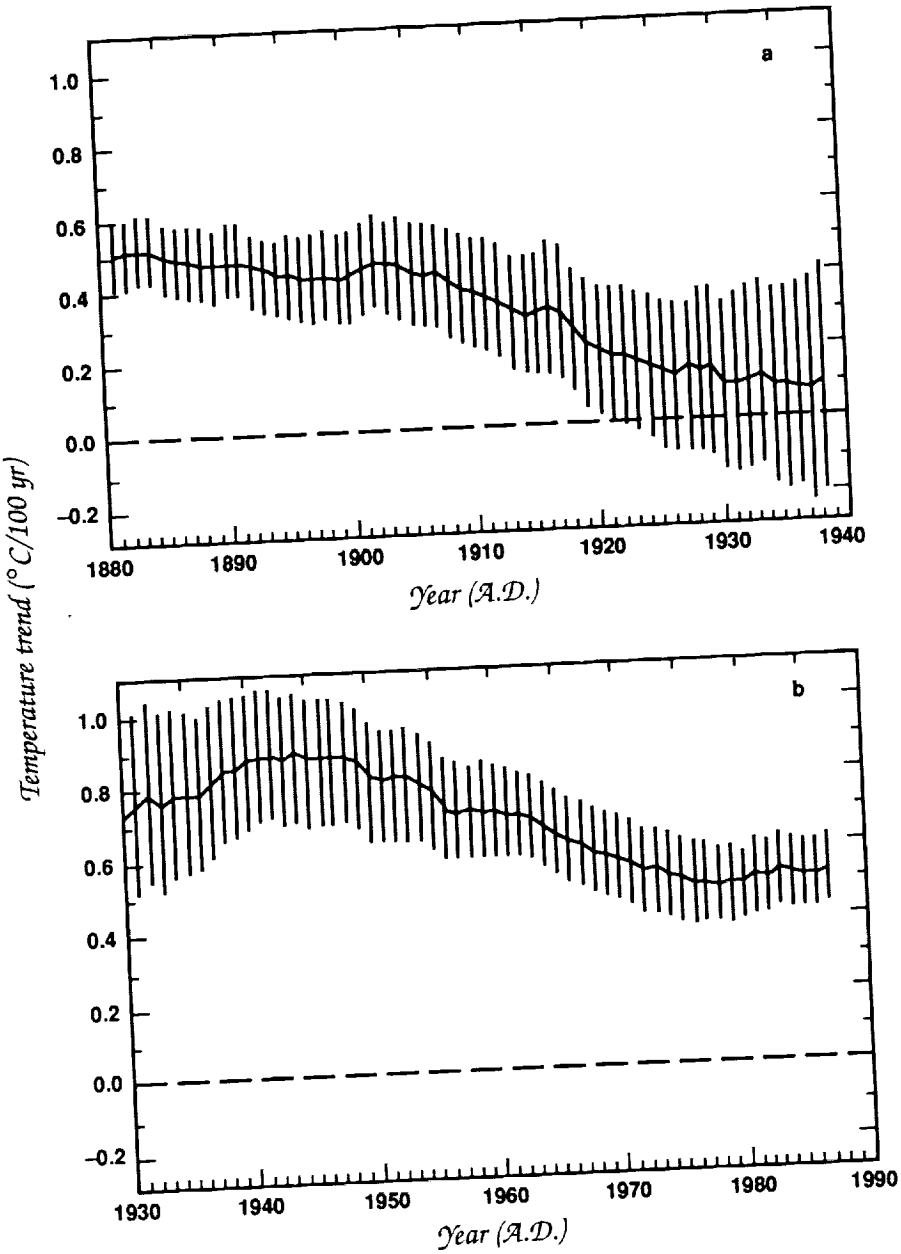

Figure 3. Linear trends of global average land temperatures based on data of Jones (1988) and their associated 95% confidence intervals expressed as rates of change over 100 years: (a) ending year for all trends is 1987, and the beginning year is given on the x axis; and (b) ending year for all trends is given along the x axis, and the beginning year is 1881. Trends reflect changes due to changes in both atmospheric composition and to other natural and human-induced factors (prepared by T. Karl for MacCracken et al., 1990; used with permission).

through inconsistent, and often conflicting, analyses (MacCracken, 1983). Natural variability may also be confounding the analysis. A 1 × CO_2 control simulation by Hansen et al. (1988), for example, shows that the climate may have an inherent natural variability that could be hiding the greenhouse signal (or, conversely, creating much of the recent warming). Without a convincing explanation, the association of the warming with the increases in greenhouse gas concentrations remains captive to uncertainties in our calculations and about the role of natural variability and the influence of other anthropogenic factors.

In addition, the observed and predicted (interpolated) latitudinal patterns of the warming are not in agreement with interpolations from equilibrium calculations (and perhaps should not be expected to be in agreement). Much of the recent warming has been in middle and even low latitudes rather than in high latitudes, as suggested in equilibrium perturbation simulations. However, recent simulations with coupled ocean-atmosphere models suggest that the high-latitude warming may be delayed for very long periods due to the deeper mixing of heat in polar regions. Thus, the importance of this inconsistency may be fading as more realistic calculations become available. Overall, about all that can be said is that warming has occurred over the last century and that some fraction of it (the fraction may range from small to larger than unity) must be due to the increased concentrations of greenhouse gases.

Equally difficult problems arise when considering changes in stratospheric temperature and sea ice extent (for both of which the record is much less complete) and for sea level (for which the prediction and record are both of limited certainty), as explained in the next section. None of the analyses of individual records provides the unequivocal association that is being sought.

The Multivariate Approach

The shortcomings of the individual records suggest that it might prove useful to search for a combination of changes that could be uniquely associated with changes in the concentrations of greenhouse gases (as opposed to volcanic, solar, or other natural influences). Such a *signature* or *fingerprint* approach has great appeal, but has proven quite difficult in practice, because it requires accurate records of multiple variables over comparable periods (the records of the array of variables may not be as long, however, negating some of the benefit of a larger set of variables) and accurate model projections for multiple variables and for all important internal and external changes that may be influencing the climate. As a

C-5,

balance to these difficulties, however, the approach enriches consideration of the set of variables by allowing consideration of relative magnitudes and signs of the changes, spatial and seasonal patterns and gradients, correlations, and other aspects.

Elements of a possible signature for the greenhouse gases are shown in Table 2. These indicators have, of necessity, been drawn from equilibrium rather than from transient model simulations. As a result, more comprehensive model simulations may change the fingerprint (and not all characteristics listed have yet been confirmed even in all equilibrium simulations). Three important additional problems exist. First, the records for many of these variables are quite limited; second, it remains difficult to provide quantitative theoretical estimates of these changes; and third, it is not clear that these elements create a sufficiently unique fingerprint for greenhouse gas–induced changes to allow at least some fraction of past changes to be distinguished from changes due to natural variability and to other factors.

Table 2: Possible components of a greenhouse gas–induced climate signal

Increasing surface temperature
Strong latitudinal gradient over land
Larger changes over land than over the ocean
Larger changes during the winter in high latitudes than during the summer
Reduced diurnal temperature range
Warmer troposphere
Weaker latitudinal gradient
Cooling middle and upper stratosphere
Increasing atmospheric water vapor concentrations
Increasing global precipitation
Largest relative change in high latitudes
Retreating sea ice cover
Retreating snow cover and mountain glaciers
Rising sea level

Despite these difficulties, there are preliminary indications that at least some of these changes are occurring; at least, none of the elements are changing strongly in an unexpected direction. The sea level record, for example, appears to be showing a relatively rapid increase (Figure 4).

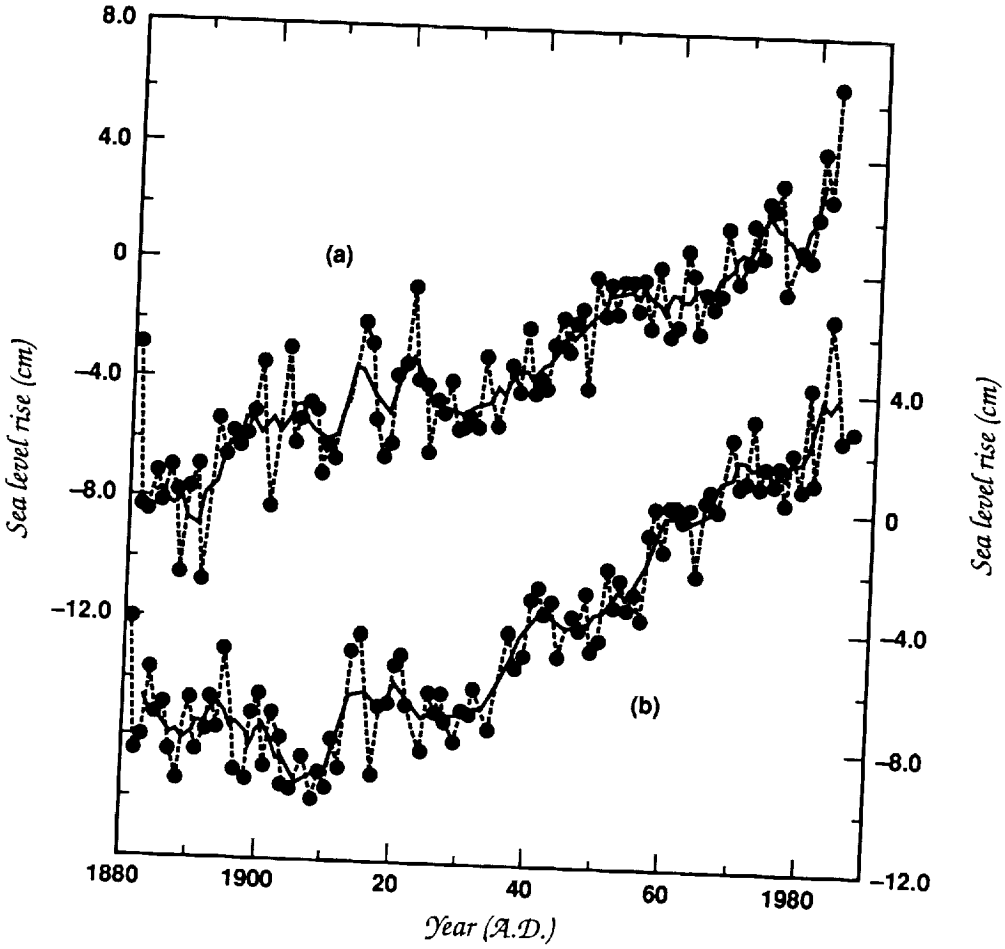

Figure 4. Estimates of global mean sea level rise over the last century. The baseline is arbitrarily selected as the average for the period of 1951 to 1970. The dashed lines connect the annual mean changes (dots); the solid line represents five-year running mean. Data are from (a) Gornitz and Lebedeff, 1987, and (b) Barnett, 1988 (from MacCracken et al., 1990; used with permission).

Again, however, there is not yet quantitative and unequivocal association of the changes with the changes in atmospheric composition.

Conclusions

Observations clearly indicate that the climate has warmed since the mid-19th century—but then, it has warmed before, and the warming since 1850 has not been spatially consistent and temporally monotonic. Clearly, changes due to other factors are also

occurring, and we have not been able to quantitatively and uniquely associate the temperature or other climatic changes with the increasing concentrations of greenhouse gases. The collective set of changes that are occurring, however, is certainly suggestive that the enhanced greenhouse effect is starting to have an effect, even though we cannot yet use this determination to narrow our estimates of future change. The situation suggests that we are, in qualitative terms, closer to a civil conviction of the greenhouse gases (i.e., a preponderance of evidence) than to a criminal conviction (i.e., beyond a reasonable doubt) and that, in quantitative terms, there is still homework to do and observations to be gathered before we can substantially strengthen the case.

Acknowledgments

This work was supported by the U.S. Department of Energy Atmospheric and Climate Research Division and performed by the Lawrence Livermore National Laboratory under Contract No. W-7405-ENG-48.

References

Barnett, T.P. 1988. Global sea level change. In *Climate Variations Over the Past Century and the Greenhouse Effect.* A report based on the First Climate Trends Workshop, 7–9 September 1988, Washington, D.C. National Climate Program Office/NOAA, Rockville, Maryland.

Bradley, R.S., H.F. Diaz, J.K. Eischeid, P.D. Jones, P.M. Kelly, and C.M. Goodess. 1987. Precipitation fluctuations over Northern Hemisphere land areas since the mid-19th century. *Science 237,* 171–175.

Bretherton, F.P., K. Bryan, and J.D. Woods. 1990. Time-dependent greenhouse-gas-induced climate change. In *Climate Change: The IPCC Scientific Assessment* (J.T. Houghton, G.J. Jenkins, and J.J. Ephraums, eds.), Cambridge University Press, Cambridge, England, 173–193.

Gibbons, A. 1990. What's the sound of one ocean warming? *Science 248,* 33–34.

Gornitz, V., and S. Lebedeff. 1987. Global sea level changes during the past century. In *Sea Level Change and Coastal Evolution* (D. Nummedal, O.H. Pilkey, and J.D. Howard, eds.), Special Publication No. 41, Society of Economic Paleontologists and Mineralogists, Tulsa, Oklahoma, 3–16.

Grotch, S.L. 1987. Some considerations relevant to computing average hemispheric temperature anomalies. *Monthly Weather Review 115,* 1305–1317.

Grotch, S.L. 1989. The distribution of the correlation between large scale average and component members. In *Proceedings of the Fourteenth Annual Climate Diagnostics Workshop*, Scripps Institution of Oceanography, La Jolla, California, 16–20 October, 1989. University of California Press, Berkeley, A34–A56.

Grotch, S.L., and M.C. MacCracken. 1991. The use of general circulation models to predict regional climatic change. *Journal of Climate 4(3)*, 286–304.

Hansen, J.E., and A.A. Lacis. 1990. Sun and dust versus the greenhouse. *Nature 346*, 713–719.

Hansen, J.E., and S. Lebedeff. 1988. Global surface air temperatures: Update through 1987. *Geophysical Research Letters 15*, 323–326.

Hansen, J.E., I. Fong, A.A. Lacis, D. Rind, S. Lebedeff, R. Reudy, and G. Russell. 1988. Global climate changes as forecast by the Goddard Institute for Space Sciences three-dimensional model. *Journal of Geophysical Research 93*, 9341–9364.

Jones, P.D., and P.M. Kelly. 1988. Hemispheric and global temperature data. In *Long and Short Term Variability of Climate* (H. Wanner and U. Siegenthaler, eds.), Springer-Verlag, New York, 18–34.

Jones, P.D., T.M.L. Wigley, and G. Farmer. 1991. Marine and land temperature data sets: A comparison and a look at recent trends. In *Greenhouse Gas-Induced Climatic Change: A Critical Appraisal of Simulations and Observations* (M.E. Schlesinger, ed.), Elsevier, Amsterdam, 153–172.

Lorenz, E.N. 1984. Irregularity: A fundamental property of the atmosphere. *Tellus 36A*, 98–110.

MacCracken, M.C. 1983. Have we detected CO_2-induced climate change? Problems and prospects. In *Proceedings: Carbon Dioxide Research Conference: Carbon Dioxide, Science and Consensus*, Berkeley Springs, West Virginia, 19–23 September 1982. DOE Conf. Report, CONF-820970, February 1983, U.S. Department of Energy, Washington, D.C., v.3–v.45.

MacCracken, M.C., A.D. Hecht, M.I. Budyko, and Y.A. Iztael (eds.). 1990. *Prospects for Future Climate.* US/USSR Special Report on Climate and Climate Change, Lewis Publishers, Chelsea, Michigan, 270 pp.

Schneider, S.H., and S.L. Thompson. 1981. Atmospheric CO_2 and climate: Importance of the transient response. *Journal of Geophysical Research 86*, 3135–3147.

Shine, K.P., R.G. Derwent, D.J. Wuebbles, and J.-J. Morcrette. 1990. Radiative forcing of climate. In *Climate Change: The IPCC Scientific Assessment* (J.T. Houghton, G.J. Jenkins, and J.J. Ephraums, eds.), Cambridge University Press, Cambridge, England, 41–68.

Spencer, R.W., and J.R. Christy. 1990. Precise monitoring of global temperature trends from satellites. *Science 247*, 1558–1562.

Vinnikov, K.Ya., P.Ya. Groisman, and K.M. Lugina. 1990. Empirical data on contemporary climate changes (temperature and precipitation). *Journal of Climate 3*, 662–677.

Wang, W.-C., M.P. Dudek, and X.-Z. Liang. Can we use *effective* CO_2 to simulate the combined greenhouse effect of CO_2 and other trace gases? *Nature*, in press.

Watson, R.T., H. Rodhe, H. Oeschger, and U. Siegenthaler. 1990. Greenhouse gases and aerosols. In *Climate Change: The IPCC Scientific Assessment* (J.T. Houghton, G.J. Jenkins, and J.J. Ephraums, eds.), Cambridge University Press, Cambridge, England, 1–40.

Wigley, T.M.L., and M.E. Schlesinger. 1985. Analytical solution for the effect of increasing CO_2 on global mean temperature. *Nature 315*, 649–652.

Wigley, T.M.L., J.K. Angell, and P.D. Jones. 1985. Analysis of the temperature record. In *Detecting the Climatic Effects of Increasing Carbon Dioxide* (M.C. MacCracken and F.M. Luther, eds.), U.S. Dept. of Energy DOE/ER-0235, Washington, D.C., 55–90. Available from NTIS.

Modeling Earth System Changes of the Past

John E. Kutzbach

Introduction

The earth's climate and related components of the earth system have always been changing and will no doubt continue to change. The earth system has a past and a future. The state of the earth system of the future is unknown, but major efforts are under way to estimate the changes that may be associated with increases of greenhouse gases. Until fairly recently the state of the earth system during the past has only been described qualitatively. This situation is now changing. New and more detailed and accurate information is available from analyses of historical records and from environmental records that provide accurate annual dating, such as tree rings, laminated lake or ocean sediments, glacial ice, and coral. Although lacking annual time-scale resolution, new observational techniques are also being used to obtain long-term environmental records from soils, other lake and deep ocean sediments, and ice strata. These records are accurately dated by radiometric methods and are being obtained worldwide, so that near global coverage is possible. As a result, we are gaining detailed information about the evolution of the atmosphere and ocean, of shifts of continents and rise and fall of mountains, and of the wax and wane of ice sheets, forests, lakes, and deserts.

This wealth of new knowledge has in turn activated efforts to simulate climates of the past with the aid of climate models. These modeling studies serve a number of purposes. First, modeling studies help us identify potential causes of climatic change by testing the sensitivity of the model's climate to changes in external forcing or orographic

and geographic boundary conditions. For example, the possible sensitivity of climate to changes of earth's orbital parameters was suggested more than a century ago (Croll, 1864), but the idea received serious consideration only decades later when quantitative estimates of the climatic effects of the orbital changes were made with the aid of a zonal-average energy budget climate model (Milankovitch, 1920). Second, modeling studies help us explore the internal mechanisms of climate change, such as the coupled interactions of the atmosphere, oceans, ice sheets, and biosphere as the climate shifts between glacial and interglacial states. Third, comparisons of the results of simulations of past climate with observations of past climate help us evaluate the adequacy and accuracy of climate models.

This review outlines some of the challenging problems to be faced in understanding the causes and mechanisms of large climatic changes and gives examples of initial studies of these problems with climate models. The review covers climatic changes in three main periods of earth history: (1) the past several centuries, (2) the past several glacial-interglacial cycles, and (3) the past several million years. The review will concentrate on studies of climate but, where possible, will mention broader aspects of the earth system.

All of the modeling studies described here are called climate sensitivity experiments. In such experiments, we analyze the response of a climate model (and up to now an incomplete climate model) to some known or hypothetical change in forcing. Qualitative comparisons of the modeled outcome with observations help to evaluate the possible importance of the change in forcing for explaining the observed climatic change. Climate sensitivity experiments have proven to be very helpful for identifying causes and mechanisms of climate change. Alternatively, if all external and surface boundary conditions are properly prescribed and if the model is an appropriately complete representation of the coupled climate system, then the studies are called climate simulation experiments. In climate simulation experiments, the model results should agree rather closely with the geologic evidence, provided, of course, that both the model and the geologic estimates are accurate. Achieving this level of climate simulation experimentation remains largely a task for the future.

Studies of past climates use a broad range of models. Atmospheric general circulation models (AGCMs) or AGCMs coupled to ocean mixed-layer models are being used to explore the full three-dimensional structure of past climates, including details of the hydrologic cycle. However, the extensive computing resources required for AGCMs have precluded, until now, very long simulations. For similar reasons, extensive work with fully coupled AGCMs and ocean general circulation models (OGCMs) remains largely a task for the future.

Simplified climate system models, such as energy budget models, are often used to explore the long-term evolution of climate.

This chapter is limited to a brief introduction to climate sensitivity experiments pertinent to the study of past climates; more comprehensive overviews are in Saltzman (1985, 1990). Frakes (1979) and Crowley (1983) provide excellent and concise summaries of the geological records of climatic change. Both observations and model studies are treated extensively in the report of the 1989 Global Change Institute (GCI) on Global Changes of the Past (Bradley, 1991a) and in Crowley and North (1991). This chapter draws extensively on material from the 1989 GCI report.

Changes of the Past Several Centuries

The environmental records of the past several centuries have the potential to provide detailed information about the natural decade- to century-scale variability of the earth system. Environmental records are available from historical accounts, tree rings, annually laminated lake or ocean sediments containing fossil pollen or planktonic records, high-resolution ice cores, coral, and mountain glaciers (Bradley, 1991b).

One example of the kind of information forthcoming from these records is illustrated in Figure 1, where the $\delta^{18}O$ records from a north-south transect of ice cores show the centuries-long Little Ice Age event that existed from about A.D. 1550 to 1850–1900 (Thompson, 1991). While many independent records corroborate this evidence for a cold period, detailed regional analyses of decade- to century-scale changes of climate are possible only for North America, Europe, and East Asia (Hughes, 1991). These regional analyses are derived primarily from tree-ring and historical records and provide estimates of temperature and precipitation, drought frequency, and other climatic extremes. What is needed now is a synthesis of existing spatial and temporal records that will allow regional or continent-wide analyses in some areas and also highlight those areas where more work needs to be done (Hughes, 1991).

Although records of the climate of the Little Ice Age are incomplete, the global average temperature of recent decades is estimated to be perhaps 0.4–0.5°C higher than it was during the Little Ice Age. It would be of great interest to know the cause of this recent century-scale warming. The cooling and subsequent warming marking, respectively, the onset and the termination of the Little Ice Age must be part of a natural climatic cycle, because events like the Little Ice Age occur in records from previous millennia. However, this most recent century-scale warming may also have been influenced by the

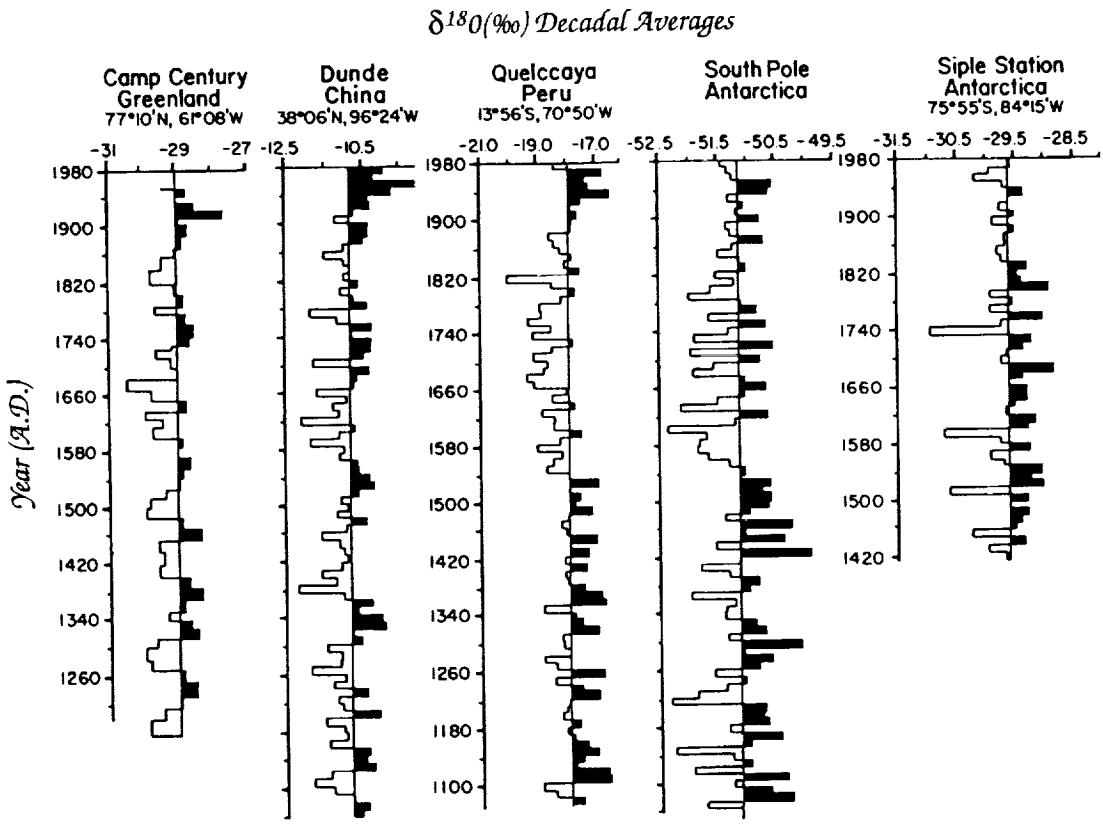

Figure 1. Decadal averages of the $\delta^{18}O$ records in a north-south global transect from Camp Century, Greenland, in the north to the South Pole. The shaded areas represent isotopically less negative (warmer) periods and the unshaded areas isotopically more negative (colder) periods relative to the mean of the individual records. Values shown with reference to the long-term mean at each station for the periods shown (from Thompson, 1991).

increasing concentration of greenhouse gases which grew from preindustrial levels of about 270 ppmv to 350 ppmv at present.

Are decade- to century-scale changes of climate the result of internal oscillations of the coupled system (atmosphere, ocean, ice, etc.), or are they triggered, at least in part, by external changes? Overpeck (1991) has summarized various hypotheses for explaining the occurrence of the Little Ice Age. Two "external" mechanisms suggested frequently are increased volcanic aerosols and decreased solar irradiance (Schneider and Mass, 1975; Hansen and Lacis, 1990). Examples of internal mechanisms that might be associated with longer-term climate changes are natural oscillations of the ocean or of the coupled ocean-atmosphere-cryosphere system.

Major volcanic eruptions produce small decreases in land surface temperature that persist for one or more years following the erup-

tion (Hansen et al., 1978; Rampino et al., 1988; Bradley, 1988). Observations of recent eruptions, such as El Chichon, are helping to calibrate the relationship between eruptions, increased stratospheric aerosol loading, decreased solar radiation reaching the surface, and lowered temperature. At somewhat longer time scales, Porter (1986) has found that Northern Hemisphere glacier advances of the past two centuries appear to follow closely after major volcanic eruptions as recorded in the Greenland ice sheet acidity profile. Conversely, glacier retreats during an earlier warm period (A.D. 1100–1200) occurred at a time of decreased acidity in Greenland ice. Although acidity records in ice cores are a useful qualitative index of volcanic activity, allowance must be made for the effect of the distance of the erupting volcano from the ice sheet on the acidity level in the core. If such bias errors could be removed, then acidity records would be even more useful as a quantitative global index of volcanic activity.

Experiments with AGCMs or coupled models could be used to test climate sensitivity to externally imposed stratospheric volcanic aerosol loadings. These kinds of experiments have not been used extensively, perhaps because of uncertainties about the chemical and radiative properties of the aerosol and its likely vertical and horizontal distribution. However, Wigley (1991) used a simple global average energy balance climate model to illustrate that a Little Ice Age–scale temperature reduction on the order of 0.4°C would require 20 eruptions the size of the Krakatau event: one every 5 years for 100 years. He assumed that a Krakatau-size eruption had an aerosol loading effect equivalent to a 2% reduction in solar irradiance. The size of the temperature response depends, of course, on the climate sensitivity of the model. Because there is no evidence for so many large eruptions, Wigley concluded tentatively that volcanic eruptions alone are not likely to explain fully the observed temperature lowering during the Little Ice Age.

Solar variability has also been proposed as an external cause of climatic change on the decade to century time scale (Eddy, 1976; Eddy et al., 1982). For example, the coldest periods of the Little Ice Age correspond approximately to extended periods of sunspot minima. However, the possible magnitude of variations in solar irradiance has until recently been unknown. Over the past decade, radiometric observations from satellites have documented that the total solar irradiance decreased by about 0.1% between the sunspot maximum in 1981 and the minimum in 1986. Foukal and Lean (1990) have used the recent radiometric data to develop an empirical model of total solar irradiance variation between 1874 and 1988, and this time series is now available for climate studies.

For many years prior to the era of satellite measurements, the evidence for longer-term solar variability came primarily from observations of sunspots or auroras. Now, two other independent lines of evidence are available, $\delta^{14}C$ records from tree rings and ^{10}Be concentrations in ice cores (Stuiver and Braziunas, 1991; Beer et al., 1988). Both ^{14}C and ^{10}Be variations are produced by variations in cosmic ray flux, and the cosmic ray flux varies due to changes in the solar wind or earth's magnetic field. The two radioisotopic records agree fairly well with each other, and with historical records of sunspot number. This agreement offers encouragement that a reliable index of solar variability covering the past several centuries may be achievable.

Wigley and Kelly (1990) have used a simple energy budget climate model to estimate the solar irradiance reduction required to produce a Little Ice Age–scale global average temperature reduction of 0.4°C. In their model, the required irradiance reduction is between 0.2 and 0.5%, depending again upon the assumed climate sensitivity coefficient for the model. These hypothetical irradiance changes are small, but nevertheless significantly larger than recent measurements of total solar irradiance variability over the 11-year sunspot cycle. Therefore, if solar irradiance changes played a major role in producing the cooling of the Little Ice Age, or the subsequent warming into the 20th century, then either those solar irradiance changes were larger than the shorter-term (11-year-cycle) changes observed recently with satellites, or the model's sensitivity is too small.

Borisenkov et al. (1985) calculate that there are additional small perturbations (on the order of 0.05%) of the latitudinal and seasonal solar irradiance associated with an 18.6-year period of nutation of earth's rotational axis. There are also very small seasonal trends (on the order of 0.1% per century) associated with the slowly changing Milankovitch cycles (see following section).

In summary, climate sensitivity experiments with energy budget climate models suggest that external forcing changes associated with volcanic activity or solar irradiance would have to be larger than is now indicated by observations in order to explain fully the cause of the Little Ice Age. Nevertheless, and in view of all the uncertainties, changes in volcanic and solar activity remain candidates for producing climate variability on the scale of decades to centuries. Further experimentation with external forcing changes is needed, especially with AGCMs and coupled models incorporating feedbacks associated with components of the climate system not explicitly calculated in energy balance climate models. Improved data sets of decade- to century-scale climate change and accurate measures of volcanic and solar variability are also needed.

While this section has focused on possible external factors that might cause decade- to century-scale climate change, the internal operation and oscillations of the climate system could also be responsible for climate change, or could amplify or modify the effects of external changes. There is considerable evidence, particularly in the Atlantic, that the oceans are strongly involved in these decade- to century-scale variations. Long records of sea ice (Mysak et al., 1990) and salinity (Dickson et al., 1988) show decade- or century-scale variability, and model studies illustrate the possibility of long-term variability in the thermohaline circulation (Bryan, 1986; Manabe and Stouffer, 1988). Isotopic records recovered from corals show promise of providing long decade- to century-scale records of El Niño–Southern Oscillation events (Cole and Fairbanks, 1990).

Changes of the Past Several Glacial-Interglacial Cycles

Observational studies have shown that variations of earth's orbital parameters are pacemakers of glacial-interglacial cycles (Hays et al., 1976) and of wet-dry cycles in the tropics (Rossignol-Strick, 1983; Prell, 1984; Prell and Kutzbach, 1987). A significant fraction of the variance in time series of the estimated volume of glacial ice and indicators of temperate-latitude vegetation and tropical monsoons is phase-locked with the orbital cycles. Illustrations of this kind of phase-locking are in Figure 2.

The discovery that large climatic changes are apparently paced by relatively small changes in the earth's orbital parameters presents a major opportunity and challenge: namely, to analyze and explain the processes and feedbacks that produce the observed large climatic response to the precisely known changes in external forcing that modify the seasonal and latitudinal distribution of insolation. If we are successful, we will have learned a great deal about the internal workings of the climate system. Variations of the earth's orbital parameters include changes in the axial tilt (range, 22 to 24.5 degrees; period, about 41,000 years), season of perihelion (range, all times of the year; period, about 22,000 years), and orbital eccentricity (range, 0 to 0.06; period, about 100,000 years). In this section, several topics related to these orbital changes and climate modeling studies are reviewed.

6000–9000 Years Ago

A recent time of substantially altered orbital parameters was around 6000 to 9000 years ago (6–9 ka), when perihelion was reached during northern summer (it is now reached in northern

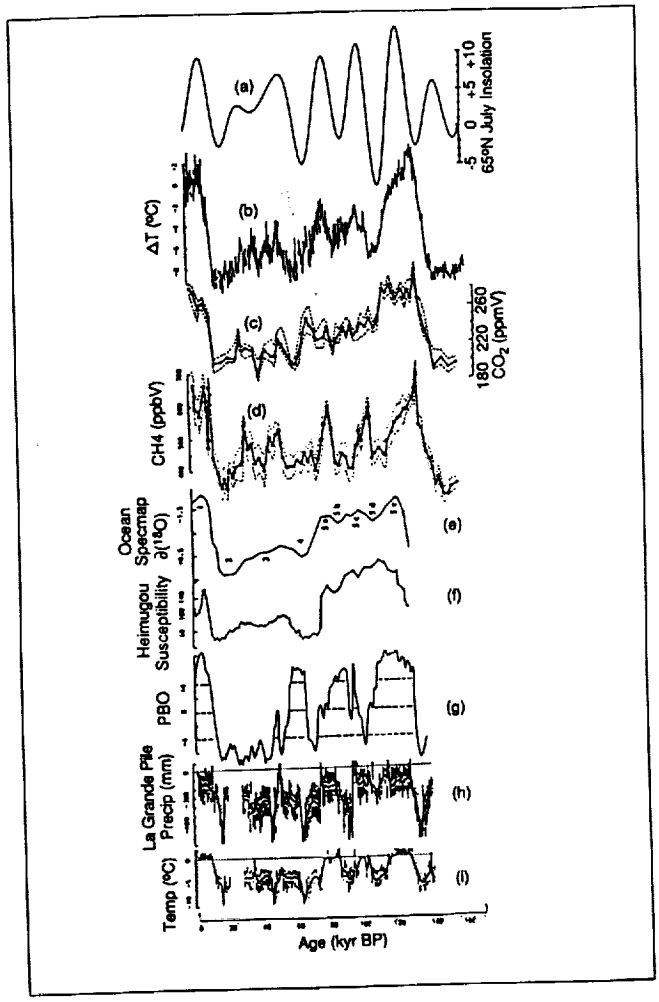

Figure 2. Examples of data on global forcings and earth system responses. (a) July insolation at 65°N (the Milankovitch forcing parameter) expressed as the percentage deviation from the present value (from Berger, 1978). (b–d) Records of temperature deviations from present in °C, based on oxygen isotope data (Jouzel et al., 1987), atmospheric CO_2 (Barnola et al., 1987), and atmospheric CH_4 (Barnola et al., 1987) determined on gas trapped in the Vostok (Antarctica) ice core (from Houghton et al., 1990). (e) SPECMAP O isotopic record (Imbrie, 1984), indicating major isotopic stages (from An et al., 1990). (f) Magnetic susceptibility profile from Heimuguon loess section, Loess Plateau, central China (from An et al., 1990). (g) Palaeogeoclimatic operator (PBO, or best possible climate profile of fossil vegetation changes) time series reconstructed from la Grande Pile pollen records (from Guiot et al., 1989). (h-i) Annual total precipitation and mean temperature reconstructions (expressed as deviations from modern values) for la Grande Pile, based on determination of modern analogue for fossil pollen assemblages (from Guiot et al, 1989).

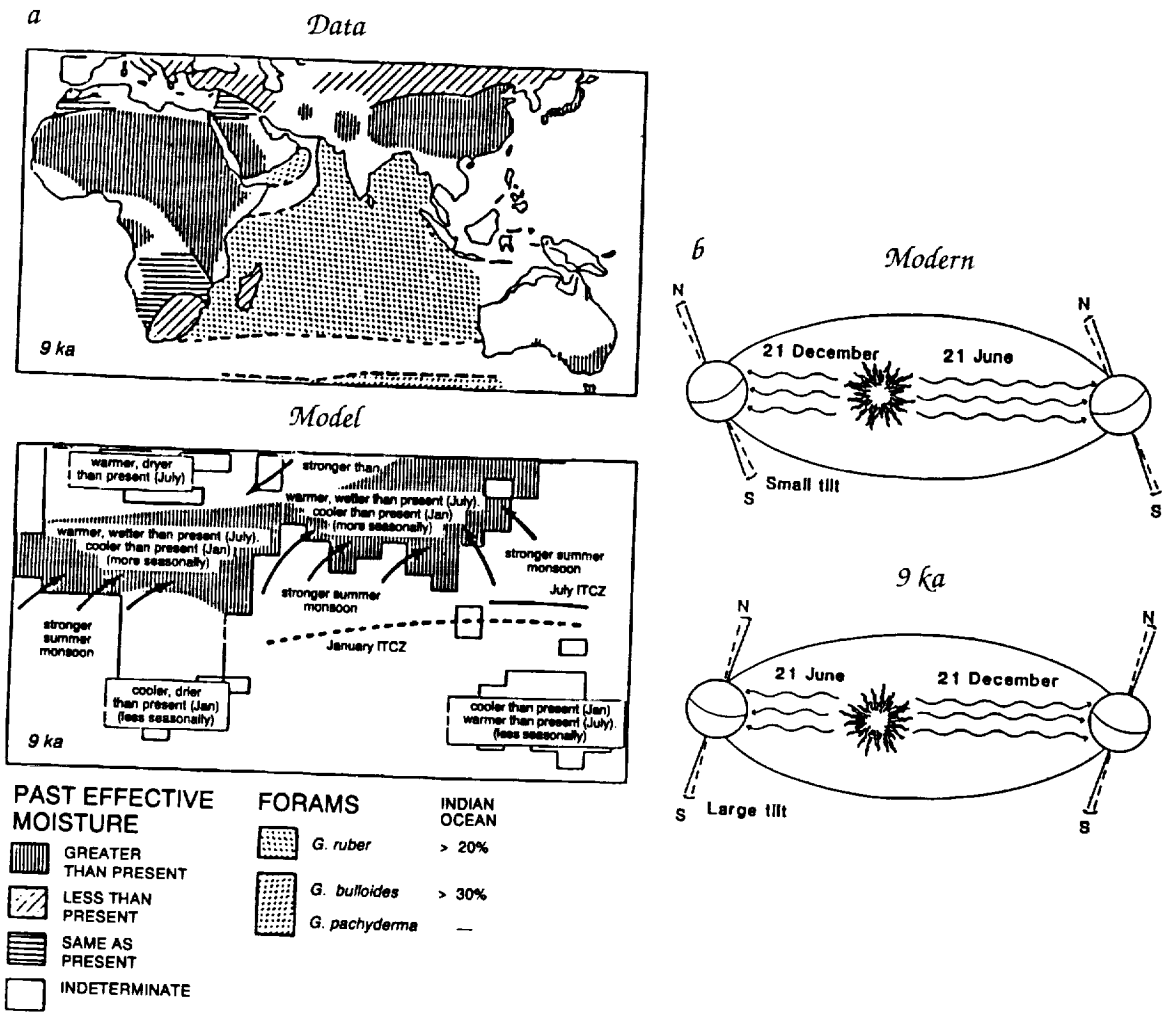

Figure 3. (a) Features of the earth's climate around 9 ka based on geologic and paleoecologic evidence (top panel) and climate model simulations of enhanced monsoonal circulations (bottom panel). (b) Changes in the earth's orbit from the present configuration, where perihelion (minimum earth-sun distance) is reached in northern winter, to the configuration for 9 ka, where perihelion was reached in northern summer and the axial tilt was 24° (from COHMAP Members, 1988).

winter) and the axial tilt was greater than at present. The solar radiation in July of 9 ka, averaged over the Northern Hemisphere, was about 7% (30 W/m^2) greater than it is at present. In January of 9 ka, solar radiation was correspondingly less than present (Figure 3). Climate sensitivity experiments have helped to show how the orbitally caused changes in the seasonal cycle of solar radiation interact with the different thermal properties of land and ocean to cause large climatic changes. These climate sensitivity experiments

were made first with AGCMs with prescribed (modern) sea surface temperature. They have subsequently been made with AGCMs coupled to mixed-layer ocean models. The only coding changes required, relative to control (modern) simulations, are adjustments of the axial tilt, season of perihelion, and orbital eccentricity.

The change between the orbital configuration of 6–9 ka and today therefore provides us with an experiment, performed by nature, for studying the climatic response to an enhanced seasonal insolation cycle in the Northern Hemisphere, and a reduced seasonal insolation cycle in the Southern Hemisphere. The enhanced seasonal insolation cycle in the Northern Hemisphere produces strengthened Northern Hemisphere monsoons (Kutzbach, 1981; Figure 3). Northern continents are warmer in summer (temperature increase of 2–4°C) and colder in winter; the temperature changes of the surrounding oceans are much less owing to their large heat capacity. In northern summer, the warming of the land relative to the ocean increases the land/ocean temperature contrast and produces an increased land/ocean pressure gradient (lower pressure over land relative to ocean) and a significantly expanded and intensified region of low pressure across North Africa and South Asia. Summer monsoon winds are strengthened and precipitation is increased for parts of North Africa and South Asia (Kutzbach and Guetter, 1986; Kutzbach and Gallimore, 1988; Mitchell et al., 1988; COHMAP Members, 1988). These simulated changes in the hydrologic regime of past millennia are in qualitative agreement with geologic and paleobotanical observations of changes in tropical lake levels and vegetation (Kutzbach and Street-Perrott, 1985). For example, between 12 ka and 6 ka lakes and savanna vegetation existed about 1000 km north of present limits in tropical North Africa. In the model experiment, northern continental interiors were warmer (in summer) and drier than at present, and this too agrees qualitatively with observations (Gallimore and Kutzbach, 1989). The increased insolation in northern summer, stemming both from the summertime perihelion passage and the increased tilt, produces considerable melting of Arctic sea ice. Some observational evidence also suggests reduced sea ice cover around 9 ka.

Although many features of the observed climate around 6–9 ka are in qualitative agreement with the results of the climate sensitivity experiments for orbitally caused insolation changes, the agreement is far from perfect. Much needs to be learned about the response of soil moisture, runoff, vegetation, sea ice, and ocean currents to the changed insolation. In keeping with the sense of the definition of sensitivity experiments given earlier, the simulated climate

sensitivity will change, perhaps significantly, as models of the climate system become more complete and accurate. There is also a need to refine the climatic estimates derived from the observations and, in some regions, to expand the data coverage.

125,000 Years Ago

Data from the previous (Eemian) interglacial, the period around 125 ka, indicate a climate significantly warmer than present and also warmer than the warmest period of the current interglacial (6–9 ka). Estimates of the climate of the previous interglacial have been made for parts of the middle and high latitudes of the Northern Hemisphere by Velichko (1984) and Vinnikov et al. (1988). The patterns of high-latitude warmth around 125 ka are similar to the 6–9 ka patterns, but the magnitude of the changes is larger (4 to 6°C warmer than present at 125 ka, compared to 2 to 4°C warmer than present at 6–9 ka), and in some cases the boundaries are shifted. Dramatic evidence of warmer conditions is also provided by Koerner (1989), who estimates that the Greenland ice sheet was significantly smaller, or nearly absent, during this interglacial period, and by Andrews (1991), who reviews evidence that sea level was 5 m (or more) above present. The Vostock ice-core records show relative maxima in atmospheric concentrations of CO_2 and CH_4 during this period. In the tropics, there is evidence of stronger monsoons (Prell and Kutzbach, 1987; Petit-Maire, 1986). All of these indicators of significantly altered climate provide a rationale for studying this period as an example of a climate regime warmer than present. Moreover, the phase-locking of many of the above-mentioned climate variables with insolation records at the precessional and tilt periods indicates that orbital configurations are of great importance for producing interglacials (Figure 2).

The seasonal and latitudinal changes in solar radiation caused by orbital changes are approximately twice as large at 125 ka as at 6–9 ka. This is because the eccentricity of the earth's orbit was significantly larger then (so that the earth-sun distance was significantly smaller at perihelion), and because perihelion passage occurred in northern summer around 125 ka, whereas now it occurs in northern winter. Summertime radiation was increased by more than 50 W/m^2 (12–13%), compared to present, and wintertime radiation was decreased. Owing to the increased axial tilt at 125 ka (23.9°) compared to the present (23.4°), the annual average insolation in the polar regions was increased by 3–4 W/m^2, compared to the present.

Royer et al. (1984), Prell and Kutzbach (1987), Kutzbach et al. (1990), and MacCracken and Kutzbach (in press) have reported on climate sensitivity experiments with AGCMs using 125-ka orbital parameters. High-latitude warmth, decreased sea ice extent, increased mid-

continent aridity, and strengthened tropical monsoons are among the simulated responses. More work is needed to compare model results with observations, to improve the observational records, and to repeat these kinds of studies using improved models of the climate system.

Glacial Cycles

When we address the relationship between orbital changes and the glacial portion of glacial-interglacial cycles, issues of climate sensitivity are more complicated. The geologic evidence provides us with the challenge of explaining not only the accumulation and wastage of several-kilometer-high ice sheets, but also substantial changes in ocean circulation, sea ice extent, vegetation zones, and atmospheric concentrations of carbon dioxide and methane (Figure 2). Describing in detail how this system operates will require the use of fully coupled climate system models, including descriptions of ice sheets, upper lithosphere adjustments to ice loading, and biogeochemical cycles capable of producing changes in atmospheric composition.

One aspect of the problem of explaining glacial-interglacial cycles has received considerable initial attention. Climate sensitivity experiments have shown that orbital conditions favoring cool northern summers might reduce temperatures sufficiently to prevent the melting of high-latitude snows. If snow were to persist through the summer months, glaciation could be initiated. This condition would be favored at times of large eccentricity, January perihelion, and minimum axial tilt. North et al. (1983) used an energy budget climate model to show that for these orbital conditions summer temperatures could be several degrees Celsius lower than present in northern continental interiors where present-day summer temperatures are only a few degrees Celsius above freezing. When an ice-albedo feedback was included, the cooling was enhanced. While this result lends some support to the hypothesis that certain orbital configurations favor initiation of glaciation, the role of the ice-albedo feedback mechanism remains uncertain because the energy budget model has no explicit hydrologic cycle. Similar sensitivity experiments with AGCMs, with explicit precipitation and snow cover parameterizations, are therefore needed. One such AGCM experiment produced lowered temperatures in summer and year-round, and wetter conditions in high northern latitudes and especially Canada (Royer et al., 1983). Rind et al. (1989), on the other hand, found in their AGCM experiment with orbital conditions set to favor cool summers that temperature was not lowered sufficiently to maintain snow cover through the summer. Clearly, the sensitivity of climate to the insolation changes depends upon model parameterizations, resolution, and other prescribed (or interactive) boundary conditions (see Oglesby, 1990).

18,000 Years Ago

Leaving aside, for the moment, the question of the ultimate cause of glacial-interglacial cycles, it remains of great interest to explore the characteristics of glacial-age climates because conditions were so different from those existing now. Many features of the most recent glacial-age climate have been simulated with AGCMs (Gates, 1976; Manabe and Hahn, 1977), using prescribed lower boundary conditions such as ice sheets, sea ice, sea surface temperature, and land vegetation as estimated from geologic evidence. Here, the pioneering work of the CLIMAP project (CLIMAP Project Members, 1981) has been instrumental in providing accurate lower boundary conditions for the most recent glacial maximum around 18 ka. Moreover, analysis of fossil air trapped in glacial ice and retrieved from ice cores in Antarctica and Greenland has shown that the atmospheric concentration of CO_2 was about 200 ppmv during glacial times (Barnola et al., 1987). In the simulations of glacial climates with AGCMs, large anticyclones develop over the ice sheets. Temperatures are generally lower and precipitation rates are reduced. In the middle and upper troposphere, the presence of the large North American ice sheet causes the Jet Stream to split into two branches, a northern branch along the Arctic flank of the ice sheet and a southern branch located well south of the ice sheet border (Manabe and Broccoli, 1985; Kutzbach and Wright, 1985). The details of the climatic sensitivity are a function of ice sheet size and shape (Shinn and Barron, 1989). The sensitivity of the North Atlantic ocean to upstream glacial-age ice sheet boundary conditions was explored by Manabe and Broccoli (1985). They used an AGCM coupled to a motionless ocean mixed layer in which ice sheets were prescribed but sea surface temperatures were allowed to vary. The northern branch of the split atmospheric flow brought cold Arctic air over the North Atlantic, producing cold water and extensive sea ice cover that agreed with the marine geologic evidence (CLIMAP Project Members, 1981). While many of the results of these experiments agree with paleoclimatic observations, many puzzles remain, such as the changed behavior of the ocean circulation and biogeochemical cycles, as manifested in the reduced atmospheric concentration of carbon dioxide.

Role of the Ocean and Other System Components

Learning more about the role of the ocean in large climatic changes is of particular importance. For example, observational evidence indicates that North Atlantic deep water flow was significantly reduced during glacial times; that the upper waters of the oceans, and particularly the North Atlantic, were depleted in nutrients compared to today; and that the deep ocean was cooler (Boyle and Keigwin, 1982, 1987). If

the vertically overturning thermohaline circulation of the Atlantic, described as a conveyor belt, slowed down or stopped, the climate of the North Atlantic region would be much colder than at present. Broecker et al. (1985) and Broecker and Denton (1989) have described evidence for this bimodality, both on the long-term scale of glacial-interglacial cycles and on the abrupt "event" scale of centuries. Paralleling these observational findings have been studies with ocean models of possible bimodality in the ocean's thermohaline circulation (see Bryan, 1986, and references to earlier work therein). Multiple experiments with a coupled ocean-atmosphere GCM found, with identical boundary conditions but different initial conditions, two stable equilibria: In one the North Atlantic had a vigorous thermohaline circulation and a relatively warm climate in regions bordering on the Atlantic; in the other there was no thermohaline circulation, and the regional climate of adjacent lands was much cooler (Manabe and Stouffer, 1988) (Figure 4). Birchfield (1989) has examined similar kinds of bimodality in coupled atmosphere-ocean box models. These oceanic changes are very likely linked to changes in biogeochemical cycling that may ultimately explain the glacial-interglacial differences of about 70 ppmv in the atmospheric concentration of CO_2 ($\cong$ 270 ppmv preindustrial value; $\cong$ 200 ppmv glacial-age value). Some of these indicators of ocean climate show significant amplitude variability and consistent phase relationships with orbital cycles (Imbrie et al., 1989).

Tracer studies are another important earth system linkage now being explored for past climates (Jouzel, 1991). The spatial and temporal distribution of isotope species, such as $\delta^{18}O$ in precipitation, and aerosol (desert dust, loess, marine aerosol, indicators of volcanicity) are important paleoclimatic indicators. Various modeling studies are employing tracers for isotopes and dust in AGCMs for both modern and 18-ka simulations (Jouzel et al., 1986; Joussaume and Jouzel, 1987; Joussaume et al., 1989). Tracer studies can provide a stringent test for evaluating models of present-day conditions. Tracer studies are also useful for checking paleoclimatic inferences made from the spatial and temporal distribution of isotopes or dust in geologic records and, in fact, were first undertaken by those involved in the interpretation of paleoclimatic records.

The amount and climatic importance of aerosol loading of the glacial-age atmosphere is a very important and unresolved question (Harvey, 1988). The possibility exists that significant aerosol loading could have contributed to the observed lowering of glacial-age temperature. However, improved estimates of the location, amount, and radiative properties of the aerosol are needed.

For large climatic changes, there are also significant changes in the distribution of land vegetation and soil carbon (Prentice and

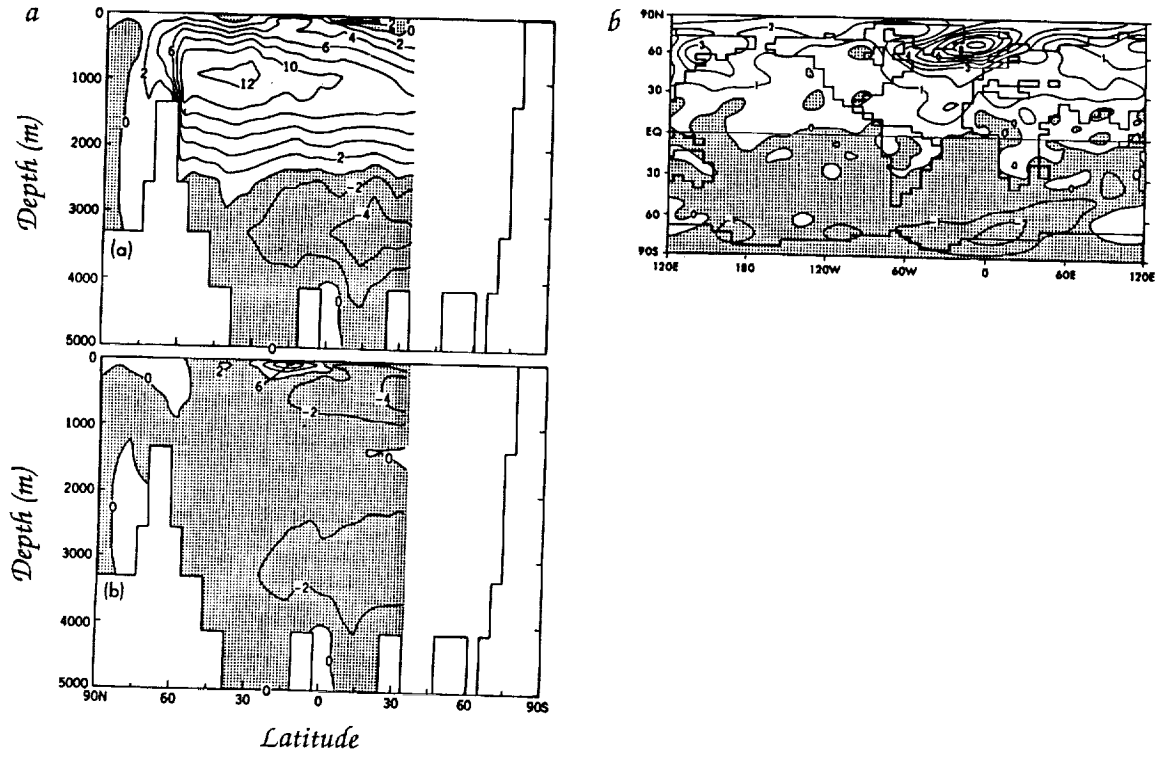

Figure 4. (a) Streamfunction illustrating meridional circulation in the Atlantic Ocean. Units are Sverdrups (10^6 m^3/s): (top) Experiment I, (bottom) Experiment II. In experiment I there is a strong thermohaline circulation, whereas in experiment II it is absent. The streamfunction is not shown in the southern Atlantic ,which is not enclosed by coastal boundaries and freely exchanges water with other oceans. (b) Difference in surface air temperature (°C) between experiments I and II. The surface air temperatures in the North Atlantic sector are significantly warmer with strong thermohaline circulation and large poleward heat transport in the North Atlantic ocean (from Manabe and Stouffer, 1988).

Fung, 1990) and possible biosphere-albedo feedbacks (Cess, 1978; Street-Perrott et al., 1990).

Evolution of Climate

In general, paleoclimate simulation experiments (in contrast to climate sensitivity experiments) are largely a task for the future because models are not yet adequate for incorporating all parts of the climate system. For the period since the last glacial maximum, however, there is detailed information on the size of the wasting ice sheets, the atmospheric concentration of carbon dioxide, and the ocean surface temperature (as inferred from information in marine sediments). Using these geologic observations to prescribe surface boundary conditions of ice sheets and ocean temperature and, in

some cases, atmospheric CO_2 levels, along with orbitally prescribed insolation, AGCMs have been used to simulate "snapshots" of the climate at 3000-year intervals from 18 ka to the present (COHMAP Members, 1988). The simulated climate agrees qualitatively with many features of the observed climate (COHMAP Members, 1988). These initial attempts at simulating sequences of paleoclimates will no doubt be repeated in coming years using more complete models and more complete observational data sets for model/data comparisons. In order to facilitate model/model and model/data comparisons, there will be a need to develop standard data sets for selected times such as 6 ka and 18 ka.

Embedded in the general deglaciation of the past 18,000 years are one or more very abrupt changes in climate (Boyle and Keigwin, 1987; Broecker et al., 1989). For example, between 11,000 and 10,000 years ago the general warming trend was interrupted by a very significant return to cold conditions that persisted for a few centuries, which was in turn followed by an equally abrupt warming. The cause of this reversal, known as the Younger Dryas, and other such abrupt events is unknown. Perhaps the climate is sensitive to small changes of ice sheet height or shape or to meltwater discharge to the Gulf of Mexico or the North Atlantic. The possible causes of these and other abrupt events are under investigation (Rind et al., 1986; Schneider et al., 1987; Overpeck et al., 1989; Oglesby et al., 1989).

The above-mentioned studies with GCMs provide detailed snapshots of the relatively fast response of the atmosphere, land surface, and upper ocean to insolation changes. The more general questions of the time-dependent behavior of the fully coupled climate system during glacial-interglacial cycles are being addressed currently with the aid of highly simplified models of the climate system. These models incorporate, often in heuristic fashion, the slow-response climate variables such as ice mass, bedrock depression, deep ocean temperature, and atmospheric concentration of carbon dioxide. Papers by Saltzman and Sutera (1984), Saltzman and Maasch (1991), Ghil et al. (1987), Pollard (1983), and Peltier (1982) illustrate this approach. These models have typically simulated the time-dependent variations of one or more climate variables, such as global ice volume; these model-derived time series are then compared with observations of ice volume variations inferred from oxygen isotope records. Some studies have focused on understanding the forced response of these coupled systems to changes of orbital parameters, while others have demonstrated that the coupled systems themselves exhibit free oscillatory behavior resembling, to some extent, observed variations (Saltzman, 1990).

In part because of computing limitations, time-dependent climate models simulating the slow-response variables use very simplified

treatments of the atmosphere. This limitation will certainly be relaxed as computing power increases. In the meantime, an intermediate class of atmospheric models, statistical-dynamical models, is efficient enough to be used in time-dependent integrations. For example, Berger et al. (1988, 1990) have performed a time-dependent integration with a two-dimensional (latitude-height) zonal average atmospheric model coupled asynchronously to mixed-layer ocean and ice sheet models. They simulate the climatic response to orbital changes of the past 125,000 years in the form of an ice volume chronology that matches the observational record quite well. With enhanced computing resources and improved and coupled AGCMs and OGCMs it should become possible to study the three-dimensional evolution of the climate system over this full interglacial-glacial-interglacial cycle.

In summary, the strong empirical evidence linking precisely known changes in external forcing of the climate system (namely, the changes in the earth's orbital parameters) to glacial-interglacial cycles in high northern latitudes and cycles of enhanced or weakened monsoons in middle and tropical latitudes provides a major opportunity to explore the internal workings of the climate system. Much has already been accomplished, but many puzzles remain. The initial studies show encouraging agreement between experiments and geologic observations and underscore the notion that we can learn a great deal about the general behavior of the climate system by parallel studies with observations and models of the large climatic changes of the geologic past.

Changes of the Past Several Million Years

The early Pliocene (roughly 3 to 5 million years ago) is the most recent period with existing observational evidence that climates were *substantially* warmer than present. For example, temperatures in high latitudes may have been 5–10°C higher than present (Zubakov and Borzenkova, 1988). Glacial-interglacial cycles similar to those of the past few hundreds of thousands of years began about 2.5 million years ago. However, compared to the more recent geologic periods mentioned in previous sections, the observational record from this period is relatively poor.

Plate movements (changing geography), crustal movements (changing orography), and associated changes in outgassing, weathering, and biogeochemical cycles must exert a strong "lower-boundary" forcing on earth's climate on the scale of millions of years. To the extent that these "solid earth" processes are viewed as external to the climate system, these more distant geologic periods also pro-

vide extraordinary opportunities for understanding the full range of behavior of the climate system in response to external change. These ancient climates are very different from the present and include periods when the earth was warmer than at present and likely experienced higher concentrations of atmospheric CO_2.

Climate sensitivity experiments performed with energy budget climate models have been particularly useful, because of their computational efficiency, in exploring the first-order effects on climate of the location and size of continents. The primary boundary condition changes are land/ocean distributions, and the primary climatic response is due to the different thermal response characteristics of land and ocean to the seasonal insolation cycle and the influence of the size of the land mass on the continentality of its climate. Crowley et al. (1986) illustrated how, over the past 100 million years, the gradual isolation and movement of Antarctica toward the South Pole and the gradual northward drift and separation of Greenland from adjacent land masses may have both lowered the average temperature and reduced summertime warmth (decreased seasonality of temperature owing to the decreased in continent size) and thereby favored the development of permanent ice sheets.

In the past several million years the overall plate movements have been relatively small; yet geologic observations suggest significant changes of climate toward cooler and generally drier conditions, with the cooling leading ultimately to the initiation of glacial-interglacial cycles around 2.5 million years ago. Since orbital variations occurred prior to this time, one interpretation is that some other factor (or factors) caused the climate to cool to the point where orbitally caused glacial cycles could occur. Mountain uplift, lowering CO_2 levels, and changes in ocean circulation are among the suggested factors. Ruddiman et al. (1989) have presented evidence that major worldwide uplift of plateaus and mountains has occurred in the past five to ten million years, with a possible doubling of heights in many regions. In a series of climate sensitivity experiments with AGCMs for no-mountain, half-mountain (perhaps approximating the situation of five to ten million years ago), and full (present-day) mountains as prescribed lower boundary conditions, but with ocean temperatures prescribed at modern values, Ruddiman and Kutzbach (1989) show that many of the patterns of regional cooling and drying that have been estimated from geologic observations can be explained by uplift (Figure 5). By comparing simulations with and without the Tibetan plateau, Manabe and Broccoli (1990) show that the modern-day Asian deserts are simulated correctly only with the Tibetan plateau present. These kinds of studies with AGCMs give useful preliminary indications of the atmospheric changes to be expected from changing

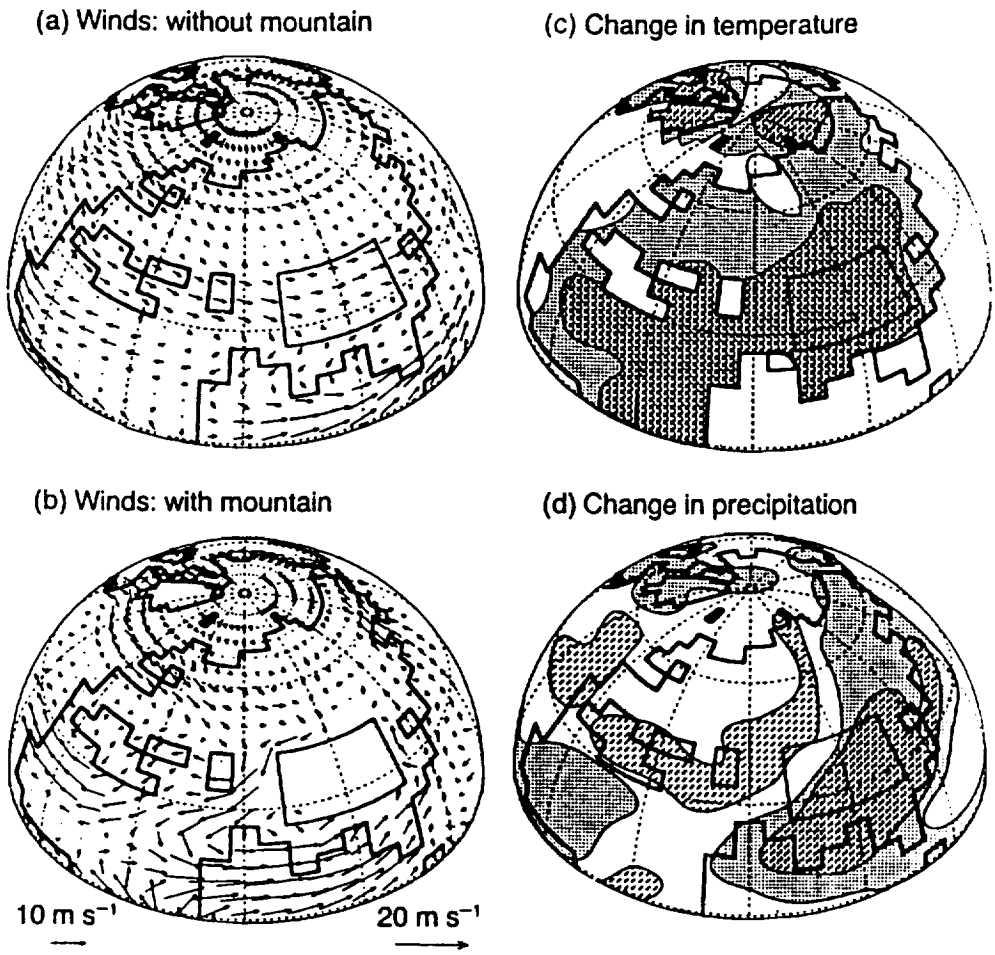

Figure 5. Model simulation of uplift-induced circulation changes in Eurasia for July. (a) Near-surface winds in "no mountain" experiment. (b) Near-surface winds in "mountain" experiment. (c) Change in surface temperature due to uplift; cooler regions stippled, warmer regions blank. (d) Change in precipitation due to uplift; wetter regions stippled, drier regions blank. Diagonal (broken-line) shading in (c) and (d) is used for areas where temperature or precipitation changes are significant at the 99% confidence level (from Ruddiman and Kutzbach, 1989).

orography but ignore the likely changes in ocean temperature and circulation that would also occur. A climate model with a fully coupled ocean will be needed to simulate more completely the response of the climate system to uplift, and the model will also likely need to include interactive coupling with biogeochemical and vegetation processes. This is so because changes in weathering associated with uplift might be expected to change the carbon cycle and lower atmospheric CO_2 concentration (Raymo et al., 1988).

Ocean gateways may also open or shut in response to otherwise subtle horizontal or vertical crustal movements. Maier-Reimer et al. (1991) have used an OGCM forced by modern observed wind stress and surface air temperature in a sensitivity experiment on the possible consequences of the closing or near-closing of the central American isthmus that is believed to have occurred over the past ten million years. They found that with an open isthmus lower-salinity waters from the Pacific dilute the salinity of the North Atlantic surface waters, and this dilution leads to drastically reduced strength of the thermohaline circulation cell and the poleward ocean heat transport in the North Atlantic.

Many questions remain concerning the causal factors that produced the general cooling of climate over the past several million years. All of the above mentioned factors (uplift, falling levels of CO_2, and changes in ocean circulation or in ocean gateways) may have played a role (Crowley, 1991). Improved data sets would provide a focus for modeling studies of this period and could lead to improved understanding of the potential behavior of the earth system during periods substantially warmer than the present.

Conclusions

The climatic history of our earth provides an increasingly data-rich environment for testing ideas about the causes and mechanisms of large climatic changes. Moreover, it may be possible in the future to use modeling studies in combination with geological observations to assess the adequacy and accuracy of climate models.

This brief overview has illustrated some of these opportunities and some of the obstacles. Of necessity, most studies have used models of the climate system that fall well short of the desired level of breadth and detail. On the one hand, studies with fully coupled models are greatly simplified and include only a few variables (global ice volume, global deep ocean temperature, etc.). On the other hand, detailed studies with individual system components (atmospheric or ocean GCMs) are likewise of limited value because they are not coupled to other important components of the climate system.

The climate sensitivity experiments that are used to infer the possible effects of past changes in orbital parameters, geography and orography, CO_2 levels, and solar irradiance are similar in methodology to the climate sensitivity experiments that are used to infer possible effects of future increases in greenhouse gases. The advantage of the former is that the paleoclimatic observations help us assess the model's response. Stated slightly differently, an advantage in studying the climates of the past is that we know (or can find out) what happened.

As we develop coupled climate models, we will need to evaluate their accuracy. One test of the accuracy of coupled climate models will be the degree to which they can simulate the observed seasonal cycle. The recent few decades and the past century of historical records are useful for testing the accuracy of coupled climate systems on the scale of interannual variability. Records of the past several centuries and the past millennia are useful for estimating and understanding decade- to century-scale variability. However, only the more distant paleoclimatic records of past millennia provide examples of climatic changes of a magnitude that might be associated with doubling or tripling of atmospheric concentrations of CO_2 and increases in other greenhouse gases over the next century. For example, the estimated global average warming from the most recent glacial maximum (around 18 ka) to the present is about 4°C—roughly the same order as the anticipated warming caused by increased greenhouse gases over the next century. Because the future changes may occur perhaps 100 times more rapidly than the deglacial warming, which occupied a period of about 10,000 years, abrupt as well as gradual changes in climate need to be studied. Another example of a period of the past that is now of substantial interest is the climate of several million years ago. This period had generally warmer conditions than present and perhaps elevated CO_2 levels. It appears to be the most recent example of a climate substantially warmer than present.

If we can construct realistic models of the coupled climate system and of the even broader earth system, we will have many opportunities to use them—not only for addressing practical questions that we face in the next century, but also for working in an interdisciplinary mode with geologists, ecologists, archaeologists, and paleontologists in solving puzzles about the earth's past.

References

Andrews, J.T. 1991. Association of ice sheets and sea level with global warming: A geological perspective on aspects of global change. In *Global Changes of the Past* (R.S. Bradley, ed.), Global Change Institute Vol. 2, UCAR/Office for Interdisciplinary Earth Studies, Boulder, Colorado, 321–339.

Barnola, J.-M., D. Raynaud, Y.S. Korotkevich, and C. Lorius. 1987. Vostok ice core periods 160,000-year record of atmospheric CO_2. *Nature 329*, 408–414.

Beer, J., U. Siegenthaler, G. Bonani, R.C. Finkel, H. Oeschger, M. Suter, and W. Wolfli. 1988. Information on past solar actvity and geomagnetism from ^{10}Be in the Camp Century ice core. *Nature 331*, 675–679.

Berger, A.H., H. Gallee, T. Fichefet, I. Marsiat, C. Tricot. 1988. *Testing the Astronomical Theory with a Physical Coupled Climate-Ice-Sheets Model.* Sci Rpt 1988/3. Inst d'Astron et de Geophys Lemaitre, G. Univ Catholique, Louvain - La-Neuve, Belgium.

Berger, A., T. Fichefet, H. Gallee, I. Marsiat, C. Tricot, and J.P. Van Ypersele. 1990. Physical interactions within a coupled climate model over the last glacial-interglacial cycle. *Transactions of the Royal Society of Edinburgh: Earth Sciences 81*, 357–369.

Birchfield, G.E. 1989. A coupled ocean-atmosphere climate model: Temperature versus salinity effects on the thermohaline circulation. *Climate Dynamics* 4, 57–71.

Borisenkov, Ye.P., A.V. Tsvetkov, and J.A. Eddy. 1985. Combined effects of earth orbit perturbations and solar activity on terrestrial insolation. Part I: Sample days and annual mean values. *Journal of the Atmospheric Sciences 42(9)*, 933–940.

Boyle, E.A., and L. Keigwin. 1982. Deep circulation of the North Atlantic over the last 200,000 years: Geochemical evidence. *Science 218*, 784.

Boyle, E.A., and L. Keigwin. 1987. North Atlantic thermohaline circulation during the past 20,000 years linked to high-latitude surface temperature. *Nature 330*, 35–40.

Bradley, R.S. 1988. The explosive volcanic eruption signal in northern hemisphere continental temperature records. *Climatic Change 12*, 221–243.

Bradley, R.S. (ed.). 1991a. *Global Changes of the Past.* Global Change Institute Vol. 2, UCAR/Office for Interdisciplinary Earth Studies, Boulder, Colorado, 514 pp.

Bradley, R.S. 1991b. Instrumental records of past global change: Lessons for the analysis of noninstrumental data. In *Global Changes of the Past* (R.S. Bradley, ed.), Global Change Institute Vol. 2, UCAR/Office for Interdisciplinary Earth Studies, Boulder, Colorado, 103–116.

Broecker, W.S., and G.H. Denton. 1989. The role of ocean-atmosphere reorganizations in glacial cycles. *Geochimica et Cosmochimica Acta 53*, 2465–2501.

Broecker, W.S., D.M. Peteet, and D. Rind. 1985. Does the ocean-atmosphere system have more than one stable mode of operation? *Nature 315*, 21–26.

Broecker, W.S., J.P. Kennett, B.P. Flowers, J. Teller, S. Trumbore, G. Bonani, and W. Wolfli. 1989. The routing of Laurentide ice-sheet meltwater during the Younger Dryas cold event. *Nature 341*, 318–321.

Bryan, F. 1986. High-latitude salinity effects and interhemispheric thermohaline circulations. *Nature 323*, 301–304.

Cess, R.D. 1978. Biosphere-albedo feedback and climate modeling. *Journal of the Atmospheric Sciences 35*, 1765–1768.

CLIMAP Members. 1981. Seasonal reconstructions of the earth's surface at the last glacial maximum. *Geological Society of America Map and Chart Series, MC-36.*

COHMAP Members. 1988. Climatic changes of the last 18,000 years: Observations and model simulations. *Science 241*, 1043–1052.

Cole, J.E., and R.G. Fairbanks. 1990. The Southern Oscillation recorded in the $\delta^{18}O$ of corals from Tarawa Atoll. *Paleoceanography 5(5)*, 669–683.

Croll, J. 1864. On the physical cause of the change of climate during geological epochs. *Philosophical Magazine 28*, 121–137.

Crowley, T.J. 1983. The geological record of climatic change. *Reviews of Geophysics and Space Physics 21*, 828–877.

Crowley, T.J. 1991. Modeling Pliocene warmth. *Quaternary Science Reviews 10*, 275–283.

Crowley, T.J., and G.R. North. 1991. *Paleoclimatology.* Oxford University Press, New York, 339 pp.

Crowley, T.J., D.A. Short, J.G. Mengel, and G.R. North. 1986. Role of seasonality in the evolution of climate during the last 100 million years. *Science 231*, 579–584.

Dickson, R.R., J. Meincke, S.A. Malmberg, and A.J. Lee. 1988. The "great salinity anomaly" in the northern North Atlantic 1968-1982. *Progress in Oceanography 20*, 103–151.

Eddy, J.A. 1976. The Maunder Minimum. *Science 192*, 1189–1202.

Eddy, J.A., R.L. Gilliland, and D.V. Hoyt. 1982. Changes in the solar constant and climatic effects. *Nature 300*, 689–693.

Foukal, P., and J. Lean. 1990. An empirical model of total solar irradiance variation between 1874 and 1988. *Science 247*, 556–558.

Frakes, L.A. 1979. *Climates Throughout Geologic Time.* Elsevier Science Publishing Company, New York, 310 pp.

Gallimore, R.G., and J.E. Kutzbach. 1989. Effects of soil moisture on the sensitivity of a climate model to earth orbital forcing at 9000 yr BP. *Climatic Change 14*, 175–205.

Gates, W.L. 1976. The numerical simulation of ice-age climate with a global general circulation model. *Journal of the Atmospheric Sciences 33*, 1844–1873.

Ghil, M., A. Mullhaupt, and P. Pestiaux. 1987. Deep water formation and Quaternary glaciations. *Climate Dynamics 2*, 1–10.

Hansen, J.E., and A.A. Lacis. 1990. Sun and dust versus greenhouse gases: An assessment of their relative roles in global climate change. *Nature 346(6286)*, 713–719.

Hansen, J.E., W-C Wang, and A.A. Lacis. 1978. Mount Agung eruption provides test of a global climatic perturbation. *Nature 199*, 1065–1068.

Harvey, L.D. 1988. Climatic impact of ice age aerosols. *Nature 334*, 333–335.

Hays, J.D., J. Imbrie, and N.J. Shackleton. 1976. Variations in the Earth's orbit: Pacemaker of the ice ages. *Science 194*, 1121–1132.

Houghton, J.T., G.J. Jenkins, and J.J. Ephraums (eds.). 1990. *Climate Change: The IPCC Scientific Assessment.* Intergovernmental Panel on Climate Change and Cambridge University Press, Cambridge, 329–341.

Hughes, M.K. 1991. The tree-ring record. In *Global Changes of the Past* (R.S. Bradley, ed.), Global Change Institute Vol. 2, UCAR/Office for Interdisciplinary Earth Studies, Boulder, Colorado, 117–137.

Imbrie, J., A. McIntyre, and A. Mix. 1989. Oceanic response to orbital forcing in the late Quaternary: Observational and experimental strategies. In *Climate and Geo-sciences* (A. Berger et al., eds.), Kluwer Academic Publishers, Dordrecht, The Netherlands, 121–164.

Jouzel, J. 1991 Paleoclimatic tracers. In *Global Changes of the Past* (R.S. Bradley, ed.), Global Change Institute Vol. 2, UCAR/Office for Interdisciplinary Earth Studies, Boulder, Colorado, 449–476.

Jouzel, J., W.S. Broecker, R. Koster, G. Russell, R. Suozzo, and J. White. 1986. Modern and 18 ka BP simulations of the HDO and $H_2{}^{18}O$ atmospheric cycles using the NASA/GISS general circulation model. In *Conference on Abrupt Climtic Changes SIO*, Ref. 86–8, 149–152.

Joussaume, S., and J. Jouzel. 1987. Simulations of paleoclimatic tracers using atmospheric general circulation models. In *Abrupt Climatic Changes: Evidence and Implications* (W.H. Berger and L.D. Labeyrie, eds.), NATO ASI series, D. Reidel, Dordrecht, The Netherlands, 369–381.

Joussaume, S., J. Jouzel, and R. Sadourny. 1989. Simulations of the last glacial maximum with an atmospheric circlation model including paleoclimatic tracer cycles. In *Understanding Climatic Change* (A. Berger, R.E. Dickinson, and J.W. Kidson, eds.), Geophysical Monograph Series 52, American Geophysical Union, Washington, D.C., 159–162.

Koerner, R.M. 1989. Ice core evidence for extensive melting of the Greenland Ice Sheet in the Last Interglacial. *Science 244*, 964–968.

Kutzbach, J. E. 1981. Monsoon climate of the early Holocene: Climatic experiment using the Earth's orbital parameters for 9000 years ago. *Science 214*, 59–61.

Kutzbach, J.E., and R.G. Gallimore. 1988. Sensitivity of a coupled atmosphere/mixed-layer ocean model to changes in orbital forcing at 9000 years BP. *Journal of Geophysical Research 93(D1)*, 803–821.

Kutzbach, J.E., and P.J. Guetter. 1986. The influence of changing orbital parameters and surface boundary conditions on climate simulations for the past 18,000 years. *Journal of the Atmospheric Sciences 43(16)*, 1726–1759.

Kutzbach, J.E., and F.A. Street-Perrott. 1985. Milankovitch forcing of fluctuations in the level of tropical lakes from 18 to 0 kyr BP. *Nature 317*, 130–134.

Kutzbach, J.E., and H.E. Wright, Jr. 1985. Simulation of the climate of 18,000 yr BP: Results for the North American/North Atlantic/European sector and comparison with the geologic record. *Quaternary Science Review 4*, 147–187.

Kutzbach, J.E., P.J. Guetter, and W.M. Washington. 1990. Simulated circulation of an idealized ocean for Pangaean time. *Paleoceanography 5(3)*, 299–317.

MacCracken, M.C., and J.E. Kutzbach. Comparing and contrasting Holocene and Eemian warm periods with greenhouse-gas-induced warmings. In *Greenhouse-Gas-Induced Climate Change: A Critical Appraisal of Simulations and Observations* (M.E. Schlesinger, ed.), Elsevier Science Publishing Company, in press.

Maier-Reimer, E., U. Mikolajewicz, and T. Crowley. 1991. Ocean general circulation model sensitivity experiment with an open Central American isthmus. *Paleoceanography 5(3)*, 349–366.

Manabe, S., and A.J. Broccoli. 1985. The influence of continental ice sheets on the climate of an ice age. *Journal of Geophysical Research 90*, 2167–2190.

Manabe, S., and A.J. Broccoli. 1990. Mountains and arid climates of middle latitudes. *Science 247*, 192–195.

Manabe, S., and K. Bryan. 1985. CO_2-induced change in a coupled ocean-atmosphere model and its paleoclimatic implications. *Journal of Geophysical Research 90*, 11689–11708.

Manabe, S., and D.G. Hahn. 1977. Simulation of the tropical climate of an ice age. *Journal of Geophysical Research 82*, 3889–3911.

Manabe, S., and R.J. Stouffer. 1988. Two stable equilibria of a coupled ocean-atmosphere model. *Journal of Climate 1*, 841–866.

Marshall, H.G., J.C.G. Walker, and W.R. Kuhn. 1988. Long-term climate change and the geochemical cycle of carbon. *Journal of Geophysical Research 93*, 791–801.

Milankovitch, M. 1920. *Théorie Mathématique des Phénomenes Thermiques Produits par la Radiation Solaire*. Gauthier-Villars, Paris, 338 pp.

Mitchell, J.F.B., N.S. Grahame, and K.H. Needham. 1988. Climate simulations for 9000 years before present: Seasonal variations and the effect of the Laurentide ice sheet. *Journal of Geophysical Research 93*, 8283–8303.

Mysak, L.A., D.K. Manak, and R.F. Marsden. 1990. Sea-ice anomalies observed in the Greenland and Labrador Seas during 1901–1984 and their relation to an interdecadal Arctic climate cycle. *Climate Dynamics 5(2)*, 111–133.

North, G.R., J.G. Mengel, and D.A. Short. 1983. A simple energy balance model resolving the seasons and the continents: Application to the astronomical theory of the Ice Ages. *Journal of Geophysical Research 88*, 6576–6586.

Oglesby, R.J. 1990. Sensitivity of glaciation to initial snowcover, CO_2, snow albedo, and ocean roughness in the NCAR CCM. *Climate Dynamics 4*, 219–235.

Oglesby, R.J., K.A. Maasch, and B. Saltzman. 1989. Glacial meltwater cooling of the Gulf of Mexico: GCM implications for Holocene and present-day climates. *Climate Dynamics 3*, 115–133.

Overpeck, J.T., L.C. Peterson, N. Kipp, J. Imbrie, and D. Rind. 1989. Climate change in the circum-North Atlantic region during the last deglaciation. *Nature 338*, 553–557.

Overpeck, J.T. 1991. Century- to millennium-scale climatic variability during the Late Quaternary. In *Global Changes of the Past* (R.S. Bradley, ed.), Global Change Institute Vol. 2, UCAR/Office for Interdisciplinary Earth Studies, Boulder, Colorado, 139–173.

Peltier, W.R. 1982. Dynamics of the ice age Earth. *Advances in Geophysics 24*, 1–146.

Petit-Maire, N. 1986. Paleoclimates in the Sahara of Mali. *Episodes 9*, 7–15.

Pollard, D. 1983. Ice-age simulations with a calving ice-sheet model. *Quaternary Research 20*, 30–48.

Porter, S.C. 1986. Pattern and forcing of Northern Hemisphere glacier variations during the last millennium. *Quaternary Research 26*, 27–48.

Prell, W.L. 1984. Monsoonal climate of the Arabian Sea during the late Quaternary; a response to changing solar radiation. In *Milankovitch and Climate* (A. Berger, J. Imbrie, J. Hays, G. Kukla, and B. Saltzman, eds.), D. Reidel, Hingham, Massachusetts, 349–366.

Prell, W.L., and J.E. Kutzbach. 1987. Monsoon variability over the past 150,000 years. *Journal of Geophysical Research 92*, 8411–8425.

Prentice, K., and I.Y. Fung. 1990. The sensitivity of terrestrial carbon storage to climate change. *Nature 346*, 48–51.

Rampino, M.R., S. Self, and R.B. Stothers. 1988. Volcanic winters. *Annual Review of Earth and Planetary Science Letters 16*, 73–99.

Raymo, M.E., W.F. Ruddiman, and P.N. Froelich. 1988. Influence of late Cenozoic mountain building on ocean geochemical cycles. *Geology 16*, 649–653.

Rind, D., D. Peteet, and G. Kukla. 1989. Can Milankovitch orbital variations initiate the growth of ice sheets in a general circulation model? *Journal of Geophysical Research 94*, 12,851–12,871.

Rind, D., D. Peteet, W. Broecker, A. McIntyre, and W. Ruddiman. 1986. The impact of cold North Atlantic sea surface temperatures on climate; Implications for the Younger Dryas cooling (11–10K). *Climate Dynamics 1*, 3–34.

Rossignol-Strick, M. 1983. African monsoons, an immediate climate response to orbital insolation. *Nature 304*, 46–49.

Royer, J.F., M. Deque, and P. Pestiaux. 1983. Orbital forcing of the inception of the Laurentide ice sheet. *Nature 304*, 43–46.

Royer, J.F., M. Deque, and P. Pestiaux. 1984. A sensitivity experiment to astronomical forcing with a spectral GCM: Simulation of the annual cycle at 125,000 BP and 115,000 BP. In *Milankovitch and Climate*, Part 2 (A.L. Berger et al., eds.), D. Reidel, Hingham, Massachusetts, 733–763.

Ruddiman, W.F., and J.E. Kutzbach. 1989. Forcing of late Cenozoic northern hemisphere climate by plateau uplift in Southern Asia and the American West. *Journal of Geophysical Research 94(D15)*, 18409–18427.

Ruddiman W.F., W.L. Prell, and M.E. Raymo. 1989. Late Cenozoic uplift in Southern Asia and the American West: Rationale for General Circulation Modeling Experiments. *Journal of Geophysical Research 94 (D15)*, 18379–18391.

Saltzman, B. 1985. Paleoclimate modeling. In *Paleoclimate Analysis and Modeling* (A.D. Hecht, ed.), John Wiley and Sons, New York, 445pp.

Saltzman, B. 1990. Three basic problems of paleoclimatic modeling: A personal perspective and review. *Climate Dynamics 5*, 67–78.

Saltzman, B., and K.A. Maasch. 1991. A first-order global model of late Cenozoic climatic change. II. Further analysis based on simplification of CO_2 dynamics. *Climate Dynamics 5(4)*, 201–210.

Saltzman, B., and A. Sutera. 1984. A model of the internal feedback system involved in the late Quaternary climate variations. *Journal of the Atmospheric Sciences 41*, 736–745.

Schneider, S.H., and C. Mass. 1975. Volcanic dust, sunspots, and temperature trends. *Science 190*, 741–746.

Schneider, S.H., D.M. Peteet, and G.R. North. 1987. A climate model intercomparison for the Younger Dryas and its implications for paleoclimatic data collection. In *Abrupt Climatic Change* (W.H. Berger and L.D. Labeyrie, eds.), D. Reidel, Dordrecht, The Netherlands, 399–417.

Shinn, R.A., and E.J. Barron. 1989. Climate sensitivity to continental ice sheet size and configuration. *Journal of Climate 2*, 1517–1537.

Street-Perrott, F.A., J.F.B. Mitchell, D.S. Marchand, and J.S. Brunner. 1990. Milankovitch and albedo forcing of the tropical monsoons: A comparison of geological evidence and numerical simulations for 9000 yr BP. *Transactions of the Royal Society of Edinburgh: Earth Sciences 81*, 407–427.

Stuiver, M., and T.F. Braziunus. 1991. Isotopic and solar records. In *Global Changes of the Past* (R.S. Bradley, ed.), Global Change Institute Vol. 2, UCAR/Office for Interdisciplinary Earth Studies, Boulder, Colorado, 225–244.

Thompson, L. 1991. Ice-core records with emphasis on the global record of the last 2000 years. In *Global Changes of the Past* (R.S. Bradley, ed.), Global Change Institute Vol. 2, UCAR/Office for Interdisciplinary Earth Studies, Boulder, Colorado, 201–224.

Velichko, A.A. 1984. Late Pleistocene spatial paleoclimatic reconstructions. In *Late Quaternary Environments of the Soviet Union* (A.A. Velichko, H.E. Wright, Jr. and C.W. Barnosky, eds.), University of Minnesota Press, Minneapolis, 261–285.

Vinnikov, K.Ya., N.A. Lemeshko, and N.A. Speranskaya. 1988. *Changes of Soil Wetness Induced by Global Warming (Empirical Estimates)*. State Hydrological Institute Report, Leningrad, U.S.S.R.

Wigley, T.M.L. 1991. Climate variability on the 10–100-year time scale: Observations and possible causes. In *Global Changes of the Past* (R.S. Bradley, ed.), Global Change Institute Vol. 2, UCAR/Office for Interdisciplinary Earth Studies, Boulder, Colorado, 83–101.

Wigley, T.M.L., and P.M. Kelly. 1990. Holocene climate change, ^{14}C wiggles and variations in solar irradiance. *Philospohical Transactions of the Royal Society of London A330*, 547–560.

Zubakov, V.A., and I.I. Borzenkova. 1988. Pliocene palaeoclimates: Past climates as possible analogues of mid-twenty-first century climate. *Palaeogeography, Palaeoclimatology, Palaeoecology 65*, 35–49.

Models of Atmosphere-Ecosystem-Hydrology Interactions: Approaches and Testing

David S. Schimel

Introduction

Interactions among the atmosphere, terrestrial ecosystems, and hydrological cycle have been the subject of investigation for many years, although most of the research has had a regional focus (Hewlett and Hibbert, 1967; Wood et al., 1990). The topic is broad, including the effects of climate and hydrology on vegetation, the effects of vegetation on hydrology, the effects of the hydrological cycle on the atmosphere, and interactions of the cycles via material flux such as solutes and trace gases. The intent of this paper is to identify areas of critical uncertainty, discuss modeling approaches to resolving those problems, and then propose techniques for testing. I consider several interactions specifically to illustrate the range of problems. These areas are (1) cloud parameterizations and the land surface, (2) soil moisture, and (3) the terrestrial carbon cycle.

I separate the issues of process and scale somewhat artificially but for convenience in discussing the issues more clearly. Issues of process are those where biological or physical processes are not well understood. As an example, the biological controls over ecosystem response to CO_2 fertilization are not known, although hypotheses abound. Issues of scale are familiar in both the physical sciences, where considerable problems with cloud parameterizations persist, and biology, where the problem of extrapolating from the organism level (where our understanding is concentrated) to regions and the globe is unresolved. In some cases, the issues of process and scale become entangled. An example of this was presented in Jarvis and McNaughton's (1986) classic paper on scaling from leaf to canopy:

At some scale, transpiration becomes a control over itself by influencing boundary-layer humidity. This process, whereby the vegetation influences boundary-layer physics (Avissar and Verstraete, 1990), is one that only becomes apparent when the region of study achieves some critical size, and it is dependent upon the state of the atmosphere. Similarly, CO_2 only becomes a control over climate (and hence terrestrial ecology) at the global scale, yet CO_2 exchange is mediated by single leaves and microorganisms.

The interactions discussed in this chapter are not within subsystems of the earth system but at their interfaces (Moore, 1990), and the appropriate methods of validation are often unclear. For example, in ecological modeling, a strong test of a model is considered to be the comparison of model predictions to experimental data where the experiment is a manipulation of the system different from those used in developing the model. Another test would be to evaluate the model's ability to replicate system behavior along an environmental gradient (i.e., Parton et al., 1987). Clean application of these techniques for continental and global models is difficult; the biosphere does not have replicates, and replication is difficult even for landscape- to regional-scale simulations (Hobbs et al., in press). Bretherton (personal communication) uses the expression "increasing credibility" to refer to the process whereby models are incrementally challenged and improved in cases where full testing is impractical, as is the case with models of the coupled ocean-atmosphere-biosphere system. We must work continuously to challenge every testable part of the models so that they embody our best understanding. Critical to this is that feedbacks, once identified by experiment, by theory, or in the paleorecord, should be included and their significance evaluated. I will pursue these issues below, using the examples of cloud, soil moisture, and carbon cycle interactions. These interactions impose reciprocal constraints on model resolution and parameterization in both atmospheric and ecosystem/hydrological models, adding to their interest and challenge.

Cloud Feedbacks and Biology

It is well known now that cloud feedbacks are significant in the earth radiation budget (Ramanathan et al., 1989) and that clouds are poorly represented in current atmospheric general circulation models (GCMs) (Mitchell et al., 1989). While the effect of "cloud feedbacks" is often argued to be a negative feedback to global temperature (by reflecting radiation to space), it is less clearly understood that a change in cloudiness would in and of itself have a significant effect on plant energetics and physiology, possibly affecting primary

production and the outcome of plant competition. Several factors are involved in this plant-radiation interaction. First, photosynthesis (A) is highly and nonlinearly sensitive to incoming photosynthetically active radiation (PAR), with a response curve often fitted by a hyperbola (Johnson and Thornley, 1984).

Changes between cloud and clear sky radiation will have substantial effects on photosynthetic rates and associated evapotranspiration (ET). Because these rates are highly nonlinear, the parameterization chosen for clouds in a coupled atmosphere-biosphere model will have large consequences during climate change simulations. That is, taking a grid cell with humidity greater than threshold for cloud formation and assigning an average cloudiness will result in an average radiation field. Because the photosynthesis-PAR curve is strongly nonlinear, carbon and water exchange for that grid cell will be calculated incorrectly, possibly resulting in subsequent errors in the atmospheric water.

At steady state, this problem may be resolved by implicitly parameterizing the model to take into account "typical" cloud statistics, and this is often done. For nonsteady-state simulations or those of trace gas–modified climate, a physically based cloud statistic for each grid box is more desirable. The response of the vegetation can be correctly modeled by integrating the A-PAR function over the cloud distribution field for each grid cell.

The above argument assumes that the A-PAR relationship adjusts instantaneously and that PAR is the sole control over A. In fact, plant responses include lags and are controlled by multiple factors (Knapp and Smith, 1988; Schimel et al., 1991). First, while the drop in A following a decrease in PAR is rapid, the increase in A after PAR is increased may be slow (Knapp and Smith, 1990). Thus, an increase in cloudiness could produce a larger decrease in A and evapotranspiration than predicted with a linear extrapolation as a result of the hysteresis of the A-PAR relationship in time. This effect may be small at the global scale but has not been evaluated.

In water-stressed environments, cloudiness may actually increase net carbon gain. Water-stressed vegetation at high PAR will exhibit near-total stomatal closure and high resistance (g) to water and CO_2 exchange. Thus in dry environments and under clear sky conditions, A may be near zero and ET low for much of the day, despite high photosynthetic capacity at full sunlight when well watered. Cloud passage under such conditions may allow stomatal opening and permit some photosynthesis. Knapp and Smith (1988, 1990) have shown that typical levels of cloudiness increase net daily A over that predicted for clear sky conditions in a subalpine environment.

This opens the following questions: (1) To what extent are such responses (hysteresis of A-PAR) tuned to the environment by evolutionary adaptation, or (2) how and how fast can plants respond to a changing light intensity? (3) Is the response physiological, in which case we may assume that a near-optimal response will keep pace with the changing environment, or (4) is the response genotypic, in which case the response will occur over time scales of community and evolutionary change (Field, 1990; Schimel et al., 1990).

In addition to the physiological processes, light also affects the outcome of competition between plant species. The widely used Jabowa family of models (e.g., Pastor and Post, 1986) includes the effects of light competition as a primary factor structuring forest communities. Each species included in the model has parameters describing its tolerance of high and low light levels, and shading is computed using a simple radiation model. While the response of ecosystem models to changing temperature and water has been evaluated (Schimel et al., 1990, 1991; Clark, this volume; Pastor and Post, 1988), effects of changing light environment have not been simulated. Indeed, scenarios of changing earth surface radiation from GCMs have not been widely released and may be quite unreliable (Smith and Vonder Haar, 1991). In fact, plant responses to the absolute light environment (as opposed to the relative light environment defined by shading) may not be well known.

Returning to the issue of cloud parameterizations in atmospheric GCMs (AGCMs), it is clear that simulated cloudiness structure or statistics in the AGCM not only must satisfy the requirements of correct simulation of the cloud radiation feedback on mean global and regional temperature. It also must accurately model the variability of clouds and hence the solar radiation field at the earth's surface for correct simulation of plant response. The time scales of these two requirements may well be different. For example, the earth radiation budget is normally calculated with a time step of about a month, and radiation calculations in most AGCMs are integrated at longer time steps than many other processes. For simulation of A, ET, and g, statistics describing the variability in monthly cloudiness but for morning, midday, and afternoon conditions may be required. Cloud parameterizations in AGCMs should be developed with requirements based on sensitivity analyses of ecosystem models as one criterion. In addition, the use of cloud statistics in ecosystem simulations should be investigated further.

One type of model subsystem checking is conceptual checking to insure that no important process has been omitted. The above discussion points out a series of interactions that have not been considered in the development of most models of land surface interac-

tions. Assuming that the above interactions were to be included in an earth system model, how could they be tested? This question has a number of answers. First, the physiological response of plants to cloudiness can be investigated using leaf and canopy measures of gas exchange, and some such studies are under way (Knapp, personal communication; Knapp and Smith, 1988, 1990). In addition, many data sets collected using eddy correlation measurements of water and CO_2 exchange include incoming radiation or even cloud statistics (e.g., the first ISLSCP [International Satellite Land Surface Climatology Program] Field Experiment [FIFE] Information System, NASA-Goddard Space Flight Center) and could be analyzed for effects of cloudiness and hysteresis. Cloud passage is often treated as a noise term but could be analyzed as a signal.

The physiological adaptation of plants to new cloud regimes could be simulated experimentally using growth facilities or transplants but will be difficult to relate to the field situation and to global change. The effects of changing light environment on plant competition can be modeled using improvements of extant models but will be well-nigh impossible to test in the field given the time scale of plant succession. In this area, sensitivity analysis of rigorously developed models may have to suffice, possibly augmented with field studies using analogous gradients.

Soil Moisture

Soil moisture is a key parameter linking atmosphere and biosphere. Soil moisture is a key control over decomposition (Parton et al., 1987), over leaching of nutrients, and over plant growth. The central role of soil moisture storage and of runoff to the biota and hydrology make their correct representation in earth system models crucial. In order to simulate the surface energy balance, climate models use the basic prognostic equation for soil moisture (w):

$$\frac{\partial(w)}{\partial t} = r - ET + m - f \tag{1}$$

where r is rainfall, ET is evapotranspiration, m is snowmelt, and f is runoff. Recent work has focused on improving the representation of ET (Sellers et al., 1986). This approach is acceptable for simulation of sensible and latent heat exchange over broad areas, but is it adequate for linking climate, plant growth, and biogeochemistry?

There are several issues to consider. First, plant available water (pw) is defined by the following equation in real landscapes:

$$\frac{\partial(pw)}{\partial t} = f_{t,om}[r - ET + m - f + i - d] \tag{2}$$

where pw is plant available water; t is time; om is organic matter content; r, ET, m, and f are as above; d is deep drainage; and i is run-on. The function must be converted from total water (the conserved quantity) to plant available water using the soil moisture release function, which varies largely as a function of soil texture and soil organic matter content. In many ecosystems, run-on is a significant control over landscape-scale plant production as much of the production may be concentrated in zones of run-on (Schimel et al., 1985; Noy-Meir, 1977). Similarly, trace gas efflux may be much greater from zones of water concentration than from upland areas (Schimel et al., 1985; Parton et al., 1988), both because of higher microbial activity and because of the erosional concentration of nutrients in run-on zones (Schimel et al., 1986).

The above issues raise problems of scale. The simple prognostic equation for soil water, as modified to include detailed representation of evapotranspiration, currently suffices to simulate atmospheric moisture and surface energy balance in AGCMs. These representations may also suffice for calculations of water balance for large drainages (Gleick, 1987). When the focus of interest changes to the biosphere, these representations become less satisfactory. Stored soil water is an influence over plant production in many ecosystems, and this is of course influenced by position in the runoff/run-on continuum. Field studies and simulations of nitrous oxide (N_2O) and ammonia (NH_3) flux show position in the landscape along this continuum to be of predominant importance (Schimel et al., 1986; Parton et al., 1988). Similarly, methane flux is influenced by meso- and microscale hydrology and topography (Whalen and Reeburgh, 1988). The above problems require mapped or statistical data on topography, soil properties, vegetation, land use, and engineering structures for resolution in models. Clearly, some of these problems require resolution higher than achievable or desirable in an earth system model; equally clearly, these processes (productivity, trace gas flux) are of significance to the earth system.

Improved coupling of atmospheric and hydrological models is also important to understanding the interactive role of fresh water ecosystems in the earth system. Changes in climate will have significant consequences for rivers and lakes, and these changes will undoubtedly have feedbacks, at least to regional climate and certainly to human societies. Current AGCMs include no representation of fresh water interactions and barely even include them due to coarse resolution of geography. Yet fresh water systems are critical to nutrient and organic matter transport, interact strongly with marginal wetlands, and are the dominant vector for nutrient transport to the oceans. There have been repeated critiques of the lack of

consideration of coastal and shelf regions of the oceans in global carbon cycle models; simulation of these areas will require consideration of the inputs from fresh water systems. Indeed, as Broecker (1981) has pointed out, fresh water may play a dominant role in millennial changes in ocean circulation and climate.

A critical link in the land surface–atmosphere–hydrology part of the "wiring diagram" then is the *interface* between global and regional changes in P–E, and their expression in real hydrological systems. A variety of approaches has been used to develop such interfaces. Wilks (1988) used a statistical conversion from AGCM-predicted changes to "real" weather and soil properties from a crude data base to translate between AGCMs and detailed plant models but did not address run-on/runoff and other landscape processes. Schimel et al. (1990) used a similar approach for biogeochemical cycling. Gleick (1987) used AGCM output as input to a basin hydrology model, but focused on water output rather than on distribution and effects within a watershed. Giorgi (1990) used a mesoscale atmospheric model forced by AGCM output and a land surface parameterization to examine effects of mountainous topography and sub-AGCM grid circulations; this study did not consider routing of runoff. Vörösmarty et al. (1989) used a basin-scale hydrological model to study the routing of runoff within a large drainage (the Amazon) and its effects on evapotranspiration and nutrient flux. This model could be forced by simulations such as those of Dickinson (1987) or Shukla et al. (1990) to evaluate regional hydrological consequences of a changed vegetation in the Amazon region.

The problems of including hydrology in earth system models are serious, however. Wood et al. (1990) have pointed out that most hydrological models are extensively parameterized to account for the peculiar features of topography, soils, and geology in a catchment area of interest. This is because of the complex nonlinear interactions that occur within catchments, and the detailed geographic data required to analyze those interactions. The response of catchments is also very sensitive to initial conditions (Wood et al., 1990; Figure 1), again resulting in complex responses. Work by Wood, Band, Gupta, and others (Wood et al., 1990; Wood et al., 1988; Gupta et al., 1986; Band and Wood, 1988) has attempted to develop scale-independent measures that can be used to develop simplified models of watershed response, at least above threshold sizes (*Representative Elementary Areas*: Wood et al., 1990). These theoretical approaches and simulations hold promise for developing improved representation of land surface hydrology and its interactions with biology and the atmosphere in the near future. Improvement of the representation of hydrology in earth system models will greatly aid

a

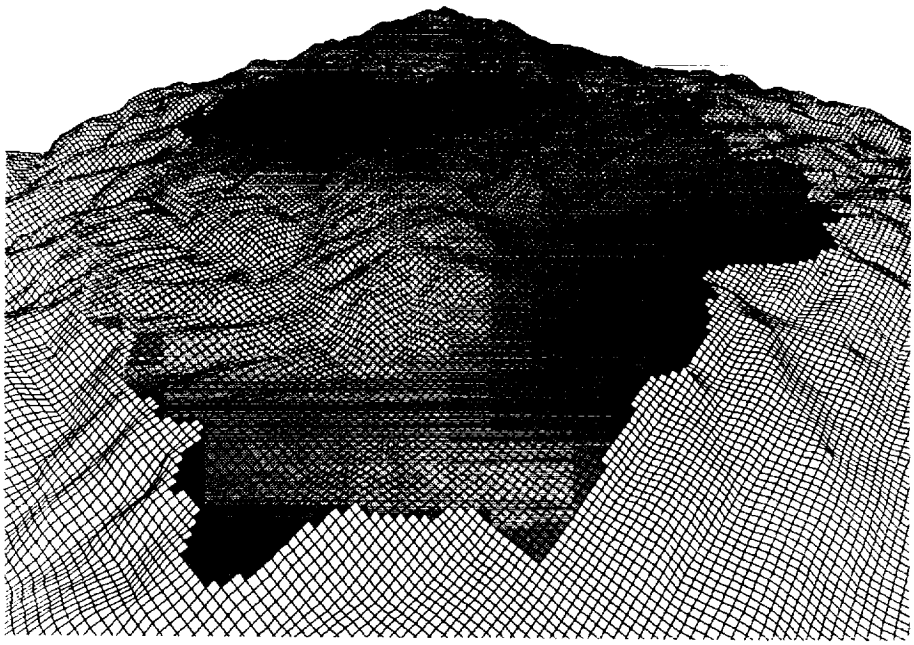

Figure 1. Results of simulations of runoff on a Kansas tallgrass prairie watershed (Konza Prairie Research Natural Area Long-Term Ecological Research Site; also, the site of FIFE. Adapted from Wood et al., 1990). Patterns are superimposed on the digital elevation model of the site. (a) Rainfall for a storm on August 4, 1987; (b) predicted runoff assuming dry initial conditions.

in improving the biogeochemistry and biology in these models, but improvements to the runoff routing will be required in addition to improved ET simulations.

Validation of earth system models including hydrology is again difficult. Replication is essentially impossible at the scales of interest and experimental manipulation unlikely. Two approaches have been used with some success. The large field experiment, exemplified by FIFE or the Hydrological Atmospheric Pilot Experiment (Sellers et al., 1988), can test parameterizations of the ET and small-scale routing issues by extensive measurements of soil moisture, stream flow, and fluxes above the canopy. Basin-scale investigations can compare model simulations to river hydrographs (Vörösmarty et al., 1989), although the validity of the internal processes remains untested. In the end, these models will have to be tested against a few intensive field studies and long-term records and then compared broadly to routinely collected data on rainfall, stream and river flow, and river biogeochemistry. Simulations of paleoevents, such as the

b

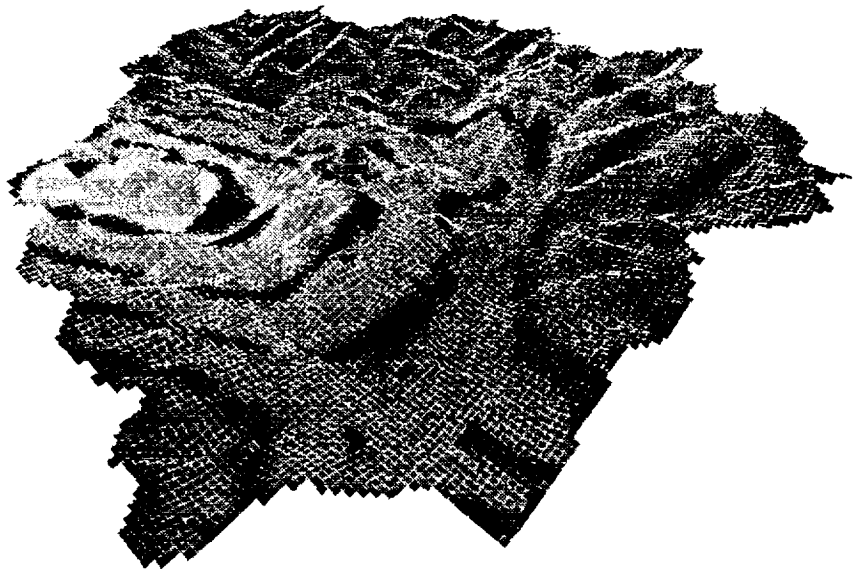

Figure 1(b).

hypothesised Younger Dryas event, will also be helpful in establishing confidence in these complex simulations. Finally, the global parameterizations should be based on extensively tested and more complex regional models.

The Carbon Cycle

Issues in the terrestrial carbon cycle have been extensively argued over the past decade or so, and many unresolved questions remain (Houghton et al., 1983; Detwiler and Hall, 1988; Tans et al., 1990). Tremendous effort has been expended on resolving the question of whether the terrestrial biosphere is a source or sink for CO_2. I will not attempt a new analysis of this question but will instead outline steps that seem necessary to resolving it, and further steps required for inclusion of an interactive terrestrial biosphere in earth system models. The questions that must be answered to address the source/sink issue seem now to be: (1) Where and when, if ever, is

CO_2 fertilization expressed? (2) What are the geography and carbon budgets for disturbed ecosystems; can these systems be a sink? (3) Can climate change (variability) over the past century have caused a directional change in carbon storage? In order to include an interactive biosphere into earth system models, the following additional questions must be answered: (1) If terrestrial ecosystems are now a sink, what are the limits to sink strength? (2) How will vegetation distribution change and how will this affect the carbon cycle? Finally, for both issues (source/sink, predictive models), how can the answers be tested at large scales?

Can the terrestrial biosphere serve as a long-term sink for carbon? Enhanced CO_2 will lead to increased photosynthesis under certain conditions. Three factors may limit the significance of this increase. First, it may be a transient, as some evidence shows that plants may acclimate to increased CO_2 and show a gradually decreasing response.

Second, the effects of CO_2 may be attenuated by constraints from other limiting factors. Nutrients or water may limit CO_2 uptake at levels only slightly greater than under current CO_2 concentrations. The interaction of CO_2 fertilization with other limiting factors requires far more study in a range of ecosystems with varying limiting factors. CO_2 fertilization has the potential to alter nitrogen and water use by allowing increased enzyme efficiencies (photosynthetic enzymes contain large amounts of N) or by increasing water-use efficiency through stomatal effects. Under most circumstances, these changes in water- or N-use efficiencies will result in the production of plant tissue with reduced content of N and other nutrients. This is because CO_2 fertilization does not enhance nutrient availability through any known mechanism and, with increased efficiency, more biomass will be produced on the same amount of nutrients. The production of plant tissue with higher C:element ratios will increase microbial uptake of nutrient when that tissue is decomposed, competing with plants and reducing nutrient availability (Parton et al., 1987; Melillo et al., 1984). This feedback will tend to reduce the effects of CO_2 fertilization on primary production, homeostatically. We have evaluated the consequences of increasing CO_2 on carbon storage in a grassland model (Figure 2) and found the behavior described above to apply; that is, feedback through plant-microbial competition for nutrients limited the effects of CO_2-induced increases in resource use efficiencies.

Third, an extrapolation of the above effect suggests that the ability of terrestrial ecosystems to store carbon is limited by the availability of other resources. If CO_2 were to increase carbon storage in some or most ecosystems, how much carbon could they store? A certain amount of C can be stored in plant biomass, especially in

wood. However, the maximum biomass of forests is constrained mechanically, by nutrients and light, and by human requirements for forest products. Carbon storage in soil organic matter is a more permanent sink, having a turnover time of hundreds to thousands of years. All organic matter, however, has nutrients associated with it, and soil organic matter is normally quite rich in nutrients. For example, N in humus is generally 5 to 20 times more concentrated than in plant biomass (Parton et al., 1987). Thus any major increase in soil carbon will constitute a major sink for N and other nutrients, eventually leading to the same sorts of restrictions on primary productivity described above. In effect, the humus becomes a competitive sink for nutrients with the plants, and production must decline. Bogs and other wetland areas where peat accumulates are the contemporary examples of this process, having high carbon storage and low primary productivity.

The use of fertilization in agriculture to support or enhance the direct CO_2 effects on primary production would seem to enhance a negative feedback to atmospheric CO_2 concentration. However, rates of decomposition are relatively high in agricultural systems and rates of carbon stabilization low. Most agricultural soils contain at the most a few percent carbon, and the carbon content tends to decline slowly or stabilize at low levels (Bouwman, 1990). Thus the negative feedback due to fertilizing agricultural soils is limited; however, carbon once stabilized in cultivated soils may have a long residence time (Parton et al., 1987; Trumbore et al., 1990).

Disturbed ecosystems may pass through a period of rapid carbon accumulation, where stocks of biomass and soil carbon are replenished (see Houghton et al., 1983). This phenomenon is evident in recently harvested forests, after burning, and following severe storm damage. The expansion of the use of terrestrial ecosystems in the past century may have "reset the clock" for many ecosystems to the point where they are accumulating organic matter rapidly and serving as a sink. While the accumulation of carbon following disturbance is included explicitly in the budgetary estimates of Houghton et al. (1983) and Detwiler and Hall (1988), our data on the geography of disturbance and recovery rates are not numerous (Botkin and Simpson, 1990).

In conclusion, terrestrial ecosystems are unlikely to be a long-term sink for CO_2, although certain areas act as sinks for some intervals. The ability of ecosystems to store carbon is limited and unlikely to accommodate the extent of atmospheric CO_2 increases projected as a consequence of industrial civilization.

If greenhouse gas emissions lead to increased temperatures, this will also affect the carbon cycle. Increased temperatures, other fac-

tors being equal, will accelerate decomposition and cause loss of stored carbon, increasing the atmospheric inputs of CO_2 (Schimel et al., 1990). In general, decomposition is quite sensitive to temperature (e.g., Parton et al., 1987). In a recent simulation exercise, we showed that across a range of grasslands, increased temperature resulted in soil carbon losses despite enhanced production due to CO_2 enrichment (Figure 2). While this result is only for one ecosystem type, other models exhibit similar behavior for other ecosystem types (Pastor and Post, 1986), suggesting it may be a fairly general result. If this is true, then CO_2 fertilization responses may not keep pace with respiration losses resulting from increases in temperature. It is also possible that climate changes over the past few centuries, including a possible greenhouse effect term, have resulted in significant changes in soil carbon storage. Substantial improvements in data and models will be required to test this hypothesis and even to establish the direction of the change; nonetheless, this would be an interesting exercise even with current process models.

Testing process-based models of the carbon cycle presents major challenges. While regional models can be developed and tested effectively, repeating this process in every ecosystem globally is precluded by logistics. Testing at the global scale is feasible using atmospheric CO_2 concentration gradients, but these tests do not test the internal dynamics of the model very well, and hence the predictive capability of the model remains in question.

I suggest a strategy based on three techniques. First, models should be based on understanding of principles that have been proven to be broadly applicable—a theory-based approach—rather than on empirical relationships (Schimel et al., in press). Real progress is being made in this area for both autotrophic and heterotrophic processes, although empirical models remain the dominant type for global representations.

Second, while traditional field tests cannot be made everywhere, remote sensing can obtain data in virtually all terrestrial ecosystems. Remote observations can serve to quantify temporal and spatial distributions of ecosystem properties with current techniques (Tucker et al., 1986). Excellent progress is being made on retrieving more quantitative information on hydrology, physiology, and biogeochemistry using satellite data (Schimel et al., 1991b; Wessman et al., 1988). While many of the traditional formulations for ecological and hydrological processes are not readily tested with remote sensing, often these models may be transformed or reparameterized to allow such testing (Schimel et al., 1991b).

Finally, the aggregate output of models already tested regionally using remote sensing and field techniques can be compared to

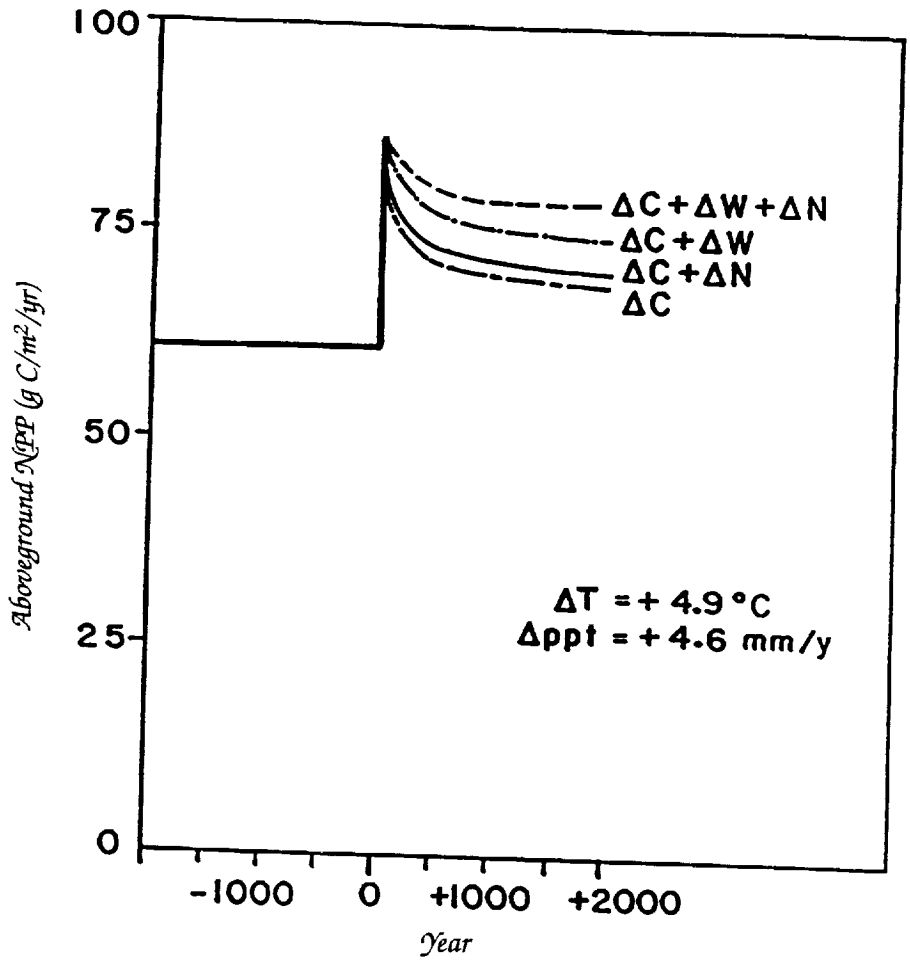

Figure 2. Century simulations showing the response to changing water-use efficiency (ΔW), nitrogen-use efficiency (ΔN), and both to simulate the direct effects of CO_2 enrichment (ΔC). The altered water-use efficiency and nitrogen-use efficiency were imposed after a step change in temperature and precipitation to a doubled-CO_2 climate. Note that despite enhanced NPP, the net effect of the temperature increase was a reduction in stored carbon due to increased decomposition.

atmospheric CO_2 and other trace gas fields. Comparison of predicted source/sink relationships may be compared to inverse calculations of those sources and sinks (Tans et al., 1990).

In summary, while no one method of testing will allow full confidence to be established in carbon biogeochemistry models, the application of a hierarchy of tests will allow comprehensive evaluation. Application of the tests proposed is contingent on continued development of theory and practice for both ecosystem analysis and

measurement techniques, especially remote sensing. Progress in these areas is very encouraging although major challenges remain.

Conclusions

Interactions of the terrestrial biosphere and hydrology with the atmosphere are a critical component of earth system modeling; these interactions will influence the trajectory both of climate, especially regional climate, and of ecosystems upon which humankind depends for sustenance. Critical gaps remain in the modeling of these interactions. In many cases these gaps arise because of the independent evolution of atmospheric, hydrological, and ecological models within those disciplines. Because of this independent evolution, connections and reciprocal requirements must now be worked out as earth system modeling emerges as a major research area.

References

Avissar, R., and M.M. Verstraete. 1990. The representation of continental surface processes in atmospheric models. *Reviews of Geophysics 28*, 35–52.

Band, L., and E.F. Wood. 1988. Strategies for large scale distributed hydrological simulation. *Applied Mathematics and Computation 27*, 23–37.

Botkin, D.B., and L.G. Simpson. 1990. Biomass of the North American boreal forest: A step toward accurate global measures. *Biogeochemistry 9*, 161–174.

Bouwman, A.F. 1990. Background. In *Soils and the Greenhouse Effect* (A.F. Bouwman, ed.), John Wiley and Sons, New York, 25–167.

Broecker, W.S. 1981. Glacial to interglacial changes in ocean and atmospheric chemistry. In *Climate Variations and Variability: Facts and Theories* (A. Berger, ed.), D. Reidel, Dordrecht, The Netherlands, 109–120.

Detwiler, R.P., and C.A.S. Hall. 1988. Tropical forests and the global carbon cycle. *Science 239*, 42–47.

Dickinson, R.E. (ed.) 1987. *The Geophysiology of Amazonia.* John Wiley and Sons, New York.

Field, C.B. 1990. Ecological scaling of carbon gain to stress and resources availability. In *Integrated Response of Plants to Stress* (H.A. Mooney, W.E. Winner, and E.J. Pell, eds.), Academic Press, New York.

Giorgi, F. 1990. Simulation of regional climate using a limited area model nested in a general circulation model. *Journal of Climate 3*, 941–963.

Gleick, P.H. 1987. Regional hydrological consequences of increases in atmospheric CO_2 and other trace gases. *Climatic Change 10*, 137–160.

Gupta, V., I. Rodrigues-Iturbe, and E.F. Wood. 1986. *Scale Problems in Hydrology*. D. Reidel, Hingham, Massachusetts.

Hewlett, J.D., and A.R. Hibbert. 1967. Factors affecting the response of small watersheds to precipitation in humid areas. In *Forest Hydrology* (W.E. Sopper and H.W. Lull, eds.), Pergamon, New York.

Hobbs, N.T., D.S. Schimel, D.S. Ojima, and C.E. Owensby. Environmental contingency influences ecosystem processes: Fire and grazing in the tallgrass prairie. *Ecology*, in press.

Houghton, R.A., J.E. Hobbie, J.M. Melillo, B. Moore III, B.M. Peterson, G.R. Shaver, and G.M. Woodwell. 1983. Changes in the carbon content of terrestrial biota and soils between 1860 and 1980. *Ecological Monographs 53*, 235–262.

Jarvis, P.G., and K.G. McNaughton. 1986. Stomatal control of transpiration: Scaling from leaf to region. *Advances in Ecological Research 15*, 1–49.

Johnson, I.R., and J.H.M. Thornley. 1984. A model of instantaneous and daily canopy photosynthesis. *Journal of Theoretical Biology 107*, 531–545.

Knapp, A.K., and W.K. Smith. 1988. Effects of water stress on stomatal and photosynthetic responses in subalpine plants to cloud patterns. *American Journal of Botany 75*, 851–858.

Knapp, A.K., and W.K. Smith. 1990. Stomatal and photosynthetic responses to variable sunlight. *Physiology Plantarum 78*, 160–165.

Melillo, J.M., R.J. Naiman, J.D. Aber, and A.E. Linkins. 1984. Factors controlling mass loss and nitrogen dynamics of plant litter decaying in northern streams. *Bulletin of Marine Science 35*, 341–356.

Mitchell, J.F.B., C.A. Senior, and W.J. Ingram. 1989. CO_2 and climate: A missing feedback? *Nature 341*, 132–134.

Moore, B. 1990. Committee on Global Change (U.S. National Committee for the IGBP). Integrated modeling of the earth system. In *Research Strategies for the U.S. Global Change Research Program*, National Academy Press, Washington, D.C., 1990, 67-107.

Noy-Meir, I. 1977. Desert ecosystems: Environment and producers. *Annual Review of Ecology and Systematics 4*, 23–51.

Parton W.J., A.R. Mosier, and D.S. Schimel. 1988. Rates and pathways of nitrous oxide production in a shortgrass steppe. *Biogeochemistry 6*, 45–58.

Parton, W.J., D.S. Schimel, C.V. Cole, and D.S. Ojima. 1987. Analysis of factors controlling soil organic matter levels in Great Plains grasslands. *Soil Science Society of America Journal 51*, 1173–1179.

Pastor J., and W.M. Post. 1986. Influence of climate, soil moisture and succession on forest carbon and nitrogen cycles. *Biogeochemistry 2*, 3–27.

Pastor, J., and W.M. Post. 1988. Response of northern forests to CO_2-induced climate change. *Nature 334*, 55–58.

Ramanathan, V., B.R. Barkstrom, and E.F. Harrison. 1989. Clouds and the earth's radiation budget. *Physics Today 42*, 22–32.

Schimel, D.S., M.A. Stillwell, and R.G. Woodmansee. 1985. Biogeochemistry of C, N and P in a soil catena of the shortgrass steppe. *Ecology 66*, 276–282.

Schimel, D.S., W.J. Parton, F.J. Adamsen, R.L. Senft, and M.A. Stillwell. 1986. The role of cattle in the volatile loss of nitrogen from shortgrass steppe. *Biogeochemistry 2*, 39–52.

Schimel, D.S., W.J. Parton, T.G.F. Kittel, D.S. Ojima, and C.V. Cole. 1990. Grassland biogeochemistry: Links to atmospheric processes. *Climatic Change 17*, 13–25.

Schimel, D.S, T.G.F. Kittel, A.K. Knapp, T.R. Seastedt, W.J. Parton, and V.B. Brown. 1991a. Physiological interactions along resources gradients in a tallgrass prairie. *Ecology 72*, 672–684.

Schimel, D.S., T.G.F. Kittel, and W.J. Parton. 1991b. Terrestrial biogeochemical cycles: Global interactions with the atmosphere and hydrology. *Tellus 43(4)*, 188–203.

Sellers, P.J., Y. Mintz, C. Sud, and A. Dalcher. 1986. A simple biosphere (SiB) model for use within general circulation models. *Journal of the Atmospheric Sciences 43*, 505–531.

Sellers, P.J., F.G. Hall, G. Asrar, D.E. Strebel, and R.E. Murphy. 1988. The First ISLSCP Field Experiment (FIFE). *Bulletin of the American Meteorological Society 69*, 22–27/

Shukla, J., C. Nobre, and P.J. Sellers. 1990. Amazonian deforestation and climate change. *Science 247*, 1322–1325.

Smith, L.D., and T.H. Vonder Haar. 1991. Clouds-radiation interactions in a general circulation model: Impact upon the planetary radiation balance. *Journal of Geophysical Research 96*, 893–914.

Tans, P.P., I.Y. Fung, and T. Takahashi. 1990. Observational constraints on the global atmospheric CO_2 budget. *Science 247*, 1431–1438.

Trumbore S.E., G. Bonani, and W. Wolfli. 1990. The rates of carbon cycling in several soils from AMS ^{14}C measurements of fractionated organic matter. In *Soils and the Greenhouse Effect* (A.F. Bouwman, ed.), John Wiley and Sons, New York, 407–414.

Tucker, C.J., I.Y. Fung, C.D. Keeling, and R.H. Gammon. 1986. Relationship between atmospheric CO_2 variations and a satellite-derived vegetation index. *Nature 319*, 195–199.

Vörösmarty, C.J., B. Moore III, A.L. Grace, M.P. Gildea, J.E. Melillo, B.J. Peterson, E.B. Rastetter, and P.A. Steudler. 1989. Continental-scale models of water balance and fluvial transport: An application to South America. *Global Biogeochemical Cycles 3*, 241–265.

Wessman, C.A., J.D. Aber, D.L. Peterson, and J.M. Melillo. 1988. Remote Sensing of canopy chemistry and nitrogen cycling in temperate forest ecosystems. *Nature 335*, 154–156.

Whalen, S.C., and W.S. Reeburgh. 1988. A methane flux time series for tundra environments. *Global Biogeochemical Cycles 2(4)*, 399–409.

Wilks, D. 1988. Estimating the consequences of CO_2-induced climatic change on North American grain agriculture using general circulation model information. *Climatic Change 13*, 19–42.

Wood, E.F., M. Sivapalan, K. Beven, and L. Band. 1988. Effects of spatial variability and scale with implications to hydrological modeling. *Journal of Hydrology 102*, 29–47.

Wood, E.F., M. Sivapalan, and K. Beven. 1990. Similarity and scale in catchment storm response. *Reviews of Geophysics 28*, 1–18.

Evaluating Models of Climate and Forest Vegetation

James S. Clark

Introduction

Understanding how the biosphere may respond to increasing trace gas concentrations in the atmosphere requires models that contain vegetation responses to regional climate. Most of the processes ecologists study in forests, including trophic interactions, nutrient cycling, and disturbance regimes, and vital components of the world economy, such as forest products and agriculture, will be influenced in potentially unexpected ways by changing climate. These vegetation changes affect climate in turn through changing C, N, and S pools; trace gases; albedo; and water balance. The complexity of the indirect interactions among variables that depend on climate, together with the range of different space/time scales that best describe these processes, make the problems of modeling and prediction enormously difficult. These problems of predicting vegetation response to climate warming and potential ways of testing model predictions are the subjects of this chapter.

Before evaluating predictions about vegetation, it is important to consider that "vegetation" encompasses many variables. These include a variety of state variables (e.g., leaf area, density, standing crop, basal area, litter), which can be measured at any given instant, and rates (e.g., growth, thinning, net primary production, decomposition), which can be estimated from repeated measurements. Because these variables are typically considered at different scales of space and time, models differ in how they treat these variables. For example, leaf area is a boundary condition in Running and Coughlan's (1988) model, while it is a prediction of gap models (Botkin et al.,

1972; Shugart, 1984). In Clark's (1990a) model, leaf production is dynamic, but, as in Running and Coughlan's (1988) model, individual trees are ignored. Gap models (Botkin et al., 1972; Shugart, 1984; Pastor and Post, 1986) consider every tree larger than a particular diameter. Treatment of such variables differs, because each model is designed for a different purpose. Consequently, each of these approaches has its strengths and weaknesses.

The variables contained in models and the selection of boundary conditions are influenced by the complexity of the process, which is largely determined by the number of ways in which different processes are related. These vegetation variables depend on climate directly and on other factors that also depend on climate. Temperature, for example, has direct effects on rates of photosynthesis and respiration. It also influences the microbially mediated mineralization of N, and hence the accumulation of organic matter in the forest floor; the probability of fire at several time scales; soil moisture storage; and the growth rates of all other plants within a stand that compete for light, water, and N. Temperature effects on these other variables that influence growth rate complicate the response of vegetation to temperature. Similarly, although physiology of seedlings responds to CO_2 concentration (Norby et al., 1986a), it is difficult to extrapolate these results to landscapes of trees of different ages. Increased water use efficiencies of individual trees at elevated CO_2 concentrations are expected to have many indirect effects on stand dynamics (e.g., Jarvis and McNaughton, 1986; Eamus and Jarvis, 1989; Graham et al., in press). Associated changes in litter quality and thus N cycling, for example, could have complex and protracted influences on vegetation composition (Norby et al., 1986a, 1986b). The composite effect of climate on vegetation therefore includes effects on many state variables and fluxes by many indirect and correlated pathways.

This complexity of the climate's control over so many important processes represents perhaps the greatest challenge for prediction of how a change in one or several climate variables in the future may influence vegetation. This complexity may be so severe as to frustrate efforts to predict even what might be the sign of a given response. The fact that increasing temperatures might decrease growth of moisture-limited plants while increasing growth of plants not limited by moisture is one of the simplest such examples—temperature variability potentially has opposing consequences as a result of the indirect effects on moisture availability. In this case, knowledge of the sign of direct and indirect effects is not sufficient for predicting the sign of the composite effect. Either direct or indirect pathways may prevail, depending on the many indirect linkages and correlated

causes, functional forms of each dependency, and initial conditions. Nonlinearities in these dependencies result in variable sensitivities of predictions to parameter values. This complexity makes it important to test model output under a range of environmental settings, to test a range of predictions, and to explore sensitivities to the variability in parameter values that may exist in the real world.

Pastor and Post's (1988) predictions of composition change in Minnesota under doubled CO_2 represent an example from climate change literature of the potential importance of indirect effects of climate on vegetation change (Figure 1). The area considered in this example is predicted to become warmer and drier (Manabe and Wetherald, 1986; Kellogg and Zhao, 1988; Rind, 1988). Sandy soils

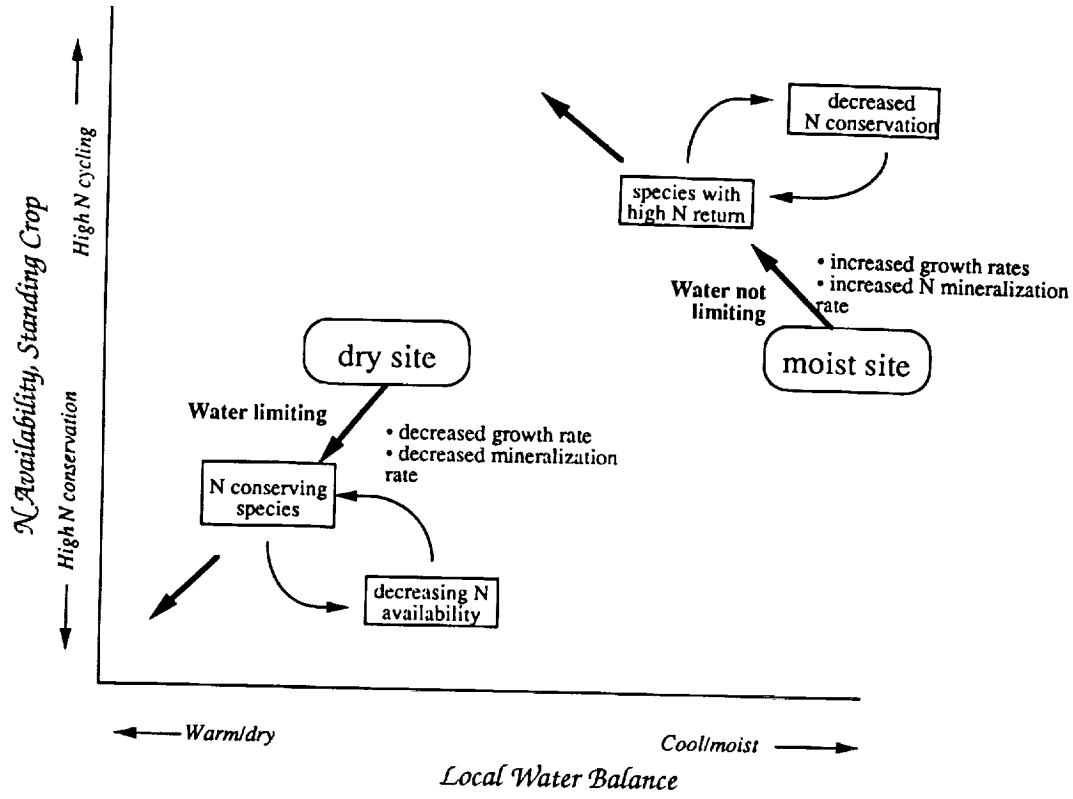

Figure 1. Potential feedback effects of warmer and drier climates on forests suggested by simulation models of Pastor and Post (1988). Sites that initially are rather similar could become increasingly different when subjected to warm/dry conditions as a result of modest initial differences in local water balance. On the moist site, higher temperatures lead to increased mineralization rate, while on the dry site moisture is limiting, and mineralization rate decreases. Subsequent changes in species composition, and thus litter chemistry, provide feedback effects that exaggerate these differences (from Clark, 1991a).

in the region hold little moisture, and the rate of N mineralization is limited by moisture availability; finer-textured soils hold more moisture, and N mineralization rates are higher.

Simulation models predict that future warmer and drier conditions would affect vegetation and nutrient cycling on these different types of Minnesota soils in distinctly different ways. On coarse soils, moisture limitation of N mineralization would become more severe as precipitation decreased and atmospheric demand for soil moisture increased. Decreased mineralization rates would lead to lower N availability and to a shift to species more conservative in their use of N. The change in species composition represents a positive feedback on the nutrient cycle, because N-conservative species return smaller amounts of N to the soil in litterfall. On finer-textured soils that hold more soil moisture, however, the negative effect of drier conditions might be less important than would be the positive effect of higher temperatures. If moisture is not limiting to microbial populations responsible for N mineralization, higher temperatures allow higher mineralization rates. Here again, a positive feedback may come into play, because higher N availability promotes species that cycle larger quantities of N (Chapin, 1980; Vitousek, 1982; Pastor et al., 1984). Mineralization rates increase further with the larger quantities of N returned in litterfall.

Thus, a change to warmer and drier conditions could have opposite effects on different parts of the landscape, and this is indeed what Pastor and Post's (1988) models suggest. In their simulations, similar vegetation types on silty clay loam and on sandy soils changed in opposite directions under warmer conditions. Productivity of dry sites decreased as mixed hardwood and conifer forests shifted to a depauperate oak savanna. On finer soils, stands became *more* productive, as mineralization rates increased and species that cycle larger amounts of N became of increasing importance.

These complex interrelationships present difficulties that are compounded by the need to accommodate vastly different spatial and temporal scales. The climate models are comparatively coarse in space (grid spacing of 1° to 10° latitude by longitude), and they run at rather short time steps (roughly an hour). Many vegetation models have annual time steps on plots with sizes of only fractions of a hectare. One potential approach for integrating such models is to spatially average vegetation parameters to serve as boundary conditions for general circulation models (GCMs) over time and to temporally average climate variables for vegetation models over space. The time-averaged climate output is assumed to apply everywhere in that grid cell, and the spatially averaged vegetation output is assumed constant for many time steps of the climate model. Para-

meters could also be converted to simple functions of space or time to accommodate topographic complexity or seasonality. Another approach might be to shift the focus of vegetation models to better accommodate the scales of GCMs (Running and Coughlan, 1988). The kinds of GCM output required for biosphere models are discussed in Bretherton et al. (this volume). Below I summarize some important features of models that have been or can be used to explore vegetation responses to climate change. I then suggest some of the ways in which these models can be evaluated.

Types of Models

Several types of models have been used to address forest responses to climate change. A review of these models is beyond the scope of this chapter. Here I simply point out some of the major differences among them and some aspects that will be referenced in the next section on model evaluation.

Models that can be used to predict vegetation response to climate range from simple and highly empirical to rather more mechanistic and complex. Box (1981) applied a simple set of rules that could be used to predict vegetation "life forms" (based on growth form, seasonal habit, and leaf type, size, and structure) on the basis of water-balance variables. Maximum and minimum values of each water-balance variable (monthly totals and means) were identified for locations of each vegetation life form and used to map vegetation types globally. A more recent and independent analysis of the factors regulating vegetation types at subcontinental scales (Neilson et al., 1989) resulted in a set of "rules" that could be applied in a similar on/off fashion for predicting vegetation biomes. Neilson et al. (1989) interpreted empirical relationships between water balance and vegetation cover in terms of life histories of resident plants. They identified combinations of water-balance variables that help to explain distributions at broad scales and ways to link vegetation with macroclimate. The Holdridge life-zone classification scheme used by Emanuel et al. (1985) is a further example in which simple empirical relationships aid identification of the potential effects of climate change on vegetation. All of these studies make use of simple, empirical relationships that can have powerful predictive capabilities, and they can facilitate understanding of mechanisms at broad spatial scales. The most accurate predictions of vegetation responses to climate change might come from applying a simple set of rules regarding vegetation type and water balance.

The principal limitations of such empirical approaches are their inability to handle climate/vegetation relationships that do not cur-

rently exist on the globe and their inability to address dynamics. The first limitation is clearly a concern given the past existence of assemblages with no close existing analogs (e.g., Davis, 1981; Webb, 1988). Future climate conditions are also likely to include types of climates that do not now exist, so we cannot hope to confidently predict the assemblages of species that will co-occur in such cases. The second limitation relates to the inherent static nature of such calibration/prediction activities. Results of these models aid understanding of potential patterns, but they do not address the transient aspects of changing climate and tracking vegetation.

Contrasting with this simple approach are forest gap models (Botkin et al., 1972; Shugart and Noble, 1981; Shugart, 1984; Pastor and Post, 1986), which have been used more than other types of models for exploring effects of climate change. These models simulate the growth and development of each tree on a plot the size of one mature individual. Plant recruitment, growth, and mortality depend on resource availabilities, regional climate, and disturbance regimes (Shugart and Noble, 1981). The landscape is assumed to consist of a mosaic of such patches that are independent of one another. Thus, the landscape patterns are summarized from a number of separate runs of the same model, each subject to a different random number sequence, which influences recruitment and mortality processes. As in real forests, recruitment tends to occur most strongly following disturbances, such as the canopy gaps that result from mortality of a large individual. Because plots are independent, gap processes on different plots are out of phase. Recent incorporations of an N cycle (Aber et al., 1982; Pastor and Post, 1986) permit exploration of the role of fertility in the climate response. This class of models is most useful for understanding effects of different equilibrium climates on forest structure. Existing versions of the model would not address protracted transient climate conditions particularly well, because most do not allow for broad spatial processes, such as species migration. The water balances in existing models (e.g., Thornthwaite in Pastor and Post's Linkages model) are semiempirical. The space and time scales used in these models reflect the fact that some of the interesting and important dynamics of forest vegetation are best described at scales much different from those that describe the atmosphere. Resources (light and N) that are the basis for much of the dynamics in these models depend on local neighborhoods measured largely at annual rates (e.g., decomposition and N mineralization), while GCMs have short time steps over large areas.

A much different approach of Running and Coughlan (1988) uses leaf area as a boundary condition in a model that focuses on energy and water balance. Stands are dynamic only in the sense that there

occurs an annual partitioning of dry matter to root and stem, which serves as a basis for net primary production (NPP) calculations. As with many ecological studies, this value is difficult to interpret, because consistently positive NPP implies an infinite standing crop. If an "aggrading forest" is implied, this value is equally difficult to interpret, for NPP changes dramatically with age until some "equilibrium" is achieved, at which point NPP is zero. An annual N cycle is included, but it is highly simplified. There are no individual trees. Because of the focus on water and energy, this model is particularly well suited for application with GCMs: Its use is not closely tied to a particular spatial scale, and it contains much detail on the climate side at the expense of stand dynamics. This model comes closest to GCMs in terms of scale, operating on a short time step over potentially large areas.

Clark's model (1990a) is intermediate between these two approaches in some ways. It uses long-term temperature and precipitation data to reconstruct water balances, which in turn drive leaf and woody detritus production, decomposition, N cycling, and fire probability. It is useful for evaluating responses of these ecosystem-level processes to annual and long-term changes in water balance, but it does not permit exploration of climate effects on stand structure. Because of the annual time step, it cannot now be directly linked to GCMs. Like Running and Coughlan's (1988) model, it is not tied to a particular spatial scale.

Evaluating Models

The problems of scale and complexity that make these models difficult to construct also make them difficult to test. Predictions about processes that operate at scales of subcontinents are not subject to tests that require experimental manipulation. The complexity of the models also means that there can be many routes (many importantly wrong) to a given prediction. Thus, tests of one or several predictions do not constitute strong support for the complete model. On the other hand, a complex model makes many predictions. By employing a range of methods it may be possible to test some predictions that can increase understanding and guide future model development.

Manipulations

Although most models of climate effects on forests are difficult to test using artificial experiments, manipulations can play a role for evaluating submodel predictions. Model predictions of vegetation composition for forests (e.g., Shugart, 1984) and nutrient cycling in grasslands (e.g., Schimel et al., 1990) would require long-term

experiments and, in many cases, land areas too large to be manipulated. Submodels dealing with recruitment responses to climate variables, and with N mineralization and immobilization and dry-matter partitioning under different water balances, can be, and in some cases have been, tested with manipulations in the laboratory and field. Many experiments dealing with the soil-plant-atmosphere system are also relevant for understanding climate change effects. Obviously, such studies are the basis for parameterizations of existing models. Pastor and Post (1986) and Running and Coughlan (1988) provide many such comparisons of submodel predictions with empirical data.

One approach to this problem is irrigation experiments. The most profound effects of climate change in many regions may result from altered water balance. Because of the complex ways in which water balance affects ecosystems, the sensitivities of ecosystem-level processes and species composition to water balance are extremely difficult to evaluate. Forecasts of future changes in water balance are tenuous for several reasons (Kellogg and Zhao, 1988; Rind, 1988; Bryson, 1988), but it is possible to explore sensitivity to water balance in several ways (Clark, 1991a). That sensitivity can be assessed by adding water to ecosystems. It is likely that processes will vary in their sensitivities and that indirect interactions among processes could result in unexpected responses. Although species composition and nutrient cycling may have long response times, irrigation for several years might be sufficient to establish whether such processes are sensitive to water balance (Aronsson and Elowson, 1980; White et al., 1988). The potential for manipulation of soil temperature is also being explored within the context of the Long-Term Ecological Research network of the National Science Foundation (W.H. Schlesinger, personal communication). Use of such an approach together with specific submodel tests should provide valuable insights into sensitivity of ecosystems to climate.

Such submodel tests are an important evaluation tool, but they do not test the full model. Submodels could make predictions that match experimental results, while larger models in which they are embedded might incorporate submodel output in ways that produce unrealistic results. Thus, it is important to test performance of submodels, but additional means for assessing predictions of full models are desirable.

Variability along Gradients

Use of spatial gradients as a proxy for response to environmental change through time has long been an invaluable tool and a favorite target for criticism. In the absence of observations over time, analy-

ses of processes along gradients may be the sole opportunity for analyzing a response to environmental change. If we predict that future climates will produce a rising sea level, for example, one source of information on vegetation changes in the coastal zone is the spatial zonation of vegetation types from low to high elevation. Likewise, if the Upper Midwest is predicted to have a climate like that of the Plains States, transitional vegetation might share some characteristics of existing vegetation that lies along a gradient between these two regions.

This method has some obvious shortcomings, but many are not as severe as those of alternatives. Existing patterns result from a possibly long and unknown past. The time scale on which these past influences operate may be vastly different than those that will dictate future climate change. The "transient" patterns may not appear anywhere on the existing landscape, and the existing patterns may themselves be transient and potentially unrelated to the environmental gradient of interest. Cultural practices have been varied and often are difficult to reconstruct. It is generally difficult to establish what lasting effects these practices have had on the modern landscape and how future climate change will interact with land use changes to come.

It is nonetheless important to test model predictions along climatic and soils gradients. Because models for predicting climate effects on forests contain boundary conditions that vary along gradients, an important test of a simulation model is the accuracy and precision with which it can predict vegetation gradients. This ability is a necessary but not sufficient test of such models. Examples of such tests include elevational gradients at Hubbard Brook (Botkin et al., 1972), elevation and fire gradients in Australian eucalypt forests (Shugart and Noble, 1981), and soil-texture variability (Pastor and Post, 1986).

The simpler the model, the easier it may be to test in this manner. The simple and empirical approaches of Box (1981) and Neilson et al. (1989) permit straightforward testing with GCMs. Neilson et al. (1989) evaluated the degree to which GCMs could predict distributions of biomes by comparing model predictions of the relevant water-balance variables with those that best explained vegetation patterns at a continental scale. The many indirect interactions contained in larger models (e.g., Shugart et al., 1986) make it more difficult to identify assumptions responsible for biased predictions.

Forest Reconstructions, Historic Documents, Chronosequences

Vegetation change and chronosequences provide a means for exploring changes over time. Comparisons of such evidence with model results represent one method for evaluating model predictions.

Evidence for actual vegetation changes through time must come from historic documents or from reconstructions from live and dead plant material still present on the site. This stand history is useful for understanding effects of changing climate if some independent record of climate is available for the appropriate spatial and temporal scales. For example, Clark (1990b) compared fire frequencies predicted by models using 20th-century climate data with correlations between 19th-century climate and fire occurrence. In general, however, such information is incomplete, and the data required to understand many processes are not preserved. Historic documents are often "snapshot" views that are difficult to interpret in terms of changes over time. Examples include the original land surveys of the Northeast and Upper Midwest (Grimm, 1984; Seischab, 1990). Forest reconstructions become less detailed as the time before the present increases. The actual evidence for forest changes is limited by mortality and decomposition (forest reconstructions) and incomplete documentation (documents). Although there are many studies of forest history, there are few that consider the effects of changing climate through the past. This is likely to be a focus for future research, and modelers might exploit these results as a basis for testing predictions.

A chronosequence is a series of stands for which different lengths of time have elapsed since the last disturbance occurred, such as fire, logging, or agriculture. Chronosequences have the advantages of containing much information that can be measured directly and offering the opportunity to conduct experiments (e.g., Robertson, 1982). Many processes change with stand age, including nutrient cycling, recruitment, mortality, and species composition, and these changes have been revealed largely through analyses of chronosequences. Unfortunately a "good" chronosequence can be difficult to identify, because the proportion of variance within the series that is due to stand age is generally uncertain. Climate change is a good example of an influence that depends on stand age, and thus its effects on stands within the sequence could depend on time since the last disturbance. This stand age–climate interaction represents a confounding bias. Spatial inhomogeneity is another source of error, as topography and soils are likely to vary within the series. Despite these confounding factors, studies from chronosequences have proved to be among the most useful tools for model development and testing (Shugart, 1984; Pastor and Post, 1986).

Pollen Analysis

Pollen data provide long records of vegetation change, and pollen grains are sufficiently abundant to permit quantitative analysis. These two attributes of pollen data make them extremely valuable in

considering the long-term effects of climate change on vegetation. Pollen grains have been analyzed from sedimentary environments over large geographic areas that have experienced a range of climate changes just since the maximum of the last glaciation (18,000 years before present, or B.P.). Vegetation responses to climate change have been documented in space and time, most fruitfully in recent years with the construction of maps of the pollen data themselves (Webb, 1981), of inferred species migrations (Davis, 1981), of changing community types (Delcourt and Delcourt, 1987), and of rates of change (Jacobson et al., 1987).

There are limitations to the method, which include the facts that pollen data represent a biased record of vegetation and that knowledge of climate changes responsible for past vegetation, and thus pollen, is coarse. The second problem has been addressed by a coordinated effort between climatologists and palynologists through the use of climate/pollen comparisons and GCM predictions of past climate that contain boundary conditions derived from independent evidence. A large data base of fossil pollen from lake and mire sediments (Webb, 1981; Jacobson et al., 1987) has been compared with GCM predictions of climate changes (Kutzbach and Wright, 1985) that have attended past changes in atmospheric CO_2 and aerosols, sizes of ice sheets, amounts and seasonality of solar radiation, and sea surface temperatures (COHMAP, 1988). Comparisons of pollen and other evidence for past species distributions with these climate predictions for past times represents one type of model evaluation.

Overpeck and Bartlein (1989) used modern relationships between surface pollen in lakes and climate variables together with GCM predictions of climate at 18,000 yr B.P. to simulate past pollen distributions. In view of all of the uncertainties associated with the approach, maps of predicted pollen and actual pollen for eastern North America agree reasonably well. This agreement suggests that the GCM captures some of the important features of the climate of 18,000 yr B.P. and that climate/pollen relationships from one time period (i.e., the present) can be cautiously applied to another time period (the past or future). Stand simulations using output from a different GCM produced maps that agreed less well with pollen evidence for forests of 18,000 yr B.P. In such a case it is difficult to determine the degree to which GCM predictions vs. stand simulation predictions might be responsible for unrealistic results. These differences between model predictions and data aid future model development, and they suggest new perspectives for ecologists engaged in attempts to explain past forest changes. Thus, pollen data have already proved a useful tool for model testing, largely because of the broad spatial and temporal domain that can be considered.

Analyzable Models

Development and application of complex simulation models have progressed well ahead of those of the simpler analyzable models that are needed to make simulation models understandable. Despite much debate regarding the relative merits of analytical and numerical models, the topic is so central to the subject of this chapter that some basic points are worth restating. Consider a response variable R that represents some aspect of vegetation. R depends on time t and n factors in the environment, call them c_i:

$$R(t;c) = f(t;c_1,c_2,\ldots,c_n) \tag{1}$$

Now if these n factors act on R independently, then a linear approximation of this dependency can be written as

$$R(t;c) = \sum_{i=0}^{n} b_i c_i \tag{2}$$

with slope coefficients b_i, and the effect of any given factor c_i is simply

$$\frac{dR(t;c)}{dc_i} = b_i \tag{3}$$

Thus we need know only the partial regression coefficient to predict how R might respond to factor i. Sensitivity to c_i is directly related to b_i, thus making the problem rather simple. If the response is importantly nonlinear, then the response to factor i may be more complex than a single coefficient, but it remains a relatively simple and tractable problem.

Now suppose that environmental factors also depend on one another. The effect of c_i on R becomes substantially more complex:

$$\frac{dR(t;c)}{dc_i} = \sum_{j=1}^{n} \frac{\partial R(t;c)}{\partial c_j} \frac{\partial c_j}{\partial c_i} \tag{4}$$

In order to predict the effect of factor i on R we now need to know the effects of i on all other j factors that affect R. Whereas in the first case the sensitivity of variable R was substantially less complex than that of the full model, now the sensitivity of R to a single variable can and usually will be substantially more complex than is the full model of the process. The predicted response to factor i in the second case is potentially subject to errors contained in every parameter, and those errors are propagated in intractable ways.

In fact, the second model represents a more realistic approach, but it may not be desirable for several reasons. First, complex models cannot be analyzed, and they are notoriously difficult to understand. By analysis, I mean the manipulation of the model to discover its behavior and the contributions of different parameters and variables.

For example, what is the relative importance of temperature, both direct and indirect, for recruitment of seedlings? Temperature may only influence growth of large trees in the model, but those growth rates influence in several ways the space/time distribution of canopy gaps where recruitment is possible. If a growth effect on soil moisture is also contained in the model, complexity is likely increased by an order of magnitude. This question can be solved explicitly in several simplified models of the shifting mosaic process (Clark, 1991b), but we cannot even write an analytical expression for the process described by gap models. Only a large factorial experiment could be used to address the problem, and we might still have only a vague impression of the effects of many parameters.

Second, a complicated model requires much information that we likely do not have. Nothing is gained by adding relationships that must be parameterized by guesswork. There are situations where a Thornthwaite water balance may be preferable over Penman-Monteith simply because stomatal conductance and wind speed, required by the latter, are unknown. Although Penman-Monteith is more realistic, lack of information can neutralize this advantage. Simple vegetation models (e.g., Box, 1981) may be preferable to gap models in many situations for the same reason.

The inability to conduct comprehensive sensitivity analyses is a drawback that makes this guesswork dangerous. If we could fully analyze the implications of a particular functional form or parameter value, we would know when to be suspicious of uncertain assumptions. But these assumptions are propagated in such intractable ways through complex models that we may never identify the cause for unrealistic predictions. These effects may simply be tuned out during initial model runs, in which case the "mechanistic" interpretation of the model could be wrong. If so, the increased mechanistic detail simply confuses the issue.

The answer is not to focus only on simple models or only on large models with much detail. Results of large numerical models function in many ways like empirical data from observations and experiments: They suggest or support simple models that then can be analyzed. For example, distributions in space and time of leaf area generated by gap models could be analyzed in simpler models with respect to the dominant environmental conditions. The same distributions could be incorporated in GCMs. Summary and derived parameters, such as distributions of fire regimes in different climatic settings (Clark, 1989), can be analyzed, and they can also be incorporated in slightly more complex models that retain the virtue of analyzability. Such models can be used in ways not altogether different from the simple empirical relationships of Box (1981) and

Neilson et al. (1989). Despite the fact that they are less "mechanistic" than the complex gap models, they can often contribute more to understanding simply because they ignore tremendous complexity at lower levels of organization. Seasonality of precipitation in these simple models explains the distribution of a particular vegetation type. The same answer might emerge from a costly and protracted analysis of a more complicated model, but it would be more difficult to identify than it would from a simple empirical approach.

Simple models have long been an important tool in many disciplines, and it is likely that they could contribute much to the understanding of climate effects on forests. A potentially important research step in the future could involve the parameterization of analyzable models from output of less simple simulation models. Much progress has been made toward the construction of numerical models linking vegetation to climate. Simpler analyzable models represent an area for future development.

Conclusions

There are several kinds of models now available for exploring consequences of climate change for vegetation. These models operate at different spatial and temporal scales, and they focus on different aspects of vegetation and climate. The time steps and landscape areas of some are more compatible with GCMs than are those of others. Given the range of scales at which climate affects vegetation, however, this diversity of modeling strategies is to be encouraged and perhaps expanded to include more attention to analyzable models. Thus far, there seems to have been more effort devoted to complex models with much detail. There are a number of reasons that simpler models may be preferable for many problems, including potentially better predictive potential and more understandable results at higher levels of organization.

One of the more pervasive difficulties associated with the assessment of many models is general lack of documentation concerning model tuning. Much effort has been devoted to validation of the models, but these tests are difficult to evaluate and to extrapolate to future, no-analog conditions without knowledge of how models have been tuned to various situations. More effort devoted to documentation of parameter sensitivity and to model tuning would greatly increase the usefulness of the models for individuals not involved with their actual development.

The large-scale and protracted nature of the climate change responses makes many of these models inherently difficult to test. Each of these methods for evaluating model output has some

unique advantages and many limitations. The logistical problems of spatially large and long-term manipulations limit the potential for experimental approaches. Many submodel predictions are testable, however, and more emphasis on sensitivity of processes to climate variables would aid understanding of what aspects of ecosystems are likely to be affected first and most dramatically by climate change. Experimental manipulations can aid evaluation of some submodel predictions. Gradients provide opportunities to examine model sensitivity to parameters that vary with soils and/or climate. Evidence for vegetation responses to climate change in the past (e.g., forest reconstructions, historic documents, pollen analysis) has the advantage of allowing examination of long-term changes, but this approach is limited by the availability of independent evidence for vegetation and climate changes for corresponding times and places. Because of the complementary nature of these methods, a combination of approaches provides for the most comprehensive model evaluation.

References

Aber, J.D., J.M. Melillo, and C.A. Federer. 1982. Predicting the effects of rotation length, harvest intensity, and fertilization on fiber yield from northern hardwood forests in New England. *Forest Science 28*, 31–45.

Aronsson, A., and S. Elowson. 1980. Effects of irrigation and fertilization on mineral nutrients in Scots pine needles. *Ecological Bulletins 32*, 219–228.

Botkin, D.F., J.F. Janak, and J.R. Wallis. 1972. Some ecological consequences of a computer model of forest growth. *Journal of Ecology 60*, 849–872.

Box, E.O. 1981. Predicting physiognomic vegetation types with climate variables. *Vegetatio 45*, 127–139.

Bryson, R.A. 1988. Civilization and rapid climatic change. *Environmental Conservation 15*, 7–15.

Chapin, F.S. III. 1980. The mineral nutrition of wild plants. *Annual Review of Ecology and Systematics 11*, 233–260.

Clark, J.S. 1989. Ecological disturbance as a renewal process: Theory and application to fire history. *Oikos 56*, 17–30.

Clark, J.S. 1990a. Landscape interactions among nitrogen mineralization, species composition, and long-term fire frequency. *Biogeochemistry 11(1)*, 1–22.

Clark, J.S. 1990b. Twentieth century climate change, fire suppression and forest production and decomposition in northwestern Minnesota. *Canadian Journal of Forest Research 20(2)*, 219–232.

Clark, J.S. 1991a. Ecosystem sensitivity to climate change and complex responses. In *Global Climate Change and Life on Earth* (R. Wyman, ed.), Chapman and Hall, New York.

Clark, J.S. 1991b. Disturbance and population structure on the shifting mosaic landscape. *Ecology 72*, 1119–1137.

COHMAP Members. 1988. Climatic changes of the last 18,000 years: Observations and model simulations. *Science 241*, 1043–1052.

Davis, M.B. 1981. Quaternary history and the stability of forest communities. In *Forest Succession: Concepts and Application* (D.C. West, H.H. Shugart, and D.B. Botkin, eds.), Springer-Verlag, New York, 132–153.

Delcourt, P.A., and H.R. Delcourt. 1987. *Long-Term Forest Dynamics of the Temperate Zone*. Springer-Verlag, New York.

Eamus, D., and P.G. Jarvis. 1989. The direct effects of increase in the global atmospheric CO_2 concentration on natural and commercial temperate trees and forests. *Advances in Ecological Research 19*, 1–55.

Emanuel, W.R., H.H. Shugart, and M.P. Stevenson. 1985. Climatic change and the broad-scale distribution of terrestrial ecosystem complexes. *Climatic Change 7*, 29–43.

Graham, R.L., M.G. Turner, and V.H. Dale. Increasing atmospheric CO_2 and climate change: Effects on forests. *BioScience*, in press.

Grimm, E.C. 1984. Fire and other factors controlling the Big Woods vegetation of Minnesota in the mid-nineteenth century. *Ecological Monographs 54*, 291–311.

Jacobson, G.L., T. Webb, and E.C. Grimm. 1987. Patterns and rates of vegetation change during the deglaciation of eastern North America. In *North America and Adjacent Oceans During the Last Deglaciation* (W.F. Ruddiman and H.E. Wright, eds.), Decade of North American Geology Volume K-3, Geological Society of America, Boulder, Colorado, 277–288.

Jarvis, P.G., and K.G. McNaughton. 1986. Stomatal control of transpiration: Scaling up from leaf to region. *Advances in Ecological Research 15*, 1–49.

Kellogg, W.W., and Z.-C. Zhao. 1988. Sensitivity of soil moisture to doubling of carbon dioxide in climate model experiments. Part I: North America. *Journal of Climate 1*, 348–366.

Kutzbach, J.E., and H.E. Wright. 1985. Simulation of the climate of 18,000 years BP: Results for the North American/North Atlantic/European sector and comparison with the geologic record of North America. *Quaternary Science Reviews 4*, 147–187.

Manabe, S., and R.T. Wetherald. 1986. Reduction in summer soil wetness induced by an increase in atmospheric carbon dioxide. *Science 232*, 626–628.

Neilson, R.P., G.A. King, R.L. DeVelice, J. Lenihan, D. Marks, J. Dolph, B. Campbell, and G. Glick. 1989. *Sensitivity of Ecological Landscapes and Regions to Global Climatic Change*. EPA/600/3-89/073, U.S. Environmental Protection Agency, Washington, D.C.

Norby, R.J., E.G. O'Neill, and R.J. Luxmoore. 1986a. Effects of atmospheric CO_2 enrichment in the growth and mineral nutrition of *Quercus alba* seedlings in nutrient-poor soil. *Plant Physiology 82*, 83–89.

Norby, R.J., J. Pastor, and J.M. Melillo. 1986b. Carbon-nitrogen interactions in CO_2-enriched white oak: Physiological and long-term perspectives. *Tree Physiology 2*, 233–241.

Overpeck, J.T., and P.J. Bartlein. 1989. Assessing the response of vegetation to future climate change: Ecological response surfaces and paleoecological model validation. In *The Potential Effects of Global Climate Change on the United States*, EPA-230-05-89-054, U.S. Environmental Protection Agency, Washington, D.C., 1–32.

Pastor, J., and W.M. Post. 1986. Influence of climate, soil moisture, and succession on forest carbon and nitrogen cycles. *Biogeochemistry 2*, 3–27.

Pastor, J., and W.M. Post. 1988. Response of northern forests to CO_2-induced climate change. *Nature 334*, 55–58.

Pastor, J.J., J.D. Aber, C.A. McClaugherty, and J.M. Melillo. 1984. Aboveground production and N and P cycling along a nitrogen mineralization gradient on Blackhawk Island, Wisconsin. *Ecology 65*, 256–268.

Rind, D. 1988. The doubled CO_2 climate and the sensitivity of the modeled hydrologic cycle. *Journal of Geophysical Research 93*, 5385–5412.

Robertson, G.P. 1982. Factors regulating nitrification in primary and secondary succession. *Ecology 63*, 1561–1573.

Running, S.W. and J.C. Coughlan. 1988. A general model of forest ecosystem processes for regional applications. I. Hydrological balance, canopy gas exchange and primary production processes. *Forest Ecology and Management 42*, 125–154.

Schimel, D.S., W.J. Parton, T.G.F. Kittel, D.S. Ojima, and C.V. Cole. 1990. Grassland biogeochemistry: Links to atmospheric processes. *Climatic Change 17(1)*, 13–25.

Seischab, F.K. 1990. Presettlement forests of the Phelps and Gorham Purchase in western New York. *Bulletin of the Torrey Botanical Club 117*, 27–38.

Shugart, H.H. 1984. *A Theory of Forest Dynamics: The Ecological Implications of Forest Succession Models*. Springer-Verlag, New York.

Shugart, H.H., and I.R. Noble. 1981. A computer model of succession and fire response of the high altitude Eucalyptus forests of the Brindabella Range, Australian Capital Territory. *Australian Journal of Ecology 6*, 149–164.

Shugart, H.H., M.Y. Antonovsky, P.G. Jarvis, and A.P. Sandford. 1986. CO_2, climatic change and forest ecosystems. In *The Greenhouse Effect, Climatic Change, and Ecosystems* (B. Bolin, B.R. Döös, J. Jäger, and R.A. Warrick, eds.), John Wiley and Sons, New York, 475–521.

Vitousek, P.M. 1982. Nutrient cycling and nutrient use efficiency. *The American Naturalist 119*, 553–572.

Webb III, T. 1981. The past 11,000 years of vegetational change in eastern North America. *BioScience 31*, 501–506.

Webb III, T. 1988. Eastern North America. In *Vegetation History* (B. Huntley and T. Webb III, eds.), Kluwer Academic Publishers, Dordrecht, The Netherlands, 385–414.

White, C.S., J.R. Gosz, J.D. Horner, and D.I. Moore. 1988. Seasonal, annual, and treatment-induced variation in available nitrogen pools and nitrogen-cycling processes in soils of two Douglas-fir stands. *Biological Fertility of Soils 6*, 93–99.

Report: Comprehensive System Models: Strategies for Evaluation

Christopher Field, John Kutzbach, V. Ramanathan, and Michael MacCracken

General Considerations

The task of evaluating comprehensive earth system models is vast, involving validations of every model component at every scale of organization, as well as tests of all the individual linkages. Even the most detailed evaluation of each of the component processes and the individual links among them should not, however, engender confidence in the performance of the whole. The integrated earth system is so rich with complex feedback loops, often involving components of the atmosphere, oceans, biosphere, and cryosphere, that it is certain to exhibit emergent properties very difficult to predict from the perspective of a narrow focus on any individual component of the system. Therefore, a substantial share of the task of evaluating comprehensive earth system models must reside at the level of whole system evaluations.

Since complete, integrated atmosphere/ocean/biosphere/hydrology models are not yet operational, questions of evaluation must be addressed at the level of the kinds of earth system processes that the models should be competent to simulate, rather than at the level of specific performance criteria. Here, we have tried to identify examples of earth system processes that are difficult to simulate with existing models and that involve a rich enough suite of feedbacks that they are unlikely to be satisfactorily described by highly simplified or toy models. Our purpose is not to specify a checklist of evaluation criteria but to introduce characteristics of the earth system that may present useful opportunities for model testing and, of course, improvement.

The process of evaluating comprehensive earth system models will parallel, in many respects, the process of evaluating models of individual components of the system. For example, much can be learned about both comprehensive and component models as a result of intercomparisons of models from different groups, using standard data sets (e.g., Cess et al., 1989). Another need common to both kinds of models is assessments of stability and predictability, determined from long runs without external forcing. Both component and comprehensive models need to be evaluated on time scales ranging from very short (days or months) to very long (millennia or even longer). Finally, it is crucial to integrate the processes of model development, data gathering, and model testing, to insure that the data are relevant to testing the models.

The potential for enormous physical, economic, and social consequences of global climate change, and the critical role that comprehensive earth system models will play in future scientific and policy decisions, place unusual requirements on the way validations are conducted and on the translation of model validations into assessments of confidence (Houghton et al., 1990; MacCracken et al., 1990). Here, we have not focused on issues related to assessing model accuracy and expressing those assessments to the scientific and nonscientific communities; rather, we have attempted to identify kinds of tests that facilitate broad communication in this interdisciplinary endeavor and that encourage scientific extensions and improvements in the models.

Experiments at a Range of Time Scales

One of the central complications in earth system modeling is the functional importance, for the entire earth system, of interactions among processes operating over a broad range of time scales. Much of the task of evaluating comprehensive system models must, therefore, involve the fidelity with which component processes interact to simulate realistic amplitudes and dynamics of the behavior of earth system components as well as the coupled system, over the entire range of functionally important time scales. At each time scale, earth system processes may reflect different contributions from each of their component processes; for example, a component that is relatively insignificant over the short term may be quite important over a long time scale. Therefore, analysis of whole system responses at a range of time scales may provide insight into which model components need improvement. Experiments on a range of time scales, in combination with sensitivity analyses (studies of the results of changes in the model's initial conditions or internal parameters), establish a frame-

work for assessing the quantitative role of individual component processes in earth system responses. As we discuss below, there are critical unknowns at every time scale. A focus on these unknowns will insure that model evaluation produces a sensible distribution of emphasis among the components of the comprehensive model.

The Diurnal to Annual Time Scale

Even on a time scale of hours or days, the behavior of coupled and component models may be dramatically different. One clear example of this is the difference in climate predicted by atmospheric general circulation models (GCMs) with and without mechanistic descriptions of the biosphere (Dickinson and Henderson-Sellers, 1988; Shukla et al., 1990). Another motivation for emphasizing the short end of the time scale concerns the relative ease of gathering high-quality data over short intervals.

Clouds, Radiation, and Convection

Cloud feedback is a quantitatively dominant component of existing global change scenarios. The direct radiative effect of a doubling of atmospheric CO_2 is predicted to increase global net radiation by approximately 2 W/m^2, a change likely to be amplified approximately twofold as a result of the effects of increased temperature on atmospheric moisture (Hansen et al., 1984). Increased convection due to climatic warming could, however, dry the upper and middle troposphere, although experimental evidence indicates approximately the predicted water-vapor feedback (Ravel and Ramanathan, 1989; Rind et al., 1991). Increased cloudiness caused by increased atmospheric moisture has large and uncertain effects on the water vapor amplification. In a comparison of 14 GCMs, climate sensitivity to a perturbation in sea surface temperature (SST) varied approximately threefold, primarily as a result of differences in cloud feedbacks (Cess et al., 1989).

Several issues in the general area of cloud feedbacks pose unambiguous, but relatively easily tested, challenges to the explanatory power of earth system models. Satellite data from the International Satellite Cloud Climatology Program, the Earth Radiation Budget Experiment (ERBE), and microwave sensors provide a rich data base for comparison with GCM cloud climatologies. At the daily to annual time scale, many of the cloud questions are most relevant to atmospheric GCMs, but at longer time scales they involve all components of the earth system. A primary challenge for global models should be to accurately reproduce the diurnal cycle of cloudiness and cloud effects on surface energy balance. At present, the GCMs do not do

this well, partly because they do not incorporate realistic cloud properties, as measured from satellite data, and partly for reasons not yet understood. One example of a property poorly represented in the existing GCMs is the cloud albedo, which clearly is as high as 90–95% (Ramanathan, personal communication) for thick clouds with tops above the bulk of the atmospheric water vapor, but is constrained to lower values in current GCMs.

Another poorly understood but potentially important cloud feedback involves the upper limit of 305 K on sea surface temperature in the Western equatorial Pacific. This robust cap, which is unexpected from simple energy balance considerations (Ramanathan, personal communication), appears to result from the linkages between warm SSTs, deep convection, and the formation of large, highly reflective cirrus anvils (Ramanathan and Collins, 1991). The high albedo of these cirrus anvils makes them act as thermostats with the potential to provide a strong negative feedback on global warming.

Other important unresolved questions concern the origin of clouds. To the extent that oceanic cloud formation is limited by the availability of condensation nuclei, biotic controls on dimethyl sulfide (DMS) emissions and the atmospheric sulfur cycle assume critical roles in the regulation of cloudiness (Charlson et al., 1987). Differences in cloud albedo resulting from differences in condensation nuclei potentially complicate the situation even further and further augment the biospheric and chemical controls on cloudiness. Another unexplained aspect of the control of cloudiness concerns a feedback involving storm tracks. If clouds are responsible for much of the equator-to-pole temperature gradient and if this temperature gradient drives the storm tracks, then do clouds and the storm track constitute a self-reinforcing stable interaction? A spectral analysis of the dynamics of cloudiness could go a long way toward answering this question. If the storm track is a major determinant of cloudiness, then the power maximum in the spectral analysis should approximate the two- to six-day period of the storm track.

Effects of anthropogenic sulfur emissions on clear sky aerosols and on cloudiness may also be critical. Radiative effects of increased aerosols are poorly known, but the role of sulfur chemistry in climate regulation has been emphasized by recent suggestions that the net warming from CO_2 has been largely offset by a net cooling from increased cloudiness (Wigley, 1989; Wigley, 1991) resulting from anthropogenic S emissions.

Oceans

A fully interactive ocean is a critical driver of atmospheric processes, but it also responds to forcing from the atmosphere and

cryosphere (Rintoul report, this volume). Coupling among the oceans, atmosphere, and cryosphere generates ocean signatures that can serve as indices for evaluating coupled models. Because essentially all ocean processes are sensitive to these interactions, a broad suite of processes has potential application in testing and developing coupled models. The mixed layer is especially sensitive to interactions with the atmosphere and cryosphere, and its spatial and temporal structure clearly merits focus. In addition, a coupled model should be able to reproduce observed patterns of temperature and salinity, as well as currents.

Chemistry/Tracers

The coupling of chemistry (including sources) with large-scale circulation, convection, clouds, and solar radiation generates the observed variations ("chemical signatures") in a large variety of chemical trace species in the lower atmosphere.

Seasonal cycles in large-scale transport and chemistry interact with the source distribution to produce chemical climatologies (e.g., mean concentration as a function of latitude, altitude, and season) that are unique signatures for each species. For tropospherically inert species (the chlorofluorocarbons, CO_2, krypton-85) the resulting signature is strictly a function of sources and transport. For some species there are limited chemical removal mechanisms (OH + CH_4, OH + CH_3CCl_3) or physical processes (as for water vapor) that control the seasonal cycles. For other more reactive species (carbon monoxide, oxides of nitrogen, ozone) we must include in situ sources that are chemically dependent on a suite of other species or sources (nonmethane hydrocarbons, urban air pollution, lightning-generated nitric oxide). For these latter gases, the resulting chemical climatologies are difficult to predict and verify with current models.

Chemistry interacts with the boundary layer on a diurnal cycle, and the combination of chemistry and mixing determines the net flux of some key species from the surface of the earth to the free troposphere. Less reactive species with calibrated local or regional sources (CFCs, radon, methane, and possibly water vapor) provide measures of the diurnal venting of the boundary layer, and their vertical profiles measure the extent of convective transports. More reactive species (DMS, isoprene) are destroyed rapidly in the boundary layer by reaction with the hydroxyl radical (OH) or ozone (O_3) and thus have distributions that represent a balance between surface emissions, chemical loss and mixing. Other reactive species (O_3, oxides of nitrogen, OH) are involved in very complex chemical cycles in the boundary layer. In particular, ozone loss by deposition to vegetation is an important component of the global ozone budget

and will be regulated not only by mixing of ozone into the boundary layer, but also by the coupled photochemistry within.

Hydrologic Cycle

Success in modeling the evaporation/precipitation balance depends, at the first order, on the integrated behavior of an atmospheric GCM, a surface hydrology model for estimating runoff and soil moisture, and a biosphere model, which influences albedo, aerodynamic roughness, and the surface conductance to water vapor. The hydrologic cycle provides both short- and long-term as well as small- and large-area opportunities for evaluating integrated atmosphere/biosphere/hydrology models.

At the small-area extreme, a comprehensive model should duplicate natural precipitation regimes, for both the detailed statistics of frequency and distribution and the monthly and annual totals. The current generation of atmospheric GCMs used for climate research provides precipitation sums that can be compared with measurements, but the extreme spatial and temporal variability of surface precipitation records, in combination with the GCMs' large grid cells and limited description of surface topography, brings into question the utility of any model evaluation of precipitation sums, especially for less than monthly intervals. On the other hand, as comprehensive models incorporate improved descriptions of the biosphere and of surface hydrology, detailed statistics of precipitation frequency and distribution should provide a basis for increasingly informative evaluations.

For larger regions, the spatial and temporal variability of precipitation combines with the patchy distribution of precipitation recording stations to limit the utility of model evaluations based on precipitation records. While not offering precipitation and evaporation as separate quantities, runoff in major river basins provides a powerful check on regional hydrologic balances. River basin runoff is useful not only because it integrates over large areas, but also because it integrates over the atmospheric, biospheric, and hydrological components of a comprehensive model.

Biosphere

Several lines of evidence indicate that relatively simple spectral indices derived from satellite-based multispectral sensors, for example, the normalized difference vegetation index (NDVI), when appropriately screened, provide reasonably accurate measures of net primary production, especially when integrated over an entire season (Tucker et al., 1986; Fung et al., 1987; Sellers, 1985). NDVI and other simple spectral indices clearly offer room for improvement, but their current performance and global coverage is sufficient to justify

their use as checks for a comprehensive earth system model. Specifically, an integrated model containing an internally driven biosphere component should generate a quantity and phenology (seasonality) of ecosystem production that can be checked against satellite data.

Biosphere function can also be checked against its chemical signature in the atmosphere. These tests require not only that the biosphere component be accurate and accurately driven from other models but also that atmospheric tracer and chemistry modules accurately distribute and process the chemical signatures. Useful targets for analysis include the latitude-dependent annual cycle of atmospheric CO_2 concentration (Fung et al., 1987), the pole-to-pole gradient in mean annual CO_2 (Tans et al., 1990), and the isotopic composition of atmospheric CO_2 (Keeling et al., 1989). Parallel analyses with other trace gases, especially methane and nitrous oxide, will be very useful. The power of atmospheric probes for biosphere function will increase as the frequency and spatial density of high-accuracy sampling, especially over land areas, increases (Tans, in press).

Primary Land Sites

A comprehensive earth system model should, ideally, model all portions of the earth's surface with uniformly high accuracy. In one sense, data from all sites should be equally useful for model evaluation. Areas differ, however, in several respects that influence their ability to contribute interpretive power. Important sources of this variation include (1) the prominence of climatic features that are difficult to predict with single-component models and that have major effects on the coupled earth system, and (2) historical impacts of anthropogenic forcing with important feedbacks on climate. Five regions that clearly express one or both characteristics are discussed below.

Arctic

Arctic regions should be a focus of emphasis in the development and evaluation of comprehensive models because several features of the Arctic atmosphere, oceans, and land surface, although they are difficult to predict with single-component models, have potentially major feedbacks on climate. In the atmosphere, the abundance and radiative consequences of stratus clouds present a major difficulty for existing atmospheric GCMs. These problems are due, at least partly, to the role of Arctic cloudiness in a powerful positive feedback loop. Arctic cloudiness is a major driver in the equator-to-pole gradient in solar radiation absorption at the surface, and this gradient is critical for the storm track. To the extent that the storm track is responsible for Arctic clouds, the cloudiness is self-reinforcing (see "Clouds, Radiation, and Convection," above).

Potential climatic effects of the extent, duration, and thickness of Arctic sea ice make the atmosphere/ocean interface particularly critical in the Arctic. Consequences of changes in sea ice for albedo cannot be accurately determined until cloudiness is better known. Similarly, the albedo of sea ice is critically dependent on the extent of snow cover over the ice, which depends on the extent to which heat flux into the atmosphere resulting from freezing at the ice-ocean interface generates low clouds and snow. Other important but poorly known aspects of the ocean/atmosphere interface include the role of the spatial separation of ice formation and melting in transporting heat to the pole (see Hibler, this volume) and the role of salinity stratification in limiting poleward heat transport by preventing thermal overturning.

Several aspects of the Arctic land surface also have potentially major effects on climate. Changes in albedo resulting from changes in the extent and duration of snow cover are one critical area, but, here again, interactions with cloudiness will dominate the magnitude of the consequences. Changes in the distribution of permafrost and in the active (thaw) depth of permafrost regions may have major impacts on carbon storage in the biosphere. In addition, decreased permafrost may dramatically affect the atmospheric methane (CH_4) budget, as a consequence of the release of methane hydrates currently stored in permafrost.

India

The Indian subcontinent should be a focus for intensive studies because understanding the formation and continental penetration of monsoons will require an effort integrating atmosphere, ocean, and land models. Specific factors that need to be understood include the extent to which warming in the western equatorial Pacific sea surface can prevent monsoon formation, the role of terrestrial vegetation in modulating the land surface energy balance, and the subsequent effects of such modulation on the regional atmospheric circulation.

Africa

Africa, especially northern Africa, provides excellent opportunities for comprehensive model evaluation for at least two reasons. First, the sensitivity of climate to the characteristics and seasonal movement of the intertropical convergence zone (ITCZ) is clearly documented, meaning that accurate climate prediction for the region must build from a solid understanding of the dynamics of the ITCZ. Second, biomass burning in Africa, as well as in other regions, has major impacts on the chemistry of the atmosphere.

U.S. Midwest

The midcontinental United States offers other opportunities to evaluate our understanding of the controls on continental climates because the climate in this region is so sensitive to the interaction of the storm track and pressure belts. In addition, the U.S. data base on agricultural production and consumption of irrigation water, as well as the detailed process information available for the function of many ecosystems, provides an unmatched resource for evaluating predictive models of biosphere function.

Amazon

One final region that should be an intensive focus for evaluation of comprehensive models is the Amazon basin. Weather in this region is to a significant degree internally generated and appears to be quite sensitive to the status of the vegetation (Dickinson and Henderson-Sellers, 1988), a characteristic that also has consequences for the convergence of moisture from outside the region (Shukla et al., 1990). Rapid deforestation in the Amazon is providing a test of the consequences of vegetation change.

Need for Increased Process-Level Data

The primary focus of this chapter is on opportunities for evaluating comprehensive earth system models. At the diurnal to annual time scale, taking advantage of many of the opportunities will require more than comparisons between existing data sets and results of new models or newly integrated models. For many components of the coupled earth system, the shortage of process-level data is at least as great as the need for improved models. Specific data needs include (1) continuing studies of the earth's radiation budget, with measurements analogous to those of the now-completed ERBE; (2) detailed studies of Arctic sea ice dynamics, possibly using microwave data; and (3) improved land surface hydrology, emphasizing landscape-scale evapotranspiration and major basin runoff.

The Annual to Decadal Time Scale

At the annual to decadal time scale, many of the most important unknowns concern the nature and dynamics of the feedbacks, especially feedbacks among the atmosphere, oceans, and land, that regulate major climatic features. Here, we identify six kinds of processes (i.e., El Niño–Southern Oscillation events, extreme climate events, sea ice, oceanic conveyor belt, trace gases, and volcanoes) with potentially dramatic but incompletely understood origins and/or ramifications for climate.

ENSO

The first hypothesis that the atmosphere and oceans interact as a coupled system to control climate at interannual time scales (Bjerknes, 1966) emerged from analysis of what was then called the Southern Oscillation and is now referred to as El Niño–Southern Oscillation. ENSO events, characterized by a strong increase in the eastern equatorial Pacific SST and a strong decrease in upwelling in this region, are incompletely understood but clearly involve atmospheric and oceanic components. ENSO events appear to be initiated by changes in the tropical atmospheric circulation, which lead to changes in the ocean circulation and the eastern Pacific SSTs, which lead, in turn, to large changes in the distribution of precipitation (Philander, 1990).

ENSO events in 1972 and 1976 were preceded by periods of several months of unusually strong southeasterly trade winds, leading to the hypothesis that ENSO is primarily an ocean response to changes in wind shear, the "Kelvin wave hypothesis." The 1982–83 episode, the strongest in this century, was, however, completely different (Rasmusson and Wallace, 1983), leaving the basic mechanism in doubt. Both because the events clearly involve atmospheric and oceanic components and because they have dramatic effects on climate, ENSO generation and dynamics provide an excellent opportunity for evaluating coupled earth system models. The primary test, focusing on the frequency and spatial and temporal structure of the events, will involve only atmospheric and ocean dynamic models, but the suite of component models should be expanded to include a biosphere model, to evaluate changes in abundance and frequency of organisms resulting from changes in SST and upwelling. Chemical models will be necessary to assess changes in CO_2 and CH_4 signatures resulting from changes in the distribution of sources and sinks (biotic and abiotic) as well as changes in atmosphere and ocean transport.

One useful strategy for exploring ENSO events is likely to involve coupled model runs without external forcing. Examining the dynamics of and interactions among SST, surface pressure, winds, convection, and radiation should provide a basis for testing mechanistic hypotheses as well as for comparing natural and model dynamics. For the latter objective, it will be important to focus on the temporal distribution of the inherent variability in the coupled model.

Extreme Events

Extreme events, for example, the North American drought of 1988, provide excellent opportunities for testing the competence of coupled models. Useful information should come both from tests

designed to duplicate a particular episode and from characterizations of the statistical structure of related events in runs without external forcing.

The 1988 North American drought is unusually interesting because, like ENSO, it was probably initiated by changes in winds, which altered SSTs, which then altered atmospheric circulation and the distribution of precipitation in regions far removed from the area of initial atmosphere-ocean interaction (Trenberth et al., 1988). For this and similar well-characterized extreme events, the standards for accurate simulation with a coupled model can be stated very precisely, making them excellent validation exercises.

In general, we need more information on the inherent variability of the climate predicted by coupled models. Comparisons between the distributions of natural and of model variability will provide useful information about the mechanisms driving real climate variation.

Sea Ice

Natural fluctuations in the extent and duration of sea ice are incompletely known but are critical for evaluating the performance of a coupled earth system model. High-latitude cloudiness makes it difficult to assess ice with visible and thermal satellite sensors, but microwave sensors can provide a clear picture of ice extent, though not thickness. Since ice extent is influenced by atmospheric and ocean processes, temporal patterns of ice extent, with and without cloudiness, will be useful for evaluating coupled ice/ocean/atmosphere models.

Sea ice plays a potentially critical role as an amplifier of global warming. Since the albedo of open water is less than that of ice and much less than that of snow-covered ice, any loss of sea ice extent or duration should result in further warming, promoting a positive feedback effect. This simple scenario fails, however, to account for several critical aspects of the polar, and especially the Arctic, climate. An accurate model of the role of sea ice in climate regulation will probably need to address (1) ice/cloudiness interactions, (2) the role of ice movement in heat transport, (3) the regulation of lead (open water) area in sea ice regions, and (4) the role of fresh meltwater in limiting the cooling and subsequent overturning of saline surface waters.

Conveyor Belt

As warm surface waters move into the North Atlantic, they cool by approximately 8°C, releasing a quantity of heat equal to about 30% of the solar radiation incident on this region (Broecker and Denton, 1989). This heat input warms the region, increasing ocean evapora-

tion and, consequently, increasing the salinity of the North Atlantic. Once these saline waters cool sufficiently, they sink to the ocean bottom and move equatorward, driving a massive conveyor belt that transports heat into the North Atlantic. Some evidence points to interannual and decadal-scale fluctuations of salinity, convection, and deep water formation in the northern North Atlantic. The maintenance of the conveyor belt depends on ocean/atmosphere/ice interactions, so that its operation needs to be explored with coupled models. The conveyor belt appears to be maintained by a positive feedback cycle in which the northward movement of warmer surface waters is critical to support enough evaporation to increase salinity to a level sufficient to sink the surface waters to the deep ocean. Externally forced runs with coupled models will provide excellent opportunities for characterizing the range of conditions over which the conveyor belt operates.

Trace Gas Signatures

On the annual to decadal time scale, the chemical constitution of the atmosphere can be substantially changed by anthropogenic emissions, changes in biosphere and ocean exchanges, and volcanic activity. In addition, changes in the atmospheric temperature, circulation, and composition can alter the fate and dynamics of trace species (Prinn and Hartley, this volume). The accuracy of any model designed to predict the concentration and distribution of any trace gas is critically dependent on the atmospheric circulation and on the intensity and distribution of sources and sinks. Assessments for different trace species will require simulations with models incorporating different numbers of components. For relatively inert tracers like CFCs and krypton-85, atmospheric GCM wind fields and descriptions of anthropogenic sources should suffice. Predictions of CO_2 will require a biosphere component for specifying sources and sinks as well as an ocean component for specifying air-sea exchanges. Chemically reactive species like CH_4, nitrous oxide (N_2O), and DMS will demand the integration of an interactive chemistry module.

Studies of trace gas signatures will be especially useful in model runs exploring other sources of variation. For example, ENSO events, volcanos, and the 11-year solar cycle are all associated with substantial changes in atmospheric chemistry.

Volcanos

Major volcanic eruptions have large impacts on the radiation balance and chemistry of the atmosphere. Thus, coupled model runs simulating real eruptions provide a powerful probe for evaluating model responses to short-term, high-intensity external forcing. In

the realm of atmosphere-ocean dynamics, one critical parameter to study is the time until maximum cooling. The spatial structure of the plume can serve as a tracer for an atmospheric GCM. Interactions between upper-atmosphere dynamics and stratospheric chlorine/ozone chemistry will provide useful tests for coupled atmospheric chemistry/dynamics models.

Coupled model runs including emissions from biomass burning and urban air pollution should provide useful comparisons with volcano simulations. These anthropogenic sources of external forcing will differ from volcanic forcing in continuity, spatial distribution, chemical constitution, and elevation of injection.

The Last Century

The period from approximately 1920 to the present offers a unique set of opportunities for evaluating coupled models. The primary advantage of models simulating the 20th century, as opposed to some other century, is the availability of high-quality climate data. Two kinds of additional considerations, however, motivate an emphasis on a period of several decades. First, observational records document significant climate variability within this time period. Records from meteorological stations, when combined to estimate global trends, indicate strong warming in the early 1920s, followed by nearly a decade of cooling during the 1940s. Global mean temperatures through the 1950s and 1960s were relatively stable, while the 1970s was a period of strong warming, with five-year mean global temperature about 0.6°C warmer in 1980 than in 1910 (Folland et al., 1990; Ghil and Vautard, 1991). These decades were not a period of high volcanic activity, and the eruptions that did occur were reasonably well characterized. Variations in greenhouse gases are also well known, though variations in solar forcing and anthropogenic aerosol forcing (the latter probably increasing in amount, resulting in net cooling) are not. Second, long runs of atmospheric GCMs without external forcing demonstrate inherent climate variation over a range of time scales, from a year to a century or more (Hansen et al., 1990).

Given the evidence for variability in nature as well as in atmospheric models, it is interesting to ask how the variation is modulated in coupled models of increasing complexity, with and without external forcing. A sequence of simulations beginning with atmospheric simulations without external forcing is computationally realistic as well as intellectually heuristic. For example, a comparison of models with and without fully interactive oceans will address the role of fully interactive oceans in decadal-scale climate variation. In

addition, the record of ocean heat flux imbalances in a model without a fully interactive ocean should provide a basis for understanding the differences. Adding historical forcing from greenhouse gases and, for the most recent solar cycle, solar variation will begin to address the question of how external forcing impacts the inherent variability of the climate system. With an interactive biosphere model, the coupled model should be able to generate some of the changes in greenhouse gases internally, with only the anthropogenic components applied as external forcing.

The Last Millennium

The motivation for experiments involving the last millennium is an extension of the motivation for the hundred-year time scale. As we move further back in time, the quality of the climate record deteriorates, but a range of interesting new challenges for a coupled model emerges. While climate records for the last millennium hardly compare with those for the last few decades, a combination of several sources of information can lead to high-quality reconstructions. Useful sources of climatic information include descriptions in literature, records of the extent of mountain glaciers, pollen, tree rings, coral, high-resolution sediment cores, and ^{13}C. Long records of solar diameter may give some insight into variation in the solar output, and notations concerning the aurora provide an index of sunspot activity. Based on these sources of information, periods that emerge as candidates to challenge coupled models are the Little Ice Age, from about 1600 to about 1900, and the "Medieval Warm Period" several centuries earlier.

Climate changes during these periods were substantial. The current estimate is that, during the Little Ice Age, global mean temperature decreased by 1–2°C and the cooling was global in extent, though probably confined to the winter. The Medieval Warm Period was probably less dramatic, in terms of both magnitude and areal extent (COHMAP Members, 1988). The basic question to address with studies of coupled models is whether inherent variations in the coupled earth system are sufficient to generate climate changes of this magnitude or whether they must be forced externally by solar and orbital factors or by changes in volcanism. There is some evidence for external forcing. Sunspot activity reached a minimum during the Little Ice Age (Eddy, 1976), and volcanic activity may have increased. New evidence indicates orbit-driven changes in the intensity of seasons, with periods ranging from 12 to 800 years. Yet, it is not known whether these forcings were sufficient to generate the climate changes. Neither is it known whether inherent variation is suf-

ficient. Inherent factors that might become significant at the millennium time scale include changes in atmospheric dust, driven by changes in precipitation and vegetation, and long cycles in the Atlantic conveyor belt.

The Paleo Time Scale

Moving further back in time, the level of detail in the data continues to diminish, but the magnitude of the climate changes continues to increase. Past climates and climate forcers over the era of ice ages, approximately the last 2.5 million years, are now the focus of several active modeling groups and are well enough known that standardized data sets should be developed and widely applied. Accurate simulation of at least one glacial/interglacial cycle, including the global distribution of climate change, nonlinear effects of ice development, and changes in the trace gas composition of the atmosphere, will be a critical test for a coupled earth system model.

For experiments concerning climate changes of the last five million years, the emphasis in model development and evaluation shifts from inherent variability without external forcing to model responses to external forcing. Forcing factors that need to be studied in detail include Milankovitch orbital variations (Kutzbach and Gallimore, 1988; Rind et al., 1989; Berger et al., 1990), changes in solar output (Foukal and Lean, 1990), changes in ocean barriers, and consequences of mountain building (Raymo et al., 1988; Ruddiman and Kutzbach, 1989). Feedbacks that are likely to become important with these external forcings include the role of ice sheets, the role of dust and glacial age aerosol, the role of CO_2 in amplifying radiation effects of orbital variations, and changes in the Atlantic conveyor belt. As in the present-day climate, amplification of external forcing by changes in atmospheric water vapor will be critical. Solid earth processes should be included in coupled models simulating long time scales because of such effects as crustal deformation resulting from ice accumulation.

The Last 125,000 Years

The past 125,000 years provide excellent opportunities for modeling earth system behavior because the system went through a large (interglacial–glacial–interglacial), well-documented variation and because the seasonal and latitudinally varying solar radiation changes that appear to have initiated and paced these large earth system changes are known exactly. These changes are due to changes in the season of perihelion (period of about 22,000 years) and in the tilt of the rotation axis (period of about 41,000 years).

Within the past 125,000 years there are opportunities to study three extreme states (6000, 18,000, and 125,000 years ago), the entire time evolution (125,000 years ago to present), and embedded large and abrupt oscillations (such as occurred at 11–10,000 years ago).

Extreme States

The most recent interglacial maximum, at 6000 years B.P., was a time when the Arctic was warmer and sea ice cover was reduced, when northern continental interiors were drier, and when northern monsoons were stronger. Several modeling groups have already shown that seasonal and latitudinal solar radiation changes on the order of 10 W/m^2 (due to orbital changes which placed perihelion in the northern summer and increased the axial tilt), when inserted in climate models, simulate these changes to some extent.

The most recent glacial maximum, at 18,000 years B.P., provides a contrasting example of the earth system in a glacial state with large ice sheets over North America and Europe, changed biomes, reduced atmospheric CO_2, and changed ocean circulation, including stoppage of the North Atlantic conveyor belt. Most large modeling groups have already attempted to simulate these conditions with atmospheric models and are now beginning to work with coupled models.

The previous interglacial maximum, which occurred at 125,000 years B.P., had a climate somewhat similar to that of 6000 years B.P., but the insolation changes due to orbital changes were larger and the climatic changes mentioned above were even more extreme. Atmospheric CO_2 was at a relative (preindustrial) maximum. There is some evidence that the Greenland ice sheet was significantly smaller than present.

Evolution

A new opportunity is to try to model the time evolution of the earth system, starting 125,000 years B.P. and continuing to the present. This problem has already been studied with toy models and with rather detailed latitudinally varying models that include ice sheet, atmospheric, and ocean components. The possibility now exists to use more fully coupled three dimensional models (with an asynchronous coupling scheme for ice sheets, etc.).

Abrupt Changes

The earth system experienced several abrupt and large changes of several centuries' duration that are embedded within the more slowly evolving conditions mentioned above. The most recent ex-

ample was the period between 11,000 and 10,000 years ago, when the climate cooled and then warmed again abruptly. There is evidence that atmospheric CO_2 also changed abruptly and that the North Atlantic Ocean conveyor belt may have stopped and then restarted, possibly as a result of a massive influx of fresh water from melting glaciers into the North Atlantic. Several modeling groups are studying these phenomena (e.g., Rind et al., 1986).

Additional Model Studies

In addition to modeling the coupled atmosphere, ocean, ice, and biome changes at the above-mentioned times, there are opportunities for special studies. Oxygen and hydrogen isotopes, carbon isotopes, and dust distributions are known to vary significantly between glacials and interglacials, and there are opportunities to use tracer and source/link models to study these changes. In addition to CO_2 variations, mentioned earlier, CH_4 varied significantly and at the same period as the changes in season of perihelion (about 20,000 years).

System feedbacks, such as water vapor (greenhouse) feedback and snow/sea ice feedback, can potentially be studied over a range of extreme climatic states that may help us understand better the cause of apparent temperature stability in the tropics and the nature of high-latitude feedbacks at times of apparent significant reduction in sea ice. The large swing in atmospheric CO_2 concentration between 270 ppm (interglacial) and 200 ppm (glacial), documented in the Vostok ice core, presents a special opportunity to simulate the changes in the carbon cycle that must have occurred.

2–5 Million Years Ago

The marked glacial-interglacial fluctuations described above for the past 125,000 years began to be evident around 2.5 million years ago. Prior to that time, the earth probably had a climate significantly warmer than at present. In contrast to the glacial-interglacial changes, which are believed to be caused by orbitally produced changes in seasonal and latitudinal distributions of solar radiation, the fundamental causes of the general, long-term evolution from warmer to cooler climate are not known.

The role of plate tectonics in changing land-ocean distributions, while of fundamental importance for understanding early earth climates on the scale of tens to hundreds of millions of years ago, is not likely to have been a large factor in the past several million years. However, tectonic forcing could have been important in other ways. One factor may have been the important changes in ocean circulation produced by changing ocean "gateways." The closing of the

Isthmus of Panama several million years ago may have significantly altered the ocean circulation. Another factor may have been the uplift of mountains and plateaus. The associated carbon cycle changes related to changes in weathering caused by uplift may have produced a downward trend of atmospheric CO_2 concentrations that partially explains the cooling trend. However, the details are very poorly known, as are the CO_2 levels. Modeling studies of these possibilities are beginning.

In contrast to the last 125,000 years, many fewer data are available for comparison with model results for these earlier times. Nevertheless, the earth system was so different at these times that even relatively poor data sets reveal some of the large differences from the present.

The most important reason for giving some attention to this period is that it represents the most recent time when climate was significantly warmer than during recent interglacials. Increased levels of atmospheric CO_2 may have been partially responsible for the warmer conditions. Some aspects of system behavior under these extreme conditions are therefore of interest in order to check feedback sensitivities under extreme warm conditions (open Arctic, etc.).

Model Perturbations and Future Simulations

Thus far, we have emphasized opportunities for evaluating coupled models by comparison with observations. Two other classes of experiments have great potential to advance our understanding of the coupled earth system. These are long runs without external forcing to assess climate predictability and runs with large forcing to evaluate climate responses to major perturbations. Determining the limits to climate stability should be a critical objective of both kinds of experiments.

Climate predictability is a much discussed but poorly understood topic. Small changes in initial conditions clearly lead to different climate trajectories. The differences appear to be subtle over short time periods (Hansen et al., 1990), but do they ever increase with time? Daily weather records provide a short-term perspective on the limits to the predictability of climate, but very little is known about the long term and about whether coupling of modules tends to suppress or amplify the variability inherent in individual modules.

Experiments with major perturbations have two objectives. One is to explore the responses of the coupled earth system to hypothetical but potentially realistic external forcings. The other is to explore the kinds of conditions under which the climate becomes unstable and switches between fundamentally different states. Under the first

objective, interesting experiments would include coupled model runs with CO_2 elevated to three or four times present. This would extend the CO_2 story to something approaching a possible equilibrium, in addition to exploring responses to a major perturbation. Simulations of major volcanic eruptions and of perturbations like permafrost and polar ice sheet removal would similarly probe extremes.

Watson and Lovelock's (1983) Daisyworld is a toy model that illustrates the concept of limits to climate stability. With the real earth system, climate stability is unknown. The fact that ice sheets have advanced and retreated many times argues for substantial stability, but the climate may function in wells of potential energy that separate contrasting states. Changes in flower color can only do so much to maintain temperature in Daisyworld. In the real earth system, where are the limits to, for example, the thermostat function of clouds? Or, as emissions of reactive atmospheric species continue to increase, will they eventually so completely deplete the atmosphere of OH^- that it no longer plays a significant role in removing these species? These and similar questions clearly involve multiple components of the coupled earth system and must be explored with fully interactive models.

References

Berger, A., T. Fichefet, H. Gallée, I. Marsiat, C. Tricot, and J.P. van Ypersele. 1990. Physical interactions within a coupled climate model over the last glacial-interglacial cycle. *Transactions of the Royal Society of Edinburgh: Earth Sciences 81(4)*, 357–371.

Bjerknes, J. 1966. The El Niño/Southern Oscillation (ENSO) phenomenon. *Tellus 18*, 820–829.

Broecker, W.S. and G.H. Denton. 1989. The role of ocean-atmosphere reorganizations in glacial cycles. *Geochimica et Cosmochimica Acta 53*, 2465–2501.

Cess, R.D., G.L. Potter, J.P. Blanchet, G.J. Boer, S.J. Ghan, J.T. Kiehl, H. Le Treut, Z.X. Li, X.Z. Liang, J.F.B. Mitchell, J.J. Morcrette, D.A. Randall, M.R. Riches, E. Roekner, U. Schlese, A. Slingo, K.E. Taylor, W.E. Washington, R.T. Wetherald, and I. Yagai. 1989. Interpretation of cloud-climate feedback as produced by 14 atmospheric general circulation models. *Science 245*, 513–516.

Cess, R.D., G.L. Potter, J.P. Blanchet, G.J. Boer, S.J. Ghan, J.T. Klehl, H. Le Treut, Z.-X. Li, X.-Z. Liang, J.F.B. Mitchell, J.-J. Morcrette, D.A. Randall, M.R. Riches, E. Roekner, U. Schlese, A. Slingo, K.E. Taylor, W.E. Washington, R.T. Wetherald, and I. Yagai. 1989. Interpretation of cloud-climate feedback as produced by 14 atmospheric general circulation models. *Science 245*, 523–516.

Charlson, R.J., J.E. Lovelock, M.O. Andreae, and S.G. Warren. 1987. Oceanic phytoplankton, atmospheric sulphur, cloud albedo and climate. *Nature 326*, 655–661.

COHMAP Members. 1988. Climatic changes of the last 18,000 years: Observations and model simulations. *Science 241*, 1043–1052.

Dickinson, R.E. and A. Henderson-Sellers. 1988. Modelling tropical deforestation: study of GCM land-surface parameterizations. *Quarterly Journal of the Royal Meteorological Society 114*, 439–462.

Eddy, J. 1976. The Maunder Minimum. *Science 192*, 1189–1202.

Folland, C.K., T.R. Karl, and K.Y.A. Vinnikov. 1990. Observed climate variations and change. In *Climate Change: The IPCC Scientific Assessment* (J.T. Houghton, G.J. Jenkins, and J.J. Ephraums, eds.), Cambridge University Press, Cambridge, England, 195–238.

Foukal, P., and J. Lean. 1990. An empirical model of total solar irradiance variations between 1874 and 1988. *Science 247*, 556–558.

Fung, I.Y., C.J. Tucker, and K.C. Prentice. 1987. Application of advanced very high resolution radiometer vegetation index to study atmosphere-biosphere exchange of CO_2. *Journal of Geophysical Research 92*, 2999–3015.

Ghil, M., and R. Vautard. 1991. Interdecadal oscillations and the warming trend in global temperature time series. *Nature 350*, 324–327.

Hansen, J., A. Lacis, D. Rind, L. Russell, P. Stone, I. Fung, R. Ruedy, and J. Lerner. 1984. Climate sensitivity analysis of feedback mechanisms. In *Climate Processes and Climate Sensitivity* (J. Hansen and T. Takahashi, eds.), American Geophysical Union, Washington, D.C., 130–163.

Hansen, J.E., A.A. Lacis, and R.A. Ruedy. 1990. Comparison of solar and other influences on long-term climate. In *Climate Impact of Solar Variability* (K. Schatten and A. Arking, eds.), NASA, Washington, D.C.

Houghton, J.T., G.J. Jenkins, and J.J. Ephraums (eds.). 1990. *Climate Change: The IPCC Scientific Assessment* , Cambridge University Press, Cambridge, England, 365 pp.

Keeling, C.D., R.B. Bacastow, A.F. Carter, S.C. Piper, T.P. Whorf, M. Heimann, W.G. Mook, and H. Roeloffzen. 1989. A three-dimensional model of atmospheric CO_2 transport based on observed winds: 1. Analysis of observational data. In *Aspects of Climate Variability in the Pacific and the Western Americas* (D.H. Peterson, ed.), American Geophysical Union, Washington, D.C., 165–236.

Kutzbach, J.E., and R.G. Gallimore. 1988. Sensitivity of a coupled atmosphere/mixed-layer ocean model to changes in orbital forcing at 9000 years BP. *Journal of Geophysical Research 93*, 803–821.

MacCracken, M.C., A.D. Hecht, M.I. Budyko, and Y.A. Izrael (eds.). 1990. *Prospects for Future Climate: A Special US/USSR Report on Climate and Climate Change*, Lewis Publishers, Chelsea, Michigan, 270pp.

Philander, S.G.H. 1990. *El Niño, La Niña, and the Southern Oscillation*. Academic Press, San Diego, California, 293.

Ramanathan, V., and W. Collins. 1991. Thermodynamic regulation of ocean warming by cirrus clouds deduced from observations of the 1987 El Niño. *Nature 351*, 27–32.

Rasmusson, E.M., and J.M. Wallace. 1983. Meteorological aspects of the El Niño/Southern Oscillation. *Science 222*, 1195–1202.

Ravel, A., and V. Ramanathan. 1989. Observational determination of the greenhouse effect. *Nature 342*, 758–761.

Raymo, M.E., W.F. Ruddiman, and P.N. Froelich. 1988. Influence of late Cenozoic mountain building on ocean geochemical cycles. *Geology 16*, 649–653.

Rind, D., D. Peteet, W. Broecker, A. McIntyre, and W. Ruddiman. 1986. The impact of cold North Atlantic sea surface temperatures on climate; implications for the Younger Dryas cooling (11–10 K). *Climate Dynamics 1*, 3–34.

Rind, D., D. Peteet, and G. Kukla. 1989. Can Milankovitch orbital variations initiate the growth of ice sheets in a general circulation model? *Journal of Geophysical Research 94*, 12851–12871.

Rind, D., E.W. Chiou, W. Chu, J. Larsen, S. Oltmans, J. Lerner, M.P. McCormick, and L. McMaster. 1991. Positive water vapour feedback in climate models confirmed by satellite data. *Nature 349*, 500–502.

Ruddiman, W.F., and J.E. Kutzbach. 1989. Forcing of late Cenozoic northern hemisphere climate by plateau uplift in Southern Asia and the American West. *Journal of Geophysical Research 94(D15)*, 18409–18427.

Sellers, P.J. 1985. Canopy reflectance, photosynthesis and transpiration. *International Journal of Remote Sensing 6*, 1335–1372.

Shukla, J., C. Nobre, and P. Sellers. 1990. Amazon deforestation and climate change. *Science 247*, 1322–1325.

Tans, P.P. An observational strategy for assessing the role of terrestrial ecosystems in the global carbon cycle: Scaling down to regional levels. In *Scaling Processes Between Leaf and Landscape Levels* (J.R. Ehleringer and C.B. Field, eds.), Academic Press, San Diego, California, in press.

Tans, P.P., I.Y. Fung, and T. Takahashi. 1990. Observational constraints on the global CO_2 budget. *Science 247*, 1431–1438.

Trenberth, K.E., G.W. Branstator, and P.A. Arkin. 1988. Origins of the 1988 North American drought. *Science 242*, 1640–1645.

Tucker, C.J., I.Y. Fung, C.D. Keeling, and R.H. Gammon. 1986. Relationship between atmospheric CO_2 variations and a satellite-derived vegetation index. *Nature 319*, 195–199.

Watson, A.J. and J.E. Lovelock. 1983. Biological homeostasis of the global environment: The parable of Daisyworld. *Tellus 35B*, 284–289.

Wigley, T.M.L. 1989. Possible climate change due to SO_2-derived cloud condensation nuclei. *Nature 339*, 365–367.

Wigley, T.M.L. 1991. Could reducing fossil fuel emissions cause global warming? *Nature 349*, 503–506.

omit TO END

WORKING GROUP MEMBERS

Critical Gaps

Stephen Rintoul, rapporteur
Ronald Prinn, moderator
Andre Berger
Bert Bolin
Guy Brasseur
Francis Bretherton
Peter Brewer
Wallace Broecker
Kirk Bryan
Ping Chen
Paul Crutzen
Robert Dickinson
Inez Fung
William Hibler
Jennifer Logan
James McCarthy
Berrien Moore III
Michael Prather
Steven Running
John Steele
Holm Tiessen
Eli Tziperman

Development Needs

Alan Townsend, rapporteur
Stephen Frolking, rapporteur
Elizabeth Holland, rapporteur
Inez Fung, moderator
Berrien Moore III, moderator
Brian Walker, moderator
James Clark
Paul Crutzen
Jonathan Foley
William Hibler
Dennis Ojima
William Parton
Stephen Rintoul
Steven Running
David Schimel
Alan Thorndike
Holm Tiessen

Validation

Christopher Field, rapporteur
V. Ramanathan, moderator
Bert Bolin
Francis Bretherton
Andre Berger
Kirk Bryan
James Clark
Paul Crutzen
Lydia Dumenil
Christophe Genthon
Dana Hartley
Martin Heimann
William Hibler
John Kutzbach
Michael MacCracken
William Moomaw
Dennis Ojima
Richard Peltier
Michael Prather
David Schimel
Richard Somerville
Hassan Virji

PARTICIPANTS

Bert Bolin, Co-Director
University of Stockholm
Arrhenius Laboratory
Department of Meteorology
S-106 91 Stockholm
Sweden
46-8-157731

Francis Bretherton, Co-Director
University of Wisconsin at Madison
Space Sciences and Engineering Center
1225 West Dayton Street
Madison, WI 53706
608-262-7497

Barbara Anderson
Office for Interdisciplinary Earth Studies
University Corporation for Atmospheric Research
P.O. Box 3000
Boulder, CO 80307-3000
303-497-1686

Andre Berger
Institut du Astronomie et Geophysique
2 Chemin du Cyclotron
B-1348 Louvain-la-Neuve
Belgium
32-10-47-3303

Guy Brasseur
Atmospheric Chemistry Division
National Center for Atmospheric Research
P.O. Box 3000
Boulder, CO 80307
303-497-1456

Peter Brewer
Monterey Bay Aquarium Research Institute
160 Central Avenue
Pacific Grove, CA 93950
408-647-3706

Wallace Broecker
Lamont-Doherty Geological Observatory
Columbia University
Route 9W
Palisades, NY 10964
914-359-2900, ext. 413

Kirk Bryan
Geophysical Fluid Dynamics Laboratory
U.S. Department of Commerce/NOAA
P.O. Box 308
Rt. 1, Forrestal Campus
Princeton, NJ 08542
609-452-6571

James Clark
Department of Botany
University of Georgia
2505 Plant Sciences
Athens, GA 30602
404-542-3732

Paul Crutzen
Abteilung Chemie der Atmosphere
Max Planck Institüt für Chemie
Postfach 3060
Saarstrasse 23
D-6500 Mainz
Germany
49-6131-3051

Robert Dickinson
University of Arizona
Institute for Atmospheric Physics
Physics–Atmospheric Sciences Building
Room 542
1118 E Fourth Street
Tucson, AZ 85721

and National Center for Atmospheric Research
P.O. Box 3000
Boulder, CO 80307-3000

Lydia Dumenil
Meteorological Institute
University of Hamburg
Bundesstrasse 55
D-2000 Hamburg 13
Germany
49-40-41-231

John Eddy
Office for Interdisciplinary Earth Studies
University Corporation for Atmospheric Research
P.O. Box 3000
Boulder, CO 80307
303-497-1680

Christopher Field
Carnegie Institution
290 Panama Street
Stanford, CA 94305
415-325-1521

Inez Fung
Goddard Institute for Space Studies
2880 Broadway
New York, NY 10025
212-678-5590

Christophe Genthon
Goddard Institute for Space Studies
2880 Broadway
New York, NY 10025
212-678-5627

Martin Heimann
Max Planck Institüt für Meteorologie
Bundesstrasse 55
D-2000 Hamburg 13
Federal Republic of Germany
49-40-411-730

William Hibler, III
Thayer School of Engineering
Dartmouth College
Hanover, NH 03755
603-646-3172

Elizabeth Holland
Atmospheric Chemistry Division
National Center for Atmospheric Research
P.O. Box 3000
Boulder, CO 80307
303-497-1000

John Kutzbach
Center for Climatic Research
University of Wisconsin
1135 Meteorology and Space Science
Madison, WI 53706
608-262-2839

Jennifer Logan
Division of Applied Sciences
Harvard University
108 Pierce Hall
29 Oxford Street
Cambridge, MA 02138
617-495-4582

Michael MacCracken
Lawrence Livermore National Laboratory
Building 1701
7000 East Avenue
PO Box 808
Livermore, CA 94550
415-422-1826

James McCarthy
Museum of Comparative Zoology
Harvard University
26 Oxford Street
Cambridge, MA 02138
617-495-2330

James McWilliams
Climate and Global Dynamics Division
National Center for Atmospheric Research
P.O. Box 3000
Boulder, CO 80307
303-497-1352

C-Le.

William Moomaw
Center for Environmental Management
474 Boston Avenue
Curtis Hall
Medford, MA 02155
617-381-3486

Berrien Moore, III
Institute for the Study of Earth, Oceans and Space
University of New Hampshire
Science and Engineering Research Building, 4th Floor
Durham, NH 03824
603-862-1792

Dennis Ojima
Colorado State University
Natural Resources Ecology Laboratory
Grasslands Laboratory
Fort Collins, CO 80523
303-491-1976

William Parton
Natural Resources Environmental Laboratory
Colorado State University
Fort Collins, CO 80523
303-491-1987

Richard Peltier
Department of Physics
University of Toronto
60 St. George Street
Toronto, Ontario M5S 1A7
Canada
416-978-2938

Michael Prather
Goddard Institute for Space Studies
2880 Broadway
New York, NY 10025
212-678-5625

Ronald Prinn
Department of Earth, Atmospheric and Planetary Sciences
Massachusetts Institute of Technology
Cambridge, MA 02139
617-253-2452

V. Ramanathan
Scripps Institution of Oceanography
University of California, San Diego
Mail Code A-0221
La Jolla, CA 92093
619-534-8815

Stephen Rintoul
Division of Oceanography
Commonwealth Scientific and Industrial Research Organization
P.O. Box 1538
Hobart, Tasmania 7001
Austrailia
61-02-206-393

Steve Running
School of Forestry
University of Montana
Missoula, MT 59812
406-243-6311

David Schimel
Climate Systems Modeling Program
National Center for Atmospheric Research
P.O. Box 3000
Boulder, CO 80307-3000
303-497-1610

Richard Somerville
Scripps Institution of Oceanography
University of California at San Diego
Climate Research Group, A-024
La Jolla, CA 92093
619-534-4644

John Steele
Marine Policy and Ocean Management
Woods Hole Oceanographic Institution
Woods Hole, MA 02543
508-548-1400, ext. 2220

Alan Thorndike
Department of Physics
University of Puget Sound
1500 N. Warner
Tacoma, WA 98416
206-756-3817

Holm Tiessen
Saskatchewan Institute of Pedology
University of Saskatchewan
John Mitchell Building
Saskatoon, Saskatchewan S7N 0W0
Canada
306-966-6841

Eli Tziperman
Isotopes Department
The Weizmann Institute of Science
Rehovot 76100
Israel
972-8-482544

Brian Walker
Division of Wildlife and Ecology
Commonwealth Scientific and Industrial Research Organization
P.O. Box 84
Canberra, Lyneham, ACT 2602
Australia
61-62-42-1773

Agency Representatives

J. Michael Hall
Office of Global Programs
National Oceanic and Atmospheric Administration
1335 East West Highway
R/GP, 4th Floor
Silver Spring, MD 20910
301-427-2089, ext. 28

Hassan Virji
Executive Secretary to the CEES Working Group on Climate Change
Directorate of Geosciences
National Science Foundation
1800 G Street NW
Washington, DC 20550
202-357-9762

Graduate Students

Ping Chen
Department of Atmospheric Sciences
University of Illinois at Urbana-Champaign
105 South Gregory Avenue
Urbana, IL 61801
217-333-8413

Jonathan Foley
Center for Climatic Research
University of Wisconsin
1225 West Dayton Street
Madison, WI 53706
608-262-2839

Stephen Frolking
Complex Systems Research Center
University of New Hampshire
Durham, NH 03824
603-862-4098

Dana Hartley
Department of Earth, Atmospheric and Planetary Sciences
Massachusetts Institute of Technology
Building 54, Room 1326
Cambridge, MA 02139
617-253-0136

Alan Townsend
Department of Biological Sciences
Stanford University
Stanford, CA 94305-5020
415-725-1856

Leigh Welling
Department of Oceanography
Oregon State University
Corvallis, OR 97331-5503
503-737-2296

INDEX